IAEA-TECDOC-472

GEOLOGICAL DATA INTEGRATION TECHNIQUES

PROCEEDINGS OF A TECHNICAL COMMITTEE MEETING
ORGANIZED BY THE
INTERNATIONAL ATOMIC ENERGY AGENCY
AND HELD IN VIENNA, 13–17 OCTOBER 1986

A TECHNICAL DOCUMENT ISSUED BY THE
INTERNATIONAL ATOMIC ENERGY AGENCY, VIENNA, 1988

PLEASE BE AWARE THAT
ALL OF THE MISSING PAGES IN THIS DOCUMENT
WERE ORIGINALLY BLANK

GEOLOGICAL DATA INTEGRATION TECHNIQUES
IAEA, VIENNA, 1988
IAEA-TECDOC-472

Printed by the IAEA in Austria
September 1988

The IAEA does not normally maintain stocks of reports in this series. However, microfiche copies of these reports can be obtained from

INIS Clearinghouse
International Atomic Energy Agency
Wagramerstrasse 5
P.O. Box 100
A-1400 Vienna, Austria

Orders should be accompanied by prepayment of Austrian Schillings 100,— in the form of a cheque or in the form of IAEA microfiche service coupons which may be ordered separately from the INIS Clearinghouse.

FOREWORD

The objectives of this Technical Committee are to bring together current knowledge on geological data handling and analysis technologies as developed in the mineral and petroleum industries for geological, geophysical, geochemical and remote sensing data that can be applied to uranium exploration and resource appraisal.

The recommendation for work on this topic was first made at the meeting of the NEA-IAEA Joint Group of Experts on R & D in Uranium Exploration Techniques (Paris, May 1984). In their report, processing of integrated data sets was considered to be extremely important in view of the very extensive data sets built up over the recent years by large uranium reconnaissance programmes. A Technical Committee Meeting was convened in Vienna in October 1986 in order to provide a forum for the expression of new techniques and concepts in geological data integration techniques.

With the development of large, multidiciplinary data sets which includes geochemical, geophysical, geological and remote sensing data, the ability of the geologist to easily interpret large volumes of information has been largely the result of developments in the field of computer science in the past decade. Advances in data management systems, image processing software, the size and speed of computer systems and significantly reduced processing costs have made large data set integration and analysis practical and affordable. The combined signatures which can be obtained from the different types of data significantly enhance the geologists ability to interpret fundamental geological properties thereby improving the chances of finding a significant ore body.

This volume is the product of one of a number of activities related to uranium geology and exploration during the past few years with the intent of bringing new technologies and exploration techniques to the IAEA Member States.

The Scientific Secretary of the Technical Committee is Mr. D.W. McCarn of the Nuclear Materials and Fuel Cycle Technology Section of the IAEA.

EDITORIAL NOTE

CONTENTS

GEOCHEMICAL DATA INTERPRETATION AND INTEGRATION

WORKING GROUP REPORTS

GEOLOGICAL DATABASE MANAGEMENT SYSTEMS

EXPERIENCES WITH DATABASE MANAGEMENT SYSTEMS FOR REGIONAL RECONNAISSANCE AND MINERAL RESOURCE DATA

F. WURZER, H. KÜRZL
Mineral Resources Research Division,
Joanneum Research Society,
Leoben, Austria

Abstract

Presently the main task of the Mineral Resources Research Division (MRRD), Leoben, Styria, is to collect, store and process regional geological information related to the Austrian territory. Working on government contract all available data per 1:50000 mapsheet are systematically gathered and digitized. The aim is to establish a consistent digital data processing and documentation system able to provide individual information to the public. For this purpose an elegant way of data integration supported by a database management system (DBMS) is necessary. Main applications are dedicated to detailed mineral exploration and regional resource studies, especially supporting decisions in the realm of regional planning.

Different geological, geochemical, and geophysical data as well as facts concerning the mineral inventory, mining history, claims and a bibliography shall be incorporated in the system. Datatypes and structures are manifold and require special handling by the DBMS. Until now, however, no adequate solution to that problem seems to exist. Different approaches were tested, like hierarchical structured flat file management as for example supported by the VAX/VMS operating system, index sequential file structures, and relational DBMS like GRASP. Additionally VAX-DSM an interpreter language, which supports a highly structured hierarchical storage system is in extensive use. While with this language it is possible to develop a good working system for handling alphameric information especially for bibliographic and mineral inventory data, GRASP has reasonable abilities to deal with point related numeric data. Both systems, however, offer no sufficient solution to cases where thematic information is related or assigned to certain

geographic areas. Therefore at present the applicability of commercially offered geographic information systems is examined.

Recent results of the investigation suggest a combination of different DBMS's, each especially suited to the respective data structure. Well defined interfaces have to be designed to support convenient transfer and link of data.

---

1. INTRODUCTION

Regional surveys (airborne geophysics and stream sediment geochemistry) funded by the Austrian governement were carried out during the last decade. The major aim of these projects has been to increase domestic mineral exploration activities.

When the first data became available, it was obvious, that the amount of data to be handled and processed would require a well dedicated computer system. In fact no governmental and geoscientific institution in Austria had the capacity and experience to face that problem. Therefore the MRRD outlined a concept for the implementation of hard- and software, representing the basic requirements for a modern and comprehensive data processing system, well suited to handle all different types of "geo-data".

Meanwhile additional governmental contracts have been approved to gather additional regional data. For example, it is intended to establish a mineral inventory file for the whole Austrian territory. There is also the additional aim to supply governmental authorities as well as planing institutions with regional resource assessment and basic geological data. This was not obvious when originally etablishing the data processing system, so it had to be adjusted time and again.

The data processing system itself is near the fifth year of realisation. Starting with a PDP-11/34 (Digital Equipment Corporation) we now work on a VAX 8300 with a VMS operating system (12 MB Memory, 32-bit double processor) and three hard disks with 456 MB storage capacity each. In addition to online terminals, graphic capabilities include two HP vector plotters, one digitizer, one inkjet hardcopy unit and two Tektronix graphic terminals (4115B, 4207).

Starting with a rough overview of the basic theory and definitions concerning database systems the practical experiences will be outlined in this paper.

2. BASIC CONCEPTS AND DATA TYPES

Basically the overall purpose of a database system is to store, maintain, and retrieve information (resp. data). In the following there will be no clear distinction between the terms "data" and "information", both words will be used synonymously. Of course there can be seen an important difference: one can use data to refer to the values physically recorded in a database and information to refer to the meaning of those values understood by some user.

In the following the four major components of a database system (data, hardware, software, and users) will be described and shortly commented.

2.1 Data

Large amounts of data are gathered in the field of reconnaissance surveys, mineral exploration and mining. To preserve this information for future use and to satisfy present demands of current projects, it is very advisable to store these data in one or more common pools called database systems. A list of different sources of data is given in table 1.

A lot of these data resp. information is represented on maps. This fact includes the need for handling the corresponding geographic information (coordinates of points, lines and especially information related to areas).

This information, however can be very useful for different kinds of data integration (e.g. map overlay).

TABLE 1: Different sources of data to be stored in "geo-database systems".

Topography (e.g. digital terrain models)
Geology
Petrography and Mineralogy
Geochemistry
Geophysics
Exploration and Mining
Literature
Remote Sensing

2.2 Hardware

The hardware consists of the secondary storage devices (e.g. disks, drums, tapes plus the corresponding controllers) on which the database resides. But the related aspects should not be mentioned here because these aspects form a major topic in their own and the related problems are not so peculiar to database systems themselves. Of course minimum demands have to be satisfied, especially to suit the idea of combining thematic and geographical information like the graphical output devices (plotters, CRT's). It is also necessary to specify in advance which data have to be kept on disk to guarantee online retrieval. Depending on the amount of available data and mainly on the relative frequency of inquiries different parts of the database can be kept on tape.

2.3 Software

The link between the users of a database system and the physical database itself is build by a layer of software called the database management system (DBMS) providing access to data, maintaining facilities, security mechanisms, and so on.

2.4 Users

The users of a database system can be divided into three broad groups. The first are the application programmers writing the programs which need access to stored data. The second group is the class of end users accessing the database via a query language. The third group are database administrators doing the important job of creating and establishing as well as maintaining and updating the database in connection with all the necessary organisational and adminstrative duties.

2.5 Database Architecture

The architecture of a database is exposed in three levels, the conceptual, the internal, and the external level ([1], [2]). For each level corresponding models exist.

The conceptual model describes the logical overview of all data. This has to be specified before a new database is implemented.

The internal model describes the physical organisation of the data in the computer system itself.

The external model corresponds to different views of users, i.e. different users have their own requirements like a specially structured subset of the stored data. The DBMS has to provide the facilities for the respective retrievals.

2.6 Basic Approaches

The three most commonly used approaches to database modelling are the following:

a) the network database system,

b) the hierarchical database system

c) the relational database system

At MRRD network type database systems are not used, mainly because retrieval operations become very slow, when complex data structures are present.

3. PRACTICAL EXPERIENCE

The right selection of software for a database system is very important and strongly dependend on the group of users. The main part of this group is the inhouse staff requiring quick access to data in connection with project work and documentation. In addition to that a public service for off-line retrieval (via tape or printed reports) has to be established. Based on this principal demands the following DDMS's have been used to implement various databases by the MRRD.

The hierarchical database system VAX-DSM (Digital Standard Mumps, [3]) is a non structured interpreter language with a highly structured hierarchical storage system. The most important advantage is, that defined data fields do not use any storage as long as they have no assigned actual value. This feature is very useful for highly heterogeneous information like descriptions. A rough scheme for a mineral inventory file based on a hierarchical concept is outlined in figure 1. It is realized in VAX-DSM on our DP-system. Many of the items are descriptions of variable field length, which can be easily handled without wasting storage capacity.

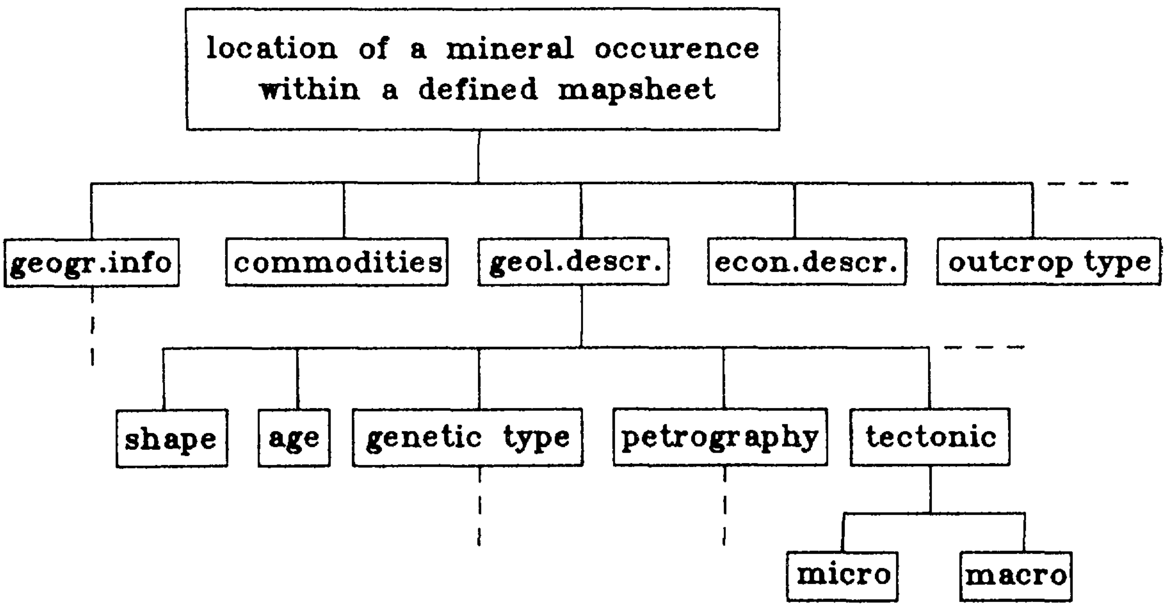

Fig. 1: Example for a hierarchical concept (mineral inventory file) - extensions are possible at any level

Another advantage of VAX-DSM is the flexibility in formulating inquiries and also in changing the hierarchical order of items.The flexibility of VAX-DSM ist based on the fact that it is not a DBMS in a strict sense but mainly a programming language. Of course this includes also the disadvantage that features usually provided by a DBMS (e.g. facilities for access restrictions) have to be written as routines. This gives the ability to design special applications but requires a lot of programming.

The state of art in computer science is represented by the relational approach. Objects and relations between them can be seen as tables. The scheme of a relational concept for a geochemical data file is given in figure 2. An existing relational system is GRASP (Geological Retrieval and Synopsis Program [4]) developed in FORTRAN at the U.S. Geological Survey. The MRRD uses a self developed system called DBS (Database System), which is based on the concept of GRASP but especially dedicated to application software and own projects.

ID	easting	northing	As	Al	...
1563	808846.	5234000.	15.	5.4	
...					

El	unit	anal.method	year	type	...
As	ppm	AAS	1984	str.sed.	
Al	%	ICP	1984	str.sed.	
...					
...					

Fig. 2: Example for a relational concept (stream sediments – analytical results)

The main advantages of relational DBMS's are the flexibility in retrieving data and in reorganizing a whole database. This is very important, because during the developement or during the lifetime of a database it is often necessary to adjust the implementation or even the whole conceptual model to fulfill new requirements. The best way to create a new database and to make it valuable and frequently used is by an iterative procedure. At first a "pilot version" of the database is implemented on the computer, based on a conceptual model, which is then transformed to an internal model. Intensive use of that pilot version should verify the usefulness of the concept and highlight additional requirements, to be incorporated in a final version.

4. ADVANTAGES OF DATABASE SYSTEMS

a) Redundancy can be reduced: if every user stores his own files belonging to his respective applications, the same data are stored several times, using up additional storage capacity.

b) Inconsistencies can be avoided: our experience shows that it is almost impossible to control the updating of multiple copies of data (sometimes one even does not know about such copies). This can create inconsistencies, i.e. some users work on corrected and others on "old" data.

c) Data can be shared: the same data can be accessed by several users at the same time. If the content of a database is well documented, which anyway is a necessity even unexprienced users, unaware of the availability of all the data, can be stimulatetd and get new ideas for further use. A good concept for a database can even foresee future requirements of applications, which should be satisfied.

d) Security restrictions can be applied with central control. Of course if these restrictions are not implemented misuse cannot be excluded and database systems can even support it.

e) Integrity can be maintained: integrity checks help to avoid errors (e.g. the sum of fractions given in percent should not exceed 100 percent).

f) Data independence: a very important advantage of data base systems is the independence between application programs and the physical file structure of the data used. Changing this structure does not necessitate rewriting whole programs because the DBMS provides access corresponding to the external model required.

5. PROBLEMS CONCEARNING GEOLOGICAL DATA

There are some basic problems which arise by setting up "geo database systems":

a) How can geographic information be handled in close connection to thematic information. For this purpose so called geographic information systems (GIS) have been developed. Those systems (e.g. ARC/INFO [5]) provide the facilities to digitize, edit, and plot geographic information. Map layouts can be designed and regionalised processes analysed in a proper and efficient way.

b) The problem of variable record length should not be neglected. Let us consider the example of the mineral inventory file, especially the geological descriptions. The length of such descriptions varies enormously from zero to many pages. For existing relational systems (like GRASP), there is no appropriate solution to that problem, because a fixed length is assigned to each data field. By cutting down voluminous descriptions, information will be lost, by defining large data fields to fit even the largest description, storage capacity will be wasted. The storage management for example of VAX-DSM provides dynamic allocation to solve this problem.

c) The problem of updating is always evident, especially if one uses a database to manage all the data for one geoscientific project. For example, the results of a statistical analysis show some grouping of geochemical data. Further analysis should be carried out within groups and the database should contain this additional information and provide the corresponding access. This was one reason, why MRRD developed it's own project database DBS, where this problem is solved.

d) One major problem for every database is the question of data quality. Inconsistencies in the source data, errors introduced by the process of data entry, measurement errors, raster information with low or inconsistent density - all these problems have to be considered. In many situations there is no clear solution to all that but it is a challenge for future work.

6. SUMMARY

Geological data have very heterogeneous forms, therefore not all the available information can or should be piled in one single database system. To guarantee transfer and link of data between different DBMS, well defined interfaces have to be designed. This is especially necessary when combining all kinds of thematic information with the corresponding geographical information (e.g. basic topographical data like drainage systems etc.). Relational DB systems, the state of the art in computer sciences, can be highly recommended but hierarchical approaches are still usefull to solve the problem of variable record length (e.g. for the incorporation of qualitative geological facts and descriptions).

REFERENCES

[1] DATE, C.J. (1981): An introduction to database systems, third edition. Addison Wesley Publ. Comp. Reading, Massachusetts.

[2] SCHLAGETER, G., STUCKY, W. (1983): Datenbanksysteme: Konzepte und Modelle. B.G. Teubner, Stuttgart.

[3] VAX-11 DSM Language Reference Manual, AA-J415B-TE, Digital Equipment Corporation, December 1982.

[4] GRASP Users Manual, Roger W. Bowen, U.S.G.S., Reston, Virginia, June 1982.

[5] ARC/INFO Users Manual Version 3.2, Environmental Systems Research Institute, Redlands California, USA, April 1986.

ADAPTATION OF THE RELATIONAL MODEL TO LARGE VOLUME GEOSCIENCE DATABASES

M.T. HOLROYD
Dataplotting Services Inc.,
Don Mills, Ontario, Canada

Abstract

Over the last half decade, the Relational model has become the preferred model for Data Base Management System (DBMS) design and the Hierarchical model has come to be regarded as obsolete. The very large volume data sets from geophysical surveys are, however, intrinsically hierarchical - in both their data structures and in the data manipulation requirements of the digital compilation and cartography processes. Converting an interpolated map grid from its conventional form to a normalised relation, would (at least) double the data storage volume and (at least) quadruple the data access time. With only moderately sized surveys this is an unacceptable penalty.

The relational model does, however, have distinct advantages over its predecessors in its clarity and simplicty of data definition and in the rigor with which data manipulation operations can be specified. These advantages could be of substantial benefit to geoscience data processing if the attendant disadvantages could be overcome.

One means to accomplish this is to employ an Algebraic data structure model in conjunction with the Relational model. The Algebraic model treats relational domains as vectors. It too employs a rigorous formal definition of data structure and manipulation processes. The relationships between domains in the same relation and between different relations are defined by arithmetical operators used in a logical sense. The data base can thus be described by an algebraic expression and data manipulation processes can exactly be modelled by algebraic manipulation of this expression.

The addition of the Algebraic model overcomes the above noted disadvantages of the Relational model as it permits Geoscience data sets to be viewed externally as fully normalised relations yet treated internally in their conventional, condensed form.

---

1. DATA BASE MANAGEMENT SYSTEMS (DBMS)

1.1 General definitions

At one time the bulk unit of data was regarded as the "file" in which all records were of the same form and content, hence simple "read and write" programs were usually adequate for data access and manipulation. Today, the bulk unit of data is the "data base" - a collection of many different interrelated "files" with different contents and structures.

Martin [1] defines a data base as follows:

"A data base may be defined as a collection of interrelated data stored together without harmful or unnecessary redundancy to serve one or more applications in an optimal fashion: the data are stored so that they are independent of programs which use the data; a common and controlled approach is used in adding new data and in modifying and retrieving existing data within the data base. One system is said to contain a collection of data bases if they are entirely separate in structure".

Date [2] provides a much briefer definition:

"A data base is a collection of stored operational data used by the application system of some particular enterprise".

Olle [3] defines the data base in contrast to the above mentioned file as follows:

"The difference between a data base and a file, in terms used prior to the advent of data processing, is perhaps analogous to the difference between a thoroughly cross-referenced set of files in cabinets in a library or in an office and a single file in one cabinet which is not cross-referenced in any way.

The relationship between the data base and the data base management system (DBMS) is described by Olle (op. cit.) as:

"A data base is a set of data stored in some special way in direct access computer storage. A DBMS is the software that handles the storage and retrieval of the records in this data base".

1.2 Data structure models and DBMS implementations

Current implementations of the DBMS fall into three general categories on the basis of the underlying structural model. The categories are "Hierarchical", "Network" and "Relational". The mathematical bases of such structures are described in detail by Berztiss [4].

Hierarchical systems are based upon the "tree" structure, and network systems on the network or plex structure. Relational systems are based upon Relational algebra. A comprensive review and comparison of the properties of the three types is to be found in Date (op. cit.)

2. THE RELATIONAL DBMS AND GEOSCIENCE DATA BASES

2.1 The characteristics of Relational data and DBMS

Relational data bases contain one or more physically independent tables - rows and columns - of data. Such a table is referred to as a "Relation". Each row or record of the relation is referred to as a "tuple" (As in "N-tuple"). The tuples of any one Relation must all have the same logical structure and content. The data items in any one column of a Relation must all belong to the same "Domain" of information.

The standard data manipulation operations available in a Relational DBMS consist simply of "SELECT", "PROJECT" and "JOIN".

SELECT operates on a single table to select certain records according to content. PROJECT operates on a single table to extract (to "project out") entire columns. Either or both of these two operations applied to a table create a new table as a row and/or column subset of the original.

The JOIN operation takes the records of two separate tables and "joins" them together wherever the same value of a specific field is found in the records of both tables. This again creates a new table. A JOIN operation is, however, only meaningful if the JOIN is made on two columns, one in each, table which both belong to the same domain.

It was shown by Codd [5], the originator of this model, that an admixture of these three basic operations, applied recursively and repeatedly as required, could isolate any definable subset of the entire data base as a single Relation. Furthermore, it is not necessary to create any predefined access paths, pointers, linkages or indices to attain this goal.

In order for these operations to proceed correctly, however, it is necessary that the following rules apply to the Relations:

1) every record must have one more fields or whose value(s) is(are) unique within the relation (a unique key).

2) all other fields within the record must be "functionally dependent" on this key.

3) all other fields must be functionally independent of each other.

These rules together constitute what is called "third normal form" and the process of putting the data base in such order is known as "Normalisation". (The phrase "The Key, the whole Key, and nothing but the key, so help me Codd" is a helpfull mnemonic for this.)

2.1.1 The general advantages of the Relational Model

The relational model offers certain potential advantages over the Hierarchical and Network models:-

1) It greatly simplies the user's view of the data base. Instead of complex graphical structures, we now have sets of simple tables - data in the form we normally conceive of it.

2) No pre-defined retrieval bias is built-in to the relational DBMS in the form of hierarchical linkages or network pointers, etc. Hence retrievals from any and all viewpoints are equally feasible.

3) Operations apply to whole tables and create new whole tables.

Consequently, the relational approach is currently very much favoured by the user community.

It must be noted though, that this is employed in practice as a conceptual model which governs the users' view of the data base and defines formally the structures of the data base and the manipulation processes applicable to it. All existing Relational DBMS's (that are acceptably efficient) rely internally, beyond the user's view, on older well proven, techniques taken straight from their Hierarchical and Network progenitors in order to function efficiently.

2.2 The characteristics of large geoscience data bases

Among the largest geoscience data bases that currently exist are those derived from large scale aero-geophysical surveys, and the volume of data gathered by such surveys is steadily increasing. This increase is exhibited by all three possible degrees of freedom - size of survey area, data acquisition rates and number of survey parameters recorded.

Bristow [6] describes an airborne gamma ray spectrometry system capable of sampling up to 1024 energy channels at rates of up to 4 samples per second. Each channel/sample is a 16 bit word, hence the maximum data acquisition rate is 8 Kbytes/second or approximately 30 Megabytes/hr. 100 hours of survey flight would therefore acquire approximately 3 Terabytes of digital data.

The Thailand aerogeophysical survey [7] currently in progress contains about 1,000,000 kilometers of survey flight line. Magnetics, gamma-spectrometry VLF and electronic navigation (ENS) data are all recorded digitally. The raw data (as recorded in-flight) volume will be several Gigabytes. The processed final data (interpolated grids, etc) will be in the Terrabyte range.

2.2.1 The logical content of survey data bases

Regardless of type, such survey data bases generally contain the following logical data entities:-

i) FIELD - A single number. e.g. A spatial coordinate, a geophysical measurement.

ii) STATION - A group of fields of different types all related to the same space/time point.

iii) LINE - An ordered sequence of stations.

iv) BLOCK - A group of lines which can be processed as an independent unit.

v) SURVEY - One or more blocks constituting an entire project.

vi) MAP - A subset of a block or survey within an arbitrarily defined polygonal boundary.

vii) GRID - A set of geodata values all of the same type arranged in grid order over all or part of the survey area.

2.2.2 The inherent structure of survey data bases

The essential function of a DBMS applied to geoscience data is to support efficient storage and retrieval of the above described logical entities.

These entities, however, clearly exibit inherent structures more suited to the oldest data model rather than the Relational model. For example "Survey - Block - Line - Station - Field" is a strictly one-to-many structure. As is "Survey - Map - Line" and "Survey - Grid - Value" i.e. all are strict hierarchies.

Furthermore, the retrieval requirements when processing this data have strictly "top-down" hierarchical search paths. i.e. The basic requirement is to retrieve the lowest level entities - a line of stations - from a specified survey and map. This writer has never encountered an application requiring an inverse search. i.e. to find the line, map and survey which contain a specific aeromagnetic field value or Uranium count.

The above considerations indicate that this type of data is inherently suited to a hierarchical DBMS. Other considerations exist which indicate its inherent unsuitability to a Relational DBMS.

2.3 Geoscience data bases and the Relational DBMS

There is nothing inherent in the types of data entities described above that would actually prevent them from being put into and served by a relational DBMS. All of the different data sets encountered in geoscience could be structured as sets of relations (it can be shown, in fact, that any data base of any kind and complexity can be restructured as a set of relations with no loss of information.)

The important question to answer is what are the advantages and disadvantages of doing so ? The general advantages of the Relational model have been described, as have certain considerations which indicate the inherent suitability of survey data to a Hierarchical model. There also exist clear disadvantages in applying a Relational DBMS to survey data.

An obvious disadvantage is one of the cited general advantages of the Relational model. i.e. the absence of pre-defined access paths. As described above, survey data bases have distinctly preferred access paths. Hence no disadvantages ensue from having these built-in, and substantial improvements in efficiency result from having them. Hence a Relational DBMS prevents exploitation of the inherent structures of the data base.

The greatest disadvantage, however, arises from the need to normalise the relations. To illustrate this, consider one of the larger data groups employed in survey data processing - the interpolated data grid.

Such grids, interpolated across and between the data traverses, are an essential prerequisite to mapping and three dimensional interpretation processes. The grids are normally stored in row or column order as sequences of binary numbers. Each number represents an interpolated value at one node of the grid. A separate "header" record defines associated grid parameters such as cell dimensions, orientation, coordinates of grid origin, data type, etc.

A single grid value can not be assumed to be unique within the set of grid values. Hence the data as usually stored violates the first rule of normalisation (section 2.1 above). In order to normalise the data, it would be necessary to store explicitly the row and column index numbers with each grid node. As no two grid nodes can have the same row/column indices, these two fields together would constitute the mandatory unique key in each record of the grid relation.

Hence, normalisation would triple the number of data items to be stored for any grid. Although it is techically simple to expand the grid data in this way, the resulting 300% increase in storage volume and retrieval time is totally unacceptable in practice.

Not all survey data groups are as intractable as grid data. The in-flight data set, for example, exists from the begining as a fully normalised relation. i.e. each record contains a fiducial which is unique, and in-flight measurements which are functionally dependent on this key and independent of each other. Even so, such data is still not acceptable as-is for manipulation by a Relational DBMS because of the pre-requisites of the JOIN operation.

Creation of a specific map as a subset of the entire in-flight data set involves "joining" this data set with another relation defining the map involved. The in-flight data as stored, however, even though it is normalised, does not contain a domain in common with the map definition data. Hence, the requisite join can not be made.

In order to facilitate the join, data from the "map no." domain would have to be added as another column to the in-flight data. Likewise, for block or survey extraction. This again would reduce storage and retrieval efficiency.

3. ADAPTATION OF THE RELATIONAL MODEL TO GEOSCIENCE NEEDS

It can be concluded from the above observations that the Relational model and current DBMS implementations of it, are generally unsuited to the needs of large geoscience survey data bases, and by extension, to any other geoscience data base with similar properties to the survey data base.

The model could, though, be extended and adapted to geoscience needs. A DBMS based on such an extension could offer the simplicity and power of the relational concept and still be highly efficient.

Any adaptation would have to resolve the problems of data storage and retrieval efficiency. The adaptation should also, in keeping with the Relational model, have a formal theoretical basis. It should not be simply an an-hoc superficial modification.

A potential candidate for the adaptation is the Algebraic data model. The properties of this model are described below.

3.1 The Algebraic data model

The Algebraic data model was derived from observation of a variety of geoscience data sets and the manipulation processes commonly applied to such data in geoscience data compilation systems.

A key feature of the model is the use of arithmetical operators to represent the logical relationships between various levels of components of the data set. This permits a data set to be represented symbolically as an algebraic expression.

It was shown that formal algebraic manipulation of such an expression exactly models all of the basic data manipulation operations carried out within the geoscience processing systems studied and permits formal derivation of subsequent data structures from the initial form of tha data set.

Detailed description of the derivation of the model is given by Holroyd [8]. A summary description follows.

3.1.1 Definition of terms

A data item is an "attribute" of some real-world entity. An attribute possesses two components - a "type" and a "value".

The "attribute type" is a real-world property of the entity. Mass and colour are two examples of real-world properties of physical objects. The "attribute value" is an observed or measured value of the property. e.g. "50 kilograms" is a possible value for the attribute type mass.

A group of attributes which all describe an individual entity is an "aggregate". A data set is composed of many such aggregates, one for each of the entities that the data set describes.

A data set is in "cardinal from" if all of the entities described by the data set belong to the same class (i.e. all are described by the same set of attribute types), and there is a unique one-to-one correspondence between entities and aggregates. Such a data set is a simple table. Each row is an aggregate describing one and only one entity. Each column contains a single type of attribute. This is similar to a normalised relation. The difference is that there is no need for a unique key.

3.1.2 Arithmetical equivalents to logical relationships

Logical relationships between data set components can be expressed as arithmetical operators. This confers algebraic properties on the data set model.

The logical relationship between attributes of the same entity is equivalent to the simple multiplication operator. The logical relationship between aggregates describing members of the same entity is equivalent to the addition operator. The logical relationship between aggregates describing members of different entity sets is the null operator.

3.1.3 Notational conventions for the data model

An attribute is represented by a letter for the type and an integer for the specific value. e.g. -

$$A7 \qquad (1)$$

A letter followed by a lower case alphabetic subscript represents the general case. e.g., if "A" represented the property of colour, then "some or any particular colour" is represented by:-

$$A_i \qquad (2)$$

An aggregate of the attributes of a single entity is represented by a string of attribute symbols separated by commas to indicate the multiplicative relationship. e.g description of a particular entity by specific values of three types of attributes is represented as: -

$$A7,B5,C2 \qquad (3)$$

A data set in cardinal form is represented by a sequence of aggregates separated by plus signs to indicate the additive relationship. e.g a data set describing three entities of the same class is represented as:-.

$$A7,B5,C6 + A2,B1,C1 + A1,B1,C9 \qquad (4)$$

A data set can be characterised by type simply by the attribute types it contains, regardless of any specific attribute values. Parentheses are used to indicate replication. e.g. the cardinal form in (4) above can be summarised as:-

$$(A,B,C) \qquad (5)$$

3.1.4 Algebraic representation of cardinal form data

An expression representing a common aerogeophysical data set is :-

$$M1,L1,F1 + M1,L1,F2 + \dots M1,L2,F_i + \dots M2,L1,F_j + \dots M_k,L_k,L_k \dots \text{etc.} \qquad (6)$$

A data set of this form is created by digitisation of the flight path maps of a survey. The entities are navigational fixes along flight lines on maps. The attributes of each entity are as follows:-

M	map number
L	line number
F	fiducial (serial) number.

The first aggregate (M1,L1,F1) describes the first entity - the first fix on the flight path - by the map and line upon which it lies and by its fiducial number. The second aggregate (M1,L1,F2) describes the second flight path point, etc, etc.

Note that, according to the notational convention, the second fix is on the same map and line as the first, but has a different fiducial number. Successive aggregates describe fixes on different lines, then on different maps.

The elipsis (...) in the expression indicates that a sequence of aggregates, unspecified in number, has been omitted for brevity. The lower case subscripts ("i", "j" and "k") indicate the general-case of the aggregate - "some/any specific value".

All of the information available for description of each entity resides in one aggregate and this aggregate contains no information descriptive of any other entity. Hence by definition this is the cardinal form of the data set. The summary representation of (6), as in (5), is:-

$$(M,L,F) \tag{7}$$

3.1.5 Algebraic development of alternative forms

The above representation of the cardinal form of the data set was derived simply by observing an actual data set then describing it symbolically according to the notational convention.

Noting that the same map number is common to many successive aggregates, and that the same line number is common to many successive aggregates within one map, and that the relationship between attributes is multiplicative, then these common values can be factored out of (6) to produce the expression:-

$$\begin{aligned} &M1(\ L1(\ F1 + F2...Fi) + L2(Fj...)\ ...\ + Li(..)) \\ &+ M2(\ L1(..)...)\ ...\ Mi \end{aligned} \tag{8}$$

- which, in summary notation is:-

$$(M(L(F))) \tag{9}$$

Expression (9) is, in fact, a hierarchical structure. This same structure is developed within data compilation programs by the first process applied to the initial digitised track data in order to economise on storage and improve retrieval efficiency.

Here, the structure was developed solely by formal algebraic manipulation of the data set expression. This briefly demonstrates the simulation capabilities of the model.

More complex manipulation procedures can be carried out which bring more powerful operators into use. These are the "dot" (inner product) and "star" (outer product) operators. The use of these operators is shown in the next section.

3.2 Combination of the Relational and Algebraic models

At the conclusion of section 2.1.1 above, it was noted that the Relational model is employed conceptually to provide a formal framework for the user's view of data base structure and manipulation processes. What actualy goes on within the workings of the DBMS is of no consequence provided that it appears to adhere to the formal rules of the Relational model.

Even so, the rules still do not permit, for example, storage of a data grid in a Relational DBMS in any other than the expanded, inefficient structure as described.

If, however, we permit a relation to be defined as an algebraic structure, it becomes possible to store a data grid in the usual efficient way and still maintain it as a fully normalised relation in the manner shown below.

The expression for the data grid with the preferred, efficient, structure is:-

$$G1 + G2 + G3 \ldots \qquad (10)$$

In summary form this is:-

$$(G) \qquad (11)$$

i.e. simply rows and columns of grid values alone.

The required relational structure is:-

$$I1,J1,G1 + I1,J2,G2 + \ldots.$$
$$+ I2,J1,Gj + I2,J2,Gk\ldots \qquad (12)$$

In summary form this is:-

$$(I,J,G) \qquad (13)$$

i.e. rows and columns of grid values each with an explicit row number (I) and column number (J).

Note that all of the aggregates in the first grid row all have the same row number I1 and that all the aggregates in the next row all have the same row number I2. The column numbers in the first row are all different. They begin at J1 and increase serially by 1 to Jm, where m is the number of columns in the grid. This sequence from 1 to m is repeated in all subsequent rows. Hence, there are many common factors in the expression.

The expression can therefore be factorised. Two hierarchical forms are possible:

(I(J,G)) (14)

or:-

(J(I,G)) (15)

In (14), the row number occurs once only at the start of each row. This is followed by a sequence of grid values each with an explicit (and different) column number. In (15) the grid matrix has been transposed to column order.

Both of these two forms reduce storage but neither is as efficient as the desired form (11). The outer and inner product operators, however, can be used to reduce the expression to essentially the desired form as:-

(I)*(J).(G) (16)

This structure consists of all unique row numbers stored once only, followed by all unique columm numbers stored once only, followed by the entire grid stored as grid values only, in the same form as (11). When (16) is multiplied out, however, it becomes the normalised cardinal form in (13).

Hence (16) is formally the equivalent of (13) but requires considerably less data storage. With a grid of M columns and N rows, the number of items L1 in (13) is given by:-

L1 = 3 x (M x N) (17)

For (16), the number of items L2 is given by:-

L2 = M + N + (M x N) (18)

For a 1000 x 1000 point grid, L2 is only 0.2% larger than the optimum achieved in (11), whereas L1 is 300% larger.

Similarly, the flight path data set in (9) is formally the equivalent of its cardinal form (7). Hence (9) can be stored in the preferred, access and storage efficient, hierarchical form and still retain its formal definition as a normalised relation.

3.2.1 Implementation considerations

In an actual implementation of an "Algebraic/Relational" DBMS, very little need be added to the user's burden beyond that already carried for a standard Relational DBMS. The user could regard all data as being in a fully normalised form at all times and hence perform all the standard Relational operations without hindrance.

The Algebraic aspects would be an additional capability totally independent of Relational operations. Provision would simply be made for the user to define the preferred algebraic structures for the relations so as to optimise storage and retrieval efficiency.

A simple but powerful data manipulation language could be created on the formal algebraic basis of the model. For example, a command as simple as:-

(M,L,F) -> (M(L(F)))

- is sufficient to define fully and invoke the factorisation process to create a hierarchy from a table.

4. CONCLUSIONS

It has been shown that commonly employed geoscience data bases have inherent structures which make them more suited to data models other than the Relational model and that Relational DBMS´s have features inherently unsuited to many common data storage and manpulation requirements of geoscience data.

Hence, it can be concluded that Relational DBMS´s as they currently exist, are essentially inappropriate for many geoscience data management needs.

Specific features of geoscience data and the Relational model were examined to determine exactly where the most severe problems lay.

The properties of a new data model, the Algebraic model, were demonstrated. These properties were employed to find solutions to the problems.

It is concluded that a DBMS could be implemented with the Algebraic model as an adjunct to the Relational model. Such a system would make the beneficial features of the Relational method applicable to geoscience data without the attendant problems that currently make Relational systems inapplicable to such data.

REFERENCES

[1] Martin, J., Computer Data Base Organisation, Prentice Hall Inc., Englewood Cliffs, New Jersey (1975), 44.

[2] Date, C.J., An Introduction to Data Base Systems, Addison-Wesley Publishing Co., Reading Mass. (1976), 1.

[3] Olle, T.N., "Data base and data base management", Encyclopedia of Computer Science, 3rd ed., Petrocelli/Chanter, New York (1976), 389.

[4] Berztiss, A.T., Data Structures: Theory and Practice, Academic Press, New York (1975).

[5] Codd, E.F., "A data base sub-language founded on the relational calculus", Proc. ACM SIGFIDET Workshop on Data Description, Access and Control (1971)

[6] Bristow, Q., "A gamma-ray spectrometry system for airborne geological research", Current Research Part C, Geological Survey of Canada Paper 79-1C (1979), 55.

[7] (Anon), Technical Specifications, Bidding Documents for Airborne Geophysical Survey No. MRDP/01/1983, (Prepared by Geological Survey of Canada) (1983)

[8] Holroyd, M.T. A System for Automated Compilation and Cartography of Earth Science Data With Special Provision for Aerogeophysical Data, Phd Thesis, University Of Ottawa, Geology Department (1984)

SAMINDABA — A SOUTH AFRICAN MINERAL DEPOSITS DATABASE

S.S. HINE, E.C.I. HAMMERBECK
Geological Survey of South Africa,
Pretoria, South Africa

Abstract

The South African Mineral Deposits database, SAMINDABA, is designed specifically to accommodate interactive computerized access to data on known mineral deposits within the Republic of South Africa. Data on a wide range of mineral deposits is being captured at present, interalia on uranium deposits of the Karoo Sequence.

The mineral deposit data is subdivided into seven major groupings: DEPOSIT IDENTIFICATION DATA identifying and locating the mineral deposit; HOST ROCK DATA a multiple data grouping describing the host rock(s) surrounding the ore body(ies); OREBODY DATA a multiple data grouping describing the geological characteristics of the orebody(ies); EXPLORATION DATA describing the history and level of exploration carried out on the mineral deposit; EXPLOITATION DATA RESOURCE DATA describing deposit resources sub-divided into the following subgroups: demonstrated economic reserves, demonstrated marginal reserves, demonstrated subeconomic resources, and inferred resources and, finally, DATA REFERENCES describing references to the sources of the mineral deposit data.

SAMINDABA'S primary functions include the capture, validation and updating of the mineral deposit data while at the same time maintaining a high level of security. Enquiries on and extraction from the database can be done on two levels, firstly using an on-line, menu driven enquiry system, SAMENQ, which allows a user, no matter what his level of computer expertise, to make enquiries using predefined search paths, key fields and output formats. The second level, using the database enquiry language, requires a specialized knowledge of the database structure and the enquiry language together with a much higher level of computer literacy, but allows a user freedom to enquire and output the enquiry results in any format that he wishes.

Due to the availability and high level of development of computer software no specific applications software was written

for SAMINDABA but rather a facility was created in SAMENQ allowing a user to output the results of an enquiry to an interface file for input to various application packages as required. These, at present, include statistical, graphical, mapping and modelling packages.

---

1. INTRODUCTION

One of the primary functions of the Geological Survey is to provide basic geological information to promote the exploration for, and mining of, minerals in South Africa.

To date the collection, compilation and dissemination of data and information on mineral occurrences and deposits has been done manually. The ever increasing volume of such data and information is making it extremely difficult to manage this function efficiently, and hence the establishment of a computerized mineral deposits database was proposed.

A study was made of various existing geological databases, in particular CANMINDEX, CRIB, DASH and G-EXEC [1,2,3,4]. This was followed by a detailed data analysis and with the help of two computer consulting firms the South African Mineral Deposits Database (SAMINDABA) was designed, written and implemented[5,6].

2. SAMINDABA DESIGN PHILOSOPHY

SAMINDABA, a menu driven, on-line system was designed to support a wide range of users with varying degrees of technical and computer expertise. Special attention was paid to the protection of confidential data down to element level. SAMINDABA functions can be broadly subdivided into three groups as depicted in figure 1.

1. Capture, validation and storage of mineral deposit data
2. Enquiries against the database and output of the data
3. Processing of the data

The first two of these functions support the whole spectrum of users and have extensive help, maintenance and system security facilities, while the processing function of SAMINDABA requires a greater technical knowledge and assumes that the user takes responsibility for the data. This processing portion of SAMINDABA is totally divorced from the database and it's con-

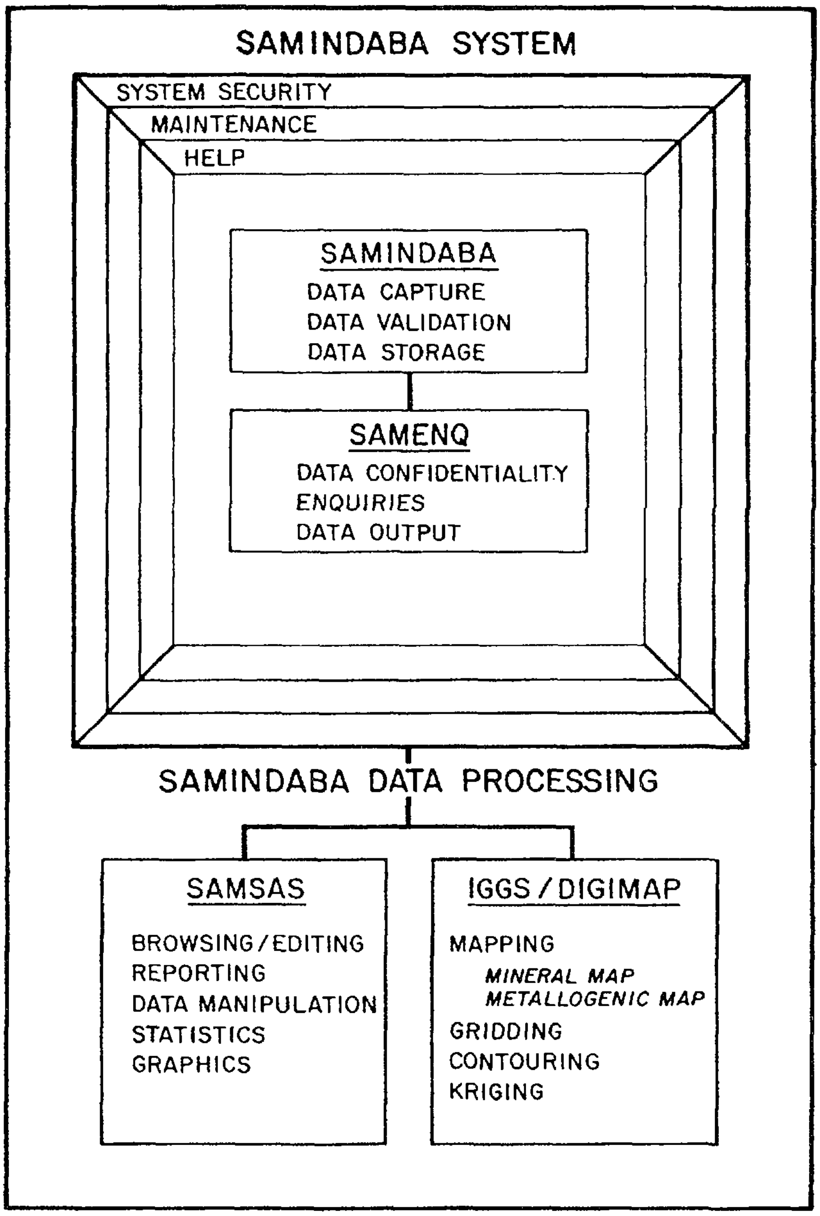

FIG. 1. Schematic representation of relationships between SAMINADABA system, output and processing facilities

tents can in no way be affected by any of the available functions.

3. GEOLOGICAL CONCEPTS

A SAMINDABA mineral deposit is defined as an identified natural concentration of minerals which is geologically, geographically or otherwise distinguishable from neighboring concentrations. The data describing the deposit have been divided into seven logical groupings as follows :

1. Deposit Identification or Header Data
2. Host Rock Data

3. Orebody Data
4. Exploration Data
5. Exploitation Data
6. Resource Data
7. Data References

3.1 Deposit Identification or Header Data

The data in this group, as shown in figure 2, primarily identifies and locates a mineral deposit and is subdivided into three groups of elements:

1. Deposit Identification
   The deposit identification data grouping consists of the deposit name, synonum names, commodities, deposit type and the deposit status.
2. Deposit Locality
   The locality data elements precisely locate a deposit both geographically and within certain boundaries.

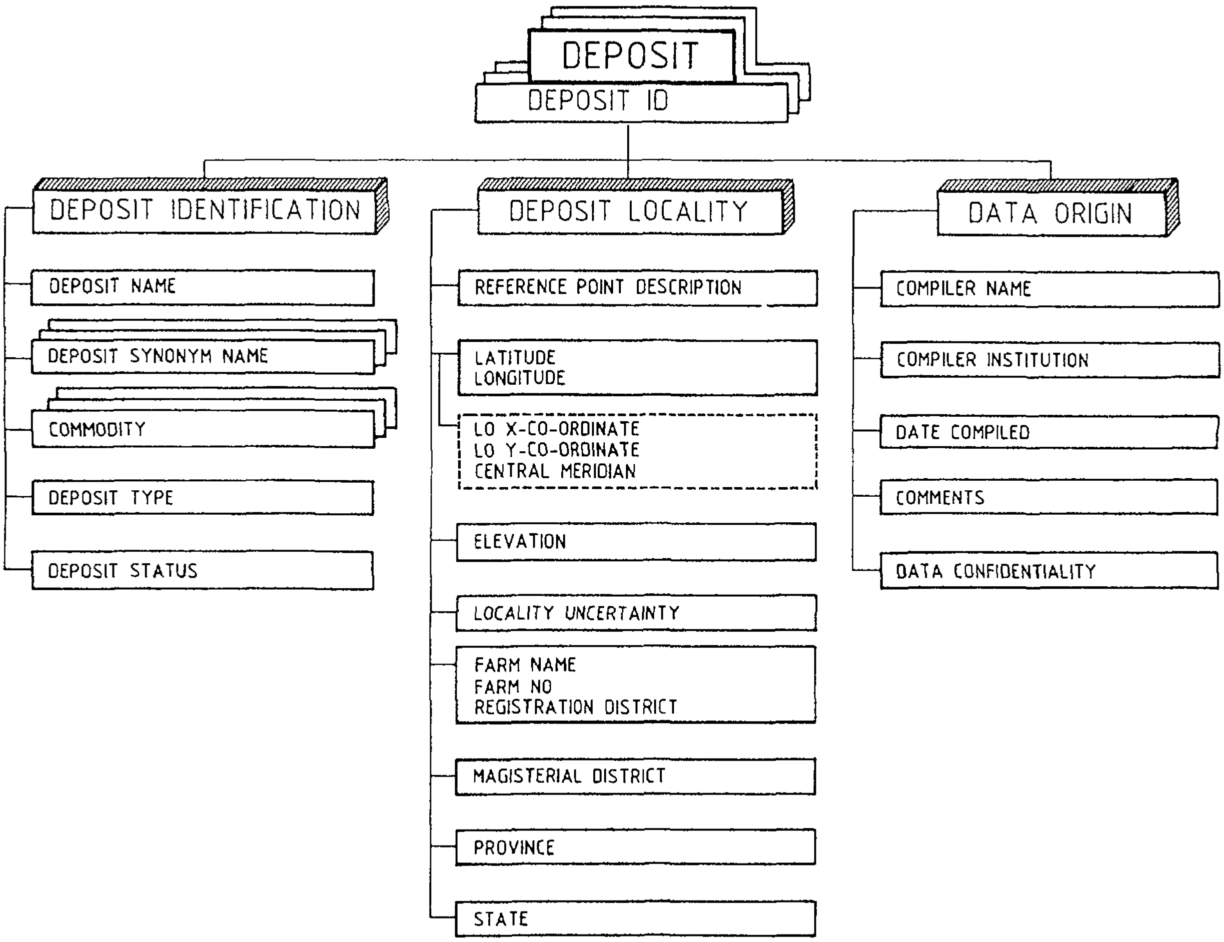

FIG. 2. SAMINDABA deposit identification data elements

(e.g. farm, province etc.). Geographically a deposit locality represents a point located approximately at the centre of the deposit within a farm boundary at surface elevation and defined by a longitude, latitude and elevation.

3. Data Origin

   This group of data elements, which is also included with all the other six data groupings describes who the contributor of the data was and what the confidentiality status of the data is.

3.2 Host Rock Data

The host rock data grouping describes the rock or rocks surrounding the mineral deposit and contains the data elements as shown in figure 3. These data elements describe the rock type, geochronology, lithostratigraphy, structure, alteration, laboratory investigations and the economic status of the host rock or rocks.

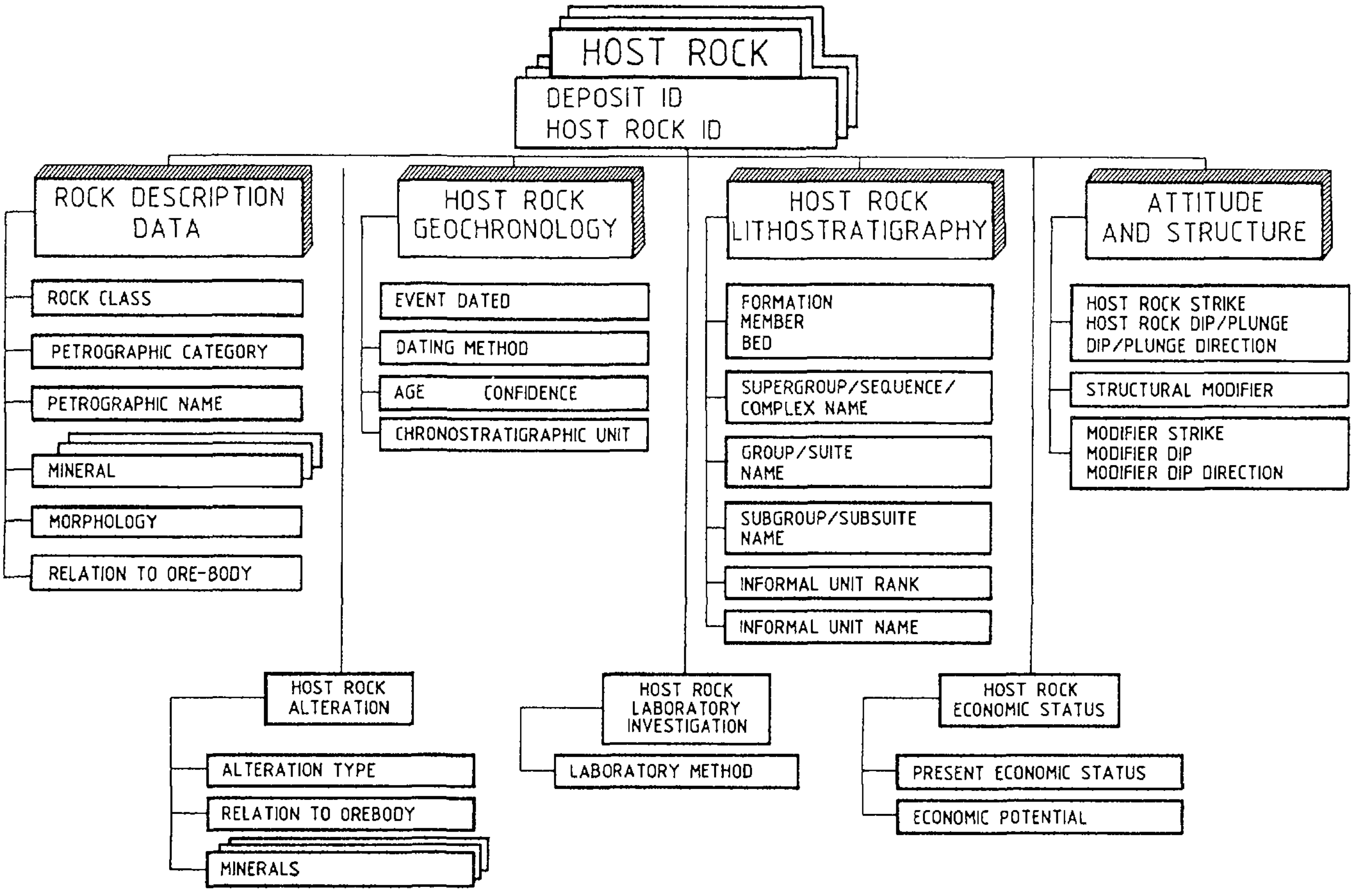

FIG. 3. SAMINDABA host rock data elements

3.3 Orebody Data

The orebody data group which can be subdivided as shown in figure 4 contains the following data: descriptive, form and structure, mineralogy, geochemistry and physical properties.

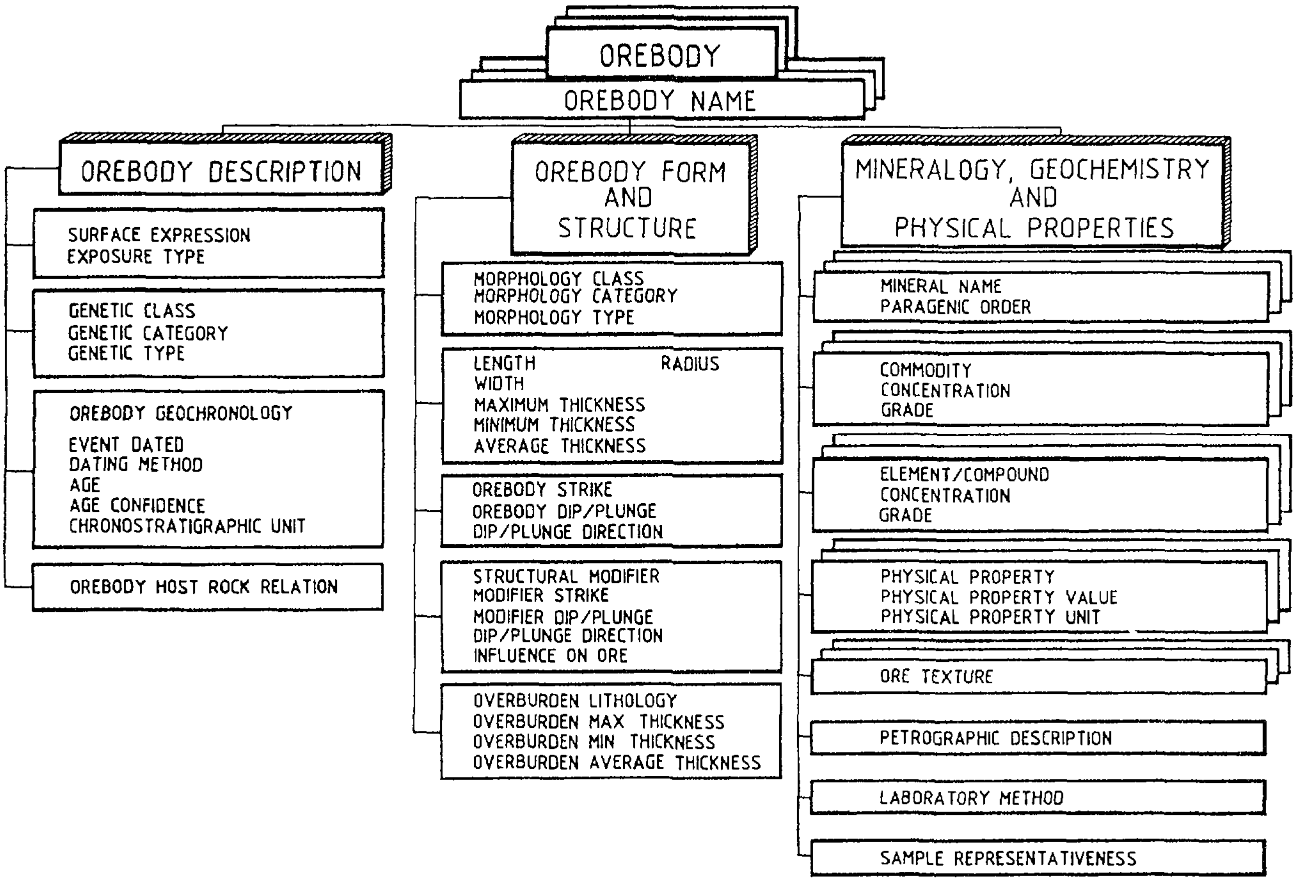

FIG. 4. SAMINDABA orebody data elements

3.4 Exploration and Exploitation

Exploration contains data elements describing when the deposit was discovered, who discovered it and by what method, who has explored the deposit, what exploration techniques were used and how well the deposit has been explored (fig. 5).

Exploitation data describes whether or not a deposit has been mined, what type of mining activity took place, what commodities were exploited, their grades, beneficiation methods, cumulative production and who owns the deposit at present (fig. 5).

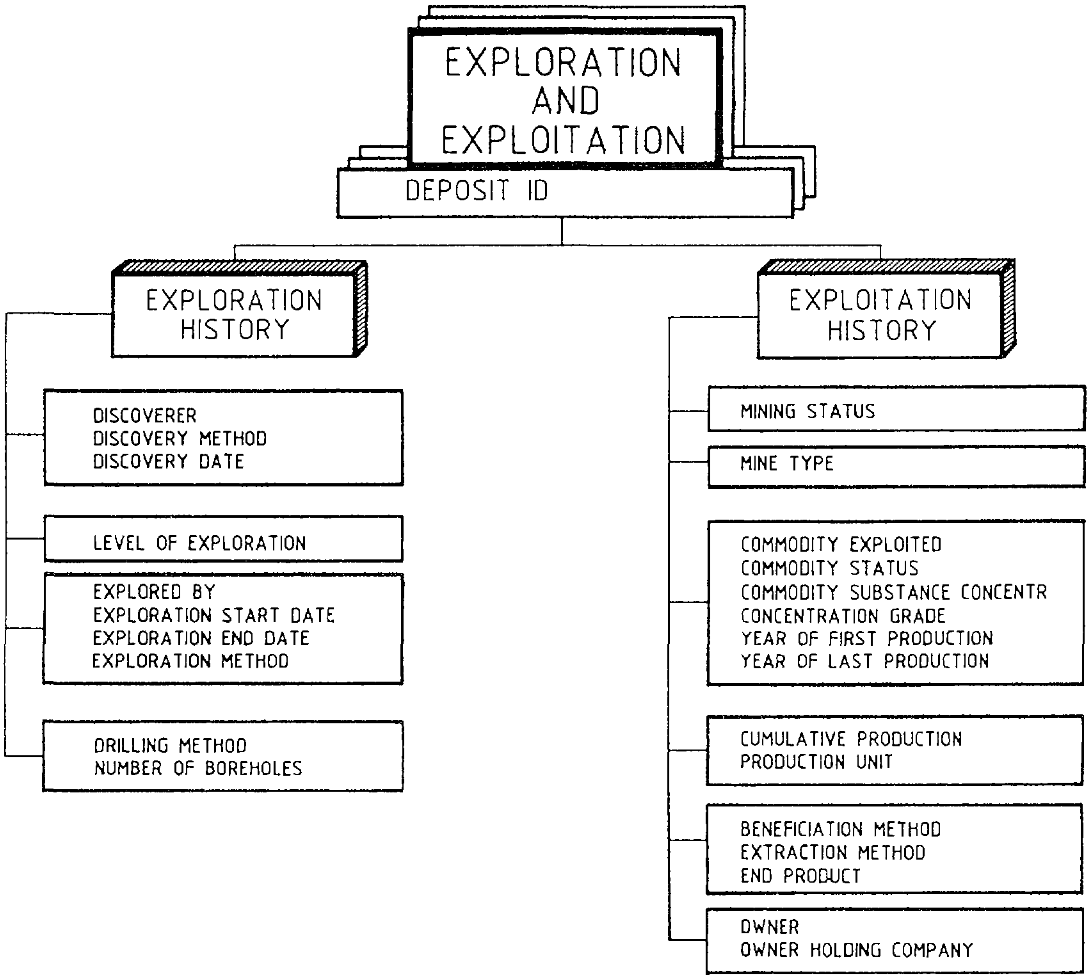

FIG. 5. SAMINDABA exploration and exploitation data elements

3.5 Resources and Reserves

The deposit resource and reserve data has been divided as follows (fig. 6):

1. Demonstrated Economic Reserves
2. Demonstrated Marginal Reserves
3. Demonstrated Subeconomic Resources
4. Inferred Resources

The data describing these reserves and resources include quantities, commodities, grades, cut-off values, physical property cut-off values and deposit dimensions and are repeated for each of the above sub-groups. In addition, a size classification and the area of influence are stored.

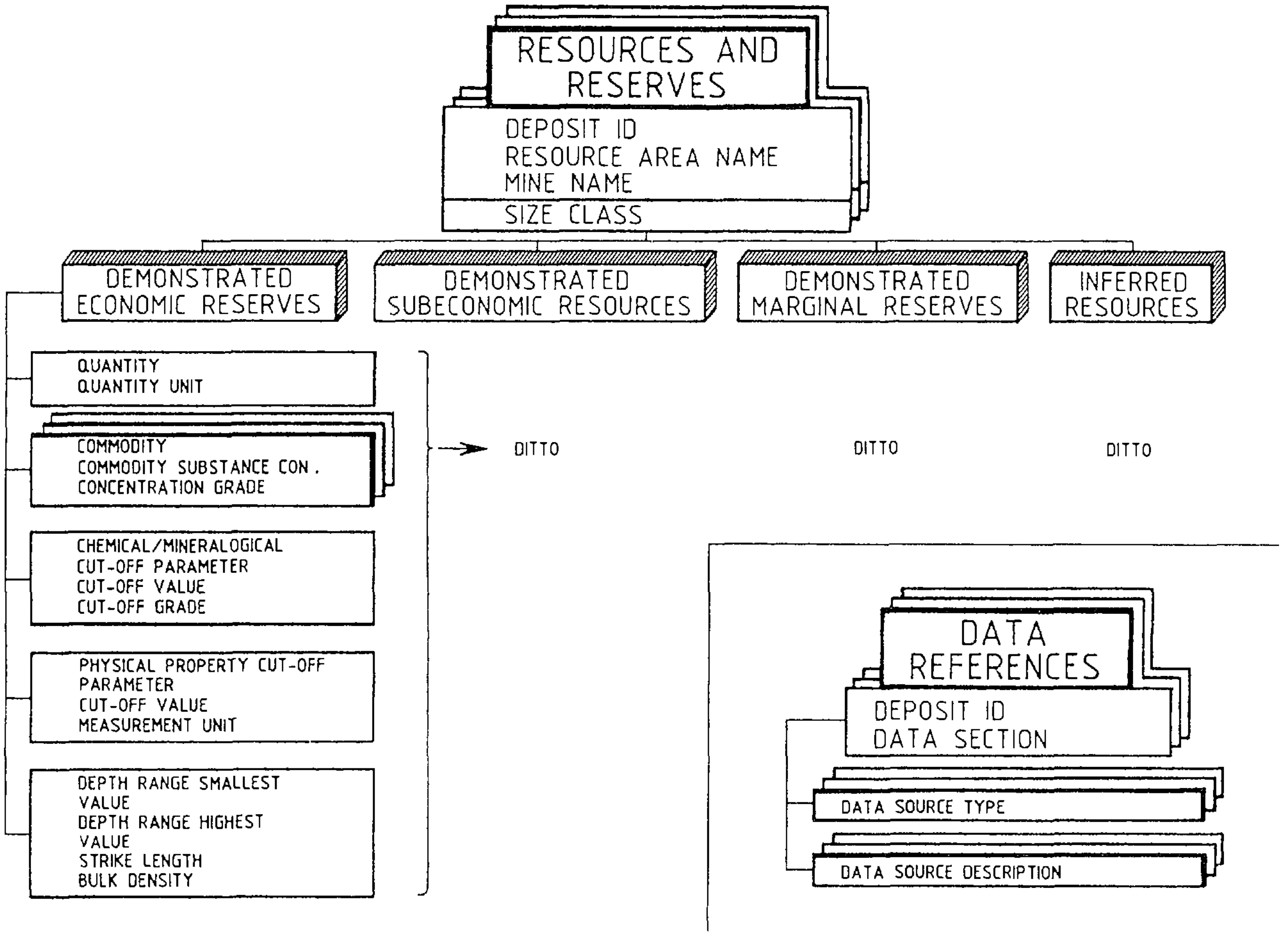

FIG. 6. SAMINDABA resource and reserve data elements

3.6 Data References

This data group contains all the references used to compile the information on the deposit. Included in this group, as shown in figure 6, is the type of reference and the data group to which the reference applies.

4. SAMINDABA MODELLING

A data model for SAMINDABA was developed employing relational data modelling, during which the geologically defined deposit was analyzed, the data reduced to simple basic elements and then grouped into logical relations with keys to each of the defined data elements. The resulting data model is schematically presented in figure 7.

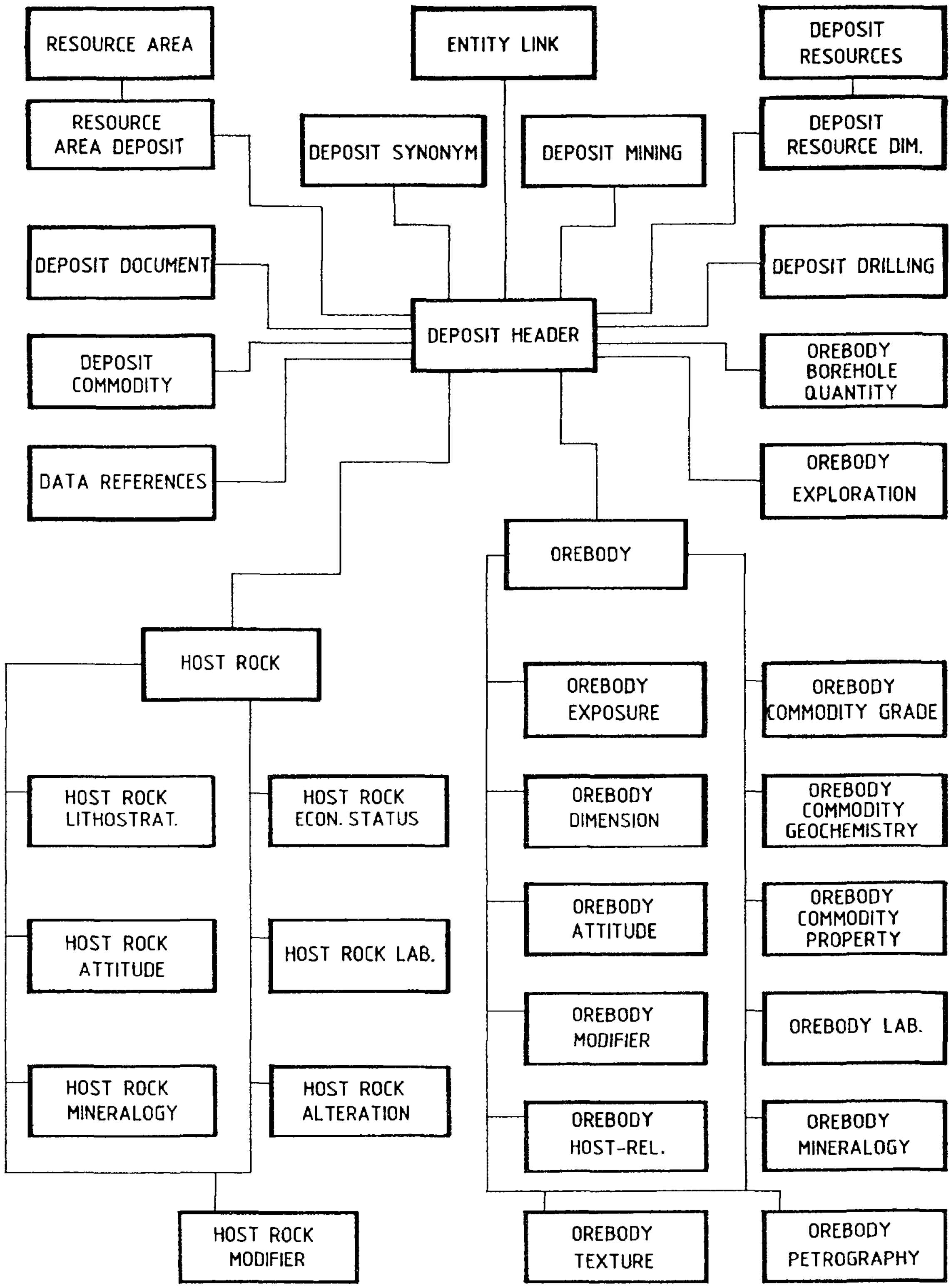

FIG. 7. Schematic outline of the SAMINDABA data model

Conceptually SAMINDABA contains only deposit area records, however, in practice this posed a large problem as much of the reserve and resource data is not calculated for a deposit area but rather for a mine lease area, as in the case of working mines, or for resource areas, in the case of resource studies. The solution to the problem was to introduce two additional records, a mine area record and a resource area record.

The resource area record, represented by a resource area reference point located at the approximate centre of a geologically defined resource area and by an x, y and z co-ordinate, can incorporate one or more mine and/or farm areas and contains the following data groupings :

1. Resource Area Header
2. Exploitation
3. Resources
4. Data References

Similarly, a mine area record represented by a mine area reference point located at a convenient locality within a mine area, e.g. the main shaft, is defined by an x, y and z co-ordinate. It may incorporate one or more farms and carries a link to a resource area containing the following information :

1. Mine Area Header
2. Exploitation
3. Resources
4. Data References

This concept of three interlinked record types is demonstrated in figure 8.

5. SAMINDABA FUNCTIONS

SAMINDABA was developed in a mainframe computer environment using a commercially available database management system and a fourth generation language. The primary SAMINDABA functions include the following :

1. Database maintenance
2. Data capture and validation
3. Database enquiries and output

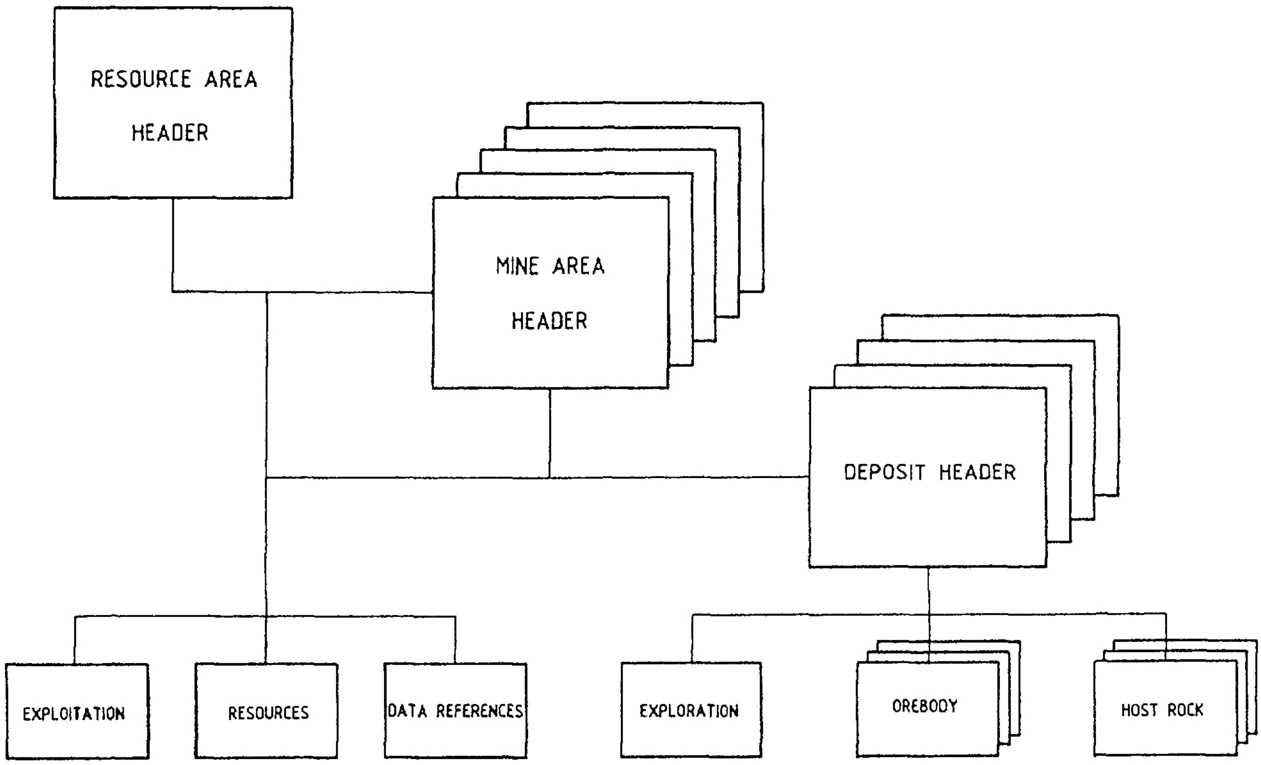

FIG. 8. Conceptual model showing the relationship between SAMINDABA resource areas, mine areas and deposits

5.1 Maintenance

All maintenance on the database which includes the registration, insertion, updating and deletion of data records, synonym tables, validation tables, user profiles, programs, menus and help text is the responsibility of the database administrator who executes these functions in an on-line, menu assisted environment. Also included is a facility to provide management information on the database usage and security violations. Only the database administrator has access to this section of SAMINDABA.

5.2 Data Capture and Validation

Due to the low volumes of data preparation, all capturing of SAMINDABA data is menu assisted and executed in an on-line environment. The data capturing process may be sub-divided into the following groups :

1. Data records
2. Validation tables
3. Synonym tables
4. Help text

The data records are the primary source of data for SAMINDABA. Data is recorded by geologists, partially in alpha-numeric code, on a comprehensive prescribed form. In order to assure consistency and standardization this is done with the help of a detailed coding manual[7].

Validation of SAMINDABA data is automatic, taking place at the time of capture and includes the following :

1. Data integrity
   The data must not violate database logic. Checks are done to ensure that key fields are entered and relationships maintained, e.g. the element concentration unit cannot exist without the element name and concentration value.
2. Data duplication
   Duplication checks are done especially on multiple data elements.
3. Data format
   Data formats, i.e. numeric, alphabetic and alphanumeric are checked so that, for example, numeric values are not entered in an alphabetic field.
4. Data sizing
   The data elements are checked that they do not exceed a certain length and that the number of characters is correct.
5. Data checks against validation tables
   Due to the nature of the data much of the validation is done by checking the entries against tables of allowed terms. SAMINDABA has 45 validation tables.

5.3 Database Enquiries and Output

All enquiries and output of SAMINDABA data are done through an enquiry system called SAMENQ (Samindaba Enquiries). This enquiry system ensures that users of the database cannot corrupt data or access data that is not available to them according to their security classification.

SAMENQ is a menu driven on-line system which allows any registered user, no matter what his level of computer experience or knowledge of the database structure is, to make enquiries against SAMINDABA.

The SAMENQ enquiry path is depicted in figure 9 showing two basic types of enquiries. The first is a simple enquiry where the user specifies area and/or commodity criteria followed by what output is required. The second type of enquiry is more complex. The user again specifies area and/or commodity criteria and then refines the search by selecting more specific criteria regarding other data elements on the database, followed by an output specification. It is envisaged that these two types of searches will satisfy 90 per cent of all enquiries made against the database.

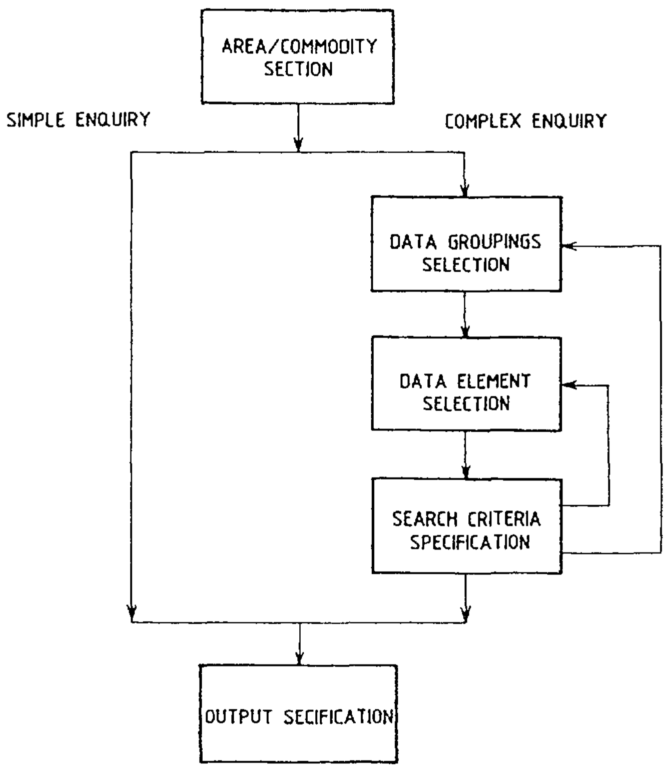

FIG. 9. Diagrammatic representation of SAMENQ enquiry paths

Output of SAMINDABA data resulting from a SAMENQ enquiry may be routed to a screen, printer or interface file in the following formats :

1. Deposit profiles (partial or complete)
2. Mineral map interface files
3. Metallogenic map interface files
4. SAS interface files

The output in the metallogenic format may be edited before being sent to an interface file while specific data elements may be selected for output to a SAS interface files.

5.4 Database Security

Due to the nature and sensitivity of the data stored on SAMINDABA one of the most important aspects of the database design was the security aspect. SAMINDABA security is applied at three levels :

1. The system level
2. The application level
3. The data level

5.4.1 System security

System level security refers to the standard security options available with the database management system (DBMS) and are in effect regardless of what applications are being used. A user is assigned a password-protected identification code (ID) which is linked to a profile specifying the files and applications to be used and the operating system and programming commands that can be executed. Thus, at this level it is possible to restrict a user from accessing applications and programming.

5.4.2 Application Security

Security at this level refers to controls programmed into the SAMINDABA system and are only effective during a SAMINDABA session. The controls operate in a similar manner to the system security in that a user is assigned a password protected ID linked to a profile. This profile is stored on a SAMINDABA database file and contains the following information :

1. The SAMINDABA user ID
2. The user password

3. Entry menu
4. SAMINDABA file access
5. Data ownership code
6. Printer identification code

The user password must be supplied before sign-on to SAMINDABA is effected. Once the user is signed on his user profile, linked to the ID, determines which files may be accessed and at what level the menu hierarchy will be entered. For example, a user who just has authority to search the database will only be allowed to enter the system via the enquiry menu where no updates, deletions or any programming can be done. The user will not be aware that these functions even exist.

5.4.4 Data Security

At the data level it is possible to indicate the confidentiality status and ownership of the data. For practical considerations data elements are grouped together and each grouping is given a security status and data ownership code. At present there are three basic confidentiality options.

1. The entire document is not confidential
2. Certain of the specified data element groupings within the document are confidential
3. The entire document is confidential

If the document is not confidential any user may access the data. If only certain of the data element groupings within a document are confidential the confidentiality indicator for that element grouping is set and the data origin code is entered. In this case only users with the same data element group may access the data. All other users will not be aware that the data exists.

In the case where an entire document is confidential, the confidentiality indicator on the deposit header record is set and the data ownership code entered. All data on this deposit can then only be accessed by users with the same ownership code on their profiles as that on the record.

6. SAMINDABA DATA PROCESSING

As stated above, the processing of data extracted from SAMINDABA is completely separated from the data input, validation, maintenance and enquiry functions.

All data extracted from SAMINDABA will have been routed via SAMENQ where all the necessary security controls have been applied. Once a user has extracted the data he may do what he wishes with that data, which cannot be put back onto the database.

At present provision has been made to process the data using SAS, IGGS and DIGIMAP, three commercially available software packages which are briefly described below.

SAS is a data analysis system containing statistical routines as well as providing data management, querying, reporting, graphics and modelling facilities all using an english-like language.

IGGS is an interactive, geo-facilities graphics support program written in fortran IV and used to develop applications for data entry, editing, updating and displaying of geograhically oriented data.

DIGIMAP, an application of IGGS, is an interactive mapping application. It provides rapid response to user requests for map displays. Several mathematical techniques are available as interpretation aids, e.g. gridding, contouring, kriging.

6.1 SAMINDABA/SAS

Once the data has been extracted from SAMINDABA a user may process it using SAMSAS, a specially developed system providing the capability to process SAMINDABA data using SAS. An interface program has been written which reads the SAMINDABA output file and converts it into a SAS dataset. Three basic methods of SAS processing are available:

1. Batch SAS processing
2. Interactive SAS processing
3. SAMSAS

Batch processing is used to processing very large data sets or run very large programs which do not require interactive intervention and take a long time to run on the computer, e.g. the interface conversion program.

Interactive SAS processing is used for program development, processing small data sets and running programs that require user intervention, e.g. creating reports, graphs etc. This system assumes that the user is familiar with the SAMINDABA data principles and the SAS language.

SAMSAS is a menu driven system which was written specifically for the inexperienced SAS users. This system allows a user to edit, browse, manipulate, statistically analyze, report and graphically process the data extracted from SAMINDABA.

6.2 SAMINDABA/IGGS/DIGIMAP

The second main type of processing currently available is a mapping function. This facility uses IGGS and DIGIMAP and gives the user the capability to produce maps. These may be simple mineral maps showing the locality of mineral deposits. Such maps may be produced on a commodity (or group of commodities) basis of selected areas, on any scale of 1:250 000 or larger. The relevant data on the mineral deposits portrayed is available in accompanying sets of complete or partial deposit profiles.

Provision will be made for the creation of more detailed metallogenic maps or complicated geological maps showing contacts, deposit boundaries etc. Using the same package the user can also create contour maps and do certain geostatistics, like gridding, trend analysis and kriging, which will permit detailed metallogenic analysis. Due to the nature of this type of processing it is a prerequisite that the user of this package has some computer and technical knowledge.

7. CONCLUSIONS

SAMINDABA is an advanced computerized storage system for South African mineral deposits data, covering a wide range of geographical, geological, historical and resource aspects on all types of deposits, e.g. precious metals and stones, ferrous and base metals, industrial minerals, as well as nuclear fuels. The primary objectives of SAMINDABA are to provide South African mineral deposit information in an efficient and timely manner in an attempt to assist in the exploration programmes, and by using this information and the processing tools available, to contribute to the further understanding of the processes taking place during the formation of mineral deposits.

The database is being implemented by various current projects of the Geological Survey, in particular metallogenic mapping, the compilation of mineral maps, and various commodity studies. Of special interest in the context of this publication is that uranium and attendant molybdenum deposits in the Karoo Sequence are receiving attention at present, while a start is also being made with the Witwatersrand gold and uranium deposits.

ACKNOWLEDGEMENTS

The authors are indebted to Mr M.D. du Plessis who played a leading part in the development of SAMINDABA. This paper is in part based on his earlier work. The Chief Director of the Geological Survey of South Africa kindly permitted publication of this article.

REFERENCES

[1] Picklyk, D.D., Rose, D.G., Laramee, R.M., Canadian Mineral Occurrence Index (CANMINDEX), Geol. Surv. Canada Paper No. 78-8, (1978), 27.

[2] Calkins, J.A., Kays, O., Keefer, E.K., CRIB-The mineral resources data bank of the U.S. Geological Survey, U.S. Geol. Surv. Circ 681, (1972), 39.

[3] Mundry, E., Ein Dokumentations-und Abfragebprogramm für Schichtenverzeichnisse (DASCH), Geol. Jb., Bd. A7, (1973), 9.

[4] Jeffery, K.G., Gill, E.M., G-EXEC: a generalized FORTRAN system for data handling in Computer-based systems for Geological field data, Geol. Surv. Canada Paper No. 74-63, (1975), 3.

[5] Hine, S.S., Vermaak, G., SAMINDABA Functional Specifications, Geol. Surv. S. Afr. Rep. (unpublished), (1986).

[6] Venter, I.M., Vermaak, G., Hine, S.S., SAMINDABA Technical Specification, Geol. Surv. S. Afr. Rep. 1986-0114 (1986).

[7] Barnardo, D.J., Bredell, J.H., Vorster, C.J., SAMINDABA Coding Manual, Geol. Surv. S. Afr. (unpublished) (1986), 105.

GEOSIS — A PILOT STUDY OF A GEOSCIENCE SPATIAL INFORMATION SYSTEM

A.L. CURRIE
Ontario Geological Survey,
Ministry of Northern Development and Mines,
Toronto, Ontario, Canada

Abstract

GEOSIS is a database system for geoscience and exploration data designed to cover Ontario. A pilot study is currently in progress to test all aspects of GEOSIS (eg data input methods for cost and throughput, data structures, response rates and user interface). The pilot study area (80km by 20km) is in north-western Ontario just north of Lake St Joseph, and is part of the Uchi belt.

The major data sets within the database are Precambrian geology and economic geology (ie assessment files, mineral occurrences data etc) with subsidiary data sets such as remote-sensing data. GEOSIS is designed so that users can access the database using a telecommunicating microcomputer without any decrease in functionality compared to a directly connected graphics workstation.

Spatial information systems are based on the concept of spatial relationships (ie map data) and attributes of objects on maps. Data structures used in GEOSIS must be able to successfully integrate several fundamentally different kinds of data: 1. structured map graphic data (geoscience maps), 2. passive raster graphics (sketch maps from field notes and property descriptions), 3. raster data from remote sensing or image processing systems, 4. structured alphanumeric data (geological structural data) and 5. unstructured text (geologists' reports, property descriptions etc).

The goal of the GEOSIS project is to provide users, in their place of work (office or field), with access to the geoscience data collected or managed by the Ministry of Northern Development and Mines.

---

1. INTRODUCTION

GEOSIS is a geoscience spatial information system that is designed to process and retreive geoscience and mineral exploration data that would eventually have Ontario-wide coverage. Spatial information systems incorporate in an integrated way the features of both map and alphanumeric data base systems. The non-digital equivalent of these systems is a map with the associated data (tabular or text) that are linked to the map by location. Spatial information systems try to mimic the functionality of a paper map and associated data as used by an experienced user.

By the end of of 1986 a pilot study, designed to test the various aspects of GEOSIS, will have been completed. The major topics to be explored are as follows:

1. data input methods for cost and throughput,
2. data structures so that user queries are able to be successfully answered,
3. response rates of system to users queries and the workstation costs in relation to response times and
4. design of user interface so that users can successfully use the system with minimum training.

The pilot study area (80km by 20km) is in northwestern Ontario just north of Lake St. Joseph, and is part of the Uchi volcanic belt. This area was selected because it had been recently mapped and the field notes were in digital form (Fig. 1). The area is also an area of active mineral exploration. The exploration history of the study area is not extensive but sufficent to test data input methods.

Spatial information systems by their very nature must be able to integrate data of different types from a wide range of sources. The pilot study is designed to investigate how the following types of data can be integrated into a system:

1. geoscience maps
2. sketch maps and drawings from field notes and property descriptions etc,
3. raster data from remote-sensing and image processing systems,
4. geological data from traditional computer data bases and
5 text from geological field notes, geological reports, property descriptions, etc.

The varied types of data within the system require that many different software products that were not designed to be used in an integrated way with other packages must be used in that manner. This means that the operating system within which the spatial information system exists must be have strong integration capabilities so that users can route data through many processes in a serial

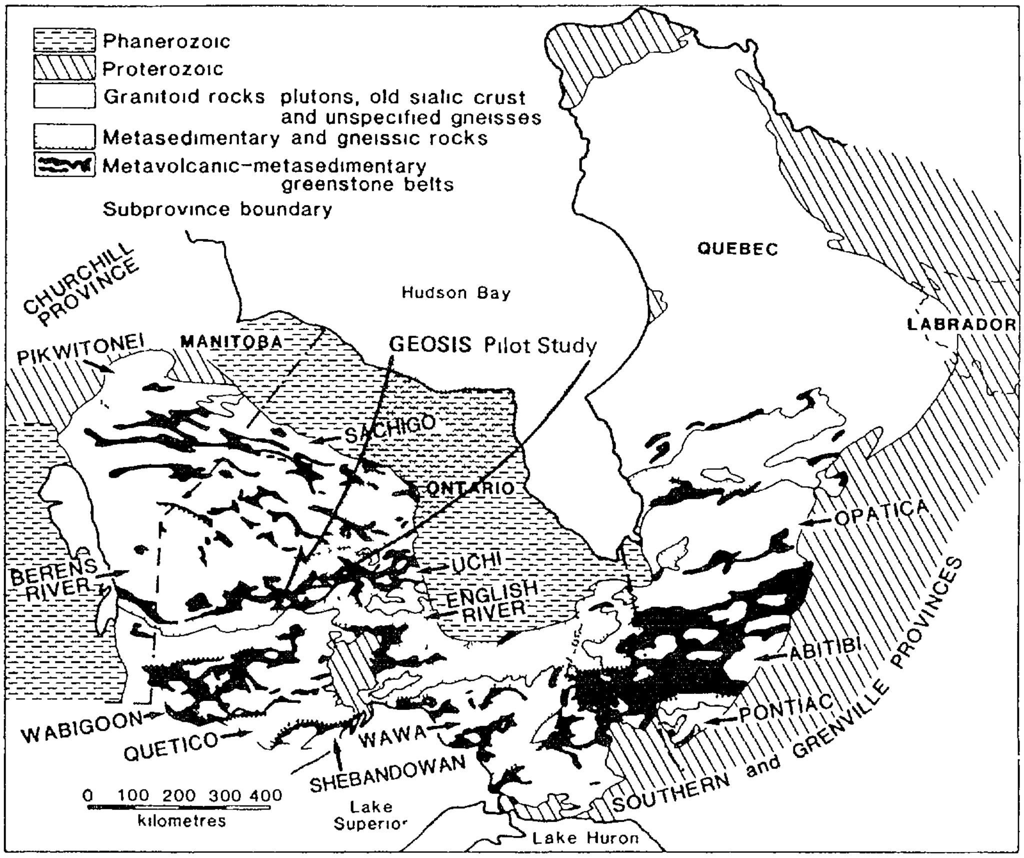

Figure 1. The GEOSIS pilot study area

fashion to obtain the results they require. The operating system used by GEOSIS is UNIX.

Integration of different types of data that cover extensive areas results in the aggregation of previously separate data bases (digital and hardcopy) to form large spatial information data bases. This creates problems during the input phase of data base when large volumes of data, especially map data, must be digitized. Scanning techniques are essential for the efficient input of both text and map hardcopy data. The testing of scanning methods forms a important part of the pilot study. Retreival from large data bases also requires particular techniques, such as the ability to split the data base into temporary subsets so that during a query session the only data searched are in the geographic area of interest to the user.

The ultimate goal of the GEOSIS project is to make more accessible to the users the varied geoscience data sets created and managed by the Ministry of Northern Affairs and Mines and to provide the search and integration tools that will enable the user to use this data to its full potential.

2 DATA INPUT AND PROCESSING

Data are in essentially two forms: digital and non-digital. GEOSIS contains data that previously existed in both forms. The greater the amount of previously digital data that is be stored in a spatial data base the cheaper the data base will be to establish. Hardcopy data bases present two major problems which are lack of organization of the data and the conversion of the data to digital form.

2.1 Digital Data Bases

The input of digital data from one system to another system relies on the capabilities of the software to use established industry standards. The end result is the eventual establishment of an automated series of processes through which files are piped from one system to another. This part of the data input task is not labour intensive as it is a transfer between digital data bases and takes advantage of the effort invested by the builder of the original data base.

2.1.1 Structured Data Bases

The structure designed into these data bases means that these data bases can be transferred to the spatial data base and used as originally designed but with the added advantage that the data can now be integrated with the other data sets in the spatial data base. At a simple level of integration the locations of selected mineral occurrences from a mineral deposits data base can now be plotted on a geological map stored in the vector map files.

2.1.2 Unstructured Text Data Bases

In GEOSIS these data bases are field notes and published geological reports. The reports can be directly transferred to the spatial data base and are used in a full text data base management system that retrieves documents using user selected key words. The field notes are text files that contain numeric codes. Using these codes it is possible to convert these files from text files to tabular files that can be entered into a relational data base management system. The geological field notes are keyed into laptop microcomputers in the field at the end of each day. The notes are deliberately left unstructured so that the field geologist has sufficient freedom to compose the notes to suit the geological context. The field notes contain the location of each observation station (UTM co-ordinates) and as a result the notes can be used as the source of all point data on the geological map (eg structural symbols, lithological codes).

2.1.3 Geophysical Map Data

To produce a map of the geophysical survey data the data are processed to produce a plot file that usually contains contour data describing the geophysical surface. These plot files are in vector format and can easily be transferred to the spatial data base. Editing of the file may be necessary to close gaps in the contours and to indicate the value of contours.

2.2 Non-Digital Data Bases

These data bases can be highly varied in their form and content are only restricted by the ways humans put information on paper. They in fact pose a tremendous problem to the establishment of spatial data bases and in the quest to create a spatial data base that will contain all relevent data on a topic or series of topics covering a selected geographic area.

The non-digital data in GEOSIS are of the following types :

1. typed text (eg geological reports, mineral property reports)
2. page-size drawings and sketches (eg from field notes, geological reports)
3. large maps-custom (ie map manuscripts created for scanning)
4. large maps-cartographic (ie printed coloured geological maps)
5. large maps-general (eg geological field maps, exploration property maps, geophysical maps)

2.2.1 Typescripts

The major source of this type of data in the GEOSIS project are the files submitted by holders of mineral claims to report work done on their claims. These files are the most detailed records of the exploration activity in Ontario and are available for public access in 18 offices throughout Ontario. These files are highly variable in quality and format so that part of the files will be able to be scanned to produce coded text files (ASCII) but a sizable minority of the data would have to be manually input or scanned as a graphic image.

2.2.2 Page-size Drawings and Sketches

These data are scanned as a bit-map graphic which is a fast process taking only a few seconds. The major problem is the storage requirements which are large (1 byte per dot in the image if image data not compacted; common resolutions are approximately 100 and 120 dots/cm). Storage systems based on laser disks are just now offering a solution to the storage problem. Some systems offer laser disks combined with data compaction done in hardware to increase the speed of access to the decompacted graphic image.

2.2.3 Large_Maps - Custom

These map manuscripts are designed to be scanned. The Ontario Geological Survey (OGS) started a program in 1984 in which the field geologist would produce in the field a map manuscript in several layers that would contain all the linear and polygon data for the geology of the field area. The point data would come from the digital field note system described in section 3.1.2. These scannable manuscripts present little difficulty in processing as they are designed solely for the scanning and digital processing. The end products of this method are a published coloured geological map and digital vector files of the map data that are provided to GEOSIS.

2.2.4 Large Maps-Cartographic

This data set is the printed coloured geological maps that were prepared by cartographic methods (ie scribe and peel coats etc in many layers) and were printed on multicolour printing presses. This highly structured artwork composed of many layers, although not designed to be scanned, is close to the ease of processing for the custom maps described above. The Ontario Geological Survey has published approximately 750 coloured geological maps and is currently looking into the feasibility of scannning approximately 500 of these maps

2.2.5 Large Maps-General

These maps are mainly from the exploration files but also include geological map manuscripts prepared by OGS geologists that were not produced as printed coloured maps. All these maps can be scanned. The quality of some of the maps is such that the raster image, that is the result of scanning, cannot be converted to vector format. These maps produce the same problems that the scanned page-size drawings have (see section3.2.2) only intensified many times, as a single map may be 1.5m by 1m. If the image quality of the map is good and objects on the map do not lie one on top of the other then the map can be vectorized and added to the data base as a fully structured set of map files.

3. TOPOLOGY AND DATA STRUCTURES

Spatial information system should explicity encode topological relationships and have the types of data structures that are a response to requirements of users.

3.1 Topology

At first sight, these systems do not look radically different from the many drafting and engineering graphic systems available today. The feature that is crucial to the proper functioning of a spatial information system is the concept of topology. A geological map defines all locations within the area of the map. This is not the case with drawings or plans created on a drafting system, which only define the objects of interest (eg. buildings). To successfully structure this spatial continuum of geological data in the data base, it is essential that the adjacency or neighbourhood relationships of each polygon or area of each map unit be included in the structure of the data base. A map user can tell at a glance that one polygon is adjacent to another on a map. One of the reasons people have been using maps for centuries is the map's capacity to store these fundamental topological relationships. If the map data in a graphic system are not topologically structured then the user will be unable to use the system to fully replace the paper map. When making searches on the basis of adjacency (ie. topological) relationship, the user receives no help from the system. The only change is that the user now does searches on the map while looking at it on a CRT instead of looking at a paper copy of the map.

3.2 Data Structures

Data strucutres used in a spatial information system for say a city government or to manage wetland areas should be quite different from those used in a system of geoscience data. Mature spatial information systems of geoscience data do not exist so that the range of data structures required to successfully respond to geoscience user's queries is not yet fully defined.

An example of the way users require data to be presented and and how this controls the data structures is as follows. A characteristic of geological data is that the descriptive data collected at the outcrop is little use to the user if the user is working with an area 100km by 50km. The requirement is that as the user's area of interest changes in size, the descriptive or attribute data and also the map data must become either more generalized or less generalized. This is akin to what geologists have traditionally done; a geological report and map covering a small area gives considerable detail even down to describing individual outcrops and showing them on the map whereas a report and map of large area give a highly generalized account of the geology. A correctly structured geoscience spatial information system should be able to provide access to the geological data at various levels of generalization but more importantly allow the user to move through the data base easily from one generalization level to another and at the same time control the geographic extent as the levels change. At any time the user should only be exposed to a volume of data appropriate to the current query.

If spatial information systems are to meet the needs of geologists the underlying data structures must be such that the systems are able to mimic the functionality of the tools currently used by geologists so that the geologist is working in an environment that is not alien.

4. DATA INTEGRATION AND APPLICATIONS

4.1 Data Integration

Integration of data sets in spatial information systems can occur in two ways. Visual integration occurs when two or more data sets are superimposed using a common geographic base. The user gives meaning to the new displayed image and the relationships between the data sets, eg a user looks at a CRT display of gold occurrences superimposed on a geological map and arrives at his own conclusions. The systems plays no active role in the linking of geology and mineral occurrences. Structured integration occurs when two or more data sets are superimposed using a common geographic base. The relationship between data sets is either explicitly stated and forms part of the data base or can be created using geographic linkages, eg a user creates a query to link selected gold occurrences to particular geological map units. The system performs a geographic search to link the two data sets and provides the user with the results. The user sets the process in motion but does not take part in the integration of the data sets as is required in visual integration. The ability of spatial information systems to integrate data sets in batch mode gives these systems the potential to perform complex integration and modelling tasks on large multiple data sets.

4.2. Applications

The production of custom maps by a spatial information system is the most obvious use of these systems. Map data are divided into files which are analagous to the layers of different data used in traditional cartographic methods. A map is made by selecting various files or parts of files covering a selected area and superimposing these data. Custom maps make the interpretation of geoscience data easier for the user, but the system is not yet mimiking the function of the experienced map user, merely providing a better map product with which to begin work. Spatial information systems can enhance the effectiveness of users only if the concept of the map is built into the structure of the data, and if users are provided with tools that perform the tasks previously done manually using paper maps and associated data.

The map graphics module of spatial information systems contains a series of tools that enable the user to perform searches of the map data base. Searches can be made on the basis of distance from a point or line; intersection of lines, of polygons, or of lines and polygons; inclusion and exclusion of points, lines or polygons within polygons. These tools can be used singly or in combination, so that searches of considerable complexity can be performed. In addition, these geographic searches can be combined with searches using topological relationships. An example of such a search is as follows: find all locations where two map units (eg. granite and mafic tuff) share a common boundary, where a fault intersects that boundary, and where known mineral occurrences (i.e. occurrences in data base) are located within 1 km of the intersection of the fault and the common boundary. Basically, this is a filtering or distilling of the data base through a sequential series of searches.

Spatial information systems also have alphanumeric data bases in which data associated with graphic objects (points, lines and polygons) are stored. These alphanumeric (attribute) data can be manipulated as in traditional data bases. The geographic search described above can be augmented by output from queries made on the attribute data. An example of this would be to change the search described above from a search of all mineral occurrences to one limited to those occurrences with assay values above a certain value that also are located within 1 km of the intersection of the fault and the contact of the two map units. A complex query of a spatial information system might involve an intermixed series of attribute queries and geographic searches that could result in a final output in either map, text, numeric format or a mix of formats.

The linkage of attribute data to graphic objects in the map graphic data base is the reason for the great manipulative powers of spatial information systems. Geoscience data are by their very nature spatial data and location is fundamental to effective interpretation of them.

5. CONCLUSIONS AND FUTURE DEVELOPMENTS

The GEOSIS pilot project has shown that the tools exist to input the various data sets required to create a spatial data base using geoscience digital and non-digital data sets created or managed by the Ontario Ministry of Northern Development and Mines. This geoscience data can be manipulated in an integrated fashion using an variety software products in a UNIX operating environment. A Province-wide graphic index to exploration data and data base of exploration data has been proposed and is in the early planning stage. An extension of the GEOSIS project to cover the complete Uchi volcanic belt (FIG. 1) is planned.

INDUGEO — INDIAN URANIUM GEOLOGICAL DATABASE

K.N. NAGARAJ, P. SRINIVASA MURTHY,
S.G. TEWARI
Atomic Minerals Division,
Department of Atomic Energy,
Hyderabad, India

Abstract

The Atomic Minerals Division is engaged in surveying for various atomic minerals in India since 1950. During the last thirty six years a large volume of geological, analytical, mineralogical and other relevant data have been generated and documented in a systematic manner. These data, are presently available on manually operated files. This conventional way of data handling though serves a limited purpose, is very slow for information retrieval and is highly inefficient for large data volumes and multiple users. An efficient way of handling information to match the speed of data generation and demand for quick information retrieval is through a computer using a data base approach. With this objective in view, Indian Uranium Geological Data Base (INDUGEO) was designed on the lines of INTURGEO 1 . The System 332 Computer where the INDUGEO has been implemented supports a network file structure. INDUGEO consists of eleven files. A base with proper logical relationships and links has been designed for easy access, quick retrieval and query. The System provides sufficient flexibility to the application programmer to change the view of the data to suit different applications. There is also provision for extending the data base to meet any future requirements. The System has been made user friendly with HELP Commands to assist those who have little programming knowledge.

Introduction

The survey for atomic minerals involves many stages from reconnaissance to exploitation. Every stage has its own associated information which has to be accessed and periodically monitored for evaluation, decision making and at times dissemination at various levels. Persons from many disciplines namely geology, geophysics, physics, chemistry, drilling, mining, management etc. are involved in the whole process who generate and use the data. It was therefore, decided to have an integrated information system and INDUGEO was designed where the data have been organised in such a way as to enable each user to view the data to suit his objective and also it can be seen in totality by the management. In fact the specifications of the users' requirement was the starting point and detailed designing has been done after several discussions with the users. This ensured continued user involvement during the designing phase.

Computer System:

The System 332 computer where the INDUGEO has been implemented has a multiprogramming, multiuser environment with the following configuration:

- 512 K byte main memory
- 600 M bytes online storage on three disc drives
- 4 tape drives (800/1600 BPI)
- Line Printer
- Card Reader
- Monochrome terminals

Compilers supported are FORTRAN, COBOL and RPG. It has a network model DBMS package. This model permits access to the data base through links and multiple pointers. The DBMS software has the facility for base generation and editing of data files.

INDUGEO Schema:

The user generally likes to view the data in a form most convenient to him and it is the job of data management software to do the translation from the logical organisation to

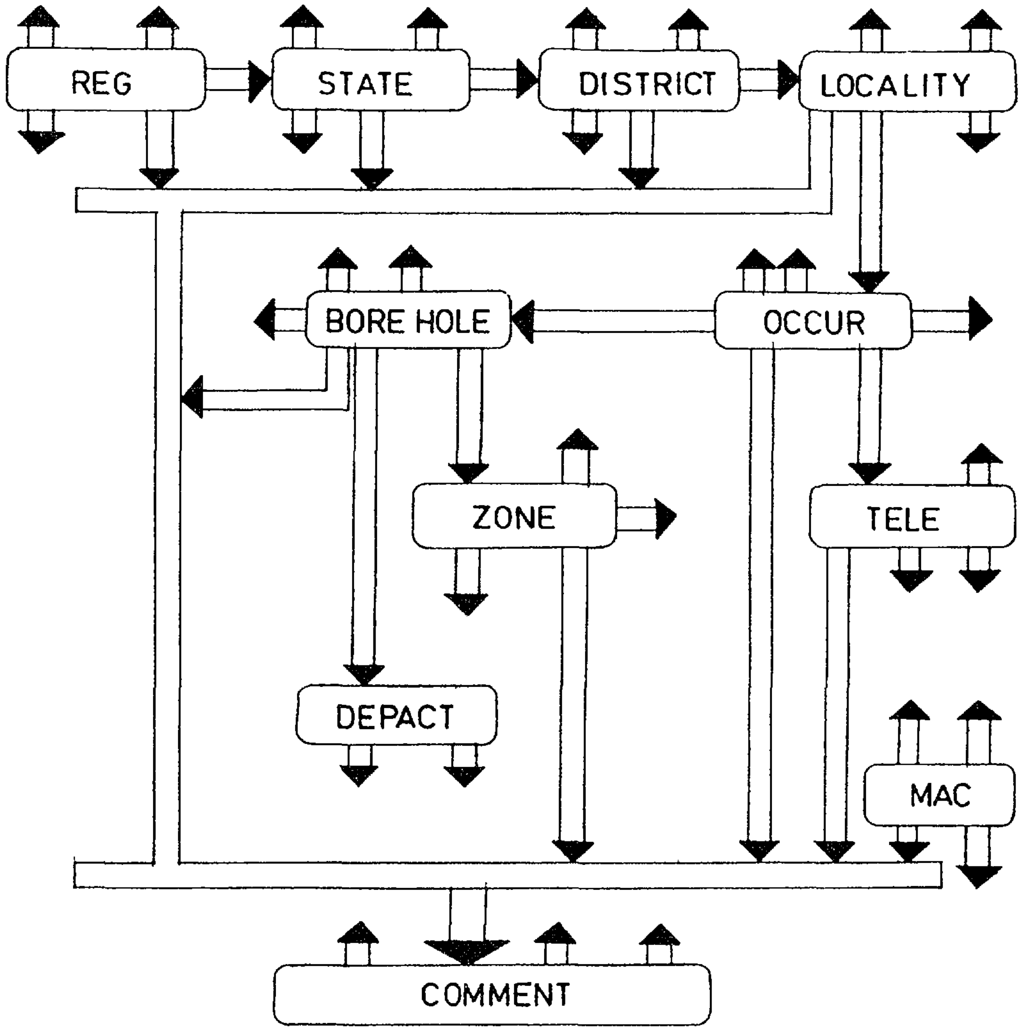

FIG.1 SCHEMATIC DIAGRAM OF INDUGEO

a physical organisation which gives the most efficient performance. Keeping this factor as a guide the Schema for INDUGEO has been designed based, however, on the principle that quality cannot be compromised for speed. The schematic diagram of the schema is shown in Fig. 1 . The entities created may be used as data sources for a wide variety of applications like having a report on Uranium occurrence, radioactive horizons of boreholes, deposit type etc. In fact the entities can be treated as seperate files and full characteristics of each file with their relationships are as follows:

1. REGION FILE :

ENTITY NAME : REG
Maximum Entities : 10

ENTITY CONTAINS :

1. R-CODE : Region Code for Identification. Unique Code
2. R-NAME : Region Name (Unique)

ENTITY LINKED TO :

1. REG-STA-LNK : Region Linked to STATE.
2. REG-COM-LNK : Region Linked to COMMENT.

EXTRA LINKS :
(For Further Use)

1. REG-ARB-LNK.
2. REG-XY-LNK.
3. REG-PSM-LNK.

2. STATE FILE :

ENTITY NAME : STATE
Maximum Entities : 50

ENTITY CONTAINS :

1. S-CODE : STATE Code for Identification (Unique)
2. S-NAME : STATE Name (Unique)
3. R-R : REG Realisation Number

ENTITY LINKS :

1. STA-DIS-LNK : STATE Linked to DISTRICT.
2. STA-COM-LNK : STATE Linked to COMMENT.

ENTITY REFERRED TO :

1. STA-REG-LNK : STATE REFERRED TO REG.

EXTRA LINKS :

1. STA-YZ-LNK
2. STA-ARB-LNK
3. STA-PSM-LNK

3. DISTRICT-FILE :

ENTITY NAME : DISTRICT
Maximum Entities: 5000

ENTITY CONTAINS :

1. D-CODE : DISTRICT Code for Identification(Unique)
2. D-NAME : DISTRICT Name (Unique)
3. R-R : REG Realisation Number
4. R-S : STATE Realisation Number

ENTITY LINKED TO :

1. DIS-LOC-LNK : DISTRICT Linked to a Locality
2. DIS-OCC-LNK : DISTRICT Linked to an Occurrence
3. DIS-COM-LNK : DISTRICT Linked to COMMENT

ENTITY REFERRED TO :

1. DIS-STA-LNK : DISTRICT Referred to STATE

EXTRA LINKS :

1. DIS-ARB-LNK
2. DIS-XXX-LNK
3. DIS-PSM-LNK

4. LOCALITY FILE :

ENTITY NAME : LOCALITY
Maximum Entities : 5000

ENTITY CONTAINS :

1. L-CODE : LOCALITY CODE for Identification (Unique)
2. L-NAME : LOCALITY NAME (Unique)
3. R-R : REG Realisation Number
4. R-S : STATE Realisation Number
5. R-D : DISTRICT Realisation Number
6. LAT : LOCALITY LATITUDE
7. LON : LOCALITY LONGITUDE
8. FREE : (for further use)

ENTITY LINKED TO :

1. LOC-OCC-LNK : LOCALITY linked to OCCUR (rence)
2. LOC-BOR-LNK : LOCALITY linked to BOREHOLE
3. LOC-COM-LNK : LOCALITY linked to COMMENT

ENTITY REFERRED TO :

1. LOC-DIS-LNK : LOCALITY Referred to DISTRICT

EXTRA LINKS :

1. LOC-ARB-LNK
2. LOC-MN-LNK
3. LOC-PSM-LNK

5. OCCURRENCE FILE :

ENTITY NAME : OCCUR

Maximum Entities : 35000

ENTITY CONTAINS :

1. OC-CODE	:	Occurrence Code for Identification(Unique)
2. OC-NAME	:	Occurrence Name (Unique)
3. R-R	:	Region Realisation Number
4. R-S	:	State Realisation Number
5. R-D	:	District Realisation Number
6. R-L	:	Locality Realisation Number
7. OC-LAT	:	Occurrence Latitude
8. OC-LON	:	Occurrence Longitude
9. STATUS	:	Mining Status of Uranium Deposit
10. TOTBH	:	Total Boreholes drilled in this occur
11. GRD-ORE	:	Grade of Ore
12. TOP-SHTNO	:	Topo-Sheet No.
13. DEP-T41 14. DEP-T42	:	Type of Deposit
15. H-ROCK1 16. H-ROCK2	:	Host Rock
17. TEC-STING1 18. TEC-STING2	:	Tect. Setting
19. HAGE-MYRS	:	Host Age in Million Years
20. MIN1 21. MIN2	:	Minerals
22. ORECTROL 1 23. ORECTROL 2	:	Ore Control
24. ALTS 1 25. ALTS 2	:	Alteration
26. LEACHTY	:	Leachibility
27. TRDEP-KMTS	:	Total Drilled Depth in K.Meters
28. TMN-KMTS	:	Total Mining in K.Meters
29. RSRV-MTNS	:	Reserve in M.Tonnes
30. INCLU 31. EXTRA 32. INT	:	(for further use)

ENTITY LINKED TO :

1. OCC-BOR-LNK	:	Linked to Borehole
2. OCC-COM-LNK	:	Linked to COMMENT
3. OCC-TELE-LNK	:	Linked to Trace Elements (TELE)

ENTITY REFERRED TO :

1. OCC-LOC-LNK	:	OCCUR referred to Locality
2. OCC-DIS-LNK	:	OCCUR referred to District

EXTRA LINKS :

1. OCC-ARB-LNK
2. OCC-GEO-LNK
3. OCC-PSM-LNK

6. TRACE ELEMENTS FILE :

ENTITY NAME : TELE
Maximum Entities : 7000

ENTITY CONTAINS :

1. T-CODE : Trace Element Code for Identification
2. ELEMENT : Trace Element Name
3. PPM : PPM of this element
4. R-O : Realisation No. of the Occurrence

ENTITY LINKS :

1. TELE-COM-LNK : Linked to COMMENT

ENTITY REFERRED TO :

1. TELE-OCC-LNK : Referred to an Occur

EXTRA LINKS :

1. TELE-GE-LNK
2. TELE-ARB-LNK
3. TELE-PSM-LNK

7. BOREHOLE-FILE :

ENTITY NAME : BOREHOLE
Maximum Entities: 500000

ENTITY CONTAINS :

1. BHNO : Borehole Number
2. LATITUDE : Borehole Latitude
3. LONGITUDE : Borehole Longitude
4. R-R : Region Realisation Number
5. R-S : State Realisation Number
6. R-D : District Realisation Number
7. R-L : Locality Realisation Number
8. R-O : Occur Realisation Number
9. INCN : Inclination of this Borehole
10. DD : Day
11. MM : Month
12. YR : Year
13. DRDEP : Drilled Depth
14. DELOG : Logging Depth

ENTITY LINKS :

1. BOR-DEP-LNK : Linked to Depat.
2. BOR-COM-LNK : Linked to COMMENT
3. BOR-ZON-LNK : Linked to Zone

ENTITY REFERRED TO :

1. BOR-LOC-LNK : Referred to a Locality
2. BOR-OCC-LNK : Referred to an Occurrence

EXTRA LINKS :

1. BOR-ARB-LNK
2. BOR-PSM-LNK

8. DEPTHS & ACTIVITIES FILE :

ENTITY NAME : DEPACT

Maximum Entities : 5000000

ENTITY CONTAINS :

1. BD-CODE : Borehole-Depths Code for Identification
2. DEPTH : Borehole Depth
3. ACTY : Activity
4. ZONE : (for further use)

ENTITY LINKS :

1. DEP-COM-LNK : Linked to COMMENT

ENTITY REFERRED TO :

1. DEP-BOR-LNK : Referred to a Borehole

EXTRA LINKS :

1. DEP-ARB-LNK
2. DEP-PSM-LNK
3. DEP-GE-LNK

9. ZONE-FILE :

ENTITY NAME : ZONE

Maximum Entities: 3500000

ENTITY CONTAINS :

1. Z-CODE : Zone Identification No.(Unique)
2. ZST : Zone Starting Depth
3. ZEND : Zone Ending Depth
4. ZLN : Zone Length
5. ZAV : Zone Avg. Activity

ENTITY REFERRED TO :

1. ZON-BOR-LNK : Referred to Borehole

EXTRA LINKS :

1. ZON-ARB-LNK
2. ZON-MSP-LNK
3. ZON-PSM-LNK

10. MACROS-FILE :

ENTITY NAME : MAC

Maximum Entities: 3000

ENTITY CONTAINS :

1. M-CODE : Macro Code
2. MACRO-NAME : Name of the Macro

ENTITY LINKED TO:

1. MAC-COM-LNK : Linked to COMMENT

EXTRA LINKS :

1. MAC-PSM-LNK
2. MAC-XXX-LNK

11. COMMENT-FILE :

ENTITY NAME : COMMENT

Maximum Entities : 75000

ENTITY CONTAINS :

1. C-CODE : COMMENT Code for Identification
2. COM-CODE : This specifies Reference/Comment etc.
3. COM 1 : Comment
4. COM 2 : Comment
5. R-R : Region Realisation Number
6. R-S : State Realisation Number
7. R-D : District Realisation Number
8. R-L : Locality Realisation Number
9. R-O : Occurrence Realisation Number
10. RT : (for further use)

ENTITY REFERRED TO :

1. COM-REG-LNK : Referred to Region
2. COM-STA-LNK : Referred to State
3. COM-DIS-LNK : Referred to District
4. COM-LOC-LNK : Referred to Locality
5. COM-OCC-LNK : Referred to Occurrence
6. COM-BOR-LNK : Referred to Borehole
7. COM-ZON-LNK : Referred to Zone
8. COM-MAC-LNK : Referred to MAC

EXTRA LINKS :

1. COM-XYZ-LNK
2. COM-GEO-LNK
3. COM-PSM-LNK

Data Input

One of the most important factors in any data handling and retrieval activity is that the data stored is errorfree. Every effort is made to ensure that the input data remains accurate from the stage it is recorded and documented to the stage it is used. This has been taken care of by proper input design and rigid validation procedures.

MACROS (Output)

The process of querying on a terminal has been made interesting since the System initiates a dialogue and converses with the user to provide the desired information. One has the option to get the reply to a query as a display on the terminal or as hard copy on the printer. A series of macros have been written to answer a wide variety of queries. For example the exploration activity could be at various localities and at various stages namely reconnaissance, drilling, exploration mining etc. Information regarding each activity can be obtained regionwise, statewise or districtwise. Similarly information can be obtained regarding mineralogy, leaching characteristics of the ore, trace element distribution etc. A file has therefore, been created named MACROS where a complete directory of macroname and its functions are available for any user. This helps in executing only the relevant macro for getting the required information.

ACKNOWLEDGEMENTS The authors are grateful to Mr. T.M. Mahadevan Director, Atomic Minerals Division and Mr.Narendar Dayal, Head, Physics Group for their constant encouragement and support for this work. They would also like to thank Mr. N.V. Surya Kumar for his continuous assistance during the implementation of the System.

REFERENCE

1 Hansen, M.V. and Trocky, L, The International Uranium Geology Information System. (Proc. of Symp. on Uranium evaluation and mining techniques, Vienna, 1979). Paper No. IAEA-SM-239/37.

AIRBORNE RADIOMETRIC INTERPRETATION AND INTEGRATION

ANALYSIS OF AIRBORNE GAMMA RAY SPECTROMETRIC DATA FROM THE VOLCANIC REGION IN THE EASTERN PART OF CHINA

Shuxin ZHAO
Bureau of Geology,
Ministry of Nuclear Industry,
Shijiazhuang, China

Abstract

Airborne spectrometric data with high sensitivity from volcanic region in eastern part of China are analyzed in this paper, some suggestions for further use of these data are made. The analysis of the relationship between geochemical fields of airborne uranium concentration and uranium deposits, investigation on uranium sources, effect of thorium concentration variation on distinguishing regional structure, petrological characteristics and potential prospecting are of specified significance for uranium exploration. Because of geological and geomorphic features, there are weak airborne anomalies in the region, at the same time, because of development of drainage system and geochemical mobility of uranium, anomalies in the form of dispersion train of radioelement of uranium deposits are frequently found, which are important clues for uranium exploration.

INTRODUCTION

China started its airborne radiometric survey in volcanic region in eastern part in 1956, and good results have been obtained. Since 1981, high sensitivity airborne gamma-ray spectrometric survey has been carried out in the region using GR-800D airborne spectrometric system mounted in Bell-212 helicopter, and the data obtained were processed on PRIME computer. The data analyzed in the paper include: K, U, Th and their ratios; analysis of geological data of several spectral variables; correlation, covariance and principal component analysis; magnetic two-dimentional filtration and depth computation of magnetic sources, etc.

ANALYSIS OF AIRBORNE GAMMA-RAY SPECTROMETRIC DATA

1. Location of uranium deposits of volcanic type in regional geochemical fields of uranium concentration

It has been proved in practice that most of uranium deposits are distributed in and adjacent to the raised regional geochemical fields (abbreviated to raised field hereafter) of airborne uranium concentration [1, 2]. The statistical result of tens of uranium districts indicates that the raised fields of uranium deposits of volcanic type are characterized by A) the raised fields have a wide range up to several hundred km^2, B) the raised fields are activated (the statistical standard deviation of uranium concentration is large) and the higher activity of the fields, the greater possibility for finding deposits, and C) the raised fields have higher uranium concentration which may reach more than 3 ppm. For comparison, average values of uranium concentration of

Table I. Computer-generated average values of airborne K, U and Th concentration of volcanic rocks in Dagao district and rocks of different type in the region

Strata	$J3m^5$	$J3m^4$	$J3m^3$	$J3m^2$	$J3m^1$	Average values in the region
K(%)	1.71	2.32	2.06	2.03	2.09	1.93
U(ppm)	3.18	3.15	3.30	3.01	3.08	2.58
Th(ppm)	23.70	23.33	18.68	18.24	19.74	13.93

volcanic rocks of Jurassic age in Dagao district and rocks of different type in the region are listed in Table I.

2. Relationship between the variation of thorium and potassium concentration and uranium deposits

Uranium concentration of uranium deposits in the region has a positive correlation to thorium. In many economic uranium districts it is always indicated that the higher the uranium concentration, the higher concentration of thorium, and thorium concentrated on the surface, and uranium enriched in the depth, which is very important to uranium exploration.

Since the geochemistry of thorium and potassium is more stable than that of uranium, and there is a correlation between these elements, therefore analysing the existence of uranium mineralization using the regularity of thorium and potassium concentration variation, significant results have been obtained from the region. Fig. 1 is the computer-plotted interpre-

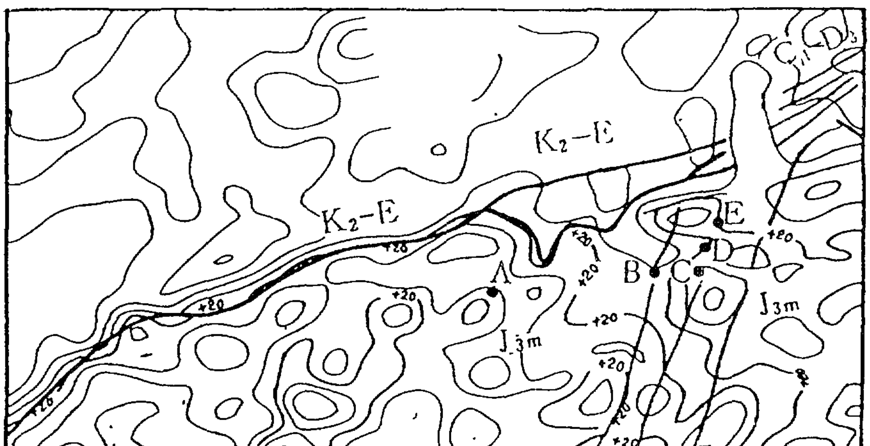

FIG. 1. Interpretation map of airborne thorium concentration in Dagao district. A-E Uranium deposits /-Structure. Contour interval 4ppm. Shading on low side 2ppm.

tation map of airborne thorium concentration of volcanic rocks in Dagao district. Solid line means the structural line, the black dots are uranium deposits. With 20 ppm thorium concentration contour, completely coincides with NE regional structure. According to the variation of thorium concentration, the J3m volcanic rocks and K-E strata on south and north sides may be distinguished. It can be seen from Fig. 1 that J3m volcanic rocks with high thorium concentration are spilled out to the south along the structure. There is a group of NE secondary structures in eastern part of high thorium concentration across 20 ppm contour, where some main uranium deposits (A-E) are just occurred.

According to the above-mentioned analysis, the increase of thorium concentration, besides geological, structral and petrological conditions and uranium anomalies to be considered, is an important criterion for uranium exploration.

3. Investigation on uranium sources in volcanic region

Through analysis it is believed that uranium mainly derived from volcanic rocks for volcanic type uranium deposits in the region, because there is a increased area of uranium content in a wide range to supply suffiecent uranium for mineralization under favourable geological conditions. This can be seen on contour map of uranium concentration and on total count rate map, Fig. 2 is the computer-generated airborne total count rate contour map of volcanics in Dagao district. The black dots are uranium deposits, Fig. 3 is the computer-generated contour map of airborne uranium concentration of volcanic rocks in Dagao district.

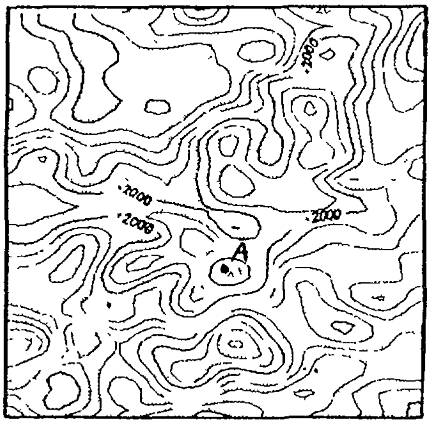

FIG. 2. Airborne total count rate contour map of uranium deposit from Dagao district. A-Uranium deposit. Contour interval 200 cps. Shading on low side 100 cps.

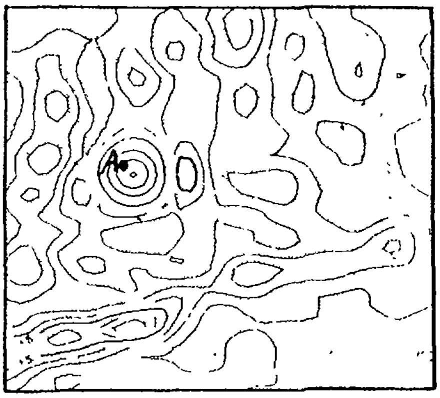

FIG. 3. Airborne Uranium concentration contour map of uranium deposit from Dagao district. A-Uranium deposit. Contour interval 1ppm. Shading on low side 0.5 ppm.

It can be seen from two figures that uranium deposits occurred near the area in which volcanic rocks contained high uranium.

Besides volcanic rocks with high uranium concentration, Yanshanian, Indo-China and Caledonian granites and Cambrian bottom strata in this region are uranium sources. Their uranium concentration is listed in Table 2.

Table 2 Airborne uranium concentration of uranium sources horizons of volcanic rocks

Lithology	Volcanic rock(J)	Granite (r_5^3)	Granite (r_5^2)	Granite (r_5^1)	Granite (r_3)	Carbonaceous -sillieeous-pellitic(Cm)	Average value in the region
Uranium concentration (ppm)	2.8-3.6	3.2-3.7	3.4-4.5	3.3-7.4	3.5-4.9	4.1-4.9	2.58

4. Normal distribution of uranium concentration of uranifeous strata (bodies)

Uranium concentration of uranifeous strata (bodies) in volcanic region is charaterized of normal distribution which appears as positive skewness [3] and extends in the direction of high uranium concentration, and, sometimes, several peaks appear on histogram. Fig. 4 is the computer-generated histogram which shows airborne uranium concentration of

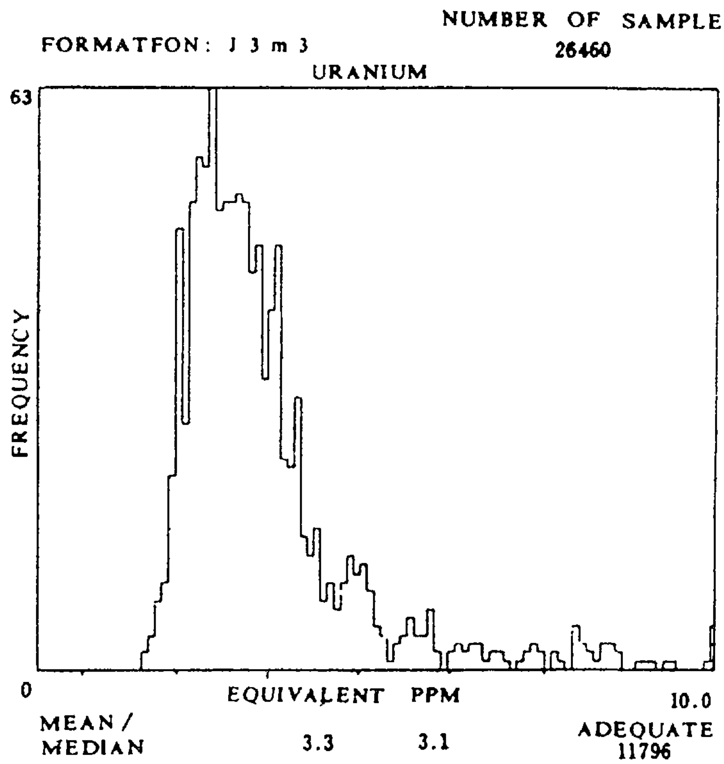

FIG. 4. Computer-generated airborne histogram of uranium concentration of uraniferous stratum in Dagao district.

$J3m^3$ volcanic rocks in Dagao district. A total amount of 26460 sampling sites were counted for this stratum in Dagao district, the mean from these sites is 3.3ppm, the median is 3.1 ppm. It may be seen that the uraniferous stratum appears as positive skewness and there are several variations in statistical frequency in direction of high uranium concentration, which shows a local re-enrichement of uranium in this stratum.

5. Spectral character of airborne anomalies of uranium deposits of volcanic type

Airborne survey in the region indicates that the spectra of uranium deposits are characterized by high total count rate and high uranium concentration, and high U/Th and U/K ratio, Fig. 5a is a computer-generated airborne spectrometric profile showing a uranium deposit in southern part of Dagao district. Airborne uranium concentration of the deposit is 11.1 ppm, and the total count rate and U/Th, U/K ratio are of high values. Fig. 5b is the airborne spectrometric profile which shows uranium deposit in another area, uranium concentration of which is 114.5 ppm. It can be seen from the two profiles that the spectra of the two deposits are similar regardless of their different uranium concentration.

6. Discrimination value of uranium anomalies

The standard deviation of uranium is generally used as a discrimination value for airborne anomalies in volcanic region. Uranium concentration of airborne anomalies in this region is usually more than 3 times of standard deviation above mean, Fig. 6 is the computer-generated interpretation map of airborne uranium anomalies counted up according to strata of volcanic rocks in Dagao district. It can be seen from Fig. 6

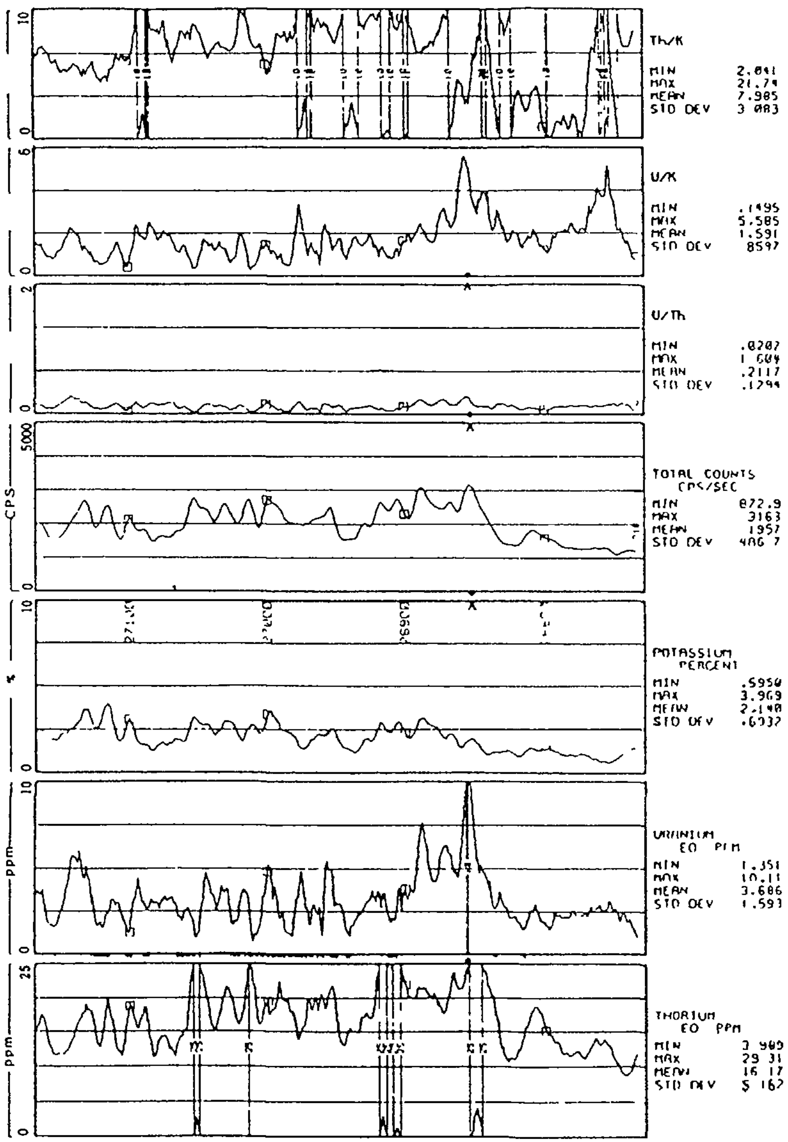

FIG. 5a. Airborne spectral profiles of uranium deposit. A-Uranium deposit.

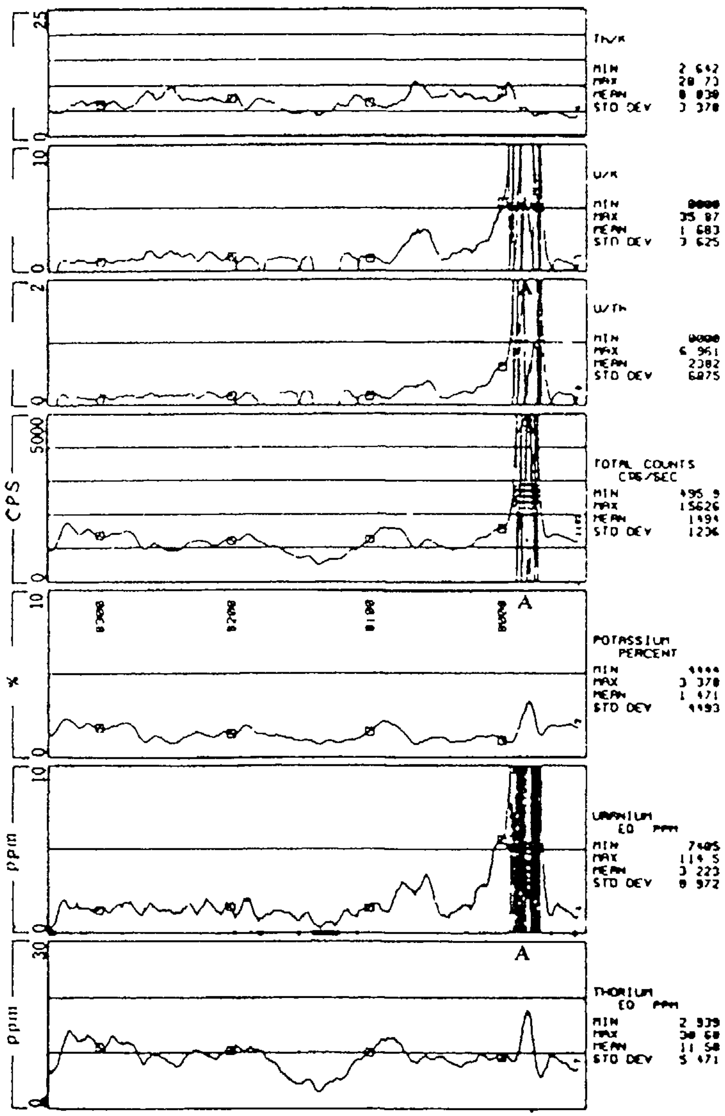

FIG. 5b. Airborne spectral profiles of uranium deposit. A-Uranium deposit.

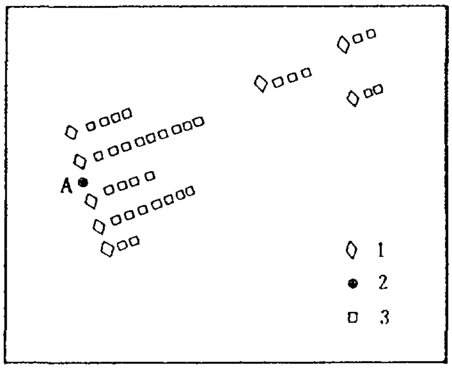

FIG. 6. Computer-generated interpretation map of airborne anomalies from Dagao district.
1 - Location of standard deviation.
2 - Location of uranium deposit.
3 - Standard deviation.

that the uranium concentration is very high, up to 9 times of standard deviation above mean.

7. Weak airborne anomalies feature of volcanic region

Generally, in volcanic region economic uranium deposits have both high total count rate and high uranium content, however, the anomalies become more weak due to following condition: poor outcrops, high terrain clearance, thick cover, absorption by surface water, vegetation shielding and geochemical process, etc. The weak anomalies usually occurred in gulches and paddy fields. This is the case in Fig. 7. Fig.7 is an airborne spectrometric profile which shows a uranium deposit of volcanic type in western part of Dagao district, which appears as a extremely weak anomaly, only 4 ppm by airborne measurement. Only two high radioactive points exist in the paddy field, which are not continuous and 20m long only. The weak anomaly was generally interpreted by analogue method under favourable geological condition.

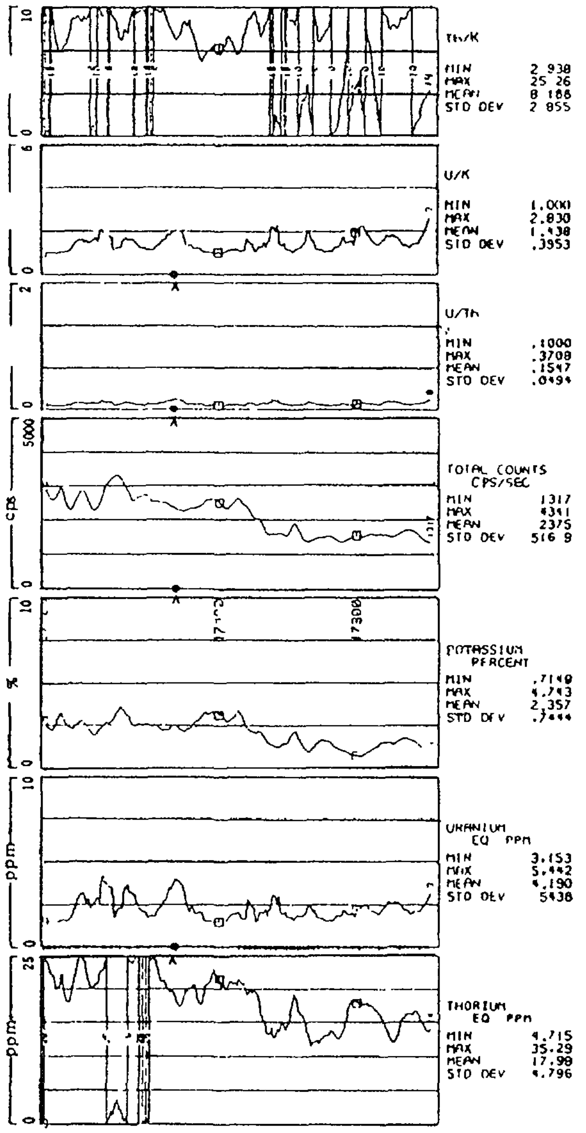

FIG. 7. Airborne spectral profiles of weak anomaly of uranium deposit. A-Uranium deposit.

It is necessary to mention "high altitude" anomalies above 200m. The anomalies at that altitude are difficult to recognized even with high sensitivity airborne measurement, because they only appeared as small projections. Judged by the discovered uranium deposits, it is desirable that terrain clearance is as low as possible, and the optimum flight altitude should not be over 120m.

8. Geomorphic features of airborne anomalies

According to statisties of locations where airborne anomalies of known uranium deposits are found, most of the anomalies were often occurred in river valleys, streamlets, paddy fields, deperssions and in the places where drainage system is developed. It is the erosional cutting of drainage that results in mineralized outcrops, and they are easy to be found with airborne radiometric measurement.

In the places where drainage system is developed and geochemical mobility is strong, in low reaches of the drainage which runs through uranium deposit, it is easy to form dispersion train of radioactive elements [4]. The dispersion train may, sometimes, extend to tens of km. The airborne radiometric survey can find the dispersion train which is an important criterion for uranium exploration. Fig. 8 shows the dispersion train anomalies of radioactive elements over 2,000 cps in volcanic region. The southern part in the Fig. is a complex terrain with high uranium concentration, the area of which is more than 1,000km^2. The dispersion train along the river is 55km, and 19 anomalies were found within the range of 55km. The black dots are uranium deposits.

9. Magnetic characteristics

Uranium deposits in volcanic region are usually related to certain magnetic bodies, therefore the structure, petrology, morphology of geological body and the depth of basement associated with uranium deposits may be investigated on the basis of magnetic field variation [4, 5].

The uranium deposits are usually controlled by structure, and regional structure may extend from a few km to several hundred km. The magnetic field of

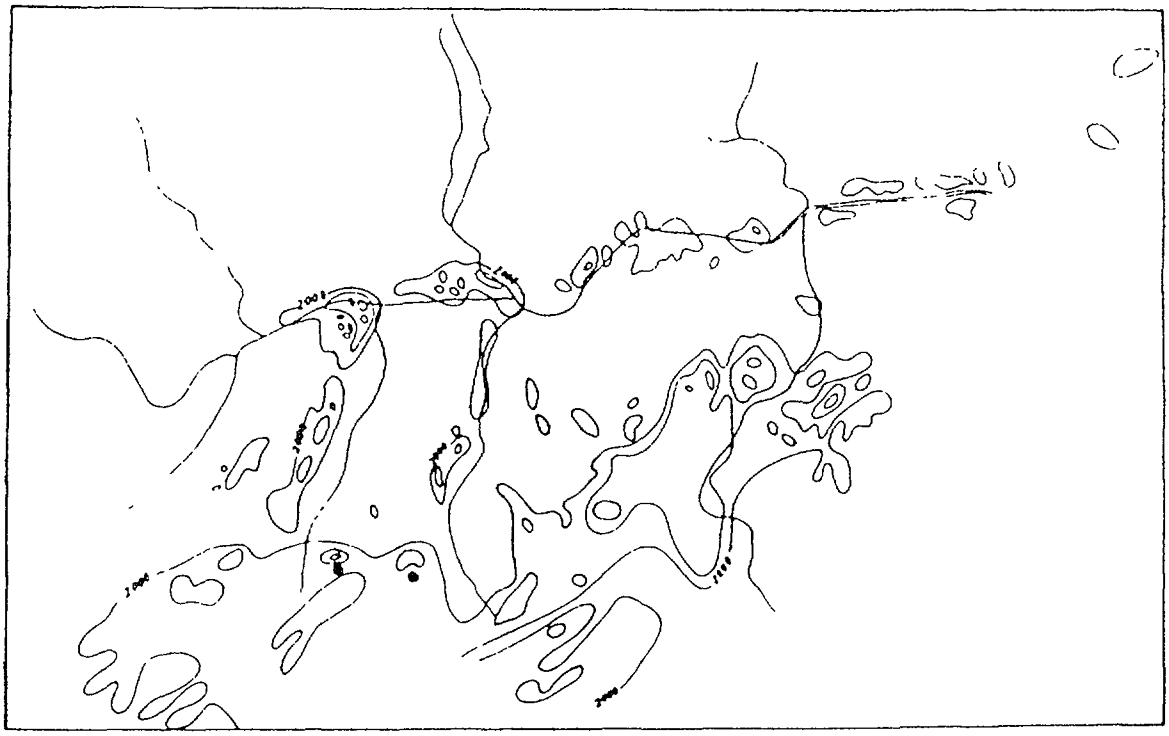

FIG. 8. Dispersion train anomalies map of airborne radioelement.
• – Uranium deposit. Contour interval 400cps.

such structure is characterized by linear and echelon array with magnetic high. In the junction of structures superimposition, intersection or transposition of magnetic field often apears. The uranium deposits are generally occurred in such places with complicated variation of magnetic field, by which the spatial and time relations between deposits and structure can be investigated and uranium mineralization traced.

The uranium deposits are also controlled by petrology, and associated with some veins, for example, lamprophyre, syenite, diabase,etc. The morpholoty, location, extending direction and buried depth of magnetic bodies, as well as their relations with uranium mineralization were analyzed by means of magnetic contrast.

Fig. 9 is the computer-generated interpetation map of residual magnetic field intensity. The black dot means uranium deposit, which is occurred in J31

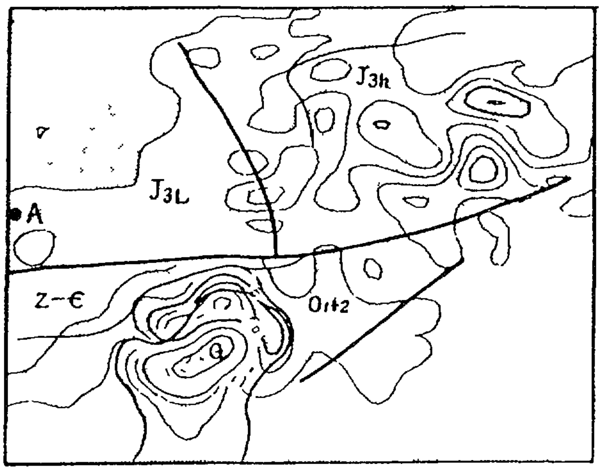

FIG. 9. Interpretation map of residual magnetic field intensity. A-Uranium deposit. /-structure. Contour interval 200 gammas. Shading on low side 100 gammas.

stratum. The solid line is structural line. The magnetic field apparently indicates the structure and completely separates J31 and J3h strata. The southern part shows a equiaxial hidden magnetic body covered by Quaternary. Fig. 10 shows the first order vertical derivative of magnetic field. It may be seen from the Fig. that the regional boundary is given more clearly, and besides equiaxial hidden magnetic body, there are hidden magnetic bodies which were not destroyed by northern structure.

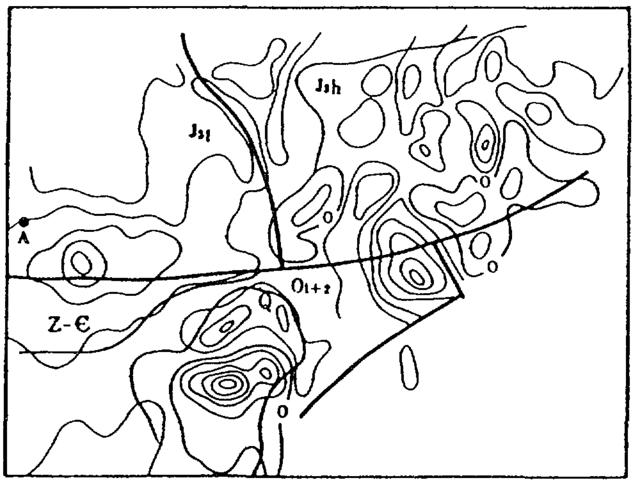

FIG. 10. First order vertical derivative of residual magnetic field. A-Uranium deposit. /-structure. Contour interval 0.001 gammas/inch.

In addition, the form of volcanic eruption and the location of volcanic vent were investigated using circular and linear features of magnetic field, and some results have been obtained.

At the end of our discussions in this paper, it should be confirmed that the high sensitivity airborne spectrometric survey in volcanic region in eastern part of China is effective and succesful. It still needs,of course, to carry out this work further in the region so that our experience will become more perfect and ripe.

REFERENCES

[1] Feng Weizhou et at. Airborne radiation field map and its explanation.

[2] A.G.Darnley et al. Distribution of uranium in rock as a guide to the recognition of uraniferous regions. IAEA-TC-25/9.

[3] Chengdu Geological College. Methods of Radioactivity Surrey. Publishing house of atomic energy, 1978.

[4] Zhao Shuxin. Airborne spectral and magnetic data processing and the application. Publishing house of atomic energy. Radioactive Geology, 3/1983.

[5] Bureau of National Geology. Introduce of methods of matched filtering. Airborne geophysical prospecting techniques, 4/1979.

DATA ENHANCEMENT TECHNIQUES FOR AIRBORNE GAMMA RAY SPECTROMETRIC DATA

S.G. TEWARI, K.N. NAGARAJA, N.V. SURYA KUMAR
Atomic Minerals Division,
Department of Atomic Energy,
Hyderabad, India

Abstract

High sensitivity airborne gamma ray spectrometric and magnetic surveys have been conducted by the Atomic Minerals Division in India since 1978. About 250,000 line kilometers of data have been obtained at 1km. line spacing in parts of Bihar, Rajasthan, Andhra Pradesh, Karnataka, Madhya Pradesh in India. This data have been processed using a library of computer programmes developed inhouse.

The first step of processing consists of making contour maps for five main parameters namely eU, eTh, K, Total cps and Magnetic and three derived parameters, eU/eTh, eU/K and eTh/K.

Statistically significant anomaly maps are prepared based on the information on the geological boundaries. This information is coded and written on the data tape for computing the mean and variance of each parameter namely eU, eTh and K for a given geological unit. Maps based on this information remove the purturbations due to geological noise and quantify the anomaly. Where geological information is lacking line anomaly maps are prepared for each flight profile based on the mean and variance of each parameter along and across the profile. These maps are prepared using a drum plotter or printer.

Alpha-numeric maps for each parameter are prepared by dividing the data set into three to four ranges based on the frequency distribution for that parameter. Combining the three most significant parameters namely, eU, eU/eTh and eU/K and dividing each parameter into three ranges say High, Medium and Low, twenty seven such combinations are obtained. A unique character is printed for a specific combination of the three parameters. This is less expensive than colour coding. The exact location of zones of interest on the base map are delineated using flight line number and grid points obtained from the flight data.

Three case studies characterised by their own rqdiometric parameters are presented using these techniques to illustrate their usefulness.

---

1. INTRODUCTION

The high sensitivity airborne gamma ray spectrometric and magnetic survey system was designed and fabricated by the Atomic Minerals Division to fulfil the specifications of the high sensitivity gamma-ray spectrometric and magnetic surveys. The requirements for such surveys are a large crystal volume ($\simeq$50 litres) a proton precession magnetometer, integrity of performance and digital data recording on a computer compatible tape. The spectrometer is capable of sensing changes in the ground surface concentrations of the order of 1 ppm eU, 2 ppm eTh and 0.2% of K. The magnetometer has a recording sensitivity of 1 gamma. The system also has provision and necessary instrumentation for monitoring atmospheric radon by measuring 214 Bi in air.

The data in digital form, is accumulated every second and recorded on a magnetic tape. Some parameters are simultaneously converted to analogue form and recorded on a six pen strip chart recorder. The system currently being used records data from two multichannel analysers with 256 and 64 channels for the two detector systems and also for four spectral channels, one for total and the other three for K, U and Th. The latter together with magnetic and altimeter data are also recorded on the chart recorder.

Each data block recorded every second consists of 1040 bytes of numeric data whose format is given in the next section.

For processing this data on a computer, a modular software package has been written using COBOL and FORTRAN. The routines are executed for data validation and editing, applying various corrections, checking for jitters in the data, assigning coordinates to the data points after flight path recovery, interpolating the data at grid points and drawing stacked profiles and contour maps of 8 parameters and in some cases 9 parameters. The 8 parameters are Total counts per second, U, Th, (in ppm), K (in %), U/Th, Th/K and Magnetic. Altimeter data is also contoured in some cases.

2. DATA FORMAT

The logical record length consists of 1040 bytes of information. The record written in EBCDIC has the following format.

Byte No.	Parameter
1-6	Date
7-8	Operator Code
9-10	Line No.
11-16	Real Time
17-19	Fiducial Number
20-24	Magnetometer reading (in gammas)
25-28	Y-Coordinate
29-34	X-Coordinate
35-39	Blank
40-43	Pressure in mb
44-46	Temperature ^{o}C
47-50	Radio altimeter
51-54	Total B.G.
55-57	U - B.G.
58-60	Cosmic B.G.
61-65	Total window counts
66-68	Thorium window counts
69-72	Potassium window counts
73-76	Uranium window counts
77-80	Blank
81-848	3 bytes for each channel count from 256 channel analyser
849-1040	Channels counts from 64 channel analyser

2.1 Data Volume

In a typical flight lasting 4 hours, the data will contain 14,400 records each having 1040 bytes. The total data length therefore, comprises nearly 14.4 million bytes on each day's flight. This is recorded on a computer compatible tape and sent from the field area to the computing laboratory.

3. PROCESSING OF DATA

The system being used for data processing is a third generation 32 bit system 332 computer with 512 K bytes of main memory, four 800/1600 BPI, 9 track tape drives, two 200 MB disc units, a high speed card reader and line printer with six monochrome terminals. For drawing contour maps and profiles an offline Calcomp 1051 plotter is being used. Maps are normally produced in 1:50,000 and 1:250,000 scale.

3.1 Software

A library of modular, largely machine independent routines, has been developed for data processing. These have been written both in COBOL and FORTRAN. All processing involving large volume of I/O, is done using COBOL routines as this results in large saving of CPU time. The source code is fairly optimised for efficient execution and is well structured and easy to follow. Since software is always evolutionary it cannot be frozen and patches are introduced to take care of some abnormal situations or when a more efficient algorithm is developed.

3.2 Brief Description of Computer routines

(a) COPY

This programme written in COBOL when executed gives a formatted list of all field tapes.

(b) VALID :

This COBOL module validates and edits the data. It checks if all the data bytes are numeric and the operator code is correct. This also removes all the unwanted data and a new file is generated which contains all the required validated data.

(c) BLOCK-MERGE :

To facilitate handling of tapes a set of files is merged into a single file. Ten logical records are blocked into one physical record and data from 8 to 9 tapes are merged into a single tape. This COBOL programme does this job for each flight line as one unit, writes a header label indicating the flight line number,

number of records to follow, date of flight and other relevant information.

(d) CORRECT with SMOOTH, SURVEY and INVERT:

This programme takes the output from (c) and applies various corrections for background, inter-channel corrections so as to eliminate the effect of Compton contribution in various windows, altitude corrections to reduce all data to one datum (122 meters ground clearance). The data is then checked for jitters using a second derivative method. After this stage, a subroutine SMOOTH is called to compute weighted average over a group of nine data points. Subroutine SURVEY computes the coordinates of each data point given the coordinates at Fiducial points. The routine INVERT is used depending on the operator code so as to write the data heading only in one direction. All these routines have been written in FORTRAN.

(e) GRID :

This programme takes the data from the output of (d) above and interpolates the data at the intersection of the grid lines which are normal to the flight lines. A linear interpolation is used to computer the data at all the grid intersections. The output of this programme is written on tape for stack profiling and contouring.

(f) PROFILE :

This programme draws stacked profiles for each flight line. Any number of parameters can be selected at one time and profiles can be drawn in four colours.

(g) CONTOUR :

This is a general purpose contouring package which is written in FORTRAN and is machine independent except for the fact that it calls plotting routines available with CALCOMP-1051 system. The scale of the map, the contour interval, writing density etc. can be selected in advance.

A single map covering any three parameters can be made in different colours after slight modification of the programme.

All the routines described above have been developed in the Atomic Minerals Division and are being regularly executed since 1978.

3.3 Specific Program for Magnetic Data Processing

Geophysicists who want to interpret aeromagnetic data require downward or upward continuation of magnetic field, computation of amplitude spectrum etc. For these jobs a computer programme has been written for handling two dimensional magnetic data. The programme uses the same methodology as given by Bhattacharya [1]. By a slight modification of the programme single magnetic profiles can be handled.

4. STATISTICAL ANALYSIS

The approach of drawing contour maps and discerning anomalous regions is successful in delineating only those areas with strong intensity contrast as compared to normal background variation. Often it happens that the total area when contoured as one block will be covering several geological units in which some units will be more radioactive than the others and this unit will appear anomalous in the map. To reduce this geological effect one approach is to compute the mean intensity of the radiation and its standard deviation for each rock unit. Z score $= (x_i - \bar{x})/\sigma$ are then computed for each data point. Contour maps are then prepared based on this dimensionless factor designated as significance factor by Potts [2].

A routine SIGFAC has been written to execute this job. The output of SIGFAC is used for drawing contour maps using the programme CONTOUR.

In an area where geological information is lacking an attempt has been made to segment various geological units in a coarse manner following the procedure of Tewari et al [3] before computing Z scores and contouring. This approach appears to be better than taking the entire area as one lithological unit.

4.1 Line anomaly maps

For quick appraisal of the area, line anomaly maps are prepared on a high speed printer. The average value of the parameter (say eU) and its standard deviation is calculated for each profile. For all the data points which are greater than twice and thrice the standard deviation above the mean value a unique character is printed. Similar job is done using a plotter where a map is drawn to the desired scale. Exactly identical procedure is followed by taking all data across the flight line and writing a character depending upon the significance of that point based on its 'Z' score value. These maps give a quick appraisal of the area for ground follow up work.

4.2 Alphanumeric maps

Two approaches have been used in making such maps one is a range map, where each parameter is taken individually and the distribution of that parameter is segmented into four ranges and a character is printed for each data point depending upon the range in which that data point lies. This is in a way, similar to contour maps drawn on a plotter except that this is done using a printer and the ranges are less to delineate rough boundaries of high ranges. The second approach of making alphanumeric maps is to combine three parameters at a time. This is being done by some workers [4,5] using image processing systems to produce coloured images from the airborne survey data. We have however, adopted a very inexpensive procedure of producing such maps based on three parameters at a time. Supposing we have to superpose three maps namely eU, eU/eTh and eU/K for a given area; each parameter can be segmented into three parts say High Value (H), Medium Value (M) and Low Value (L). Twenty seven combinations therefore are possiblewith three variables, each variable taking any of three values namely H, L or M. For each unique combination say H for U, H for U/Th and H for U/K, character 'A' is printed, similarly all other combinations in sequence can follow the English alphabetic sequence.

For all parameters in low range character * is printed. In this way 27 'colours' can be produced by the printer. This was suggested by Killeen [6]. It is much easier and faster to interpret such maps by taking three parameters at a time. Line numbers and data points can be marked on the printed map to obtain the exact location of anomalous zones on the base map.

5. SOME CASE STUDIES

(A) Devarkonda area, Andhra Pradesh: In this area 47 flight lines with 1km. separation were flown in the north-south direction covering an area of approximately 4500 sq. kms. This area has two major geological units namely massive granites and fractured granites. In addition to the production of contour maps for eight parameters, statistical techniques were applied for signal enhancement for better delineation of the area for ground followup. Three sets of statistically processed maps were prepared namely (a) z score maps based on the assumption that the entire area has one geological unit (b) similar maps based on two geological units (c) line anomaly maps based on mean and standard deviation. computed both along and across the flight lines.

Figs. 1,2,3 & 4 display the geological map of the area along with z score map of Total cps, eU, eTh and eU/eTh based on one and two geological units. These maps were made using a high speed printer. It can be seen that the area north-east of the map remains anomalous in both the cases. Some areas in the eastern side of the middle portion of the map do not show up as big cluster of anomalies when two geological units were taken compared to when computations were done based on a single unit.

Text continued on p. 99.

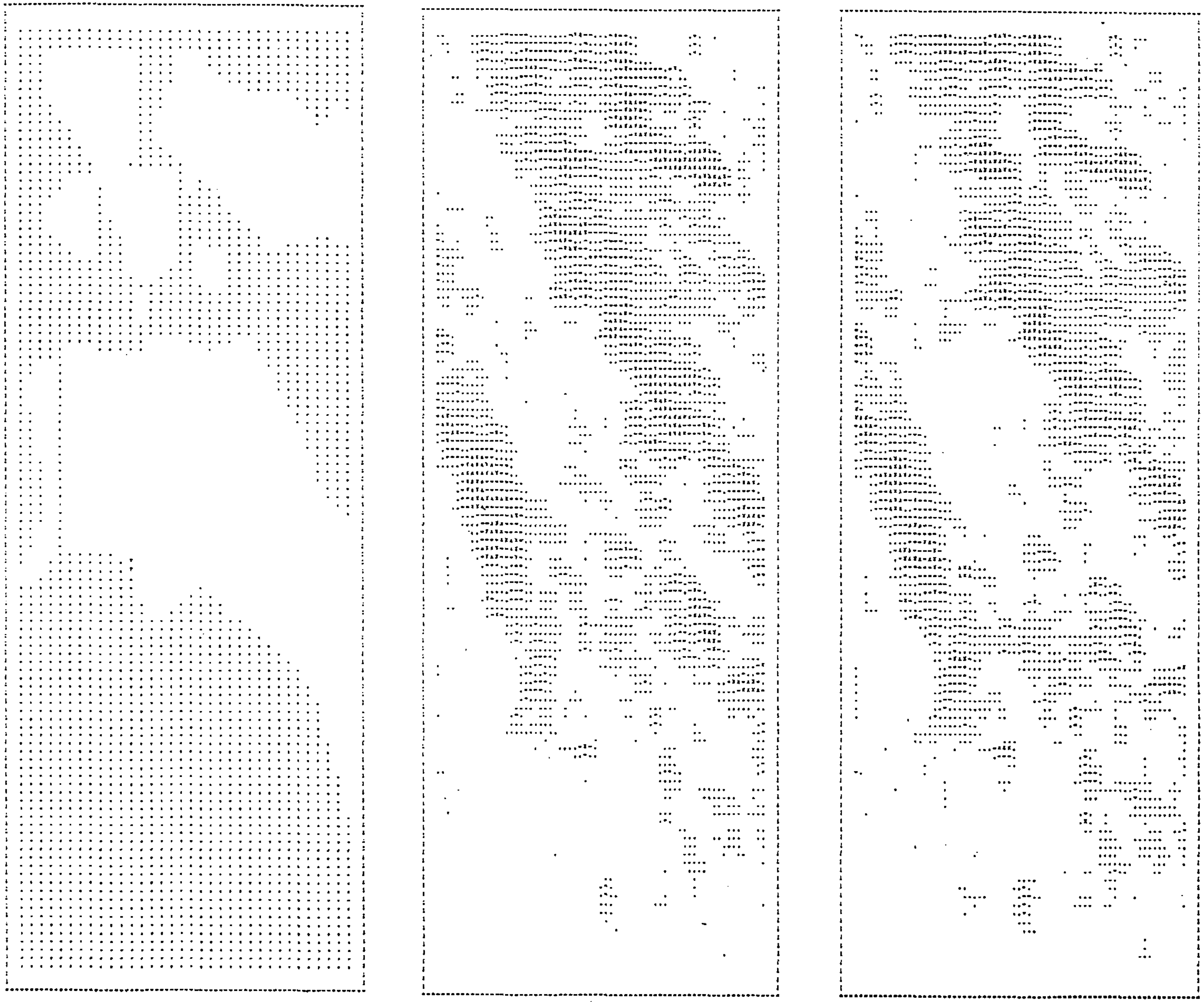

GEOLOGY MAP OF DEVARKONDA (A.P.INDIA)

SPACE - FRACTURED GRANITE
. - MASSIVE GRANITE
, - UNDEFINED

Z SCORE MAP OF TOTAL COUNTS OF DEVARKONDA (A.P.INDIA)
NO. OF GEOLOGICAL UNITS = 1
SPACE - VALUE < 0
. - VALUE (>= 0 AND < 1)
: - VALUE (>= 1 AND < 2)
, - VALUE >= 2

Z SCORE MAP OF TOTAL COUNTS OF DEVARKONDA (A.P.INDIA)
NO. OF GEOLOGICAL UNITS = 2
SPACE - VALUE < 0
. - VALUE (>= 0 AND < 1)
: - VALUE (>= 1 AND < 2)
, - VALUE >= 2

FIG.1.

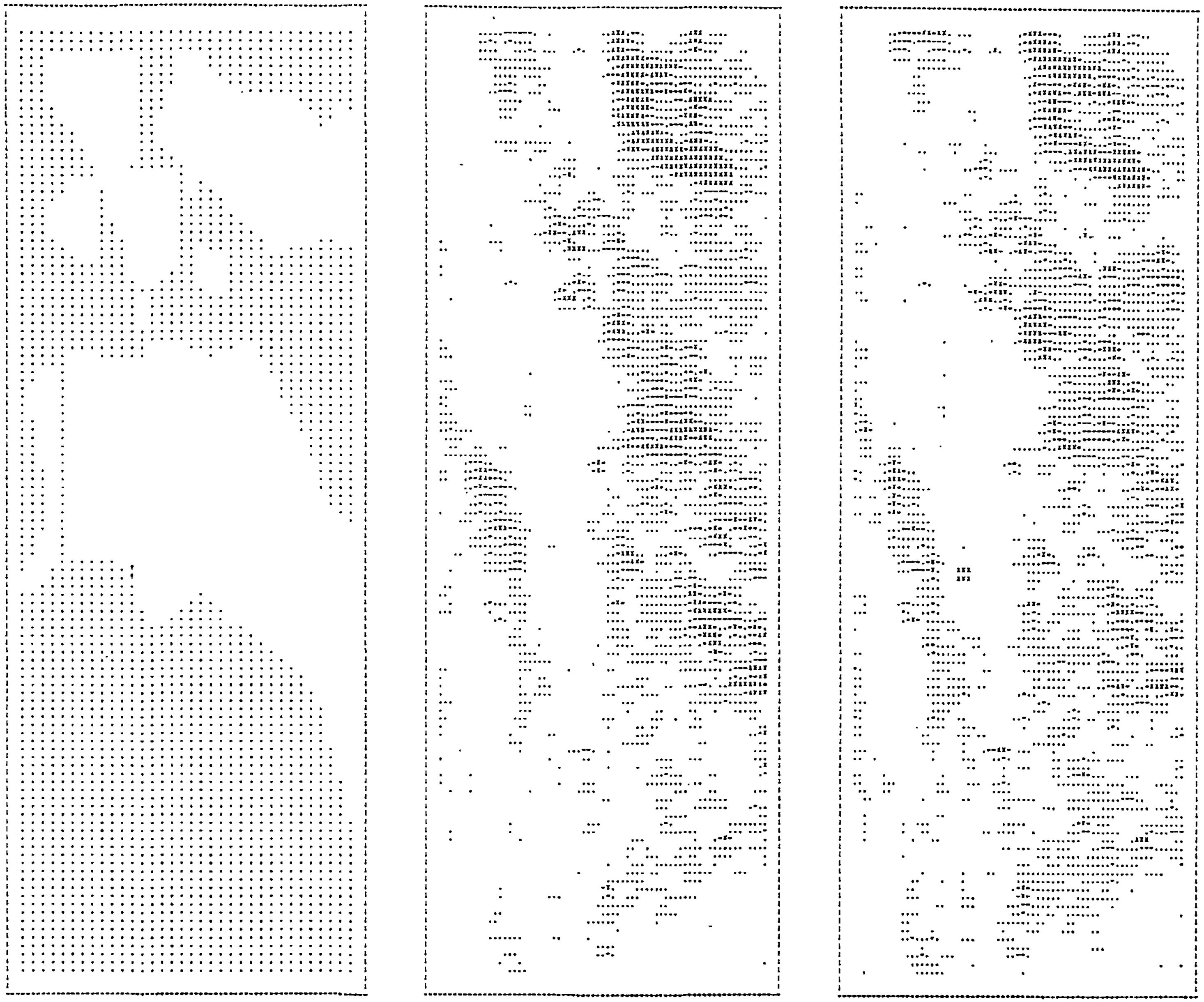

GEOLOGY MAP OF DEVARKONDA (A.P.INDIA)

SPACE - FRACTURED GRANITE
. - MASSIVE GRANITE
+ - UNDEFINED

Z SCORE MAP OF URANIUM COUNTS OF DEVARKONDA (A.P.INDIA)
NO. OF GEOLOGICAL UNITS = 1
SPACE - VALUE < 0
. - VALUE (>= 0 AND < 1)
- - VALUE (>= 1 AND < 2)
X - VALUE >= 2

Z SCORE MAP OF URANIUM COUNTS OF DEVARKONDA (A.P.INDIA)
NO. OF GEOLOGICAL UNITS = 2
SPACE - VALUE < 0
. - VALUE (>= 0 AND < 1)
- - VALUE (>= 1 AND < 2)
X - VALUE >= 2

FIG.2.

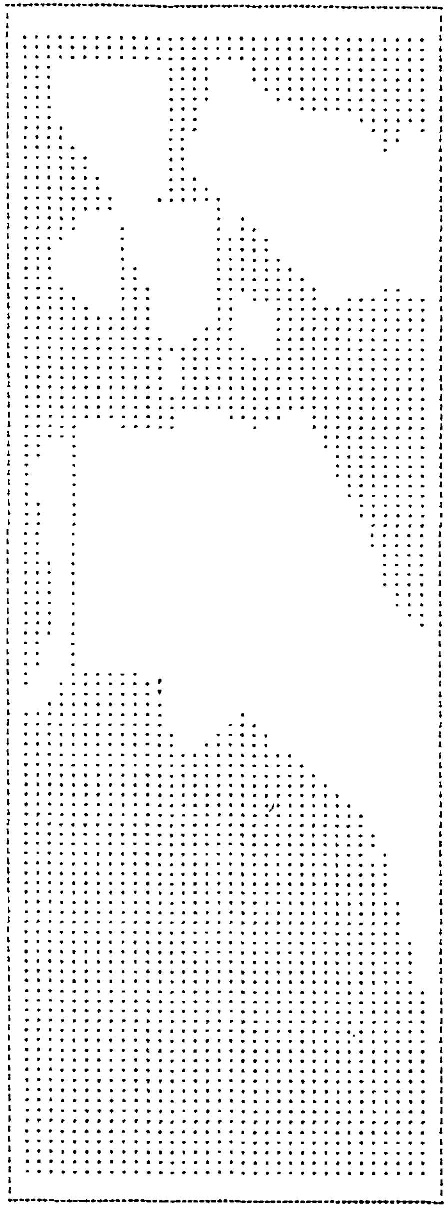

GEOLOGY MAP OF DEVARKONDA (A.P.INDIA)

SPACE - FRACTURED GRANITE
. - MASSIVE GRANITE
+ - UNDEFINED

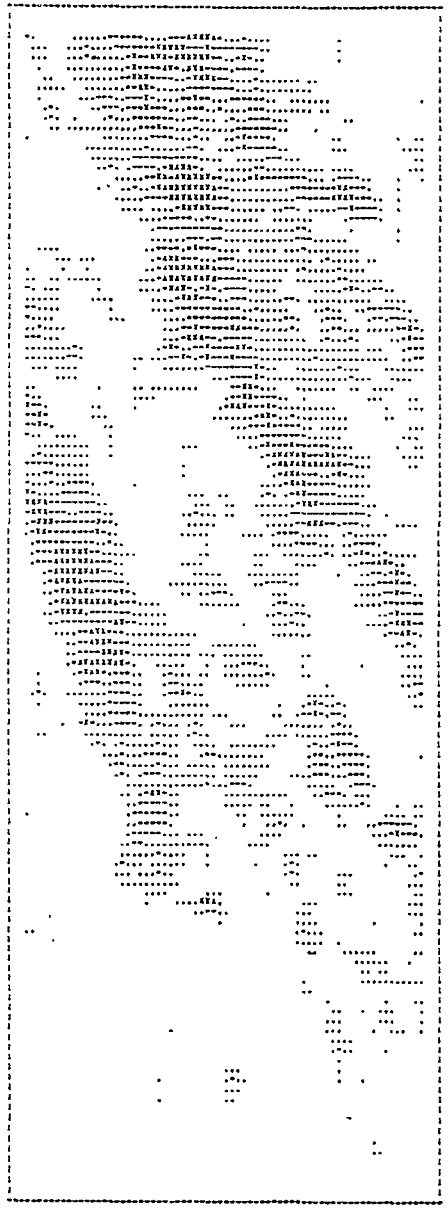

Z SCORE MAP OF THORIUM COUNTS OF DEVARKONDA (A.P.INDIA)
NO. OF GEOLOGICAL UNITS = 1
SPACE - VALUE < 0
. - VALUE (>= 0 AND < 1)
- - VALUE (>= 1 AND < 2)
X - VALUE >= 2

Z SCORE MAP OF THORIUM COUNTS OF DEVARKONDA (A.P.INDIA)
NO. OF GEOLOGICAL UNITS = 2
SPACE - VALUE < 0
. - VALUE (>= 0 AND < 1)
- - VALUE (>= 1 AND < 2)
X - VALUE >= 2

FIG.3.

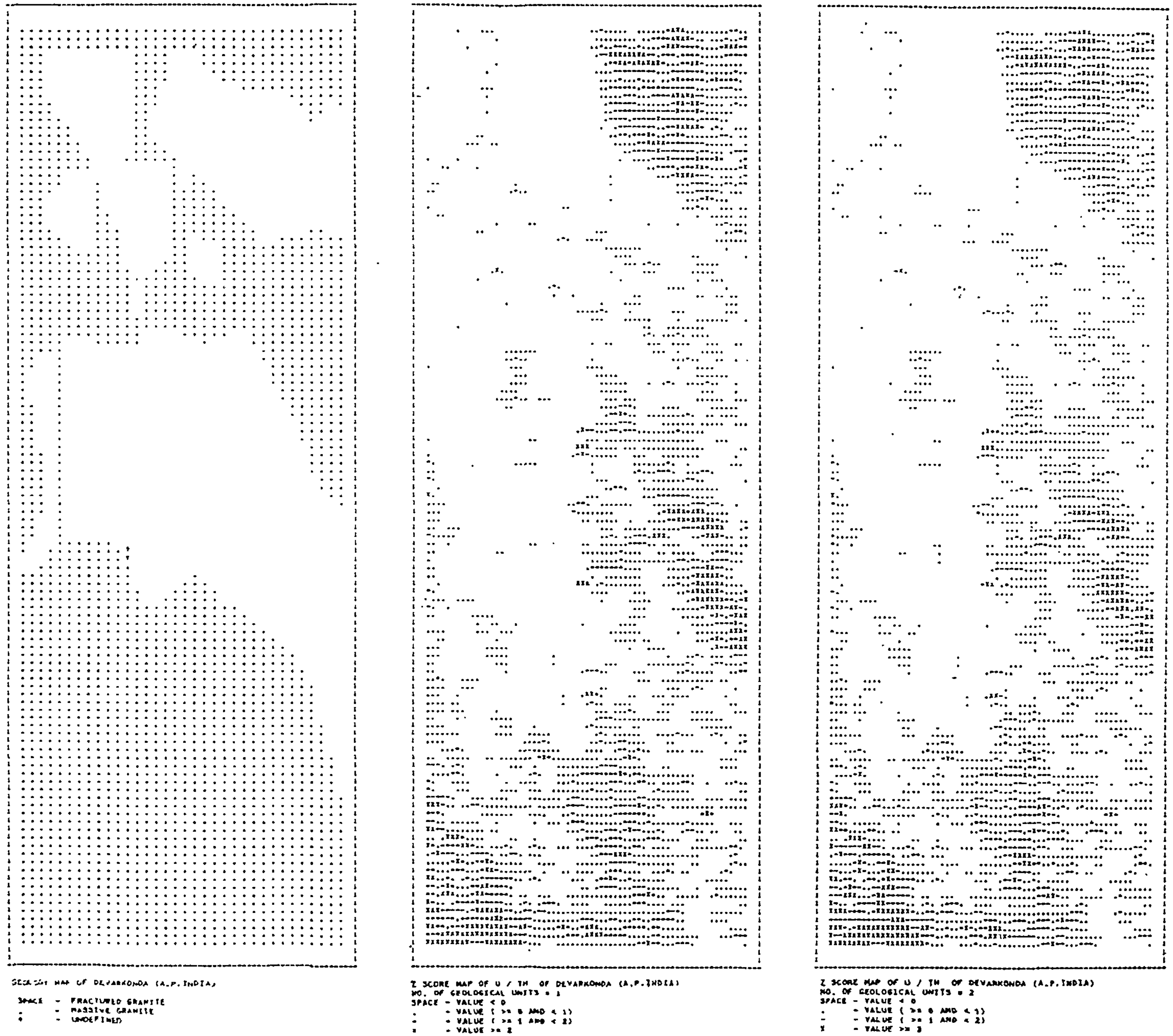
GEOLOGY MAP OF DEVARKONDA (A.P. INDIA)
SPACE - FRACTURED GRANITE
. - MASSIVE GRANITE
+ - UNDEFINED
Z SCORE MAP OF U / TH OF DEVARKONDA (A.P. INDIA)
NO. OF GEOLOGICAL UNITS = 1
SPACE - VALUE < 0
. - VALUE (>= 0 AND < 1)
- - VALUE (>= 1 AND < 2)
x - VALUE >= 2
Z SCORE MAP OF U / TH OF DEVARKONDA (A.P. INDIA)
NO. OF GEOLOGICAL UNITS = 2
SPACE - VALUE < 0
. - VALUE (>= 0 AND < 1)
- - VALUE (>= 1 AND < 2)
X - VALUE >= 3

FIG.4.

Line anomaly maps : Figs. 5 (a,b,c,d) and 6 (a,b,c,d)show a plotter drawn map identifying those data points which exceed by two and three times the standard deviation from the mean value for each parameter namely Total cps, eU, eTh & eU/eTh computed both along and across the flight lines. There is a concentration of anomalous points trending NW-SE in three separate bands. From the actual data it is seen that the average for the parameters generally increase from west to east across the flight lines and this trend continues from south to north along the flight lines. The north-eastern portion becomes a common intersect of the two sets lying between lines 32 to 43. eU/eTh map also corraborates this finding. This trend is mostly seen in the area covered by fractured granites. This seems to be the most promising area for ground investigations.

Text continued on p. 108.

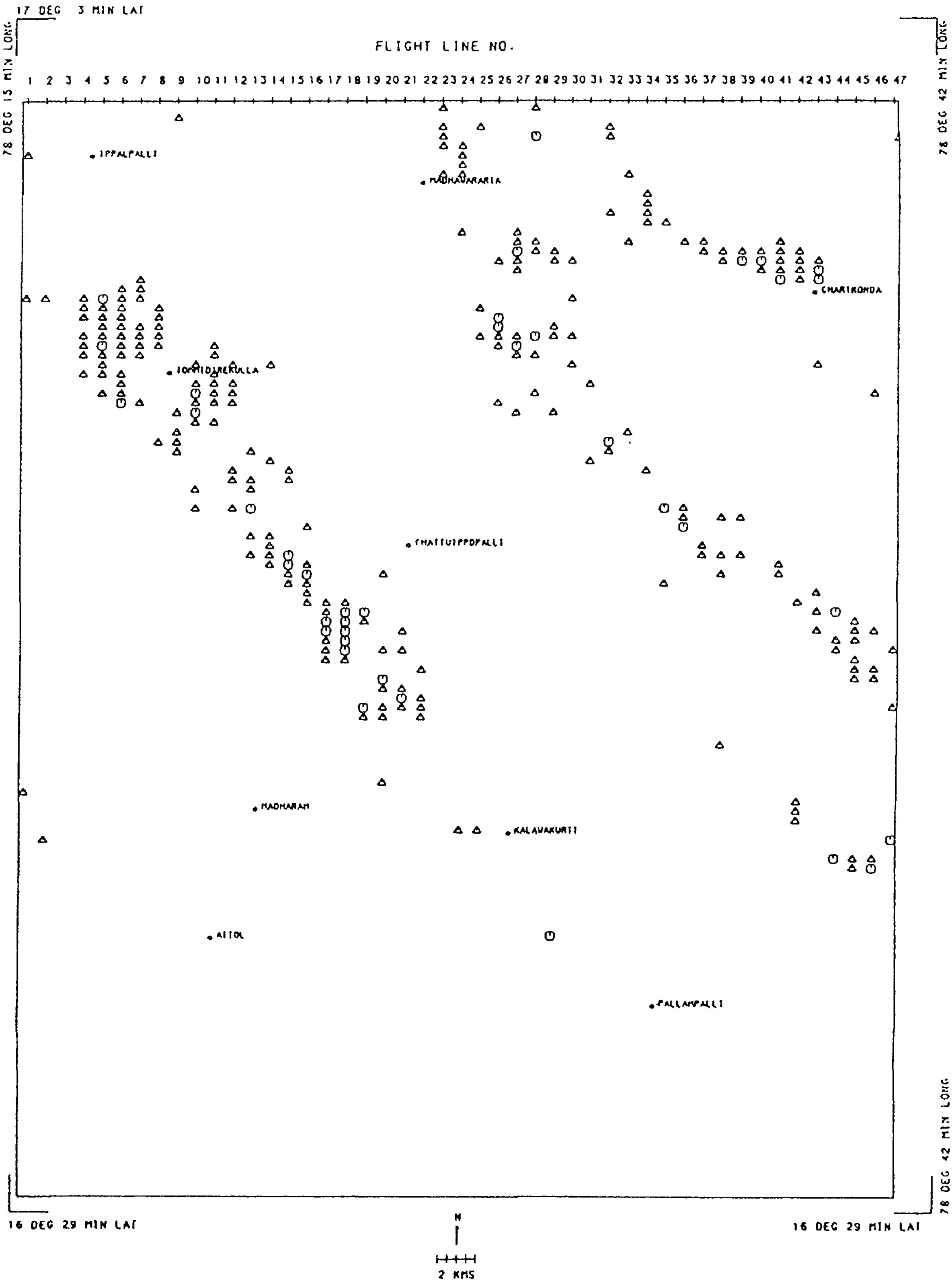

STATISTICAL ANOMALY MAP OF TOTAL COUNTS
FOR AERO-RADIOMETRIC DATA OF DEVARKONDA, INDIA
COMPUTED ALONG FLIGHT LINES
△ - VALUE > (MEAN + 2 STD.DEV.) AND < (MEAN + 3 STD.DEV.)
O - VALUE > (MEAN + 3 STD.DEV.)

FIG.5(a)

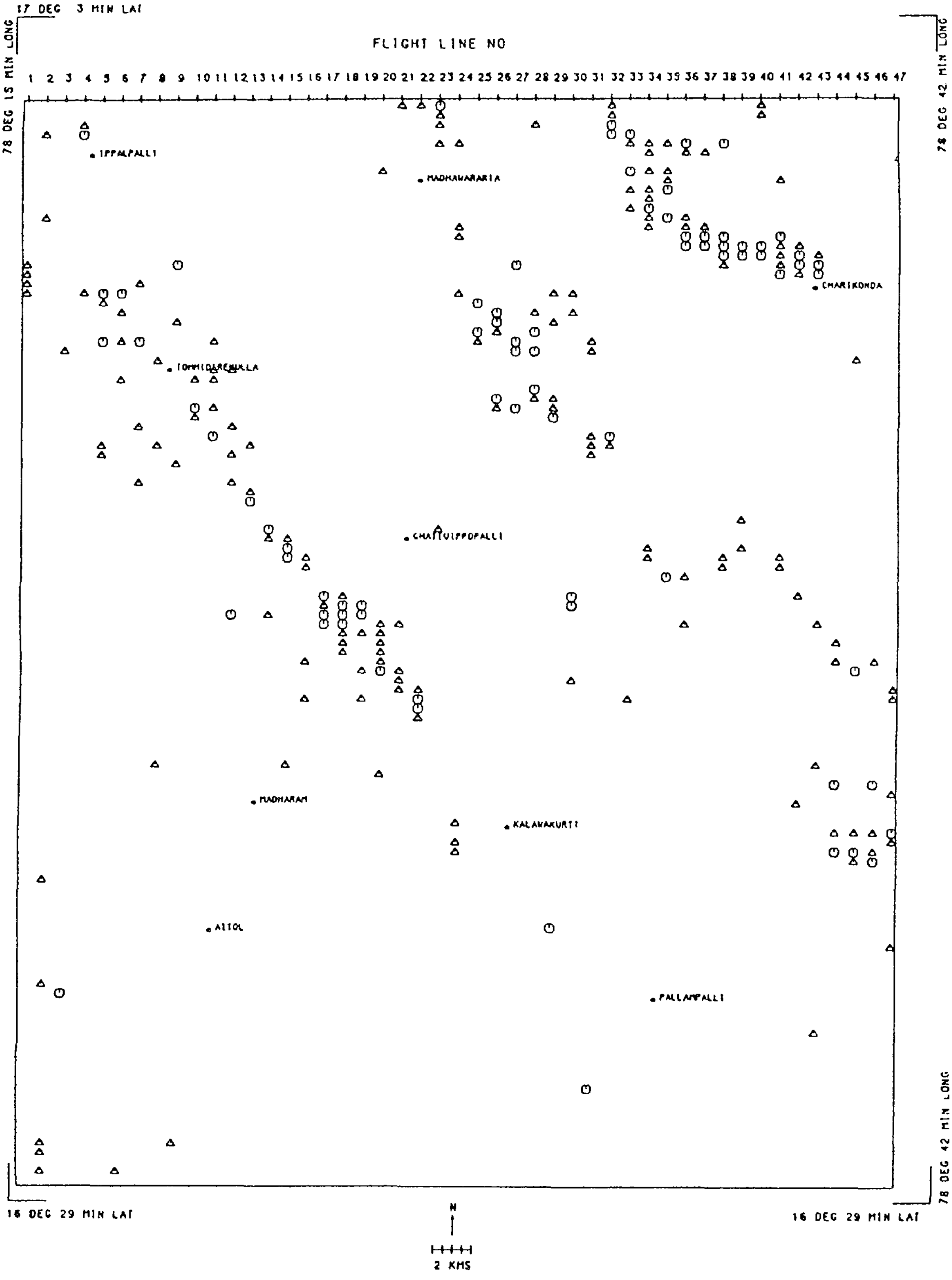

STATISTICAL ANOMALY MAP OF URANIUM COUNTS
FOR AERO-RADIOMETRIC DATA OF DEVARKONDA, INDIA
COMPUTED ALONG FLIGHT LINES
△ - VALUE > (MEAN + 2 STD.DEV.) AND < (MEAN + 3 STD.DEV.)
Ⓘ - VALUE > (MEAN + 3 STD.DEV.)

FIG.5(b)

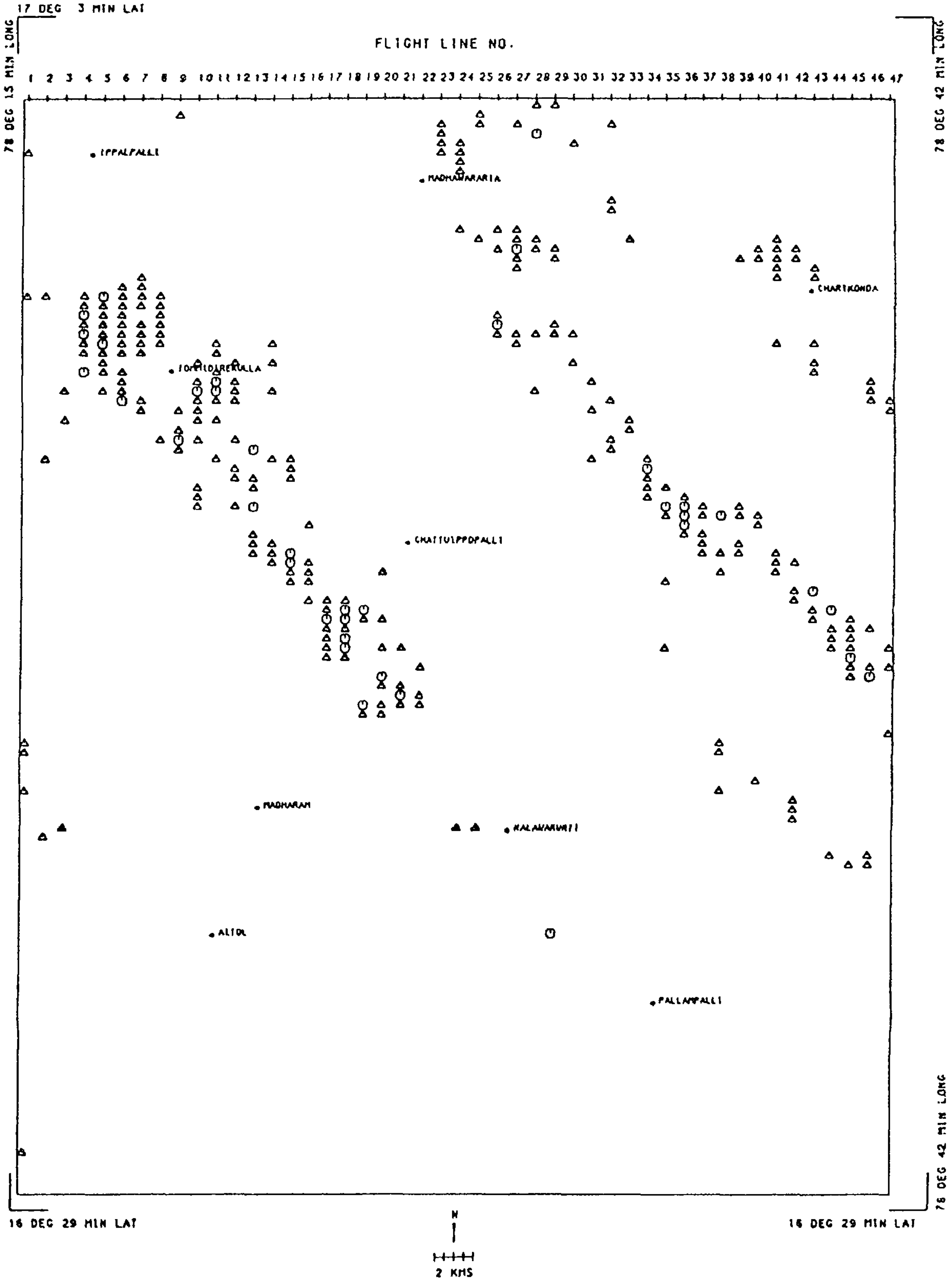

STATISTICAL ANOMALY MAP OF THORIUM COUNTS
FOR AERO-RADIOMETRIC DATA OF DEVARKONDA, INDIA
COMPUTED ALONG FLIGHT LINES
△ - VALUE > (MEAN + 2 STD.DEV.) AND < (MEAN + 3 STD.DEV.)
⊕ - VALUE > (MEAN + 3 STD.DEV.)

FIG.5(c)

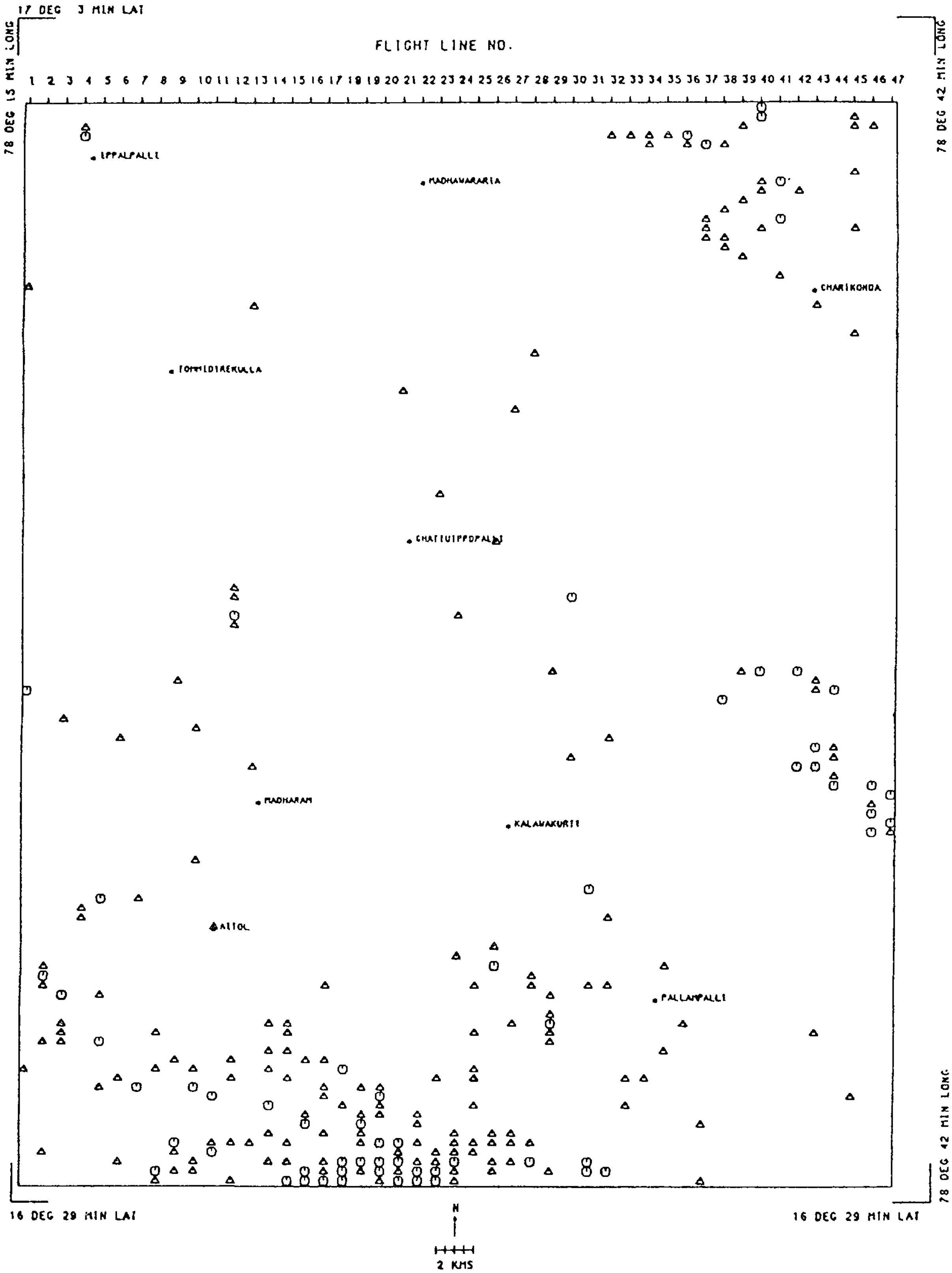

STATISTICAL ANOMALY MAP OF URANIUM/THORIUM
FOR AERO-RADIOMETRIC DATA OF DEVARKONDA, INDIA
COMPUTED ALONG FLIGHT LINES
△ - VALUE > (MEAN + 2 STD.DEV.) AND < (MEAN + 3 STD.DEV.)
Ⓞ - VALUE > (MEAN + 3 STD.DEV.)

FIG.5(d)

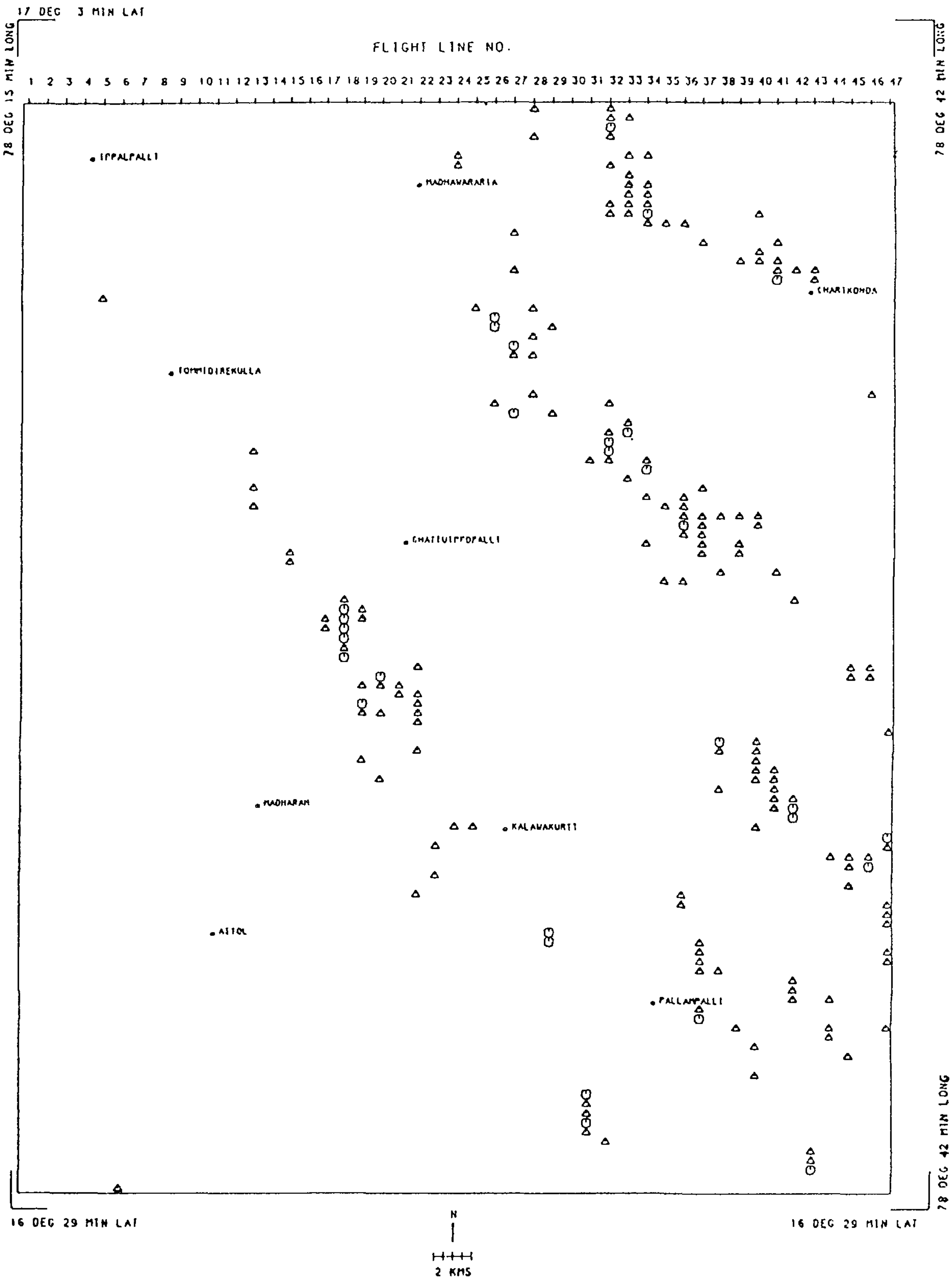

STATISTICAL ANOMALY MAP OF TOTAL COUNTS
FOR AERO-RADIOMETRIC DATA OF DEVARKONDA, INDIA
COMPUTED ACROSS FLIGHT LINES
△ - VALUE > (MEAN + 2 STD.DEV.) AND < (MEAN + 3 STD.DEV.)
○ - VALUE > (MEAN + 3 STD.DEV.)

FIG.6(a)

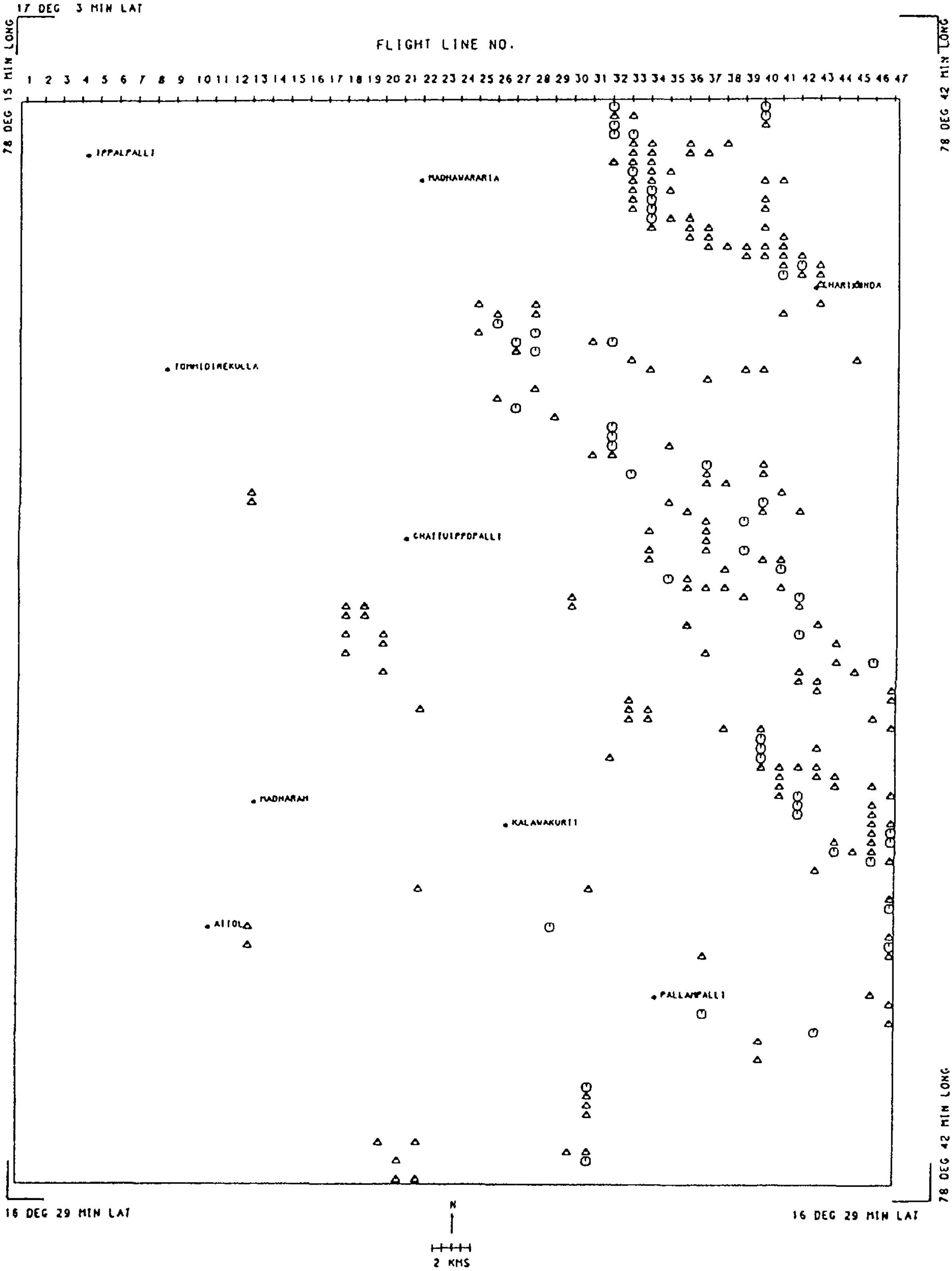

STATISTICAL ANOMALY MAP OF URANIUM COUNTS
FOR AERO-RADIOMETRIC DATA OF DEVARKONDA, INDIA
COMPUTED ACROSS FLIGHT LINES
△ - VALUE > (MEAN + 2 STD.DEV.) AND < (MEAN + 3 STD.DEV.)
O - VALUE > (MEAN + 3 STD.DEV.)

FIG.6(b)

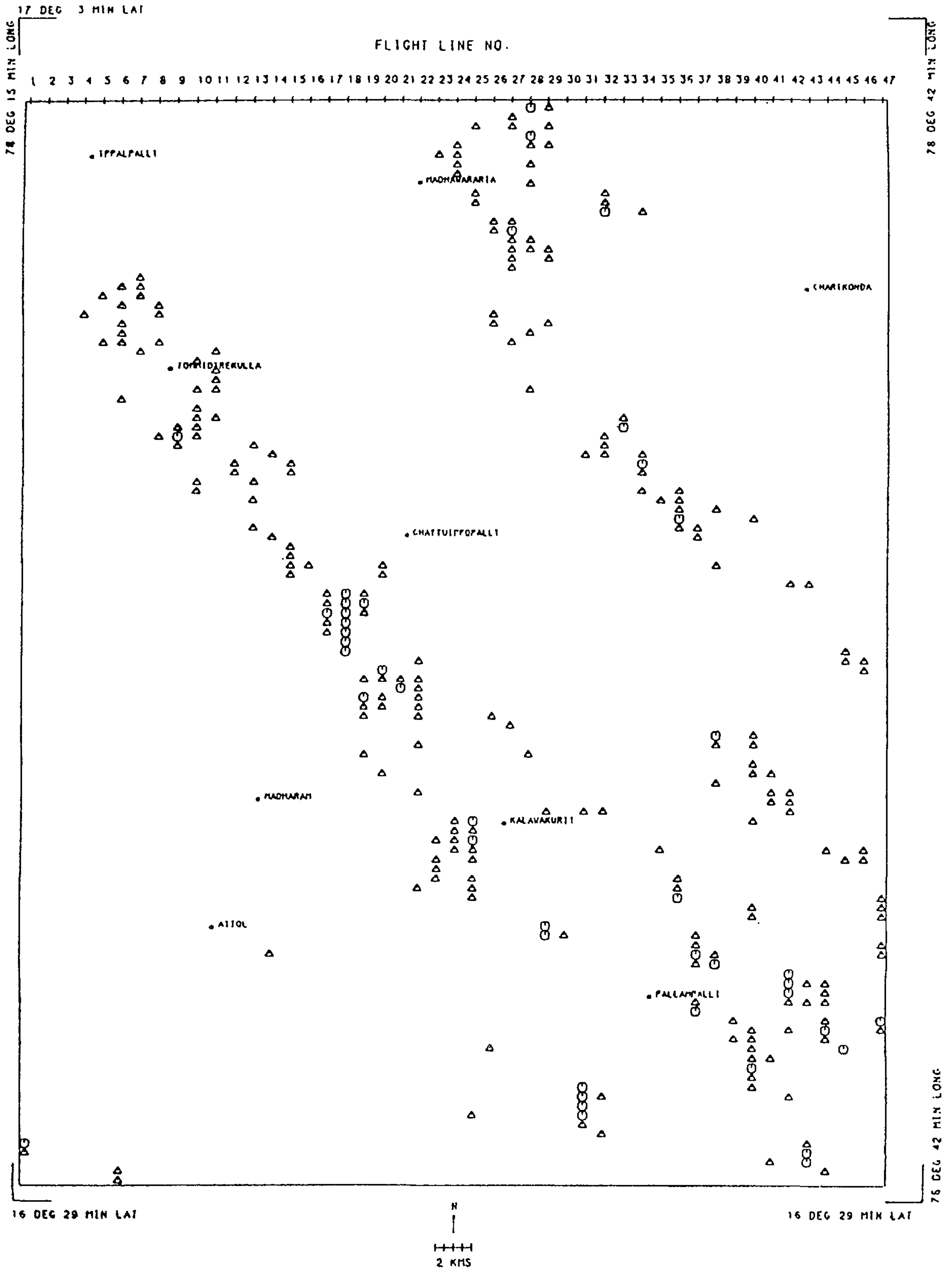

STATISTICAL ANOMALY MAP OF THORIUM COUNTS
FOR AERO-RADIOMETRIC DATA OF DEVARKONDA, INDIA
COMPUTED ACROSS FLIGHT LINES
△ - VALUE > (MEAN + 2 STD.DEV.) AND < (MEAN + 3 STD.DEV.)
O - VALUE > (MEAN + 3 STD.DEV.)

FIG.6(c)

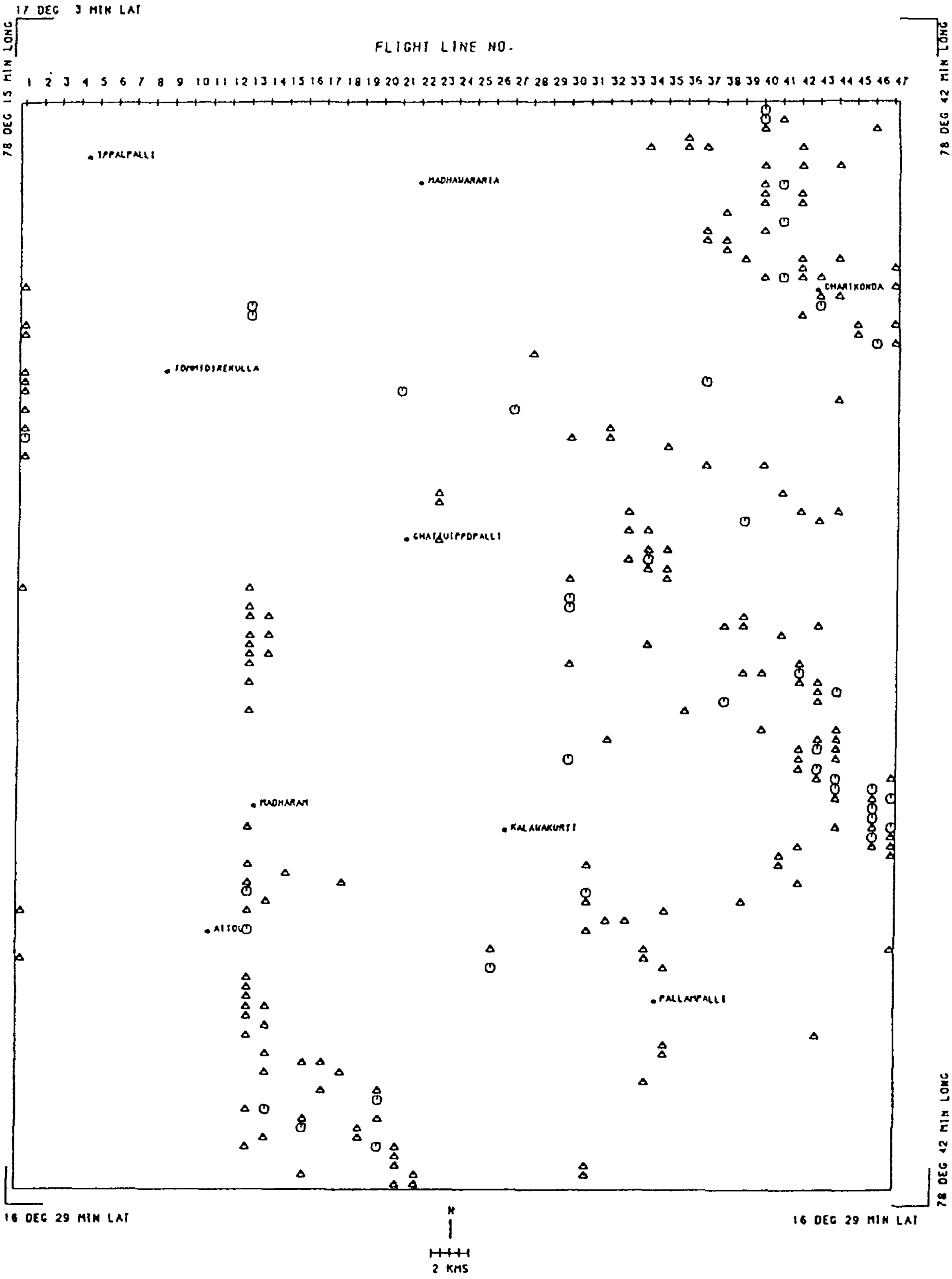

STATISTICAL ANOMALY MAP OF URANIUM/THORIUM
FOR AERO-RADIOMETRIC DATA OF DEVARKONDA, INDIA
COMPUTED ACROSS FLIGHT LINES
△ - VALUE > (MEAN + 2 STD.DEV.) AND < (MEAN + 3 STD.DEV.)
O - VALUE > (MEAN + 3 STD.DEV.)

FIG.6(d)

(B) Bastar area, Madhya Pradesh : 128 flight lines were flown in this area but for the purpose of application of statistical analysis only flight line numbers 27 to 51 flown in the N-S direction have been taken. Twelve lithological units have been demqrcated in this area based on photogeological interpretation. For the sake of comparison it is seen in Fig. 7 that if the whole area is treated as having a single lithological unit, a number of anomalous points based on total cps appear in the north west corner and a few clusters appear in the middle portion of the map. When the whole area is segmented on the basis of twelve litho-units, the number of anomalous points in the north west reduce, the middle portion maintains its anomalous character while new anomalies, which were totally missed based on a single lithological unit, appear in the south east portion. This area mostly consists of sand stones and partly of quartzites. Almost similar trend is shown for Thorium [Fig. 8]. In the Uranium anomaly map, (Fig. 9) however, the apparently anomalous portion in the north-west corner, when the whole area is viewed as a single litho-unit, almost totally disappears when all the twelve litho-units are taken separately except for a small patch between the contact of migmatites and granites. The middle portion even in this case remains anomalous while the south east portion appears clearly anomalous. In the statistical anomaly map based on eU/eTh ratio (Fig. 10) in the south-east portion we get enhancement of the anomaly. A few more portions on the southern side between flight lines 33-36 appear anomalous. Combining all these maps it can be concluded that the south-east portion of this area deserves detailed ground checkup followed by the contact between migmatites and granites in the northern portion where uranium anomalies have been discerned.

Text continued on p. 113.

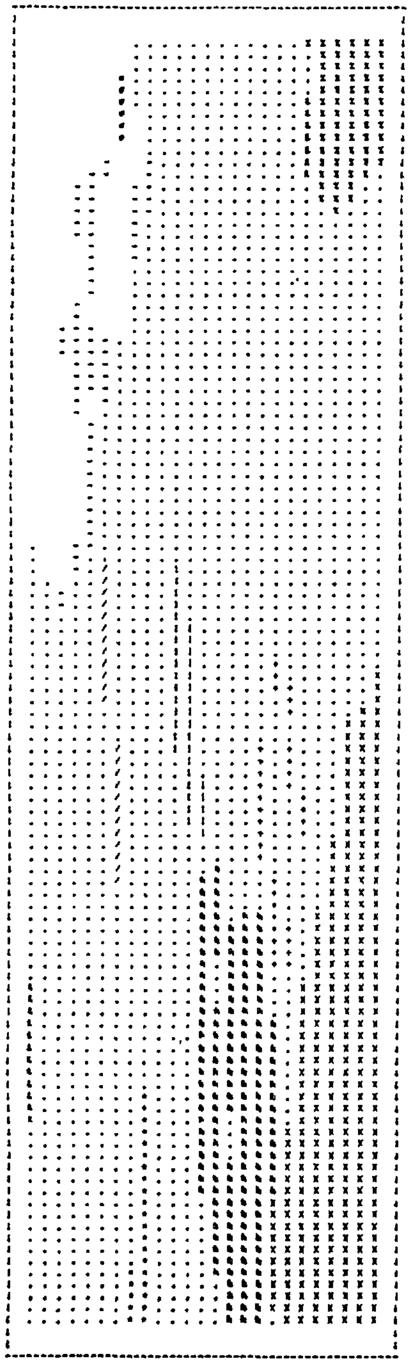

GEOLOGY MAP OF BASTAR (M.P, INDIA)

```
SPACE  -  MIGMATITE
.      -  GRANITE
-      -  QUARTZITE (1)
/      -  QUARTZITE (2)
I      -  QUARTZITE (3)
A      -  QUARTZITE (4)
+      -  QUARTZITE (5)
#      -  BASICS (1)
X      -  BASICS (2)
B      -  BASALT (1)
*      -  BASALT (2)
X      -  SANDSTONES
```

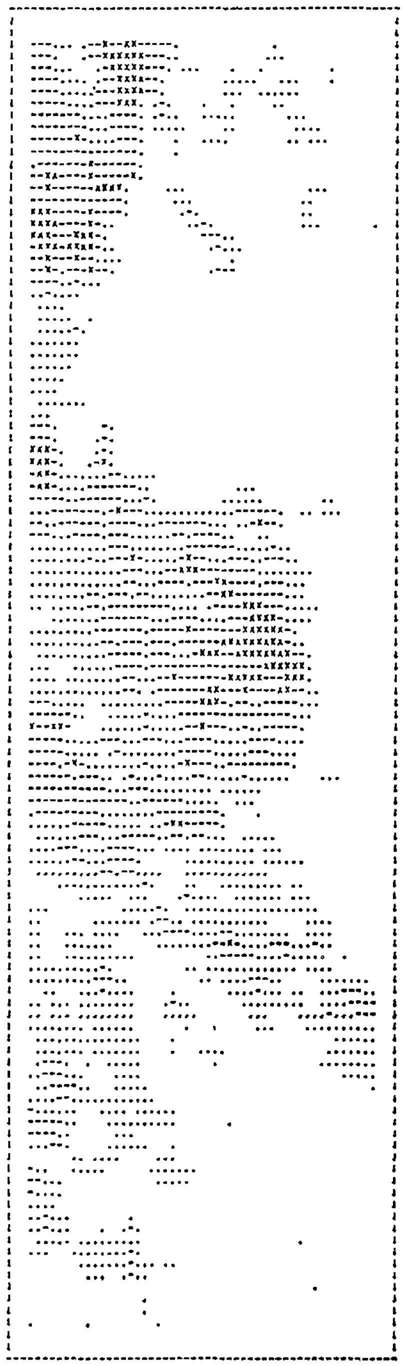

```
Z SCORE MAP OF TOTAL COUNTS OF BASTAR (M.P, INDIA)
NO. OF GEOLOGICAL UNITS = 1
SPACE - VALUE < 0
.     - VALUE ( >= 0 AND < 1)
-     - VALUE ( >= 1 AND < 2)
X     - VALUE >= 2
```

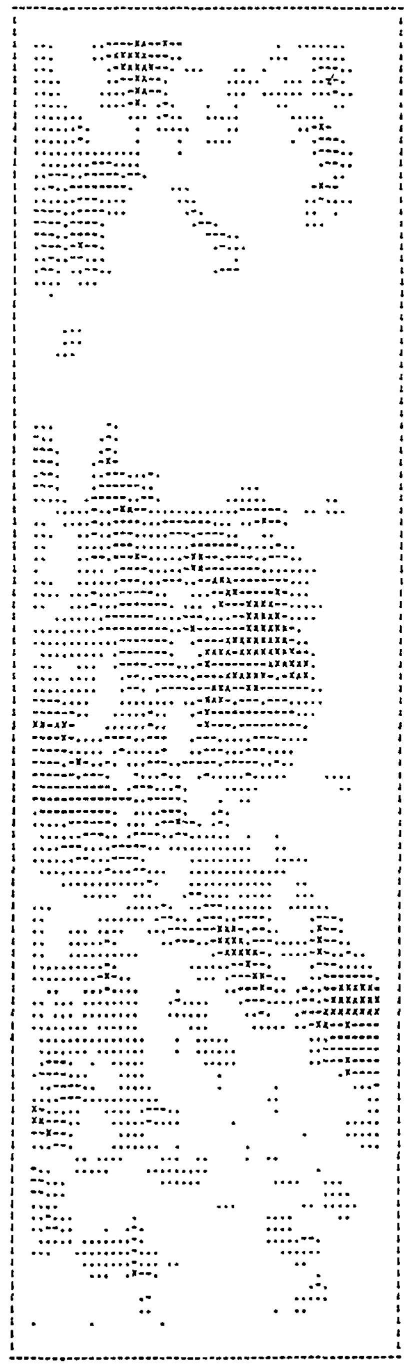

```
Z SCORE MAP OF TOTAL COUNTS OF BASTAR (M.P, INDIA)
NO. OF GEOLOGICAL UNITS = 12
SPACE - VALUE < 0
.     - VALUE ( >= 0 AND < 1)
-     - VALUE ( >= 1 AND < 2)
X     - VALUE >= 2
```

FIG.7.

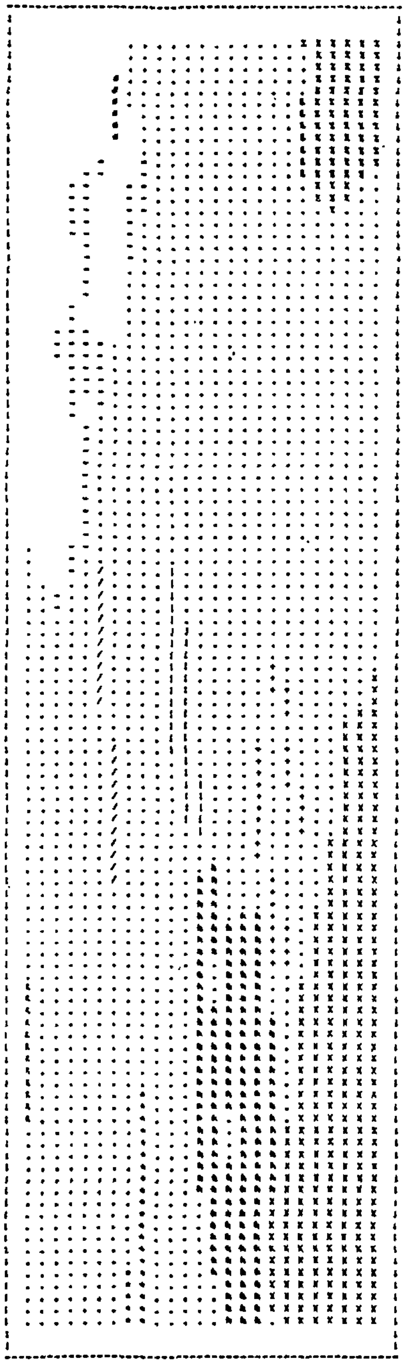

GEOLOGY MAP OF BASTAR (M.P. INDIA)

SPACE	-	MIGMATITE
.	-	GRANITE
-	-	QUARTIZE (1)
/	-	QUARTIZE (2)
I	-	QUARTIZE (3)
R	-	QUARTIZE (4)
+	-	QUARTIZE (5)
#	-	BASICS (1)
I	-	BASICS (2)
$	-	BASALT (1)
*	-	BASALT (2)
X	-	SANDSTONES

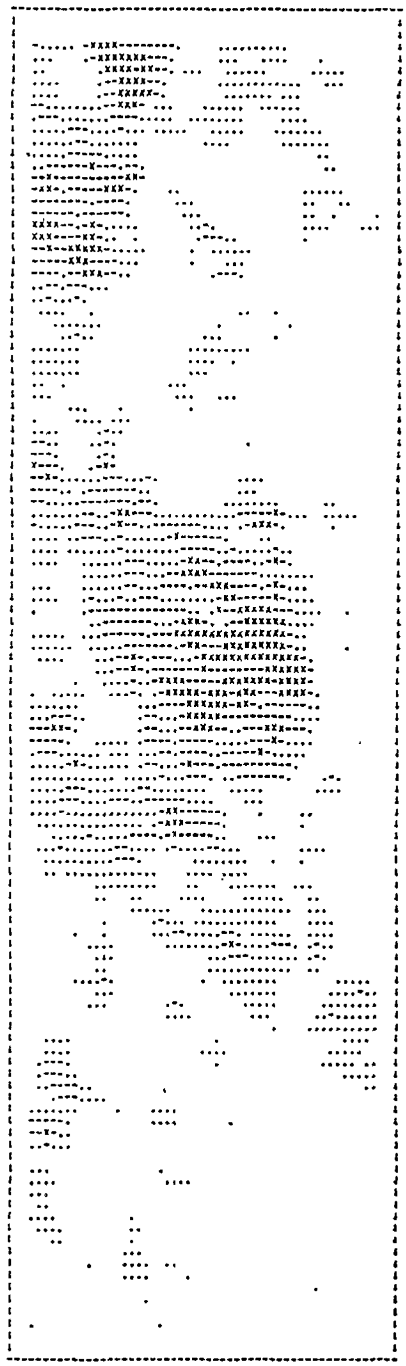

Z SCORE MAP OF THORIUM COUNTS OF BASTAR (M.P. INDIA)
NO. OF GEOLOGICAL UNITS = 1

SPACE	-	VALUE < 0
.	-	VALUE (>= 0 AND < 1)
-	-	VALUE (>= 1 AND < 2)
X	-	VALUE >= 2

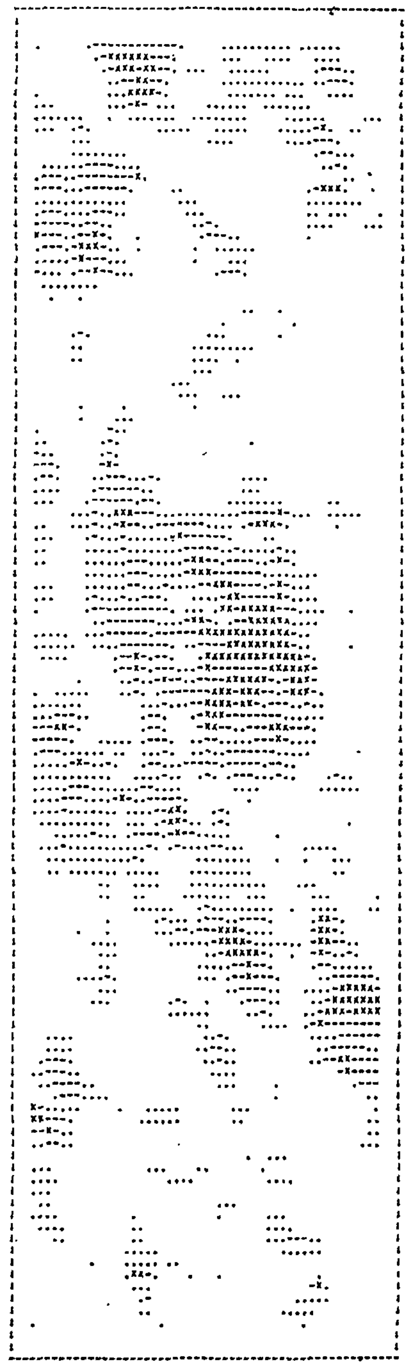

Z SCORE MAP OF THORIUM COUNTS OF BASTAR (M.P. INDIA)
NO. OF GEOLOGICAL UNITS = 12

SPACE	-	VALUE < 0
.	-	VALUE (>= 0 AND < 1)
-	-	VALUE (>= 1 AND < 2)
X	-	VALUE >= 2

FIG.8.

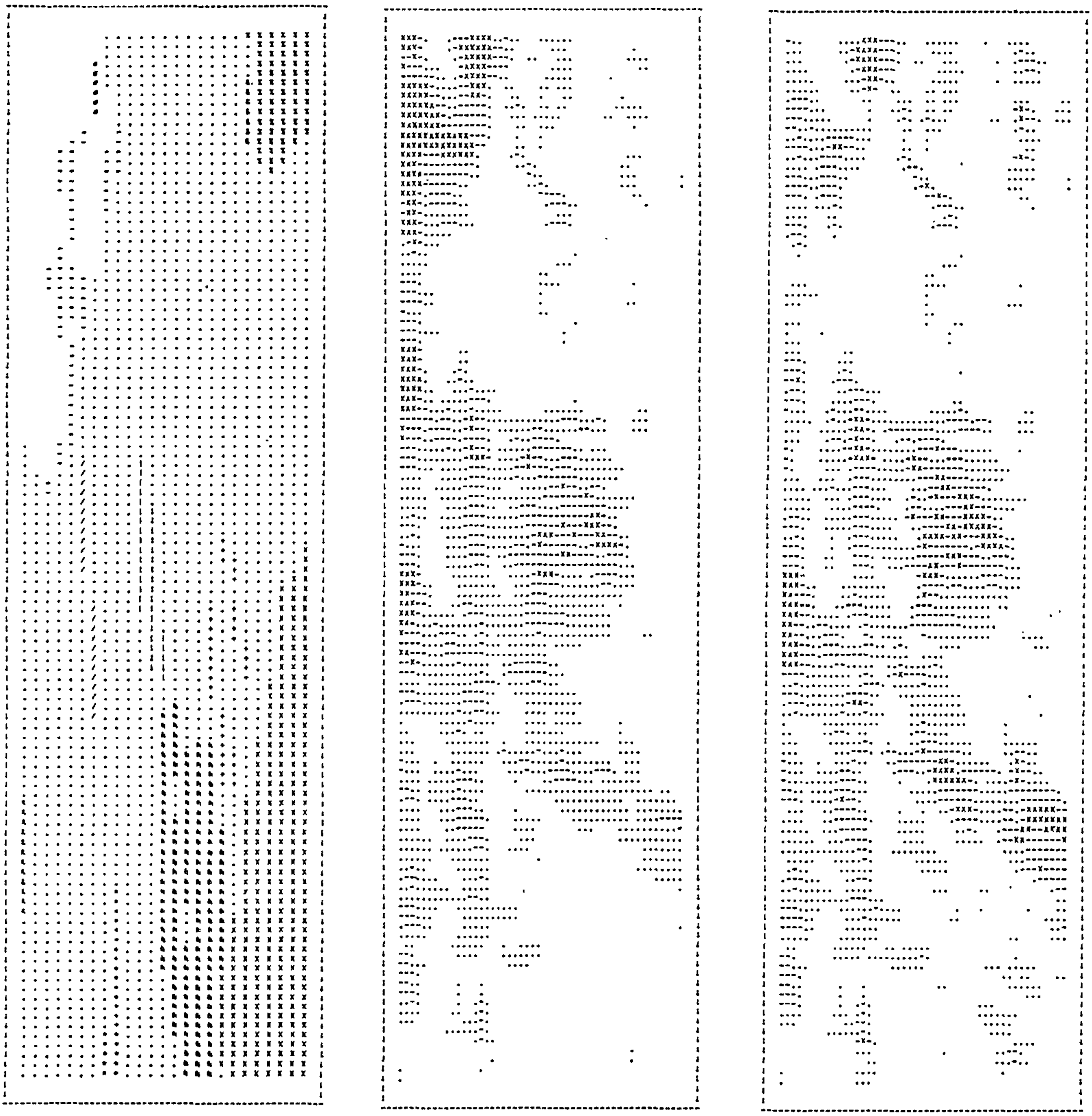

GEOLOGY MAP OF BASTAR (M.P, INDIA)

SPACE	-	MIGMATITE
.	-	GRANITE
-	-	QUARTIZE (1)
/	-	QUARTIZE (2)
I	-	QUARTIZE (3)
A	-	QUARTIZE (4)
+	-	QUARTIZE (5)
#	-	BASICS (1)
$	-	BASICS (2)
&	-	BASALT (1)
*	-	BASALT (2)
X	-	SANDSTONES

Z SCORE MAP OF URANIUM COUNTS OF BASTAR (M.P, INDIA)
NO. OF GEOLOGICAL UNITS = 1

SPACE	-	VALUE < 0
.	-	VALUE (>= 0 AND < 1)
-	-	VALUE (>= 1 AND < 2)
X	-	VALUE >= 2

Z SCORE MAP OF URANIUM COUNTS OF BASTAR (M.P, INDIA)
NO. OF GEOLOGICAL UNITS = 12

SPACE	-	VALUE < 0
.	-	VALUE (>= 0 AND < 1)
-	-	VALUE (>= 1 AND < 2)
X	-	VALUE >= 2

FIG.9.

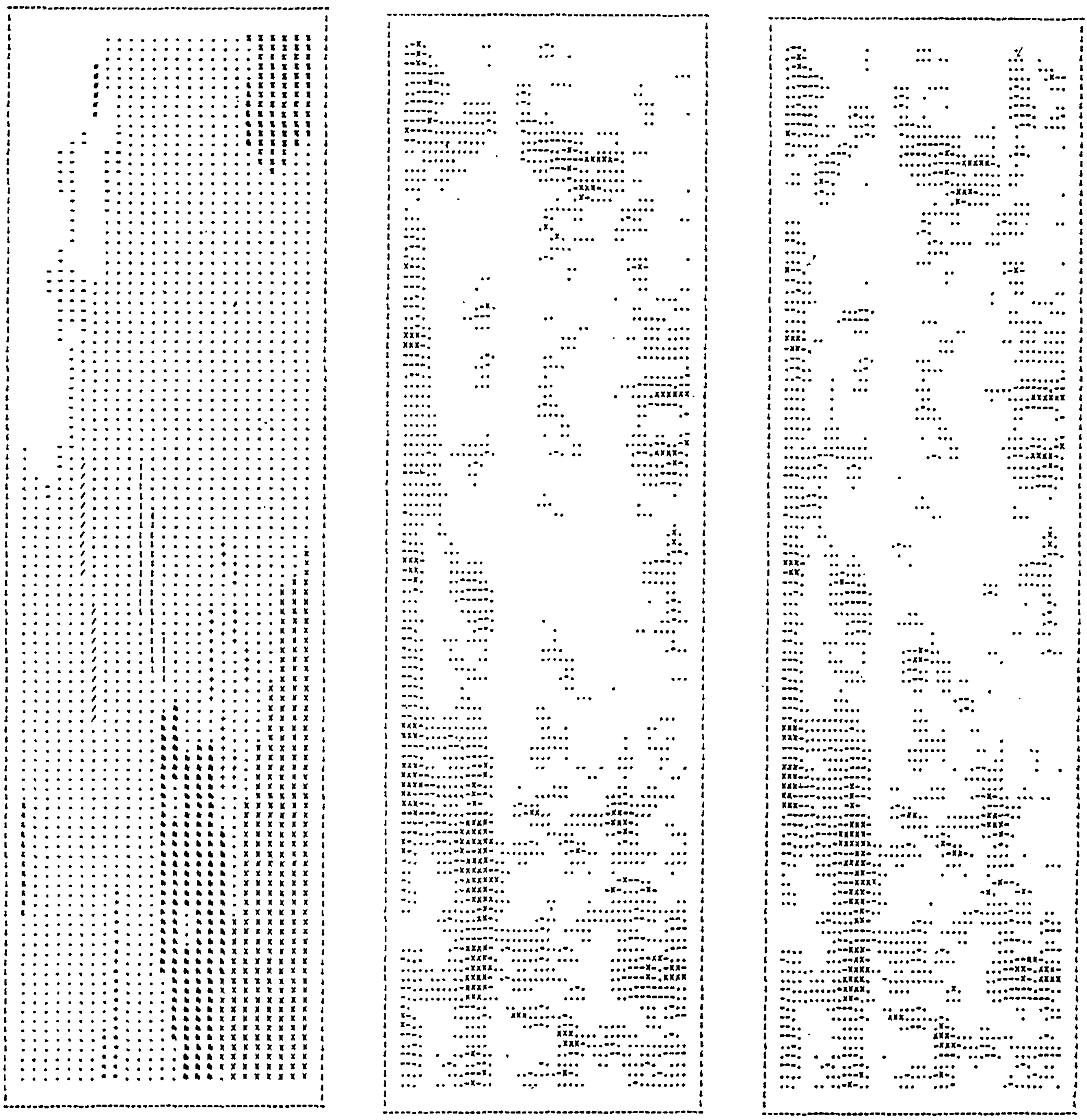

GEOLOGY MAP OF BASTAR (M.P,INDIA)

```
SPACE  -  MIGMATITE
.      -  GRANITE
-      -  QUARTZITE (1)
/      -  QUARTZITE (2)
I      -  QUARTZITE (3)
&      -  QUARTZITE (4)
+      -  QUARTZITE (5)
#      -  BASICS (1)
I      -  BASICS (2)
b      -  BASALT (1)
*      -  BASALT (2)
X      -  SANDSTONES
```

Z SCORE MAP OF U / TH OF BASTAR (M.P,INDIA)
NO, OF GEOLOGICAL UNITS = 1

```
SPACE - VALUE < 0
.     - VALUE ( >= 0 AND < 1)
-     - VALUE ( >= 1 AND < 2)
X     - VALUE >= 2
```

Z SCORE MAP OF U / TH OF BASTAR (M.P,INDIA)
NO, OF GEOLOGICAL UNITS = 12

```
SPACE - VALUE < 0
.     - VALUE ( >= 0 AND < 1)
-     - VALUE ( >= 1 AND < 2)
X     - VALUE >= 2
```

FIG.10.

(C) Bodal Area, Madhya Pradesh : For the Bodal area, another method of drawing a map using the high speed printer is illustrated. Normally drawing a set of contour maps is a time consuming process and to reduce drawing such detailed maps for the entire region one can print range maps of a given parameter for a quick appraisal of those segments which need detailed attention. Fig. 11 (a) shows such range maps where for the sake of illustration, Uranium map has been drawn. The entire set of values obtained in this area have been divided into four classes and a character is printed for each data point depending on its value. By using matrix printer with a red and black ribbon, characters can be printed in four colours by overprinting. In the present study the character 'A' indicates Uranium content above 20 ppm. A cluster of such characters can be seen in the southern portion of the first six flight lines. There is another cluster of such high values trending NE-SW in the southern part of this map. These maps are useful in delineating anomalous portions as well as marking different lithological units. Several sets of such printer drawn maps can be quickly produced using different classes for each character for better definition if necessary.

In this area alphanumeric maps based on a combination of three parameters at a time have also been prepared for illustration Fig. 11(b and c) . As mentioned earlier by dividing each parameter into three classes we get a group of twenty seven characters. In the present case eU, eU/eTh and eU/K are the three parameters chosen. The character 'A' indicates that all the three parameters are high. For a given set of high, medium and low values it is seen in Fig. 11 (b) that most of 'A' appear in the southern portion of the map. Some patches are also seen on the western margin of the map. For further reduction of the significant area, the range values can be increased and another map Fig. 11(c) has been printed where the threshold for high, medium, low have nearly been doubled. In such a case, it is seen that though the character 'A' does not appear so much as in the earlier case but the western margins and SW trending signi-

URANIUM MAP OF BODAL (M.P,INDIA)
VERY HIGH = A (> 20 PPM)
HIGH = B (>10 & (=20 PPM)
MEDIUM = C (>5 & (=10 PPM)
LOW = ' (>0 & (=5 PPM)

(a)

U, U/TH, U/K COMBINED MAP OF BODAL (M.P,INDIA)

PARAMETER SYMBOL

U	U/TH	U/K	
H	H	H	A
H	H	M	B
H	H	L	C'
H	M	H	D
H	M	M	E
H	M	L	F
L	L	L	*

K > 10 ppm

(H=HIGH, M=MEDIUM, L=LOW)

(b)

U, U/TH, U/K COMBINED MAP OF BODAL (M.P,INDIA)

PARAMETER SYMBOL

U	U/TH	U/K	
H	H	H	A
H	H	H	B
L	L	L	*

(H=HIGH, M=MEDIUM, L=LOW)

(c)

FIG.11.

ficant zones do appear characterized by character 'D' which indicates high eU, medium eU/eTh and high eU/K. This combined map using different sets of parameters can be very effectively used for delineating areas for detailed ground followup. The ranges for high, medium and low are decided based on the frequency distribution for various parameters. It may be of interest to note that detailed ground surveys in this area have proved that Bodal is a potential area for commerical exploitation for Uranium.

6. CONCLUSIONS

These methods described in the foregoing account can be used singly or in combination to discern anomalous areas from the large area generally surveyed from airborne platforms. The procedures save time and money by delineating small portions for ground followup and have been found to be quite cost effective in the surveys conducted by Atomic Minerals Division. By using a high speed printer after the area is gridded, is a much faster process and several sets of maps can be produced by slight alterations of the values of the parameters under study. Though these maps are not upto exact scale but it is very easy to mark the anomalous portion on the base map because each line separation and grid point separation is known. Detailed exact scale maps in 1:50000 or 250,000 can be produced only for those areas which need finer boundaries for detailed investigations.

ACKNOWLEDGEMENTS

The authors wish to thank Shri S.K. Das of Photogeology and Remote Sensing Group who has taken great pains in discerning the major lithological units for the areas illustrated in case studies. We would also like to thank Shri Narendar Dayal for a critical review of the paper and Shri T.M. Mahadevan Director Atomic Minerals Division who not only gave inspiration to write this paper but who was a constant source of enoourage-ment while we were executing jobs on the computer.

REFERENCES

[1] Bhattacharya, B.K., Two dimensional harmonic analysis as a tool for magnetic interpretation, Geophysics, xxx 5 (1965) 829.

[2] Potts, M.J., Computer methods for geological analysis of radiometric data (Proc. of IAEA Symposium on Exploration for Uranium Ore deposits, Vienna 1976) Paper No. IAEA. SM-208/46.

[3] Tewari, S.G., Nagaraj, K.N., Krishnamoorthy, B., Phadke, A.V. and Bhalla, N.S., Computerised significance factor analysis of aeroradiometric data, Jour. Assoc. Expl. Geophys. IV (3) (1984) 23.

[4] Duval, J.S., Composite colour images of aerial gammaray spectrometric data, Geophysics 48 6(1983) 722.

[5] Reeves, C.V., Airborne geophysics for geological mapping and regional exploration, ITC Journal (1985-3) 147.

[6] Killeen, P.G., In discussion on the paper Statistical interpretation of airborne gammaray spectrometric data using factor analysis by J.S. Duval; IAEA Symposium on exploration for Uranium ore deposits, Vienna, Paper No. IAEA SM-208/12 (1976).

INTEGRATION OF LANDSAT MSS IMAGERY WITH AEROMAGNETIC AND AIRBORNE SPECTROMETRIC DATA OVER A PART OF MOZAMBIQUE

G.R. GARRARD
Hunting Geology and Geophysics Limited,
Borehamwood, Hertfordshire,
United Kingdom

Abstract

An area within the undifferentiated Precambrian gneisses and granulites of the Mozambique Belt was studied using Landsat MSS imagery, aeromagnetic data and spectrometric data. Airborne radiometric data including total count, uranium, thorium and potassium channels and aeromagnetic data were prepared as raster scanned images, which were registered and combined with the Landsat imagery on an image processing system. In addition to study of the individual data sets the spectrometric channels were manipulated to provide ratios and composite images. These composite images provided information from the three main channels, potassium, uranium and thorium. Single channel images derived from them were colour contoured and integrated with the Landsat imagery. An interpretation of the geophysical data integrated with the Landsat imagery was compared with separate interpretations of each previously carried out.

The combined display techniques employed, substantially improved the discrimination of lithology within the area studied and provided a more detailed description of the regional structure.

1. INTRODUCTION

Landsat MSS imagery has been used since 1972 as an aid to geological mapping especially in remote areas. It offers three advantages over more conventional photogeological field techniques: a synoptic overview allowing rapid interpretation of large areas and a ready appreciation of the regional structure; a multispectral dimension which allows the discrimination of surface materials; and a digital format which facilitates manipulation of the data through image processing techniques.

Aeromagnetic surveys and gamma-ray spectrometric data have been used for even longer for regional mapping. Aeromagnetic maps reflect the interaction of the earth's magnetic field with susceptible materials in the uppermost 15 km or so of the crust and provide information not only about the nature of these materials but also about their structure.

Gamma-ray spectrometric maps show the distribution of natural gamma-radiation originating from the earth's surface and are similarly controlled by the regional disposition of rock types. The geophysical data are commonly prepared for presentation by computer and therefore, like the satellite imagery, are amenable to image processing techniques.

This study is a preliminary attempt to assess the best methods of integrating the display of all these data sets using image processing techniques [1,2,3] and to evaluate the advantages to the interpreter of these display techniques over more conventional approaches.

In 1981 the Direccao Nacional de Geologia commissioned Hunting Geology and Geophysics Limited to carry out a combined geological and geophysical survey over a large part of Mozambique. Landsat imagery was studied over most of the country while airborne magnetic and spectrometric data were collected over the two blocks, shown in Figure 1.

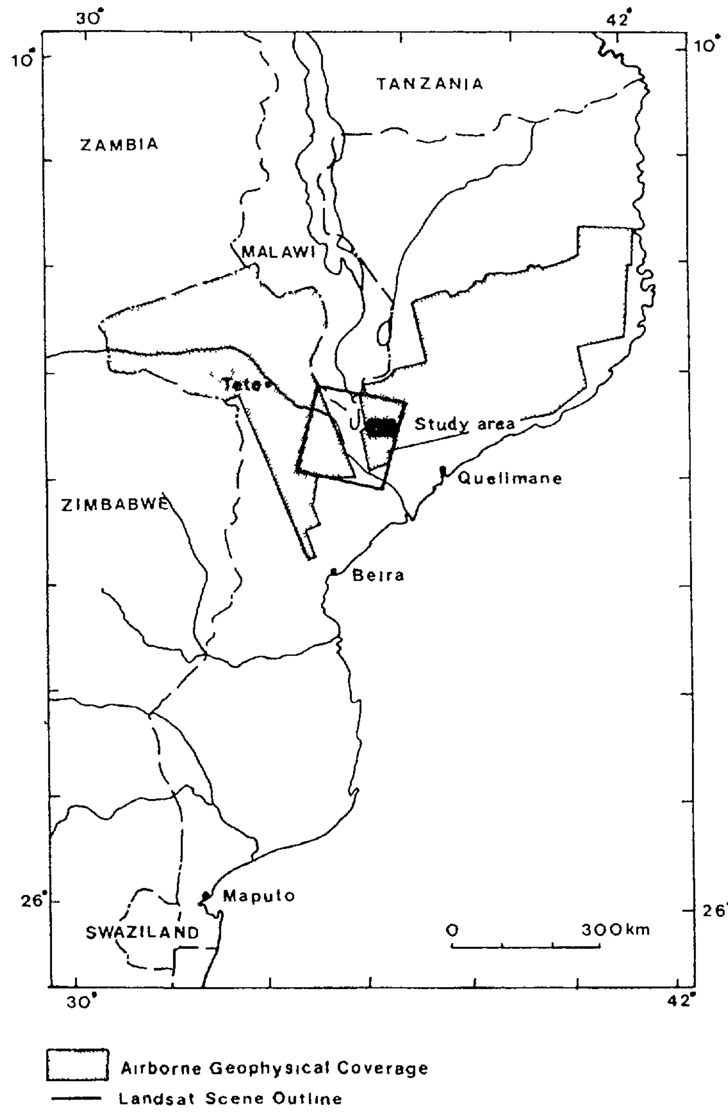

Figure 1: Location of the study area in Mozambique.

A small part of this area approximately 11 km by 21 km, was chosen to study methods for integrating data derived from:

(a) The Landsat MSS alone.

(b) The geophysical data alone.

(c) The combined data sets.

2. GEOLOGICAL SETTING

The regional geological setting is depicted in Figure 2. The study area lies within the undifferentiated Precambrian gneisses and granulites of the Mozambique Belt which trends north-south along the eastern seaboard of Africa. In Mozambique it acquired its structure during the Kibaran Epoch (Precambrian B). A major part of the belt in Mozambique comprises the

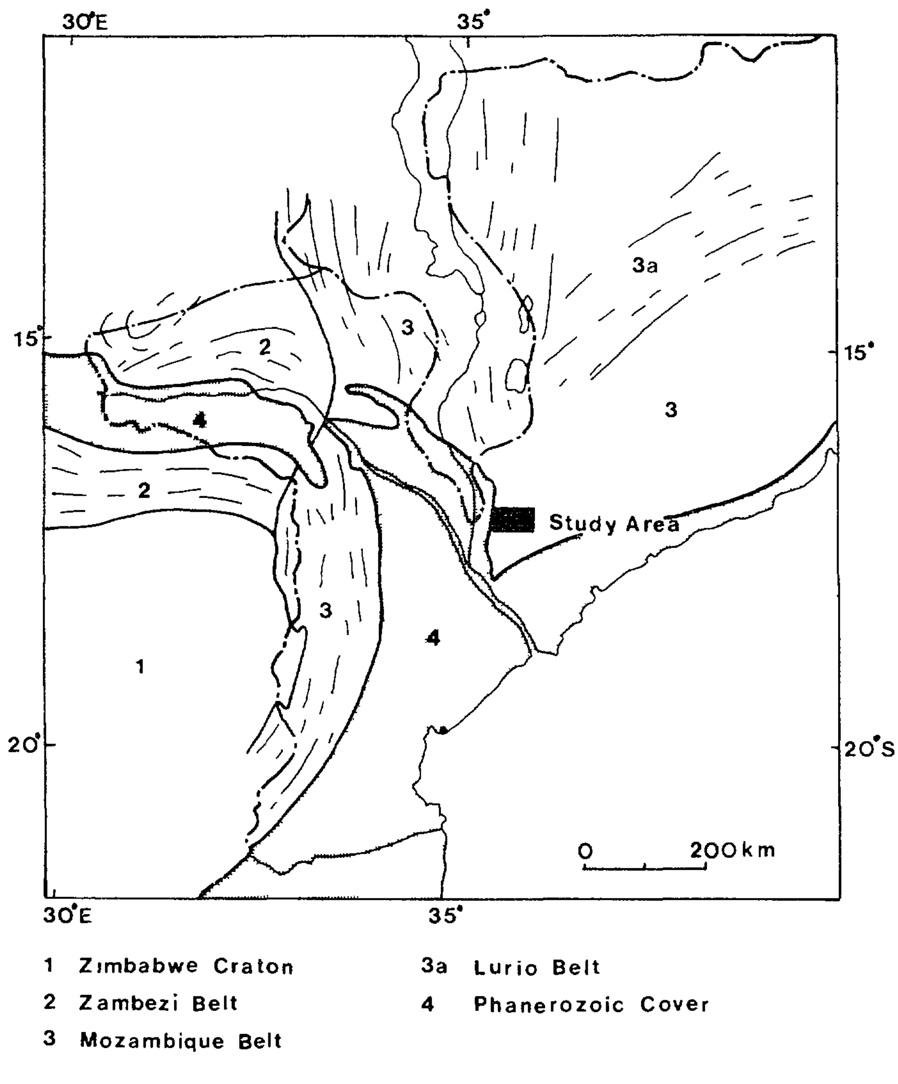

Figure 2: Geological setting of the study area.

subsidiary Lurio Belt which runs ENE-WSW across the northern part of the country [6,7]. The Lurio Belt is narrow in the east and centre but spreads out at its western end and turns more southerly along the Malawi frontier. It is a linear shear and thrust belt where the rocks have been subjected to granulite facies metamorphism.

Most of the southern boundary of the belt is well defined and has been mapped both in the field and using airborne geophysical techniques [6]. The southwestern end is more diffuse and little is known about the structural geology of this part of Mozambique.

Figure 3 shows a simplified geological map of the study area, drawn from published maps and an interpretation of air photographs [8]. It shows that the undifferentiated gneisses contain irregular bodies of charnockitic gneiss. Further subdivision was not possible due to poor exposure and extensive cover of residual soils. However the map does show major trends within the area. In the northwestern part of the area ENE trends predominate while in the south eastern part trends are variable apart from one rectilinear zone of WNW foliations. Banding and foliation are absent in areas of charnockitic gneiss but become progressively more common towards their margins.

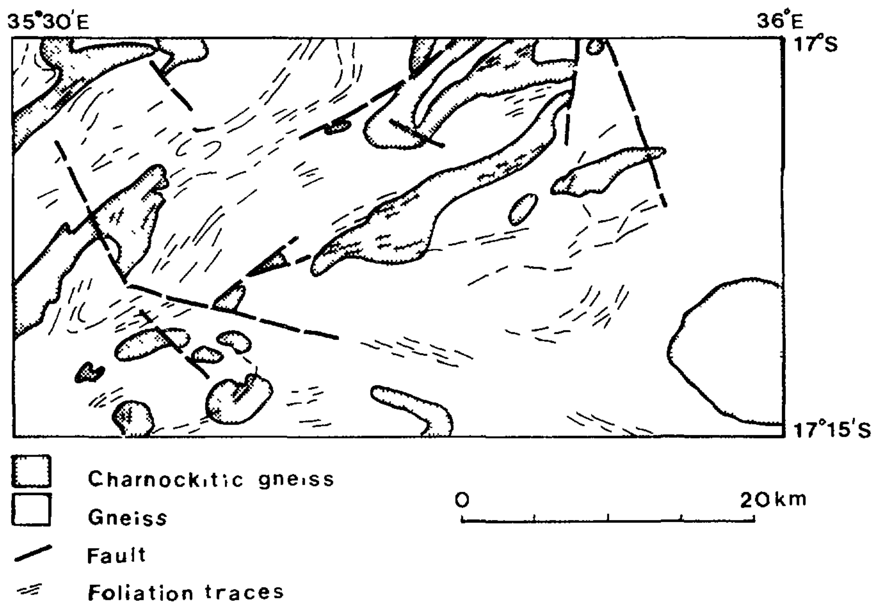

Figure 3: Simplified geological map of the study area.

3. LANDSAT IMAGERY

Landsat imagery was obtained in 1981 for the major part of Mozambique for the original work [4]. Part of the Landsat scene covered by Path 178 Row 72 acquired on the 29th August 1979 was processed using MSS channels 7,5 and 4, on the Hunting

Image Processing and Analysis System (HIPAS). Initially the data were 'destriped' to remove sixth line banding and geometric corrections were applied to rotate the image to true north and adjust it to fit the latitude-longitude projection. During this process the pixel size was enlarged from 79 m x 57 m to 50 m x 50 m [9,10]. The channels were then contrast-stretched with channel 7 in red, channel 5 in green and channel 4 in blue, to give an enhanced false colour composite image. This digital image was converted to a film product using a Color Fire 240 film writer and from the diapositive an enlarged colour print at 1:250,000 scale was produced.

Geological interpretation was carried out on a clear film overlay (Figure 4). Three major geological units were defined on the basis of the surface relief and colour. The first forms the west and north part of the image and represents areas of high relief. The second in the eastern part of the image has low relief and abundant vegetation. The last unit represents the undifferentiated bulk of the image. From comparison with Figure 3 it is likely that Unit (1) is of similar composition to charnockitic gneiss. The inability to ascribe lithologies to the other units is due to the lack of field data.

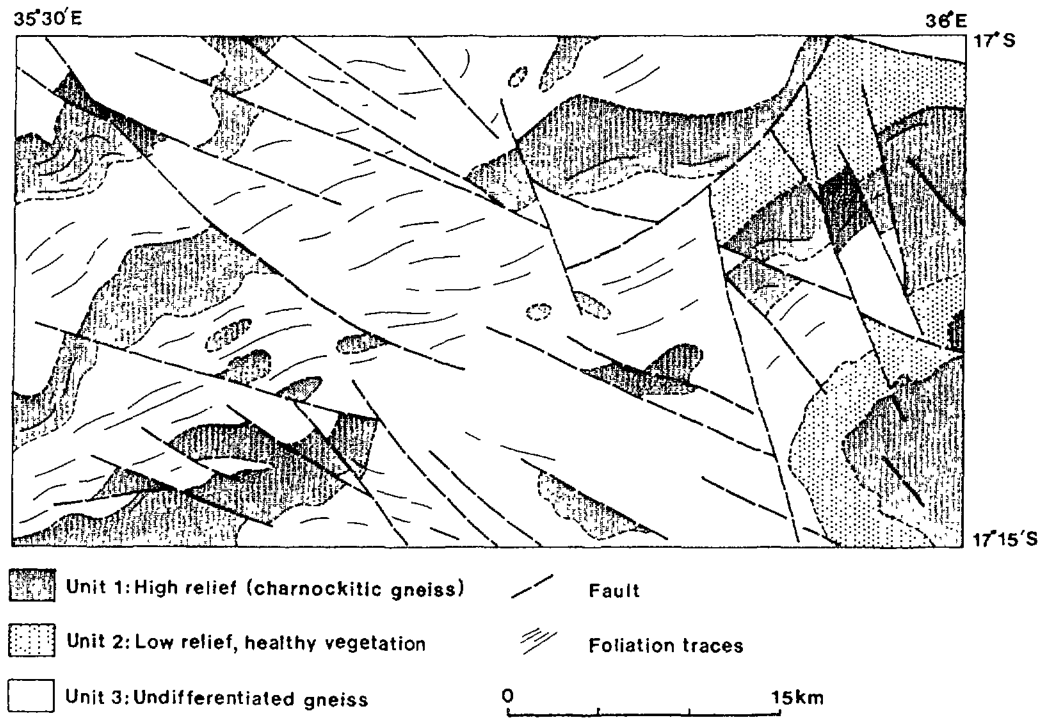

Figure 4: Geological interpretation of the Landsat image.

Structurally most of the faults lie in a WNW direction cutting the main foliation trends, which run ENE to WSW. These trends are parallel to those of the Lurio Belt further east even though the study area lies to the south of the southern limit of the Belt as it is usually mapped [6].

4. GEOPHYSICAL DATA

4.1 Aeromagnetic Data

Aeromagnetic data, primarily collected to study basement changes across the area [11,12], were produced as a colour contour map at 1:250,000 scale. The map showed a striking ENE-WSW trend which predominates in the northwestern half of the area cutting across it diagonally. The strong aeromagnetic anomalies suggest that the lithological units have well defined banding. In the southeastern half the trends virtually disappear and magnetic gradients are more gentle. The two sections of the area thus appear to be structurally different. Their boundary represents a structural and lithological discontinuity and has been interpreted as a junction between rocks thrust from the northwest across the more competent block in the southeast.

4.2 Spectrometric Data

Spectrometric data were recorded for the gamma-ray spectrum as one wide and three narrow energy windows (total count, uranium, thorium and potassium channels respectively) [11,12,13,14]. After processing or stripping, colour contour and density sliced maps were produced for each of the channels. Additional processing included production of the uranium/thorium and uranium/potassium channel-ratios and composite images [15,16].

Individual channels showed some significant features [16] but colour composite images were found to be overall more useful. In each individual image white represents the highest value and black the lowest, so that when a colour is assigned to each channel the resulting colour composite provides a range of colours representing the combined assemblages of three images. The most useful combination was found to be the potassium composite image. This image comprised the K/U ratio values in red,the K/Th ratio values in green and the potassium channel values in blue.

Film diapositives of the composite images and the single channel colour density sliced images were produced and enlarged to colour prints at 1:250,000 scale. Detailed interpretation of the composite images was carried out and is given in a paper by

Nevitt and Barr, 1985 [16]. A simplified reinterpretation to bring out the main features was carried out for this study (Figure 5).

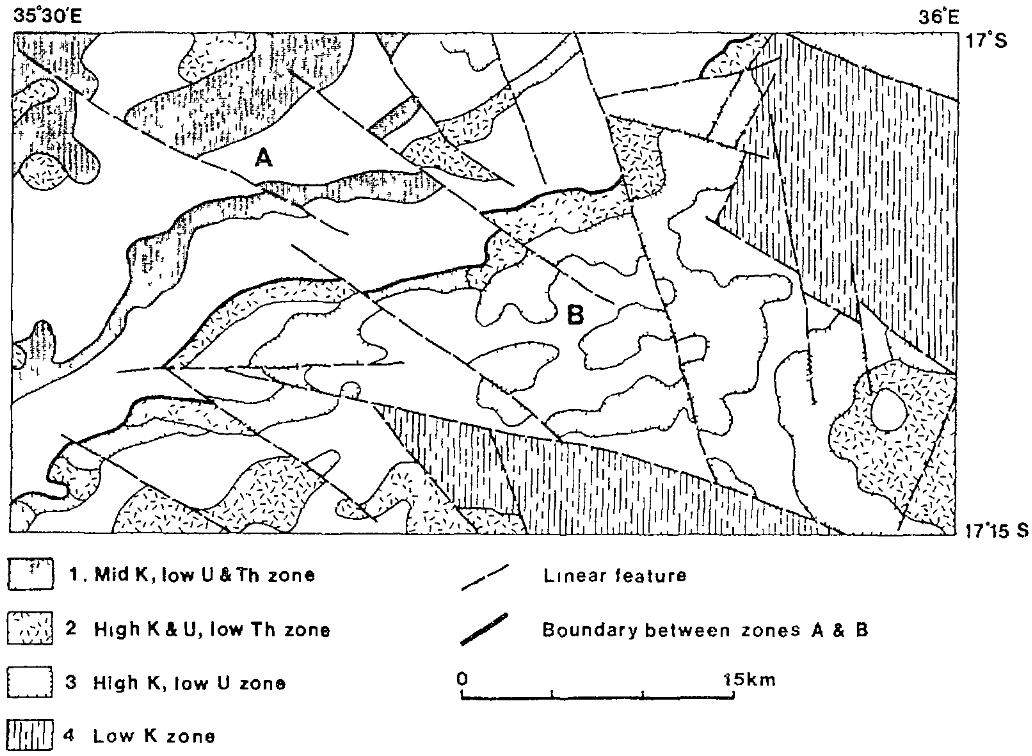

Figure 5: Interpretation from the potassium composite image.

Interpretation concentrated on the potassium composite image as it was felt that mineral and rock changes would be best discriminated by changes in potassium rather than uranium and thorium. Interpretation was carried out on the basis of colour changes and relative deviations of the elements from their mean values. Geological significance was only given to features which had previously been identified on the geological map [8].

Initial study of the potassium composite image suggested that the area could be roughly divided into two zones. The northwestern half (A) showing predominantly yellows and oranges while the southeastern half (B) had more purple and pink colours. This shows that in the southeast potassium levels and the K/U ratios are high but K/Th ratios are low in relation to mean values over the area. Thus the rocks appear to have relatively high levels of potassium and the positive deviation from the mean is higher for thorium than uranium. In the northwestern half the ratios K/U and K/Th are both fairly high while the K levels are less than those of the southeast. These northwestern rocks appear to have less potassium and the amounts of uranium and thorium deviate positively from their mean values to approximately the same extent. Structurally the two areas differ in that the northwestern one shows strong lineation with a ENE-WSW trend and the southeast half lacks foliation. This suggests that the former area contains strong lithological banding which is absent in the southeast. This may relate to differences in their metamorphic histories.

Within the two areas, four colours have been noted as distinctive. The first, an intense yellow colour, forms strong ENE trending features across the northwestern section. This colour represents areas of high K/U and K/Th and mid K values; hence the lithological unit must contain medium amounts of potassium and low amounts of thorium and uranium relative to the mean values of these elements. It is suggested that these areas represent hypersthene granite [16].

The second colour is pale blue to greenish and occurs mainly in the southeastern part of the area. Its most notable occurrence is the almost circular area in the southeastern corner of the image. This has previously been identified as charnockitic gneiss [8,16]. By inference other areas with this distinctive colour should also be charnockitic gneiss. The colour represents a rock assemblage with high K/Th ratios, mid to high K, and low K/U ratios. Thus the rock must be rich in potassium with medium uranium and low thorium content relative to their mean values.

The third colour, pinkish purple, is also found mainly in the southeastern part of the image and forms a zone separating the two areas of the fourth colour, a dark brown. The third colour represents areas with high potassium content and high K/U ratios while the fourth colour represents an area of very low potassium content. Lithological types cannot be assigned to these areas, but field checking may verify differences in rock types.

5. INTEGRATION OF DATA

Single band colour density-sliced and contoured images of geophysical data were integrated with the Landsat image by graphical overlay techniques on the HIPAS. However to obtain the combined spectrometric data integrated with the Landsat imagery required further mathematical manipulation. The spectrometric study showed the potassium composite image to be very useful and hence a single band image of equivalent information was required. Intermediate products were prepared of the ratios superimposed on the Landsat imagery.

Addition and subtraction of the two ratios (K/U, K/Th) were tried to bring out the main features and it was found that if one ratio was inverted and then added to the other a suitable product was achieved which showed most of the features being studied. To obtain the maximum amount of information two of these derived products were required. The derived products were then colour density sliced and contoured prior to combination with the Landsat data. Total information from spectrometric and aeromagnetic data combination to a single image was not achieved in this study and requires more research into the interactions between the images.

The derived products superimposed on Landsat imagery provided a useful image for interpretation. Two images were used for interpretation which was carried out on clear film overlays. These were:

(i) Landsat combined with a derived product of the potassium/uranium ratio added to the inverted potassium/thorium ratio.

(ii) Landsat combined with aeromagnetic data.

The result of the interpretation is shown in Figure 6. Interpretation was carried out on the basis of colour change in both the Landsat imagery and spectrometric data. Texture and other features on the Landsat imagery were also accounted for.

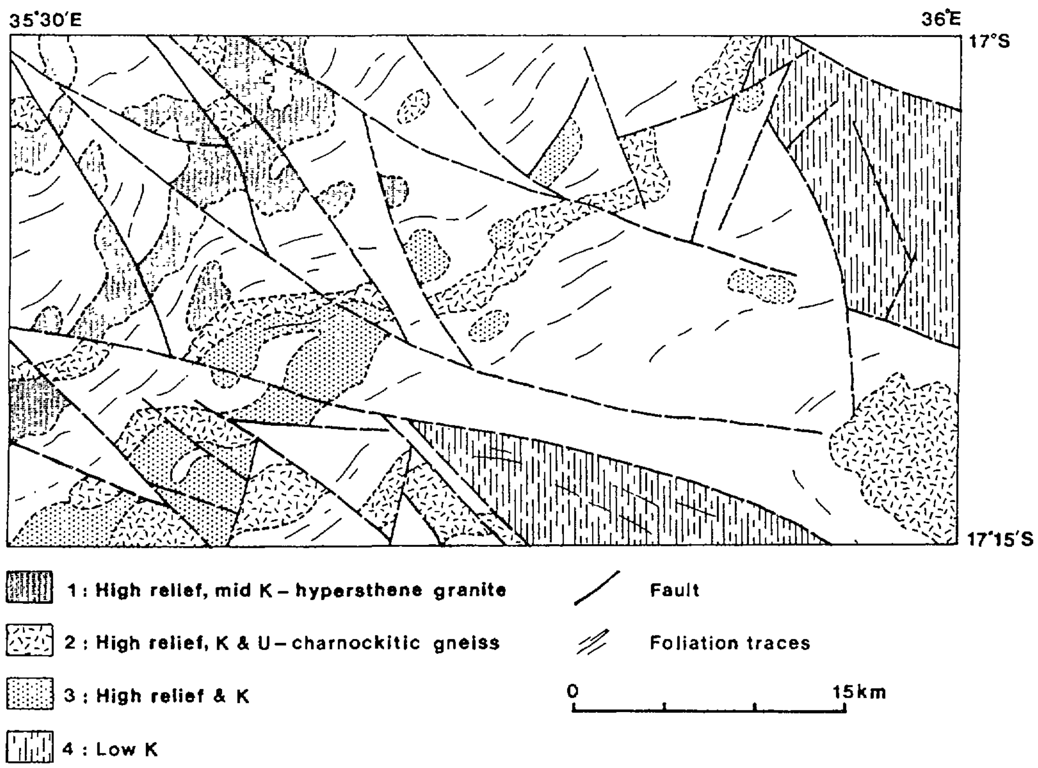

Figure 6: Interpretation from the integrated data.

Structurally, faults were inferred from high gradients in the spectrometric data and linear features visible on the Landsat imagery. Foliation trends were apparent on the Landsat imagery and banding trends were present on the spectrometric and aeromagnetic data.

The figure shows three major faults cutting ESE-WNW across the image with subsidiary faults in a NNW to NW orientation. These faults cut across the main foliation trends on the Landsat image which run from the southwest to the northeast in all areas apart from the southeastern corner. In this area the trend is from southeast to northwest paralleling the main fault direction.

Four units have been identified on the imagery and have been numbered to be equivalent where possible to those identified during the spectrometric study. The combined Landsat and derived potassium composite image indicated that some of the high relief areas identified from the Landsat imagery occurred in areas of high values on the spectrometric image while others coincided with very low values. These former areas represent lithologies with high K/U ratio values and high Th/K ratio values. This means the potassium levels were medium to high and the thorium levels showed greater relative positive deviation from their mean background level than the uranium levels. Study of these areas with aeromagnetic data provided a further subdivision of the unit into Units (1) and (3) based on the fact that Unit (1) lay in an area of mid to high aeromagnetic values with high gradients and Unit (3) lay in an area of low to mid values with low gradients. Thus although the lithologies may be similar the relationship to their surrounding rocks is different, Unit (1) being in a strongly banded metamorphosed terrain, while Unit (3) falls in a more uniform area with less banding.

Unit (2), also identified by high relief on the Landsat image, differed from Units (1) and (3) by its low values on the derived spectrometric data, i.e. high levels of potassium and low levels of both uranium and thorium relative to their mean values. Comparison with Figure 3 showed Unit (2) to be closely related to the areas of charnockitic gneiss especially in the southeast.

Unit (4) was not identified as such on the Landsat imagery, having no paricular relief features. However on the spectrometric data it forms a very strong feature by its absence of any variations. It represents areas of extremely low potassium values and appears to be fault bounded where it occurs both in the south and the northeast of the area.

Preliminary statistical analysis using a correlation matrix (Table I) show little evidence of correlation between the Landsat channels and the geophysical data. This lack of correlation is not unexpected as it is unlikely that the brightness values of a Landsat pixel will bear any relationship to the spectrometric or aeromagnetic values. This is because they represent the spectral reflectance of surface materials which in this case include: vegetation and not the lithologies. The spectrometric data are more closely related to the various lithologies of the area. Within the geophysical data the only strong correlation exists between the total count and thorium channels and to a lesser extent the uranium channel. The potassium channel showed very poor relationships with all the other geophysical sets as did the total magnetic field data.

TABLE I. Correlation Matrix

		Landsat Channels				Spectrometric Data			
		7	5	4	Aeromagnetic Data	Total Count	Potassium	Thorium	Uranium
Landsat Channels	7	1.000	0.100	0.246	0.025	0.266	0.032	0.246	0.283
	5	0.100	1.000	0.521	-0.010	-0.110	0.050	-0.112	-0.124
	4	0.246	0.521	1.000	0.005	0.039	0.088	0.023	0.039
	Aeromagnetic Data	0.025	-0.010	0.005	1.000	-0.123	-0.097	-0.089	0.099
Spectrometric data	Total Count	0.266	-0.110	0.039	-0.123	1.000	0.001	0.975	0.710
	K	0.032	0.050	0.088	-0.097	0.001	1.000	-0.212	0.001
	Th	0.246	-0.112	0.023	-0.089	0.975	-0.212	1.000	0.664
	U	0.283	-0.124	0.039	-0.099	0.710	0.001	0.664	1.000

Correlation would have been better carried out on derived products of the raw data which could be related to the physical properties of the lithologies. For example a measure of texture derived from the Landsat imagery would differentiate high and low relief areas, the former of which was suggested to be charnockitic gneiss [8]. From the total magnetic field derived products a reduction to the pole or a magnetic susceptibility map would more closely relate to lithology; and for the spectrometric data a classification map of a composite image using potassium, uranium and thorium data could provide an input relating to the chemical composition of the different lithologies. Factor or discriminant function analysis of such data might provide greater insight into the geological relationships of the area.

6. CONCLUSIONS

The integration of data allowed a geological interpretation to be carried out which was better than that achieved with either of the individual data sets.

1. Major faults across the image, defined by steep spectrometric gradients and Landsat linear features were only partially interpreted on the individual data sets.

2. Foliation trends interpreted on the Landsat imagery were confirmed and extended by both the magnetic data and spectrometric data.

3. Lithological Units (1),(2) and (3) on Figure 6 were previously assigned by texture to one unit on the Landsat imagery. Integration with the spectrometric data showed marked differences between Units (1) and (2). Use of magnetic data enabled Units (1) and (3) to be defined.

4. Broad units interpreted from the spectrometric data were more clearly defined by integration with the Landsat texture information.

The mapped boundaries interpreted by integrating the data will enable follow up geological mapping to define lithologies and structure more precisely in the area.

ACKNOWLEDGEMENTS

The author would like to thank the Ministry of Mineral Resources of the People's Republic of Mozambique for permission to publish these data and Hunting Geology and Geophysics Limited for the use of their image processing facilities.

REFERENCES

[1] BOLIVAR,S.L.et al. Multisource data set integration and characterisation of uranium mineralisation for the Montrose Quadrangle, Colorado, Los Alamos Sci.lab.LA 8807.M.S.(1980).

[2] MOORE,G.R. Computer correlation of exploration data for the Pennine Orefields. Remote Sensing in Mineral Exploration. Commission of the European Communities (Resources) Report EUR 10334 EN Cat.No. CD-NS-85-002-EN-C(1986).

[3] SINDING-LARSEN,R.,STRAND,G. Quantitative integration of mineral exploration data. I.U.G.S. Episodes 1 (1981) 9-12.

[4] HUNTING GEOLOGY AND GEOPHYSICS LIMITED, Final Report - Mineral Inventory Project. Report on Landsat and Geophysical survey (1981-1983). Direccao Nacional de Geologia. Unpubl.report (1984).

[5] HUNTING GEOLOGY AND GEOPHYSICS LIMITED, Airborne geophysical survey Zambezia area - Mineral Inventory project. Direccao Nacional de Geologia. Unpubl.report (1983).

[6] JOURDE,G.,VIOLETTE,Y. La Chaine du Lurio (Nord Mozambique). Un temoin de l'existence de chaines Kibariennes (800-1350 MA) en Afrique Orientale. BRGM Unpubl.Rep.(1980).

[7] JOURDE,G. La chaine du Lurio (Mozambique): un temoin de l'existence de chaines Kibariennes en Afrique Orientale.Proc.12th Coll.African Geol. Terruren Abs.(1983) p.50.

[8] ARAUJO,J.R.,PINTO,A.F.,PINTO,M.S. Geologia e prospeccao geral das areas de Milange, Mongue, Chire, Derre e Morrumbala (Zambezia). Direccao Nacional de Geologia, Maputo. Unpubl.Rep.No.C830 (1971).

[9] SABINS,F.F.Jnr. Remote Sensing Principles and Interpretation (Cox,A.Ed.) W.H.Freeman and Company, San Francisco (1978).

[10] SIEGAL,B.S.,GILLESPIE,A.R. Remote Sensing in Geology. John Wiley and Sons, New York.

[11] TELFORD,W.M.,GELDART,L.P.,SHERIFF,R.E.,KEYS,D.A. Applied Geophysics. Cambridge University Press, Cambridge. (1976).

[12] PARASNIS,D.S. Principles of Applied Geophysics, Chapman and hall 'A Halsted Press Book' John Wiley and Sons, New York (1979).

[13] GRASTY,R.L. Uranium measurement by airborne gamma-ray spectrometry. Geophysics 40 (1975) 503-519.

[14] KILLEEN,P.G. Gamma ray spectrometric methods in uranium exploration-application and interpretation.

(HOOD,P.J.Ed.). Geophysics and Geochemistry in the search for Metallic Ores. Geological Survey of Canada, Economic Geology Report No.31 (1979) 163-226.

[15] WILKES,P.G. Acquisition, processing and interpretation of airborne gamma-ray spectrometry data. Bureau of Mineral Resources, Geology and Geophysics Report 186. Australian Government Publishing Service.

[16] NEVITT,C.,BARR,M.W.C. Composite colour images of airborne spectrometric data. Mining Magazine 152 3 (1985).

INTEGRATED REMOTE SENSING APPROACH TO URANIUM EXPLORATION IN INDIA

N.V.A.S. PERUMAL, S.N. KAK,
V.J. KATTI
Atomic Minerals Division,
Department of Atomic Energy,
Hyderabad, India

Abstract

Integrated data from remote sensing and other conventional geophysical methods has helped to accelerate the pace of uranium exploration in a wide variety of geological environments in India during the last two decades. The integration involves data from Landsat MSS and TM, airborne multispectral scanner, air-photos, high sensitivity airborne gamma-ray spectrometry, airborne magnetics and ground gravity surveys.

Landsat MSS images in black and white and false colour composites in different scales and in 70 mm chips have been critically analysed through visual interpretation techniques for a regional geological assessment of different areas and selection of target areas for high sensitivity gamma-ray spectrometry and other airborne surveys. Computer processing of digital Landsat MSS and airborne MSS data supplemented with data from detailed photo-interpretation and Landsat TM analysis aided selection of areas for ground surveys. The information obtained from remotely sensed data when integrated with data on distribution of U, Th and K and U/Th, U/K and Th/K ratios obtained by airborne high sensitivity gamma ray spectrometry has helped in the precise mapping of structural lineaments, shears, thrusts, lithological units and transition zones having significant bearing on uranium mineralization, identification of local litho-structural controls of mineralization and location of similar litho-structural traps elsewhere. In several regions the interpretative possibilities of the remotely sensed data are greatly enhanced when synthesised with high sensitivity gamma-ray spectrometric estimations and aero-magnetic and ground gravity data.

This paper presents some case histories illustrating the usefulness of integrated remote sensing approach in uranium exploration in different geological environments, such as the Dharwarian rocks in Southern India, the intra-mobile belts of migmatite-granitoid complexes traversed by major shear zones in Central India, the interfaces of Archaean cratonic regions with Proterozoic mobile belts characterised by deep crustal fractures as in Eastern India and the Tertiary Siwalik molasse deposited along the Himalayan foredeep.

---

1. INTRODUCTION

As a part of its uranium exploration programme the Atomic Minerals Division (AMD) of the Department of Atomic Energy has been carrying out airborne radiometric surveys since 1956. Aerial photographs, the very first remotely sensed data available to the scientific community have been routinely used for planning of the survey flights, geological mapping, evaluation of radioactive anomalies and as navigational aids. When total count radiometric surveys were the order of the day until nearly the late Sixties, use of aerial stereo-photographs became indispensable for discriminating a large number of total count radioactive anomalies and identifying the appropriate ones based on their geological significance for detailed uranium investigations on the ground. Apart from considerable time and manpower required for such an arduous exercise there were other limitations like the availability of airphotos and trained photo-interpreters. With the advent of space photography and Landsat remote sensing many of these problems are simplified and limitations overcome to a large extent besides significant saving in the turn-around time.

Since radiometric and remote sensing techniques essentially relate to the surficial phenomena of the earth's crust, and the need is for location of concealed ore bodies, it is imperative that the use of other conventional geophysical techniques like magnetic and gravity, is sought for a meaningful evaluation of these data and proper understanding of the geological phenomena in the third dimension. The integrated approach utilizing data from Landsat imagery analysis, airborne gamma-ray spectrometry and magnetics, and airphotointerpretation as well as data from other available ble/compatible techniques wherever necessary during different phases of intestigations forms an essential element in the uranium exploration strategy of this Organization (Fig.1).

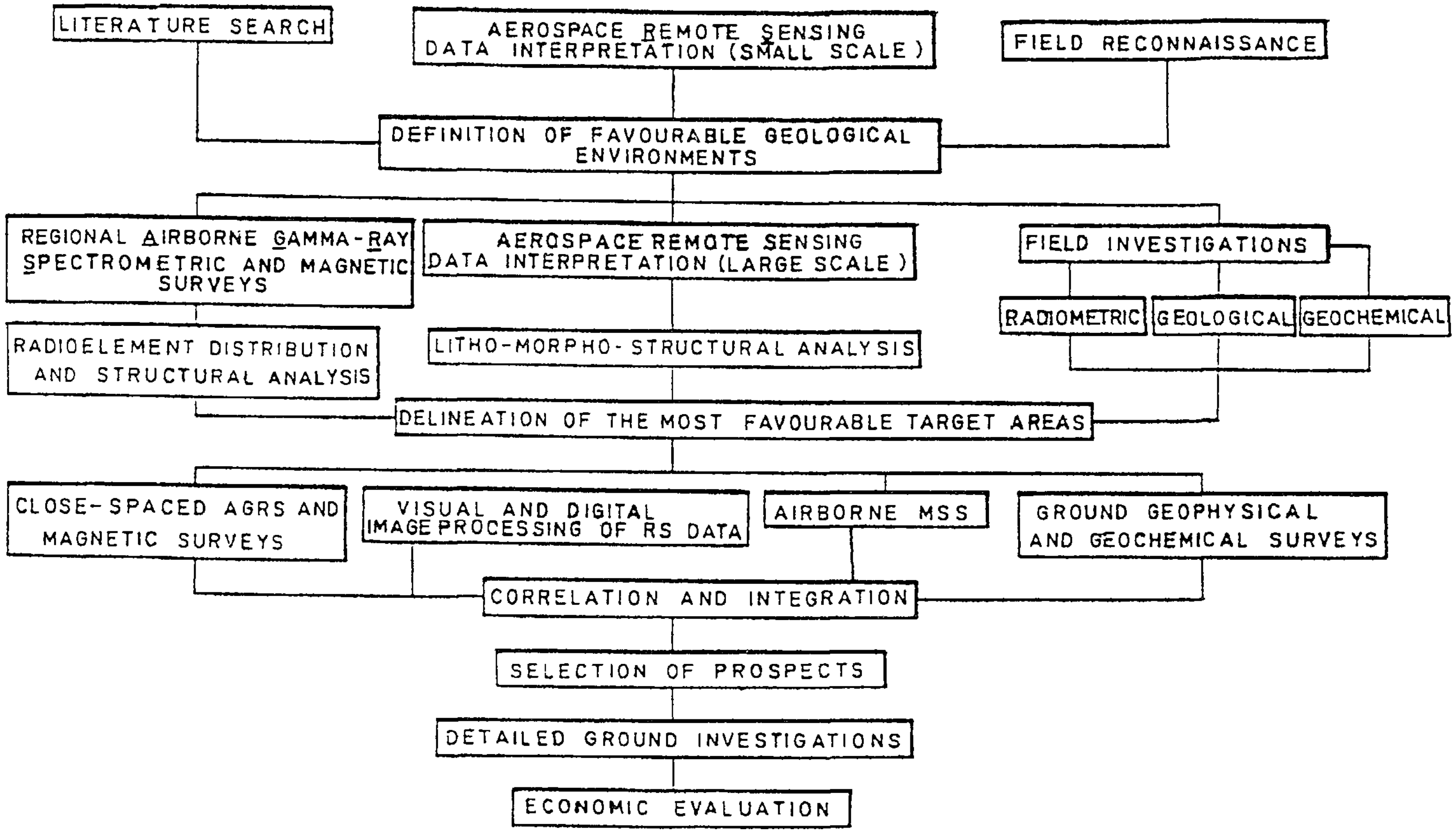

FIG.1. Uranium exploration strategy.

2. AIRBORNE GAMMA-RAY SPECTROMETRY AND REMOTE SENSING

Airborne gamma-ray spectrometry (AGRS) although does not fall under conventionally accepted definition of remote sensing, yet it cannot also be excluded from its purview as the technique relates to the remote sensing of radiant energy in gamma-ray region of the EM spectrum only. The AGRS technique involves measurement of emitted gamma-ray flux from the naturally occurring radionuclides of U, Th and K from remote distances, generally not more than 250 m above ground level, through suitable detector systems placed on airborne platforms [1]. With spectacular advancements in electronics and developments in instrumentation during the past couple of decades, these systems have evolved from simple total count to highly sophisticated and high sensitivity gamma-ray spectrometers with computer compatible digital multi-channel data acquisition and analysis capable of producing different thematic maps (eU, eTh, K, eU/eTh, eU/K, eTh/K and total count) based on radioelement distribution in the surface materials of the earth's crust. These systems are generally integrated with airborne magnetics for getting simultaneously magnetic field data without additional survey expenditure. Such a system [2] with AMD is suitably backed up by a test strip and five calibration pads for rigorous calibration and standardization. During the last decade > 0.26 million sq km area was covered in airborne surveys, 95% area with one km line spacing.

The last two decades also witnessed a number of major developments in the application of remotely sensed data to mineral exploration including that of uranium. Capability of extracting sound geological information from digital data in different spectral bands has considerably improved through machine processing as compared with the conventional visual analysis [3] of hard copy imagery.

A comparative overview of these two data sets brings forth many similarities and limitations in the fundamental characteristics of their acquisition, analysis and interpretation. Both the techniques exploit EM Spectrum, though in different regions, and are essentially related to the sensing of surface phenomena of the earth's crust. The complex nature of the physical principles underlying remotely sensed data particularly the reflection, absorption and emission and the interaction between this energy and the intervening matter have very close analogies to the emission of gamma-rays, their scattering and attenuation through matter, before their detection through respective sensor systems (TABLE-I).

Despite that the data sets from both these techniques provide information only on surficial materials of the earth's crust, integration of the two has great potential in the search for uranium in general and critical evaluation of the geological environments and regional structures favourable for the occurrence of uranium in particular.

Various data materials used in the investigations carried out in different regions as referred to in the case histories are given in the Table-I.

3. METHODOLOGY AND DATA EVALUATION

Visual photo-interpretation techniques based on the well-established photo-criteria of tone, texture, colour, shape, size, vegetation, drainage and other associated features are used in the interpretation of various Landsat hard copies including the enhanced outputs from computer processed digital MSS data. These studies are duly supported at every stage by the available published and unpublished data.

The first step in the integration process is to bring different data sets to a common scale(50,000-250,000)

TABLE I

	AIRBORNE GAMMA-RAY SPECTROMETRY (AGRS)	AERO-SPACE REMOTE SENSING (ASRS)
1.	GAMMA RAYS (10^{-7} TO 10^{-4} MICRONS) EMS	UV, V, IR, MW (10^{-1} TO 10^{-3} MICRONS) EMS
2.	NUCLEAR TRANSITION	ELECTRONIC/MOLECULAR TRANSITION
3.	CRYSTAL DETECTOR	PHOTOGRAPHIC FILM, RADIOMETER, THERMAL DETECTOR THROUGH OPTOMECHANICAL SCANNERS
4.	DIRECT DETECTION OF RADIOACTIVITY EMANATING $\simeq$ 30 CM OF SURFACE	DETECTION OF REFLECTED AND EMITTED RADIATIONS EMANATING - MICRONS TO METRES OF SURFACE
5.	DATA ACQUISITION FROM < 250 M ABOVE GROUND LEVEL	DATA ACQUISITION FROM ANY DISTANCE ABOVE GROUND LEVEL
6.	SURFICIAL PHENOMENON, ATTENUATION THROUGH ATMOSPHERE	SURFICIAL PHENOMENON DETECTABLE THROUGH SELECTIVE ATMOSPHERIC WINDOWS
7.	DATA COLLECTION IN ANALOGUE AND DIGITAL FORM	DATA COLLECTION ON PHOTOGRAPHIC FILM AND IN DIGITAL FORM

and the preparation of transparent overlays of the data sets, Transparent overlays of computer generated thematic (contour) maps of eU, eTh, K, eU/eTh, eU/K and eTh/K, are superimposed individually on the geological maps. Normally, 250,000 scale maps are used for regional assessment of radioelement distribution and study of geochemical characteristics of the major stratigraphic/lithic units, and 50,000 scale maps for detailed litho-structural evaluation and delineation of potential uranium target areas. Simultaneously overlays of locales of known mineralization are also studied. Locations of known mineralization are often directly plotted on the geological maps. Overlays of aeromagnetic contour maps facilitate structural and lithological correlation through qualitative analysis of the data.

An iterative study to define threshold value considered anomalous for each radioelement and their ratios in each study area (fifteen minute quadrangle) follows. This step involves some amount of discretion but is largely guided by the available ground radiometric data for the rock units present in the area, and their mean crustal values, and the general level of radioactivity recorded from the air. Areas above the threshold levels for each parameter are considered to be anomalous. Integration of anomalous areas of the three important parameters viz. eU, eU/eTh and eU/K, are regarded as high potential target areas and those of eU and eU/eTh, the next potential. Depending on the geological environments and favourable litho-structural associations, anomalous areas of eU and eU/eTh are also individually considered for ground investigations. Experience in several areas has shown that integration of the three parameters is quite adequate to delineate all potential target areas which generally indicate regions of actual enrichment of uranium vis-a-vis thorium and potassium. Such areas often transgress lithological boundaries. Thematic maps of K and eTh/K are used to outline areas of hydrothermal alteration and/or potash metasomatism [4].

Statistical analysis techniques are also employed for gamma-ray spectrometric data presentation and delineation of potential target areas [2]. The technique most commonly used is the Significant Factor Analysis or the preparation of uranium map of standard deviations [5]. Nevertheless, presentation of data in an integrated manner based on the three important parameters, eU, eU/eTh and eU/K, has been found to be very satisfactory, the target areas finding good correlation with the known occurrences, and also with those discovered later on in the region. The target areas thus delineated often limit to less than 15% of the survey areas.

Once any significant mineralization is located on the ground, appropriate investigations specific to the areas, including digital image processing of Landsat data and airborne MSS are undertaken. Integration of different data sets from remote sensing and conventional geophysical techniques helps to arrive at the most potential target selection through the age-old conventional procedure of "convergence of evidence", and leads to a comprehensive and meaningful understanding of the mineralization and its probable behaviour in the sub-surface.

4. CASE HISTORIES

Figure 2 shows the location of areas for which brief case histories are given [6].

4.1 Dharwars of Karnataka, Southern India:

The study area exhibits structurally disturbed low grade metamorphic suite in the Archaean-Proterozoic

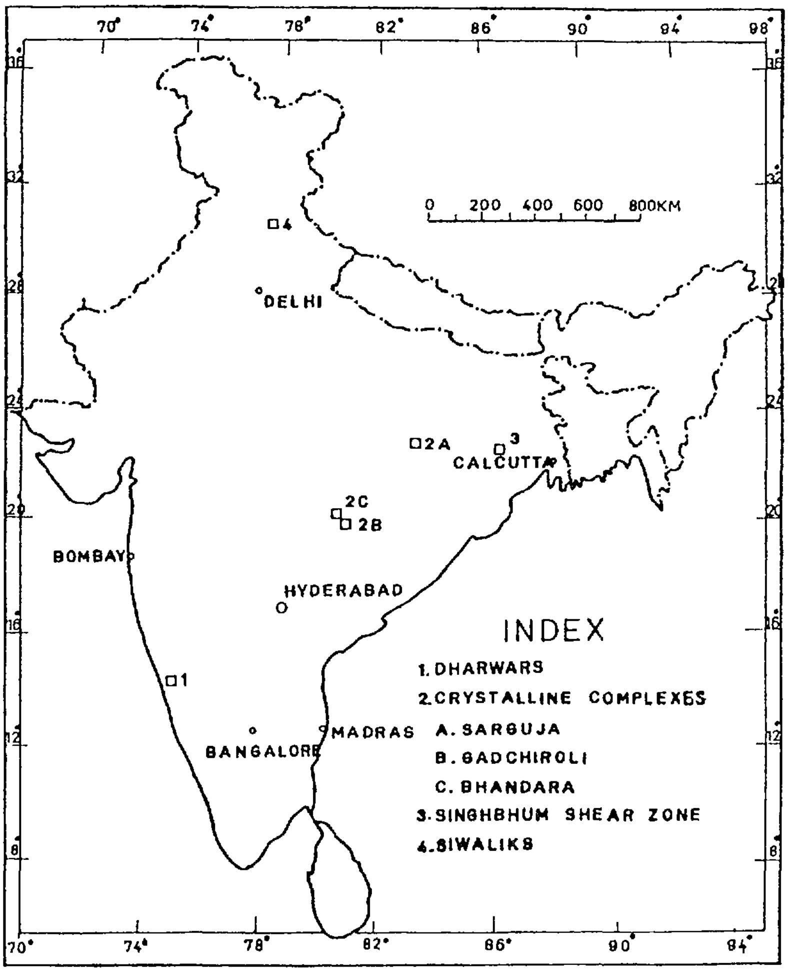

FIG.2. Location map of study areas.

meta-volcano-sedimentary rocks which form a part of the younger supra-crustal Chitradurga Schist Belt in the north-western part of Karnataka in southern Peninsular India [7].

Significant uranium mineralization has been located in the sulphide-rich litho-units of lower schistose member of the Chitradurga Group, often exposed at lower contours along the river sections. The younger member of greywackes underlain by Fe-Mn formation and limestone occupy the higher reaches. Deep lateritization, thick vegetal cover and massive overburden in this picturesque but otherwise highly rugged terrain, have imposed several limitations in ground investigations.

An attempt has been made to integrate satellite and aircraft remote sensing data with the available conventional inputs for a meaningful geological evaluation to aid the uranium exploration programme in the region. Visual analysis of Landsat data, stereo-airphotos and integration of different data sets duly aided by ground data and critical traverses in the areas, have helped not only in deciphering the tectonic overprint and the local litho-structural frame work, but also in assessing the significance of specific structural elements delineated in the area [8].

The tectonic overprint on the terrain is vividly manifested by the straight river courses in different directions, entrenched meanders, flareups in major streams, non-integrated drainage and anomalous curves and turns. Very tight folding with sub-vertical dips and superimposition of younger tectonism off-setting the earlier structural fabric, and their relative chronological order have been assessed from Landsat and airphoto studies. N-S and NNW-SSE structural linears appear to represent the pre-mineralization fractures and faults, while the N-S system was partially reactivated and mineralized. Most of the NE-SW linears in the study area around Arbail appear to be post-mineralization faults, some of them being responsible for the dislocation of the mineralized zones at Dabguli and Shevkar (Fig-3).

Integration of data from AGRS, Landsat and airphotos has brought out some promising horizons along the N-S structural trends. Since the mineralized horizon underlying the Fe-Mn formation is not always manifest on the surface, aeromagnetic data has been of particular help in the delineation of sub-surface continuity.

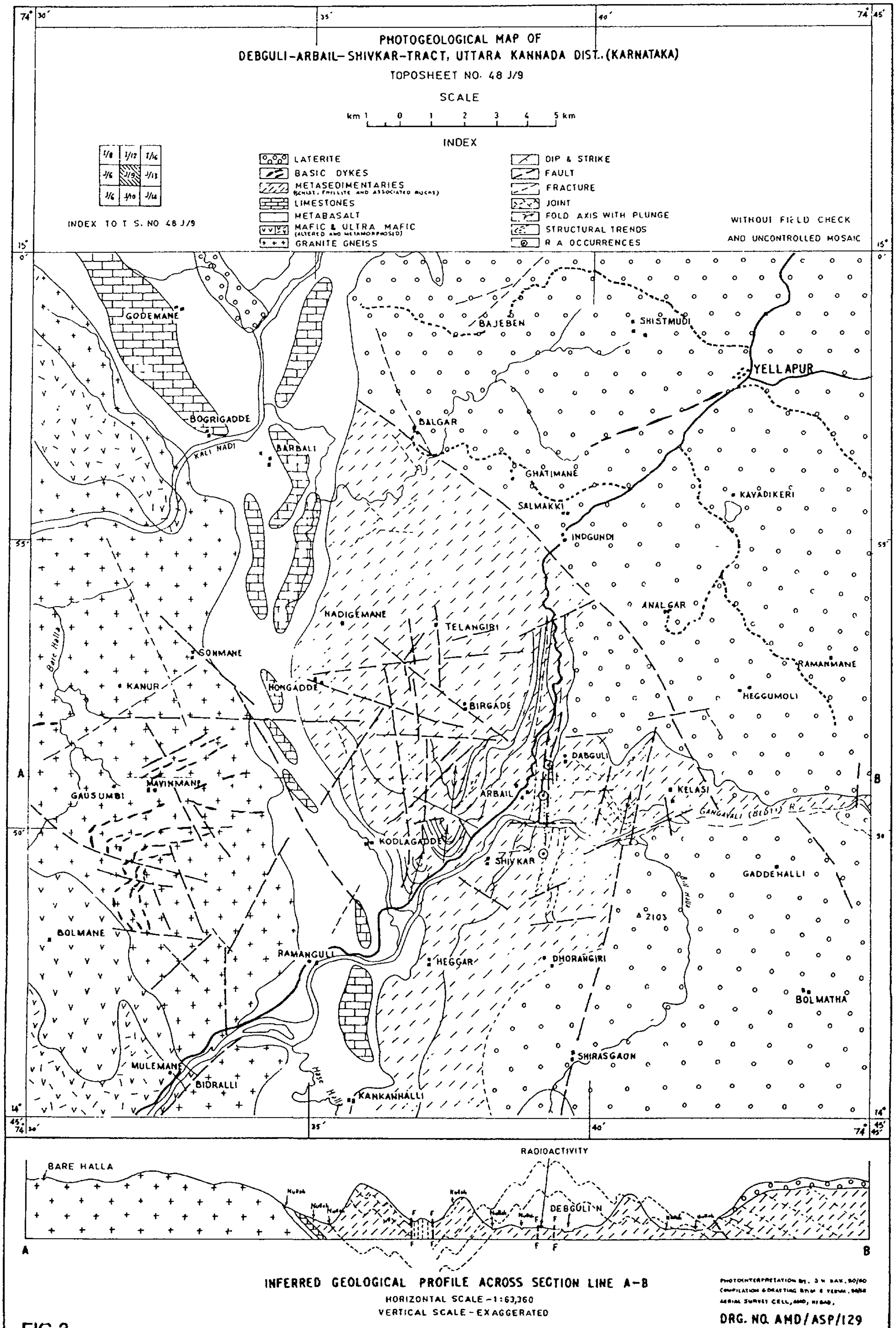
PHOTOGEOLOGICAL MAP OF
DEBGULI-ARBAIL-SHIVKAR-TRACT, UTTARA KANNADA DIST. (KARNATAKA)
TOPOSHEET NO. 48 J/9
SCALE
INDEX
LATERITE
BASIC DYKES
METASEDIMENTARIES
LIMESTONES
METABASALT
MAFIC & ULTRA MAFIC
GRANITE GNEISS
DIP & STRIKE
FAULT
FRACTURE
JOINT
FOLD AXIS WITH PLUNGE
STRUCTURAL TRENDS
R A OCCURRENCES
INDEX TO T. S. NO 48 J/9
WITHOUT FIELD CHECK AND UNCONTROLLED MOSAIC
GODEMANE
BAJEBEN
SHISTMUDI
YELLAPUR
BOGRIGADDE
KALI NADI
BARBALI
BALGAR
GHATIMANE
SALMAKKI
KAVADIKERI
INDGUNDI
ANALGAR
NADIGEMANE
TELANGIBI
SONMANE
KANUR
HONGADDE
BIRGADE
RAMANMANE
HEGGUMOLI
DABGULI
KELASI
MAVINMANE
GAUSUMBI
ARBAIL
GANGAVALI (BEDTI) R.
KODLAGADDE
SHIVKAR
GADDEHALLI
2103
BOLMANE
RAMANGULI
HEGGAR
DHORANGIRI
BOLMATHA
SHIRASGAON
MULEMANE
BIDRALLI
KANKANHALLI
BARE HALLA
RADIOACTIVITY
DEBGULI
INFERRED GEOLOGICAL PROFILE ACROSS SECTION LINE A-B
HORIZONTAL SCALE - 1:63,360
VERTICAL SCALE - EXAGGERATED
DRG. NO. AMD/ASP/129

FIG.3.

The area around Arbail has been taken up as a test site for digital image analysis of Landsat MSS data and detailed ground geophysical studies. Since it was established that the fracture/fault systems, especially the mineralized N-S and the later NE-SW, had a definite role in the control of mineralization in the region, lineament mapping through convolution techniques [9] for the extraction of different directional elements has been carried out with digital Landsat MSS data. Preliminary analysis of line printout maps of the directional elements has shown that most of the directional elements in N-S and NE-SW direction are correlatable with the mapped fractures and faults.

The linear stretched MSS data was used to generate film-write colour composites, colour-coded band ratios, and printer-plotter character printouts for detailed geological interpretation and data integration studies. These studies brought forth a wealth of information on fold geometries and associated fracture systems, as shown in Figures 4 and 5. Integration of this information with other data on lithology and mineralization may be able to guide further sub-surface prospecting operations in the area. The study shows that the printer-plotter character outputs which are very inexpensive and available immediately after digital processing are as good as the film-write colour composites for litho-structural analysis. Apart from cost, film-write products take several weeks to be available for study.

Ground gravimeter surveys carried out at a sampling interval of about one kilometer in an area of about 600 sq km around Arbail prospect (R.L. - Narasimha Rao - Personal communication) have, apart from helping in the delineation of the basement configuration useful for planning sub-surface drilling

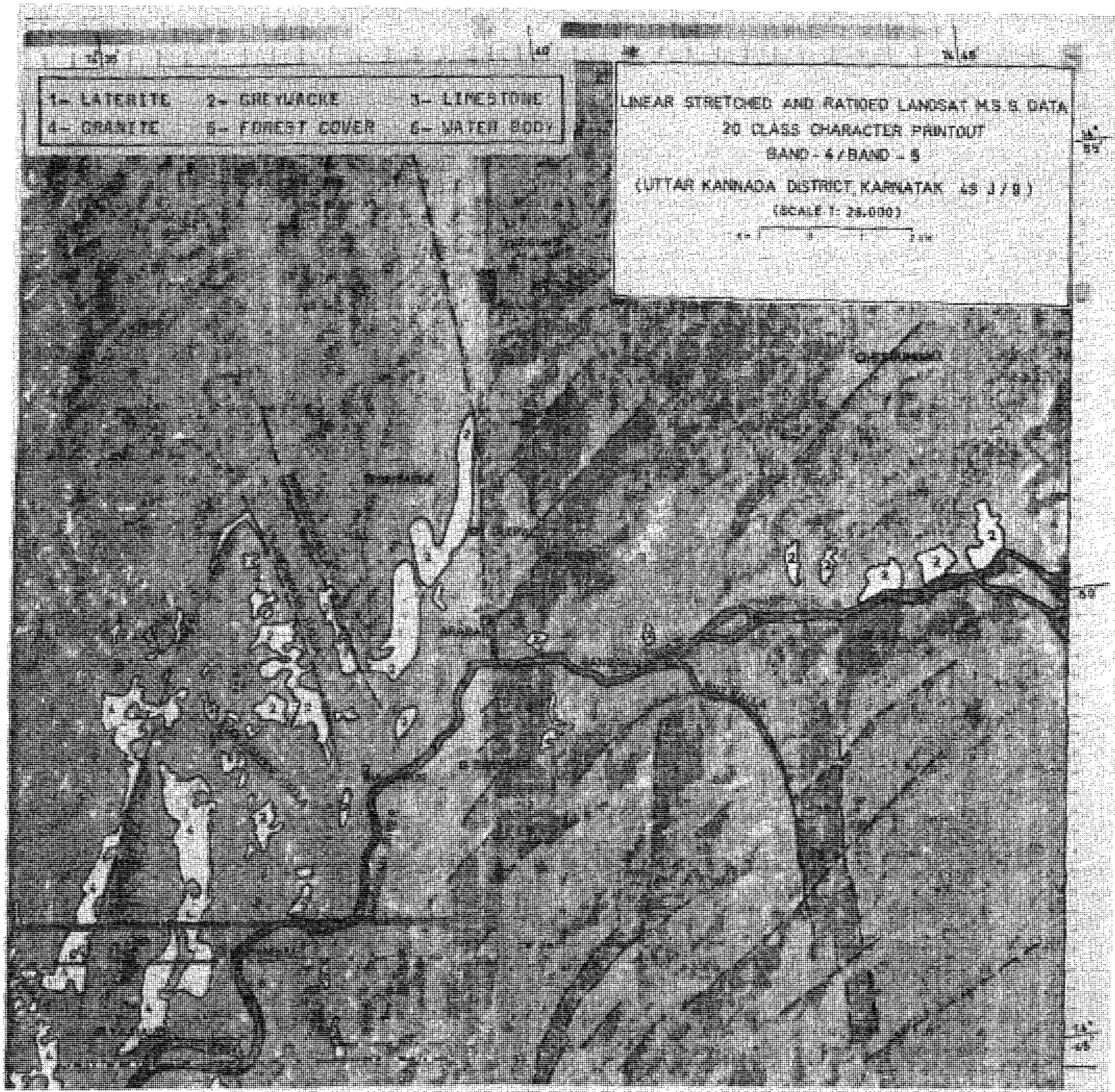
1- LATERITE
2- GREYWACKE
3- LIMESTONE
4- GRANITE
5- FOREST COVER
6- WATER BODY
LINEAR STRETCHED AND RATIOED LANDSAT M.S.S. DATA
20 CLASS CHARACTER PRINTOUT
BAND - 4 / BAND - 5
(UTTAR KANNADA DISTRICT, KARNATAK 48 J / 8)

FIG.4.

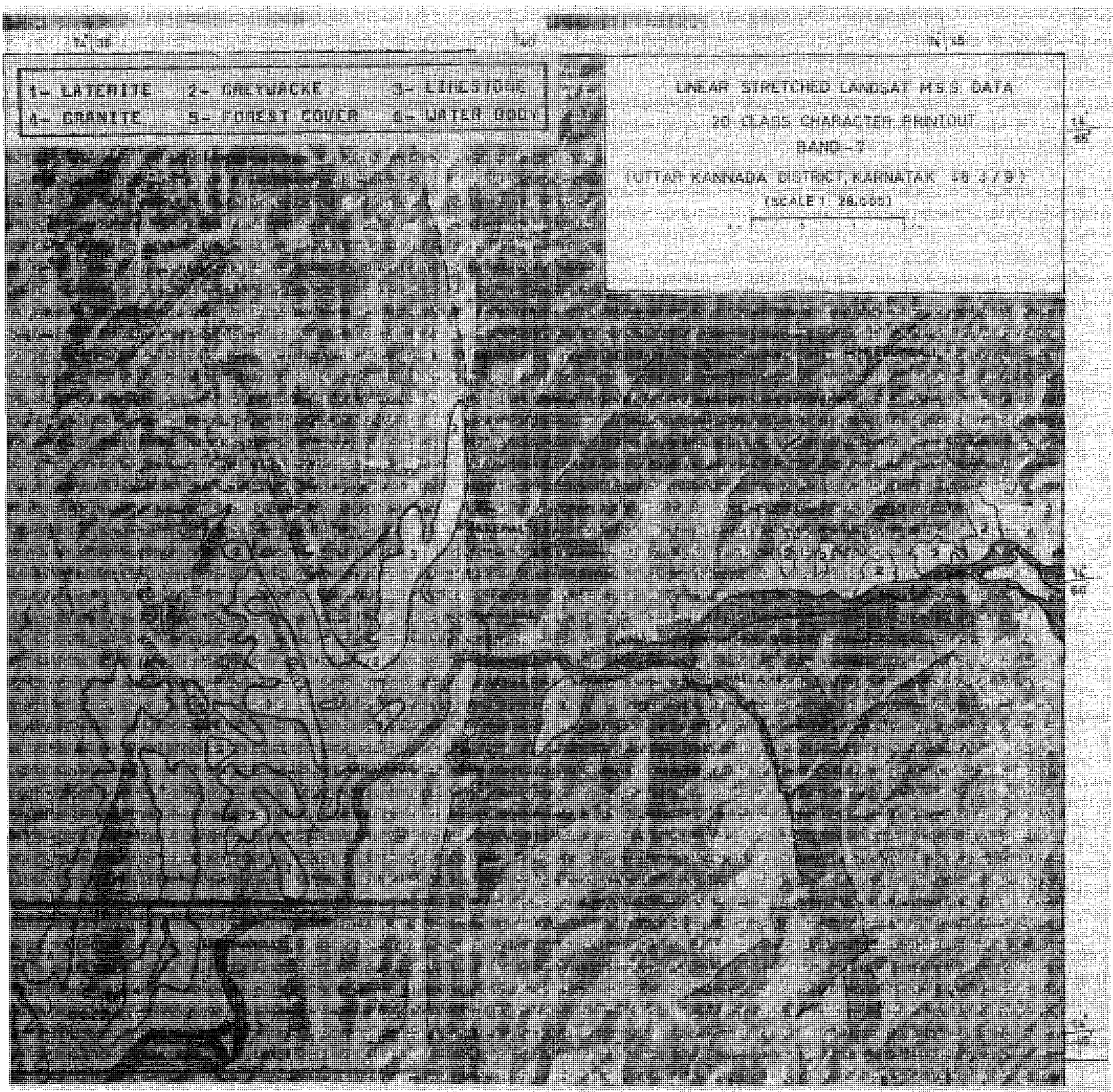
1- LATERITE 2- GREYWACKE 3- LIMESTONE
4- GRANITE 5- FOREST COVER 6- WATER BODY
LINEAR STRETCHED LANDSAT M.S.S. DATA
20 CLASS CHARACTER PRINTOUT
BAND-7

FIG.5.

operations, indicated several distinct gravity highs and lows in the area. Integration of gravity contour map (2 mgal interval) with the litho-structural map shows good correlation of highs with ferruginous quartzites at Ghatimane and ultrabasics at Dhorangiri, and lows with thin pile of metasediments over the basement at Arbail (as proved by sub-surface drilling), Kalasi-Kodki and Magod Falls regions. Alignment of these three areas also correlates with a structural lineament interpreted in the region.

Inference on the uraniferous horizons associated with sulphides and their displacement along the Gangavali River have also found good agreement with the data from Induced Polarization (IP) surveys in the area.

4.2 Crystalline Complexes, Central India.

(A) Sarguja district, Madhya Pradesh:

It is commonly observed that significant amounts of uranium get concentrated by complex processes of weathering, transportation and deposition along favourable fracture systems developed in the granitic gneisses and the associated schistose formations of Proterozoic age. Such deposits occur very close to major erosional unconformities developed during orogenic periods, generally believed to be of world-wide phenomenon, and are called unconformity related vein deposits. These occurrences are generally protected from erosion by sedimentary cover and are exposed when the sediments are removed by weathering processes. Such geological environments are recognizable in the synoptic scenes provided by Landsat missions. One such area has been located in part of Sarguja district, M.P. Here the Gondwana sedimentary cover has been partly eroded exposing the underlying Proterozoic Crystalline complex and the associated meta-sedimentary rocks [10].

A limited area of 2,200 sq km was selected for airborne gamma-ray spectrometric surveys on the basis of known mineralization at a single locality and favourable geological setting. Spectrometric data indicated correlation of significant uranium and uranium-thorium source anomalies along an ENE-WSW fracture delineated from airphoto interpretation.

Study of Landsat scenes revealed that the ENE-WSW trending fracture was only a part of a major shear zone extending over 120 km in that direction. Subsequent field investigations confined to the shear zone have brought to light mineralization at some more localities and led to subsurface drilling and development. Further airborne surveys covering the entire shear zone by high sensitivity gamma-ray spectrometer and proton-precession magnetometer have shown uranium enrichment intermittently all along the shear zone (Fig.6). Study of enlarged Landsat imagery on 250,000 scale and airphoto-interpretation of a limited area on 60,000 and 30,000 scale showed that the shear zone is made up of several parallel shears, and the mineralized and anomalous uranium areas fit into this tectonic frame work running along the northern limb of a major anticline plunging to the west. Figure -7 shows an integrated map of aero-gamma-ray spectrometric data and Landsat interpretation of northern part of the study area. Integration of data from photo-interpretation and airborne gamma-ray spectrometry and subsequent field investigations have shown that the nodes of intersection of minor transverse fractures with the main shears are the locales of intense mineralization. Landsat has also helped to extrapolate the shear zone beneath the

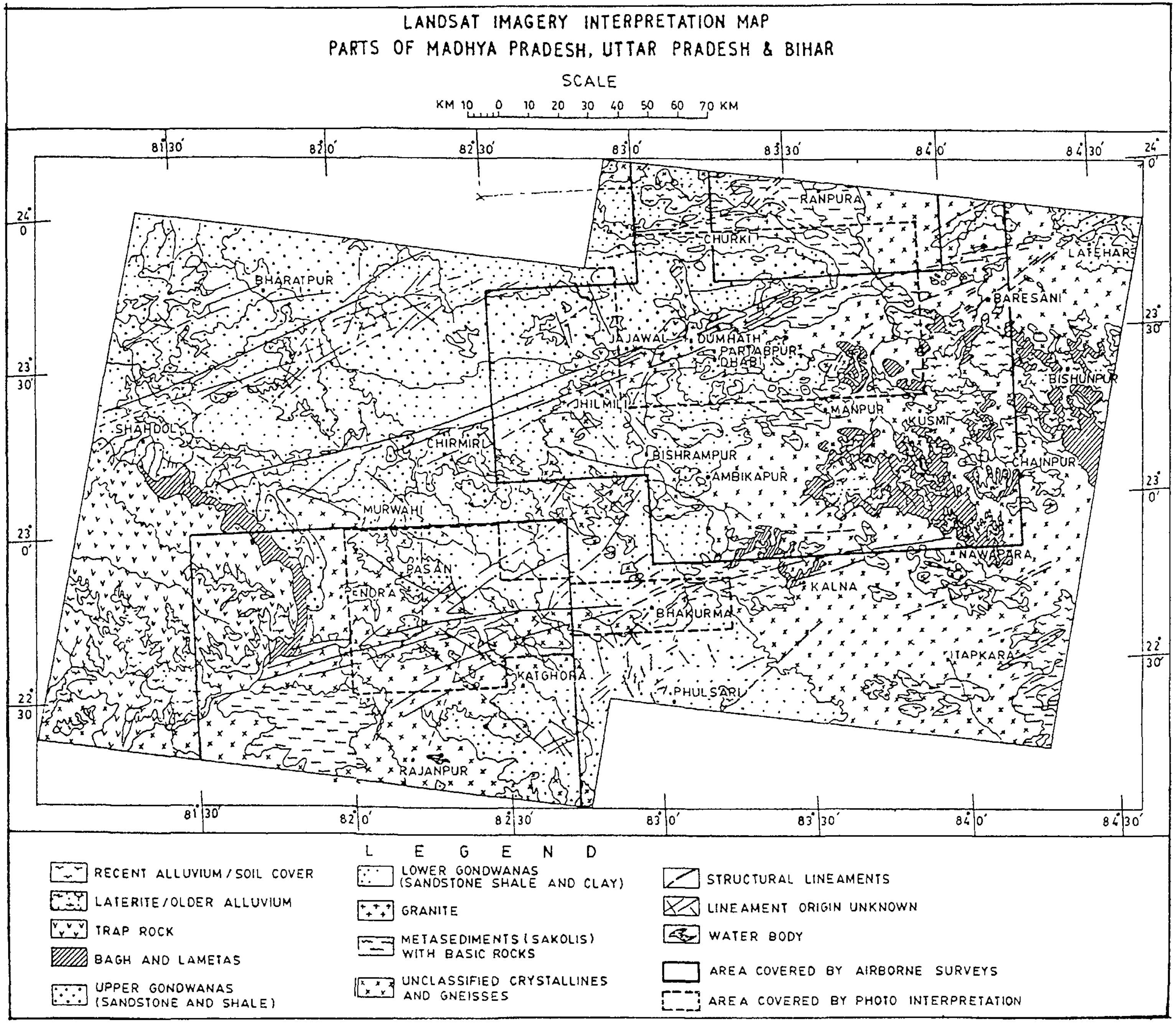

FIG.6.

DRG NO. AMD/ASP/281

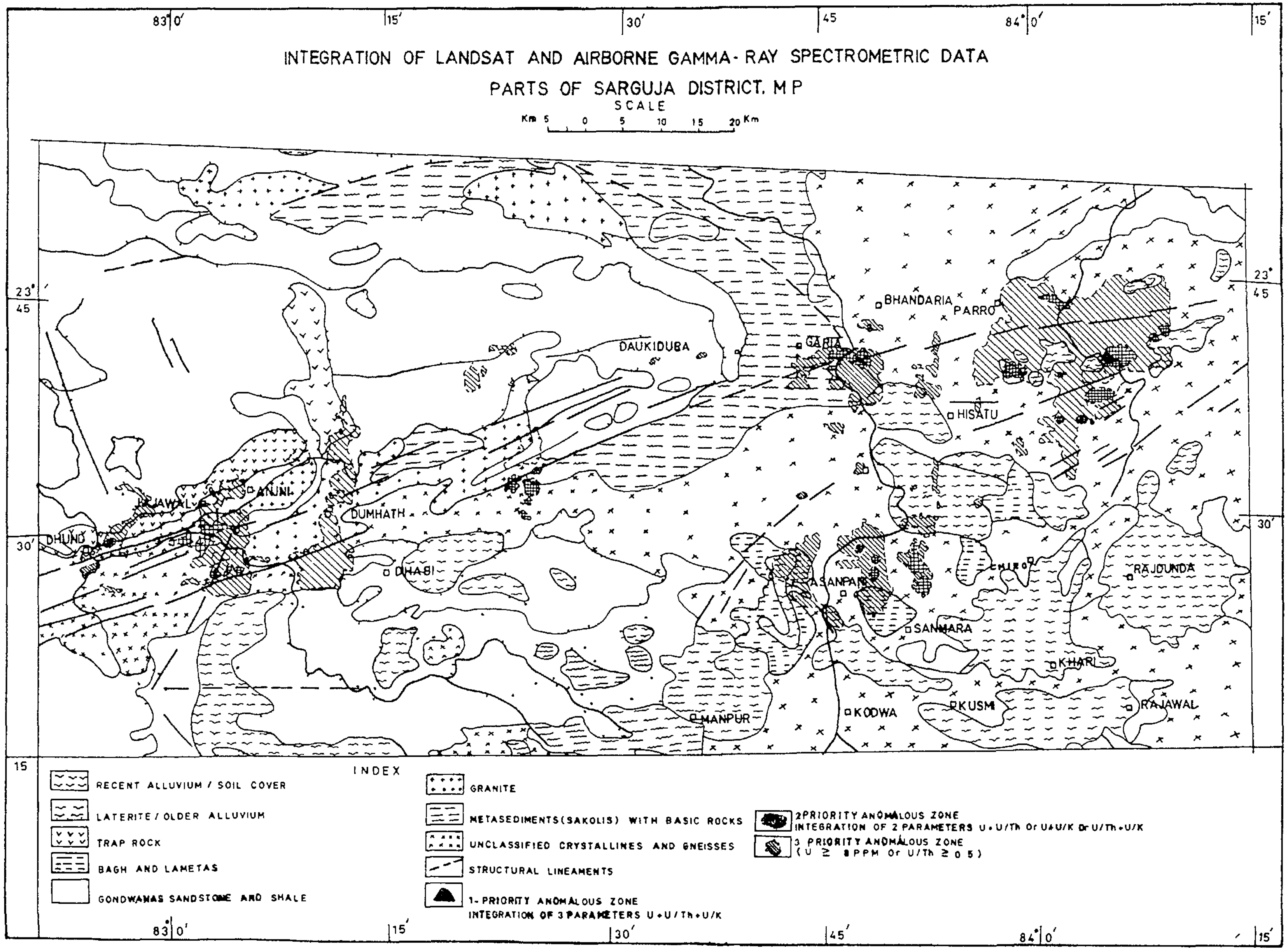
INTEGRATION OF LANDSAT AND AIRBORNE GAMMA-RAY SPECTROMETRIC DATA
PARTS OF SARGUJA DISTRICT, M P
SCALE
Km 5 0 5 10 15 20 Km
83°0′
15′
30′
45
84°0′
15′
23° 45
30′
15
BHANDARIA
PARRO
GARIA
DAUKIDUBA
HISATU
ANJNI
RAJAWAL
DHUND
DUMHATH
DHABI
ASANPANI
CHIRO
RAJDUNDA
SANMARA
KHARI
KUSMI
RAJAWAL
KODWA
MANPUR
INDEX
RECENT ALLUVIUM / SOIL COVER
LATERITE / OLDER ALLUVIUM
TRAP ROCK
BAGH AND LAMETAS
GONDWANAS SANDSTONE AND SHALE
GRANITE
METASEDIMENTS (SAKOLIS) WITH BASIC ROCKS
UNCLASSIFIED CRYSTALLINES AND GNEISSES
STRUCTURAL LINEAMENTS
1- PRIORITY ANOMALOUS ZONE
INTEGRATION OF 3 PARAMETERS U+U/Th+U/K
2 PRIORITY ANOMALOUS ZONE
INTEGRATION OF 2 PARAMETERS U+U/Th Or U+U/K Or U/Th+U/K
3 PRIORITY ANOMALOUS ZONE
(U ≥ 8 PPM Or U/Th ≥ 0.5)

FIG.7.

Gondwana cover and also led to the delineation of a parallel shear zone with identical geological setting 70 km to the south in Bilaspur and Raigarh districts (Fig-6). Airborne gamma-ray spectrometric surveys and subsequent field investigations in this part have brought to light mineralization at several places along the shear zone.

Since mineralization is associated with red alteration and/or potash metasomatism (as indicated by K, eU/K and eTh/K thematic maps and field data) an area of about 600 sq km where excellent ground truth data have been available, was subjected to digital image processing using Landsat MSS CCT for delineating such areas. No isolation of such areas was seen in colour ratio composites, histogram equalized colour composites and linear stretched colour composites. Further tests are underway for the generation of compound ratio colour composites.

(B) Gadchiroli-Chandrapur districts, Maharashtra:

In an another part of Central India significant uranium mineralization has been located in the granitic and migmatitic rocks in parts of Gadchiroli and Chandrapur districts of Maharashtra State. The areas being quite inaccessible and highly inhospitable, visual analysis of Landsat was undertaken in an area of 20,000 sq km for geological mapping and identification and documentation of litho-structural features associated with uranium mineralization on the ground. This study was supported by air-photo-interpretation of selected areas (2695 sq km) followed by further ground investigations. Six distinct rock types have been delineated in the areas generally mapped as Archaean "Crystalline Complex" and many structural linears, folds and circular features mapped. Integration of known mineralised areas with remotely sensed data has shown that the fractured granitic and migmatitic rocks are responsible for uranium mineralization which is closely associated with NW-SE and N-S fracture systems in these rocks. Fractured granitic rocks in contact with the limbs and nosal parts of the folded iron ore series rocks often recorded higher radioactivity. These investigations have helped to mark out an area of 14,500 sq km for airborne high sensitivity gamma-ray spectrometric and magnetic surveys, and an area of 2522 sq km for digital image processing of Landsat data [1]. Linear Contrast Stretching has helped to discriminate fractured granitic rocks from the associated metasediments. But fractured migmatitic rocks could not be discriminated. This may possibly be due to the inhomogeneity of the gneisses as compared with the granites.

Scrutiny of data from the airborne gamma-ray spectrometric analogue charts indicates complete correlation of uranium and uranium-thorium sources anomalies with migmatitic and granitic rocks, as well as close association of anomalous zones with N-S and NW-SE fracture systems as was made out in the earlier integrated studies.

(C) Bhandara district, Maharashtra:

Yet in another part of Central India where airborne high sensitivity gamma-ray spectrometric surveys were carried out, detailed estimations of radioelements eU, eTh and K% (Table II) in different lithic units mapped from Landsat imagery analysis, have been found helpful in the precise delineation of uranium-bearing sandstone and perphyritic rhyolite (quartz porphyry) in the area.

TABLE II. MATERIALS USED

S. No.	Data source and format	Dharwars Southern India	Crystalline complexes Cent. India	Singhbhum Shear zone Eastn. India	Siwa-like N.India
1.	Available literature, maps and Topo sheets	Y	Y	Y	Y
2.	Orbital Data (Landsat)				
	a) M S S				
	i) Hard copy B/W; FCC	Y	Y	Y	Y
	ii) Band positive	N	N	Y	Y
	iii) 70 mm Chips	Y	Y	Y	Y
	iv) Diazo colour films	Y	Y	N	Y
	b) T M				
	i) Band positives	Y	N	N	N
	ii) FCC	Y	Y	N	N
	c) CCT (MSS) (4-Band digital data electronically processed, enhanced and ratioed)				
	i) Character printout	Y	Y	N	Y
	ii) FCC	Y	Y	Y	Y
	iii) Colour coded single band and/or Ratioed hard copy	Y	N	N	Y
3.	Airborne Data				
	a) Stereo photos (B&W)	Y	Y	Y	Y
	b) MSS (Visicorder -3 Bands)	N	N	Y	N
	c) Gamma-ray spectrometry and magnetics	Y	Y	Y	Y
	i) 4-Channel (U, Th, K and Total) Analogue Data	Y	Y	Y	Y
	ii) eU, eTh (ppm), K%, eU/eTh, eU/K, eTh/K and total count contour maps	Y	Y	Y	N
	iii) Total magnetic intensity contour maps	Y	Y	Y	N
4.	Other data				
	a) Gravity	Y	N	Y	N
	b) Field Spectroradiometer	N	N	N	Y

Note: Y = Used; N = Not used

Computer systems used: i) Landsat Data — HP-1000, M-DAS, PDP-11; DIPIX

ii) Aero-gamma-ray spectrometric and magnetic data — System -332

TABLE III. RADIOELEMENT DISTRIBUTION IN MAJOR ROCK UNITS, BHANDARA DISTRICT

ROCK TYPE	eU(ppm)*	eTh(ppm)*	K(%)*
ANDESITE	2	7	.6
SANDSTONE	4	10	1.2
GRANITE	4	23	1.6
PORPHYRITIC RHYOLITE	6	15	1.4
RHYOLITIC CONGLOMERATE	5	18	1.5

* Arithmetic Mean

LANDSAT IMAGERY INTERPRETATION AND AERO-GAMMA-RAY SPECTROMETRIC DATA

PARTS OF BHANDARA DISTRICT CENTRAL INDIA

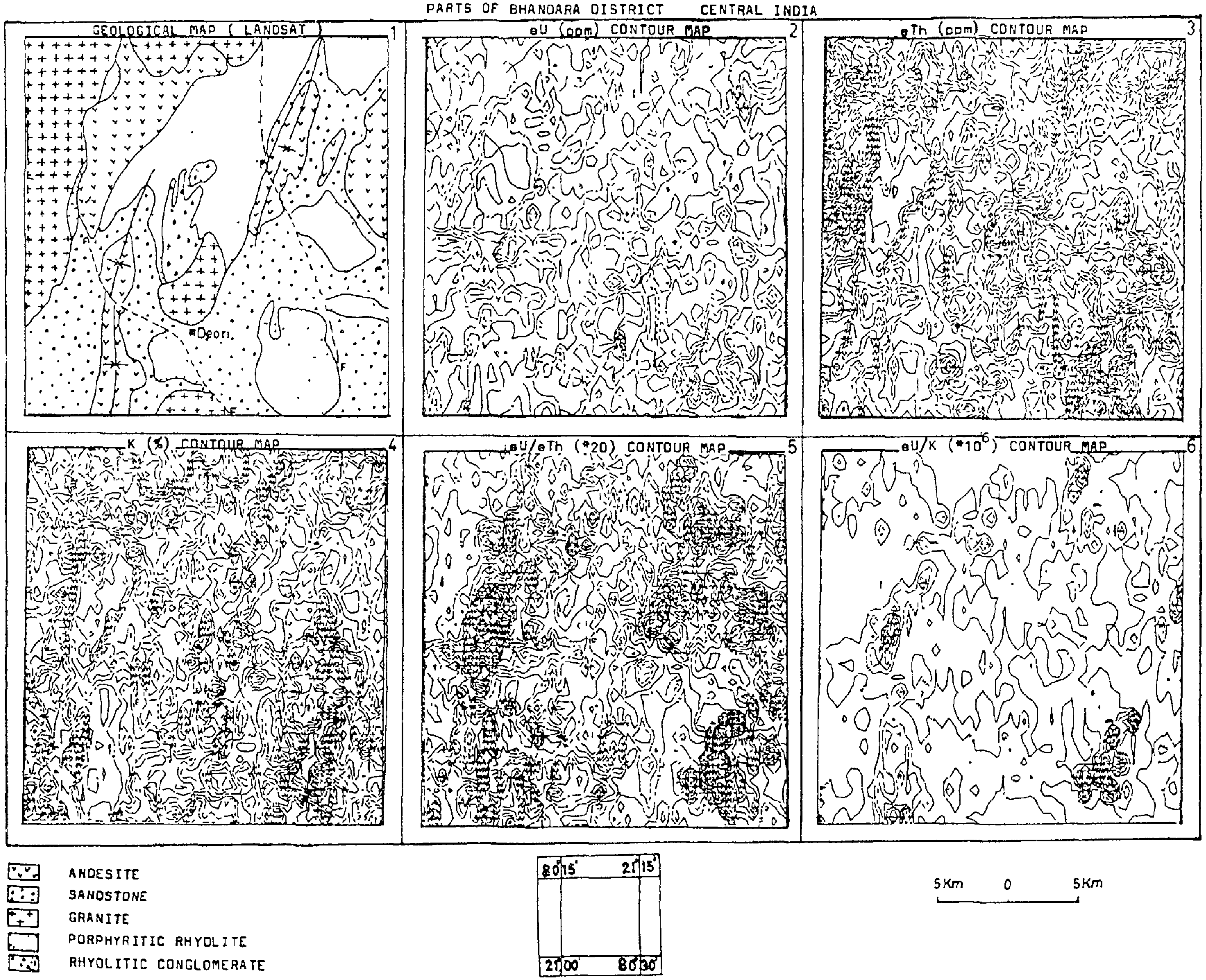

FIG.8.

Figure 8 shows Landsat imagery analysis of a fifteen fifteen minute quadrangle and the corresponding computer generated thematic maps of AGRS data in five parameters viz. eU, eTh, K, eU/eTh and eU/K. Integration of different data sets cleqrly brings out that the sandstone and porphyritic rhyolite are the most significant lithic units for uranium investigations in the area. Figure-9 shows an integrated map of geology and the three significant raciometric parameters, eU, eU/eTh and eU/K.

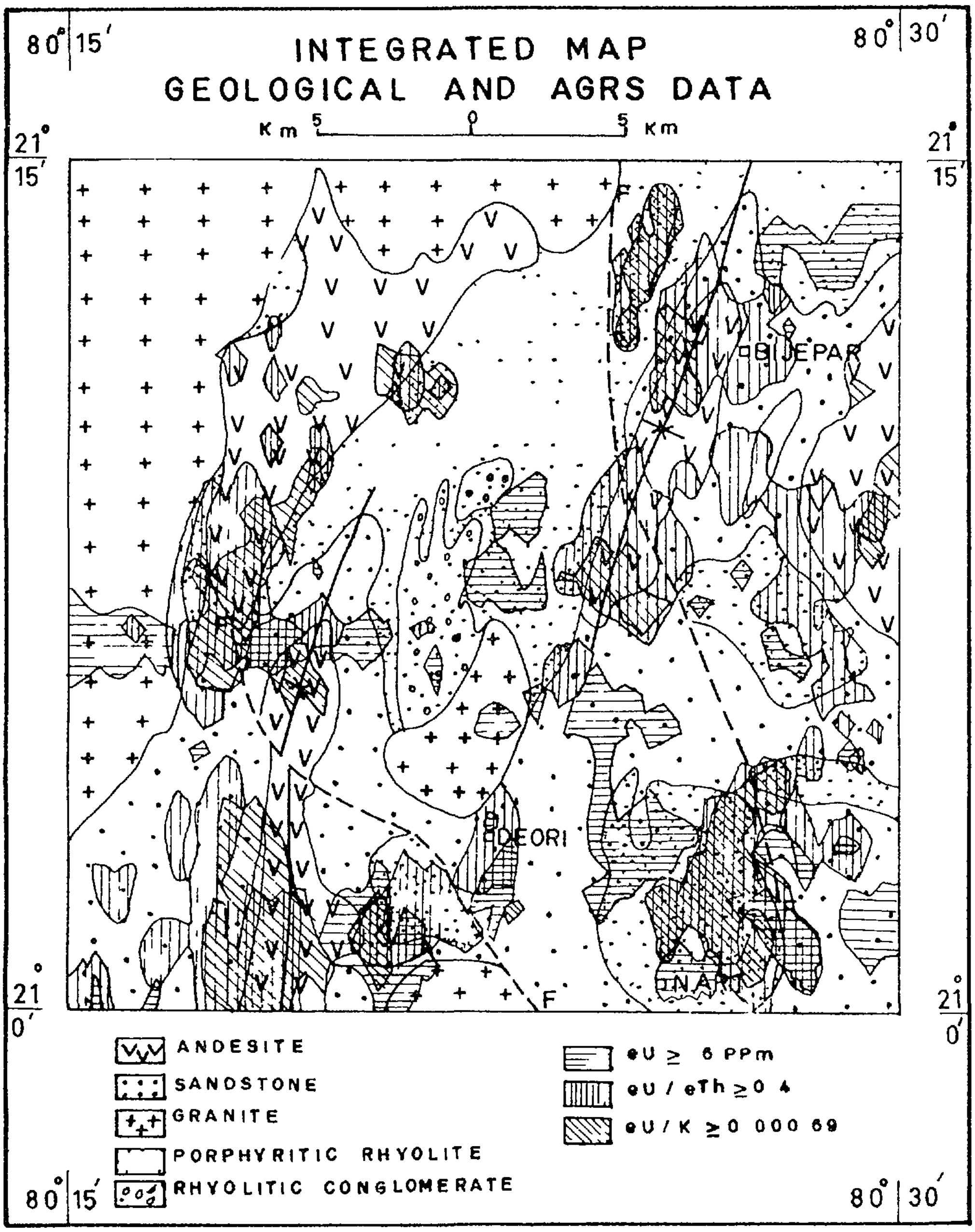

FIG.9.

4.3 Singhbhum Shear Zone, Bihar, Eastern India.

The Singhbhum metallogenic province represents a part of the poly-orogenic Precambrian crustal segment in the eastern parts of India. The area is dissected by two major shear zones of interest from the point of metallogeny. The most prominent one, the Singhbhum Shear Zone (SSZ), is the 200 km long arcuately disposed shear zone characterised by deep crustal fracturing, acid and basic volcanism and hydrothermal metasomatism. Cu, U, Ni, Mo and other element mineralization has been known to be closely associated with the SSZ. The tectonic setting of the (late Archaean) Singhbhum Craton with the associated (Proterosoic) mobile belts and the sedimentary basins associated with them, is clearly displayed in the synoptic Landsat scenes [12]. Figure 10 is a Landsat interpretation map integrated with aero-gamma-ray spectrometric anomalies. For a major part, the SSZ skirts around the granitic Singhbhum Craton to the north and more or less limits the southern boundary of the mobile belt [13]. Landsat analysis has brought to light several geological features which were not mapped earlier. The most significant is the delineation of extension of the SSZ and the associated Iron Ore Super Group (IOSG) rocks for another 20 km beyond Baharagora in the eastern sector, besides precise delineation of the entire shear zone itself which is quite significant from the point of uranium mineralization. The eliptical Singhbhum granitoid, the wedge-shaped Chakradharpur granitoid and the oval-shaped Kuilpal granitoid could also be mapped precisely.

Synthesis of AGRS data with various litho units has indicated that the older meta-volcano-sedimentary unit (Iron Ore Formation) in the IOSG is the most important uranium host rock closely associated with the SSZ. Other significant uraniferous lithic units

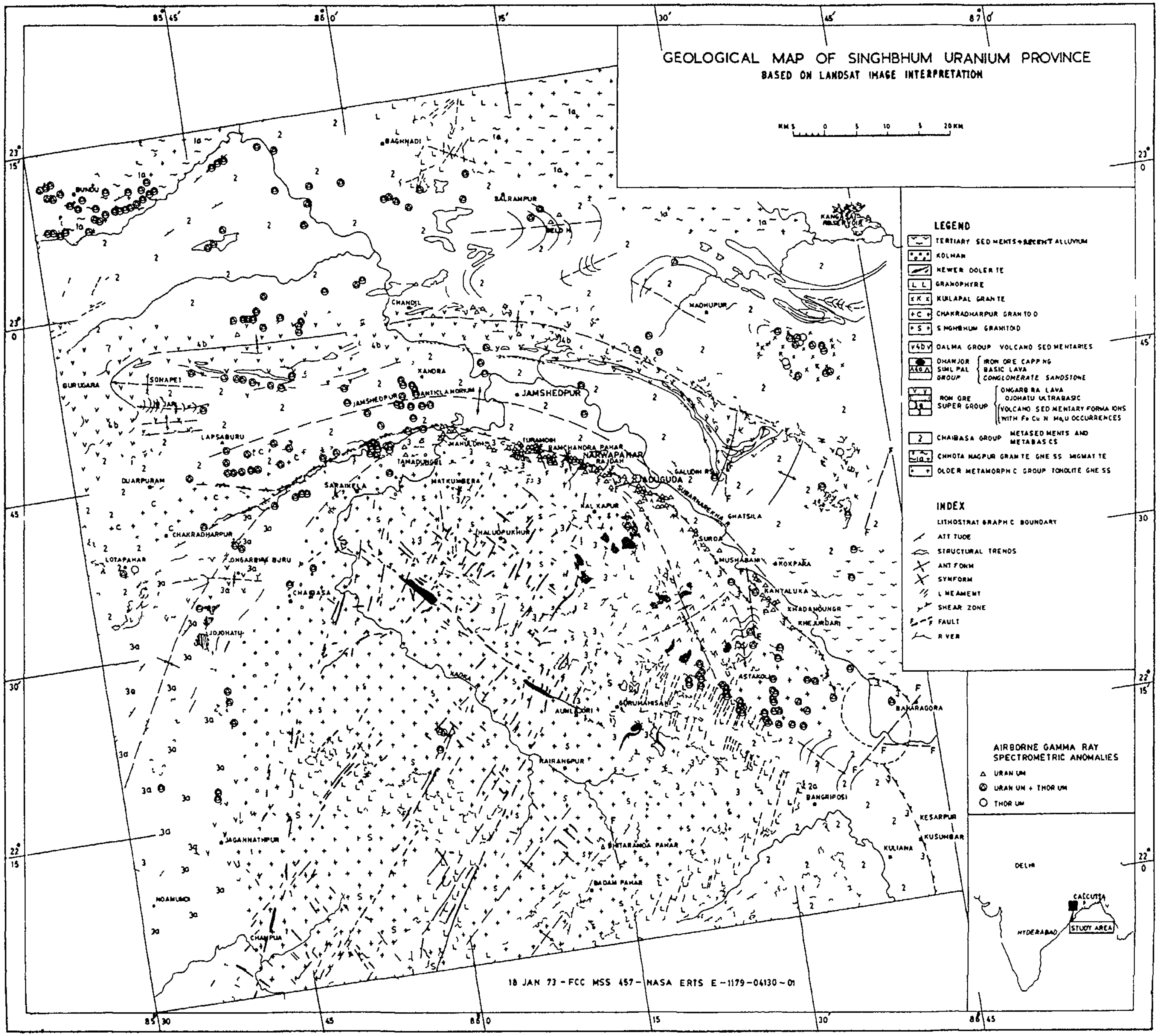
GEOLOGICAL MAP OF SINGHBHUM URANIUM PROVINCE
BASED ON LANDSAT IMAGE INTERPRETATION
KMS 0 5 10 15 20 KM
LEGEND
TERTIARY SEDIMENTS + RECENT ALLUVIUM
KOLHAN
NEWER DOLERITE
GRANOPHYRE
KULAPAL GRANITE
CHAKRADHARPUR GRANITOID
SINGHBHUM GRANITOID
DALMA GROUP VOLCANO SEDIMENTARIES
DHANJORI SIMLIPAL GROUP
IRON ORE CAPPING
BASIC LAVA
CONGLOMERATE SANDSTONE
IRON ORE SUPER GROUP
ONGARBIRA LAVA
OJOHATU ULTRABASIC
VOLCANO SEDIMENTARY FORMATIONS WITH Fe Cu Ni Mo U OCCURRENCES
CHAIBASA GROUP METASEDIMENTS AND METABASICS
CHHOTA NAGPUR GRANITE GNEISS MIGMATITE
OLDER METAMORPHIC GROUP TONOLITE GNEISS
INDEX
LITHOSTRATIGRAPHIC BOUNDARY
ATTITUDE
STRUCTURAL TRENDS
ANTIFORM
SYNFORM
LINEAMENT
SHEAR ZONE
FAULT
RIVER
AIRBORNE GAMMA RAY SPECTROMETRIC ANOMALIES
URANIUM
URANIUM + THORIUM
THORIUM
DELHI
CALCUTTA
HYDERABAD
STUDY AREA
JAMSHEDPUR
BAGHNADI
BALRAMPUR
BUNDU
CHANDIL
MADHUPUR
SONAPET
GURUGARA
LAPSABURU
DUARPURAM
CHAKRADHARPUR
LOTAPAHAR
ONGARBIRA BURU
CHAIBASA
JOJOHATU
SARAIKELA
MATKUMBERA
TAMADUNGRI
HALUDPUKHUR
JADUGUDA
NARWAPAHAR
RAKHA
GHATSILA
SURDA
MUSHABANI
KOKPARA
KANTALUKA
KHEJURDARI
ASTAKOLI
BAHARAGORA
BANGRIPOSI
KESARPUR
KUSUMBAR
KULIANA
RAIRANGPUR
BADAM PAHAR
JAGANNATHPUR
NOAMUNDI
CHAMPUA
18 JAN 73 - FCC MSS 457 - NASA ERTS E-1179-04130-01

FIG.10.

are the carbon phyllites in the Dalma Volcanics and the basal conglomerate-sandstone horizon in the Dhanjori Basin. Delineation of these sub-stratigraphic units which was not possible from Landsat analysis has been accomplished through large scale (30,000) air-photo-interpretation duly aided by visicorder data on the same scale from airborne MSS surveys. Minor shears and other structural linears appearing to have local control on uranium mineralization have been identified from a synthesis of photogeological and AGRS data. Surficial indications show that the highly radioactive Kuilapal granitoids are predominantly thoriferous [13].

The mutual complementary nature of aeromagnetic data to Landsat data and vice-versa has been well-exemplified in this area. Integration of magnetic anomaly patterns as recognised on the total intensity aeromagnetic contour maps broadly confirms the delineation of various litho-stratigraphic units, the SSZ, several major structural trends and fold patterns from Landsat analysis (Fig. 11). The Iron Ore Formation which is composed predominantly of mafic, ultramafic and volcano-clastic sediments hosting uranium mineralization is well-marked by high amplitude contours, and its contacts with the underlying granitoids could be precisely marked and its persistence in depth could be quantitatively estimated. Intricate fold patterns in the Dalma volcanics delineated from Landsat are well-matched by the high amplitude magnetic contour patterns which also suggest probable northern extension of the folded (anticlinal) strata abutting the overlying Chaibasas. Here the Landsat and field data indicate abrupt and of the Dalmas due mostly to soil and alluvial cover. Hence sub-surface continuity of the Dalmas under the cover is postulated. Low amplitude contours define the granitic bodies and the sub-surface extension of Kuilapal granitoids under shallow

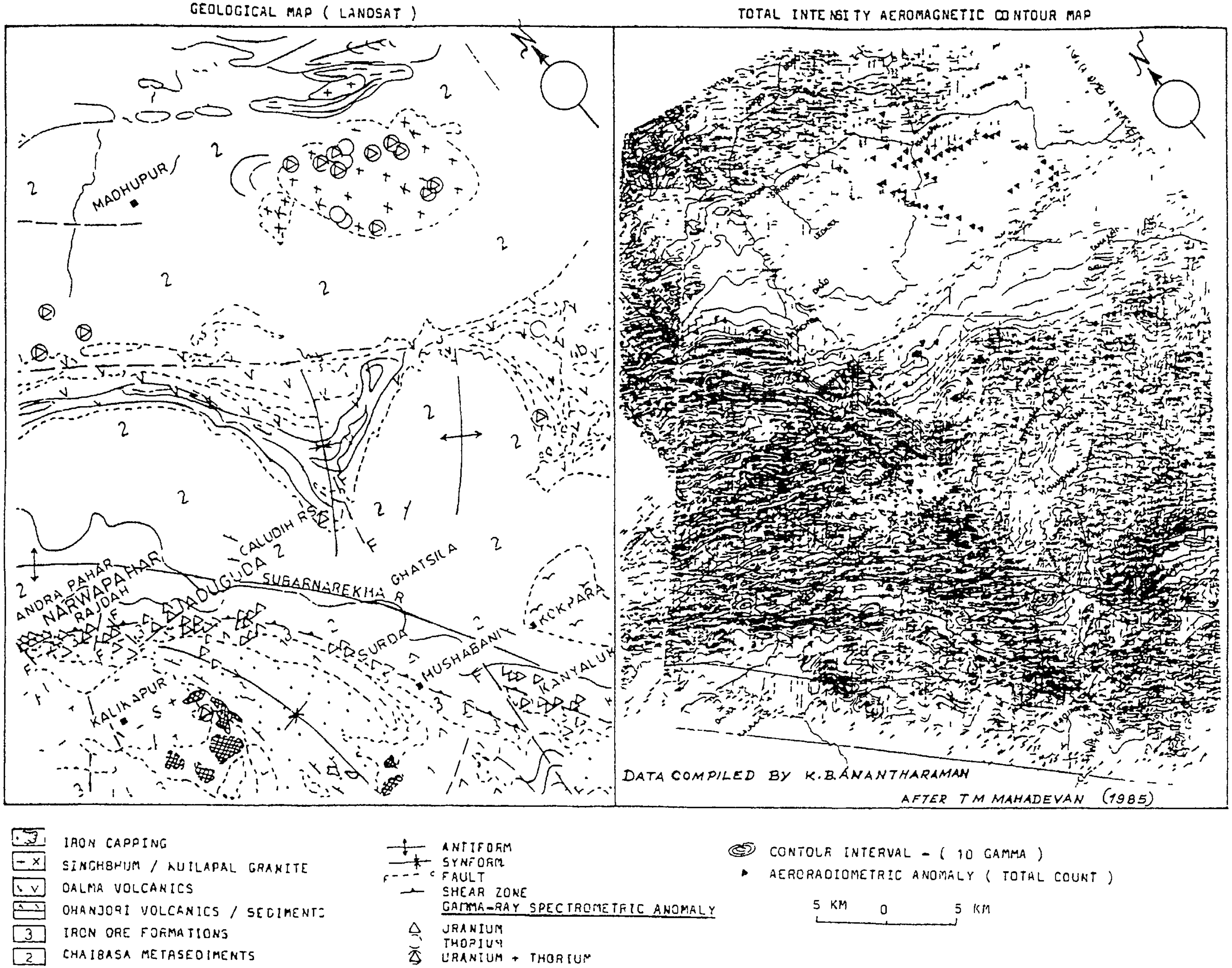
GEOLOGICAL MAP (LANDSAT)
TOTAL INTENSITY AEROMAGNETIC CONTOUR MAP
MADHUPUR
CALUDIH RS
ANDRA PAHAR
NARWAPAHAR
RAJDAH
JADUGUDA
SUBARNAREKHA R
GHATSILA
SURDA
MUSHABANI
KCKPARA
KANYALUKA
KALIKAPUR
DATA COMPILED BY K.B.ANANTHARAMAN
AFTER T M MAHADEVAN (1985)
IRON CAPPING
SINGHBHUM / KUILAPAL GRANITE
DALMA VOLCANICS
DHANJORI VOLCANICS / SEDIMENTS
IRON ORE FORMATIONS
CHAIBASA METASEDIMENTS
ANTIFORM
SYNFORM
FAULT
SHEAR ZONE
GAMMA-RAY SPECTROMETRIC ANOMALY
URANIUM
THORIUM
URANIUM + THORIUM
CONTOUR INTERVAL - (10 GAMMA)
AERORADIOMETRIC ANOMALY (TOTAL COUNT)
5 KM 0 5 KM

FIG.11.

cover towards west and south is clearly indicated by these low amplitude contours.

Since uranium mineralization is often associated with iron staining and red (hydrothermal) alteration, it may be possible to delineate such areas through digital processing of airborne MSS data [14] with resolution of 5-6 meters. An area of 540 sq km is selected for computer processing of digital MSS and AGRS data to delineate such altered areas as well as confirm anomalous areas already delineated through visual integration techniques. Since the surface expression of altered areas is not large, digital Landsat MSS data (with resolution of 79 meters) will not be useful for such studies.

4.4. Siwaliks of Himachal Pradesh, Northern India:

The tertiary Siwalik fluviatile molasse deposited along the long narrow trough developed between the rising Himalayas and the Peninsular mass, often referred to as the "Himalayan foredeep", hosting significant uranium mineralization has been the scene of active prospection for the last several years [15]. Helicopter-borne regional gamma-ray spectrometry, ground reconnaissance radiometrics and regional geochemical sampling have brought out a general picture of radioelement distribution in the area. Detailed ground follow-up has shown that the sandstone formation in the transition zone between the middle and the upper Siwaliks are mineralized. Landsat analysis and photogeological studies of selected areas have indicated the possibility of the transition zone being delineated on spectral reflectance characteristics. These studies have readily helped the local exploration programme by furnishing vital structural information in the difficult rugged terrain and prompted field spectro-radiometric (0.4-1.1 μm) surveys in the area.

A small area (512 pixels X 512 lines) was selected for digital processing of Landsat MSS data. A false colour composite (blown up to 62,500 scale) generated from linear stretched bands (4,5 & 7) was found to contain very valuable information on lithological boundaries, disposition of thrusts and faults and fold geometries, all of which could be utilized to correct the existing maps, and integrated with the known uranium mineralization. The transition zone, the favourable lithic units, specific thrust zones and synclinal structures associated with mineralization have been identified. This experiment in a known area near Hamirpur will go a long way in assessing the potentialities of the entire Siwalik foot-hill range running for several hundred kilometers, perhaps in a quite short period. Accordingly, a programme for the entire Siwalik belt with the definite aim and firm conviction of delineation (i) Transition Zone, (ii) Thrust zones, (iii) Synforms and (iv) favourable lithic units, has been initiated.

Field spectro-radiometer studies carried out on an experimental basis indicate that it may be possible to distinguish the host rocks (sandstone) exhibiting 20% - 30% reflectance characteristics at 0.9 μm (Fig. 12 E & F) from the other surface materials in the transition zone.

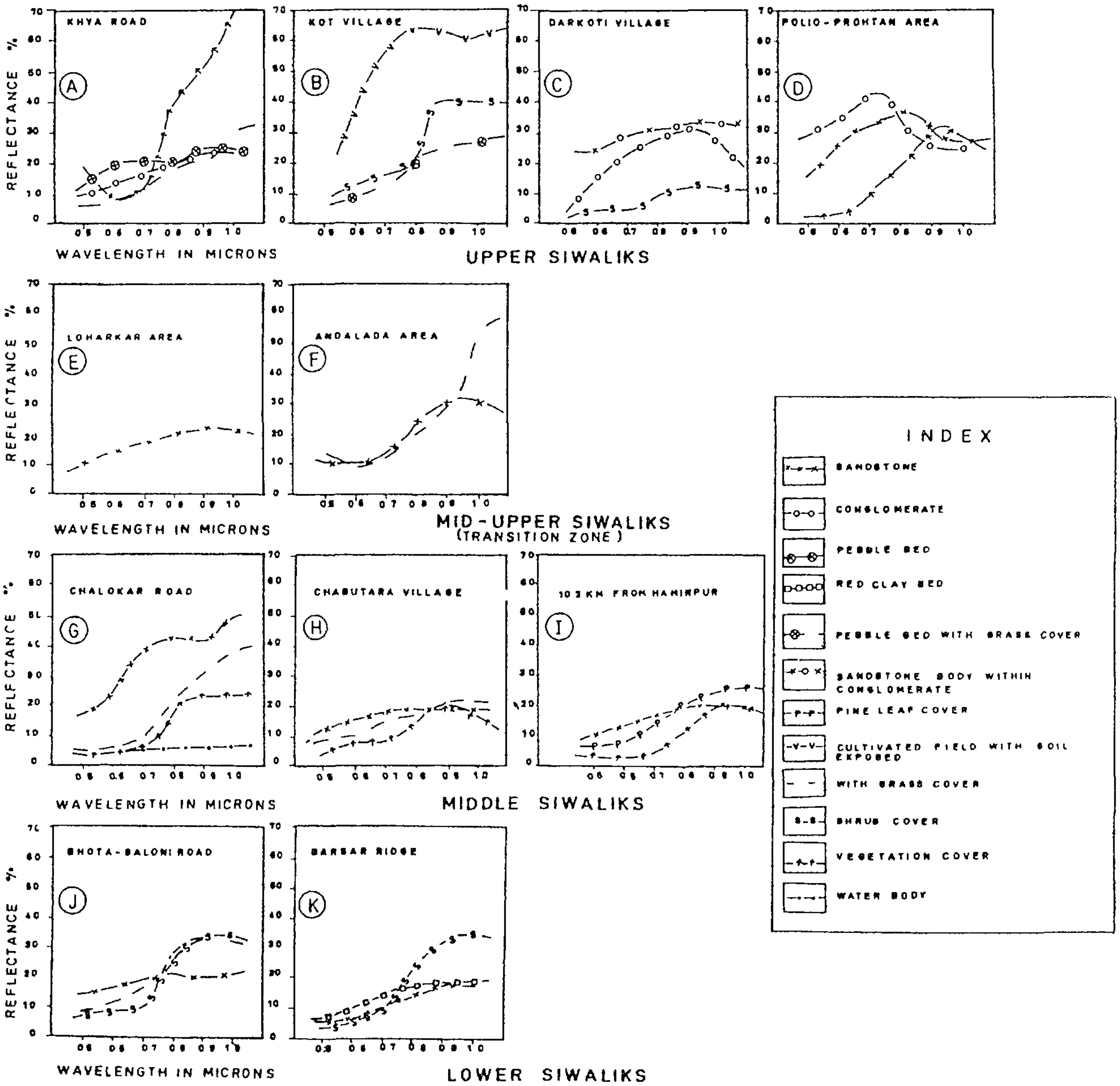

FIG.12. Field spectral data
Hamirpur-Nadau Tract (H.P.).

5. CONCLUSION

The usefulness of Landsat data in the selection of geologically favourable target areas for limiting the expensive airborne geophysical surveys as well as in formulating meaningful exploration guides for undertaking investigations in geologically analogous areas has been demonstrated. That proper integration of litho-structural information that could be extracted from Landsat imagery interpretation and photogeological studies, with data from other conventional techniques like airborne gamma-ray spectrometry and magnetometer at different phases of uranium exploration could considerably accelerate the pace of investigations in different geological environments has been amply evident from the above case histories, although it is difficult to estimate quantitatively the anormous savings made in the turn-around time, manpower and money through such integrated approaches. It is also evident that further savings in time and manpower can be affected if such laborious integration processes now being undertaken manually, are carried out through computer processing. Thus remotely sensed data from orbital and aerial platforms if properly applied and diligently integrated with other geoscience data sets constitute an effective tool in uranium exploration programme.

ACKNOWLEDGEMENTS

The authors express their sincere thanks to Shri T.M. Mahadevan, Director, AMD, for his sustained interest and encouragement in the application of remotely sensed data in uranium exploration programme and for valuable suggestions during the preparation of this paper. The authors are very grateful to the Department of Atomic Energy for permission to present the paper. The authors also express their thanks to their colleagues in the Airborne Survey, Photogeology and Remote Sensing Group for useful discussions and cooperation during the preparation of the paper. Typing of the paper by Shri K.S. Murthy, preparation of diagrams by Shri M.R. Murthy and photographic work by Shri D.S.R. Prasad are gratefully acknowledged.

REFERENCES

1. Darnley, A.G., Airborne Gamma-ray Survey Techniques - Present and Future; Uranium Exploration Method (IAEA, PL-490/15, Vienna) (1973) 67-108.

2. Tewari, S.G., Nagaraja, K.N., Surya Kumar, N.V., Data enhancement techniques for airborne gammaray spectrometric data, IAEA, Tech. Com, Vienna (1986) (Personal communication).

3. "Remote Sensing in Uranium Exploration, Basic guidance", Tech. Rep. series 208, IAEA, Vienna (1981).

4. Saunders, D.F., and Potts, M.J., Manual for the Application of NURE 1974-1977, "Aerial Gamma-Ray Spectrometer Data ERDA" Open File GTBX-13(78), (1978).

5. Potts, M.J., Computer methods for geological analysis of radiometric data in "Exploration for Uranium Ore Deposits"; (Proc. Series, IAEA, Vienna) (1976) 55-69.

6. Mahadevan, T.M., Space-time controls in Precambrian Uranium Mineralization in India; Jour. Geol. Soc. Ind., Bangalore 27, (1986) 47-62.

7. Radhakrishna, B.P., "Archaean Granite-Greenstone Terrain of the South Indian Shield", Precambrian of South India, (Proceedings of the INDO-US Workshop, Hyderabad (1982) 1-46.

8. Kak, S.N., Perumal, N.V.A.S., Rao, S.R.S.N., Krishnamoorthy, B., and Phadke, A.V., "Three case studies illustrating the use of Remote Sensing Techniques in Uranium exploration"; (NNRMS Nat. Sem., Hyderabad) (1983) III-50, 51, 52-1 to 15.

9. Moore, G.K., Objective procedure for lineament enhancement and extraction; Photogram. Eng. and Remote Sensing (1983); 49, 5, (1983) 641-647.

10. Krishnamoorthy, B., Rao, S.R.S.N. and Perumal, N.V.A.S., "Remote Sensing Applications in Uranium Exploration", (Proc. symp. on Remote Sensing for Hydrology, Agriculture and Mineral Resources, S.A.C., ISRO, Ahmedabad M-10 (1977) 177-182.

11. Perumal, N.V.A.S., Rajagopalan, V, and Phadke, A.V., Geological Mapping and Discrimination of Mineralised Granite and Migmatite Areas from Remotely Sensed Data Analysis and Correlation of Radioactive Occurrences in Chandrapur - Gadchiroli Area, Maharashtra, India", (Sixth Asian Conference on Remote Sensing, Hyderabad) (1985) 324-328.

12. Mahadevan, T.M., "Characterisation and Genesis of the Singhbhum Uranium Province, India", IAEA Technical Committee Meeting on Recognition of Uranium Provinces, London) (1985) (In Print).

13. Perumal, N.V.A.S., Shanti Kumar, C., and Mahadevan, T.M., "Integrated Multisensor Airborne Remote Sensing and Landsat Studies in Singhbhum Uranium-Copper Belt, Bihar, India"; (Sixth Asian Conference on Remote Sensing, Hyderabad) (1985) 593-598.

14. Rowan, L.C., Goetz, A.F.H., and Ashley, R.P., Discrimination of hydrothermally altered and unaltered rocks in visible and near infrared multispectral image; Geophysics, 42, (1977) 522-535.

15. Kak, S.N., Perumal, N.V.A.S., and Mahadevan, T.M., "Sedimentary Environments, Uranium Mineralization and Remote Sensing" (Abstract), (Ind. Asso. of Sedimentologists, Hyderabad) (1985) 67-68.

URANIUM EXPLORATION IN THE PRECAMBRIAN OF WEST GREENLAND USING INTEGRATED GAMMA SPECTROMETRY AND DRAINAGE GEOCHEMISTRY

(Summary)

A. STEENFELT
Geological Survey of Greenland,
Copenhagen, Denmark

In the past decade the Geological Survey of Greenland has undertaken uranium exploration in West and South Greenland. At a reconnaissance level the principal methods used are airborne gamma spectrometry (contour flying with average flight line density of 2 km, ground clearance 100 m) and low density sampling of stream sediment (analyzed for U by delayed neutron counting, and 18 other elements by X-ray fluorescence) and stream water (analyzed for U, pH and conductivity).

Both the gamma spectrometry and the geochemistry show that South Greenland is enriched in uranium and thorium (fig. 1 and 2). Further exploration in South Greenland lead to the discovery of three types of uranium mineralization.

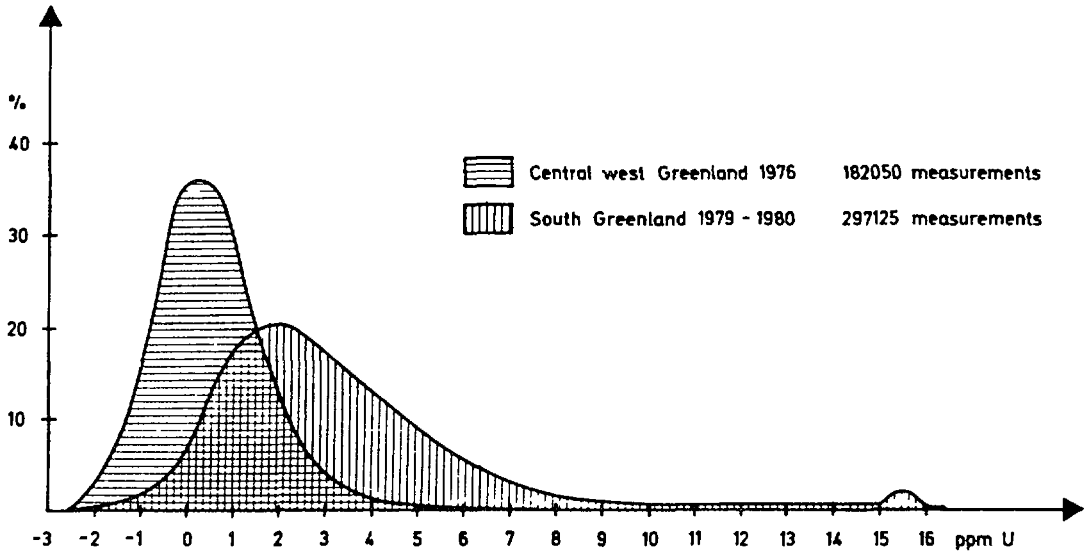

FIG. 1. Frequency distributions of eq U in gammaspectrometric surveys in the Precambrian of West Greenland and South Greenland.

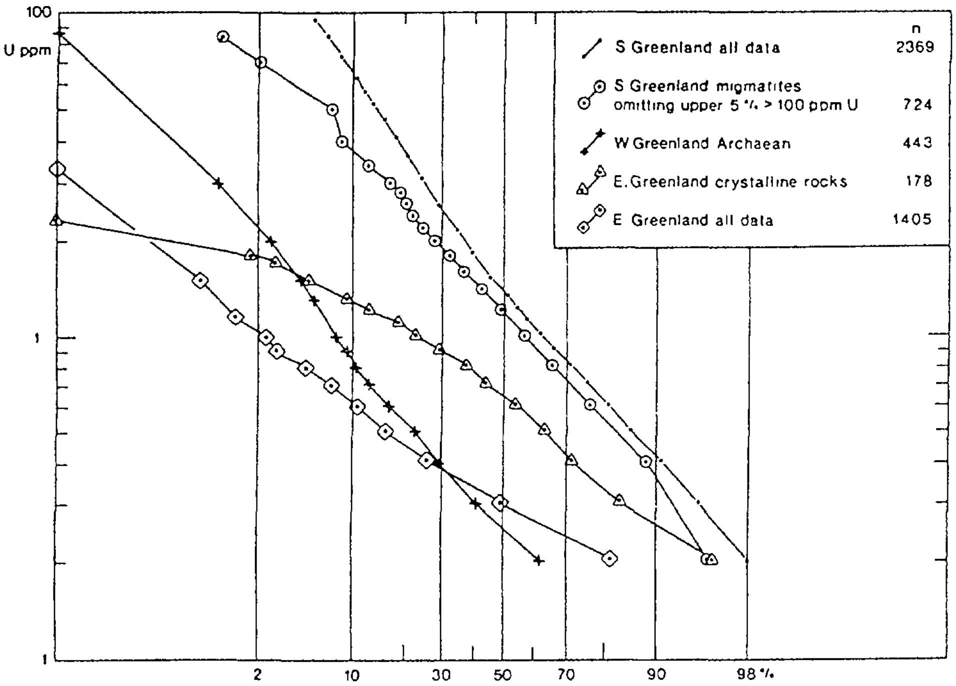

FIG. 2. Cumulative frequency distributions of U in the fine fraction of stream sediments from East Greenland, West Greenland, and South Greenland.

The airborne gamma spectrometry map for eq. U (fig. 4) and eq. Th show large anomalies over two of the alkaline intrusive bodies (I and M on fig. 3). Both intrusions are well exposed and contain uranium deposits of the disseminated magmatic type.

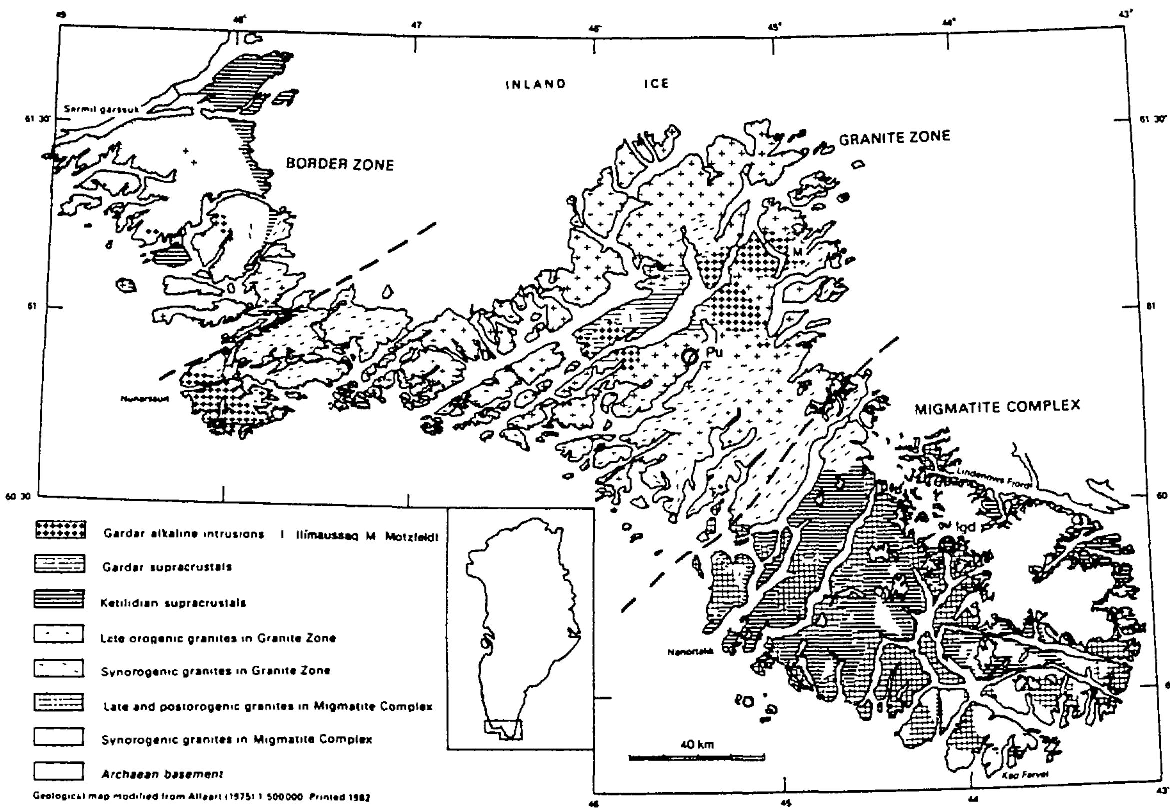

FIG. 3. Simplified geological map of South Greenland, modified after Allaart.

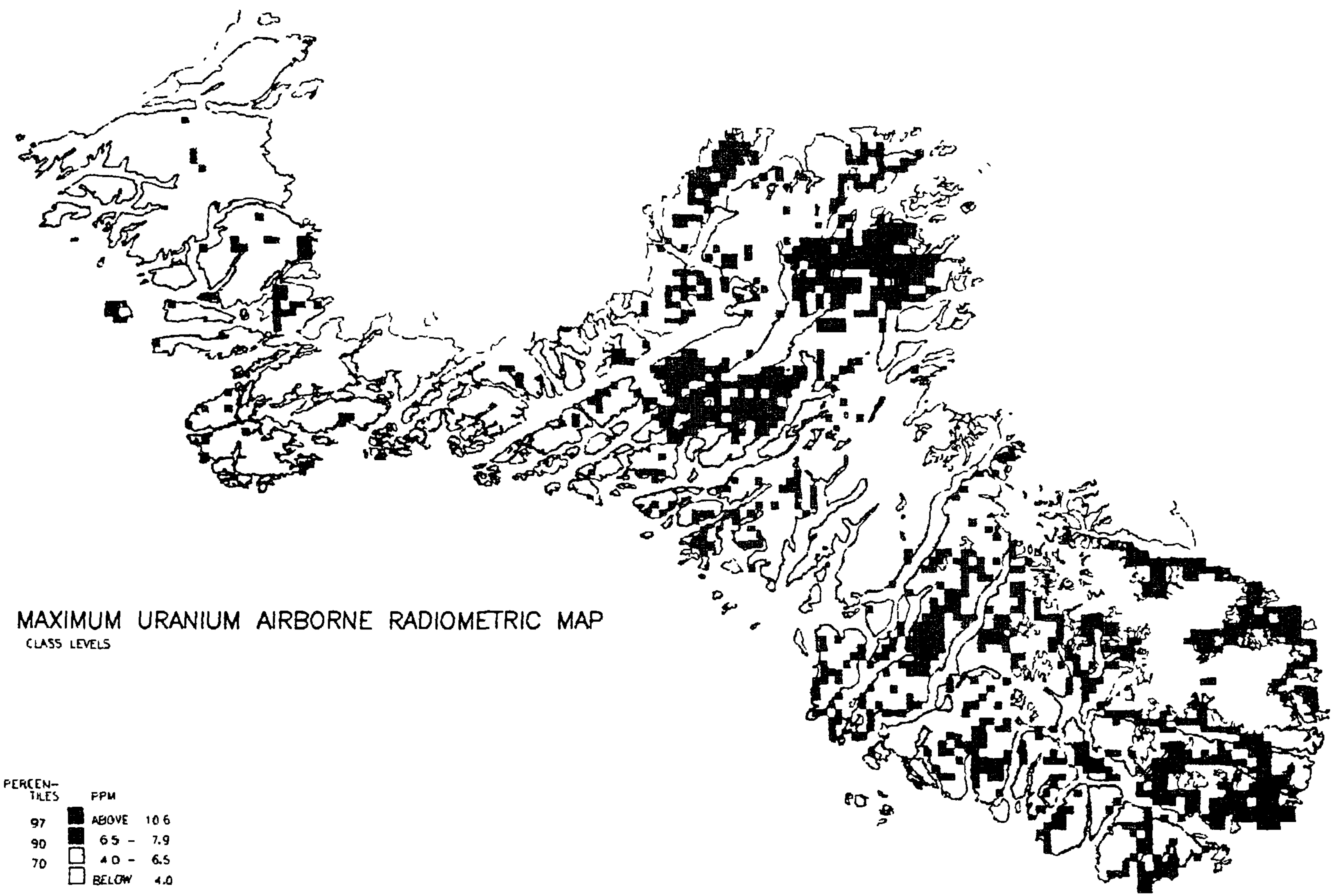

FIG. 4. Maximum uranium values from the airborne gamma-spectrometer data in each 2 km × 2 km cell in South Greenland. From Armour-Brown et al.

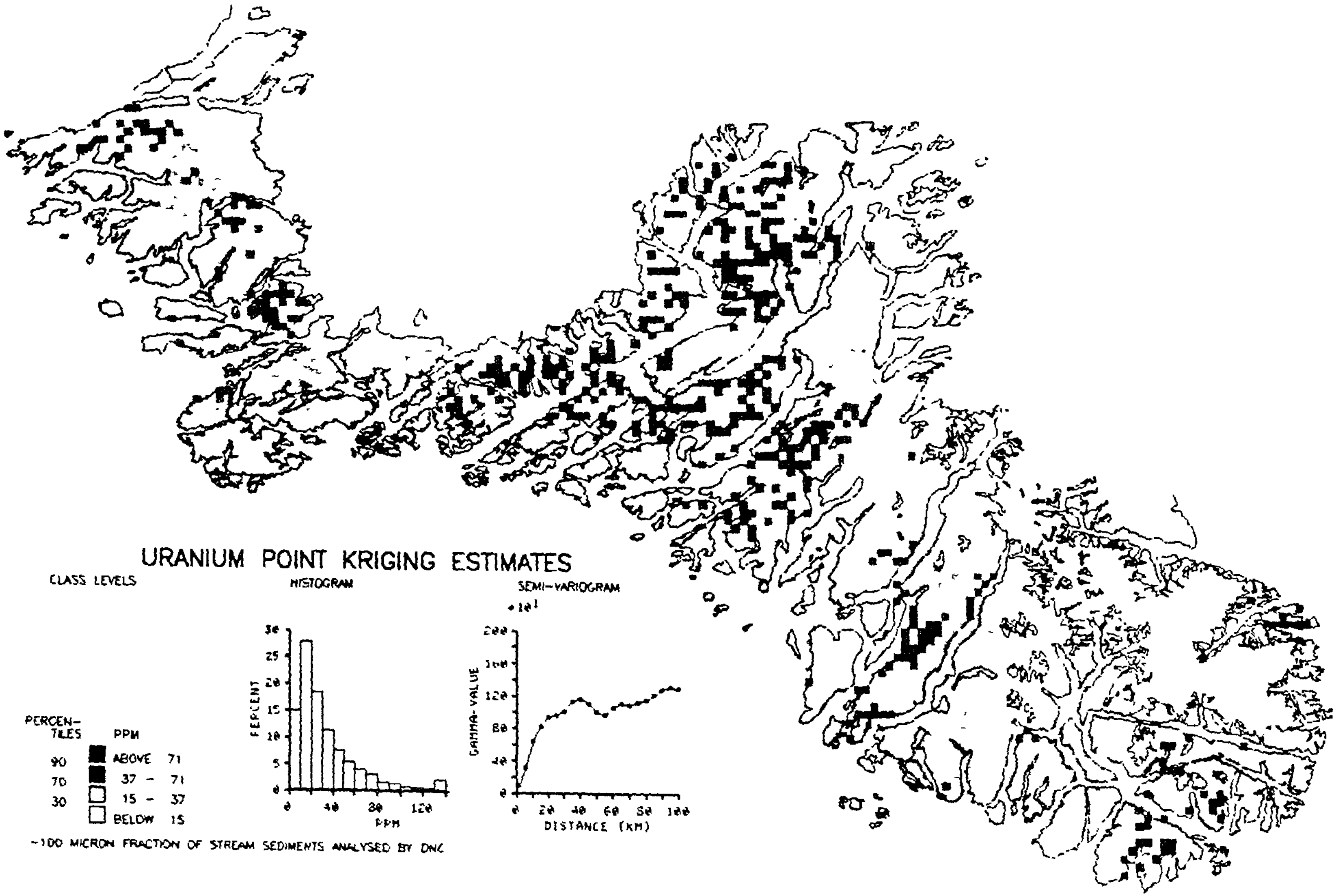

FIG. 5. Uranium in stream sediment in South Greenland smoothed by point kriging. From Amour-Brown et al.

The two magmatic disseminated deposits are also distinguished by high Nb values recorded in stream sediment, wheras the response in the uranium values in stream sediments is very weak (fig. 5).

The distribution pattern for uranium in stream sediment (fig. 5) is very different from the pattern shown by eq. U. High values occur in the Granite zone (fig. 3), and they reflect the occurrence of vein type uranium mineralization. The same pattern is also shown by the uranium in stream water, which shows the presence of soluble uranium (pitchblende). The pitchblende localities discovered so far are shown in fig. 6.

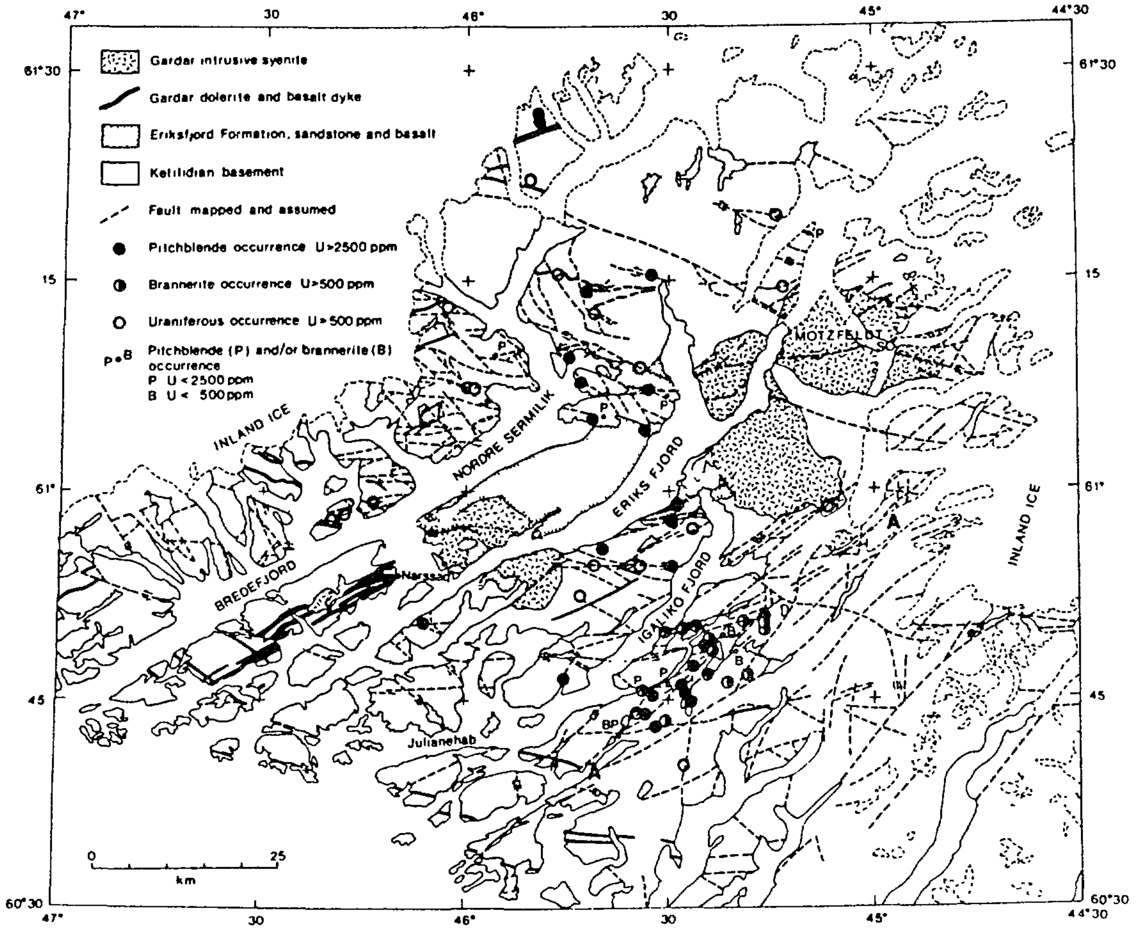

FIG. 6. Faults and lineaments and vein type uranium occurrences in the Granite Zone, South Greenland.

The sedimentary hosted uranium pitchblende mineralization in the Migmatite complex (fig. 1) is reflected both in the gamma spectrometry survey and the stream sediment survey (fig. 5) by scattered occurrences of local anomalies, some very strong. Fig. 7 shows the geological setting of one of the mineralized occurrences found.

The three types of uranium mineralizations can be distinguished by studying the differences in the distribution patterns for uranium and other elements as recorded on a regional scale by gamma spectrometry and drainage geochemistry respectively.

By computer integration of various kinds of exploration data it is important to preserve the information lying in these differences of the distribution patterns.

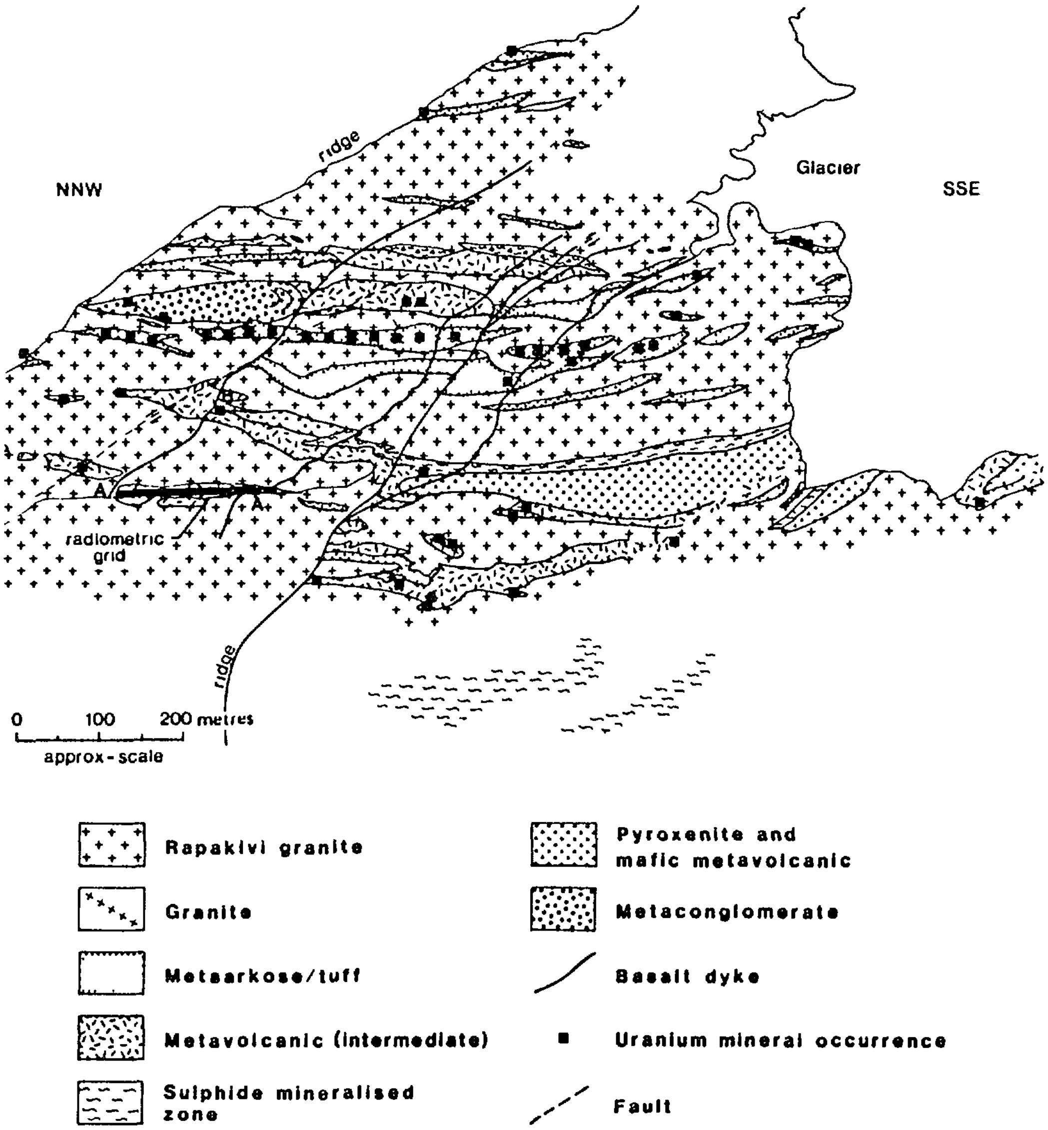

FIG. 7. Sketch of the geological setting at the Igdlorssuit uranium mineralization in the migmatite complex, South Greenland.

ANALYSIS OF INTEGRATED GEOLOGIC DATA FOR URANIUM EXPLORATION IN EGYPT

M.E. MOSTAFA
Nuclear Materials Corporation,
Cairo, Egypt

Abstract

Geologic information system(GIS) related to Nuclear Raw Materials is in current development in the Scient. Inform. Dept.(NMC). Processing of data follows developed criteria in U-exploration.

Two case studies are presented :

CASE 1 : TECTONICS OF THE FRACTURES BEARING U-MINERLIZATION IN THE YOUNGER GRANITOIDS, CENTRAL EASTERN DESERT (CED), EGYPT.

Landsat image interpretation, photo lineaments, field measured joints, faults, folds, foliation, lineation, and deformed pebbles when properly integrated and computerized have pointed out a comperhensive tectonic model related to the CED of Egypt.

The area seemed to be subjected to three deformative stages, in the first two; rocks undergone plastic deformation, while in the third one, rocks failed in brittle mode where the Red Sea Transevrse Tectonic Trend (ENE - WSW) was developed intersecting the older plastically developed linear elements (NW-SE). Further rejuvenations permit opening the mentioned fractures and occupied by siliceous materials and jasperoid viens and lastly by U-type mineralization,best depicted in the plutons of El Missikat, El Erediya, Um Had and Kab Amiri.

CASE 2 : FACTORS CONTROLLING U-DISTRIBUTION IN THE OLIGOCENE CARBONACEOUS SHALE, NORTH WESTERN DESERT (NWD), EGYPT.

The Oligocene Qatrani Formation, north of Lake Qarun, NWD of Egypt is a typical example of fluviatile deposits. The middle clayey member is enclosed between two porous sandy members. The carbonaceous shale related to the clayey member shows abnormal U-concentrations.

Statistical analysis of the distribution of uranium and other trace elements in the carbonaceous shale shows that U,Y,Mn and Ca obey the lognormal law while Sr,Rb,Zr,Cr and Ti obey the normal law. A geologic factor is derived that normally distributed elements are stationary, indeqinous probably of detrital origin. Meanwhile, other lognormally distributed elements are active and mobile. Subsurface mapping shows that uranium tends to concentrate in the troughs of the flexured carbonaceous shale suggesting an epigenetic origin.

CASE 1
TECTONICS OF THE FRACTURES BEARING U-MINERALIZATION
IN THE YOUNGER GRANITOIDS, CENTRAL EASTERN DESERT (CED), EGYPT

INTRODUCTION

In the last few decades, the Central Eastern Desert of Egypt (Plate 1) was chosen on the basis of some field criteria for intensive geologic and radiometric studies.

The first systematic aeroradiometric survey in the area was conducted by the airborne team of the Nuclear Materials Corp. in 1970 (Ammar, 1973). This is followed by detailed surface and subsurface mapping and mining working in some selected targets at the plutons of El Erediya (El Kassas, 1974) and El Missikat (Bakhit, 1978).

The intensive ground geologic and radiometric studies are put under the disposal of the Scientific Information Dept. at the Corporation. Field measured structures including joints, faults, foliations, lineations, deformed pebbles and minor folds all are statistically treated and refined using computer programs designed for this purpose.

The available geologic and radiometric information all are compiled on a base map of satellite images scale 1 : 250,000 (Plate II) Folding analysis of foliations yields the alligned pattern of fold axes located on the map. In addition, lineations, deformed pebbles and mesoscale folds measured in W. Atalla area are treated for preferred orientation. Azimuthal analysis using overlap technique are applied to screen out significant trends of photolineaments and joints measured in younger granitic plutons e.g. Um Had, El Erediya, El Missikat, El Fawakhir and Kab Amiri.

DISCUSSION

The concerned part of the C.E.D is mainly covered with basement rocks as shown on the regional map (Plate II).Folded beds and or foliations were measured in W. Ziedon (El Ghawaby, 1973), W. Arak (Assaf, 1979), W.Kariem South Atalla area (Mostafa, 1979) and W.Atalla (El Kassas,1974).
These planar elements were analyzed to get the principal axes of folding after successive rejection of poles that are significantly deviates from being plotted on the fold girdle.

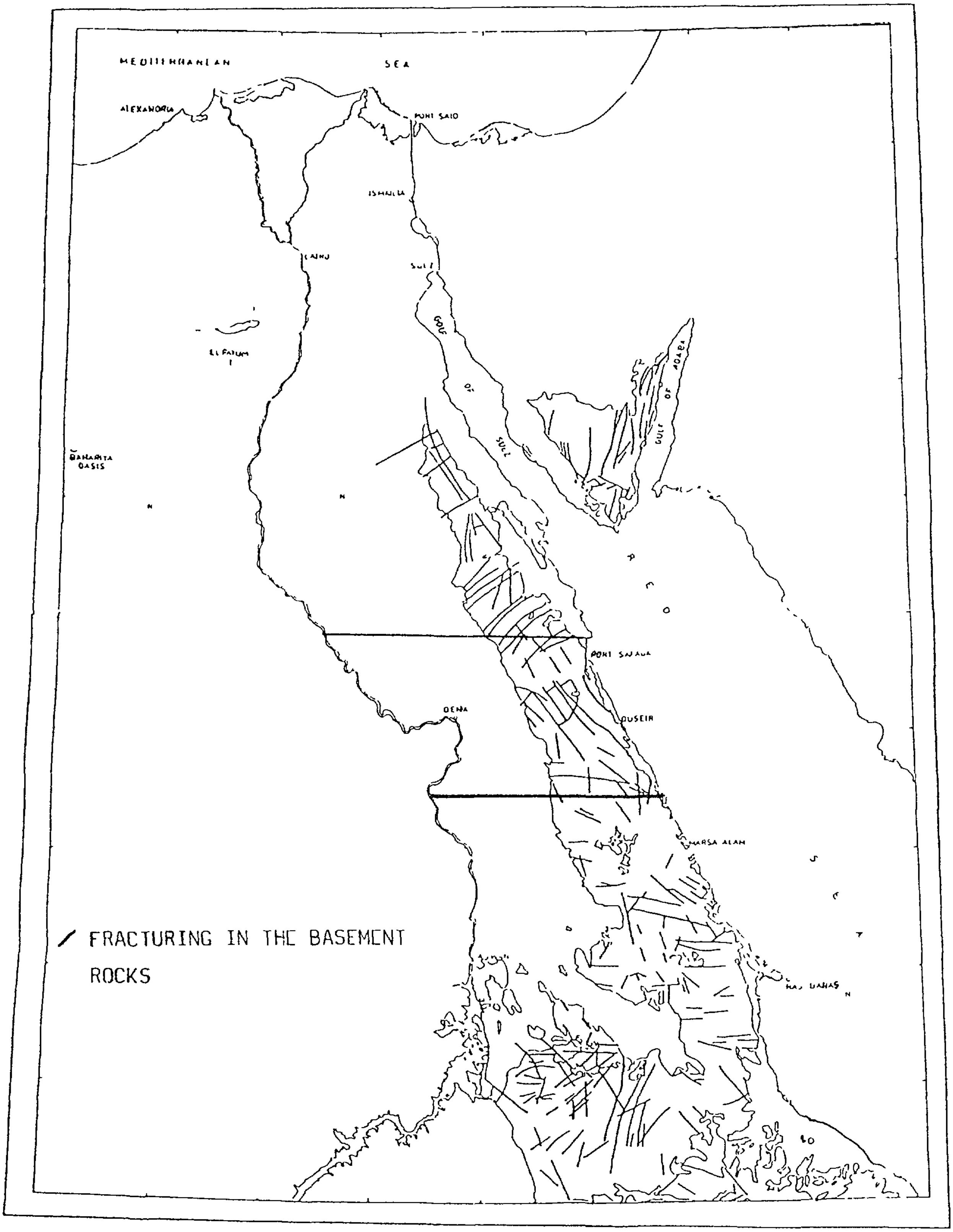

PLATE I. Location of the Central Eastern Desert, Egypt.

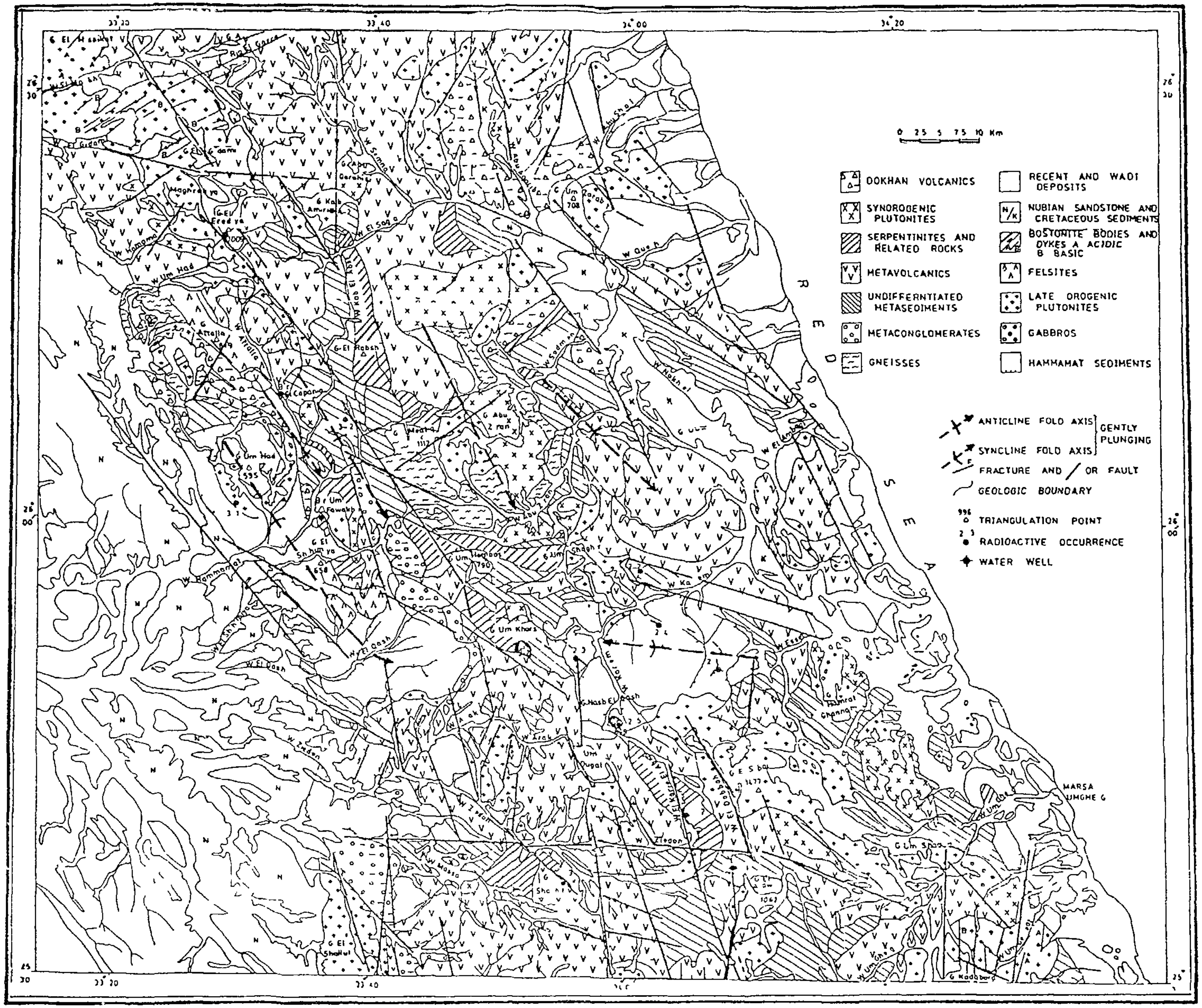

PLATE II. Geologic–structural map, Central Eastern Desert.

However the tectonic history in the area is well imprinted on structural elements (foliations and lineations) penetrate mainly the texture of the metasediments and to some extent the Hammamet sediments.

Folds in the present study are scaled into large scale,mesoscale and minor folds. In the first two scales folding axes are computed from the measured planars, while the last one ; the axes are directly measured.

Major fold axes in the area are shown plotted on the regional map (Plate II). Mesoscopic folds, lineations and deformed pebbles are shown on Plates (III, IV, V, VI).

The overlap technique used by Mostafa (1979) is a good method for azimuthal analysis of photolineaments and strike direction of field measured fractures. It permits enhancement of peak to noise ratio and to pick up significant trends at a given level of significance.

Significant trends of photolineaments are thus shown in plate (VII) and counted twice, by number and by length. The fractune pattern has mainly two trends. The NW-SE is by far the large scale trend and frequently found along the regional folding hinge and accompanied by thrusting. The other NE-SW to ENE-WSW is small scale subpenetrative closely spaced trend, mostly occupied by younger dykes and veins.

Significant trends of joints measured in some younger granitoids and felsite bodies are shown in Plate (VIII). In addition the N-S fractune trend are clearly depicted. The same trend is also reported at Um Had pluton (Plate IX) where the N-S and FNE-WSW trends are most frequently occupied by hematitization and radioactivity.

The fracture pattern at El Missikat pluton and the surrnounding is shown in Plate (X). The ENE-WSW is by far a sound trend. According to Bakhit (1978), veinletts of secondary U-mineralizations are reported along the nominated fractures when crossing longitudinally some of the aplite dykes and jasperoid veinlettes.

The other N-S set of fractures at Elerediya pluton was found occupied by jasperoid veins with further longitudinal fractures invaded by secondary U-mineralizations. The same setting is less reported along ENE-WSW (El Kas (El Kassas, 1974).

Text continued on p. 182.

SOUTH ATALLA AREA

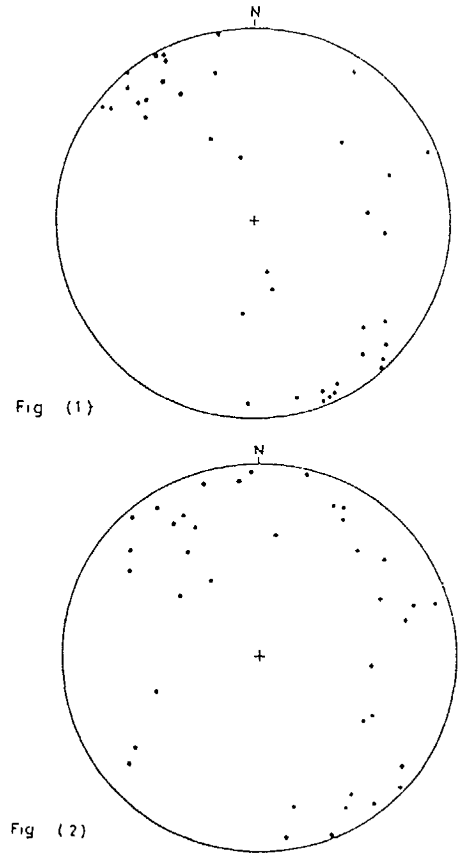

Fig (1) 34 fold axes in quartzite schist
Fig (2) 39 fold axes in quartzite

PLATE III. Stereograms for computed axes of mesoscale folds in metasediments.

SOUTH ATALLA AREA

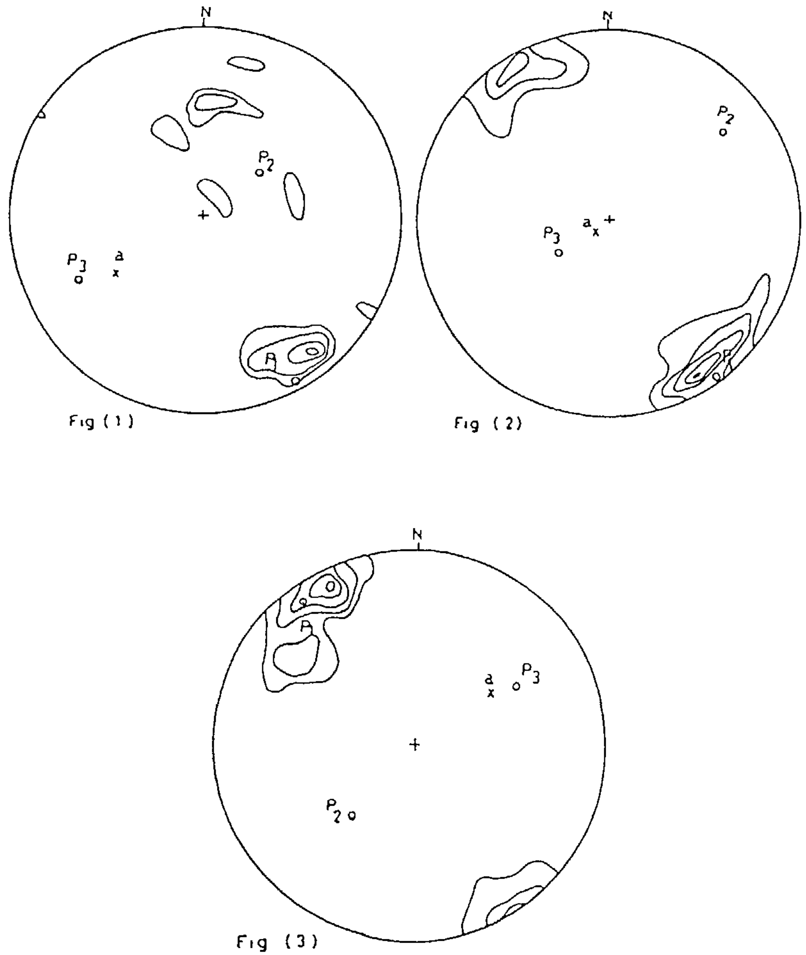

Fig (1) 17 Lineations in quartzite schist Contours, 23.5%, 15 %, 10 %, 4.9%, per 1% area
Fig (2) 144 Lineations in quartzite Contours, 15 %, 12 %, 9 %, 6 %, 2.9 %, per 1% area
Fig (3) 65 Lineations in metamudstone Contours 30%, 20%, 10 %, 7 %, 2.9%, per 1 % area
The lowest contour defines a critical value at 95 level of confidence

o principal axis of fold , X best fit fold axis

PLATE IV. Stereograms for lineation measurements in metasediments.

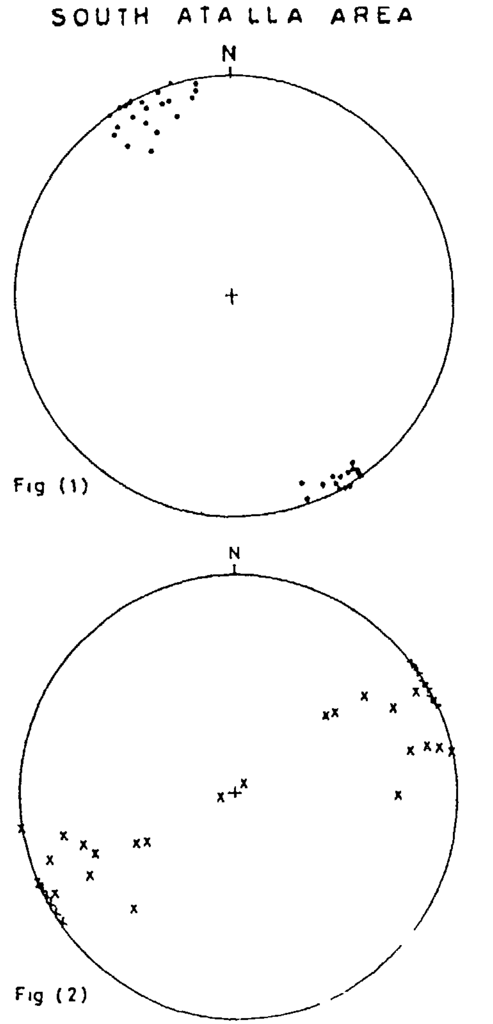

Fig . (1) 35 long axes
Fig . (2) 35 poles to principl planes (X–Y planes)

PLATE V. Stereograms for attitudes of deformed pebbles in quartzite.

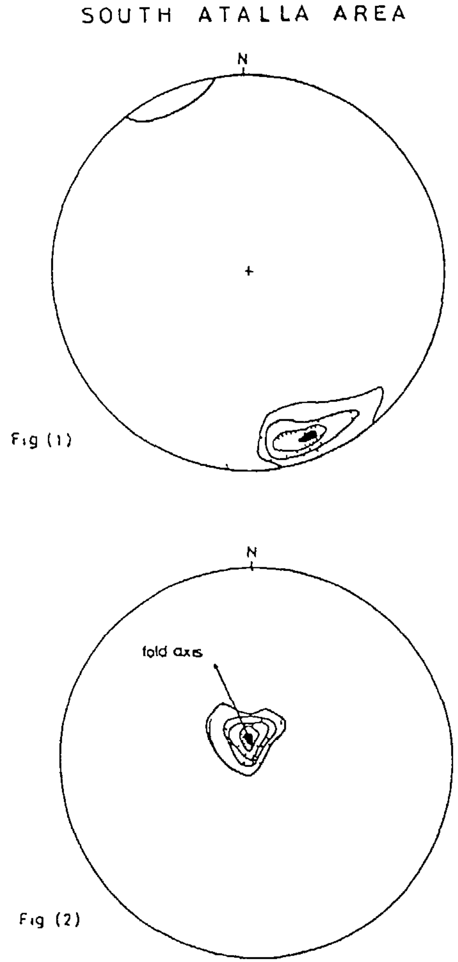

Fig (1) 24 poles to folded contacts of dykes Contours, 20 %, 15 %, 10 %, 4.7 %, per 1 % area
Fig (2) β– diagram for 283 lines of intersection of planes in fig(1) Contours 10%, 8 % 6 %, 4 %, 2.1 % per 1% area
The lowest contour defines a critical value at 95 level of confidence

PLATE VI. Stereograms for folded dykes in Um Had granite.

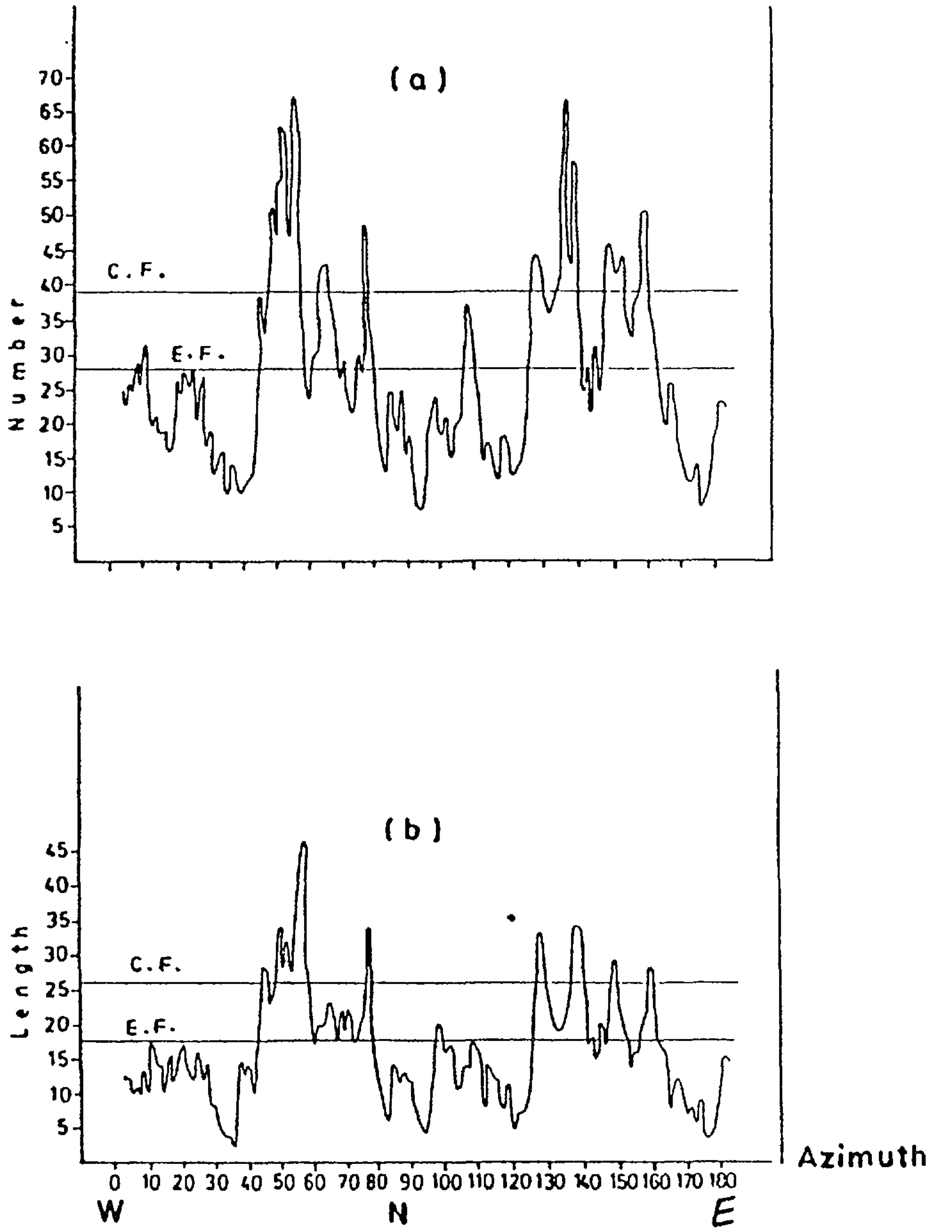

(a) COUNTED BY NUMBER

(b) COUNTED BY LENGTH

C.F. = CRITICAL FREQUENCY

E.F. = EXPECTED FREQUENCY

PLATE VII. Photolineaments, Central Eastern Desert.

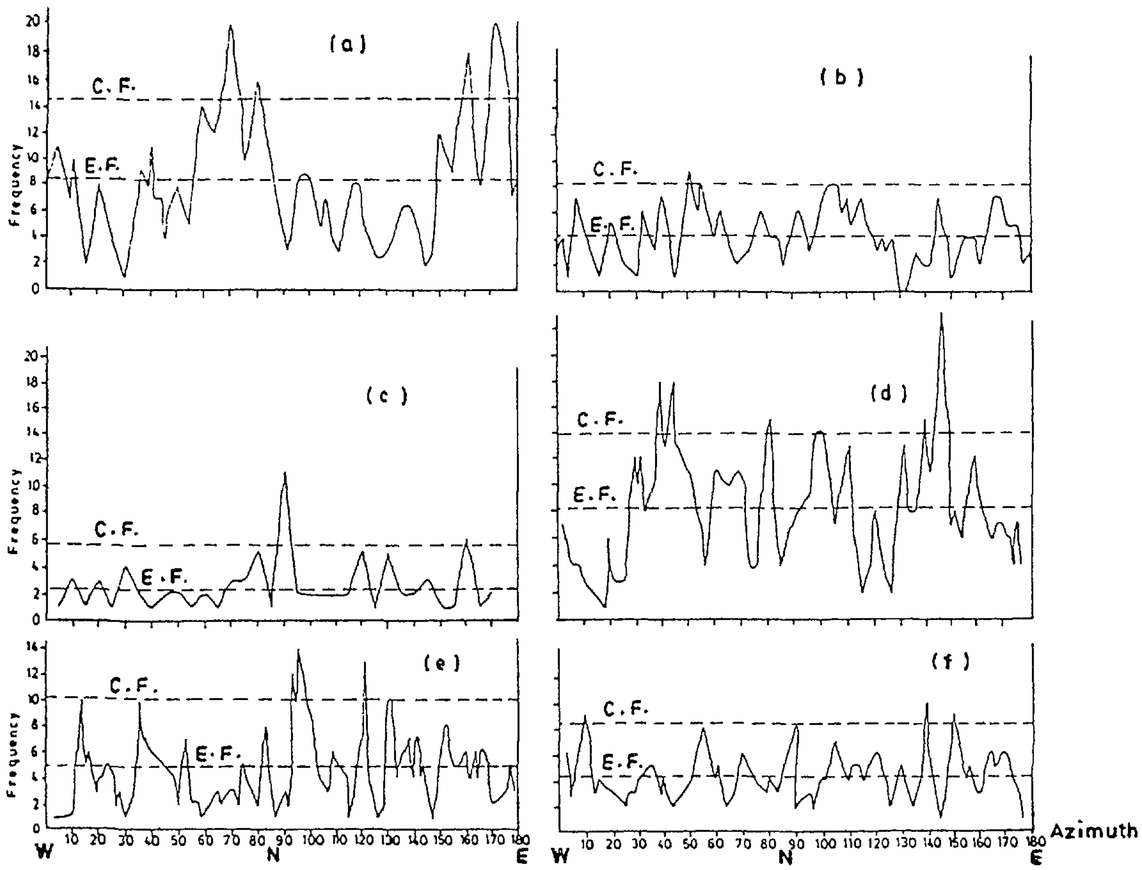

(a) FWAKHIR (b) SOUTHWEST EL EREDIYA (c) EL GIDAMI

(d) KAB AMIRI (e) EL EREDIYA (f) ATALLA FELSITE

MEASUREMENTS AFTER EL KASSAS (1974)

PLATE VIII. Joints, younger granitic plutons.

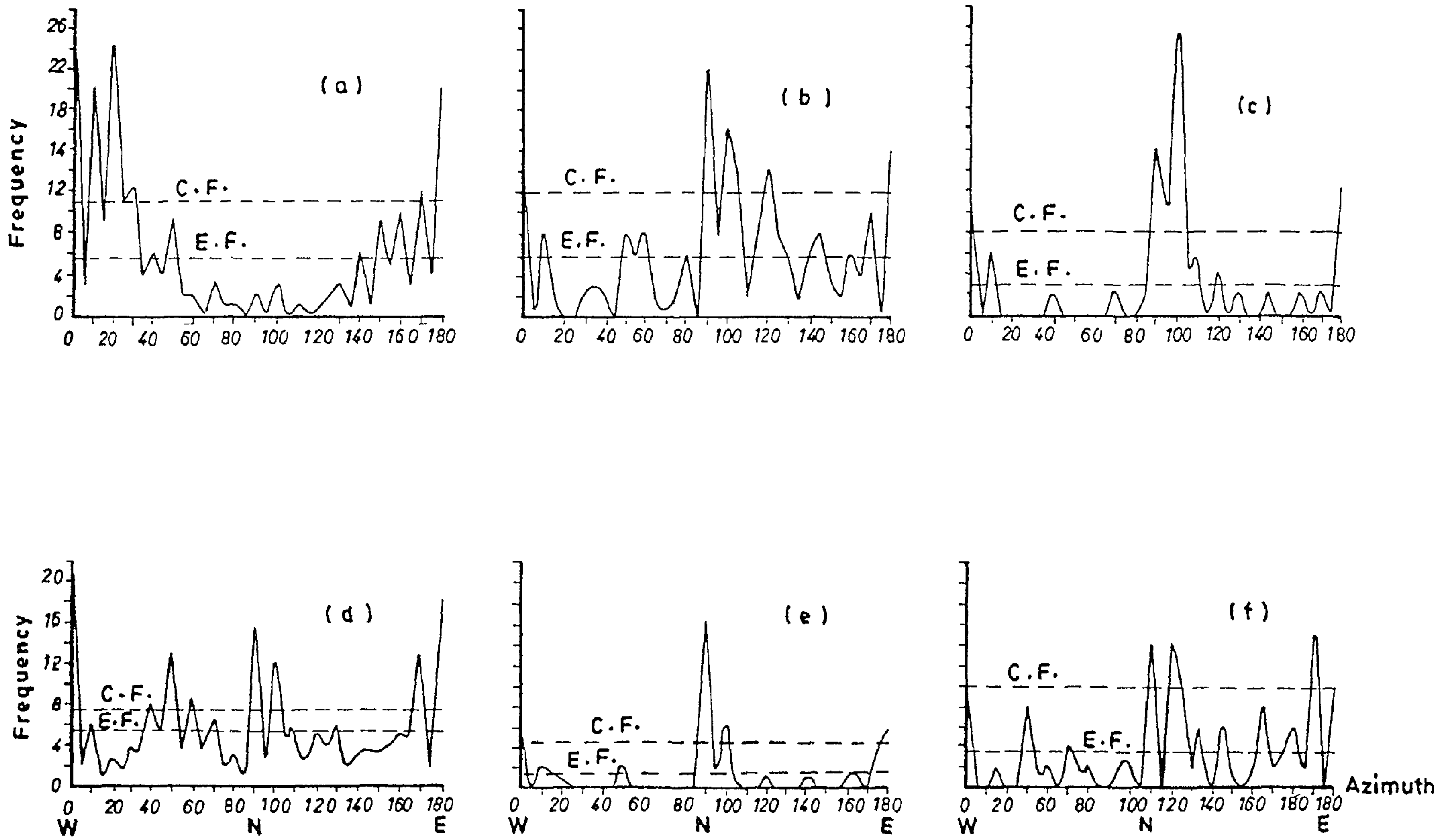

(a) SHEETING CLEAVAGE (b) HEMATITIZED JOINTS (c) QUARTZ VEINS

(d) NORMAL JOINTS (e) FAULTS (f) RADIOACTIVE JOINTS

AFTER EL SHAZLY ET AL. (1979)

PLATE IX. Fractures, Um Had pluton.

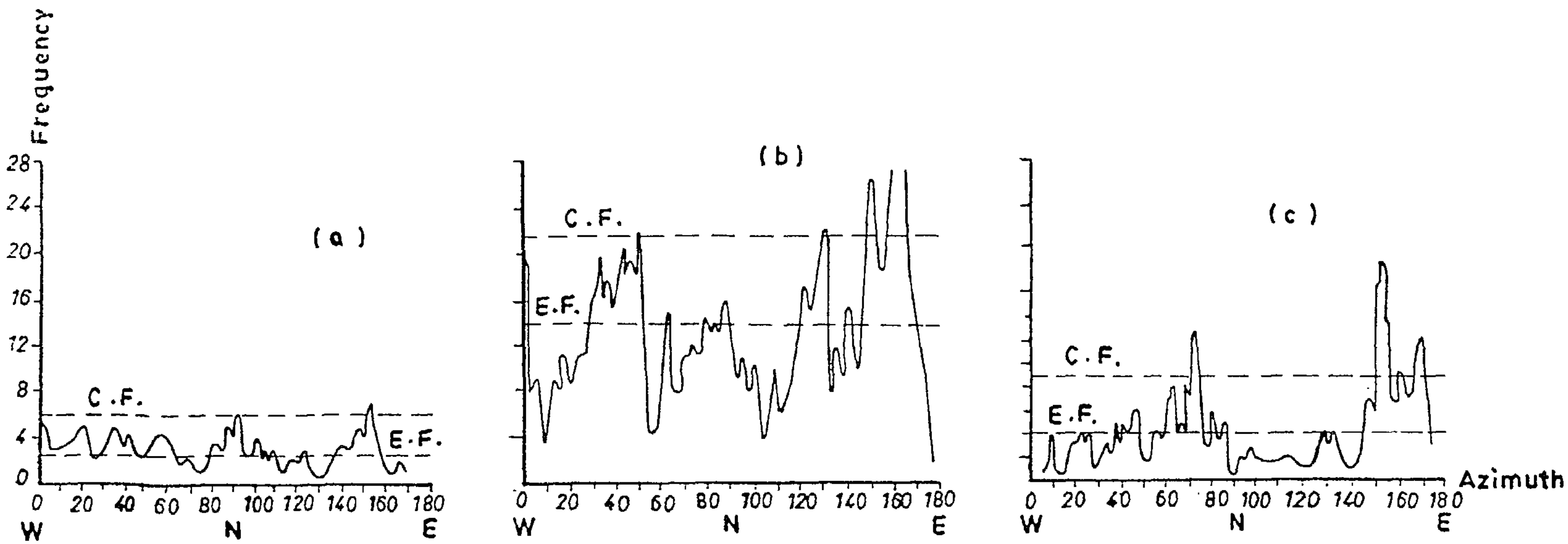

(a) GRANITE PLUTON

(b) SURROUNDING ROCKS
AFTER EL SHAZLY ET AL (1981)

(c) APLITE ROCKS

PLATE X. Joints, El Missikat area.

Regional scale fold axes are directed WNW-ESE in Wadis Ziedon and Kariem and gently plunge 10^0 - 20^0 towards the WNW. To the north, at Abu Ziran, Wadi Atalla and G. Um Had fold pattern is more regular, trending NNW-SSE and gently plunging few degrees to the SSE diretion. The fold trend in most cases are accompanied by fracturing of thrust and reverse types along the hinges. This trend was occupied by ultrabasic bodies as well as the Dokhan volcanics have been poured along it. This is best exemplified by Atalla rhyolite to the west of G. Atalla. In Wadi Atalla area, hinges of minor folds, lineations and long axes of deformed bodies are having the same trend in harmony with the large scale fold pattern. In addition, granitic bodies in general show stretch along the NNW-SSE direction. These features have occurred during the first and second plastic deformation stages which folded the older rocks and the Hammamat sediments respectively. The basement rocks have been intensely eroded, where the products have formed the Foreland sediments. This in turn has markedly decreased the lithostatic pressure, initiating the third brittle deformation stage. The developed fractures are subvertically disposed, striking in more or less N-S, ENE-WSW and NE-SW. In the northern parts, the ENE-WSW trend is dominant as fractures and regular spaced, semipenetrative joints. Meanwhile, the N-S trend is mainly depicted as joints. These two trends are commonly occupied by acidic dykes and veins, while basic dykes are nearly occupying the ENE-WSW trend. In the southern parts, the N-S trend forms a master set of large fractures as well as joints; while the ENE-WSW trend is subdominant, but as joints.

Alkaline and basic dykes are frequently encountered along the N-S fractures in Wadis Kariem and Ziedon.

A simple stress pattern may be assumed, where the major and minor axes are driected in NE-SW and NW-SE respectively. The intermediate axes is in vertical position. Under this pattern, during plastic stages the older and younger sediments have been folded about $\pm$ NW-SE subhorizontal axes. This is also the trend of stretched granitic bodies . In the brittle stage, the same tress was also acted upon, where rupturing occurred along the N-S and ENE-WSW sets of conjugate shears. Slippage on these sets is compatible with the postulated stress. The flexuring of some basic dykes in Um Had granite has yield fold axes in harmony with the surrounding old axes. Elongated bodies, fold axes, lineations and long axes of deformed pebbles all are in parallel allignement to the Red Sea. The opening of the Red Sea since the early palaeozoic coupled with sea floor spreading initiated the compressive stress normal to the coastal line the various structural features all are witnesses on this postulate.

In El Erediya and El Missikat plutons, Hussein et al (1986) recorded hy hydrothermal U- mineralization controlled by ENE-WSW shear fractures.

CONCLUSION

The younger granitic plutons in the central Eastern Desert of Egypt are characterized by higher levels of radioactivity and marked low of Th/U ratio to reach less than unity. However, stains of U-mineralizations are frequently found along longitudinal fractures and / or joints in jasperoid veins and aplite dykes. The latters are found filling the discussed fractures trending N-S and ENE-WSW. This is best developed at El Erediya, El Missikat and Um Had Plutons.

These two sets are interpretted as two conjugate shear fractures as a result of the compressive front normal to the Red Sea coast. In this stage, rocks failed by rupturing rather than folding as in the early two stages. Granitic plutons idealy failed by rupturing giving rise to clean fractures. In the course of released stresses, residual magmatic solutions invaded such fractures to form post granitic dykes and veins. The recurrency of the same stresses rejuvenated the old fractures to cause longitudinal fracturing in the filling materials (jasperoid veins and aplites) where they are highly brittle compared with the enclosed rocks.

The final release of stresses allowed these fractures to be good conduits for the ascesending solutions whether charged with U-mineralizations or leached them from the host rocks.

A mechanical model for El Missikat pluton using finite element method is developed to define the spatial distribution of fractures pattern for developing drilling and further mining work. Fractures are actually curved surfaces, these when undergone relative movement, vugs or sigmoidal shapes are developed. They are good traps for hosting mineralizations and they are the targets, the mechanical model is intented to locate.

REFERENCES

Abdel Aziz, M.G. (1968) : Geology of Wadi Kariem area, Eastern Desert, Ph.D. Thesis, Faculty of Science, Cairo University, Cairo, Egypt.

Ammar, A.A. (1973) : Application of a erial radiometry to the study of the Geology of Wadi El Gidami Area, Eastern Desert (with aeromagnetic application) Ph. D. Thesis, Faculty of Science, Cairo University.

Bakhit, F.S. (1978) : Geology and raidoactive mineralization of G.El Missikat area, Eastern, Egypt, Ph.D. Thesis, Faculty of Science, Ein Shams University, Cairo, Egypt.

El Ghawaby, M.A. (1973) : Structures and radioactivity of Wadi Ziedon area, Central Eastern Desert, Egypt. Ph.D. Thesis, Faculty of Science, Ein Shams University, Cairo, Egypt.

El Kassas, I.A. (1974) : Radioactivity and geology of Wadi Atalla area, Eastern Desert Ph.D. Thesis, Faculty of Science, Ein Shams University Cairo, Egypt.

El Shazly, E.M., El Kassas, I.A. and Mostafa, M.E., (1979) : Comparative fracture analysis and its relation to radioactivity in the pink granite of Um Had pluton, Central Eastern Desert, Egypt. J.Geol., Vol. 23, No. 1-2, PP. 95 - 110.

El Shazly, E.M., Bakhit, F.S. and Mostafa, M.E., ((981) : Significant Structural trends and the relation to radioactivity in El Missikat granite plution, Central Eastern Desert, Egypt. Proceeding of the Sixth Inter. Cong. for Statistics, Computer Science, Social and Demographic Research, Ain Shams Univ., Egypt, Vol. II, PP. 399-417.

Hussein, H.A., Hassan,M.A., El-Tahir, M.A. and Abou-Deif, A.(1986) : Uranium-Bearing Siliceous Veins in Younger Granites, Eastern Desert, Egypt. IAEA - TECDOC. 361, Vienna

Mostafa, M.E.(1979) : Computerized analysis of geologic structure in the Central Eastern Desert, Egypt and their role in the distribution of radioactive mineralization, Ph.D. Thesis, Faculty of Science, Cairo Univ., Egypt.

CASE 2
FACTORS CONTROLLING U-DISTRIBUTION IN THE
OLIGOCENE CARBONACEOUS SHALE, NORTH WESTERN DESERT (NWD), EGYPT

INTRODUCTION

Qatrani area is located in the Western Desert of Egypt and forms the northern part of Fayum depression between Lake Qarun to the south and Gebel Qatrani ridge to the north (Plate I).

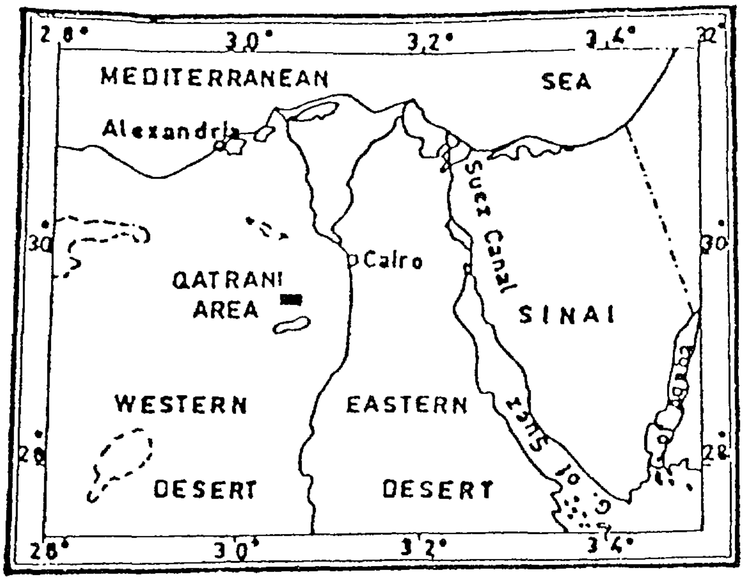

PLATE I. Location map of Qatrani area.

Radioactive occurrences were discovered in Qarrani area in 1957 by the field group of the Geology and Nuclear Raw Materials Dept., A E E, Abu Zeid and Abdel Monem (1957) and Higazyet al. (1958). The area was later aeroradiometrically surveyed by Fouad et al (1966). Detailed geologic surface and subsurface work had been carried out by mostafa (1972) to study the geology for uranium in the area. Zayed (1971) studied the geochemistry of uranium with major elements and its leachability. El Shazly et al (1971) found that uranium in the shale is acid and alkaline soluble. El Shazly et al (1974) mentioned that uranium in Qatrani area was derived from hot brines and associated with other trace elements.

Pejatovic (1968) discussed the sedimentation in Oligocene-Qatrani Formation. He explained that sedimentation took place in fluviomarine environoment under arid condition. This gave rise to rythmus of oxidation and reduction conditions, the latter represent 10% of the total thickness of Qatrani Formation.

According to Mostafa (1972) the carbonacous shale layer in enclosed in the middle clayer member of Qatrani Formation. Qatrani Formation (200-250m thick)is conformably overlying the Eocene-Qasr El Sagaha Formation and unconformably overlained by post Oligocene-pre Miocene basalt. The shale layer contains appreciable amount of immature organic matter (peats and to some extent lignite). The present shale is quite different from the typical black shale in that the environment in Qatrani area is fluviatile to fluviomarine. In the reduction rythme, it gives rise to thin layer of organic shales ranging from few cm up to 150 cm. The layer is characterize by lenticlar shapes and most probabaly deposited in swampy, land locked water bodies.

Mostafa and Zayed (1982) studied the geochemsitry of Qatrani shale.

Fifty two channel samples were collected from the shaly layer and distributed on anomaly occurrences (Plate II) as follows :

Anomaly occurrence	1E	2E	3E	1	3	4	7	12	14	22	28
Total number of samples	6	3	4	4	2	4	12	5	5	6	1

All elements were analysed by X-ray flourescence, while uranium content was determined by radiometric and flourimetric techniques. The equivalent radium was also determined radiometrically to define the state of equelibrium-disequilibrium of uranium.

The present study deals with statistical analysis of some elements U,Zr,Y,Sr,Rb,Mn,Cr,Ti and Ca. This aims to investigate factors controlling U and the other trace elements in the distribution of studied shale.

DATA PROCESSING AND COMPUTATION

Measurements are arranged in a row data matrix of nine columns(variables) and fifty five rows (samples). A computer program written by the author is used to compute ordinary statistics (means and measures of dispersions) after screening data from anomalous values. Normal readings simply fall in the range of three times of standard deviation around the mean. Chi-squared test (X^2) is applied to check the distribution of variables whether it obeys the normal or lognormal law. This is done by comparing the observed frequencies of a distribution with the theoritical normal curve having the same mean, standard deviation and total number of samples. Neter et al (1978) stated that the problem of choice the class range of a distribution is lacking theoritical basis. However in the present study, frequency distribution is carried out on different number of classes (class range). The optimal class range is chosen corresponding to the least calculated X^2-value.

Geometric means are only calculated for those elements obey the lognormal law.

The refined data matrix is thus free of anomalous values while variables are normally distributed. The correlation matrix is then computed.

Futhermore, factor analysis program is applied. It's a technique by which variables measured on a set of samples are linearly combined giving rise to a new fundemental quantities (factors) which can be named and simply interpreted in the light of sound geological reasoning. The program extracts eigenvalues and eigenvectors from the correlation matrix using a library subprogram named "FPROOT 1". Through matrix manipulation (Comery,1973), the principal factors are extracted and rotated to a position where each factor would have a large variance of the squared loading, thus the values are maximally spread out.Comery (1973) states that the most interpretable factor has high and low but few intermediate sized loadings. Scores of the original data are calculated, but related to the principal factors.

DISCUSSION

Single variate analysis (Table 1) and the histograms with the fitted theoritical curves (Plate II) show that U,Y,Mn, and Ca possess the highest measures of dispersion. Their distribution are not normal and characterized by tailing towards higher values. Meanwhile,those elements are normalized when the data undergone log-transformation with the exception of Mn-element. Ahrens (1954) states that major elements exibit normal distribution, while trace elements do lognormal behavior. It seems to the author that an element obeys the lognormal law might eventually undergone complex setting in deposition or in diagenesis. Such an element are chemically active, mobile and may be polyvalent. Uranium is a good example, where uranyl has a hexavalent soluble form under oxidation condition and tetravalent insoluble form in reduction condition, a case which is well proved in Qatrani shale.

Zayed (1971) reported that Ca is associated with a phase of dolomitization charged with U. This is evidenced from Table (2) where U is correlated with Ca.

In addition, the polyvalence nature of Mn led to intensive mobilization in diagenesis, thus it disobeys even the lognormal law.

On the other hand Zr,Sr,Rb,Cr and Ti exhibit normal distribution and low measures of dispersion. Those can be regarded as stationary elements, i,e, less mobile. The three elements Zr,Cr and Ti are probably of detrital origin, and they show mutual correlations (Table 2).

Table (1): Statistics of uranium and other elements in 52 samples from carbonaceous shale, Qatrani area .

Statistic / Variable	Range	$\bar{X}$*	Sd	Cv	Se	Skw	Kurt	Test Arithm.	Test Log.
U	6 - 340	34	0.42	27	0.06	0.34	2.87	N.N	N
Zr	96 - 541	264	91.0	34	12.6	0.6	3.6	N	
Y	4 - 61	19	0.26	20	0.04	-0.66	3.44	N.N	N
Sr	3 - 499	192	125.0	65	17.3	0.4	2.8	N	
Rb	14 - 99	50	17.8	36	2.5	0.3	4.0	N	
Mn	5 - 435	106	0.31	15	0.04	-1.08	7.81	N.N	N.N
Cr	14 - 291	124	57.8	46	8.0	0.5	3.2	N	
Ti	237 - 11227	6232	2677	43	371.3	-0.2	2.2	N	
Ca	0.17 - 19.70	3.3	0.42	81	0.06	-0.42	3.34	N.N	N

X = Arithmetic mean
Sd = Standard deviation
Cv = Cofficient of variability
Se = Standard error of estimate
Skw = Skewness
Kurt = Kurtosis
X - test
N = Normal
NN = not normal

* Geometric means are only calculated for lognormal distributions.

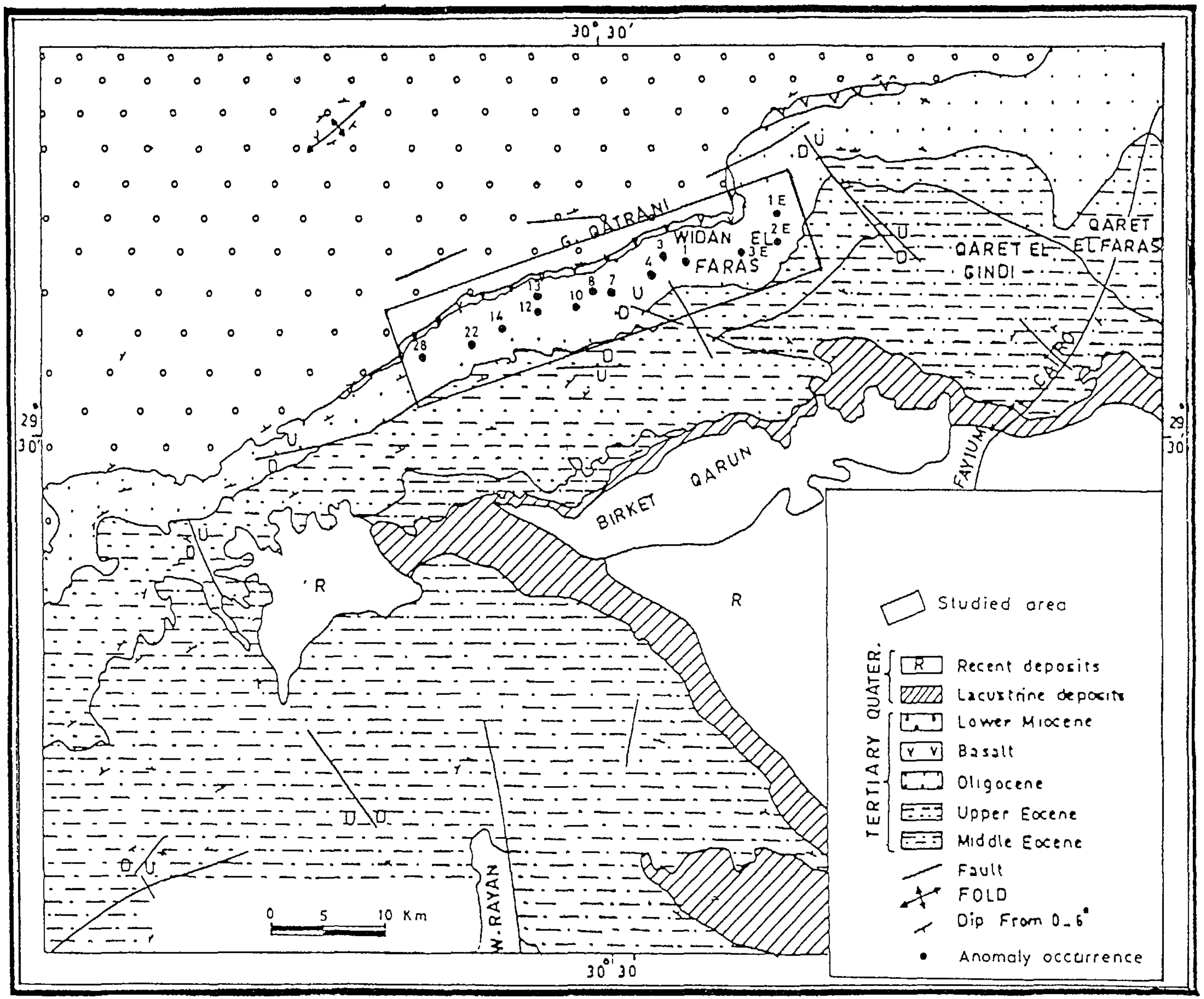

PLATE II. Geologic map of Qatrani area, Fayum district.

Table (2) : Correlation coefficients for uranium and other elements in 52 samples from carbonaceous shale Qatrani area.

element	U	Zr	Y	Sr	Rb	Mn	Cr	Ti
U								
Zr	-0.03							
Y	0.05	-0.32						
Sr	-0.07	0.35	-0.20					
Rb	0.03	0.14	-0.17	0.25				
Mn	-0.15	-0.18	0.13	-0.36	-0.17			
Cr	-0.05	0.19	-0.14	-0.05	-0.27	0.21		
Ti	-0.37	0.29	-0.26	0.13	0.11	0.20	0.45	
Ca	0.29	-0.34	0.24	-0.13	0.04	-0.10	-0.48	-0.65

Correlation coefficient les than 0.273 is insignificant at 5% level of confidence, Dixon and Massey (1957).

It is worthy to mention that Ti-U and Ti -Ca both exhibit-ve relations as if the presence of Ti prohibits deposition or adherence of both U and Ca ions.

Some - ve relations are reported between elements of mobile and stationary nature.

In factorial study, Mn is dropped fron the correlation matrix, since it disobeys even the lognormal law. Table (3) shows the extracted eigenvalues and their cummulative percent. Factor loadings of variables on each of the unrotated factors are also given.

The 8-Dimension factor space can be reduced without sound loss of information into 3-D space which is quiete interpretable. It will represent 65% of the total information.

Table (4) shows the three principal factors extracted from the previous table and they are rotated using Varimax method to occupy an interpretable

Table (3) : Unrotated factor matrix controlling distribution of U and other elements, carbonaceous shale, Qatrani area.

FACTOR	1	2	3	4	5	6	7	8
Eigenvalue	2.58	1.56	1.05	0.80	0.72	0.57	0.41	0.31
%	32.29	19.56	13.08	9.98	8.98	7.10	5.11	3.91
Cumm.%	32.29	51.85	64.93	73.91	83.88	90.98	96.09	100.00
Variable								
U	0.40	0.17	0.79	0.15	0.32	0.10	0.20	0.11
Zr	-0.59	0.38	0.33	-0.27	-0.01	-0.56	-0.10	0.02
Y	0.50	-0.35	-0.25	-0.44	0.59	-0.13	-0.02	0.00
Sr	-0.35	0.63	-0.01	-0.55	0.01	0.43	0.00	0.03
Rb	-0.09	0.73	-0.26	0.42	0.41	-0.01	-0.15	-0.16
Cr	-0.59	-0.52	0.38	0.02	0.15	0.21	-0.40	-0.14
Ti	-0.82	-0.15	-0.21	0.17	0.22	0.04	0.04	0.42
Ca O	0.82	0.23	0.03	0.00	-0.15	0.00	-0.42	0.28

Table (4) : Factors controlling distribution of U and other elements, Carbonaceous shale, Qatrani area.

Variable	F A C T O R S		
	F1	F2	F3
U	-0.117	0.131	0.886
Zr	-0.173	0.756	-0.035
Y	0.111	-0.649	0.051
Sr	0.293	0.648	-0.096
Rb	0.615	0.461	-0.117
Cr	-0.836	0.164	-0.166
Ti	-0.366	0.362	-0.689
Ca	0.522	-0.362	0.568

Factor names are discussed in the text.

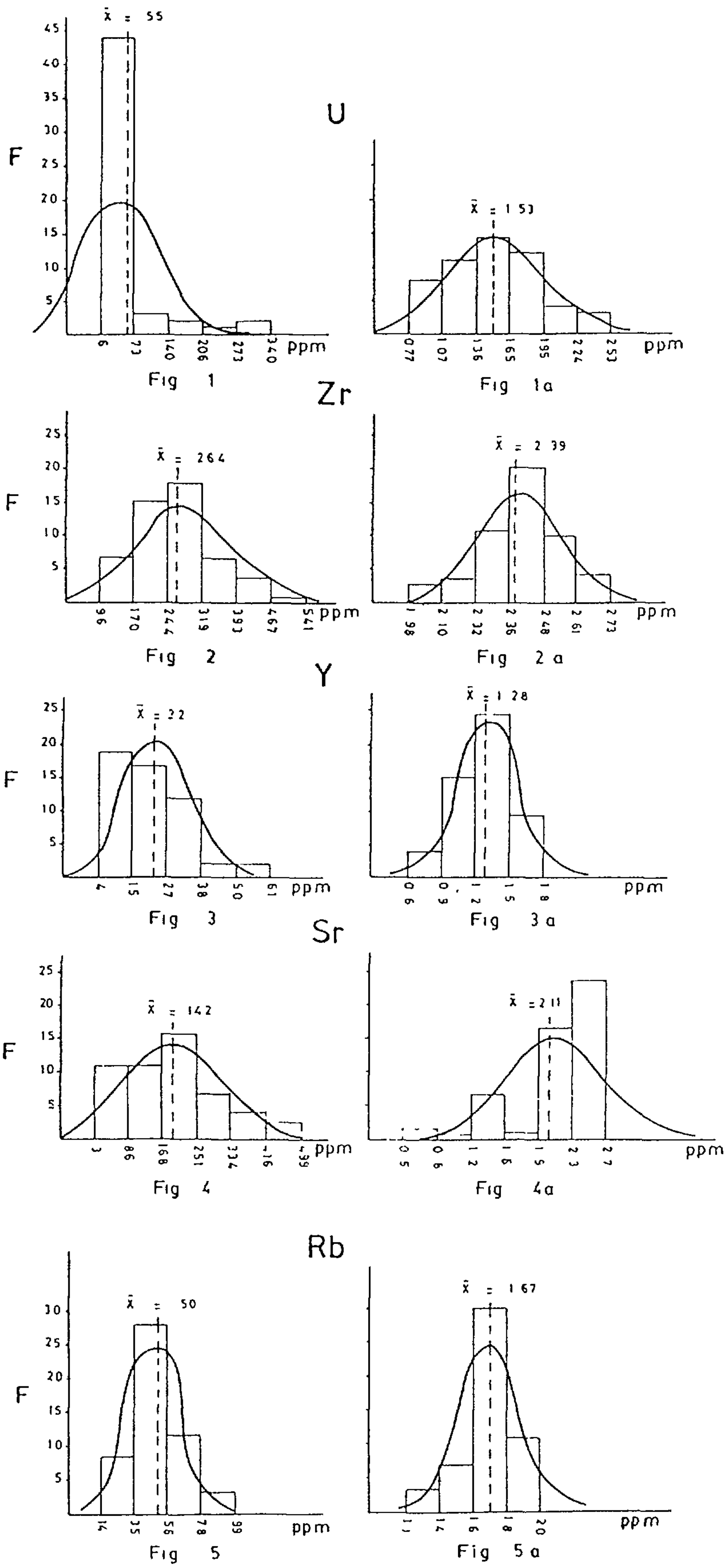

PLATE III. Frequency histograms with fitted normal curves for different
elements in the carbonaceous shale of Qatrani area, Western Desert, Egypt.

PLATE III (cont.)

Mn

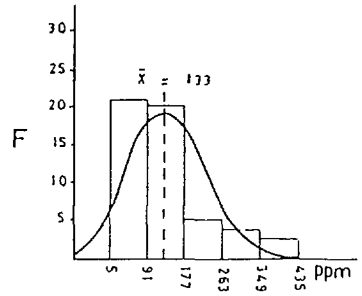

Fig 6

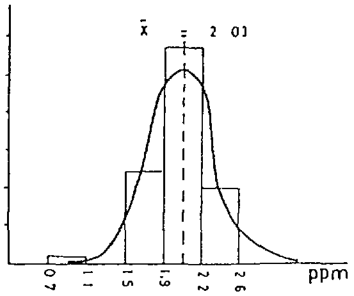

Fig 6 a

Cr

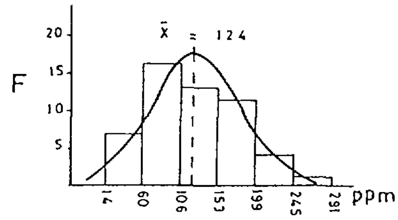

Fig 7

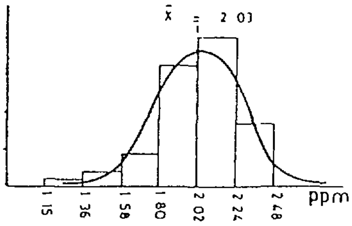

Fig 7 a

Ti

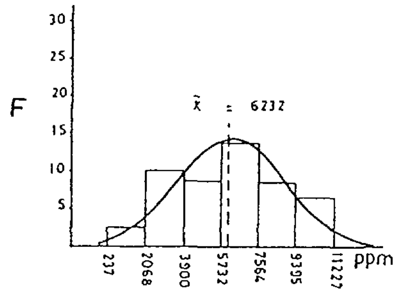

Fig 8

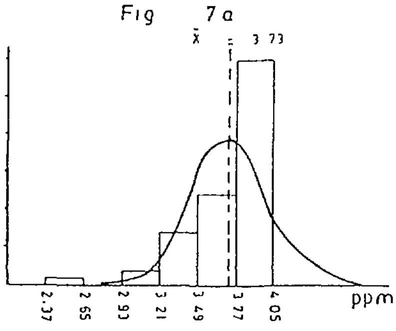

Fig 8 a

Ca

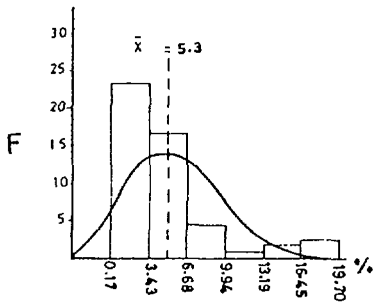

Fig 9

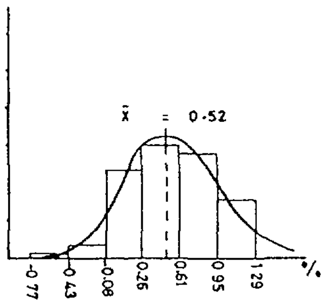

Fig 9a

Figs. 1 - 9 arithmetic scale

Figs. 1a - 9a logarithmic scale to the base 10

F ≡ Frequency

ppm ≡ part per million

position . It is worthy to notice that correlated variables are found loaded on one of the factors extracted.

The first factor (F1) is inversely correlated with Cr and Ti i,e, those elements of detrital origin. Both Ca and Rb are positively loaded on F1, F1 may differntiate between soluble and insoluble derived elements.

The second factor (F2) is correlated with Zr,Sr,Rb and Ti and inversely correlated with both Y and Ca. F2 seems to need further study to be interpretted.

However, F3 shows an expected +ve relationship with U and Ca and-ve with Ti, a fact which is previously explained. It states that Ca is associated with a phase of dolomitization.

Mostafa and Zayed (1982) state that uranium was found to be the main contributor to radioactivity, its great variability and wide range, all indicate the instable nature and the chemical affinity of uranium for mobilization.

Zayed (1971) mentioned that uranium in Qatrani shale is soluble in weak alkalies and acids. It has no discrete mineralogic form and found adhered on clays and as organo - compounds. Uranium shows high concentrations where reductants such as organic materials, iron oxides, sulphides and sulpher prevails.

El Shazly et al (1974) assumed a subvolcanic origin for uranium bearing solutions in Qarani area associated with active fault lines considered as conduits or channels. The presence of alteration products, ferrugination, silicifications all are in favour for such assumption. In addition the clastic nature of the Oligoncene Qatrani sediments plays an important rule as pervious medium for circulating solutions whether meteoric or of subvolcanic origin. The carbonaeous shale with its higher content of reductants form a suitable contition for pericipitating uranium and other trace elements from their solutions.

Subsurface mapping (Mostafa, 1972) indicated the abnormal concentration of uranium in the troughs of the flexured carbonaceous shale.

CONCLUSION

It is apparent that uranium in Qatrani shale is partially derived from an external source. It was proved that shale was attacked by a dolomitization phase charged with U,Mg and Ca. Other stable elements, Zr,Cr and Ti exhibit normal patterns of distribution and they assumed as if of detrital origin. It was also shown that the presence of Ti prohibits deposition or adherence of U and / or Ca.

The stratigraphic position of the carbonaceous shale being enclosed between thick and pervious sandy members makes it surrounded by circulated solution which meteoric or of subvalcanic origin. Its appreciable content of organic materials, reductants all are suitable conditions for capturing uranium and other trace elements fron their solution.

However, factor analysis permits extracting some few factors controlling the complex deposition and diagenesis of the carbonaceous shale. There a factor which could differntiate between elements of detrital origin and other elements derived in solution. The other factors (F3) reported the relation of U and Ca which is prohibited in the presence of Ti.

To target the uranium source, it needs a rather systematic work includes the integration of geochemical and radiometric mapping.

ACKNOWLEDGEMENTS

The author is greatly indebted to prof. Sayah, T.A., vice president of Nuclear Materials Corporation, Egypt for help and encouragement in this work. The discussion and criticism about Qatrani field study with my Collegue Mr. M.A. Morsi are greatly acknowledged.

REFERENCES

Abu Zeid, S and Abdel Monem A.A.(1957) : The discovery of uranium-bearing quartizitic veins at Gebel Qatrani area. Internal Rep., Geology and Nuclear Raw Materials Dept., A E E, Egypt.

Ahrens, L.H.(1954) : The lognormal distribution of the elements. Geochem. Cosmochim. Acta, pare 1, Vol. 5,pp. 49-73, part 2, Vol. 6, pp. 121-131.

Comery, A.L.(1973) : A first course in factor analysis. Academic press, New York.

Dixon, W.J. and Massey, F.J.(1957) : Introduction to statistical analysis Mcgraw Hill Book Company, New York.

El Shazly, E.M., El Hazek, N.M.T. and Zayed, Z.M.(1971) : Leaching experiments on uraniferous shales and sandstones fron Qatrani, Western Desert, URR,IAEA,Vienna, SM-135/35.

El Shazly,E.M., El Hazek, N.M.T., Abdel Monem, A.A.,Khawasik, S.M. Zayed, Z.M., Mostafa,M.E. and Morsi, M.A.(1974) : Priqin of uranium in Oligocene Qatrani sediments, Western Desert, Egypt, IAEA, Vienna, SM-183/1.

Higazy,R.M., Au Zeid, S. and Khattab, Kh.m.(1958) : The discovery of uranium ores in Egypt. Proc. Un Inter. Conf. peaceful Uses Atomic Energy, 2, 97,.

Fouad, K.M., Ammar, A.A., Meliek M.L., Abdel Hadi, H.M. and Soliman, S.(1966) : Airborne radiometric prospection of Qatrani area, Western Desert, Egypt, Internal Rep., Geology and Nuclear Raw Materials Dept, A E E, Egypt.

Miller, R.L. and Kahn, J.S. (1954) : Statistical analysis in the geological ciences. John Wiley and Sons Inc. New York.

Mostafa, M.E.(1972) : Geological studies of uranium occurrences, Qatrani area, Western Desert Egypt. M.SC Thesis, Faculty of Science Cairo Univ., Cairo, Egypt.

Mostafa, M.E. and Zayed, Z.M.(1982) : Statistical Approach to the Geochemistry of Uranium in the Carbonaceous Shale of Qatrani Area, Eqypt, the 17 th, Annual Conference of Statistics, Computer Science, Operations Research & Mathematics, Vol. 17, No 1 Cairo, Egypt.

Neter, J., Wasserman, W. and Whitmore, G.(1978) : Applied statistics. Allyn and Bacon Inc., Boston.

Pejatovic, S,(1968) : Geological regularities in situation of coaly clay bearing uranium manifestation at Gebel Qatrani area, Fayum District. Internal Rep., Geology and Nuclear Raw Materials Dept., A E E, Egypt,

Zayed, Z.M.(1971) : Studies on geochemistry and uranium concentrations of Qatrani uranium ores, Egypt.M.Sc. Thesis. Faculty of Science, Cairo Univ., Egypt.

ANORTHOSITE RELATED POLYMETALLIC THORIUM-URANIUM DEPOSITS IN THE NAMAQUALAND METAMORPHIC COMPLEX, SOUTH AFRICA

M.A.G. ANDREOLI*, N.J.B. ANDERSEN,
J.N. FAURIE
Atomic Energy Corporation
of South Africa Ltd,
Pretoria, South Africa

Abstract

Since 1980 detailed geological, geophysical and geochemical investigations have been carried out in the Namaqualand Metamorphic Complex of South Africa in the search for a suitable site for the disposal of low- and intermediate-level radioactive waste. The Vaalputs site, which was ultimately selected is located 100 km south of the town of Springbok in the northwestern Cape.

During the investigation, detailed geological mapping as well as airborne radiometric and magnetic surveys were conducted. The anomalies located by the airborne surveys were followed up on the ground by geophysical surveys and by further mapping and drilling.

The airborne surveys indicated that the basic and anorthositic intrusives gave clear radiometric and magnetic anomalies. The syntectonic granite gneisses also proved to contain anomalous concentrations of uranium and thorium. The trend of these radiometric anomalies follows the regional distribution pattern of the intrusive anorthosites.

The anorthosite-enderbite intrusives in the Vaalputs area are compared with those found in "steep structures" in the Okiep and Steenkampskraal districts and a north-south metallogenic zoning is proposed.

---

* Present address: Schonland Research Centre for Nuclear Science, University of the Witwatersrand, Johannesburg, South Africa.

1 INTRODUCTION

The ca. 1 100 Ma. old Namaqualand Metamorphic Complex, which outcrops in the western part of South Africa, has been the subject of many geological investigations, especially since major base-metal occurrences are located near the towns of Springbok and Aggeneys (Joubert, 1986; Lombaard et al., 1986; Ryan et al., 1986; Fig 1).

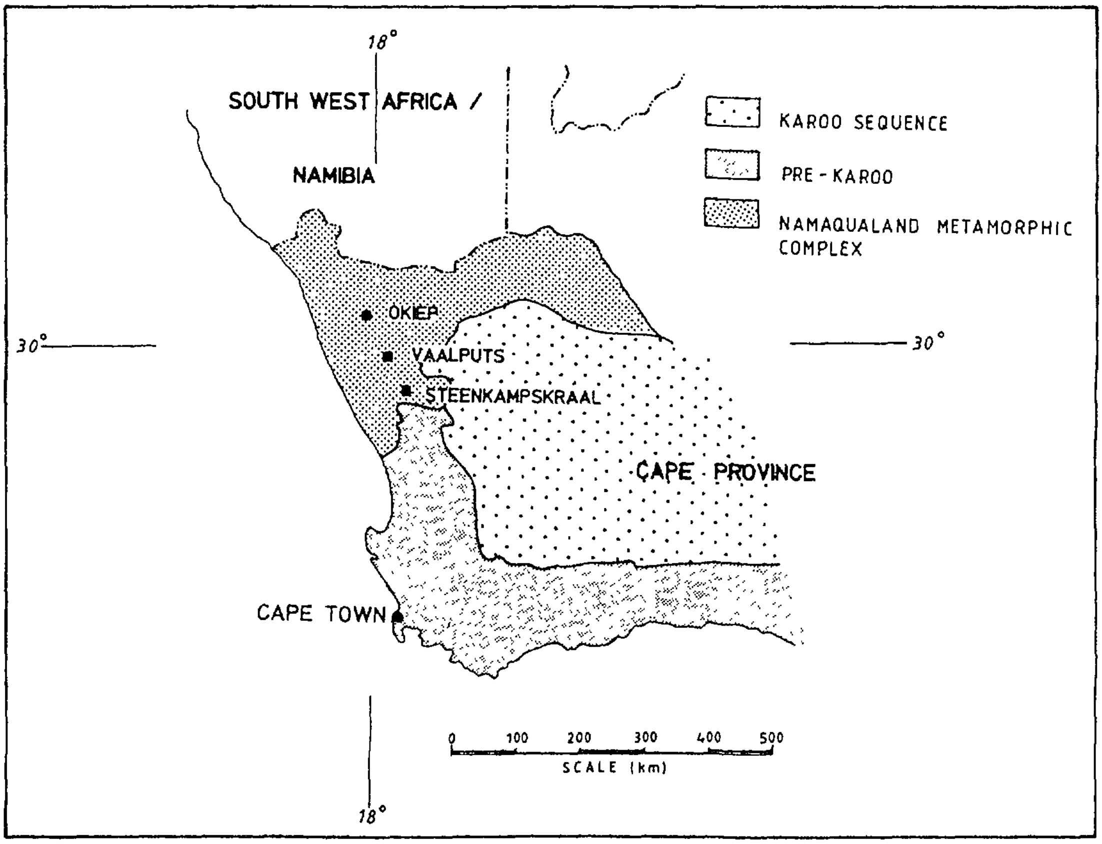

Figure 1 Generalized regional geology

Since 1980 an area approximately 100 km south of Okiep has come under the spotlight in a detailed geological/geophysical investigation to prove its suitability for the disposal of low- and intermediate-level radioactive waste as well as for the ultimate storage of high-level radioactive waste. The site that was eventually chosen covers an area of ca. 200 km^2 and became known as the Vaalputs National Radioactive Waste Disposal Site.

Airborne magnetic and radiometric surveys were carried out to resolve the structure and geology in areas where the rocks were covered by younger Kalahari sands and to evaluate the mineral potential of the area. Amongst other anomalies, the airborne surveys clearly identified basic and anorthositic intrusives as bull's eye anomalies. In the Springbok area some 100 km to the north such intrusives form exploration targets for copper orebodies which in many cases also have abnormally high concentrations of radioactive elements (Andreoli and Hart, 1986a; 1986b).

Furthermore, a detailed investigation of the old monazite (copper) mine of Steenkampskraal (Andreoli, 1984; Andreoli and Hart, 1986b) revealed a genetic relationship of the orebody with enderbitic anorthosite dykes quite similar to the ore bodies of the Springbok district. It is the purpose of this study to provide a progress report on this regionally extensive type of polymetallic mineralization (that may contain up to 2 % uranium) by making use of the geophysical surveys carried out for the development of the Vaalputs radioactive waste depository. A comprehensive model of this type of mineralization forms the theme of a joint research project between the AEC and the University of the Witwatersrand and will be reported elsewhere (Andreoli et al., in prep.).

2 THE GEOLOGY OF THE RADIOACTIVE BASE-METAL DEPOSITS OF WESTERN NAMAQUALAND

2.1 Regional Setting

The Namaqualand Metamorphic Complex (NMC) includes metasedimentary, metavolcanic and intrusive rock units which are predominantly gneissic in character. This complex is bounded in the east by the Archaean Kaapvaal Province, by younger cover rocks in the south and by the Atlantic coastline in the west (Fig 1).

TABLE 1 LITHOSTRATIGRAPHIC SUBDIVISION OF THE NAMAQUALAND METAMORPHIC COMPLEX IN THE VAALPUTS AREA

Suite	Lithology
Syntectonic Intrusive Suites:	
Koperberg	Hypersthenite, norite, anorthosite, diorite,
Spektakel	K-rich garnetiferous leucogranite, alaskite
Hoogoor	Pink, quartzo-feldspathic gneiss
Little Namaqualand	Biotite-rich granitic augen gneiss
Gladkop	Fine-grained grey gneiss, granodioritic, megacrystic in places.
Pretectonic Supracrustals	
Okiep Group	Biotite/quartzo-feldspathic gneisses; magnetite and/or feldspathic quartzite; sillimanite-rich schists

TABLE 2 GEOLOGICAL HISTORY OF THE VAALPUTS AREA

Event	Age (Ma)*
- Erosion, uplift	120-65
- Development of NW plunging open folds with emplacement of pegmatites	1 000
- Anorthosite-norite Koperberg Suite intrusions and mineralization with development of steep structures	1 070 $\pm$ 20
- Disturbance of Rb-Sr isotope system by oxygen-rich fluids (?)**	
- Emplacement of syntectonic granite suite during E-W open folding	1 166 $\pm$ 26
- Granulite facies metamorphism (P $\pm$5 K bar, T $\pm$800 ^{o}C), accompanying fecumbent folding	1 213 $\pm$ 22
- Deposition of metasediments, banded ironstones over older basement (not recognized)	1 500

* Joubert (1986)

** Andreoli (in preparation)

The lithostratigraphic subdivision of the NMC in the area under consideration is presented in Table 1. In addition, petrographic observations around Vaalputs and Springbok, together with pertinent geochronological data, provided a model for the evolution of the complex in the area under investigation that is presented in Table 2. (Hart and Andreoli, 1985).

2.2 Morphology of the Ore Bodies

The predominantly irregular dyke-like form of occurrence of the Koperberg Suite, suggested by its outcrop pattern, has been confirmed by mapping, diamond drilling and mining activities in a large area of the NMC from Springbok to Steenkampskraal. Plug-like bodies are much less common and sill-like occurrences are rare. The width of most dykes falls in the 50 m to 100 m range and continuous length seldom exceeds 1 km. A prominent feature of the distribution pattern is the arrangement of discrete bodies in linear zones.

These easterly-trending, often irregularly pinching and swelling, branching and coalescing dyke-like bodies, some of which are ore-bearing, have a predominantly near-vertical to steep northerly dip throughout the region. The maximum vertical extent over which a steep branching dyke zone has been traced continuously is 1 575 m, basic rock still extending below this depth. In contrast, many bodies appear to pinch out completely. Results of diamond drilling and mining activities have, however, substantiated that at some places a subvertical dyke may narrow downward along an extremely flat plungeline before continuing downward at a steep plunge to greater depth. Examples of this were identified at the Hoits, Koperberg, Okiep and Steenkampskraal mines (see Pike, 1958 for the last-mentioned locality).

2.3 Structural Controls

The association of these rock types with high-amplitude and short-wavelength brachyanticlines (locally referred to as steep structures) are additional features of the Koperberg Suite. These steep structures, which pierce vertically or at a steep angle to the regional shallowly dipping fabrics, generally trend easterly, and can be traced over distances ranging from 100 m to 7 km. Their amplitude is usually large relative to their width and they commonly show evidence of shearing. Within these structures, lithologic units may have moved in a diapiric fashion from 100 to 200 m above or below their normal position in the succession. Associated with many of the steep structures, and possibly confined to local areas of increased deformation, are roughly oval and steeply plunging pipe-like bodies of breccia locally referred to as megabreccias. These are composed of heterogeneous rock cemented by granitic material, or occasionally by an anomalous U, Th (quartz $\pm$) phlogopitic, biotite-rich rock called glimmerite (Andreoli and Hart, in prep.).

Anorthositic rocks of the Koperberg Suite are frequently associated with these steep structures, a fact which may possibly reflect zones of weakness and magma emplacement. In places, most strikingly so at East Okiep Mine, pipe-like bodies of megabreccia appear also to have been favoured by basic intrusives in their upward migration. The most prominent steep structures found near Vaalputs in close association with Koperberg Suite rocks are reported by Andreoli et al., (1986).

2.4 Lithological Associations

Many basic bodies are entirely uniform in composition. Others are composite, the contacts between the different types being either gradational or sharp. Where the contacts are sharp, and where one member of the basic suite is held as inclusions in another, sequential emplacement, invariably of a less basic variety followed by more basic types, can be established.

A detailed study of the lithological associations (Andreoli et al., in prep.) indicates that certain differentiation sequences, listed in Table 3, have great economic importance in the Springbok and Steenkampskraal mining districts, as well as possibly in the Vaalputs area. The structural controls, the petrology and the (REE-)geochemical signature of the Steenkampskraal ores were found to be identical to those of many barren and copper (Ni, REE, Mo, Zr, Th) bearing anorthosite, norite, diorite and glimmerite bodies scattered throughout Namaqualand from Kliprand to Steinkopf (Andreoli et al., unpublished data; Andreoli and Hart, 1986a).

TABLE 3 PROPOSED DIFFERENTATION SEQUENCES OF THE KOPERBERG SUITE AROUND VAALPUTS AND STEENKAMPSKRAAL

SEQUENCE	STAGE	MINERAL ASSEMBLAGE	PETROGRAPHIC NAME	PETROGENETIC PROCESS
B	6	hypersthene ± Plagioclase ± zircon ± REE-Th rich accessories ± apatite	Norite, Hypersthenite	Separate magma pulse
A	5	Hypersthene + quartz + K feldspar + plagioclase ± monazite ± zircon, ± sulphide	Charnockite	Carbothermal alteration of gneiss by (U, TH, REE bearing) CO_2-rich volatiles (after A-3)
	4	Quartz ± feldspar	High-silica liquid)	Segregation of two immiscible liquids
	3	Monazite + apatite + Fe, + Ti, + Zn spinel ±Fe-, Cu-, Mo-, Pb-sulphides + volatiles	Low-silica, Fe-, P-rich) liquid (nelsonite))	
	2	Plagioclase + quartz ± K-feldspar ± hypersthene + monazite	Enderbite)	Fractional crystallisation
	1	Plagioclase ± zircon ± REE-Th rich phase ± hypersthene ± quartz	(Norite) anorthosite)	

3 EXPERIMENTAL RESULTS IN THE VAALPUTS AREA

3.1 Generalities of the Airborne Geophysical Surveys

During the screening phase and in the subsequent search for a suitable site for the disposal of radioactive waste in South

Africa it became clear that the area of the Namaqualand Metamorphic Complex stretching from Springbok to Steenkampskraal was unusual in that the base metal ore occurrences also contain radioactive elements. As a result of the presence of such unconventional ore forming processes, the area became the focus of geological, geophysical and geochemical investigations.

As part of the radwaste investigations, an area of 2 100 km^2 was covered by a detailed medium-sensitivity airborne magnetic survey. This was done in order to resolve the structure and geology in those parts where the rocks are covered by windblown sands of the Kalahari Group. The radiometric survey, which covered a much larger area, was flown by the Geological Survey of South Africa as part of their regional economic mineral investigation programme.

3.2 Airborne Magnetic Survey

The aeromagnetic survey covered an area of 2 100 km^2 and was flown at an altitude of 100 m with flight-line and tie-line spacings of 300 and 1 200 m respectively. Using a Geometrics G813 magnetometer with a sensitivity of 0,1 nanotesla a noise envelope of less than 0,5 nanotsela was achieved. Computer-contoured and coloured maps were produced at scales of 1:25 000, 1:50 000 and 1:100 000.

Spectral filtering was applied and it was possible to separate the longer-wavelength magnetic data representing a deep basement from the shorter-wavelength data of the overlying supracrustal rocks. Separate magnetic maps were compiled of these two horizons.
Major magnetic anomalies that appear in the vicinity of the Vaalputs radioactive waste disposal site include:

- Magnetic linears, some recognized by their displacement of magnetic trends and others by their magnetic low character. These are typical anomalies caused by faults. The magnetic lows associated with some faults are a direct result of the leaching out of magnetite in the fault zone by ground water. The largest of these anomalies occurring in the Vaalputs area is the Garing linear, which can be followed for a distance of about 30 km on the airborne magnetic survey contour map.

- Small scale features such as high-low pairs, which are typical of the late tectonic Koperberg Suite intrusions which are known to occur in the area. Two such prominent anomalies occur on Vaalputs, with a larger one just beyond the northeastern corner of the boundary.

3.3 Airborne Radiometric Survey

As mentioned previously, the Geological Survey of South Africa flew a regional airborne radiometric survey which included the Vaalputs site. The survey was flown in 1983 at 100 m above surface and an aircraft speed of 240 km/h. The uranium channel was set at 1,66 - 1,86 MeV and the results were plotted as counts per second (cps) contour maps with both the background and the interference from the thorium channel removed. These maps are available on open file at the Geological Survey (Figure 2).

Radiometric high zones appear on the western boundary of the Vaalputs site as well as to the south-west of the site. The north-easterly trending anomaly follows the outcrop pattern of the syntectonic Vaalputs granite gneiss around the edge of a megasynform plunging easterly at a shallow angle. Anomalies along these trends give an average of 60 cps (uranium channel) above background while the highest count rate encountered was 100 cps above background (uranium channel) about 2 km north of the north-western boundary of Vaalputs. In this area a cluster of anorthosite-enderbite intrusives was found to cause the anomaly.

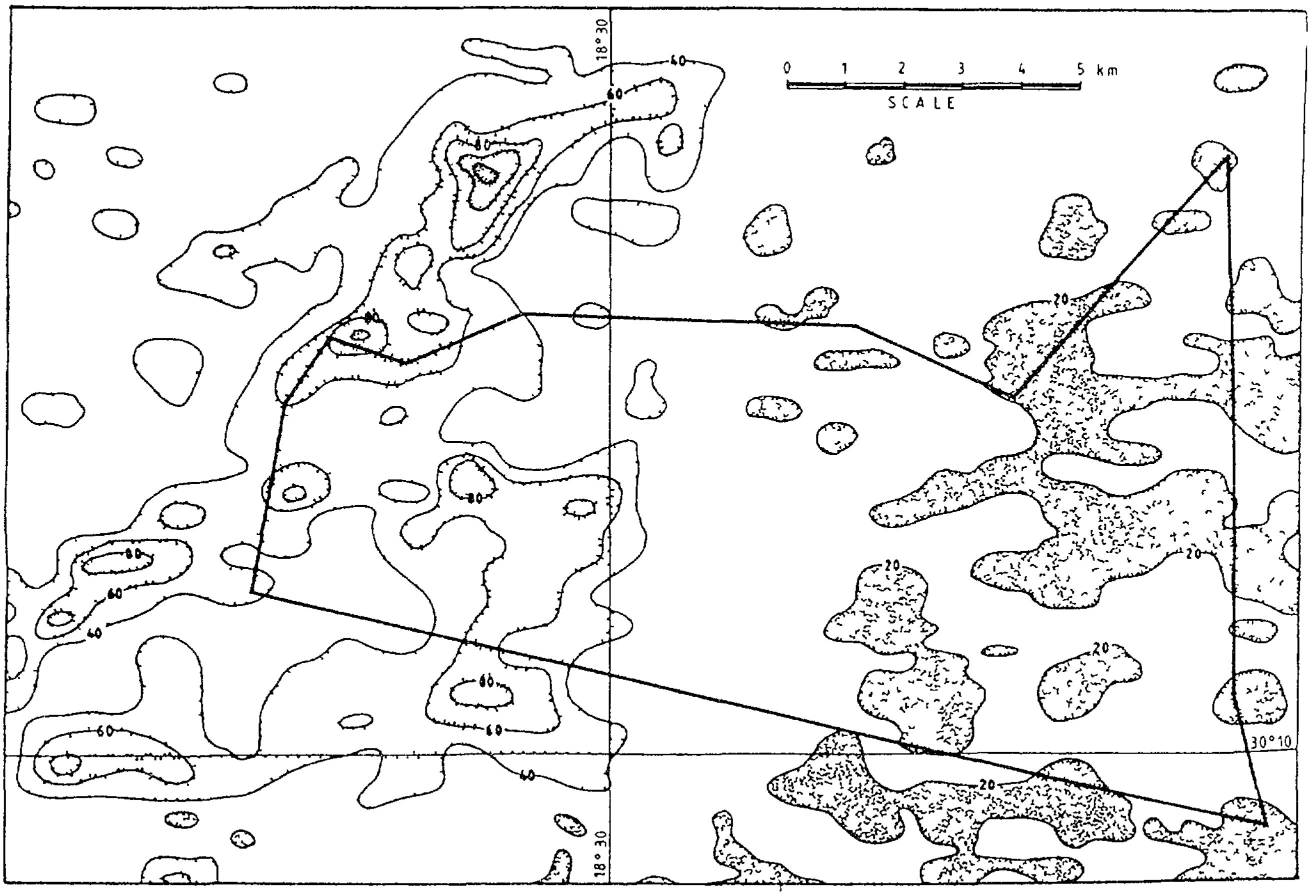

Figure 2

Airborne radiometric survey of Vaalputs area (uranium channel 1,66-1,86MeV) contours in 20cps increments from 20cps to 100cps

A large anomalous zone with count rates of the order of 60 cps above background (uranium channel) also appears in the western portion of Vaalputs, where it is directly associated with a megacrystic granite gneiss.

The Kalahari sand cover increases in thickness towards the east and this screening effect of the sand is mainly responsible for the lack of recorded anomalous areas in the eastern part of the block.

4 GROUND MAGNETIC SURVEYS

The three high-low pair magnetic anomalies as recorded by the airborne magnetic survey were located on the ground using a Scintrex MP-3 proton magnetometer. These anomalies were drilled and in all cases enderbite-anorthositic bodies were intersected.

These bodies were rich in magnetite but generally lacked minerals of economic importance. A small amount of molybdenite was found in one borehole. Since these magnetic bodies lie along a magnetic linear, there is a strong possibility that they occur in a steep structure under the sand cover. This structural aspect is yet to be investigated.

5 RADIOMETRIC SURVEYS

A regional survey was undertaken to measure the radiometric surface concentrations of uranium and thorium of some lithologies in the area surrounding Vaalputs. The lithologies present on the Vaalputs site itself were investigated in more detail using a borehole spectrometer. Both spectometers were calibrated at the Pelindaba calibration facility. It was not possible to obtain consistent results for potassium because of the high background generated on its channel by the high uranium content of the rocks.

5.1 Surface Radiometric Survey

A Geometrics DISA-400A gamma-ray spectrometer equipped with a 21 cubic inch thallium-activated sodium iodide crystal was used throughout the survey. The individual rock types were sampled at 10 or more different stations, with 5 readings being taken at each station. Counting times were governed by the radiometric concentrations present, with longer counting times being used for lower concentrations. Table 4 shows the values that were obtained. The rocks show a relative thorium enrichment with decreasing age from early syntectonic to late syntectonic.

5.2 Borehole Radiometric Survey

The radiometric borehole logging that followed after the exploration drilling was conducted in two phases. In the first phase 81 shallow boreholes, totalling 1 894 m, were drilled and logged and radiometric values were obtained for the overburden.

TABLE 4 SURFACE RADIOMETRIC VALUES* IN SELECTED LOCALITIES OF WESTERN NAMAQUALAND

Lithology/ Suite	Locality	eU_3O_8 $\pm$ SD**	$eThO_2$ - SD**	ThO_2/U_3O_8	No of samples
Enderbitic anorthosite/ Koperberg	Vaalputs	10 $\pm$ 14.7 33***	292 $\pm$ 223 560***		25
Leucogranite/ Spektakel (Late syntectonic)	Ons Vaalputs	7.6 $\pm$ 4.3	33 $\pm$ 22.5	4.3	28
Granitic gneiss/ Syntectonic granite	Riembreek (Vaalputs)	28.3 $\pm$ 9	135.8 $\pm$ 10.3	4.8	50
	Norabees se Vlei (Vaalputs)	14.1 $\pm$ 3.1	86.9 $\pm$ 3.1	6.2	12
Quartzo-feld spathic gneiss/Hoogoor (Early syntectonic)	Roodekloof Hoek Kat se Vlei	20.6 $\pm$ 5.8	31.5 $\pm$ 11.0	1.5	79
Nababeep-type augen gneiss/ Little Namaqualand (Early syntectonic)	Roodekloof Hoek Kat se Vlei	29.2 $\pm$ 2.9	24.1 $\pm$ 3.4	0.8	80

* Measurements by Andersen and Faurie (1986) in equivalent U_3O_8 and ThO_2 All values in ppm.
** SD: Standard Deviation
*** Maximum Values; measurements by Andreoli and Hart (unpublished data)

(Andersen and Faurie, 1986). In the second phase 29 deep boreholes, totalling 3 456 m, were drilled and radiometric values were obtained for the underlying bedrock lithology, the results of which are summarized in Table 5.

A Geometrics BLW-2000E differential gamma-ray spectrometer equipped with a 2 cubic inch thallium-activated sodium iodide crystal was used for the logging. Radiometric uranium and thorium values were calculated at 1 m increments in each borehole. These

TABLE 5 BOREHOLE RADIOMETRIC VALUES*

Lithology	Suite	eU_3O_8 $\pm$ SD**	MV***	$eThO_2$ – SD**	MV***	ThO_2/U_3O_8	No of samples
Enderbitic anorthosite	Koperberg (Late tectonic)	9 $\pm$ 10	60	61 $\pm$ 72	500	7	259
Leucogranite	Spektakel Suite (Late syntectonic)	19 $\pm$ 12	45	66 $\pm$ 35	170	3	41
Vaalputs granite gneiss	(Syntectonic granite suite)	17 $\pm$ 9	Coarse-grained 45	102 $\pm$ 73	350	6	853
		14 $\pm$ 6	Fine-grained 35	91 $\pm$ 37	400	7	200
Fine grained biotite gneiss	Garies Subgroup	25 $\pm$ 7	45	109 $\pm$ 46	225	4	62

* Values from Andersen & Faurie (1986)
in equivalent U_3O_8 and ThO_2
All values are ppm and integrated over borehole intervals of 1 m
** SD: Standard Deviation
*** MV: Maximum Value

data were then compared with the geological log of each hole and mean values were calculated for each lithology encountered.

6 DISCUSSION

6.1 Ground Radiometric Survey

On studying the results of the surface radiometric surveys as summarized in Table 4, the following conclusions can be drawn:

- Enderbitic anorthositic and related rocks revealed anomalously irregular values of uranium and thorium even in the same outcrop. It is possible that there might be a positive correlation between the count rates and the magnetite/ biotite content of these rocks. Higher concentrations than those reported here were measured in the Steenkampskraal area in massive monazite ore (up to 2 percent equivalent U_3O_8).

- Values obtained from the radiometric analysis of the leucogranites compare very well with neutron activation analysis carried out by Hart and Andreoli (1985) on the same rocks.

- The radiometric traverse over the Riembreek syntectonic granite suite was unfortunately, done over an airborne radiometric anomaly. It is therefore not surprising that the measured values are twice as high as those obtained elsewhere by analytical methods of the same rock (Hart and Andreoli, 1985). In contrast to this, the granitic augen gneisses of Norabees se Vlei cannot be differentiated on the bases of their uranium and thorium contents from the group III granites as analysed by Hart and Andreoli (1985) in the Vaalputs area (average values of 10 ppm uranium and 60 ppm thorium). These values obtained for the Norabees se Vlei granites can also be correlated with the Spektakel Suite rock for which Robb (1982) obtained analytical values of 20 ppm uranium and 100 ppm thorium.

  Muller and Smit (1983), on the other hand, studied similar syntectonic granites, e.g. the Concordia granites in the Springbok/Okiep area, and reported equal values for uranium but thorium values about 25% lower.

Quartz feldspathic rock from the Hoogoor Suite were not chemically analysed. However, the values as stated in Table 4 appear distinctly enriched in uranium relative to similar rocks from the Okiep and Aggeneys areas. The thorium values correlate favourably with values obtained elsewhere for the same rock suite. (Muller and Smit, 1983, and Duncan, pers. com.)

The uranium and thorium values for rocks of the Little Namaqualand Suite as measured around Vaalputs (Table 4) were compared with values obtained by Muller and Smit (1983) and Reid and Barton

(1983) of similar rocks in Namaqualand. The rocks around Vaalputs seem to be enriched in uranium by a factor of three and ten respectively. The thorium values on the other hand are lower by a factor of two.

In summary, the data presented in Table 4 indicate that uranium and thorium concentrations reach their highest values in rocks of the Koperberg Suite. This was confirmed by investigating two airborne radiometric anomalies on the ground in the Vaalputs area, which were found to be caused by dykes of monazite/zircon/etc. bearing enderbite and enderbitic anorthosite (Andreoli et al., in preparation).

The uranium and thorium concentrations for rocks of other lithologies (leucogranites and granite gneisses) compare favourably with observations elsewhere, while the abnormal values obtained for the Roodekloof Hoek, Kat se Vlei and Riembreek granites are indicative of abnormal geological processes in the area.

6.2 Borehole Radiometric Survey

The borehole radiometric survey by Andersen and Faurie (1986) confirms the results of the ground survey, in that the most highly radioactive lithologies are represented by the more differentiated end members of the Anorthosite Suite. Figure 3 shows the frequency distribution for uranium and thorium. It is interesting to note that thorium has a distinct bimodel distribution, indicating that it is not randomly distributed but has a specific petrogenetic control.

In general there is a very good correlation between the results obtained by the surface radiometeric survey and the down-the-hole radiometric survey for rock suites around Vaalputs (Table 5). The relatively small discrepancies that do occur (values obtained for the leucogranites) indicate a higher concentration of both uranium

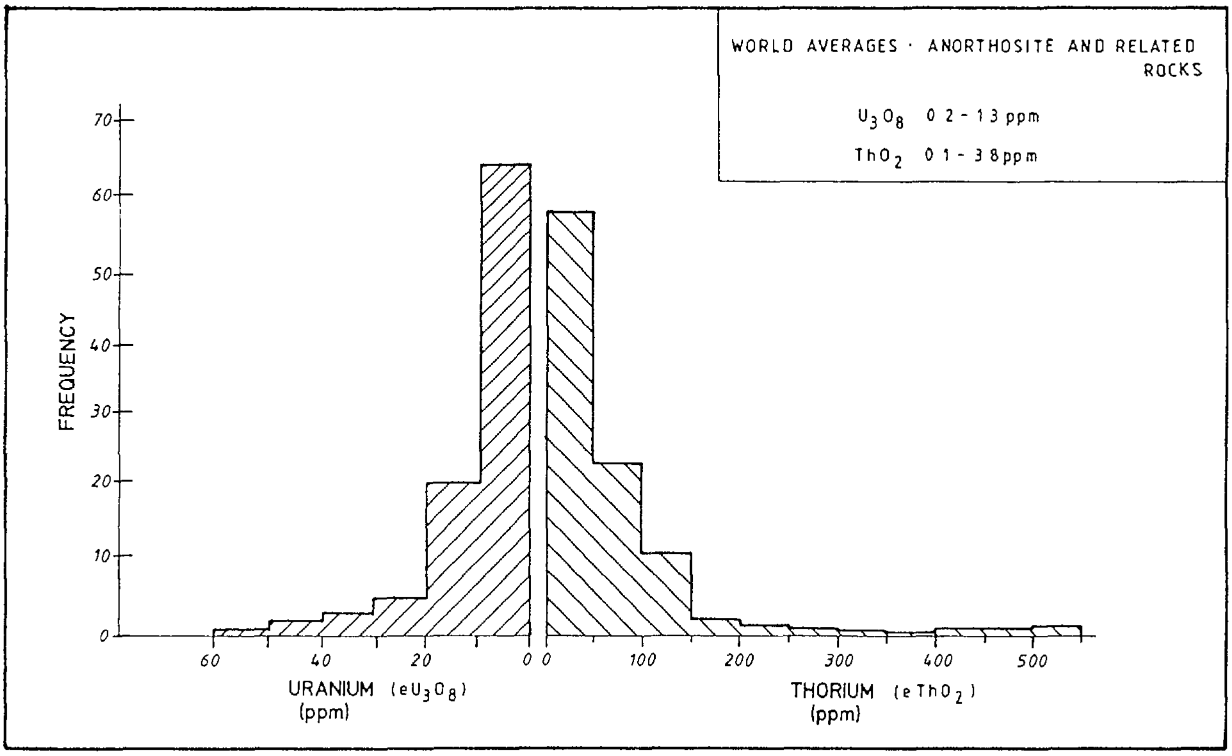

Figure 3

Frequency distribution of uranium and thorium values from radiometric borehole logs of fresh Koperberg Suite rocks from the Vaalputs site

and thorium in the boreholes measurements, which can be attributed to weathering and leaching out of these elements from the surface rocks.

The thorium/uranium ratios (Table 5) indicate that the enderbitic anorthosites have experienced complex geochemical processes which led to the decoupling of thorium from uranium. The control of this decoupling is at present the subject of a study being carried out at Steenkampskraal by Andreoli et al., (in preparation).

7 SUMMARY

The results of the study indicate a strong enrichment in uranium in all rock suites of igneous origin in the Vaalputs area relative to similar rocks worldwide. Adams et al. (1959) show that typical uranium concentrations range between 1-7 ppm in silicic igneous rocks and between 0,3 and 2 ppm in basic intrusions .

The spectacular enrichment of the anorthosites around Vaalputs as compared with typical anorthosites from Proterzoic mobile belts of America and Scandinavia is clearly indicated in Figure 3.

Although other workers, e.g. Robb and Shoch (1985), observed that the granites of Namaqualand were enriched in both uranium and thorium, proof of the exceptional enrichment of these elements and their pertinent association with the anorthosite suite is a direct result of the studies carried out on the Vaalputs block and surrounding areas (Andreoli, 1984; Andreoli and Hart, 1986a).

Our results indicate further that western Namaqualand was intruded (1 000 Ma ago) by anorthosite related magmas which were enriched in a great number of elements of specific economic value. There seems to be a broad regional zonation (see Fig. 4) in that the anorthosites of Okiep differ from those of Steenkampskraal by the relative proportions of copper vs the radioactive elements and rare earths.

Available data support the hypothesis that the K, REE, P, U, Th -enriched norites and anorthosites of the Koperberg suite are the terrestrial equivalent of the Lunar KREEP norite and basalt suite (Andreoli and Hart, in prep.).

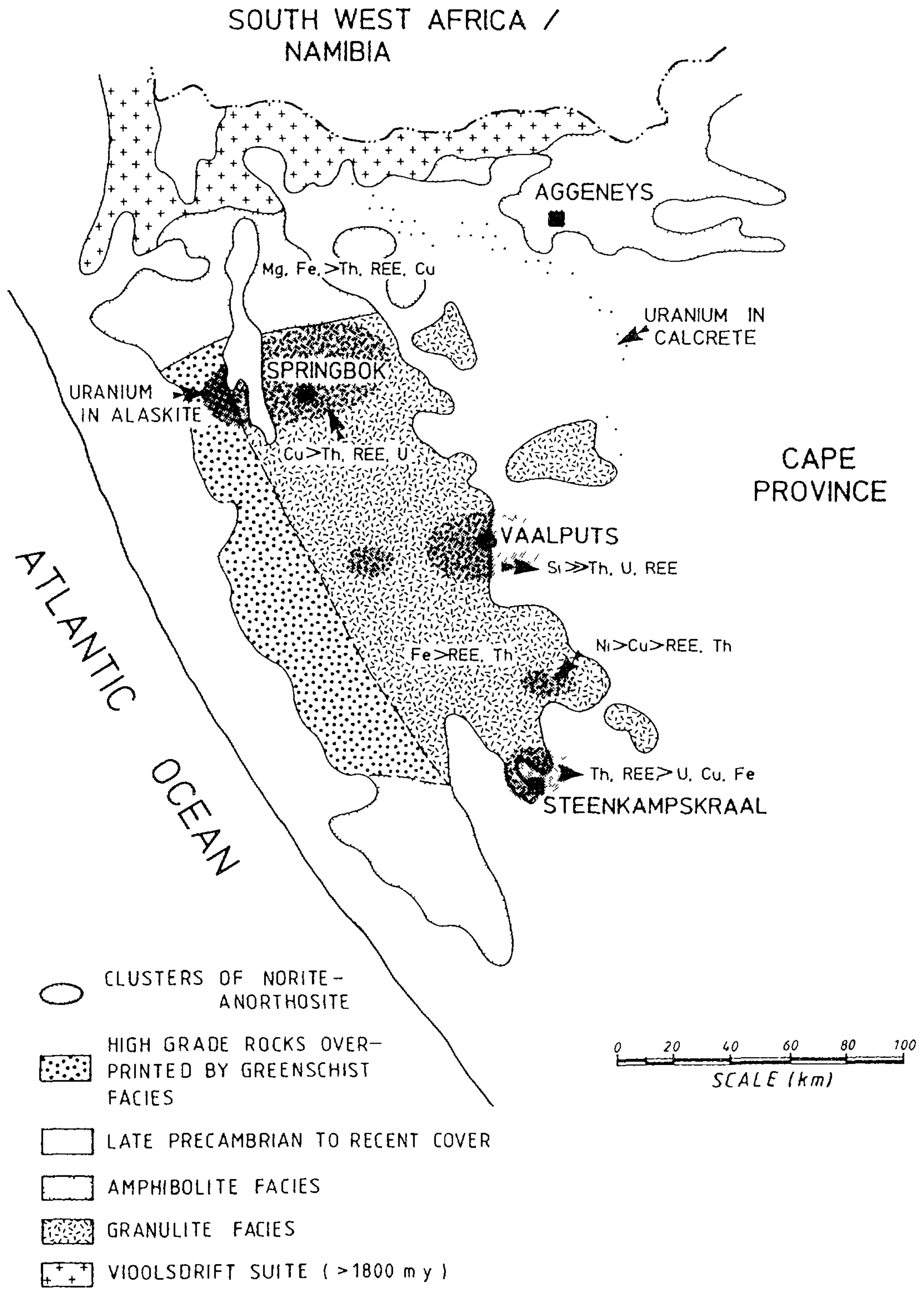

Figure 4 Metallogenetic specialization of norite-anorthosite $\pm$ enderbite and associated rocks in Western Namaqualand

REFERENCES

ADAMS, J.A.S., OSMOND, J.K., and ROGERS, J.J.W. (1959). The geochemistry of thorium and uranium. Phys. Chem. Earth, 3, pp. 298-348.

ANDREOLI, M.A.G., (1984). K-REE-P-U-Th-metasomatism in kibrara, charnockite and anorthosite suites of Mozambique, Malawi and South Africa. Proceedings, 27th International Geological Congress, Moscow, 1984, Vol. VI. Section 12, p. 7-8.

ANDREOLI, M.A.G., and HART, R.J. (1986a). Evidence for LIL-fertilisation of the lithosphere: Part I, scapolitised granulites of the Mozambique belt. The Geol. Soc. Australia Spec. Publ., in press.

ANDREOLI, M.A.G., and HART, R.J. (1986b). A charnockite-anorthorite related "HIGH-TECH" metal deposit in the Namaqualand Metamorphic Complex. Workshop on metamorphism and metamorphic processes in mineralization, Geol. Department, University of the Witwatersrand, 4-5 September 1986. Abstracts Volume.

ANDREOLI, M.A.G., ANDERSEN, N.J.B., RAUBENHEIMER, E., and NIEMAND, N. (1986). Geological map of the Vaalputs National Radioactive Waste Disposal Facility, Northwestern Cape, South Africa (with explanatory notes). Proceedings Volume to the Radwaste '86 Conference 8-12 September, 1986, Cape Town.

ANDERSEN, N.J.B., and FAURIE, J.N. (1986). Geophysical investigations on the Vaalputs Radioactive Waste Disposal Site in the Republic of South Africa. Proceedings Volume to the Radwaste '86 Conference, 8-12 September 1986, Cape Town.

DUCHESNE, J.C. et al. (1974). Rare-earth data on mononoritic rocks related to anorthosites and their bearing on the nature of the parental magma of the anorthositic series. Earth and Planetary Science Letters, 24, 1974.

DUNCAN, A. Personal communication.

HART, R.J. and ANDREOLI, M.A.G (1985). Geochemical and petrographic classification of the granitic rocks in the Vaalputs area. Site Selection Program for the Disposal/Storage of Radioactive Waste in South Africa. Site Suitability Phase Progress Report No. 31. June 1985. (GEA 622), (PER-134). Unpublished report.

GOLDBERG, S.A. (1984). Geochemical relationships between anorthosite and associated iron-rich rocks, Laramie Range, Wyoming. Contrib. Mineral Petrol. 87, 1984.

JOUBERT, P. (1986). The Namaqualand Metamorphic Complex - a summary. In: C R Anhaeusser and S Maske, (Eds). Mineral Deposits of Southern Africa (Vols I and II). Geol. Soc. S. Afr., Johannesburg, pp. 1395-1420.

LOMBAARD, A.F., and the EXPLORATION DEPARTMENT STAFF OF THE O'OKIEP COPPER COMPANY LIMITED (1986). The copper deposits of the O'okiep district Namaqualand. In: C.R. Anhaeusser and S. Maske (Eds.). Mineral deposits of Southern Africa (Vols I and II). Geol. Soc. S. Afr., Johannesburg, pp. 1421-1445.

MULLER, J.A. and SMIT, G.J. (1983). A geophysical study along a profile from Garies to Vioolsdrif across the copper district. Geol. Soc. S. Afr., Spec. Publ. 10. pp. 139 - 146.

PIKE, D.R. (1958). Thorium and rare-earth bearing minerals in the Union of South Africa. Ref. P/1107. Proc. 2nd Int. Conf. Geneva. Peaceful Uses of Atomic Energy.

REID, D.L., and BARTON, E.S. (1983). Geochemical characterisation of granitoids in the Namaqualand Geotraverse. Geol. Soc. S. Afr., Spec. Publ. 10. pp. 67 - 82.

ROBB, L.J. (1982). A review of magmatic differentiation in granites from the Springbok region, Namaqualand. Report submitted to the AEC. Unpublished.

ROBB, L.J., and SCHOCH, A.E. (1985). Deuteric alteration and uranium mineralisation processes in leucogranite intrusions from the Namaqualand Metamorphic Complex, South Africa. Proceedings Volume to the conference on: In high heat production (HHP) granites, hydrothermal circulation and ore genesis. The Institution of Mining and Metallurgy, London, pp. 301 - 314.

RYAN, P.J., LAWRENCE, A.L., LIPSON, R.D., MOORE, J.M., PATERSON, A., STEDMAN, D.P., and VAN ZYL, D. (1986). The Aggeneys base metal sulphide deposits. Namaqualand district. In: C R Auhaeusser and S Maske (Eds.). Mineral Deposits of Southern Africa (Vols. I and II). Geol. Soc. S. Afr., Johannesburg, pp. 1447 - 1473.

WEIS, D., and DEMAIFFE, D. (1983). Pb isotope geochemistry of a massif-type anorthosite-charnockite body: the Hidra Massif (Rogaland, S.W. Norway). Geochem. et Cosmochim. Acta, Vol 47, 1983.

APPLICATION OF THE GEOSTATISTICAL ANALYSES TO URANIUM GEOLOGY

(Ore reserve estimation and interpretation of airborne magnetic survey data)

Shenghuan TANG, Yuxuan XUE, Jinqing MENG
Bureau of Geology,
Ministry of Nuclear Industry,
Beijing, China

Abstract

A method for treating the uranium geological data of different types using geostatistical analyses (Kriging analysis and/or factor kriging analysis) is described in the paper. The original data are stored in data bank and can be taken out for analysis.

The uranium reserves are estimated by kriging analysis. A complete system of programs suitable for uranium reserve estimation is developed, beginning with input of original gamma-logging data in order to transfer them into ore grades in computer and to calculate uranium grade variograms and, then, to estimate uranium reserves. A case example is presented.

In order to develop a new method of analysis for regional geophysical and geochemical data processing, the factor kriging analysis in combination with the essential ideas of kriging analysis and principle component analysis is used.

This method enables the regionalized variables to split into the components of different frequency intervals corresponding to different ranges, and, then, on the basis of major component analysis several (usually two) major ranges are determined in order to infer the geological structure related to these major ranges.

According to the formula of magnetic frequency spectrum and by using fourier inverse transform of

2-dimension, covariance function and variogram are drived. The preliminary results obtained by treatment and analysis of a large number of airborne magnetic data using factor kriging analysis are given.

Kriging method for uranium ore reserve estimation

The distribution of regionalized variables ($Z(x_i)$ are the distribution variables of the ore grades in space for example) within any given deposit bears both structural and random characteristics as summarized by geostatistical analyses. It means there appear some regular pattern of random distribution and, also, certain correlation.

G. Matheron, the french scholar, found the theory of geostatistical analyses which, in fact, is used for solving the geological problems concerned by means of describing regionalized variables by variograms.

Variogram is written as following formula: [1]

$$2\gamma(h) = \frac{1}{N(h)} \sum_{i=1}^{N} \left[Z(x_i + h) - Z(x_i)\right]^2 \ldots\ldots(1)$$

Where $Z(x_i + h)$ and $Z(x_i)$ are the variable values of any two given points in space, and $N(h)$ are the numbers of the measured data pairs with distance h from each other.

From the spherical variogram model the regionalized variables can be obtained within a range of distance "a" with certain correlation to the latter. If the distance exceeds "a", the variables lose such a certain correlation.

Below are given the results of the uranium reserve estimation of the deposit No.I using the kriging method and their comparison with that of other conventional estimation method.

1) Summary of No.I deposit

No.I deposit is occured in rocks of Jurassic age, Mesozoic, which are composed of sandstone and conglomerate at the bottom, rhyolite in the middle and tuff and purple siltstone in the upper part and andesite in the top. There are three groups of the faults, i.e. NE, NW and EW. The ore body is located along the EW fault and have lenticular forms with relatively big dimension, 320m long, 110 m wide and 5 m thickness on average. The ore grade is high. The projection plan and the estimated blocks of the orebody are given in FIG. I.

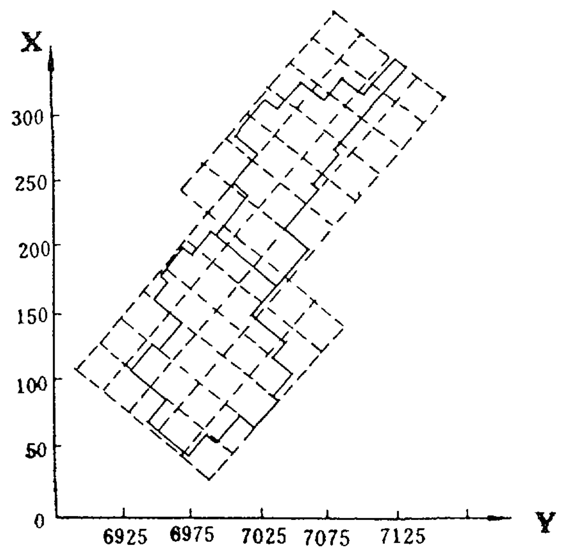

FIG. I Horizontal projection of the orebodies and estimate blocks
The solid line shows the orebodies, the dashed line shows the estimate blocks.

2) The space variation of uranium mineralization in No.I deposit

In order to find out the space variation characteristics of uranium contents in No.I deposit in each direction, and to determin the continuity of uranium mineralization, the variogram $\gamma(h)$ curves of uranium contents in orebody have been calculated separately at each level and along different direction in space by means of interpretation of the thin ore bed using the gamma-logging data obtained from 41 drilling holes with 25 X 25 m^2 grid. The $\gamma(h)$ curves of each horizontal and vertical directions are belonging to an instant variation model and can be simulated by a spherical model.

By analysing average $\gamma(h)$ curves for 41 holes along vertical direction (FIG. II) and the theoretical curve of spherical model for simulation, the structure parameters are gained as follows:

Sill = 0.10692, C_0 = 0.01, a = 4.6,

σ_k^2 = 0.07409

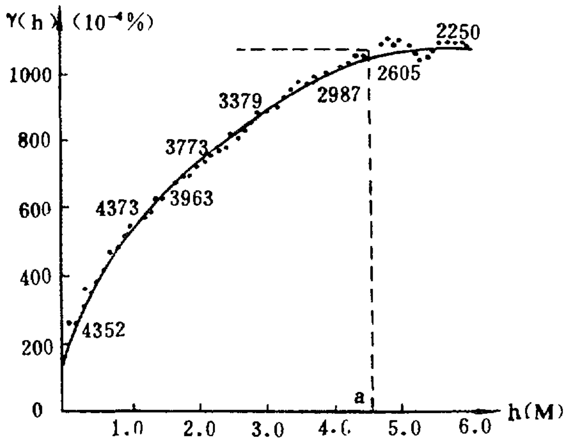

FIG. II The curve of the average variogram $\gamma(h)$ along vertical direction based on the data from 41 drill holes
The solid circles show the points of experimental estimation and the pairs; the solid line is a curve of theoretical simulation.

Where sill is the value, if h exceeds a certain distance (range) and the variogram is stabilized within a limitation; C_0 is a nugget effect indicating a discontinuity of the variogram at the original coordinate points; a is range; σ_k^2 is estimated variance.

A $\gamma(h)$ curve along 45° direction of major axis of the orebody was calculated. Because the drilling grid is 25 m^2, the $\gamma(h)$ curves calculated reflect only the big structure. The $\gamma(h)$ curve can be simulated by using the spherical model and the structure parameters can be gained as follows:

Sill = 0.02796, C_0 = 0.0062, a = 225,

σ_k^2 = 0.0485

From the above it can be seen that the "a" is relatively big,while the "sill" relatively small, that is in consistence with the characteristics of a relative continuity and small variation of the mineralization along the major axis of the orebody. But if the calculation is based on the gamma-logging data from drill holes at a certain grid, it is difficult to determine the small structure variation in space caused by relatively big distance between the drill holes. In order to obtain precisely the $\gamma(h)$ curves along the minor axis of the orebody and within a small area, we took the gamma-logging data of 930 blast-holes at the spacing 2-5 m for calculation of the $\gamma(h)$ curves along the vertical and various horizontal directions for the ladder blocks at 30 m and 20 m levels separately. The calculation results were regularized.

After interpreting the $\gamma(h)$ curves of the ladder block at 30 m level, it is obvious that the $\gamma(h)$ curves of the orebodies along the major axis (direction 45°) possess the isotropy structure, and the sill and C_0 are essentially similar. In the zone near the 80 m the $\gamma(h)$ curves along these two directions are strongly jumpy, indicating existence of an obvious discontinuity there (FIG.III). It was proved by mining operation that the middle part of the 30 m level ladder-block is just located in the saddle of the orebody. In the central part of the saddle there appear the overlying strata--purplish red siltstone.

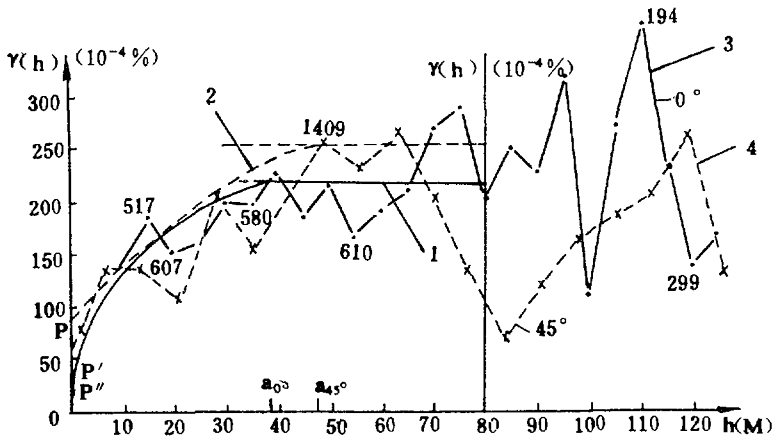

FIG. III $\gamma(h)$ curves of the ladder block At 30m-level along 0° and 45° directions, 1 and 2 are the curves of theoretical simulation; 3 and 4 are the curves of experimental estimation.

The $\gamma(h)$ curves along the minor axis direction (135°) also possess identical structure (FIG.IV). The value "a" obtained by variogram in 135° direction is smaller than that in the 45° direction showing the existence of real mineralization continuity. The structure parameters are:

In 0° direction: sill = 0.02202 a=39
$C_0 = 0$ $\sigma_k^2 = 0.0328$

In 45° direction: sill = 0.02554 a=48
$C_0 = 0.0055$ $\sigma_k^2 = 0.0242$

In 90° direction: sill = 0.01651 a=34
$C_0 = 0.0011$ $\sigma_k^2 = 0.0298$

In 135° direction sill = 0.01663 a=17
$C_0 = 0.0044$ $\sigma_k^2 = 0.0292$

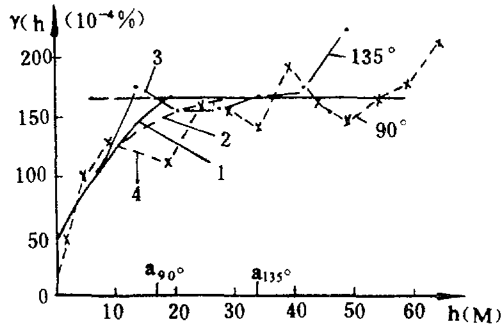

FIG. IV $\gamma(h)$ curves of the ladder block
At 30m-level along 90° and 135° direction,
1 and 2 are the curves of theoretical simulation; 3 and 4 are the curves of experimental estimation.

At the 30 m - level along the vertical direction the $\gamma(h)$ curve is smooth and fits a standard spherical model. After simulating by the theoretical curve of spherical model, the structure parameters are gained as follows:

sill=0.04 $C_0=0$ a=5.6 $\sigma_k=0.02796$

It can be seen from calculation of the $\gamma(h)$ along the vertical direction that "a" also fits the mineralization limits along the vertical direction of the orebody. Both the $\gamma(h)$ curves of the ladder blocks at 20m- and 30m-levels are essentially similar.

As we can see from the $\gamma(h)$ curves for different drilling grids and different levels, the $\gamma(h)$ curves obtained from the 25m-grid drilling data reflects the big structure of orebody variation, and the $\gamma(h)$ curves taken from the blast-holes data at 2-5m spacing show the orebody variation in small area.

3) Comparison of the estimated results

Because of the difference in orebody delineation, block classification and extrapolation for both kriging and conventional methods of ore reserve estimation, there are also a lot of such differences as the reserves with the cut-off grade 0.03% are selected for comparison.

The ore reserves of the No.I deposit have been originally estimated by vertical section method, and then verified by geoblock method. As the conventional methods do not consider the space variation of mineralization between drill holes, the tonnage of uranium metal increased at 17% in comparison with that estimated by conventional methods.

When kriging method is used, the variogram is selected in consideration of not only the space variation of the orebodies along the 0°, 45°, 90°, 135° and vertical directions, but also the variations of big and small dimension structures. So the local concentration of the mineralization between drill holes may be taken into account. The uranium reserve estimated by kriging method is bigger at 20-25% than that by conventional methods, and also bigger at about 3% than the tonnage of uranium metal mined out later. The tonnage of ore estimated by kriging method is greater at 20-26% than that by conventional methods, so the estimated result of kriging method is near to the figure of mined-out tonnage.

On the base of original gamma-logging data bank and computer processing the uranium contents for each thin ore bed can be gained. The variogram curves used for reserve estimation based on original gamma-logging data reflect not only the randomness, but the structure of the orebody, and, therefore, the spatial variation of the orebody along the various directions can be precisely determined, and, finally, the working program for estimation is made according to the actual configuration of the orebody, and thus geostatistical method can be used. It is obvious that the uranium reserve estimation system is the more perspective method.

Application of kriging method in data interpretation for airborne magnetic survey

1) Principles of factor kriging method [2]

The factor kriging method is based on the essential ideas synthesized from both kriging method and major component analysis. As a new method it can be used for processing regional geophysical and geochemical data.

This method can decompose regionalized variables into the different components with various frequences in correspondence with different ranges, and then according to major component analysis several (usually two) major ranges are recognized, and thus the geological structures correlated with these major ranges can be inferred.

As well known geophysical (geochemical) data represent the results synthesized by influence of different physical reflection in the space. These data can be regarded not only as the superposition of the regional components with the local ones, but also as the synthesized reflection of the anomalies arisen by shallow and deep geological bodies (structures). So decomposition of geophysical (geochemical) anomalies is considered as the bases for carrying out the inferential interpretation of geophysical (geochemical) data.

After making structure analyses for the variogram represented by measured field data, the regionalized variables are decomposed by factor kriging method using the following mathematical model:

$$Z(x) = \sum_{i=1}^{h} \alpha_i \, A_i \, (x) \quad \ldots\ldots\ldots\ldots (2)$$

Where "α" is the factor load of i-th space variation; $A_i(x)$ represent the space variation of the i-th variable dimension; $Z(x)$ is the value measured at point $Z(x_i)$. In the formula (2) there is required to calculate $A_i(x)$[2] for different dimensions, it is, thus, necessary to use co-kriging method. In this case we have:

$$A_i^{\bullet}(x) = \lambda^{ij} Z(x_i) \quad \ldots\ldots\ldots\ldots (3)$$

Where λ^{ij} is an unknown coefficient of kriging weight. Corresponding to the first variation dimension $A_1^{\bullet}$ it is need to estimate by kriging method in order to have the estimated values unbiased and to satisfy $\sum \lambda^{ij} = 1$. At this moment the corresponding kriging equation system are:

$$\begin{cases} \sum\limits_j \lambda^{ij} C(x_i - x_j) + \mu_1 = C_1(x_i - x) \quad i = \overline{1,n} \\ \sum \lambda^{ij} = 1 \end{cases} \quad \ldots (4)$$

and the variance is:

$$\mathrm{Var}\,[A_1^{\bullet} - A_1(x)] = C_1(0) - \sum_j \lambda^{1j} C_1(x_j - x) - \mu_1 \quad \ldots (5)$$

Based on the principles of the co-kriging method and corresponding to second variation dimension $A_2^{\bullet}$, the co-kriging estimation method should be used satisfying $\sum \lambda^{2j} = 0$, so the corresponding kriging equation system are:

$$\begin{cases} \sum \lambda^{2j} C(x_i - x) + \mu_2 = C_2(x_i - x) \quad i = \overline{1,n} \\ \sum \lambda^{2j} = 0 \end{cases} \quad \ldots (6)$$

and their variance is:

$$\mathrm{Var}\,[A_2 - A_2(x)] = C_2(0) - \sum_j \lambda^{2j} C_2(x_j - x) - \mu_2 \quad \ldots (7)$$

It is necessary to point out that the factor analysis from the multiple analyses is selected for the purpose to decrease the number of the dimensions in the case of lossing less information . For kriging method the idea of introducing major component analysis can be expressed factually in recognizing multiple ranges as multiple variables, and in carrying analysis of covariation matrix composed of multiple variations, in order to gain major component loads corresponding to the major characteristic values of the matrix. The physical meaning of the major component loads indicates their proportion among the measured values. Therefore can be given the ways to combine both factor analysis and kriging method, and to decompose the measured variations.

In order to process magnetic survey data using factor kriging method, it is recommended to definite a mathematical model of variograms according to variation characteristics of magnetic fields.

In the case of a magnetic source with regular configuration, parallelepiped for example, if a magnetization intensity is I, the buried depth is $\bar{h}$, the thickness is t, the width is 2a, the lenth is 2b, in the columnar coordinate the magnetic spectrum by theoretical calculation is:[3]

$$E(\rho,\varphi) = 4\pi^2 I^2 e^{-2\bar{h}\rho} \times (l - e^{-tb\rho})^2 S^2(\rho,\varphi) R_T^2(\rho) R_K^2(\varphi) \quad \ldots(8)$$

Where $\rho = \sqrt{u^2+v^2}$, $\varphi = \mathrm{arctg}\,(u/v)$

$$S^2(\rho,\varphi) = \left[\frac{\sin(a\rho\cos\varphi)}{\rho\cos\varphi} \times \frac{\sin(b\cos\varphi)}{\rho\cos\varphi}\right]^2$$

$$R_T^2(\varphi) = n^2 + (l\cos\varphi + m\sin\varphi)^2$$

$$R_K^2(\rho) = N + (L\cos\rho + M\sin\varphi)^2$$

Where u and v are the circle frequencies, l, m and n are the cosine directions of the magnetic field, L, M and N are the cosine directions of magnetization intensities.

By simplifying the formula (8) it can be obtained that:

$$E(\rho) = 2\pi\bar{h}^2 \exp(-2\bar{h}\rho) \text{ [4]} \quad \ldots(9)$$

In order to get the covariance expression introduced from the formula (9) we use the 2-dimensional fourier inverse transform, the essential principles of which can be expressed as follows:

As everyone knows, for each pair of random variables $\{Z(x),\ Z(x+h)\}$ the covariance c (h), if it exists, only depend on the interval (h) between the two of the points, i.e.:

$$C(h) = E\{Z(x+h) \cdot Z(x)\} - m^2 \qquad \ldots(10)$$

Where the E is the mathematical expected symbol, m is the average value.

If the covariance is expressed by interval between the original points so m=0, in this case we have:

$$C(h) = E\{Z(x+h) \cdot Z(x)\} \quad \ldots\ldots\ldots(11)$$

The formulae (10) and (11) are taken for discretic variables, if it is for continuous variables, it should be expressed by integral expression. In this case, if the 2-dimension is concerned, the corresponding covariance is:

$$c(\xi,\eta) = \int_{-\infty}^{\infty}\int_{-\infty}^{\infty} Z(u,v)\cdot Z(u+\xi, v+\eta)\,du\,dv \qquad \ldots(12)$$

Where $\xi^2+\eta^2=h^2$

According to the theory of the fourier inverse transform the integral expression of the formula (12) is a 2-dimensional autocorrelation function and, also, a fourier inverse transform of the spectrum function, thus, if the spectra of magnetic field fit the formula (9), it s covariance is:

$$c(h) = \frac{1}{2\pi}\int_{-\infty}^{\infty}\int_{-\infty}^{\infty} E(\rho)\, e^{i(u\xi+v\eta)}\,du\,dv$$

$$= \frac{1}{2\pi}\int_{-\infty}^{\infty}\int_{-\infty}^{\infty} a e^{-2\bar{h}\rho}\, e^{i(u\xi+v\eta)}\,du\,dv$$

$$= \frac{\alpha}{2\pi} \int_{-\infty}^{\infty} \int_{-\infty}^{\infty} e^{-2\bar{h}\sqrt{u^2+v^2}} \cdot e^{i(u\xi + v\eta)}\, du\, dv \quad ..(13)$$

By means of the 2-dimensional fourier inverse transform, we have:

$$\frac{1}{2\pi} \int_{-\infty}^{\infty} \int_{-\infty}^{\infty} e^{-\beta(u^2+v^2)^{1/2}} \cdot e^{i(u\xi+v\eta)} du\, dv = \frac{\beta}{(\beta^2+\xi^2+\eta^2)^{3/2}} \quad ...(14)$$

If we put the formula (14) into the (13), we obtain:

$$C\ (h) = \frac{2\bar{h}\,\alpha}{(4\bar{h}^2+\xi^2+\eta^2)^{3/2}} = \frac{\alpha'}{4\bar{h}^2+h^2} \quad ...(15)$$

Where $\alpha' = 2\bar{h}\alpha$, $\alpha = 4\pi\bar{h}^2$

From the formula (15) it is not difficult to calculate and to get the formula of the theoretical variograms. From the formula (15) we have:

$$C(0) = \pi,\ C(h) = \pi\left[1 + \frac{h^2}{(2\bar{h})^2}\right]^{-3/2}$$

If $2\bar{h} = a$,

$$\gamma(h) = C(0) - C(h) = \pi\left[1 - \left(1 + \frac{h^2}{a^2}\right)^{-3/2}\right] \quad ....(16)$$

According to the formula mentioned above, variation "a" is equal to the two-fold value of the average buried depth of the magnetic body.

2) Interpretation of magnetic anomalies using the factor kriging method.

The area II is selected as a test area. Some carbonaceous limestone and slate occure in the central part of the area, upper Cretaceous sandstons in the west, Lower Permian sandstone, slate, conglomerate in the north-east, Eocene argillite in the east, the rest zones are covered by Quarternary sediments. There are also some late Variscian intrusive rocks such as diorite-porphyrites and granites distributed along northeast 45° strike to the east of the test area, and some carbonatite bodies arranged in E-W trend to the north-west of the area. There appear some E-W-striking faults.

The variograms of the four directions in the area, i.e. 0°, 45°, 90° and 135°, are calculated (FIG. V). It is noted that the variogram curves along 45°, 90° and 135° three directions are essentially coincided with each other, so they are isotropic, and the variogram along 90° direction may be taken as the representative of the three. The variation value of the variogram along the 0° direction is greatly less than that along the 90° direction, it is because of that the 0° direction is the main structure strike of the region with a good continuity of the magnetic anomalies. The direction along the structure should give the smallest value of the variograms, so we should take in mind only the variograms along 0° and 90° directions.

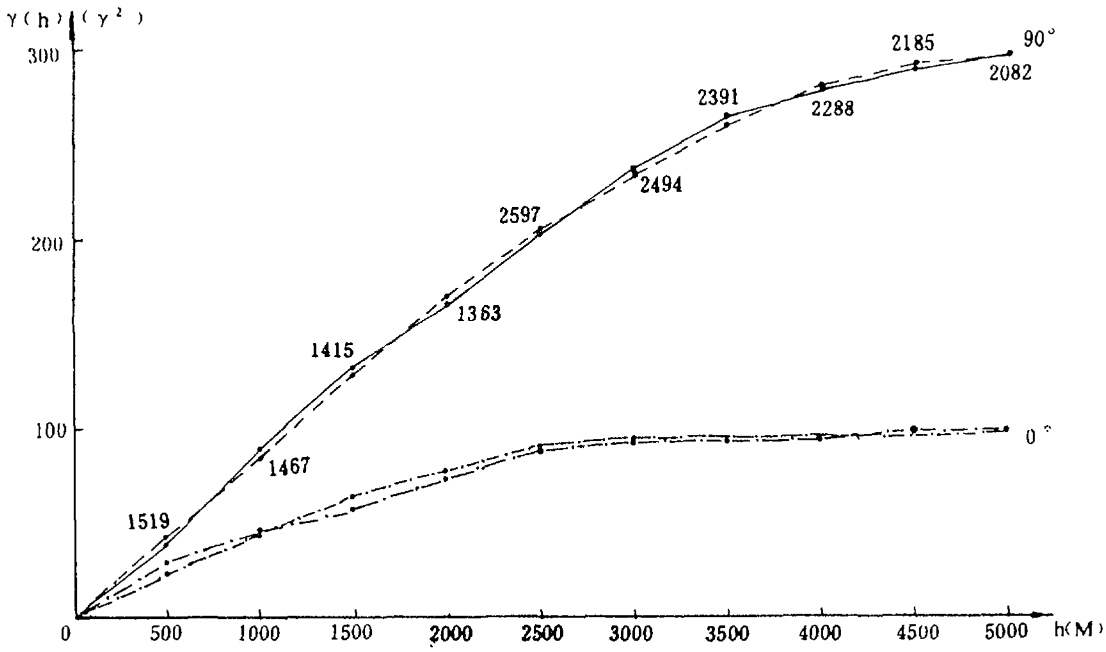

FIG. V Variogram curves
The dashed line shows the simulation curve.

After simulation using the theoretical model the structure parameters can be given as follows:

For 0°: a_1 = 500m, a_2 = 1500m, a_3 = 3000m

$sill_1$=29.51, $sill_2$=57, $sill_3$=92.35

For 90°: a_1 = 500m, a_2 = 3000m, a_3 = 5000m

$sill_1$=40.21, $sill_2$=238.91, $sill_3$=297.71

Where $sill_{1-3}$ are the Sill values of every range.

In consideration of the 0° direction being the major structure direction, the variograms indicate that there exist some correlations between the magnetic parameters within the 3000m interval, so two major ranges (500m and 3000m) are selected.

Using the variograms the covariances of each range are obtained. The factor loads of each range along different directions can be gained by resolving covariance matrix:

For 0°: α_1= 0.08, α_2= 0.17, α_3= 0.75

For 90°: α_1= 0.19, α_2= 0.59, α_3= 0.22

Where α_{1-3} are the factor loads of every range

It is, thus, clear that if a=3000m in spite of whether 0° or 90° direction, the factor load has the maximum value which makes up 59-75% of the total variance of magnetic field, and may be recognized as the first major component range, according to the theoretical calculation formula the magnetic anomalies calculated from the given range mainly reflect the variation of a magnetic field at the depth about 1500m. If a=500m, the factor load is the minimum which makes up 8-19% of the total variance of magnetic field, and may be recognized as the second major com-

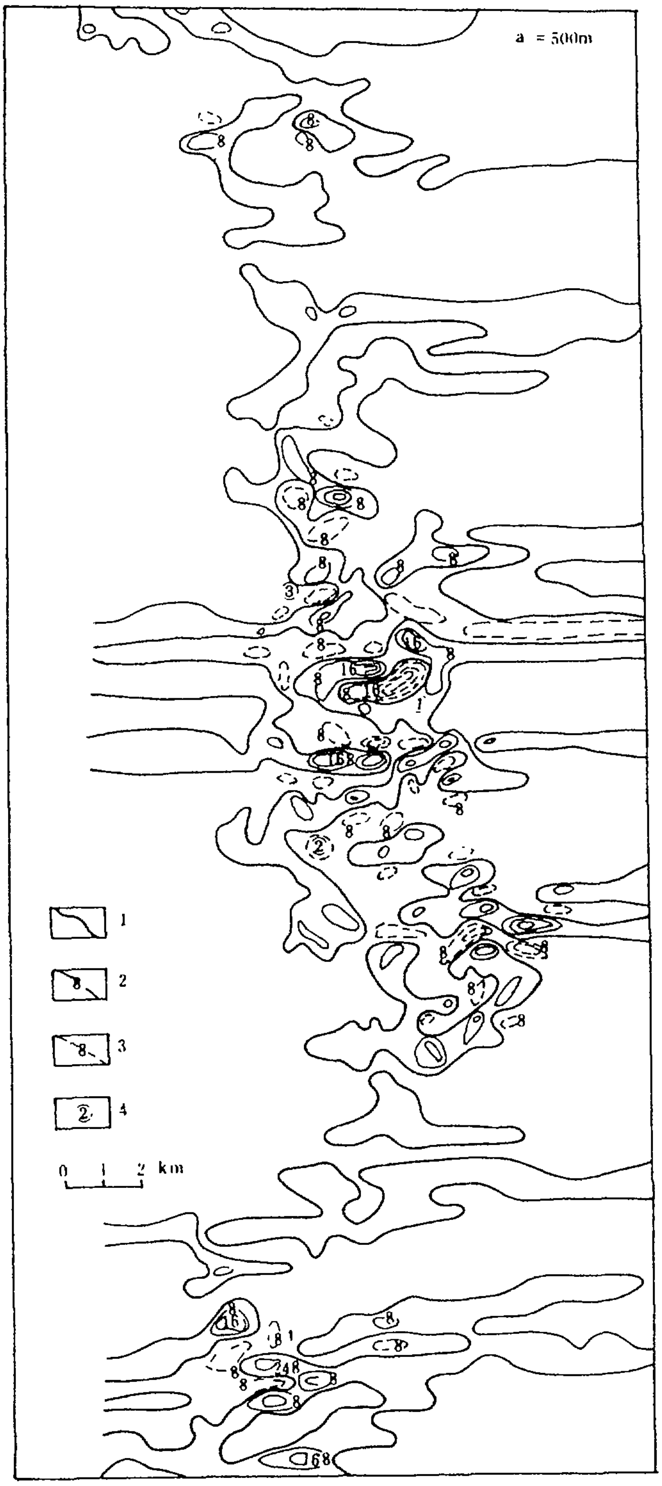

FIG. VI The ΔT isogram

1-- zero isoline; 2-- positive isolines; 3-- negative isolines; 4-- numbers of the anomalies.

Note: the actual values are twenty-fold to the numbers of the isolines.

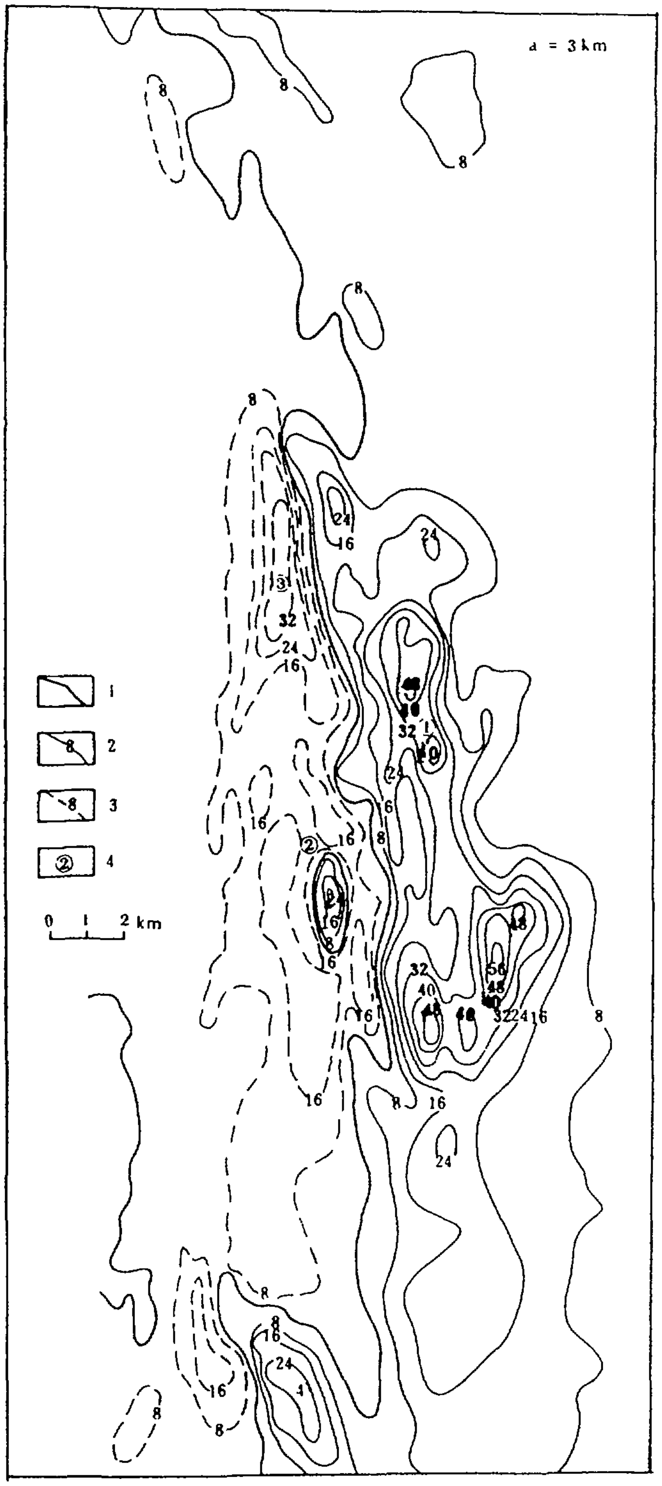

FIG. VII The ΔT isogram
1-- zero isoline; 2-- positive isolines;
3-- negative isolines; 4-- numbers of the anomalies.

Note: The actual values are twenty-fold to the numbers of isolines.

ponent range. The magnetic data calculated from that range mainly reflect the variation of a magnetic field at the depth about 250m.

The magnetic anomalies of different ranges are calculated by co-kriging method. The shallow (a=500m) magnetic anomalies are given in FIG.VI, reflecting the depth about 250m, where can be seen a group of small intrusive bodies with different magnetism arranged along EW trend. FIG.VII is the map of deep magnetic anomalies, reflecting the depth about 1500m, from that it is clear, that there appeares an apparent change from the negative to positive magnetic field from the west to the east in the central part of the region, to the north of the survey area the anomalie gradually got the NW strike, which can be inferred as a reflection of a big structure. At the shallow zone this structure is not evident, and according to a series of local small positive anomalies alternating with negative along the structure strike it may be inferred that the structure is mainly developed at the depth. This can be regarded as a reflection of an inferred big structure zone caused by different intrusive bodies in the deep.

REFERENCES

[1] Mining Geostatistics, Huijbregts Ch. and Journel A, 1977.

[2] Alain GallI., Gerdil-Neuillet. et Dadou C. Factorial kriging analysis: a substitute to spectral analysis of magnetic data; proc. NATO-ASI "Geostat-Tahoe 1983", D. Reidel publ. Dordrecht. Hollande. 1984.

[3] Bhattacharrya, B. B., Continuous spectrum of the total-magnetic-field anomaly due to a rectangular prismatic body, ≪Geophysics≫, Vol.31, No.1, 1966.

[4] Chiles. J. P. et Guillen, A., Variogrammes et krigeages pour la gravimetric et le magnetisme, ≪SCIENCES de la TERRE INFORMATIQUE GEOLOGIQUE≫, part 2 No.20, Nov. 1984.

INTERPRETATION OF AIRBORNE RADIOMETRIC DATA TO PREDICT THE OCCURRENCE OF URANIUM

J. TALVITIE, H.M. ARKIMAA
Geological Survey of Finland,
Espoo

O. ÄIKÄS
Geological Survey of Finland,
Kuopio

Finland

Abstract

Uranium pegmatites and associated uneconomic uranium mineralizations have been found in Central and Southern Finland in connection with granitoid rocks and migmatites.

Because of the glaciated terrain, where only three per cent of the bedrock area is exposed, the variation in radiation intensities reflects the variation in the thickness of the overburden, in its moisture content and in the ground-water level.

When the ratios of different energy levels of radiation are used, "the fingerprint ratio" for a certain type of uranium deposit can be found.

---

1. INTRODUCTION

Uranium pegmatites are met in Central Finland in connection with the large Middle Proterozoic granitoid complex and with highly metamorphosed migmatites. The uranium occurrences found so far are too small or of too low a grade to be of economic interest at present [1]. However, they represent a type with potential worth prospecting, but their wide areal distribution calls for a proper methods to find them effectively.

2. TEST AREA

In order to evaluate the airborne radiometric methods for prospecting, a test area of 35 km x 30 km was selected at the northeastern border of the granitoid complex. In the test area, the ground truth is formed by three uranium mineralizations connected with the uranium pegmatites. In the pegmatites, the ratio U:Th is always 2:1 or more, and the main uranium minerals are uraninite and its secondary alteration products. Also chalcopyrite and molybdenite are generally met with [2]. The lithological map of the area has been checked and reestimated by field surveys.

3. GLACIATED TERRAIN

The γ-radiation intensities of each of the three channels (U, Th, K) have been corrected for the preparation of intensity maps [3]. The intensity distribution does not reflect, however, the distribution of the lithological units. The reasons for this are that the bedrock is seldom exposed and that different kinds of radiation attenuators occur on the bedrock:

1) The test area is a typical drumlin and fluting landscape. The mechanical transport of the loose mineral material has been intensive and there seldom lies any basal till or loose mineral matter in situ on the bedrock. In this case, the radiation emitted from the till does not reflect the properties of the underlying bedrock. Instead, the overburden is a considerable attenuator, depending on its thickness.

2) The ground-water table, when lying above the bedrock surface, is a complete attenuator.

3) Peat bogs with a high moisture content covering the overburden are strong attenuators.

The distribution of the highest radiation intensities in each channel marks the exposed bedrock hills and related areas with a thin and/or dry till cover.

4. RADIATION RATIO BETWEEN CHANNELS

It has been supposed that when the radiation in different channels attenuates, the ratio between them remains

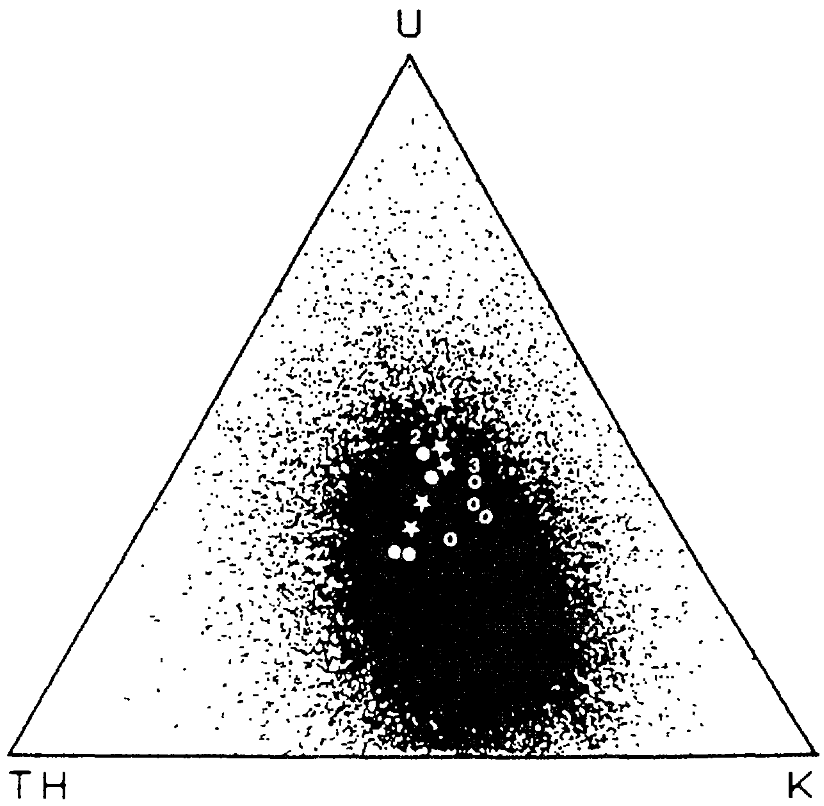

FIG. 1 The airborne radiometric data yielded by the test area represented as pixels in a triangular diagram. The known uranium mineralizations are 1. Lemmetty, 2. Kettukallio, 3. Kinturi. The pixels coinciding with the mineralizations have been indicated by 1, 2 and 3, respectively. The neighbouring pixels have been indicated by the same unnumbered symbols.

rather constant. Therefore, it may be possible to find a fingerprint ratio for a certain type of deposit.

The ratios between the data in each channel can be easily inspected in a trianglular diagram of U, Th and K (Fig. 1). All the measured pixels of the test area, as calculated in a grid of 100 m x 100 m, are shown in the diagram. The main part of the pixels forms an ovoidal distribution figure in the middle and lower parts of the diagram. The pixels coinciding with the targets or the three known uranium mineralizations are located on the uranium corner side of the ovoidal distribution figure. The pixels adjacent to the targets are located farther away from the uranium corner.

It seems obvious that the uranium occurrences in pegmatites have a certain fingerprint ratio between U, Th and K. All the other pixels having this ratio can easily be displayed on a TV-screen, using any correlation map.

REFERENCES

[1] Räisänen, E., Uraniferous granitic veins in the Svecofennian Schist Belt in Nummi-Pusula, Southern Finland, IAEA-TC-571 (1986).

[2] Yli-Kyyny, K., Geology and radioactive pegmatites in Lemmetty, Keitele, Pro gradu-Thesis, University of Turku, Dept. of Geol. and Min. (1986) (in Finnish).

[3] Virtanen, K. and Vironmäki, J., Aerogeofysikaalisten matalalentomittausten käytöstä soiden arvioinnissa, Turveteollisuus, vol. 3 (1985).

GEOCHEMICAL DATA INTERPRETATION AND INTEGRATION

GRAPHICAL DISPLAYS OF MULTIVARIATE GEOCHEMICAL DATA ON SCATTERPLOTS AND MAPS AS AN AID TO DETAILED INTERPRETATION

H. KÜRZL
Mineral Resources Research Division,
Joanneum Research Society,
Leoben, Austria

Abstract

Geological data analysis is currently undergoing major changes. It seems crucial to collect as many data as possible and to consider several variables at a time to uncover geological processes with their inherent complexities and peculiarities. Several data processing systems with capabilities for handling and analysing large sets of multivariate data do exist. Since many years diverse relative complex multivariate mathematical/statistical methods have been used. The application of these methods, however, led quite often to results, where interpretation was extremely difficult. One reason is that the strong parametric models based on certain assumption, generally implied in these methods, are not always valid for empirical data. Thus, prior to the advanced stage of multivariate data analysis, it seems absolutely necessary to know more about general data behavior.

For that purpose a new way of looking at data is suggested by the so called "Exploratory Data Analysis" techniques. They include resistant order statistics, robust statistics and a variety of relatively simple graphical methods. Basically they refer to the univariate case, which should never be neglected before looking at the relationships and common characteristics of two or more variables together. Graphical methods especially for analysing multivariate data use symbolic scatterplots and multiple code symbols. The construction of the symbols and the different possibilities of graphical displays are explained.

In examples using a set of multivariate data, derived from the regional stream sediment survey of Austria, different multiple

code symbols will be compared and the possibility of identifying patterns and relationships will be demonstrated. By looking at several multivariate displays the inherent data structure can be uncovered. In some cases a distinct aid to interpretation and essential additional informations for further classical numerical statistical analyses can be gained.

---

1. INTRODUCTION

In the realm of earth sciences and especially in mineral exploration many techniques for sampling the geological phenomenon have been developed and are routinely in use. Nealy everybody has learned about the ability of these data acquisition techniques to gather enormous amounts of data within a short time and at relatively low costs. Data integration and adjustments to modern data processing systems have been constantly advanced in close connection to hardware and software improvements. However, digital data storage, integration of different data types and computer-aided interpretation are fields where further developments seem to be necessary and distinct enhancements can still be expected. This paper focuses on some aspects of data analysis and interpetation of multivariate data. Several formal numerical techniques have been widely accepted and used in geoscience for many years. They follow the conventional statistical theories of estimation and hypothesis testing. Practical experiences with these techniques, however, showed that their models and objectives are quite often too narrow and formal to satisfy empirical data behavior. Thus results generated were often difficult to explain, and sometimes led to misinterpretations.

Looking deeper into the problem the question arises, "Why do these techniques fail?" It will be soon very clearly visible that the main reasons lie in unanticipated data structures, inadequate data models, and a lack of understanding of basic data characteristics and realationships.

One way to overcome these difficiencies, is the preliminary examination of data by the use of diagrams and multiple code symbols. By doing so, direct interpretation is sometimes possible. It will at least be an essential prerequisite to a more formal analysis.

The graphical techniques presented, originate from the quite recently developed "Exploratory Data Analysis" as described for the first time by J.W. Tukey (1977) [1]. This method works with a set of data in a fairly informal way, without any strong statistical assumptions, incorporating resistant and robust statistics. Graphical displays for inspecting data play a central role. They are based on techniques developed and partly improved significantly during the last ten years as described and published by B. Everitt (1978) [2], V. Barnett (1981) [3] and J.M. Chambers et al. (1983) [4]. Some of these techniques have been already introduced to exploration geochemistry in test applications as described by Garrett (1983) [5] and Howarth (1984) [6].

The routine use of computer graphics in data analysis has evolved only a few years ago, when graphical hardware took advantage of the rapid developments in micro electronics and basic graphical software became standardized. That means that the techniques described have a practical relevance to a broad range of potential users at this time and will multiply as soon as announced improvements, especially at the PC-level (enhanced graphic-capabilities, software for graphical data analysis), are realized.

2. TEST AREA AND DATA

To be able to show some practical applications of modern, graphically aided data analysis, actual geochemical data derived from a regional stream sediment survey in Austria are used. For this survey the -80 mesh fraction of more than 30.000 stream sediment samples has been analysed for 36 elements. For practical presentation purposes data from a small area of about 25 km (17 samples) have been chosen. The map in fig.1 shows the generalized geology of the area. The region in the south consists of orthogneises overlain by metaarenites (permian) and sericite quartzite schists of the same age. As part of another tectonic unit palaezoic

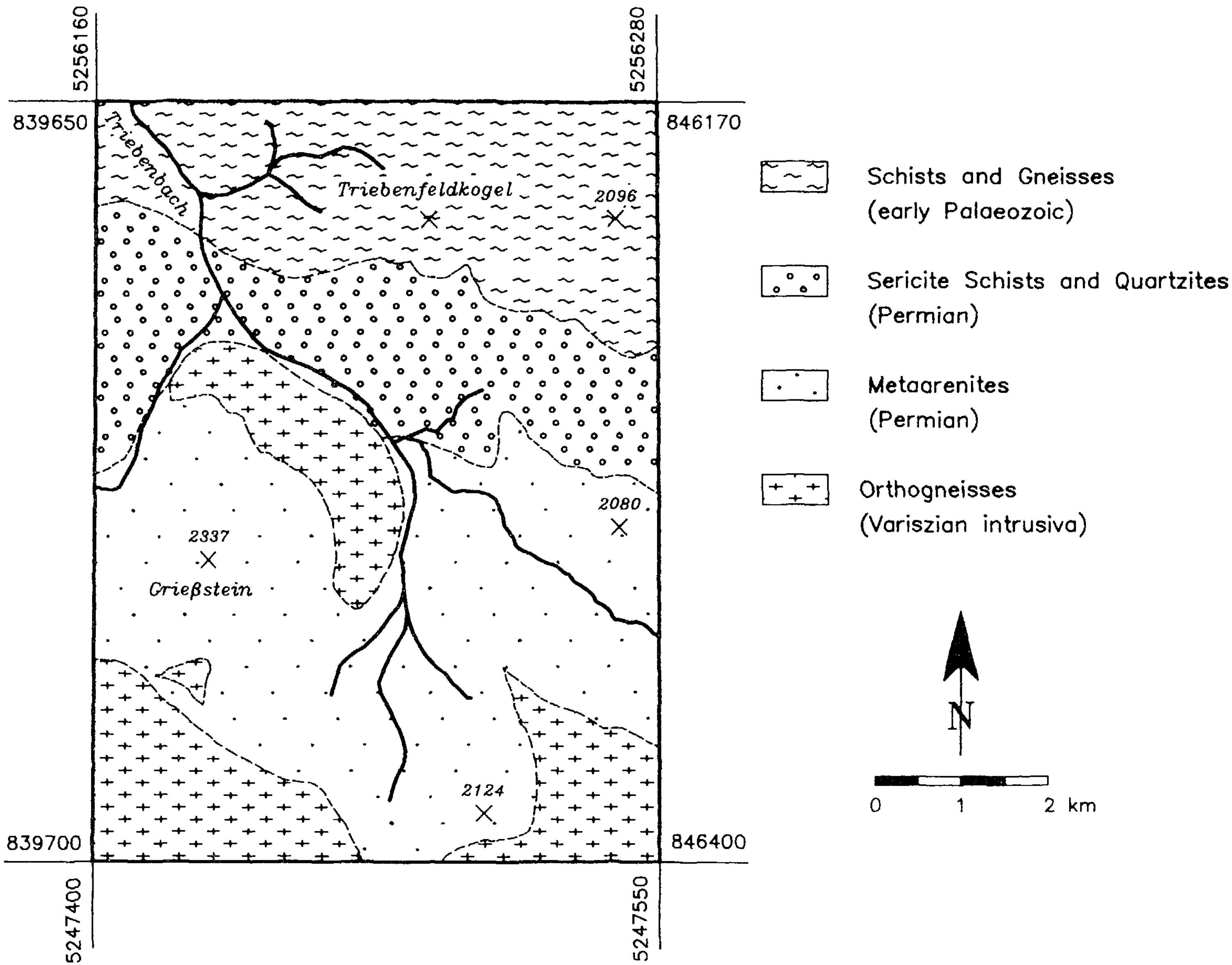

Fig. 1 Map showing geology of test area.

schists can be found in the north. The topographic relief is generally high providing a high energy hydrologic environment.

3. SCATTERPLOTS

3.1 Multiple scatterplots

The simple scatterplot of a pair of original variables is widely used and presents a two-dimensional view of the data only. However, by modifying the plot or by arranging more than one scatterplot in a special way the information content displayed can be significantly increased.

By generating an array of pairwise scatterplots including three and more variables, the drawings that a draftsman makes are copied. For this reason, following [8], [9] these arrays are called draftsman's displays. The plots are easyly to describe and to generate. They relate directly to the original data and do not require explanation of any intermediate transformation (Fig. 3). The main drawback of the technique is that the number of plots becomes impractically large for a large number of variables. The limit seems to be around 10 variables at a time [10]. However, if one is not limited in size by the available plotting device, plots incorporating much more elements can be produced. The plot is actually the graphical resolution of the correlation matrix [Tab.1]. It supports the interpretation of the correlation matrix significantly and uncovers certain bivariate element behaviors (e.g. groupings, non linear trends) which cannot be recognized by studying the correlation coefficients alone.

3.2 Symbolic scatter plots

Additional information can be included within a conventional scatterplot by coding the symbol. Such a variable is called

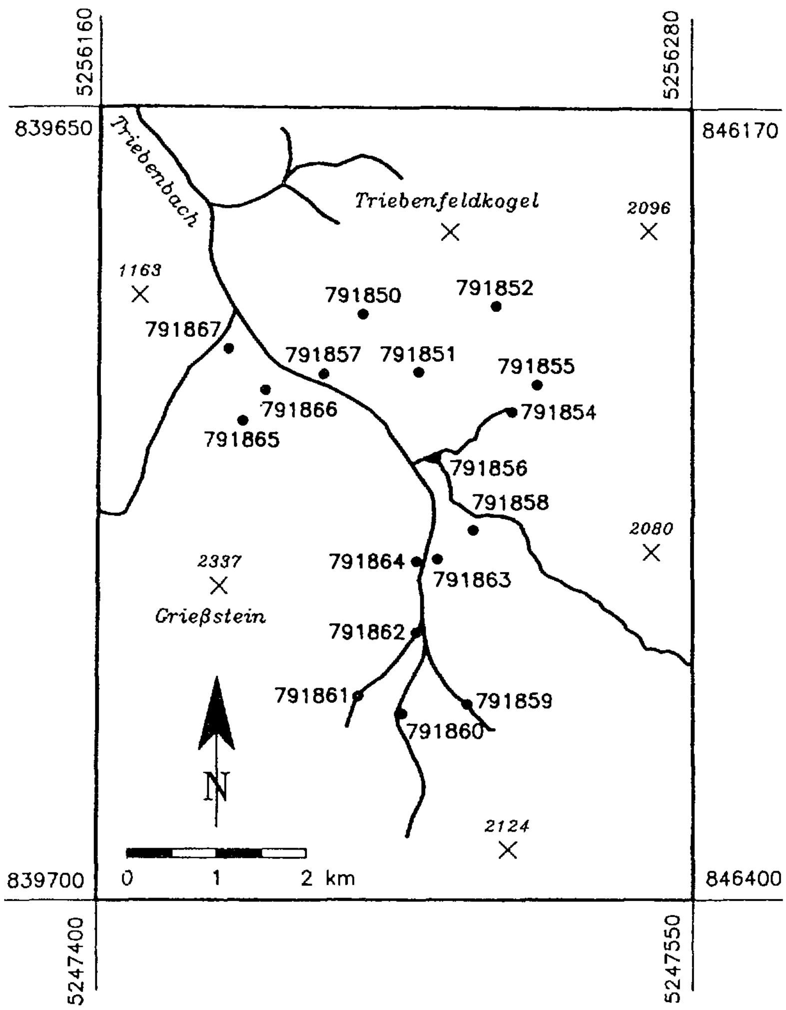

Fig. 2 Map showing stream sediment sample locations with sample numbers on a generalized drainage system.

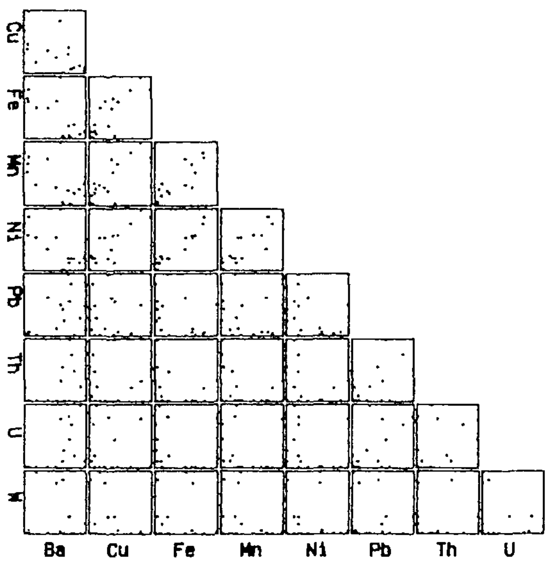

Fig. 3 Draftman's display of geochemical stream sediment data from test area - the corresponding correlation matrix can be found in tab. 1.

Tab. 1 Correlation matrix corresponding to the draftman's display in fig. 3

Cu	-0.620							
Fe	-0.742	0.830						
Mn	-0.632	0.831	0.907					
Ni	-0.686	0.861	0.969	0.878				
Pb	0.462	-0.135	-0.386	-0.232	-0.368			
Th	0.346	-0.119	-0.398	-0.403	-0.325	0.349		
U	0.505	-0.055	-0.282	-0.198	-0.218	0.612	0.385	
W	-0.057	-0.267	-0.059	-0.304	-0.102	-0.052	0.019	-0.223
	Ba	Cu	Fe	Mn	Ni	Pb	Th	U

indicator variable and can represent the sample number or indicate the rock type from which the sample was originally drawn. Additionally a division of samples into groups, priorily assigned to the data, can be displayed. Interactive editing of the scatter plots on the graphic screen facilitates the assignment of dummy variables (e.g. group numbers, symbol type) in a direct way during the data analysis procedure, supporting a quick interpretation of certain features. Further enhancements can be gained by the introduction of well suited different symbol types and the extensive use of color. One way of including variables, measured on a continuous scale, is to code the variable into the size of the plotted symbol. That means, that the size of the symbol corresponds to the absolute value of the respective variable to be included (fig.4). The absolute symbol size (maximum, minimum), defined and optionally chosen by the user, reflects the range of the values of the encoded variable. To get a readable display, the absolute symbol size must be adjusted to the scale of the plot and the number of samples presented.

4. Multiple code symbols

In the previous section various possibilities have been discussed to increase the number of variables displayed on a scatter plot to at least four. An additional continuous variable can be added by introducing color classes for the range of values for the element in

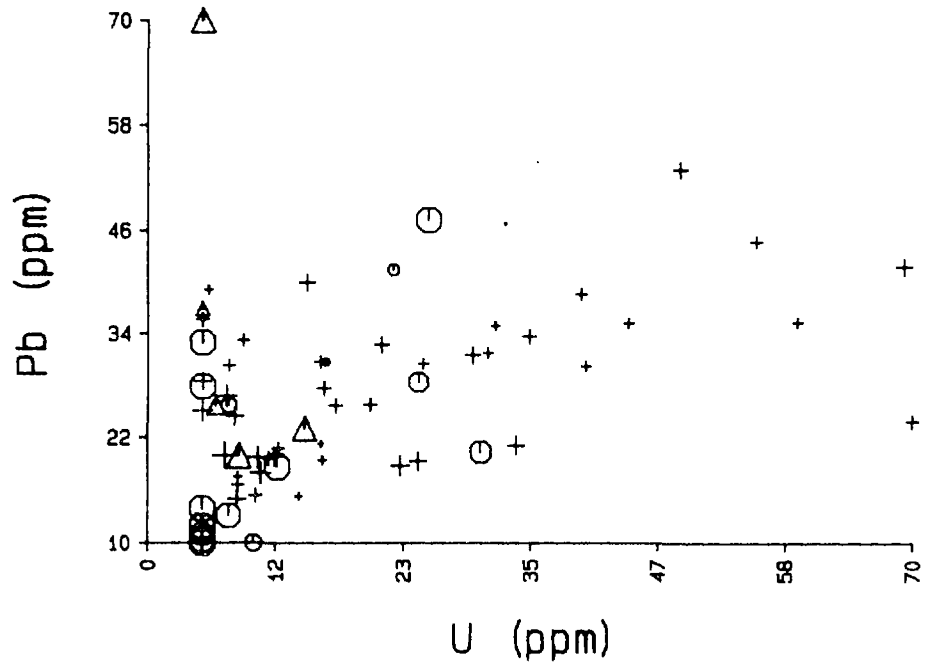

Fig. 4 Symbolic scatter plot of Pb (ppm) against U (ppm) with two variables encoded into the symbol. Diameter of the symbol represents Th (ppm) and the symbol type indicates different geochemical groups (circle refers to test area).

question. The symbols are then displayed in the corresponding color. The whole graphical display, however, becomes more and more difficult to interpret. In addition there is no elegant way to increase dimensionality with this type of presentation.

Higher dimensionality can be displayed in an elegant way by introducing more complex plotting symbols. A large number of coding schemes has been described in the literature [3,4]. Practical application to geological data, however has been very limited. Therefore a variety of symbols have been tested and those reflecting significant enhancements to interpretability will be described shortly.

4.1 Profiles

Any number of arbitrarily chosen variables can be plotted along a horizontal line in constant distances. To each variable a height is assigned proportional to the analytical value of the respective element. To get a clear picture for element comparisons the resulting profile is based on certain scaling procedures. With this method distinct features and peculiarities can be displayed in a straight forward way.

For example the base line drawn through the profile can represent either the minimum value of each variable or display a measure of a significant central value (e.g. median). The set of variables, to be incorporated in the symbol is optional. The size of the symbol is depended on the absolute length, assigned to the scaled maximum values and the assined distance between the variables along the profile. If a large number of variables is available per observation, this symbol has its limitations to the human perception. Thus it is recommended to apply it to certain meaningful subsets of variables only. Symbol patterns generated can be interpreted directly and visual comparison is easily possible.

Common profile shape reveals high similarity of pairs of samples or even groups. Outlayers - individual observations that differ significantly from the majority of the data set - will be recognized immediately.

Fig.5 displays 6 geochemical variables (0 - 1 range transformed) as profile symbols in a table. In this presentation the base line of the symbol represents the minimum. In contrast to that the values in fig.6 have been standardized so that the baseline reflects the median. In this display the standardization procedure allows a simple way of discrimination between multivariate background samples and samples showing significant geochemical enrichments. In the example, Uranium shows some clearly visible outliers. The annotation of the sample numbers in the table supplies a quick reference to the sample location map. In addition, the symbols can be displayed directly on maps (fig.7). This necessitates that the sample density is not too high and/or the scale of the map can be ajusted to the necessary symbol size so that symbols do not overlap too much.

The presentation of multivariate symbols in a table however has turned out to be very helpful in the first visual examination and interpretation of data behavior. Afterwards the mapping facility provides an easy mean to study the distribution of the detected features in the area under investigation.

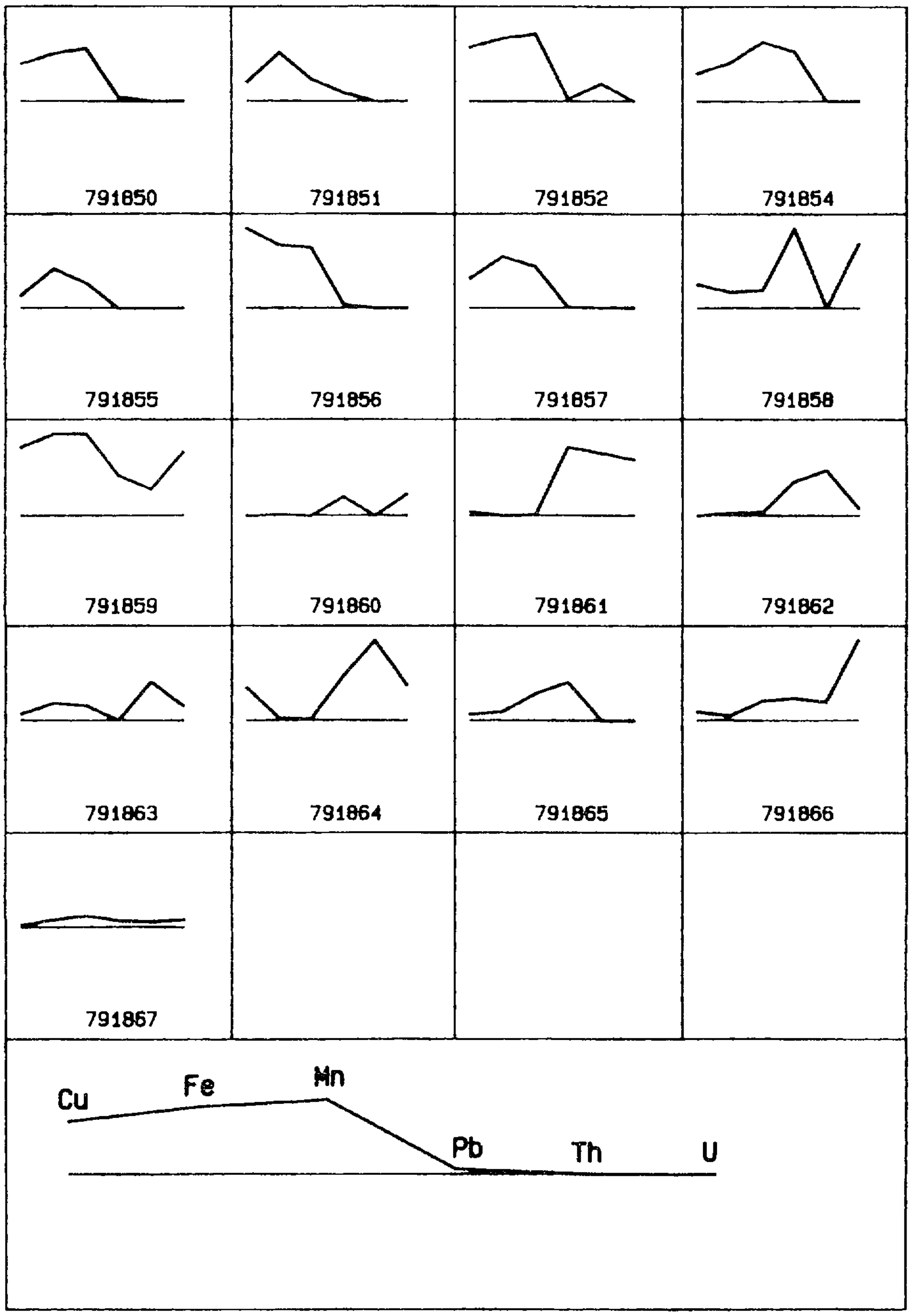

Fig. 5 Table of profile symbols for the 17 stream sediment samples from test area with annotation of sample numbers. Key at the bottom shows the assignment of the 6 chemical variables (0-1 range transformed) to position along a profile.

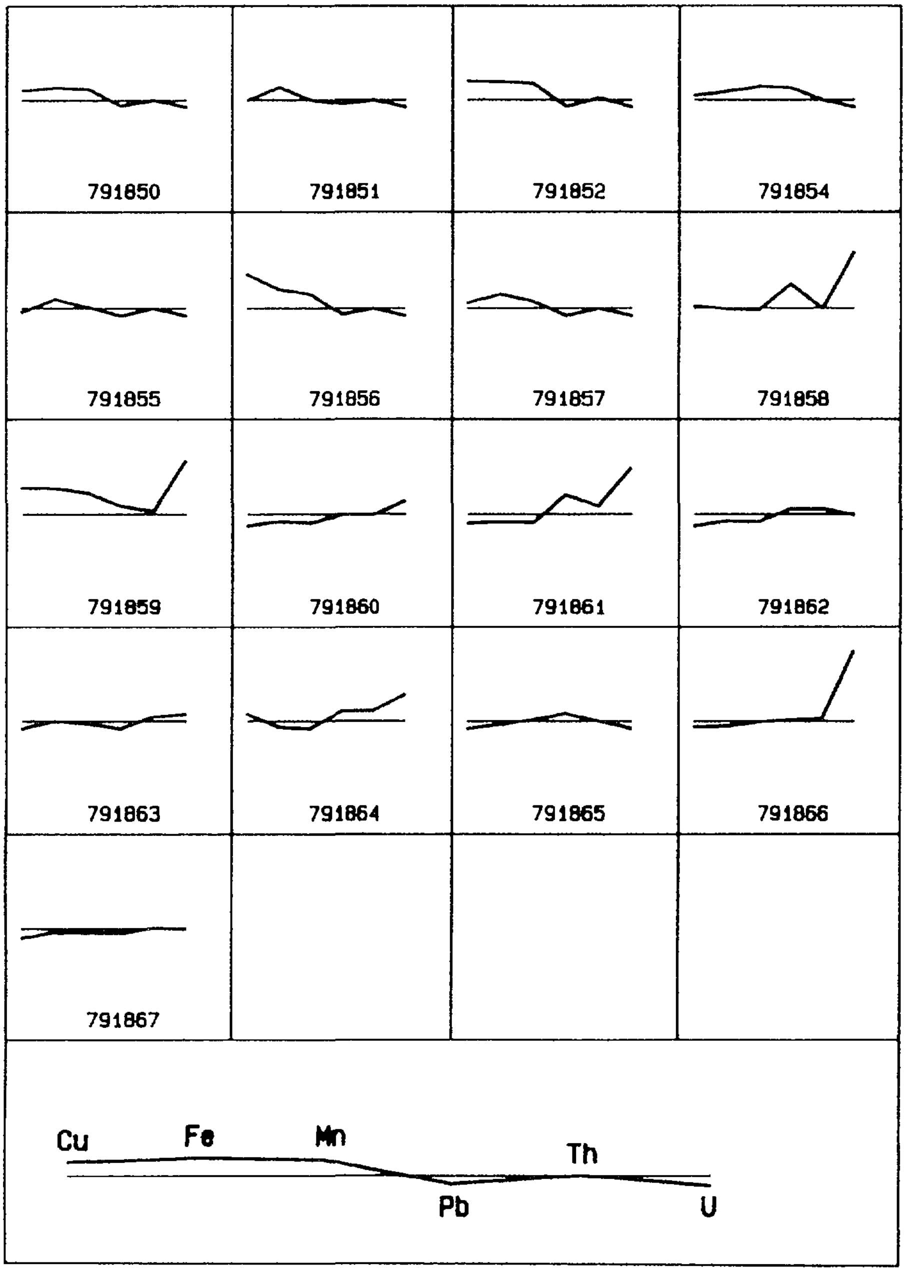

Fig. 6 The same profile symbol table as in Fig. 5 but with standardized variables.

4.2 Suns and stars (polygons)

These symbols present each variable as a value along equally spaced radii from a common center. Leaving the endpoints of the rays unconnected, one refers to suns. If they are connected by straight lines the symbols turn into stars or polygons. For presentation in this plot all data have to be nonnegative. Therefore each variable has to be rescaled after certain transformations have been applied to the data in advance.

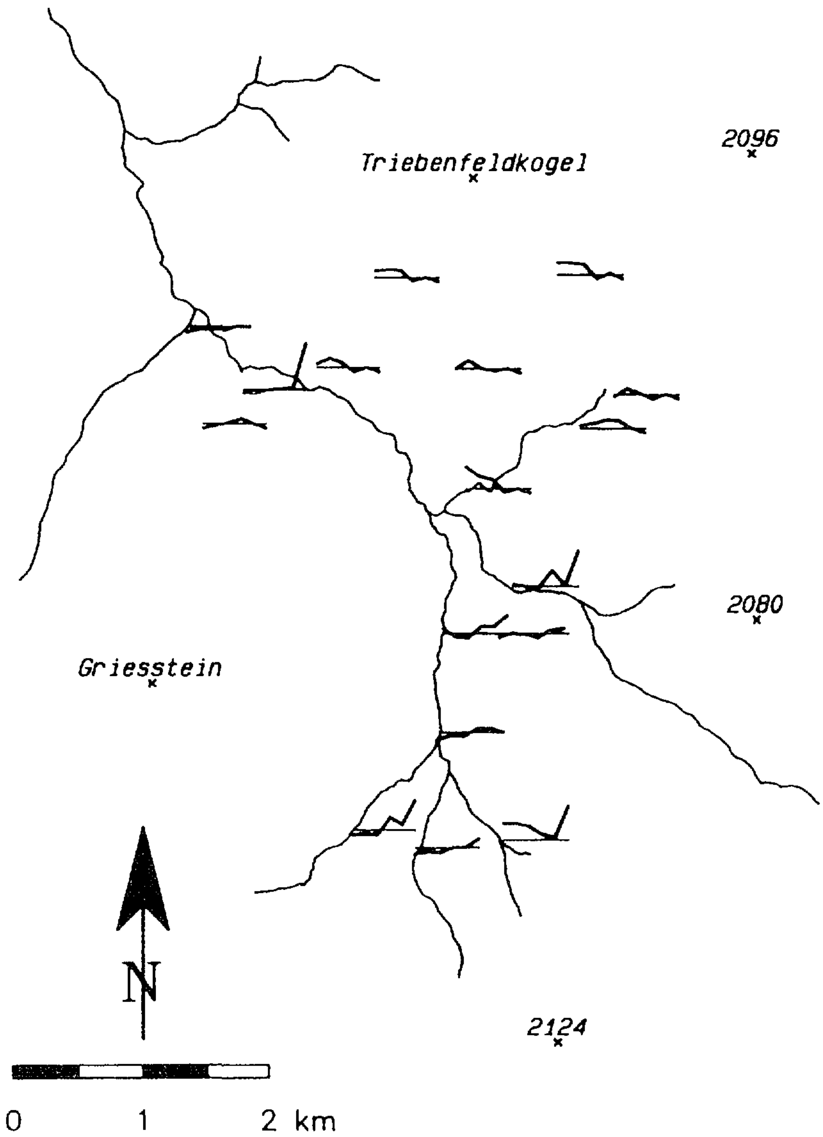

Fig. 7 Map display of profile symbols of Fig. 6 at original sample locations.

This allows also to plot the maximum and minimum of each variable with the same absolute length of rays. The computational simplicity and the compact display of information around a center are features to make this symbol very useful for a wide range of applications.

Fig.8 shows sun symbols of the major elements in a table. The assignment of the elements to the respective ray is documented at the bottom of the figure. Two distinctly different symbol patterns can easily be recognized. To gain such good results the data had to be transformed and standardized before. It is one of the major

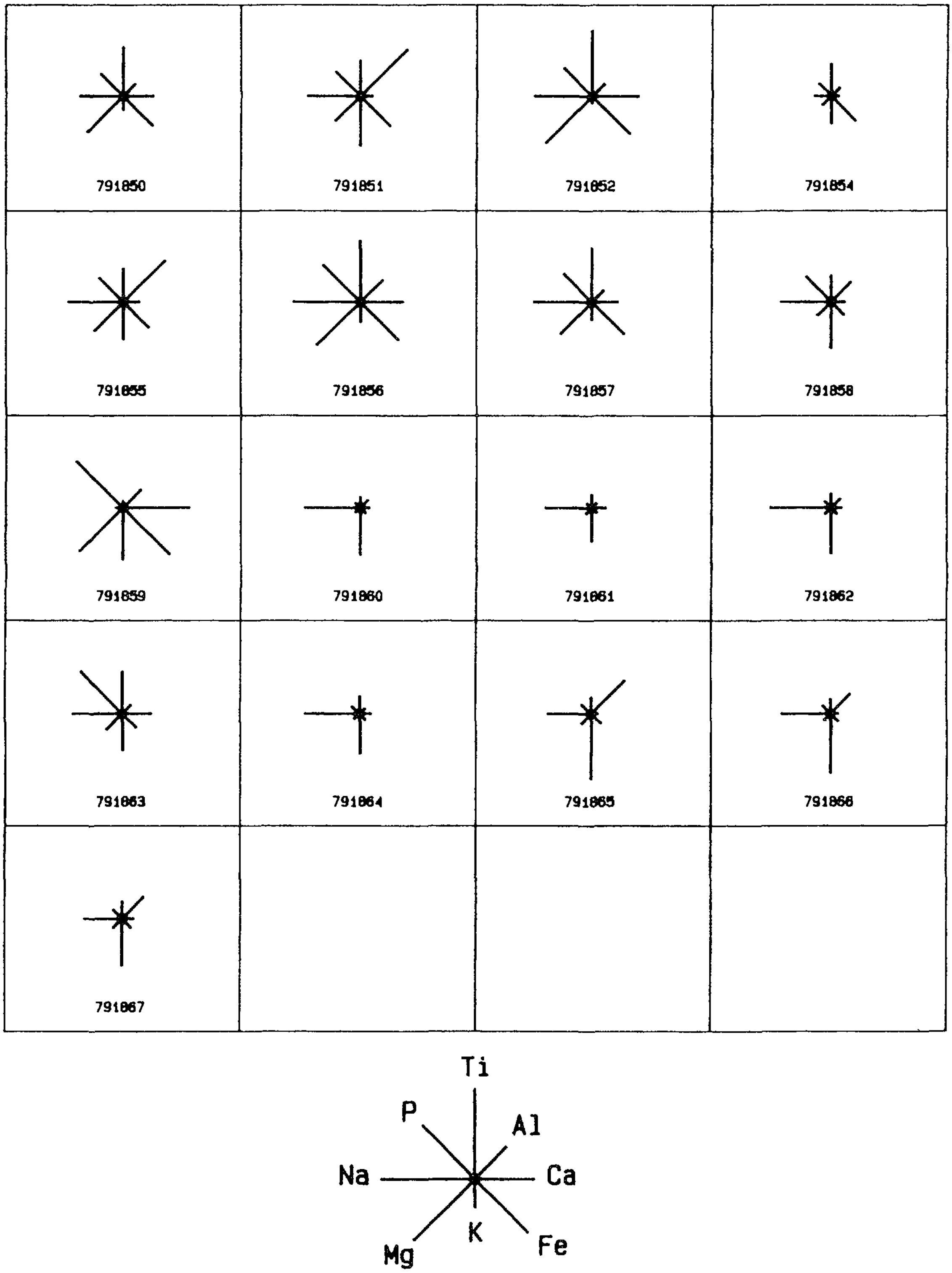

Fig. 8 Table of sun symbols with eight major elements (standardized) for the 17 samples from test area with annotation of sample numbers. Key at the bottom shows the assignment of the 8 variables to the rays of the sun symbol.

features of EDA that different approaches even to data preparation have to be tried and tested before choosing the one combination giving the best results. In this case the element associations indicated by the symbols can be related to rockforming minerals of the lithologies present. The geographical display (fig.9) allows a direct correlation to the geological situation of the area as shown in fig.1. Several points reveal a clear presence of Na and K and a depletion of all other elements incorporated in the symbol. These samples have obviously a direct relation to the othogneises and metaarenites. The geochemical signature can be regarded as a result of the abundance of feldspar and mica in the stream sediments. The samples from the north eastern part of the test area exhibit a

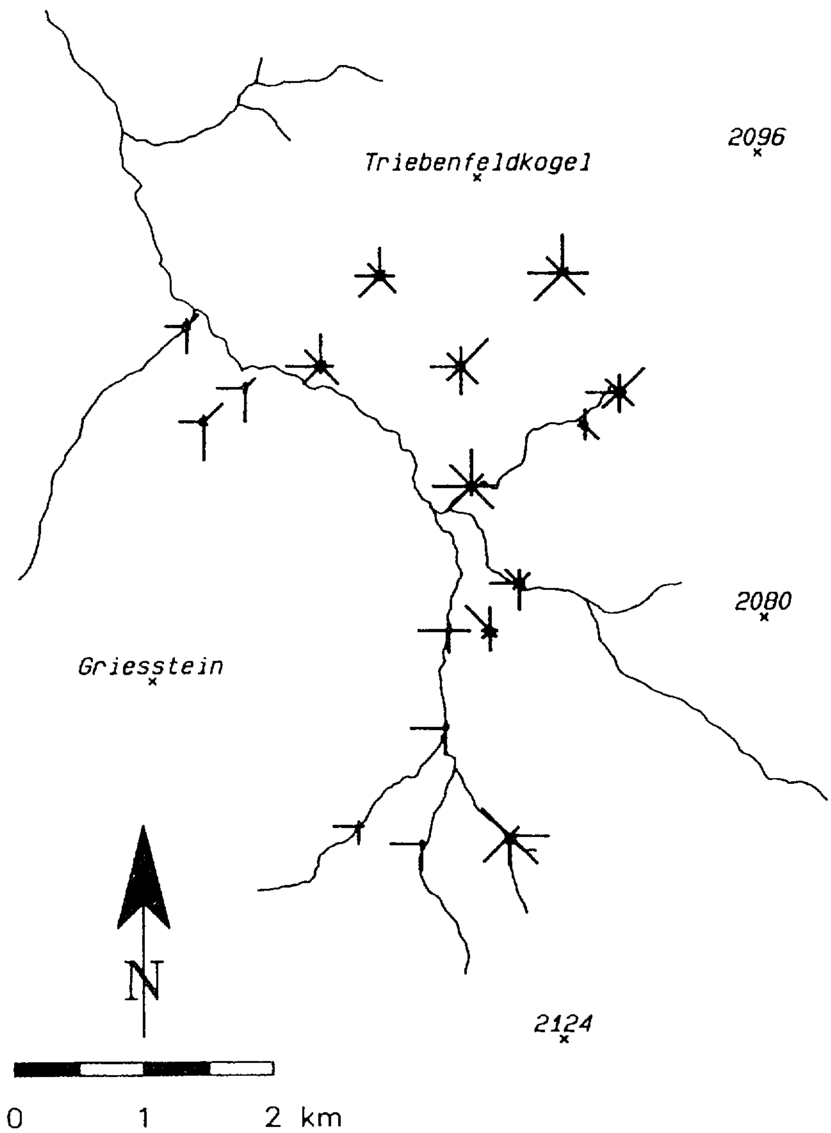

Fig. 9 Map display of the sun symbols of Fig. 8 at original sample locations.

different more complex pattern. Fig. 1 shows, that these areas are underlain by different rock types.

Fig.10 gives an example of the star symbols using ore indicating elements. The key at the bottom of the table gives the assignment of the elements to the symbol. In contrast to the profile plots (fig.6) two further elements have been added. A clear distinction

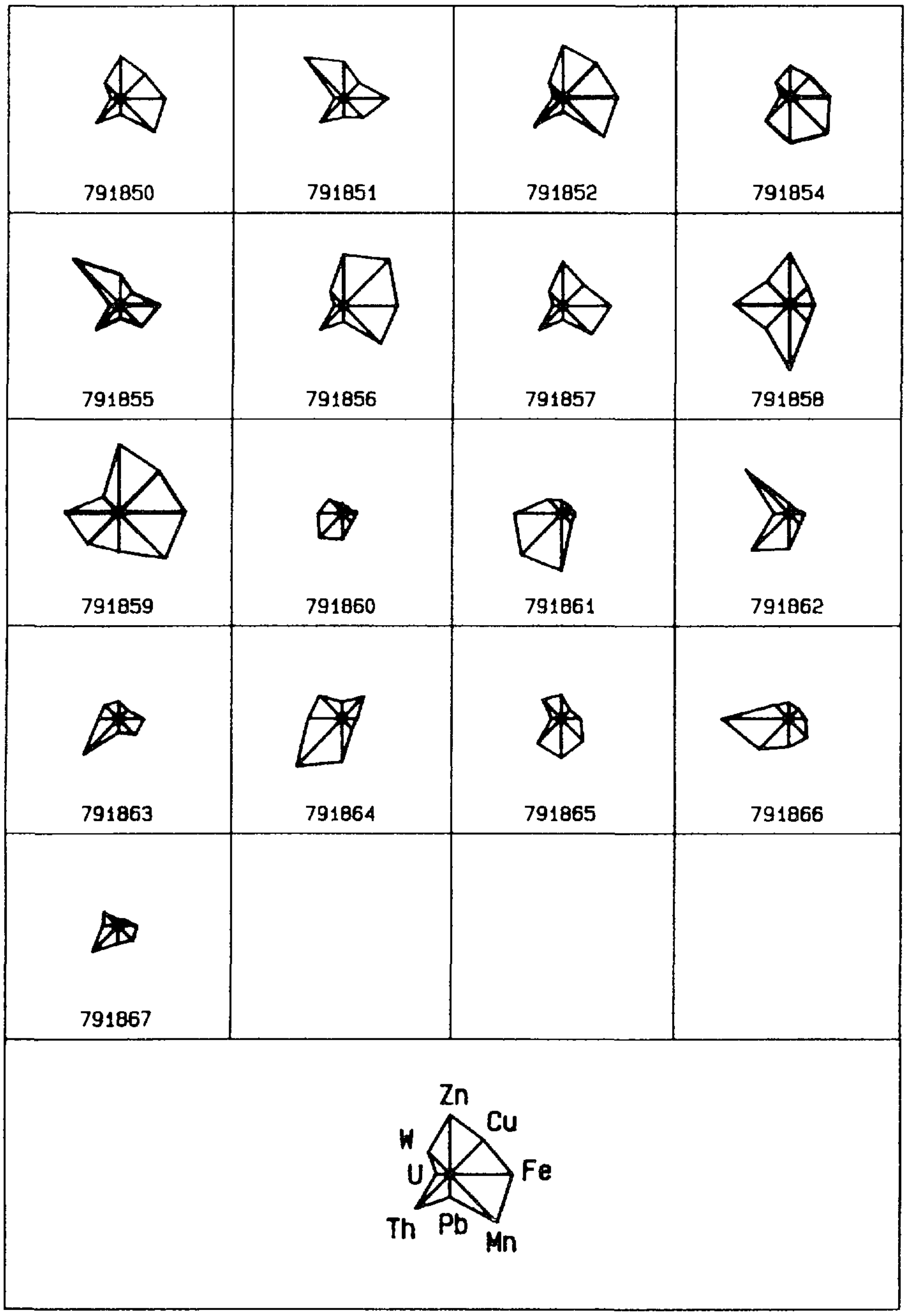

Fig. 10 Table of star symbols with elements indicative for mineralizations (standardized) for the 17 samples from test area, with annotation of sample numbers. Key at the bottom shows the assignment of the 8 variables to the symbol.

between geochemical background and multivariate outliers is not as obvious as observed in the profile plot. However single element variations and paragenetic associations can be studied more easily. The correlation to lithology is again supported by mapping the symbols (fig.11). Similar symbol patterns become more obvious, and cluster together. Symbol patterns in the southern part of the map reveal higher multivariate variations by their changing shape and seize.

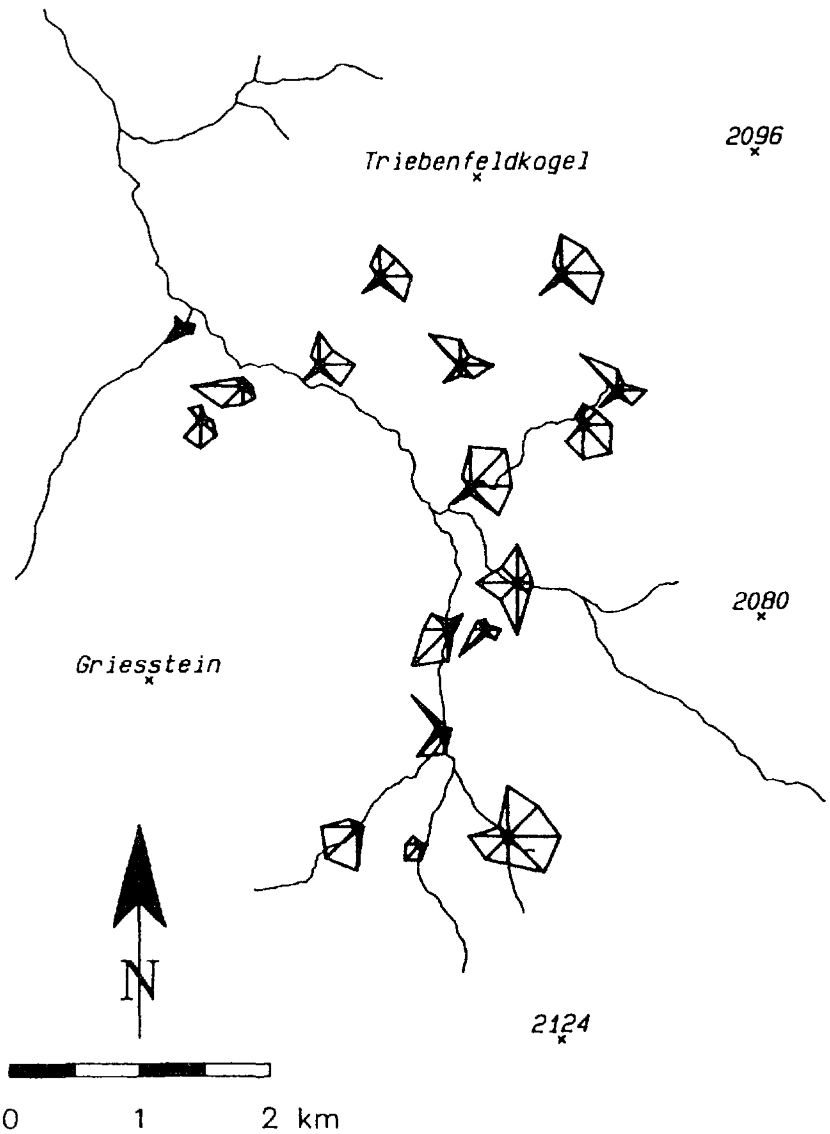

Fig. 11 Map display of the star symbols of Fig. 10 at original sample locations.

4.3 Trees, castles and boxes

The major advantage of these symbols is their ability to incorporate many variables at a time. In addition they can express certain relationships among the variables. These can be gained by calculating similarity measures in combination with an hierarchical clustering. The structure of the symbol itself is then set into a direct relation to these features (e.g. correlation and element clusters).

Clustering procedures offer different measures of multivariate distances like the Euclidian Metric or the Mahalanobis Distance. Additionally there are several sorting strategies forming clusters, like the complete linkage, the single linkage or average linkage method [11]. The best method adjusted to the data batch to be displayed, is generally found empirically, comparing the graphical results of different combinations in the cluster procedure according to the primary aim of the analysis. The main advantage of these multivariate symbols is their ability to concentrate a lot more information at one sample point than the techniques mentioned above. The interpretation of the plots, however, is not straight forward and may need more practice and experience.

4.3.1 Trees

The structure of tree plots is based on the dendrogram of a hierarchical clustering. According to it each variable is assigned to one branch of a stylized tree. The lengths of the branches are determined by the standardized values of the variables. In addition, the length of each internal limb is determined by the average of all the branches that it supports. Based on that, certain instructions are set up, how to put clustered variables together and how to avoid overlapping branches. For a detailed description of the technique see [12].

The possibility to see several features of the data at a time in the symbol enables one to get a good insight to data structure and changing data behavior. It has distinct advantages to the previously described symbols if more than 6 variables shall be incorporated. Because a good resolution of this symbol needs a certain size, it is best suited for relative small data sets and large scale maps. This guarantees that overlaps of symbols can be avoided and readability is preserved.

Fig.12 represents a table of tree symbols for the 17 test samples. Fig.13 shows the assignment of the variables to the branches of the tree. The same 8 elements have been used as in the star plot. All of them can have relations to mineralisations. The assignment of

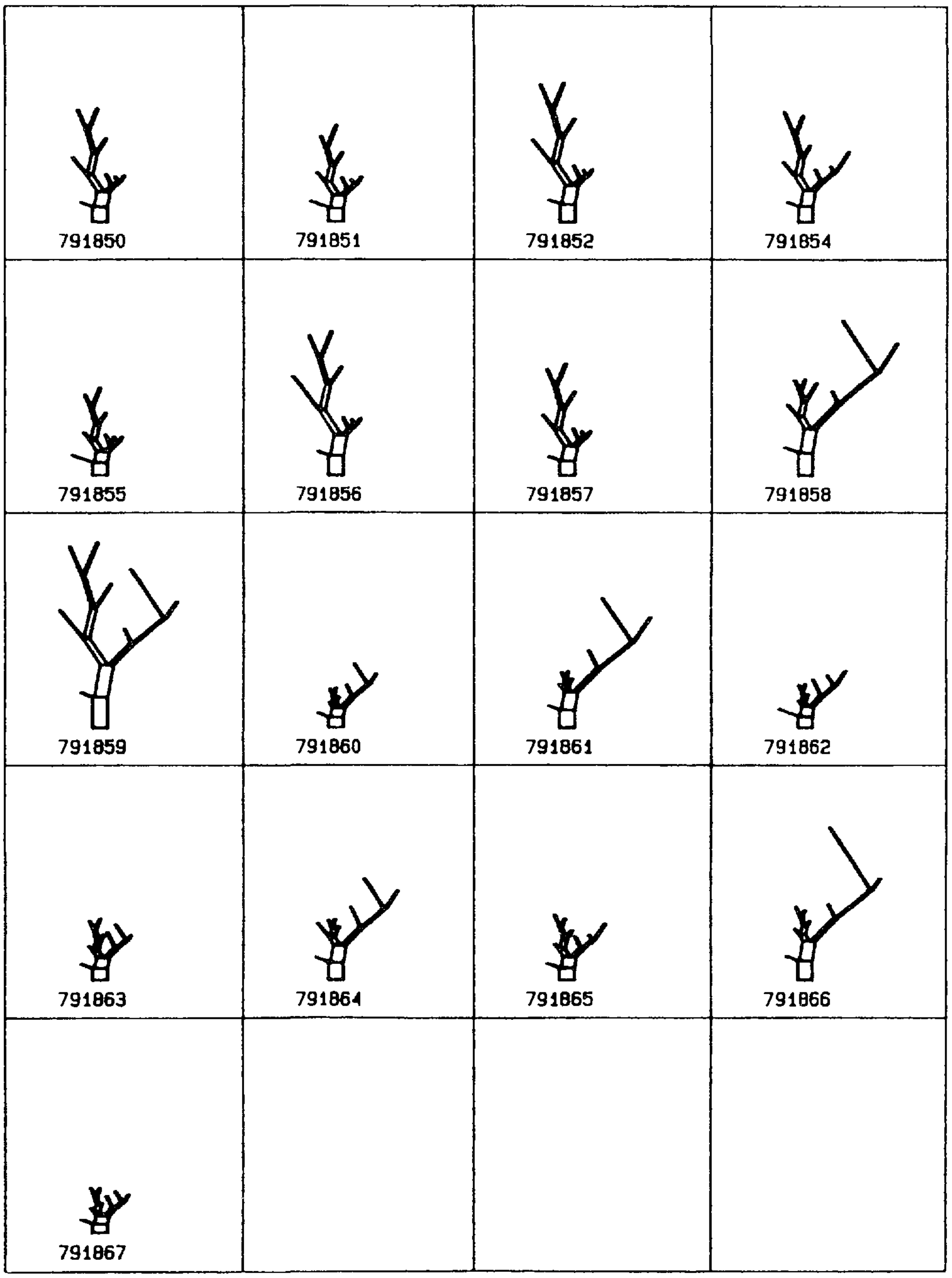

Fig. 12 Table of tree symbols with 8 elements indicative for mineralizations and annotated sample numbers. Key is shown in Fig. 13.

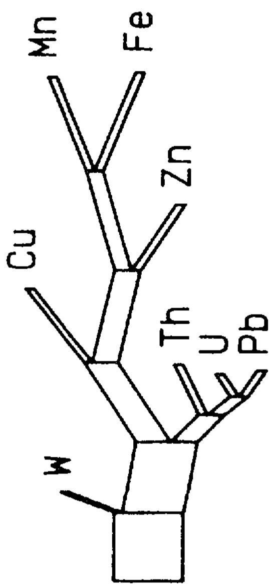

Fig. 13 Key of tree symbols used in Fig. 12 and 14. 8 elements are assigned to the branches, according to an hierarchical clustering of the variables.

the elements to the cluster tree shows some significant features. It can be observed for example that tungsten is uncorrelated to all other elements and therefore appears as single branch at the bottom of the symbol. One cluster consists of Pb, Th and U, reflecting their close geochemical relationship. It is also visible that U correlates stronger with Pb than with Th. The simultaneous display of correlations and absolute element values as shown here can provide important information concerning exploration criteria for different types of mineralisations. The other cluster of the tree symbol reflects the common relation between Fe and Mn and base metals. Scavenging effects are often observed, creating false anomalies. The detection of such situations can be very much supported by multivariate graphical displays. In this case, however, there is no significant enrichment of Cu and Zn, where the cluster with Fe and Mn dominates the symbol. This is clearly visible in the symbol table (fig.12). The consLusion in that case is that changes in this specific cluster pattern are mainly due to the different lithologies present in the area. Another type of trees, that be can observed in the table, reveals the dominating Pb - Th - U cluster with degenerated Cu-Fe-Mn-Zn branches. This geochemical group carries several multivariate outliers generally enriched in U. The geographical distribution of these tree symbols can be studied in fig.14. It is easily to recognize that group one (dominating Cu-Fe-Mn-Zn cluster) lies in the northern part of the area consisting of palaeozoic schists. The second group appears to the south, where orthogneises and metaarenites dominate the lithology. If these results are compared with fig.9, where major elements have been plotted, it can be easily seen that the same geochemical discrimination occurs.

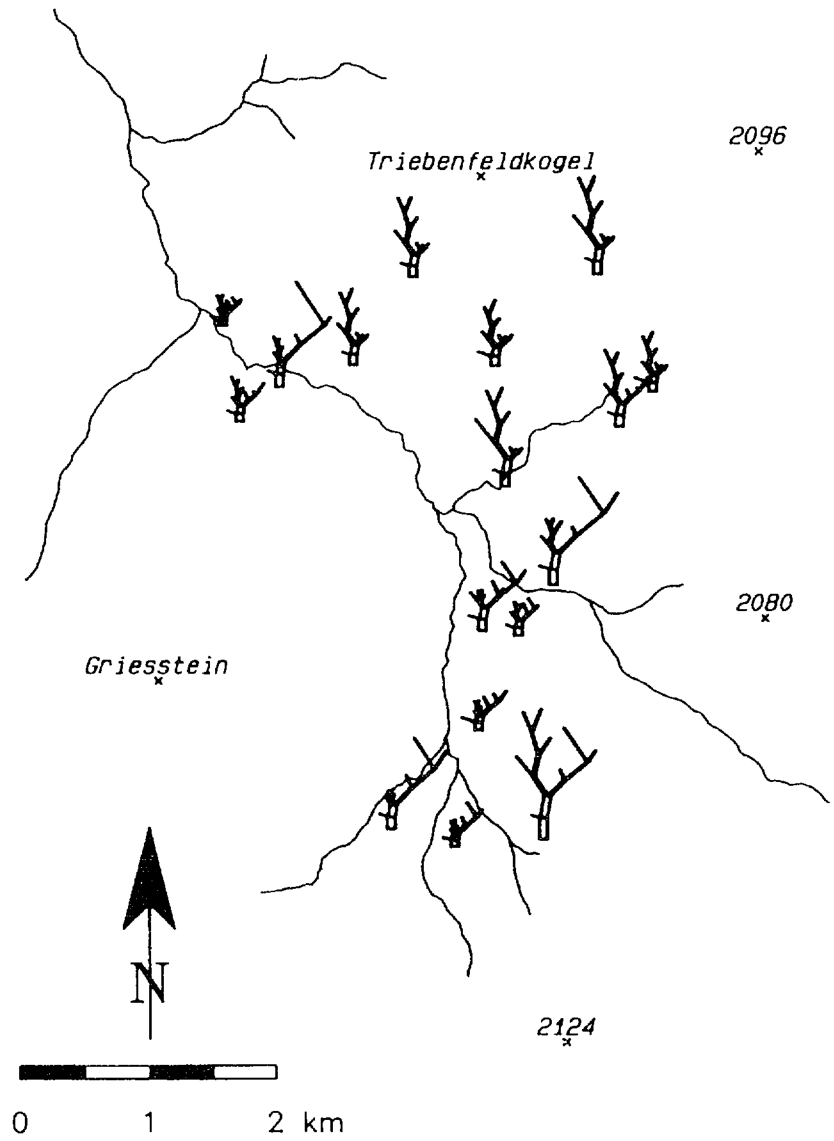

Fig. 14 Map display of the tree symbols of Fig. 12 at original sample locations. Key is shown in Fig. 13.

In some samples the uranium cluster shows a strong deviation from the background samples. The dominating outlier is sample 791859, which is generally enriched in elements indicative for mineralizations as well as major elements (fig.9). In the area of influence of this sample there is no apparent change in lithology. Thus a simple explanation of the unusual feature is not possible. Such samples should find special attention and the anomalous behavior should be studied in detail in follow up work.

4.3.2 Castles

This technique assigns a bar to each variable. These bars are afterwards assembled to a multicode symbol quite similar to the way a tree is generated. The main advantage of this plot is the possibility to directly compare the different variables of each sample. The arrangement of variables within the symbol is based on a hierarchical cluster analysis by complete linkage using Euklidian Distance measures. In contrast to the construction of trees the width of each bar is proportional to the number of variables above it and the angle between the bars is constantly zero. For a further detailed description of the technique see [12]. If more than 30 variables are used to construct trees, overlaps within the trees themselves are frequent. The castle technique avoids overlaps and is therefore especially suited for higher dimensional data. However, to be able to read the detailed information compacted into the symbol the absolute size of the symbol has to be significantly larger than trees, limiting the application to detailed studies with a small number of samples and to larger map scales.

Fig.15 represents a castle symbol plot in a table. Fig.16 shows the corresponding key symbol. Although the shape of the castle is very different to trees, the division of the samples into two geochemical groups is quite similar. It can be easily recognized that several samples are dominted by the Cu-Fe-Mn-Zn association. This symbol supports the recognition of changes in the relations among the elements, within a single geochemical cluster as well as between the clusters themselves. In the example the relations within the clustered geochemical associations remain remarkably constant. The same is valid for the second cluster, where U is dominating and accompanied by Pb and Th. The highest variation is visible for U. Where U is enriched it is correlated with Pb. W, the single element of the third group, and

Th are only present at a very low background level and show nearly no variation at all. All samples dominated by the U-association are generally low in all other elements used for constructing the castle symbol. Only sample 791859 is enriched in all elements but still exhibiting the same relations in the symbol.

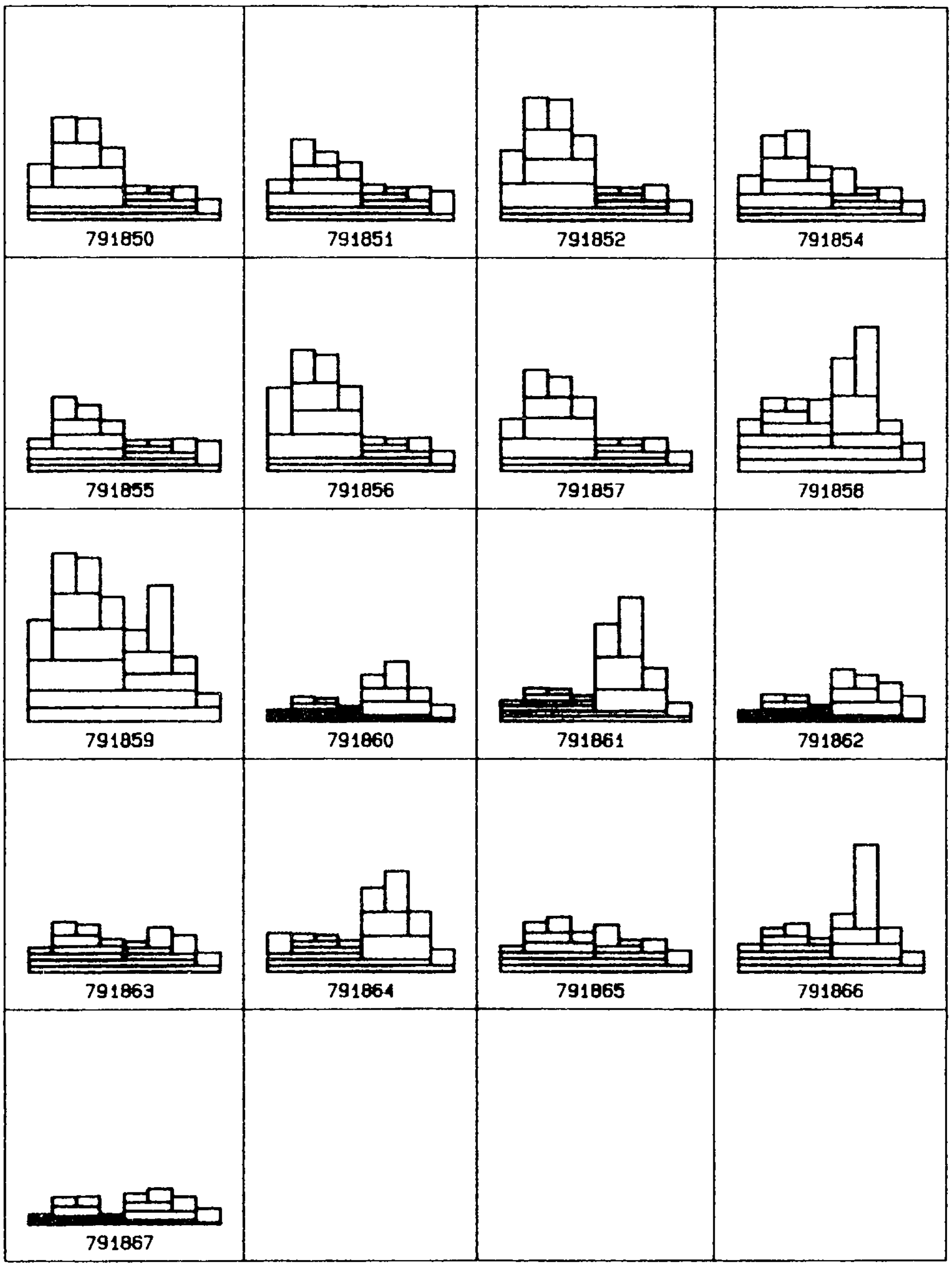

Fig. 15 Table of castle symbols with 8 elements indicative for mineralizations and annotated sample numbers. Key is shown in Fig. 16. Because of very low element contents in some samples the base lines drawn are very close to each other, resulting in a black bar at the bottom of the symbol.

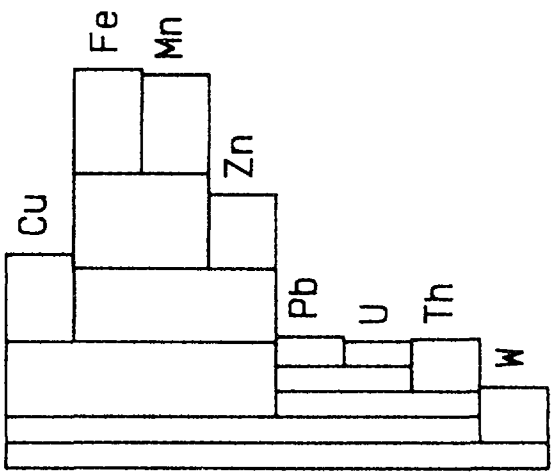

Fig. 16 Key of the castle symbols used in Fig. 15. 8 elements are assigned to the bars, according to an hierarchical clustering of the variables.

4.3.3 Boxes

Based on a hierarchical clustering using the complete linkage sorting strategy, the variables are partitioned into three subgroups. These groups are then attached to the three dimensions of a box [13].

The way the variables are arranged within a group corresponds to the sequence of the variables in the datamatrix. The edges of the boxes are proportional to the sum of the respective values. The angle, displaying the depth of the box is not fixed. It can be changed to find an optimal perspective view. To enhance interpretability the group with the highest number of variables is always attached to the height and the group with the fewest variables always to the depth. Boxes can be interpreted more directly than trees and castles. They should however, be limited to a smaller number of variables than the other two symbols, to get clusters with meaningful homogeneous element subgroups.

Fig.17 displays box symbols in a table. The key is given in fig.18. In this case Cu, Pb, Zn, Th and U were chosen as variables, because these elements did show a high geochemical variability or showed interesting associations in the other displays. The key shows that Cu-Zn as cluster one has been attached to the height, Pb-U

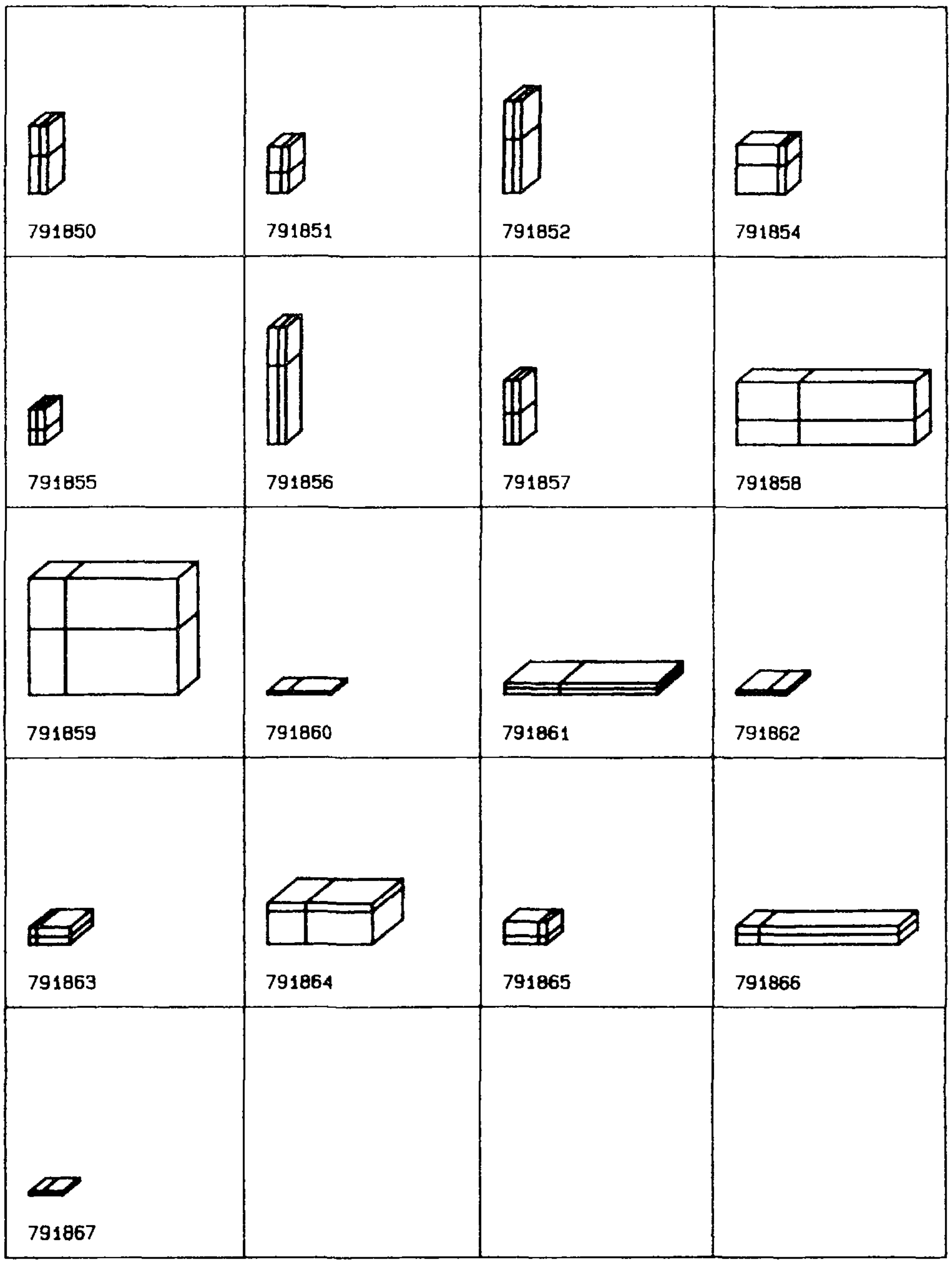

Fig. 17 Table of box symbols with 5 elements indicative for mineralizations and annotated sample numbers. Key is shown in Fig. 18.

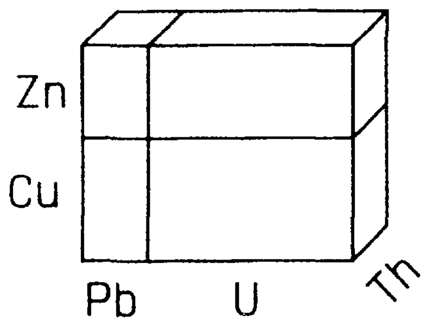

Fig. 18 Key of the box symbols used in Fig. 17 and 19. 5 elements are assigned to the three dimensions of a box according to an hierarchial clustering of the variables.

to the width and Th to the depth of the box. Again we can easily recognize the two geochemical groups present in the test area. One exhibits a column like feature, caused by a slight enrichment of Cu and Zn. The shape of the second group is more like an horizontal bar with considerable variation in the height. This variation is mainly due to changes in the background values of Cu and Zn. The barlike shape is caused by high U-contents of the samples. Fig.19 shows the plot of the box symbols at their original sample location. It reflects the expected geographical distribution of the geochemical groups. In this presentation attention is immediately drawn to several samples displaying a distinct enrichment in Uranium.

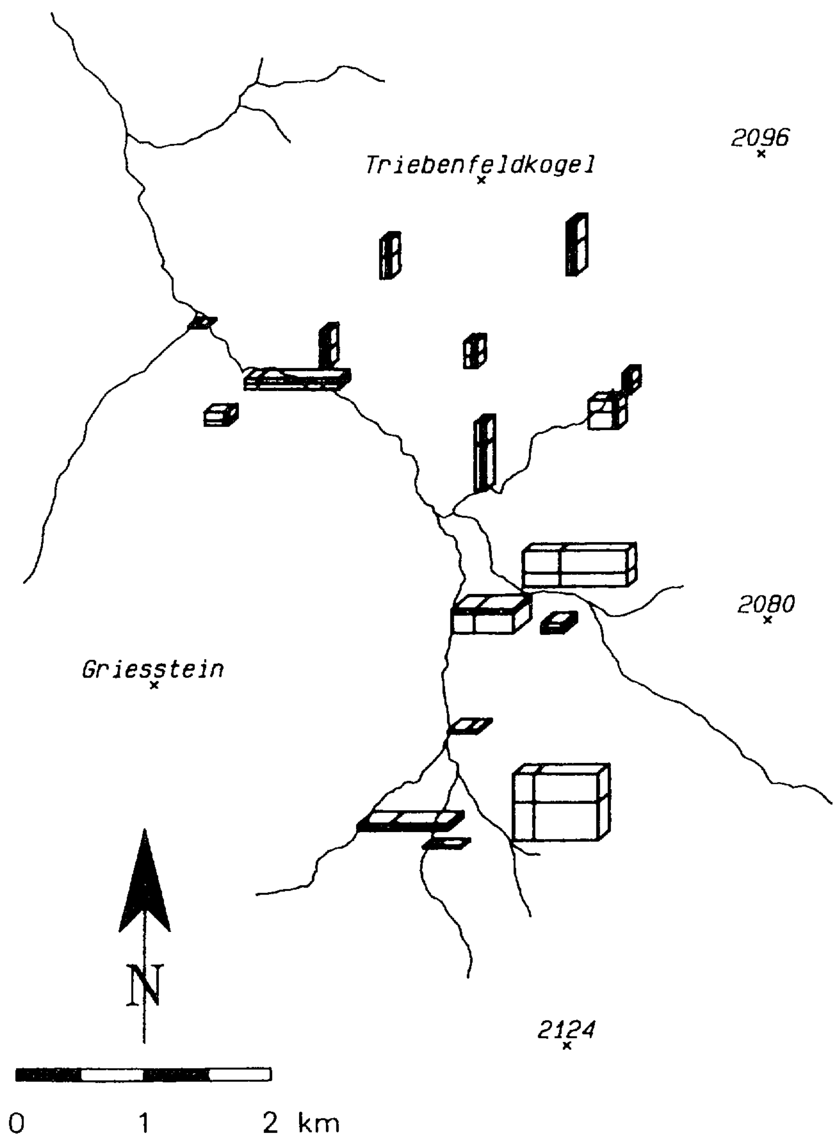

Fig. 19 Map display of the box symbols of Fig. 17 at the sample locations. Key is shown in Fig. 18.

5. CONCLUSION

The three general objectives of modern data analysis can be described as [2]:

1. Display and Description
2. Analysis and Interpretation
3. Summarization and Exposure

The corresponding graphical aids may be viewed as ranging from presentation of raw data, presentation of the results of fairly complex analyses, to graphical outputs which provide both a summary of the information content of the data and an exposure of unanticipated characteristics, such as possible inadequacies of the assumed model [2]. Graphical techniques for univariate data analysis, like the histogram or the cumulative frequency plot, are common knowledge and broadly used. In this paper techniques have been presented, which have proved to be especially useful in investigating multivariate data. These selected techniques consists of two typs: multiple scatter plots and multiple coded symbols, like profiles, suns and stars as well as trees, castles and boxes.

Variables incorporated in the described plots are usually continuous variables (original raw data). A combination with additionally coded indicator variables is possible. Any plot or symbol described can be applied also to derived variables as well, if one is willing to sacrifice the direct interpretability of the original variables or if a more advanced stage of data analysis is reached. To avoid misinterpretation and to be able to select a successful way in detailed data analysis a visual check of the original raw data and their relations to each other seems to be absolutely necessary. Therefore graphical techniques have become an essential part of modern data analysis and interpretation.

Examples with regional geochemical exploration data show that multiple scatter plots and multiple code symbols are very efficient tools in highlighting common and uncommon data behavior. Insight to data structures can be gained easily and unusual features can be pronounced if the right data preparation and displays have been chosen. If geochemical models for certain exploration strategies in specific areas have been developed, multiple code symbols can be directly interpreted according to such concepts. With this techniques important details can be provided for the selection of areas of interest and further detailed exploration work.

REFERENCES

[1] TUKEY, J.W., Exploratory Data Analysis, Addison Wesley Publ. Compl., Reading, Mass. (1977) 688.

[2] EVERITT, B., Graphical Techniques for Multivariate Data, North-Holland, New York (1978) 117.

[3] BARNETT, V., Interpreting Multivariate Data, John Wiley & Sons, New York (1981) 374.

[4] CHAMBERS, J.M., CLEVELAND, W.S., KLEINER, B., TUKEY, P.A. Graphical Methods for Data Analysis, The Wardsworth Statistics/Probability Series, Duxbery Press, Boston (1983) 395.

[5] GARRETT, R.G., Opportunities for the 80s, Math. Geol. 15 (1983) 385 - 398.

[6] HOWARTH, R.J., Statistical Applications in Geochemical Prospecting: a Survey of Recent Developments, J.Geochem. Explor., 21 (1984) 41 - 61.

[7] GNANADESIKAN, R., Methods for Statistical Data Analysis for Multivariate Observations, John Wiley & Sons, New York, (1977) 311.

[8] TUKEY, P.A., TUKEY, J.W., Graphical Displays of Data Sets in 3 or More Dimensions, in: Graphical Techniques for Multivariate Data, Barnett, V. (ed), North-Holland, New York, (1981) 374.

[9] TUKEY, J.W., TUKEY, P.A., Some Graphics for Studying Four-dimensional Data, Computer Science and Statistics: Proceedings of the 14th Symposium on the Interface, Springer Verlag, New York, (1983) 60 - 66.

[10] CHAMBERS, H., KLEINER, B., Graphical Techniques for Multivariate Data and for Clustering, in: Handbook of Statistics 2, KRISHWAIAH, P.R., KANAL, L.N., (ed), North-Holland, Amsterdam, (1982) 209 - 243.

[11] HAND, D.J., Discrimination and Classification, J. Wiley & Sons, New York, (1981) 218.

[12] KLEINER, B., HARTIGAN, J.A., Representing Points in Many Dimensions by Trees and Castles, J. Amer. Statist.Assn. 374, 76 (1981) 260 - 276.

[13] HARTIGAN, J.A., Printer Graphics for Clustering, J. Stat. Comp. and Sim., 4 (1975) 187 - 213.

GEOHYDROLOGY AND ITS APPLICATION IN DEFINING URANIUM AND OTHER METALLOGENIC PROVINCES

M. LEVIN, F.A.G.M. CAMISANI-CALZOLARI,
B.B. HAMBLETON-JONES
Atomic Energy Corporation
of South Africa Limited,
Pretoria, South Africa

Abstract

In South Africa, ground water samples are collected regularly from existing and newly drilled boreholes during the evaluation and development of ground water resources for domestic, agricultural, mining, radioactive waste disposal and industrial purposes. About 8 200 ground water samples have been analysed routinely for the major components as well as for uranium but on certain samples trace metals have also been determined.

By plotting the locality and the uranium data of all these samples on a national basis it is possible to delineate regions within which potential uraniferous target areas could exist. Three major zones have emerged, concentrated mainly in the northern and northwestern Cape Province, with several minor ones scattered elsewhere in the country. In certain instances, the anomalies coincide with known uranium occurrences in a variety of geological environments. These broadly include the suite of granitic and ultrabasic rocks of the Namaqualand Metamorphic Complex, sandstones and tillites of the Karoo Sequence and surficial deposits of Upper Tertiary Kalahari age.

During the site selection phase of the radioactive waste disposal project approximately 850 ground water samples were collected in a 30 000 km^2 region of the semi-arid northwestern Cape. The purpose of this investigation was (i) to attempt to delineate potential mineral occurrences such as base metals and uranium that are covered by a veneer of surficial material, (ii) to evaluate the regional quality of the water, and (iii) to determine from physical parameters the regional flow pattern and rate of ground water movement. Up to 34 variables were analysed for each sample, all of which were geostatistically kriged. The data showed a poor correspondence between ground water anomalies and base-metal

and uranium occurrences but nevertheless metallogenic subprovinces or zones could be identified within these large areas for future target selection.

It is further concluded that the methods used demonstrated that potential source and host rocks under thick non-uraniferous surficial cover could be outlined. In leached areas, where surface sampling has failed to detect uranium occurrences, this approach was successful.

1 INTRODUCTION

Much of South Africa is covered with thick successions of Tertiary to Recent surficial deposits which effectively conceal potential uranium mineralization within the underlying rocks. A long-term National Hydrogeochemical Project was therefore initiated in 1974 with a view to delineating target areas for future uranium prospecting. This project would also augment the State airborne radiometric survey, flown at that time, especially in the areas covered with surficial deposits where radiometric anomalies would be entirely masked. It was envisaged that the various state organizations involved with the development of ground water resources for a variety of purposes would participate in the project. Water samples would be collected according to prescribed procedures and submitted for uranium analyses in addition to the standard chemical analyses for water. The participating organizations included the Department of Water Affairs who provide a drilling service firstly to the farming community for irrigation, livestock and domestic use, and secondly for the development and assessment of water resources for large projects, which include agriculture, industrial and municipal applications. The Geological Survey has undertaken extensive hydrogeochemical projects in the Permo-Triassic sediments of the Karoo Basin as a follow-up on the airborne radiometric surveys. The Atomic Energy Corporation has had a two-fold approach, the first being the evaluation of the uranium potential of areas under surficial cover and the second the siting of nuclear facilities such as radioactive waste disposal and power plant sites.

2 URANIUM PROVINCES OF SOUTH AFRICA

Uranium mineralization is present in rocks which encompass almost the whole of the geological history of South Africa (Toens, 1981). However, significant mineralization is restricted to five fairly well-defined time periods constituting the uranium provinces (Fig. 1). Each period is characterized by a distinct type or combinations of types of uranium mineralization. The oldest are those which are hosted by quartz-pebble conglomerates which fall in the time range from 2 900 to 2 400 Ma. Uranium-bearing alkaline complexes cover a wide time scale, from 2 000 (Phalaborwa) to 1 400 Ma (Pilanesberg). Uranium is also found in granite gneisses which span a similarly large time period from 1 950 to 1 000 Ma.

A hiatus in the occurrence of uranium in South Africa exists between 1 000 and 300 Ma. It is only with the onset of Karoo sedimentation that uranium mineralization reappears in the South African stratigraphic column. Uranium occurs both in coal seams and in sandstones of the Karoo Sequence. The youngest uranium mineralization occurs in a variety of Tertiary to Recent sediments, which include calcretes, peaty diatomaceous earths, beach sands and phosphates (Camisani-Calzolari et al, 1986).

3 REGIONAL DISTRIBUTION OF GROUND WATER URANIUM ANOMALIES

Approximately 8 500 water samples have so far been collected throughout South Africa, the distribution of which is shown on Fig. 2. The 25 and 100 ppb U contours have outlined ten anomalous areas that can be grouped into three large potential uraniferous zones.

Anomalies 1, 2 and 3 constitute the Kalahari zone, which includes the Piet Plessis Block (anomaly 1) and the Gordonia Block (anomalies 2 and 3) (Levin et al, 1983, Levin et al, 1982, Levin, 1981). With the exception of mountains in the central portion and

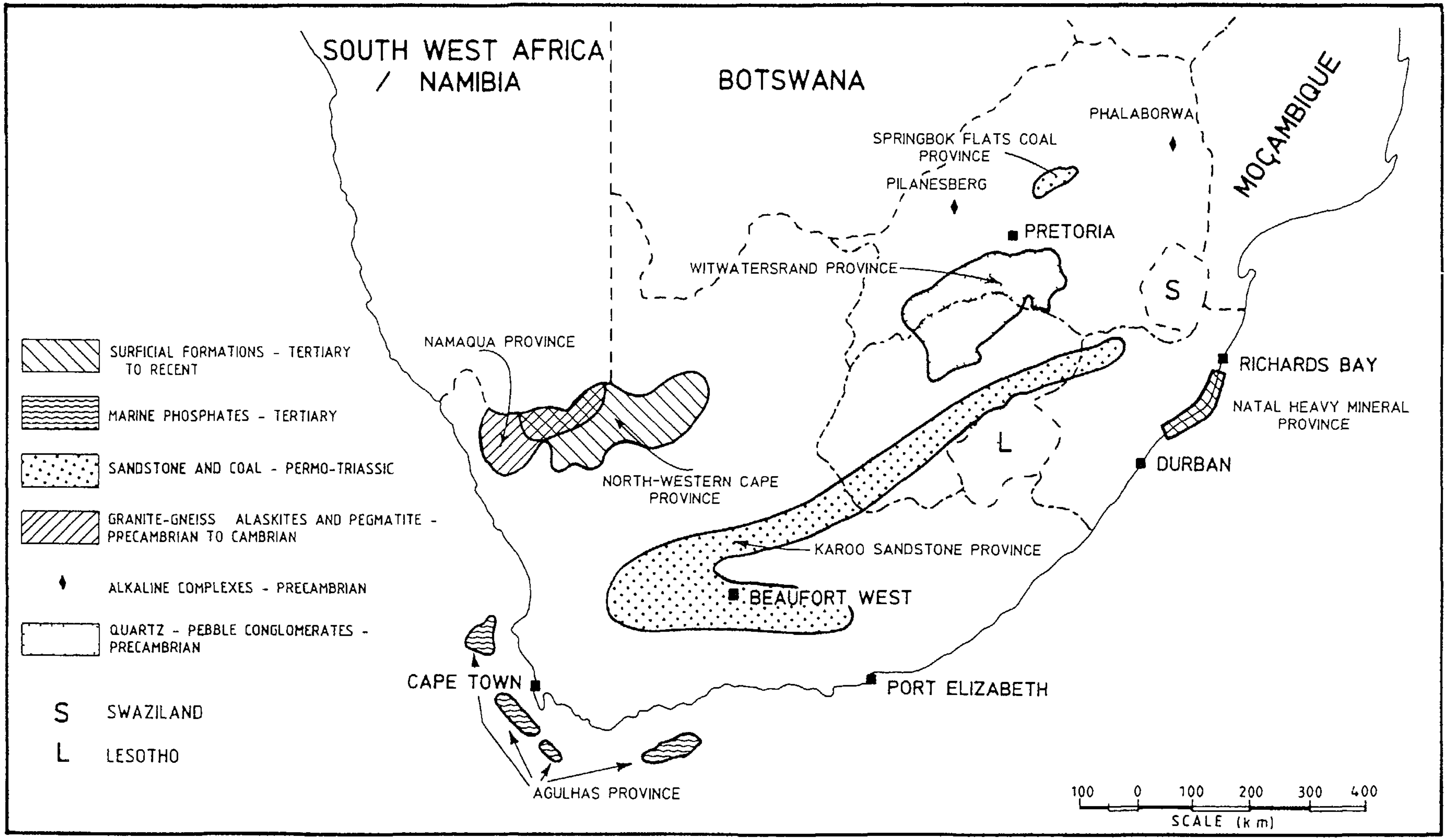

Fig. 1 Uranium provinces in South Africa

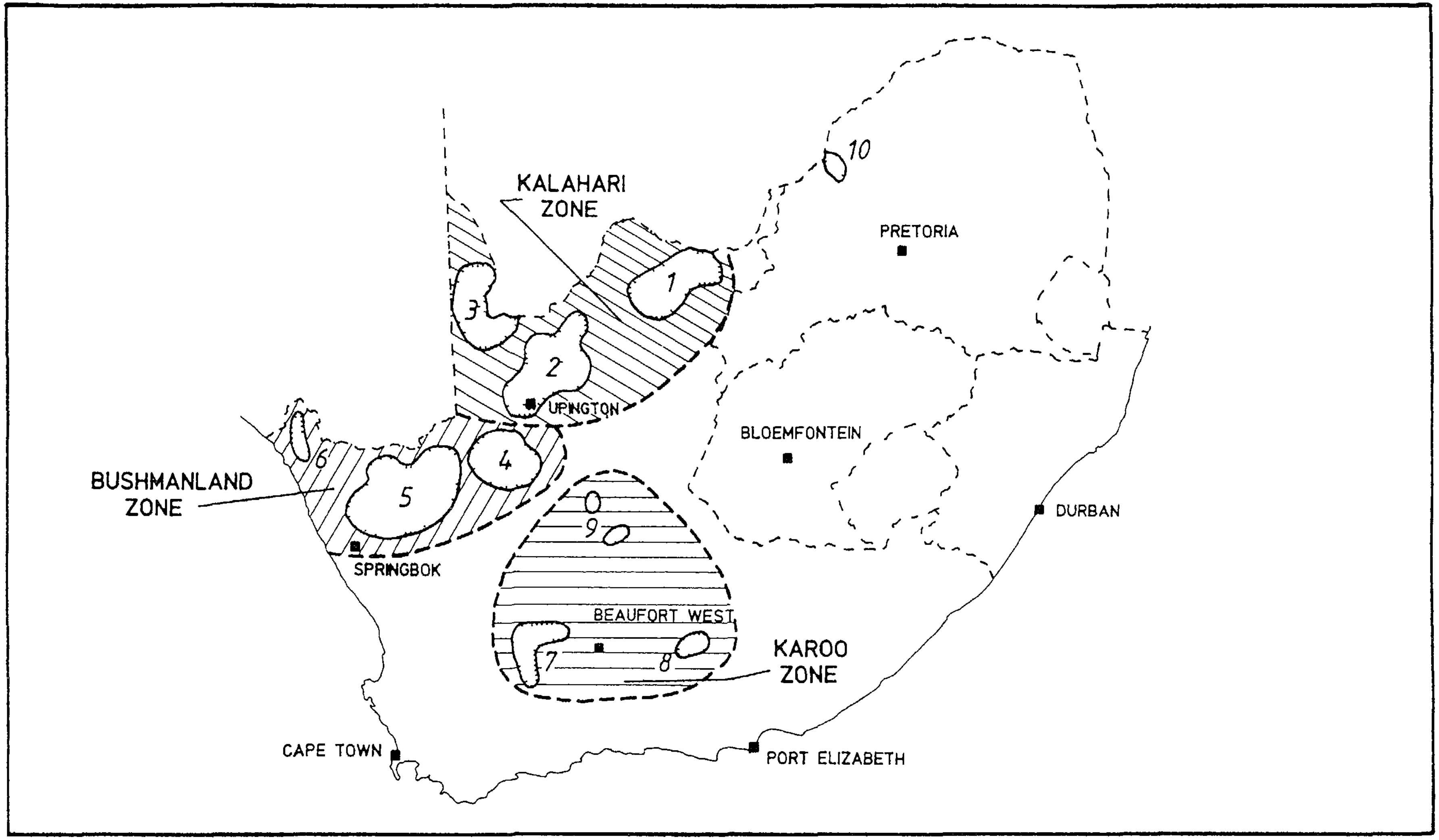

Fig. 2 Ground water uranium anomalies in South Africa. Ten anomalies have been defined by the 25 ppb U contour with the major ones being clustered into the Kalahari, Bushmanland and Karoo zones

the few isolated outcrops, the entire region is covered by the Tertiary to Recent deposits of the Kalahari Group. About 75 % of the area is covered by aeolian sand which attains thicknesses of up to 30 m. Underlying the sand is a calcretized and silcretized sandstone followed by clays and basal gravels.

A thin veneer of the Kalahari Group in the vicinity of anomaly 3 overlies the Dwyka Formation of the Karoo Sequence which consists of horizontally bedded mudstone, shale, siltstone and tillite and which outcrops mainly in pans. These anomalies do not have a corresponding uranium province (Fig. 1) and to date, only traces of uranium mineralization have been found in this area. Anomalies 4, 5 and 6 constitute the Bushmanland zone, with anomalies 4 and 5 being the most important, corresponding to the Namaqua and Northwestern Cape uranium provinces (Fig. 1). The latter are associated with surficial formations and the granitic rocks of the Proterozoic Namaqualand Metamorphic Complex (Frick, 1986, Camisani-Calzolari and Levin, 1986, Camisani-Calzolari, 1985, Levin, 1983a), while anomaly 6 is associated with Cambrian granitic plutons in the Richtersveld (Levin, 1983b).

Anomalies 7, 8 and 9 constitute the Karoo zone and are associated mainly with sandstones and siltstones of the Karoo uranium province (Brunke, 1977). Anomaly 10 is associated with Archaeozoic granitoids but no uranium mineralization is known from this area.

In order to illustrate some of the methods employed in the hydrogeochemical investigations two case studies will be discussed which will include the ground water uranium anomalies in the Kalahari and Bushmanland zones.

4 GROUND WATER ANOMALIES IN THE KALAHARI ZONE

Discussion on the Kalahari zone will deal firstly with the regional hydrogeochemistry of uranium in the ground water in anomalies 1, 2 and 3 and secondly with a description of a more detailed investigaition of the ground water in the Madala palaeodrainage channel.

4.1 Regional Hydrogeochemistry of Uranium in the Kalahari Zone

The Kalahari zone covers some 70 000 km^2 within the sand-covered area of the northern Cape (Fig. 2). The topography varies from a monotonous undulating landscape consisting of grass-covered red Kalahari sand dunes in the Gordonia Block to the flat savannah-type plains north of Vryburg and Kuruman (Piet Plessis Block). The only topographic features are the Kuruman Hills and the Koranna Mountains, both striking north-south (Fig. 3).

The climate is semi-arid, with extremes in day and night temperatures, especially in Gordonia. Annual rainfall decreases from 300 mm in the east to about 200 mm in the west. The greater part of the precipitation occurs as thunderstorms between February and April each year.

The area investigated includes the catchment areas of the Kuruman and Molopo Rivers. Both these rivers are ephemeral, draining westwards, to join in Gordonia.

A multidisciplinary approach was adopted and the study entailed an evaluation of the distribution of uranium in the ground water using all the relevant geological, geophysical and hydrological data. Much of the hydrological information was obtained from records of old boreholes drilled for agricultural and for regional ground water assessment purposes. Due to the aridity of the Kalahari much effort has gone into increasing the agricultural potential of the area by attempts to provide adequate ground water supplies. The pre-Kalahari geological map is given in Fig. 3 and the locations of the pre-Kalahari palaeodrainage channels eroded into the basement rocks are shown in Fig. 4.

Approximately 2 200 ground water samples were taken and the anomalous uraniferous areas, shown in Fig. 5, have been defined by values in excess of 25 ppb U.

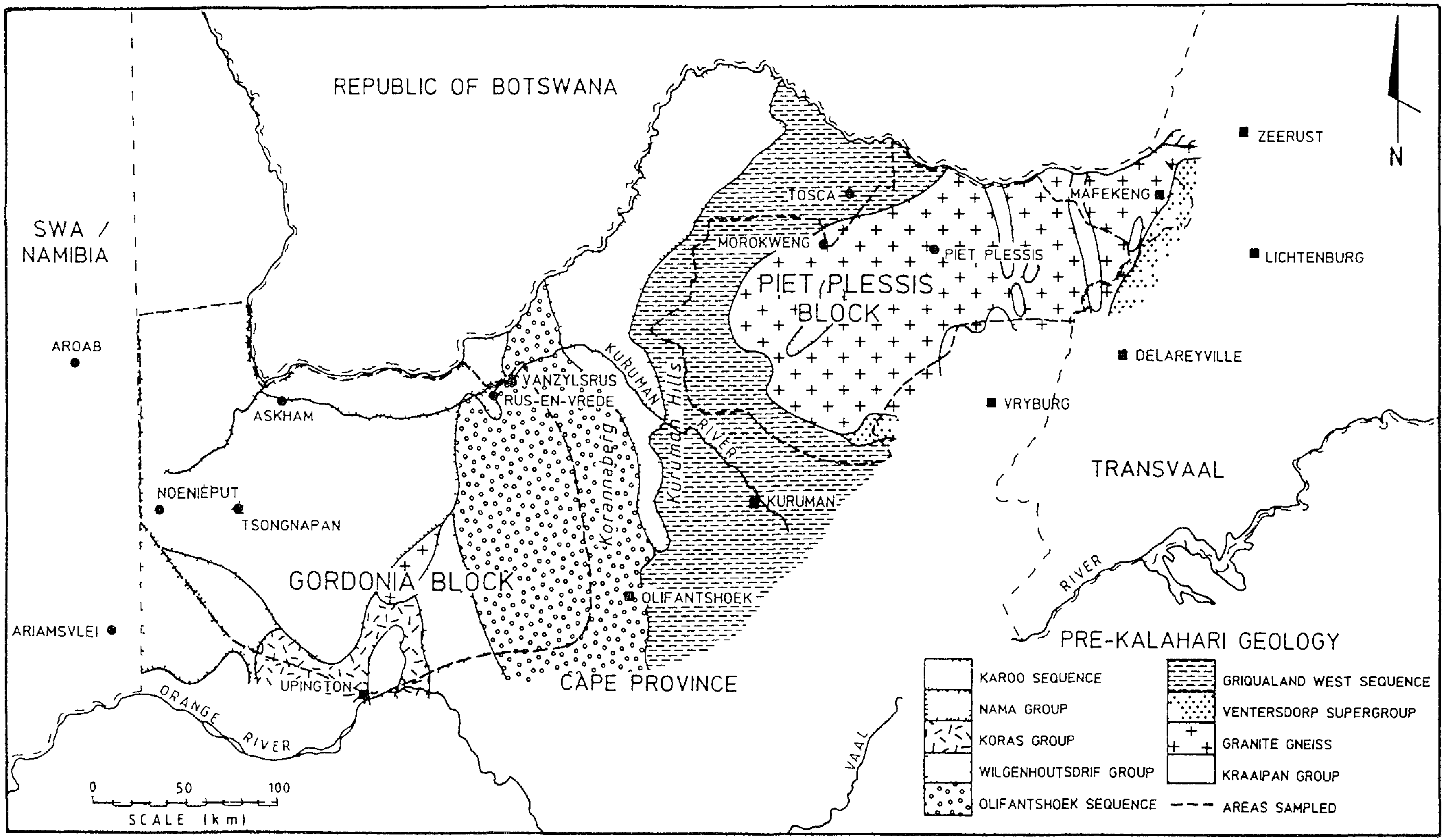

Fig. 3 The pre-Kalahari geology of the northern Cape in the Kalahari zone

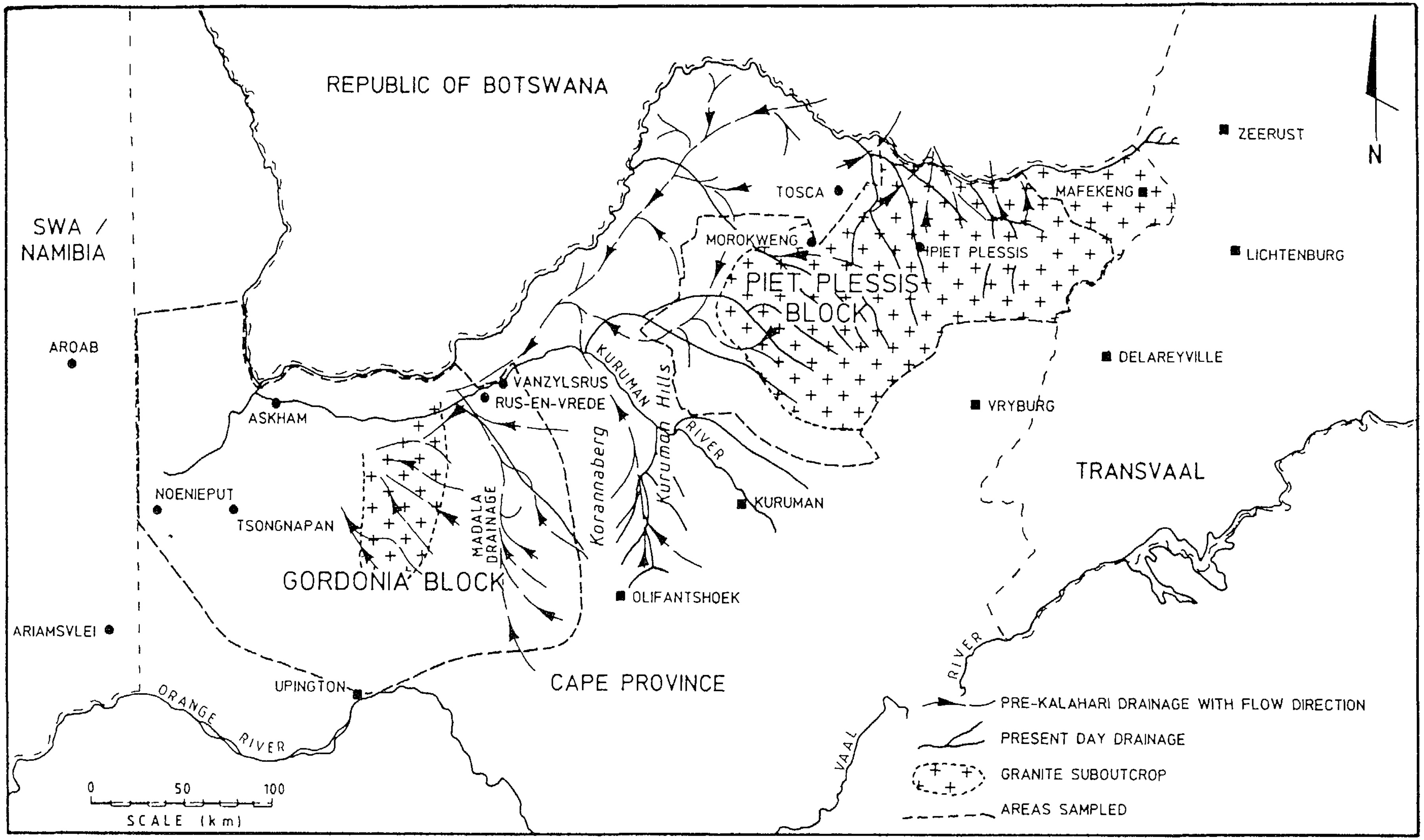

Fig. 4 The pre-Kalahari palaeodrainage channels in the Kalahari zone

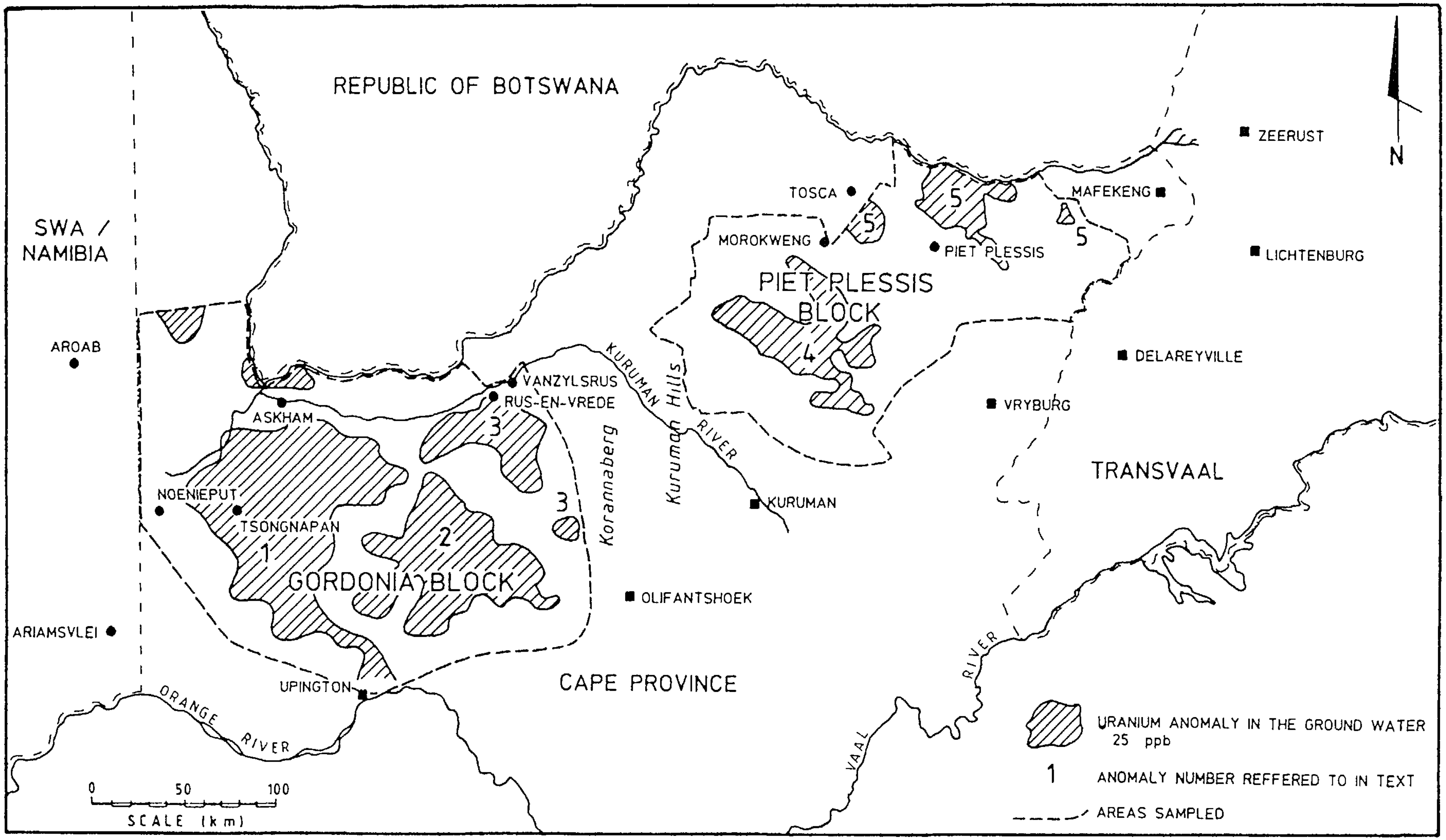

Fig. 5 Uranium anomalies in the Gordonia and Piet Plessis Blocks in the Kalahari zone

In order to divide the areas sampled into ground water regimes, all the analyses were plotted using the Piper method. Three main regimes were recognized which correspond to the distribution of the total dissolved solids (TDS) (Fig. 6):

Group I (Fig. 7) are waters originating from the recharge areas of the Kuruman River and the Koranna Mountains. The waters are relatively high in bicarbonate and low in uranium, the latter corresponding to TDS of less than 2 500 ppm. There are no uranium anomalies in this group.

Group II (Fig. 8) are waters originating from outcrop areas and where surficial cover is usually less than 30 m. Uranium correlates with TDS between 2 500 and 5 000 ppm.

Group III (Fig. 9) are waters restricted largely to western Gordonia and are generally very saline, with more than 5 000 ppm TDS but with a relatively low bicarbonate content. There is a correlation between uranium and bicarbonate, possibly due to the formation of the uranium-bicarbonate complex.

This data suggests that uranium tends to accumulate in basinal areas or in palaeochannels that are closely associated with granitic rocks. A very prominent relationship is that of anomaly 4 in the Piet Plessis Block (Fig. 5), which is situated within a circular palaeodrainage system. Radiometric logging of a few available boreholes has indicated anomolous concentrations of uranium within the area. However, additional drilling will be required to substantiate the grade and extent of the uranium anomaly. Other borehole radiometric anomalies were found at 225 m in the Dwyka Formation of the Karoo Sequence in the Tsonga Pan area of anomaly 1 (Fig. 5). No radiometric anomalies were found in the overlying Kalahari Formation of the Piet Plessis Block, which illustrates the importance of determining the position of palaeodrainage channels which are incised into a granitic basement. However, in the Gordonia Block anomalous radiometric concentrations were found in basal gravels and calcretes. Near Vanzylsrus uraniferous surface

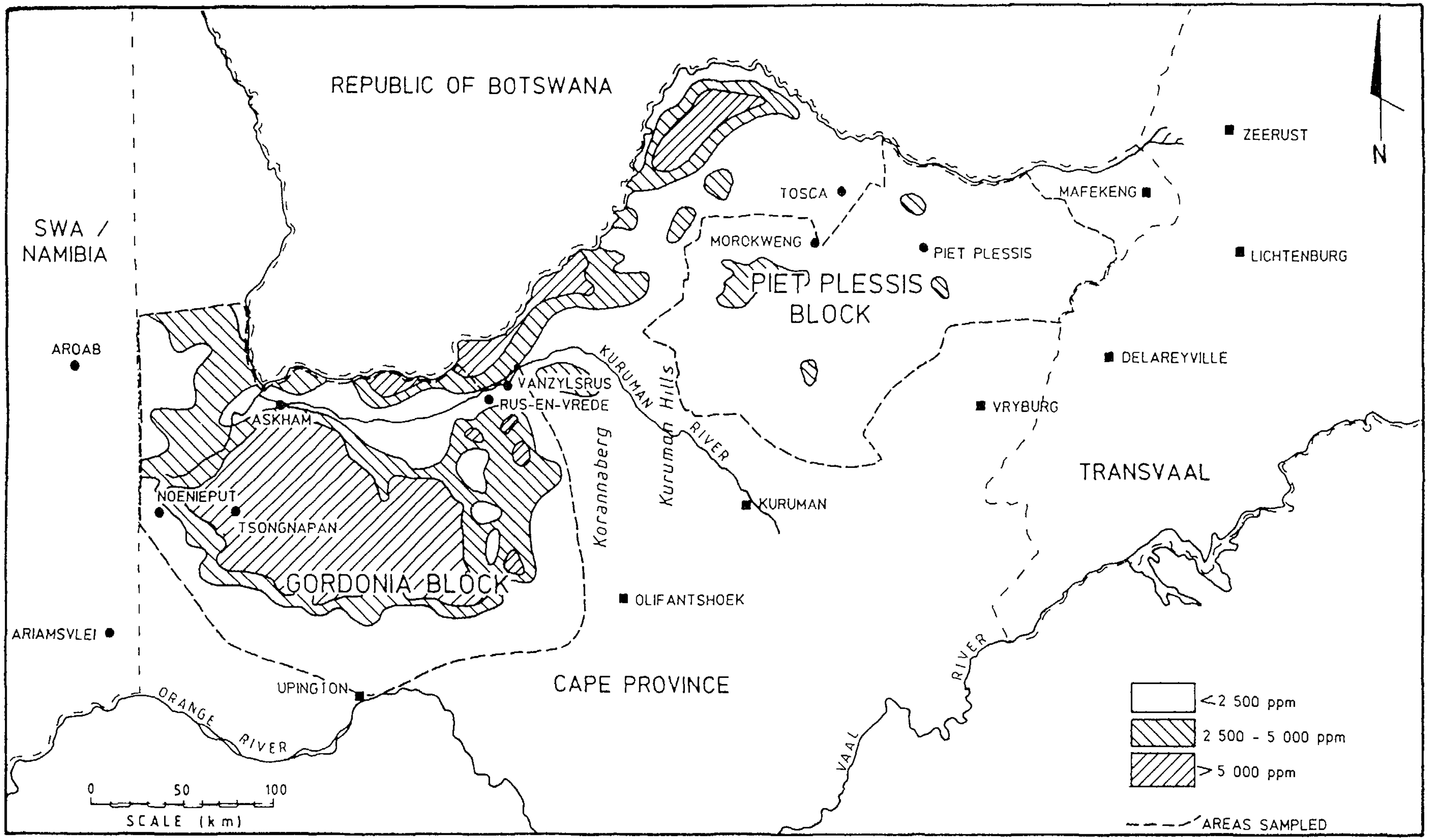

Fig. 6 The distribution of total dissolved solids in the ground water in the Kalahari zone

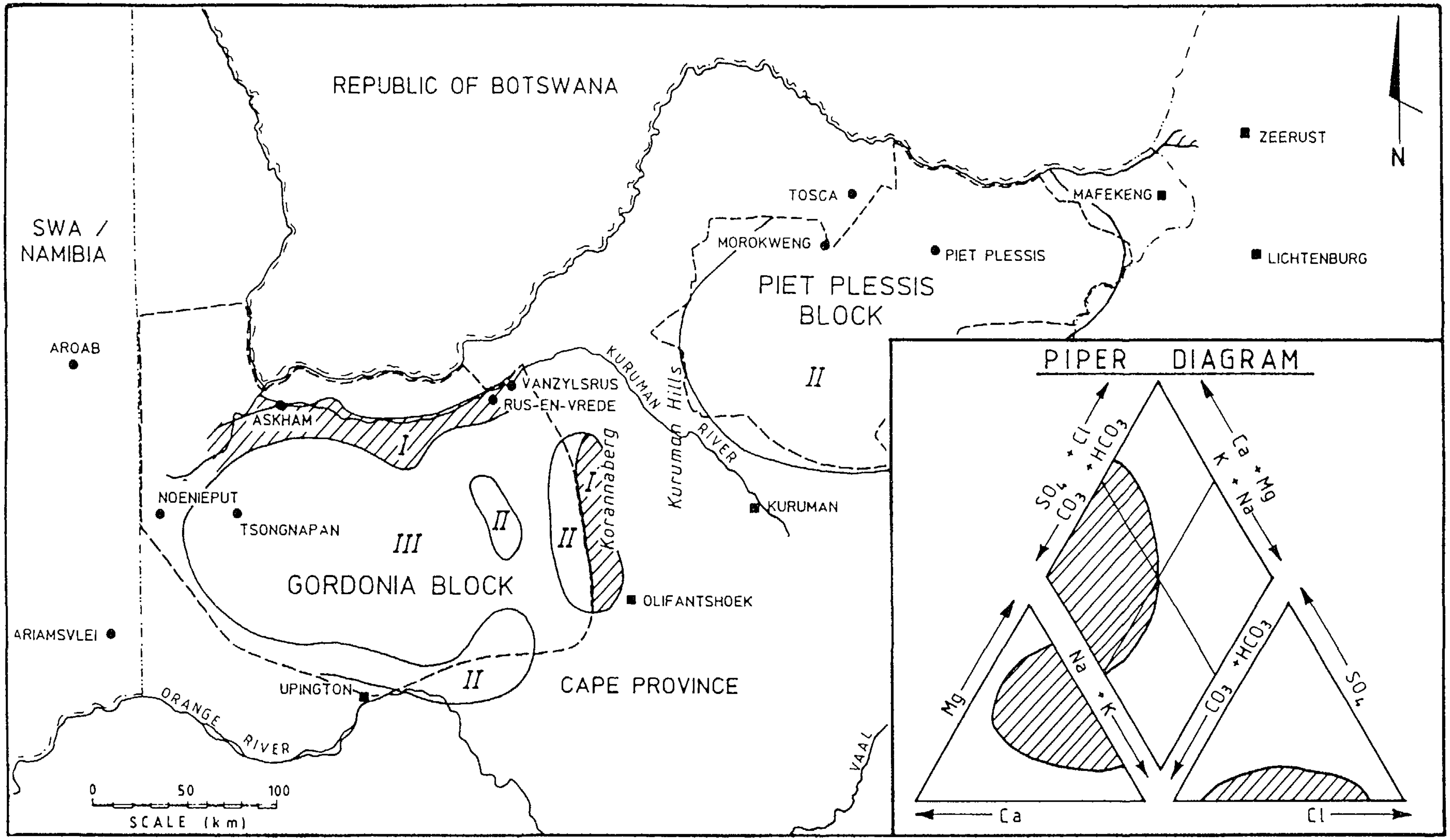

Fig. 7 Group I ground waters as defined by their relative position on the Piper diagram for the Kalahari zone

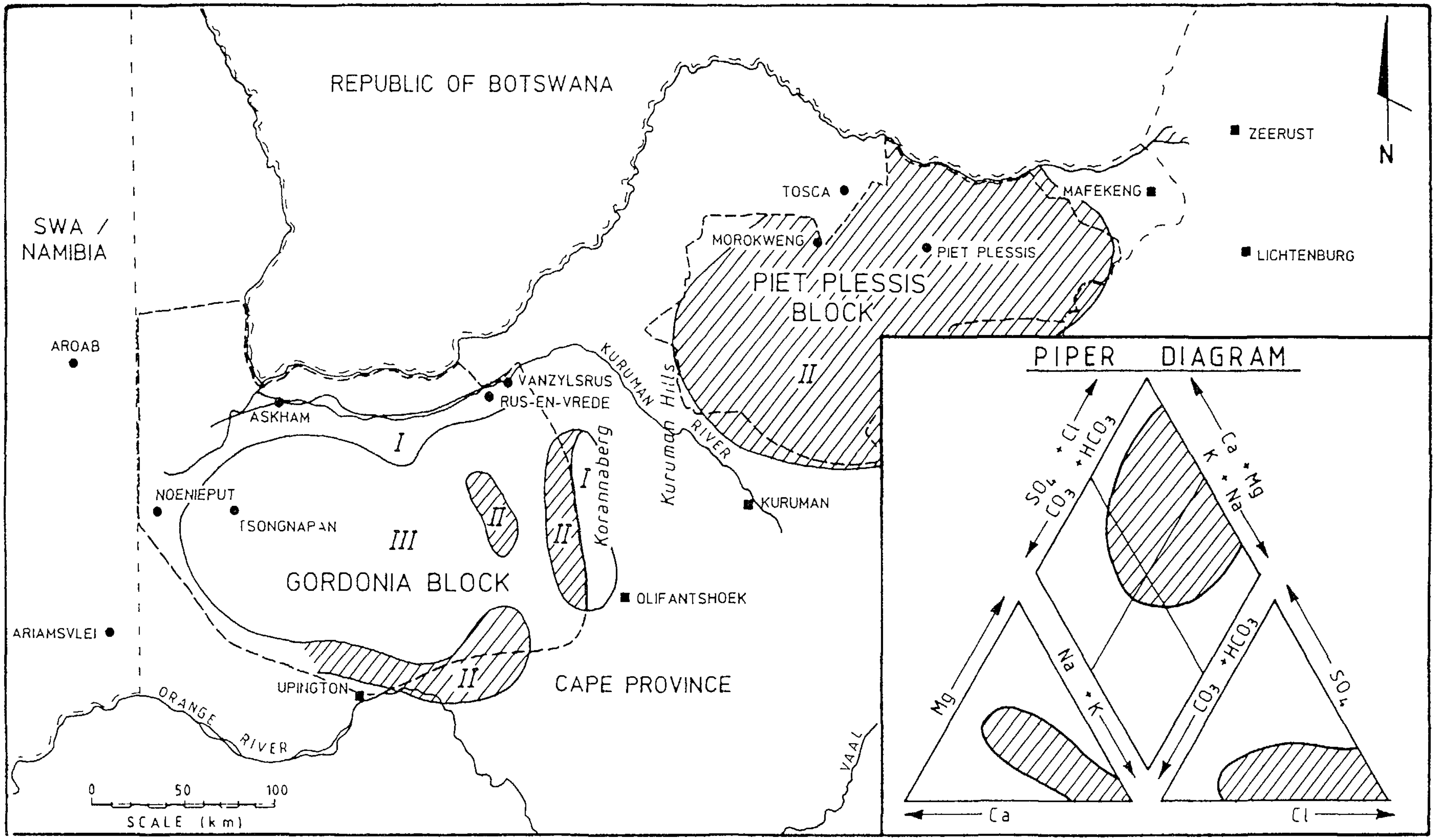

Fig. 8 Group II ground waters as defined by their relative position on the Piper diagram for the Kalahari zone

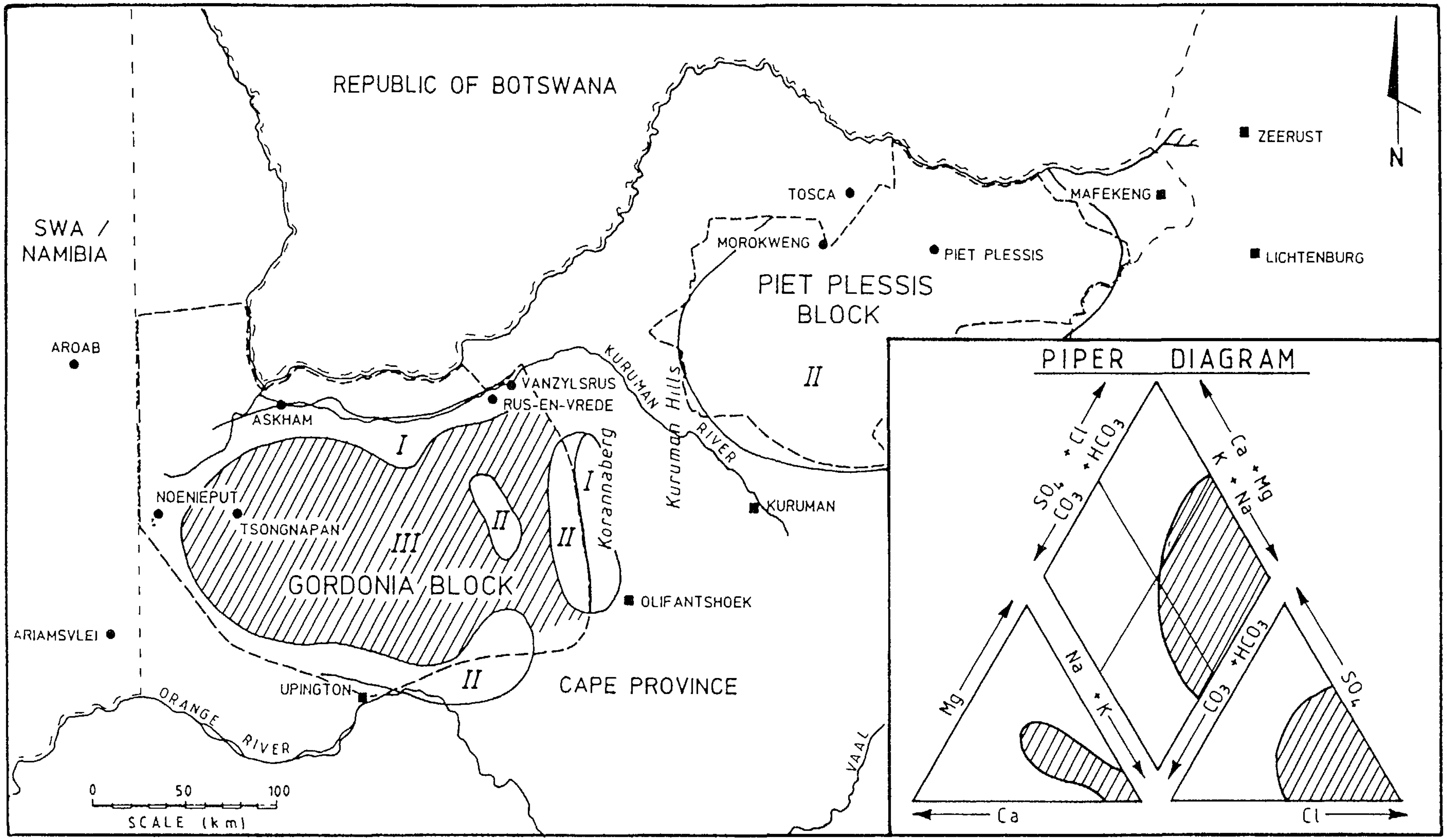

Fig. 9 Group III ground waters as defined by their relative position on the Piper diagram for the Kalahari zone

accumulations of diatomaceous earth were found in the Madala drainage channel.

Although no major new uranium deposit was located as a result of this study, several new occurrences of uranium were indicated in the basement granite, the Dwyka Formation and the Kalahari Group, thereby enhancing the uranium potential of the Kalahari zone.

4.2 **Detailed Investigations of an Uranium Anomaly in the Madala Palaeodrainage Channel**

The locality of the Madala palaeodrainage channel is shown on Fig. 4. It corresponds to the ground water uranium anomaly 3 of the Gordonia block (Fig. 5).

An airborne radiometric survey located an anomaly in the vicinity of Vanzylsrus associated with organic-rich diatomaceous earth.

Following this discovery, a ground water sampling program was initiated and a significant uranium anomaly was found along the whole course of the Madala palaeodrainage, with the highest values occurring behind a dolerite dyke a few kilometres south of the confluence with the Kuruman River. Together, the radiometric and ground water uranium anomalies constituted a likely target area for the location of a hidden uranium deposit. A multidisciplinary approach incorporating geohydrology, ground water geochemistry, isotopic data and radiometric borehole logging studies was used to evaluate its potential.

The Madala drainage rises in the Koranna Mountains about 100 km to the southeast (Fig. 4). The generalized geology of the area is given in Fig. 10 and consists of basement quartzites which are overlain in places by the Dwyka Formation which has been preserved in glacial troughs (Smit, 1972). A dolerite dyke occurs in the northern portion of the area. Faulting is common and probably controlled the direction of the palaeodrainage channel as well as displacing the dolerite dyke.

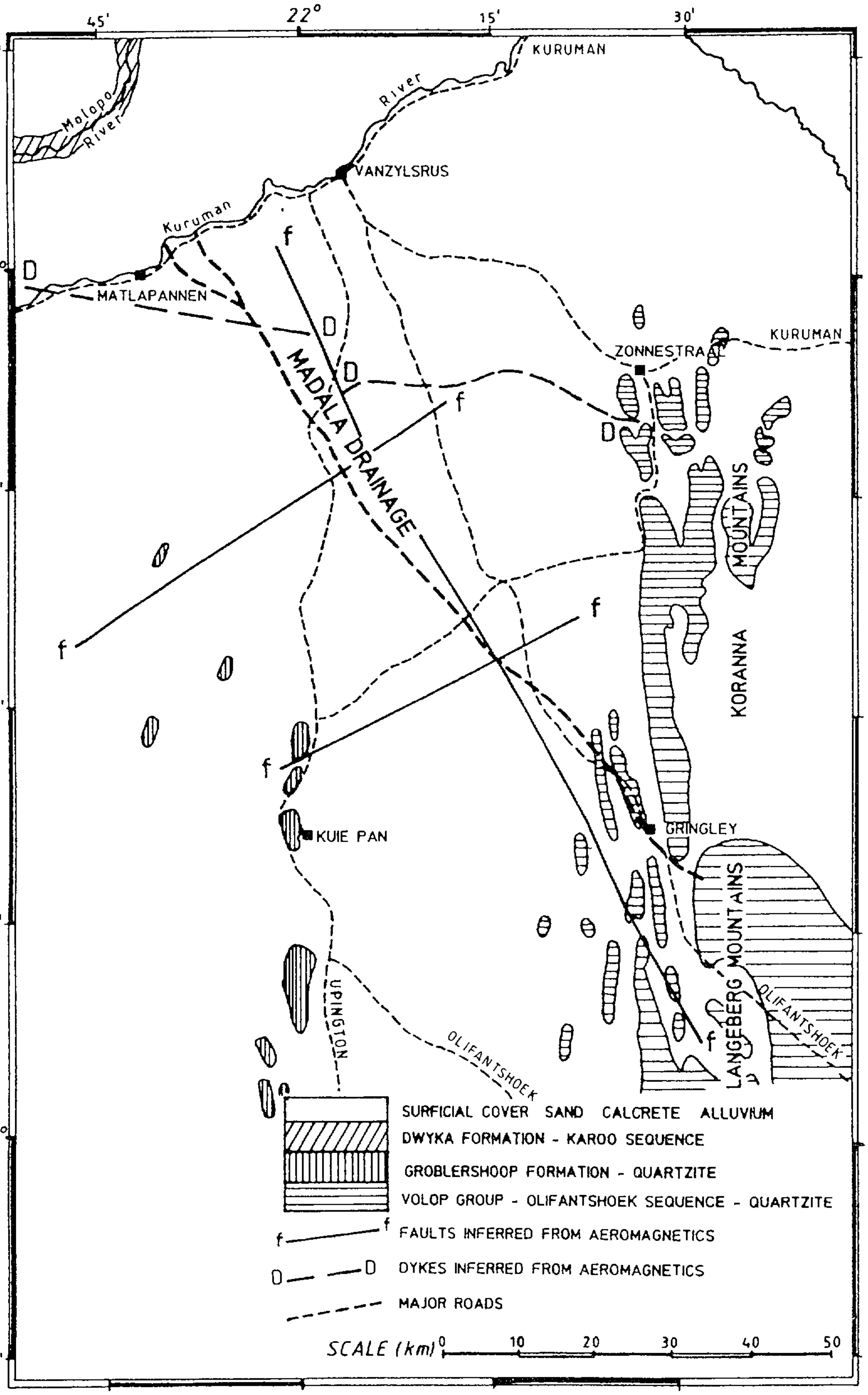

Fig. 10 The geology of the Madala palaeodrainage and environment

In the vicinity of the Kuruman River, close to the outcrop area at Kuiepan and along the mountains in the east, shallower depths to the ground water are encountered (Fig. 11). Along the Kuruman River ground water occurs in the Kalahari Group where good yields are experienced. Near the mountains and outcrop areas good ground water yields are also encountered in the quartzites of the Olifantshoek Sequence. Away from the above areas low-yielding boreholes intersect deep poor-quality water in shales of the Dwyka Formation and quartzites and schists of the Olifantshoek Sequence.

A contour map of the ground water elevation above mean sea level (Fig. 12) suggests that southward flow from the Kuruman River and westward flow from the mountains may occur. The existence of a deep ground water basin between the Kuruman River and the mountains can only be ascribed to a ground water regime that has not yet attained equilibrium.

Chloride has concentrated in the central portions of the palaeodrainage, mainly to the south of the dolerite dyke well away from the recharge areas to the north and east, and underlies the thickest portions of the Kalahari sediments. In a similar manner uranium has concentrated mainly behind the dolerite dyke but to a lesser extent southwards in the palaeodrainage channel (Fig. 13). To explain these phenomena Verhagen (1983) proposed that the recharge to these areas is vertical through the kalahari sediments rather than a regional underflow from the Kuruman River and higher lying areas such as the Koranna Mountains. Similar conclusions were reached by Levin et al, (1982) in their study of the ^{18}O contents of the ground water. In addition the $^{234}U/^{238}U$ activity ratios in the ground water in the vicinity of the uranium anomaly suggest that this is an area of uranium accumulation. However, radiometric borehole logging did not reveal any significant accumulations of uranium.

It therefore appears that the uranium anomaly in the ground water of the Madala drainage is not associated with a uranium deposit as originally thought but is the result of a localized concentration

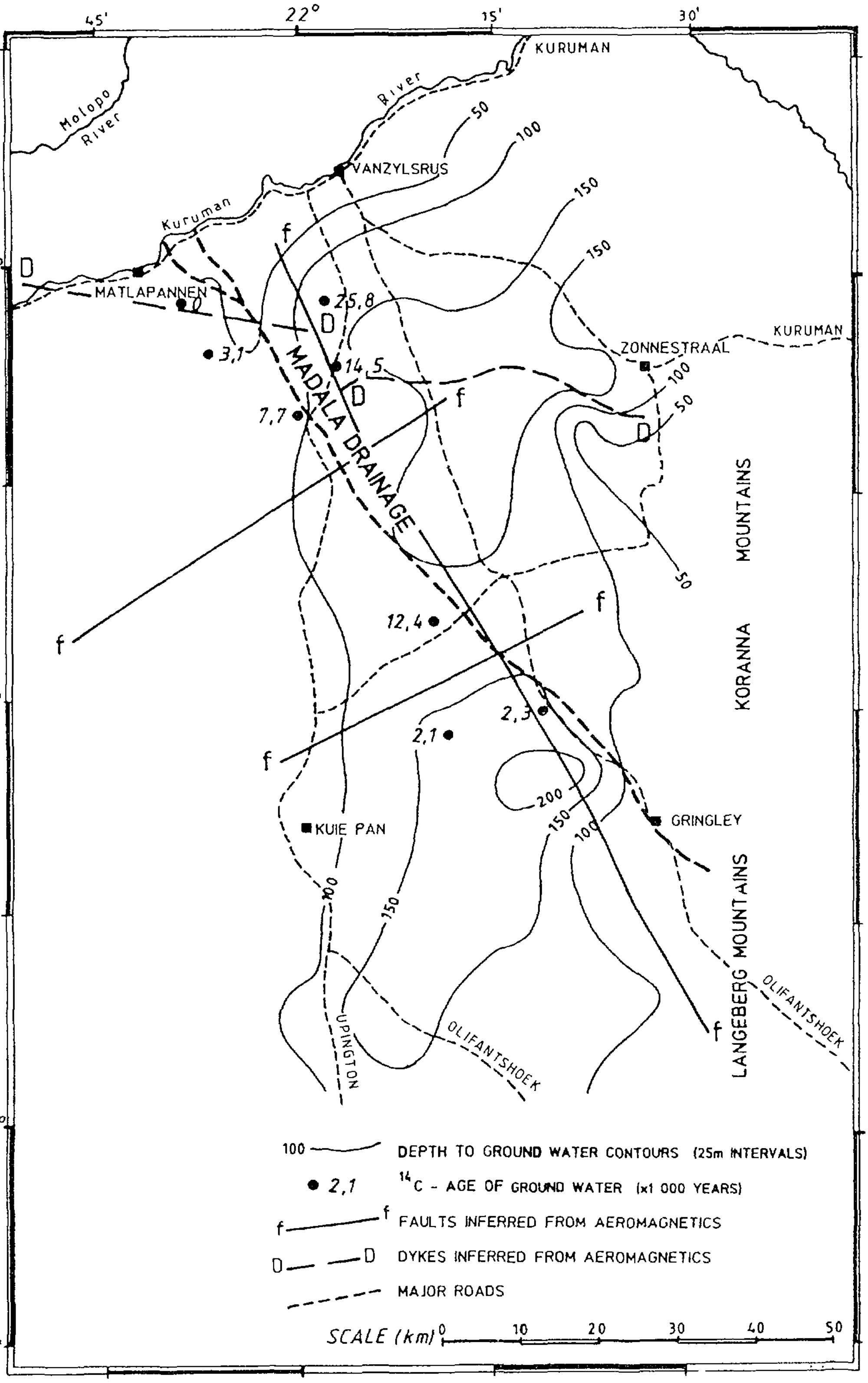

Fig. 11 Contours of the depth to the ground water and ^{14}C ages of the ground waters in the Madala palaeodrainage

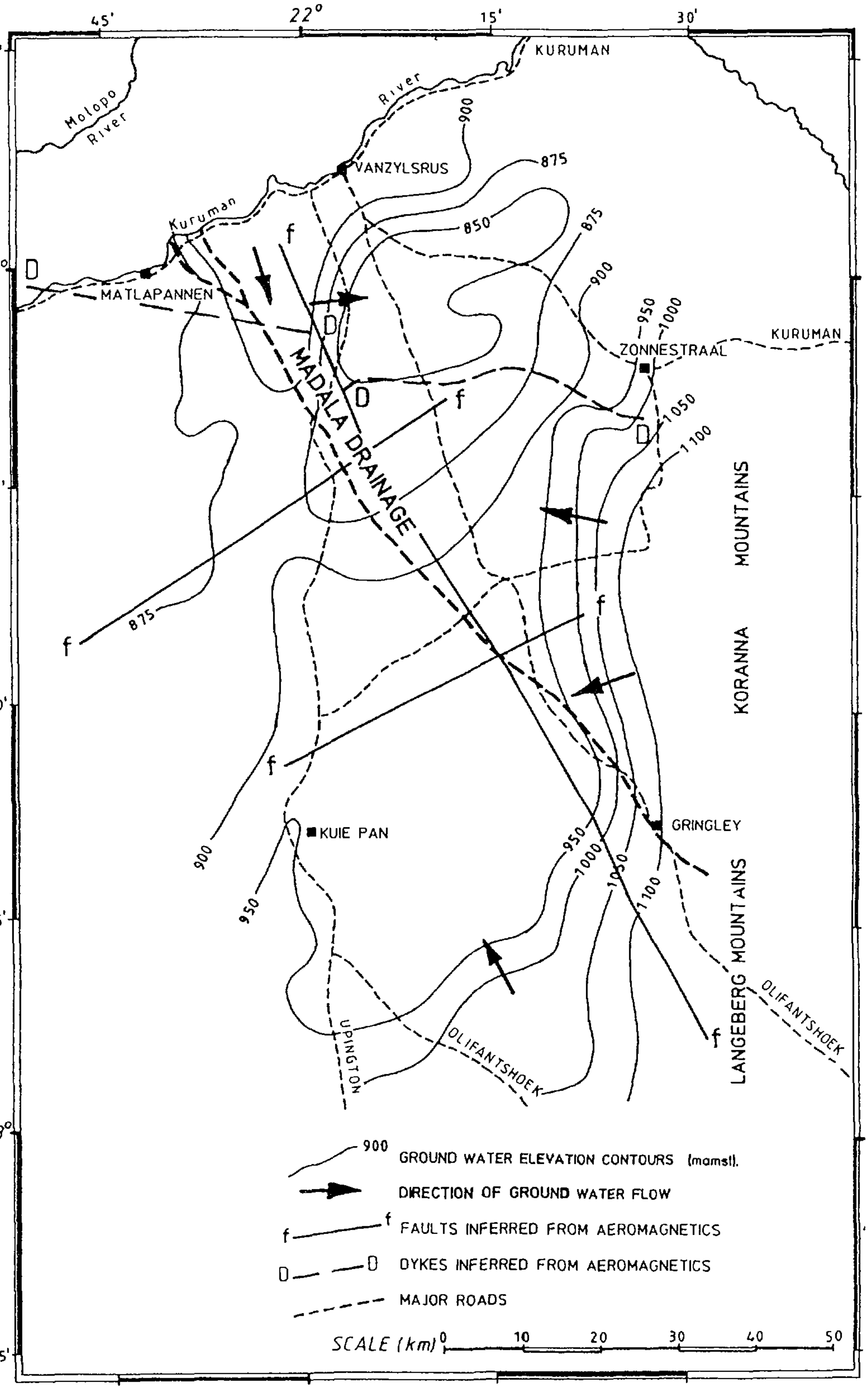

Fig. 12 Contours of the ground water elevation above mean sea level for the Madala palaeodrainage

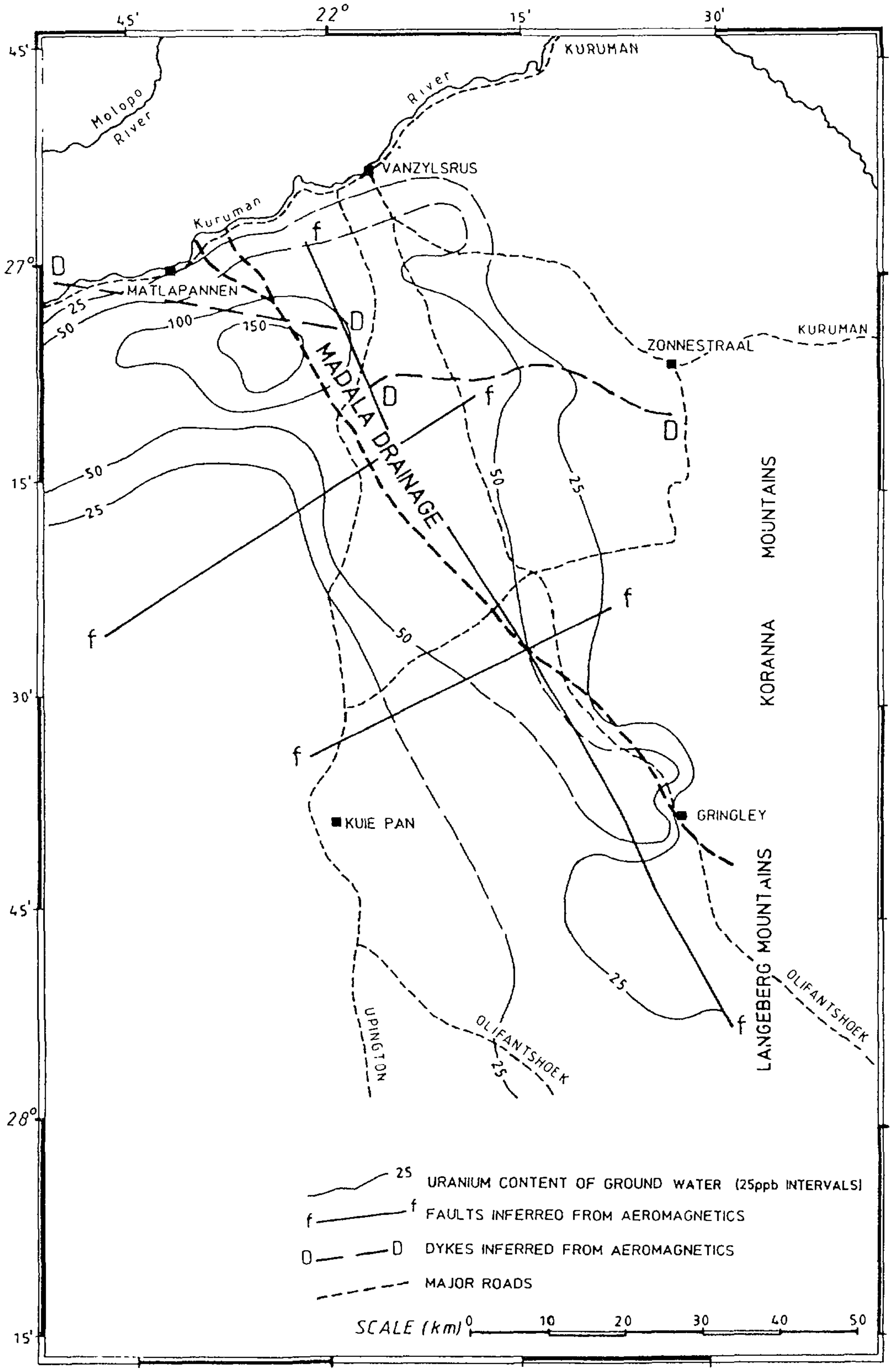

Fig. 13 Contours of the uranium concentration in the ground waters of the Madala palaeodrainage

effect by vertical recharge, probably from sources within the sediments of the Kalahari Group.

5 HYDROGEOCHEMISTRY OF THE BUSHMANLAND ZONE

Hydrogeochemical investigations of the Bushmanland zone commenced in mid-1980 as part of the regional studies relevant to the site-selection phase of the low- and intermediate-level radioactive waste disposal project. The aims of the investigation were firstly, to determine the regional quality and hydraulic gradients of the ground water and secondly, to use the trace-element information to delineate potential mineral deposits possibly underlying the surficial material. This information was used to augment existing geological and geophysical data.

The area investigated is anomaly 5 (Fig. 2), which is situated in the northwestern Cape and is bounded by an irregularly triangular polygon covering an area of approximately 30 000 km^2 within which 850 water samples were collected and analysed for 34 variables. The catchments of the Koa, Buffels and Olifants Rivers are the main hydrological features of the region (Fig. 14). Geologically the area is underlain by terraines of the Namaqualand Metamorphic Complex which consist mainly of metamorphites of volcano-sedimentary origin, quartzo-feldspathic gneisses and intrusive gneisses and granites. A number of major shear zones also traverse the area.

The data were treated statistically by kriging in order to determine whether patterns in the chemistry of the ground waters emerge and if they can be correlated to mineral occurrences or structural features (Camisani-Calzolari, 1985).

5.1 Distribution of Mineral Occurrences in Bushmanland

The northwestern Cape is well endowed in base metal mineral deposits, with the economic ores centred around Springbok containing mainly copper, and those around Aggeneys containing lead, zinc and copper. There are numerous smaller occurrences, including uranium

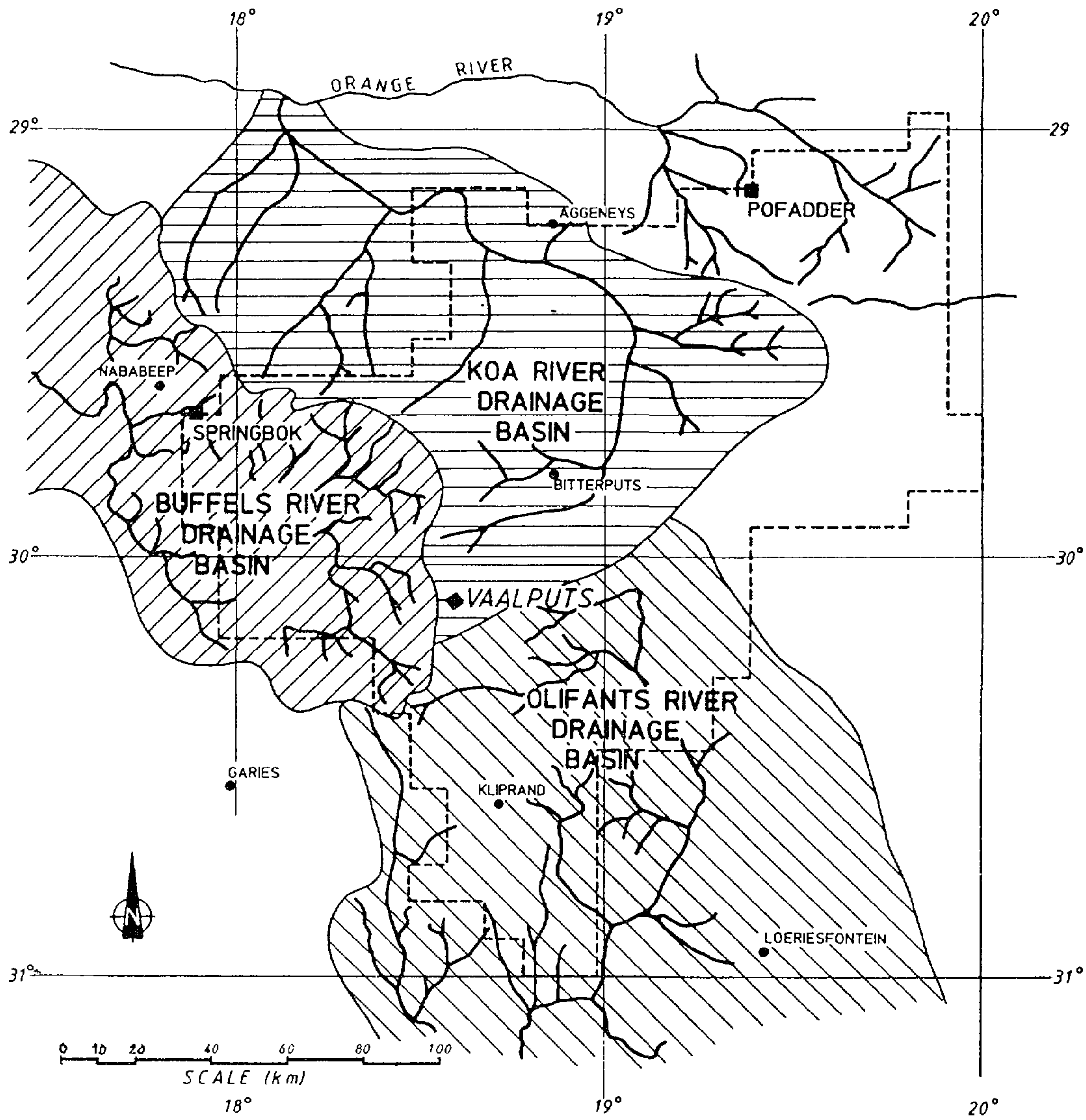

Fig. 14

Drainage basins in the area covered by anomaly 5 (Fig. 2) of the Bushmanland zone of the north-western Cape

scattered throughout the region, which together constitute the northeasterly trending Namaqualand metallogenic province (Fig. 15).

5.2 Hydrogeochemistry of the Base Metals and Uranium

Kriging of the data has resulted in contour maps of which copper, zinc and uranium are the most representative (Figs. 16, 17 and 18).

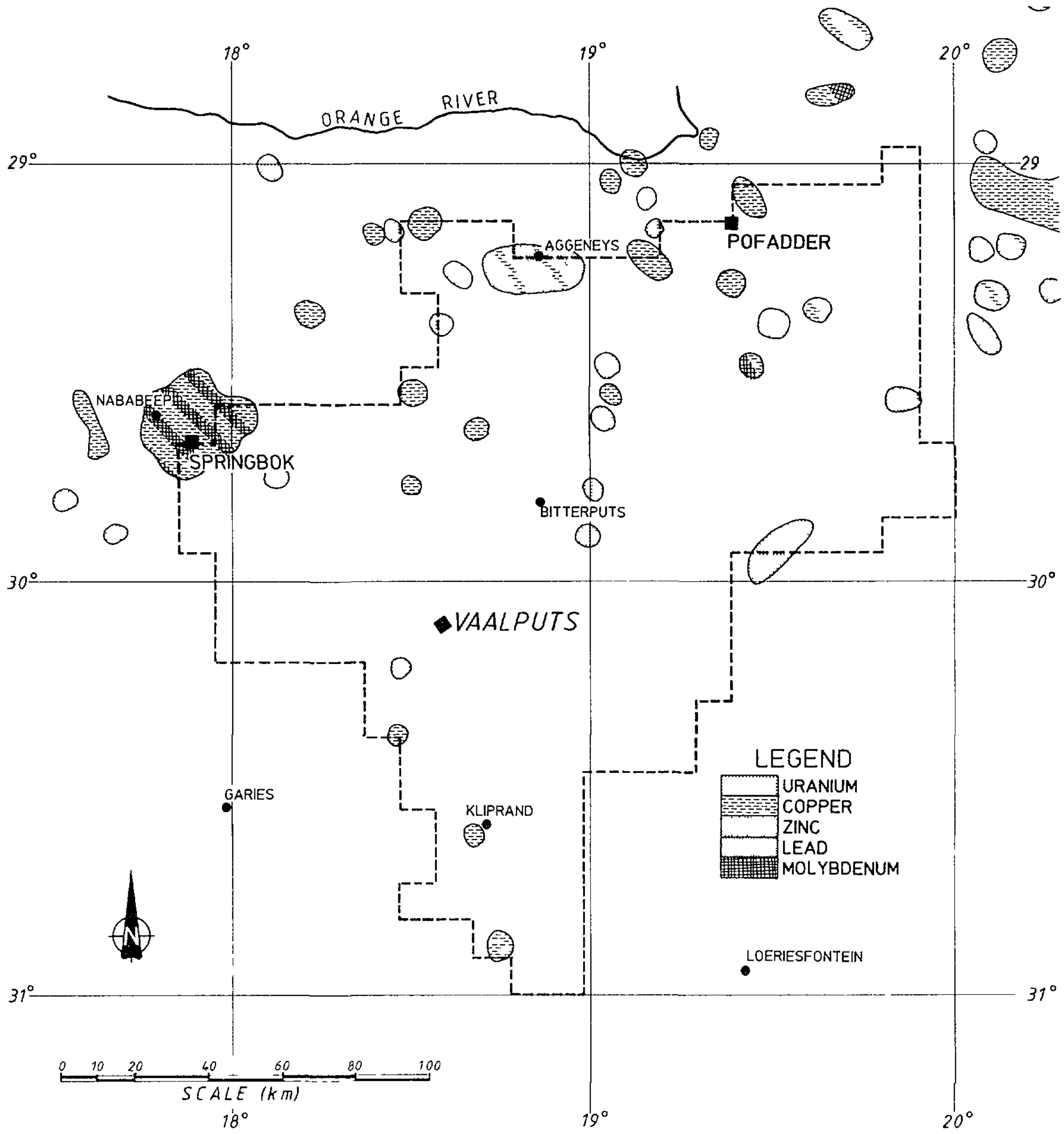

Fig. 15

Mineral occurrences in the Bushmanland zone of the north-western Cape

The distributions of both copper and zinc in the ground waters have some very distinct bulls-eye anomalies which do not necessarily coincide with each other or with known base-metal mineralization. Of significance however, is that the regional trends for both elements are the same, which also corresponds to the ground water trends of molybdenum and nickel (not shown). These parallel the northeasterly direction of the metallogenic province of Namaqualand.

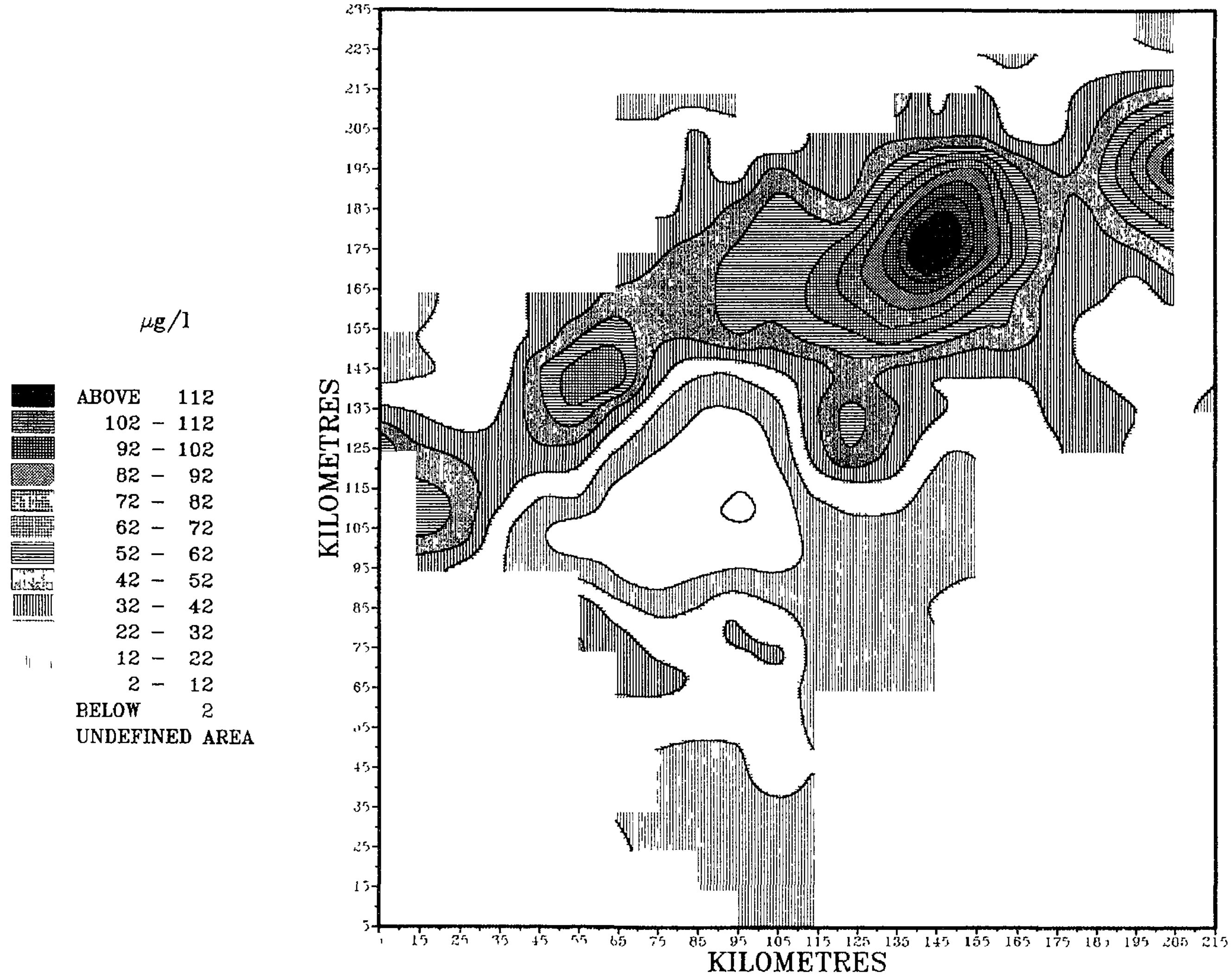

Fig. 16 Contours of kriged copper concentrations in the ground water of the Bushmanland zone

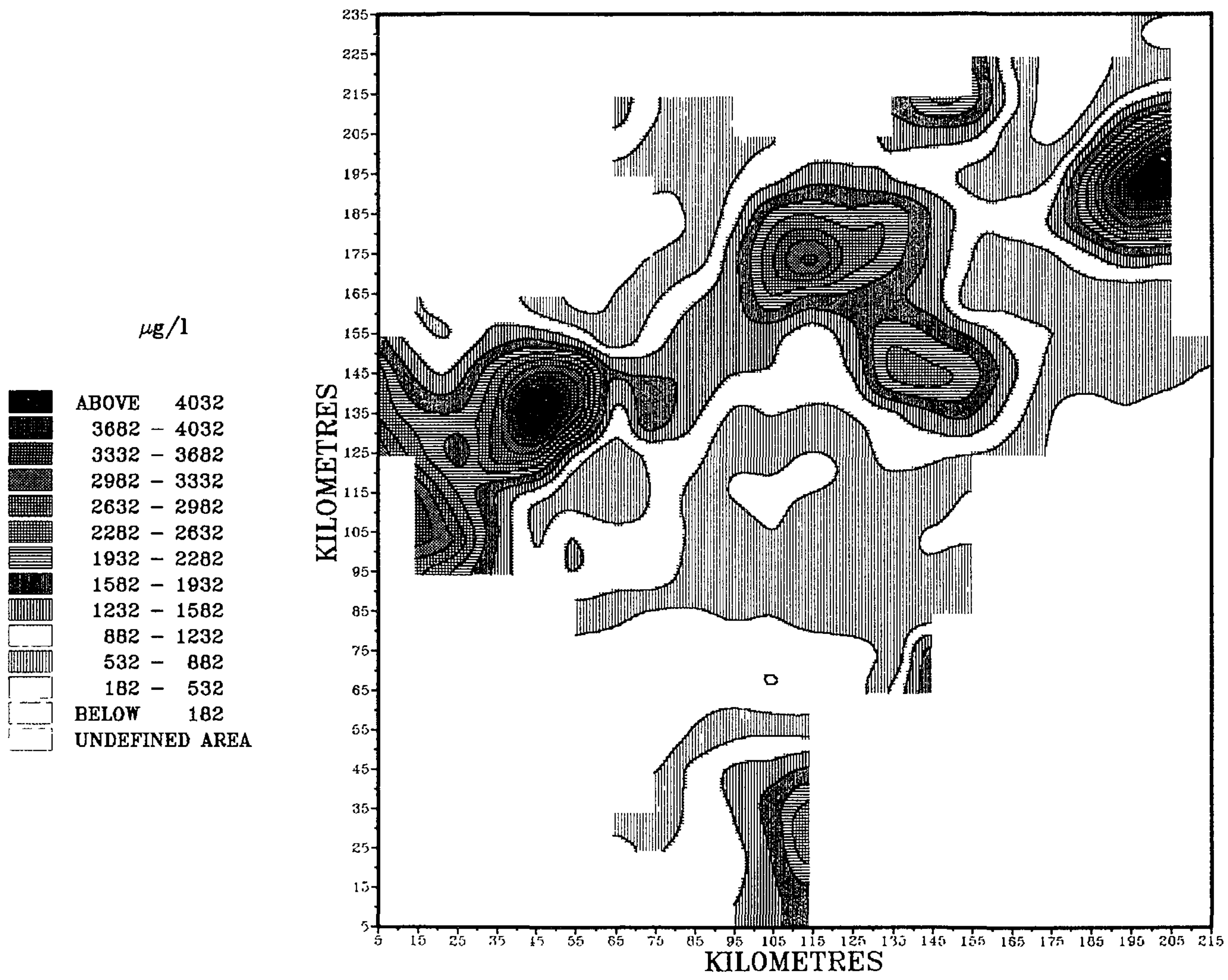

Fig. 17 Contours of kriged zinc concentrations in the ground water of the Bushmanland zone

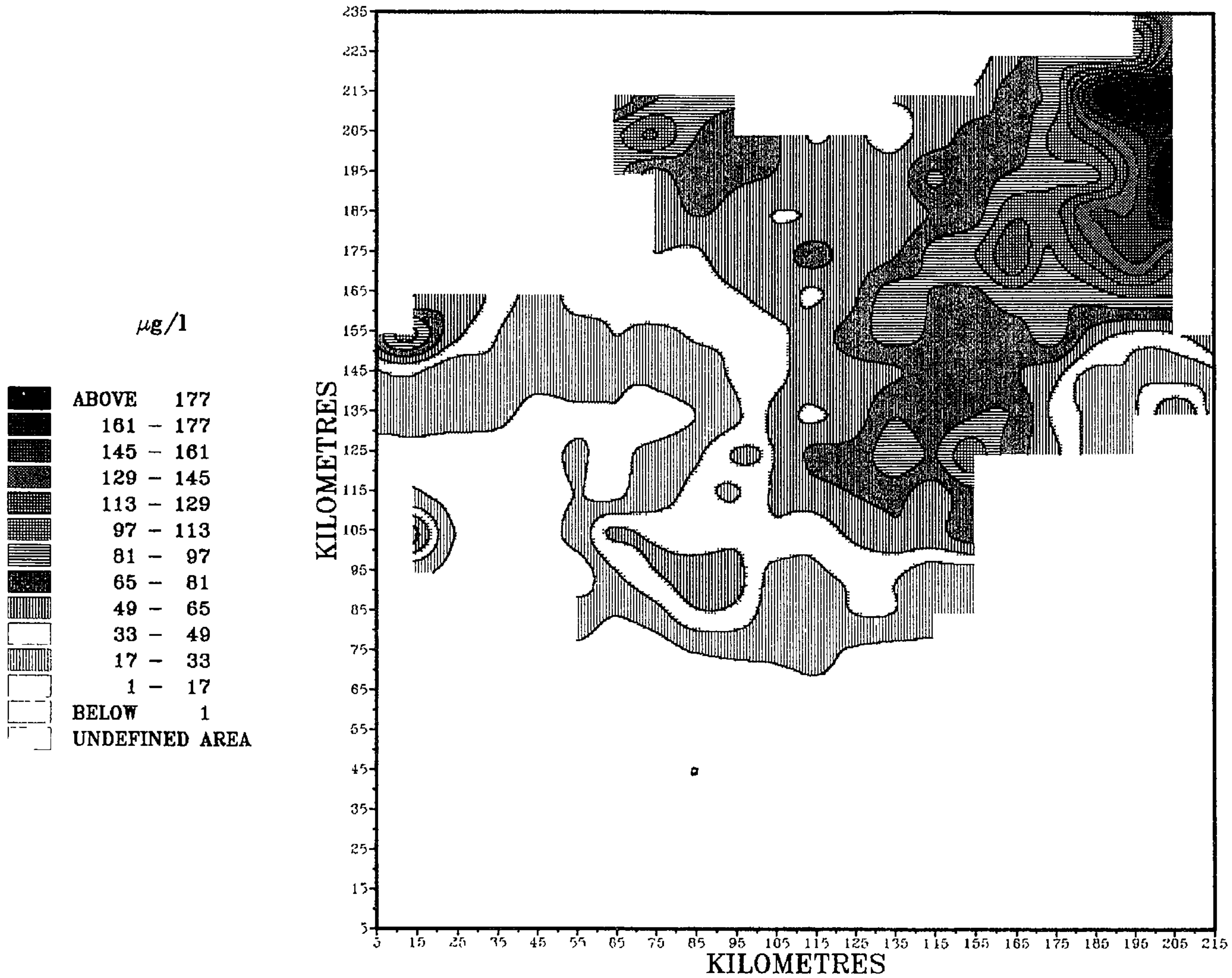

Fig. 18 Contours of kriged uranium concentrations in the ground water of the Bushmanland zone

The uranium distribution pattern in the ground water (Fig. 18) is different to that of the base metals. Generally it tends to be concentrated more to the northeastern and eastern portions of the investigated area. Most of the uranium occurrences located in this region are of the surficial type containing the mineral carnotite (Hambleton-Jones, 1984). The Koa River palaeodrainage channel contains a number of uranium occurrences but these are not clearly reflected in the kriged data in Fig. 18. This is chiefly because it is an extensive dune-covered area having an extremely low agricultural potential and therefore there is a lack of available sampling points.

In general, it appears that the base metal trace element anomalies in the ground water are not related to major palaeodrainage features although the major elements are. A similar conclusion was obtained by Frick (1986), who found that significant amounts of uranium had been leached from the upper portions of granitic source rocks in the area. Uranium anomalies in the relevant host rocks cannot be recognized by surface sampling alone and subsurface sampling using a lithogeochemical approach is necessary. Ground water however, contains much of this leached uranium and thereby shows the presence of potential source rocks demonstrating the usefulness of hydrogeochemistry as a prospecting tool for uranium in these highly leached semi-arid environments.

6 CONCLUSIONS

Analyses of ground water samples taken for domestic, agricultural and industrial applications in various parts of South Africa have led to a better understanding of the respective ground water regimes. In addition, areas have been delineated, such as the Kalahari and Bushmanland zones, that could potentially host uranium deposits within the thick sedimentary formations overlying the basement. Kriging of the analytical data for the northwestern Cape has had the tendency to smooth the data but nevertheless has outlined the main mineralized areas.

Therefore the methods used during the National Hydrogeochemical Project in the semi-arid areas of the northern Cape have demonstrated that-

a) potential source and host rocks under thick non-uraniferous surficial cover could be outlined; and
b) in leached areas where surface sampling has failed to detect uranium occurrences the hydrogeochemical approach was successful.

REFERENCES

BRUNKE, E.G. (1977) Hydrogeochemical orientation surveys at two uranium deposits in the Beaufort West area. Geological Survey of South Africa, Report No. 1978-0074.

CAMISANI-CALZOLARI, F.A.G.M. (1985) Geostatistical investigation of the hydrogeochemistry of the ground waters in the north-western Cape. Volume 1. Methods applied and discussion of results. PER-140.

CAMISANI-CALZOLARI, F.A.G.M.; AINSLIE, L.C.; VAN DER MERWE, P.J. (1986) Uranium in South Africa 1985. The Atomic Energy Corporation of South Africa Ltd., ISBN 0 86960 825 8.

CAMISANI-CALZOLARI, F.A.G.M.; LEVIN, M. (1986) A multivariate geostatistical investigation of the ground water hydrogeochemistry of an area in the northwestern cape. In, Geocongress '86 extended abstracts. 7-11 July 1986. Johannesburg, ISBN 0-0620-09820-1, 1007-1011.

FRICK, C. (1986) The behaviour of uranium, thorium and tin during leaching from a coarse-grained porphyritic granite in an arid environment. Jour. Geochem. Explor., 25, 261-282.

HAMBLETON-JONES, B.B. (1984) Surficial deposits of South Africa. In, Surficial Uranium Deposits, IAEA TECDOC-322, Vienna, 221-230.

LEVIN, M. (1981) The geology, hydrology and hydrogeochemistry of an area between the Kuruman and Orange Rivers, north-western Cape. Trans. Geol. Soc. S.Afr., 84, 177-190.

LEVIN, M.; HAMBLETON-JONES; B.B., SMIT, M.C.B. (1983) Uranium in the ground water of the Kalahari region south of the Molopo River. Seminar on the Mineral Exploration of the Kalahari, Gaborone, Botswana.

LEVIN, M.; TALMA, A.S.; VOGEL, J.C. (1983) Geohydrological investigation of an uranium anomaly near Vanzylsrus in the northern Cape Province. Symposium, Groundwater '82, University of the Witwatersrand. (To be published in the Transactions of the Geological Society of South Africa).

LEVIN, M. (1983a) Geohydrological investigations of the Vaalputs radioactive waste disposal site and environs. PER-112.

LEVIN, M. (1983b) A preliminary hydrological assessment of the Richtersveld. PER-104.

SMIT, P.J. (1972) The Karoo System in the Kalahari of the northern Cape Province. Ann. Geol. Surv. S.Afr., 9, 78-81.

TOENS, P.D. (1981) Uranium provinces and their time-bound characteristics. Trans. Geol. Soc. S.Afr., 84, 3, 293-312.

VERHAGEN, B.T. (1983) Environment isotope study of a ground water supply project in the Kalahari of Gordonia. Proceedings Symposium, Isotope Hydrology, Vienna, p 871.

INTERPRETATION AND EVALUATION OF REGIONAL GEOCHEMICAL ANOMALIES OF URANIUM

C. FRICK, S.W. STRAUSS
Geological Survey of South Africa,
Pretoria, South Africa

Abstract

In arid terrains where physical weathering predominates regional geochemical stream sediment maps generally reflect the chemical composition of the bedrocks. As an exploration tool these maps, even when the sampling grid is one sample per square kilometre, can at best serve to delineate large regional anomalies. During the present investigation five regional uranium anomalies were studied using a multivariate regression technique in order to develop criteria whereby the potential economic significance of these regional anomalies can be evaluated.

The anomalies studied were identified on the basis of U grey scale maps and four of them are located on intrusive granite plutons in the Northwestern Cape Province. The remaining anomaly occurs on a sequence of sediments with a provenance of a U-rich granite. Uranium can be concentrated in accessory minerals such as monazite, apatite, sphene and zircon, or it could be hosted in uraninite and thorianite. Anomalies resulting from the latter minerals are presently more attractive exploration targets, whereas the former are generally less attractive.

During the stepwise multivariate regression study a total of 20 elements were regressed against U, and the elements which yielded the most significant regression coefficients were identified and ascribed to specific mineral phases. It was possible to show that 80 to 90 percent of the uranium present in three of the intrusive plutons could be accounted for by U hosted in zircon, sphene, iron oxides and biotite, and consequently only a small U-residual results. In the fourth pluton, however, it was possible to show that only 10 percent of the U can be accounted for by U hosted in fluorite and iron oxides, and that the large U residual may be ascribed to the presence of uraninite or thorianite. The latter pluton is thus a more significant anomaly and should be studied further. Stepwise multivariate regression showed that 90 percent of the U in the Schwarzrand basin is hosted either in zircon or calcite, thus causing this regional anomaly to be unattractive. A fission tract study of the stream sediment samples from one of the regional anomalies showed that the mineralogical constraints established during the stepwise multivariate regression are valid.

By plotting the calculated U concentration, based on the regression coefficients against the analysed U contents it is possible to identify samples which contain U in excess of that which could be accounted for by the identified U-bearing constituent mineral phases. The fact that these samples contain more U thus suggests that a U-mineral may be present or that two populations of the U-bearing minerals may be present, with one of the populations being relatively enriched in U. The identification of samples with higher determined U-contents than calculated contents can be used to define specific exploration targets within a large regional anomaly.

---

1. INTRODUCTION

During the past decade the Geological Survey of South Africa has been conducting routine geochemical mapping of South Africa using stream sediment samples collected from first order streams on a one kilometre grid. The minus 200 mesh size fraction of these samples were analyzed for 25 elements using an X-ray fluoresence spectrometer. The analytical data are presented as a series of 1:250 000 geochemical grey scale maps, which are released on Open File. Apart from the production of the geochemical maps, the Geological Survey has also been engaged in the development of a number of geological and mathematical interpretation techniques which could be applied to this data in order to identify possible exploration targets (Frick and Strauss, in press).

As a consequence of the routine geochemical mapping programme, a number of geological units, either intrusive granite plutons or specific sedimentary formations were identified, which yielded large regional uranium anomalies. In an attempt to evaluate the significance of some of these anomalies a study was undertaken to develop a mathematical technique, which can be applied to the data, in order to grade the economic potential of the anomalies. Five large regional anomalies were selected for further investigation. These anomalies occur in the north-western Cape Province, and their distribution is shown in Figure 1.

Since U usually substitutes in a large number of mineral phases as a trace constituent such as zircon and monazite and only occasionally forms U-bearing minerals, it is of crucial importance to establish in which mineral phases uranium is hosted in the stream sediment samples. Should it be possible to use the existing geochemical data to establish the mineralogical

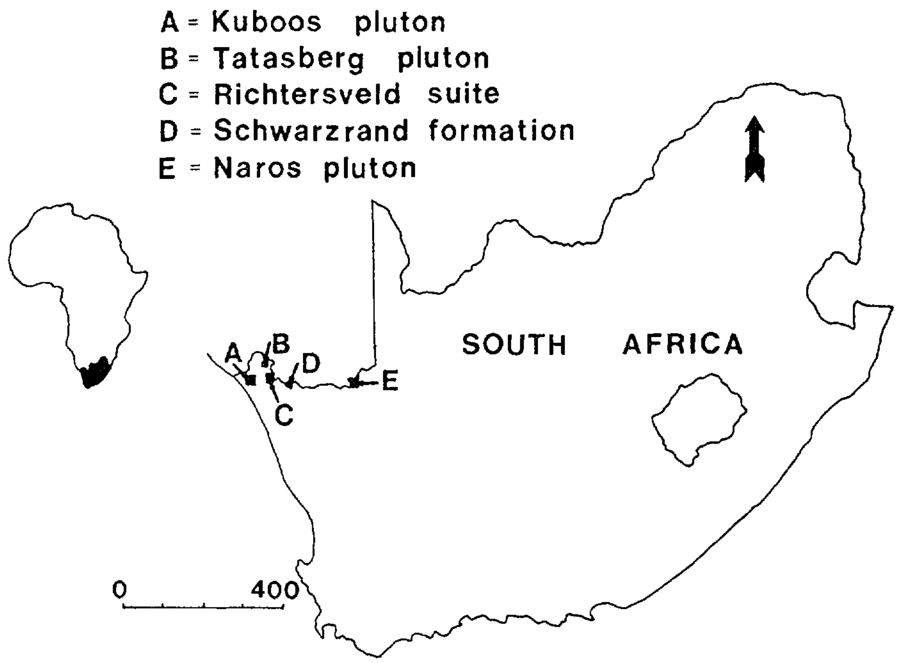

FIG. 1.

The localities of the regional anomalies studied.

hosts for the uranium it may be possible to classify insignificant (zircon etc. hosted) from significant (uraninite hosted) U-anomalies. The study area is located in a semi-desert terrain where physical weathering presently predominates. The geochemistry of the stream sediments will thus largely reflect the geochemistry of the bed rock. An understanding of the distribution of uranium between the mineral phases in the stream sediment samples will allow an assessment of the distribution of uranium in the mineral phases of the source rocks.

The anomalies studied during this investigation include the Kuboos and Tatasberg granite plutons (550 Ma), the Richtersveld Suite (920 Ma), the Naros granite pluton (1100 Ma) and the calcareous Schwarzkalk Member of the Schwarzrand Formation (700 Ma).

II SAMPLING, ANALYTICAL AND INTERPRETATION TECHNIQUES

A composite stream sediment sample, consisting of five one kilogram samples, was taken from the active parts of first order streams on a one kilometre grid. The minus 200 mesh size fraction was pressed into a powder briquette and analysed for 25 elements by means of an X-ray spectrometer using the analytical technique of Nisbet et al (1979). The USGS, CANMET and NIM rock standards were used during calibration, and the recommended values after Abbey (1983) were accepted for these standards during calibration.

The regional anomalies were identified visually on the 1:250 000 grey scale uranium geochemical maps and the multi-element data of all the stream sediment samples from these anomalous areas were used during the investigation. The complete data set for each of these anomalies were investigated using a stepwise multi-regression technique, by regressing U against the other elements using the linear equation given below.

$$U = C + A_1X_1 + A_2X_2 + A_3X_3 \ldots\ldots\ldots + A_MX_M$$

where U = Uranium concentration

A_1 = Most significant contribution to the regression

X_1 = Regression coefficient for element A_1

C = The regression constant

During each successive regression cycle, one element was added at a time, and the relative contribution of that element to the regression equation was evaluated. This procedure was continued until the relative contribution by successive elements became insignificantly small. The elements which contributed to the regressing equation were then evaluated in terms of the mineralogical composition of the source granite and combinations of elements were interpreted as possible mineral phases in which U can be hosted.

The theoretical U-concentration in the different samples was then calculated using the regression coefficients of those elements which made the most significant contributions, and compared to the observed U-concentrations. This procedure allowed the identification of samples in which more U is present than what could have been expected for the mineral phases which host uranium. Such samples may thus carry uraninite or thorianite and require further study.

III GEOLOGY

In Figure 2 the geology of the Kuboos and Tatasberg plutons, together with the Richtersveld Suite and the Schwarzrand Formation are shown on a generalized geological map of the Alexanderbay area. A generalized geological map of the Naros pluton, which occurs further to the east, is shown in Figure 3.

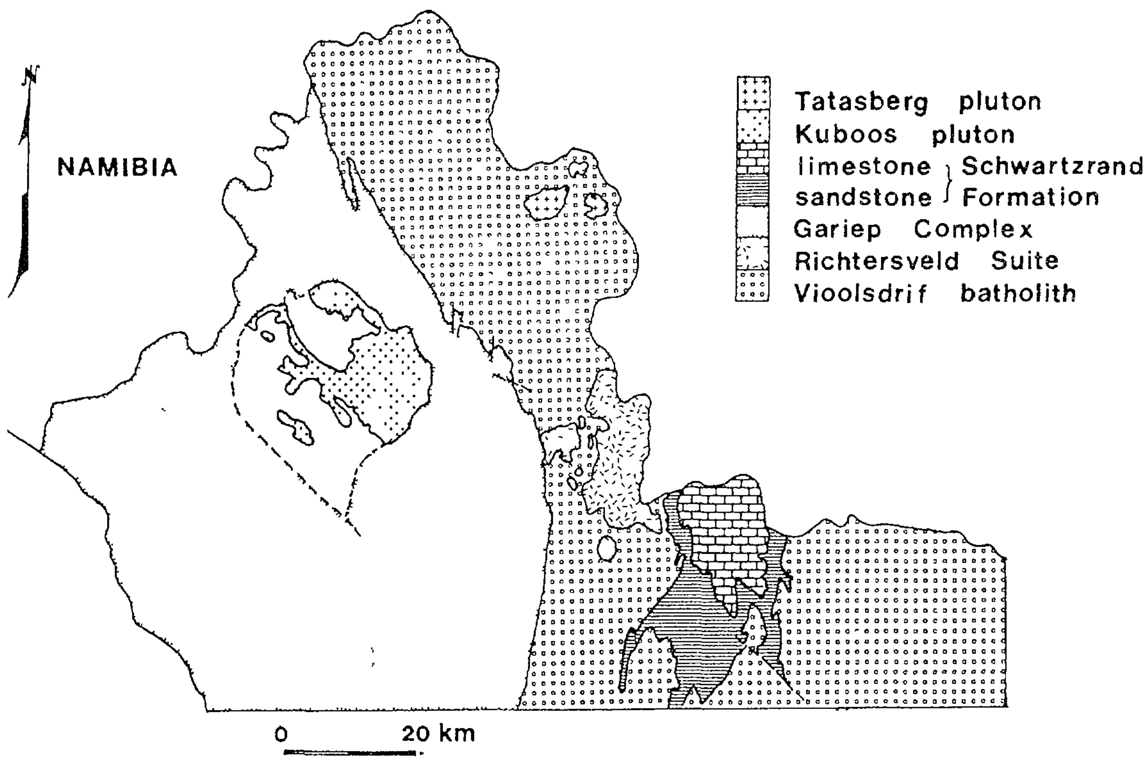

FIG. 2.

The geology of the Kuboos and Tatasberg plutons, the Richtersveld Suite, and the Schwarzrand Formation.

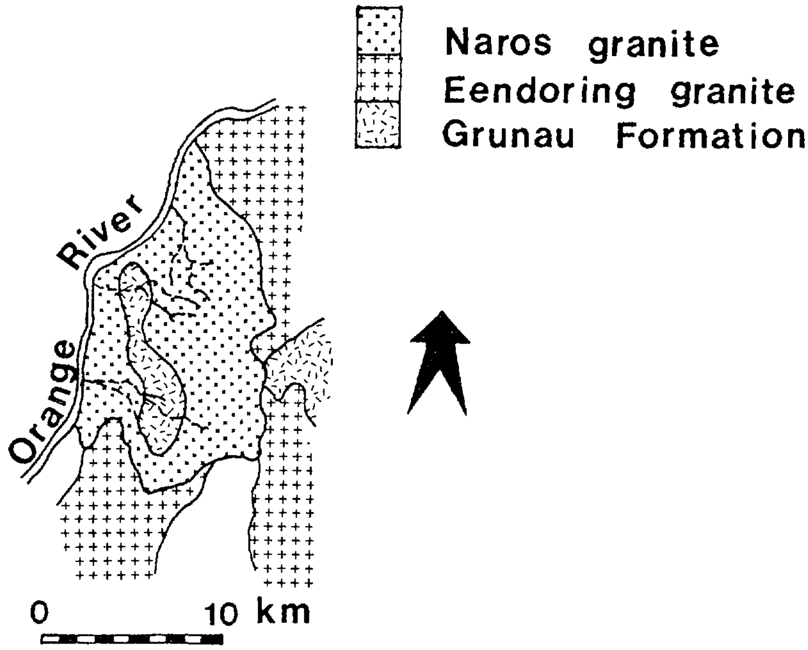

FIG. 3.

The geology of the Naros pluton.

A KUBOOS PLUTON

The Kuboos pluton is a composite intrusion which is elliptical in shape and measures approximately 26 by 30 kilometres. It occupies roughly 600 square kilometres and occurs in the Central Richtersveld where it intruded into the Garlep Complex. It consists of four separate granitic intrusions, with each successive intrusive phase either intruding into or enclosing the earlier phases. The oldest intrusion consists of a medium to fine-grained granite, which is associated with a stockwork of aplite dykes. This granitic phase has been intruded by a syenite, which occurs in the centre of the medium to fine-grained granite. The third intrusive phase consists of a coarse-grained porphyritic granite with a granite--porphyry and aplitic marginal chilled phase. This coarse-grained granite constitutes the bulk of the Kuboos pluton and is in part poorly exposed. The last phase of igneous activity consists of the intrusion of a large number of bostonite, lamprophyre and aplitic dykes, which occur both in and around the Kuboos pluton. The granite has an age of 520 + 20 Ma (De Villiers and Burger, 1967).

The medium to fine-grained granite has an equigranular texture and consists of porphyres of orthoclase and less commonly plagioclase, set in an allotriomorphic matrix of microcline-microperthite, plagioclase and quartz. Accessory amounts of biotite, zircon, sphene, magnetite and ilmenite are also present. The syenite is a leucocratic rock consisting of microcline microperthite with subordinate amounts of albite. The grain-size of the feldspar is variable. Accessory minerals include sphene, biotite, hornblende, zircon and rare apatite. The coarse-grained granite consists of large porphyres of microcline perthite set in a fine-grained matrix of microcline, quartz, oligoclase and biotite. The accessory minerals include zircon, hornblende, sphene, chlorite, magnetite and epidote.

B TATASBERG PLUTON

The Tatasberg pluton consists of three relatively small intrusive bodies, which are spatially separated from one another. The largest of these bodies, described by De Villiers and Sohnge (1959) as the southwestern mass, consists of a composite intrusion, which has an oval shape and measures 8 by 5 kilometers in diameter. The other two intrusions are much smaller. The southwestern mass consists of an outer rim of coarse-grained granite and an inner core of fine-grained granite. The other two bodies consist of a fine-grained granite, which locally becomes porphyritic in texture. Of the two smaller intrusive bodies only the northwestern one outcrops, whereas the southeastern one is almost completely covered by windblown sand, and consequently this body was not included in the present study.

Although no age determinations are available for the Tatasberg intrusions, the petrographic and chemical similarities between the Kuboos and Tatasberg granites suggest that the latter may be a correlative of the former. SACS (1980) also classified the Tatasberg intrusion with the Kuboos pluton as part of the Cape Granite Suite.

The coarse-grained granite of the southwestern mass consists of large, porphyres of perthite set in a medium-grained, equigranular matrix of microcline microperthite, quartz, plagioclase and biotite. The accessory minerals consist mainly of zircon and magnetite. The medium-grained granite is mineralogically and texturally similar to the coarse-grained granite, with the exception that the phenocrysts are finer-grained.

The fine-grained granite, which constitute the two smaller granite bodies, consists of porphyres of perthite set in a cryptocrystalline matrix of quartz and microcline, with accessory amounts of plagioclase, sericite and biotite. Zircon and magnetite are the main accessory minerals.

C RICHTERSVELD SUITE

The Richtersveld Suite occurs in the eastern portion of the Richtersveld area and is a large composite intrusion consisting of multiphase granitic and syenitic intrusions. In South Africa, where the smallest portion of the Richtersveld Suite is situated, it measures roughly 12 by 20 kilometres, but its distribution is much larger in Namibia (De Villiers and Sohnge, 1959). Beside the main intrusion, a number of smaller associated cupolas of granite and syenite, belonging to the same phase of igneous activity, occur to the west and south of the main development of the Richtersveld Suite. In the west it is overlain by sediments of the Gariep Complex. During the present investigation only samples from the main development of the pluton were studied.

The granitic phase of the Richtersveld Suite comprises the largest portion of the intrusion and despite the variation in texture, it is mineralogically fairly uniform. The syenite occurs as a number of intrusive bodies in the granite and are associated with inclusions of metalava and amphibolite. The latter were derived from the Orange River Group, and form roof pendants in the syenite. In addition to the syenite and granite, a number of aplite, granite porphyry, lamprophyre and bostonite dykes also intruded into the Richtersveld Suite and represent the terminal phase of emplacement. The age of the Richtersveld Suite is 920 Ma (Allsopp et al., 1979).

The syenite consists of phenocrysts of microcline perthite and anorthoclase, which is altered to albite and orthoclase. These phenocrysts are set in a matrix of microcline and quartz, with the latter varying from 2 percent in the syenites to 10 percent in the quartz syenites. Biotite, alkali-amphibole and chlorite occur in variable quantities, and the accessory minerals include epidote, apatite, fluorite, opaque oxides and minor amounts of sphene and zircon. The granites of the Richtersveld Suite vary from porphyritic and coarse-grained and fine-grained granites. They contain large porphyres of microcline perthite, quartz and occasionally plagioclase, set in a fine grained matrix of quartz, microcline and biotite. Accesory amounts of biotite, opaque oxides, epidote, chlorite, muscovite, fluorite and apatite are present, with sphene and zircon being rare.

D SCHWARZRAND FORMATION

The Schwarzrand Formation consists of an upper limestone succession, known as the Schwarzkalk Member and a lower arenaceous sequence, the Nudaus Member. The quartzitic succession was deposited in a shallow to moderately deep sea, which had formed on the stable Namaqualand craton. With continued deposition the pre-Nama embayments became submerged and the Schwarzkalk Member was subsequently deposited in relatively shallow water (Germs, 1972). Subsequent to deposition, the Nama sediments have been subjected to very low grade regional metamorphism, and moderate folding.

During the present investigation only stream sediment samples collected on the Schwarzkalk Member were studied. The Schwarzkalk Member consists predominantly of shale with intercalated limestone at the base. The proportion of limestone increases progressively towards the top of the succession with the shale component decreasing. Locally within the succession, thin layers of white quartzite and a clay pebble conglomerate have developed.

E NAROS GRANITE PLUTON

The Naros granite pluton occurs further to the east in the vicinity of Warmbad. It consists of a large multi-stage granitic intrusion and measures approximately 21 by 10 kilometres. Du Plessis (1979) mapped the pluton and established that it is intrusive into an older porphyritic granite, the Eendoorn Granite, and into kinzingites belonging to the Grunau Formation. Large xenoliths of the latter are present in the pluton. The younger Witwater Granite is intrusive into the Naros pluton. In parts of the Naros pluton, particularly the southern portion, a large number of pegmatite stockworks are present which contain substantial concentrations of beryl, cassiterite, columbite, tantalite and sphene (Hugo, 1970).

Along the Orange River, the Naros granite is well exposed, but further away it is covered by sand. Beside the waterlain and windblown sand, non pedogenic calcrete nodules are occassionaly present in these stream sediments.

The Naros granite has an equigranular texture and consists of microcline, plagioclase, quartz, biotite and hornblende. Accessory amounts of zircon, allanite, apatite and sphene are commonly present. In the pegmatitic stockworks, however, a larger variation of accessory minerals are present. The Naros granite is a syntectonic granite and intruded roughly 1100 Ma ago (Du Plessis, 1979).

IV REGIONAL GEOCHEMISTRY

In Figures 4 and 5 the regional geochemical U grey scale maps for the Alexanderbay and Warmbad areas are presented respectively. Figure 4 includes the areas where the Kuboos and Tatasberg plutons, the Richtersveld Suite and the Schwarzrand Formation occur, whereas Figure 5 covers the area where the Naros pluton outcrops. It should be noted that the grey scale interval used in the construction of these maps are based on percentile values using the entire sample population for the area. It is thus clear that any geological unit and/or formation, which is relatively enriched in U compared to the mean of all the other formations in the area would show up as regional anomalies.

Since a portion of the area is covered by Quaternary and Tertiary windblown and waterlain sand, which would, due to the dilution effect by the high percentages of quartz, cause the stream sediment samples to yield lower uranium concentrations, with the result that the uranium signatures of the different

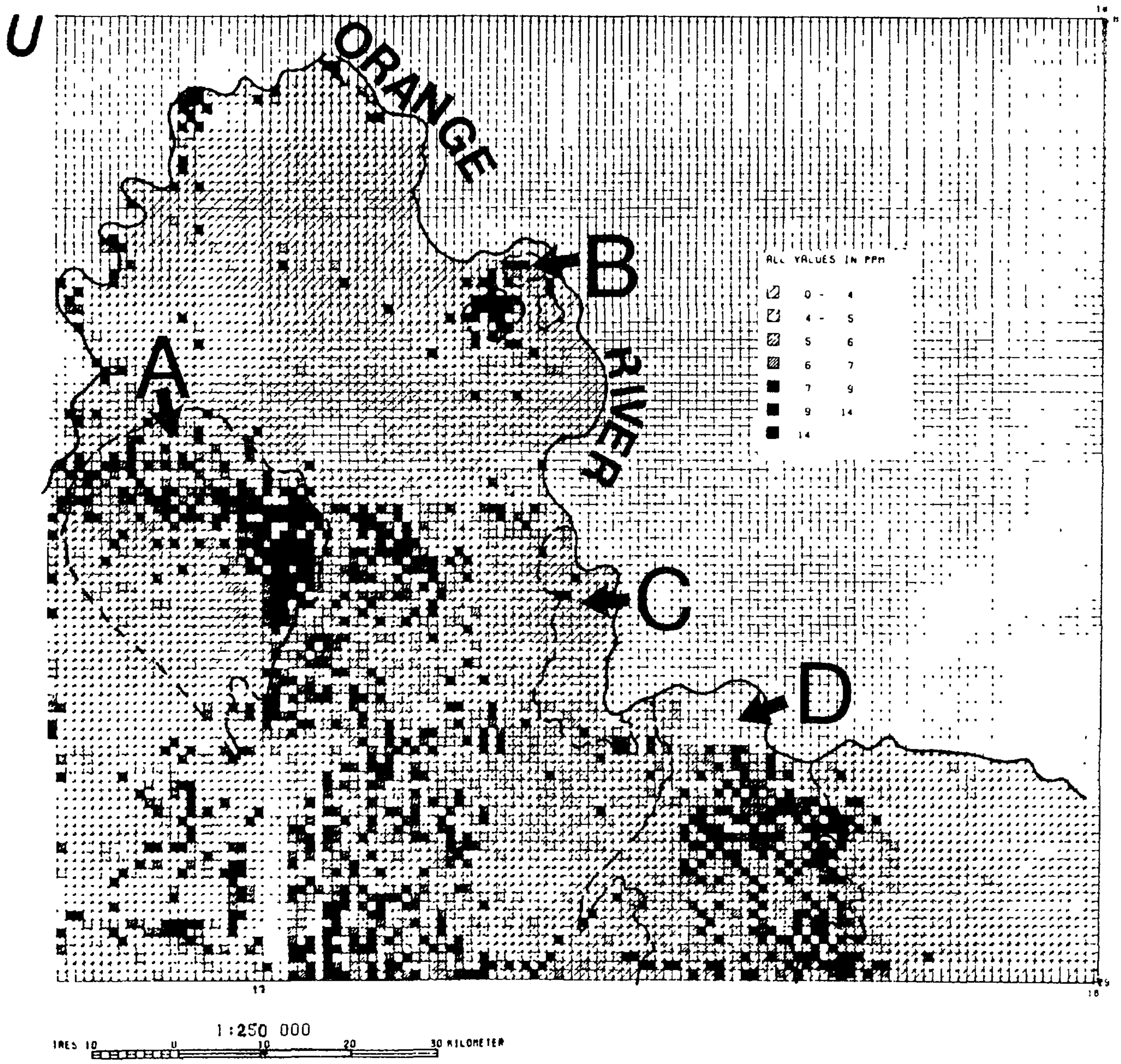

FIG. 4.

The uranium grey scale map of the Richtersveld area showing the distribution of the regional geochemical haloes studied.

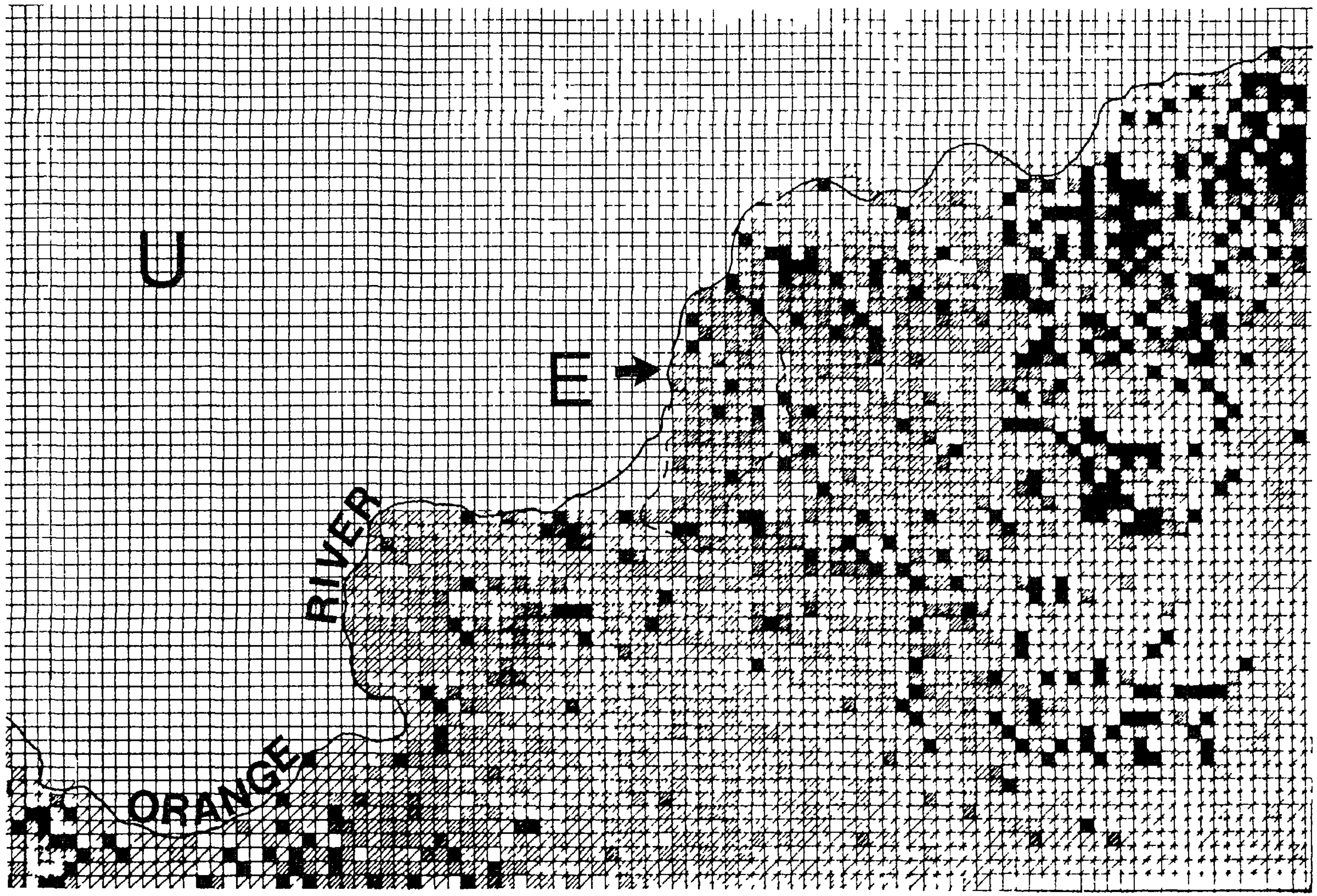

FIG. 5.

The uranium grey scale map of the eastern portion of the Warmbad area showing the regional anomaly on the Naros pluton.

geological units are often masked. In order to overcome this, only samples collected from areas of good outcrop were taken into consideration during the identification of the regional anomalies.

These grey scale maps show that an U-anomaly exists over the Kuboos pluton and that this anomaly is particularly well developed along the eastern and northern margins of the pluton, where the granites outcrop. The central and western portions are sand covered, and hence the anomaly contrast is fairly faint. The mean U-content recorded along the eastern and northern margins of the pluton is 18 ppm, suggesting that the pluton as a whole can be regarded as an anomalously enriched granite (Darnley, 1982), which could serve as an exploration target.

The Tatasberg pluton, which consists of three spatially separated intrusive bodies yields a pronounced uranium anomaly over the main, northwestern body. The northernmost one of the smaller bodies also shows an U-anomaly, but unfortunately samples were only collected over the southern portion of this intrusion. The southeastern body shows a very faint U-anomaly. This is due to the fact that this body is poorly exposed and partly overlain by wind blown sand. In the vicinity of the main outcrops of the Tatasberg granite the mean U-content of the stream sediment samples is 13 ppm, indicating that this granite too, is anomalously enriched and that it can be viewed as a possible exploration target.

The Richtersveld Suite also shows a large regional U-anomaly, but it is clear from Figure 4 that the U-values are significantly lower than in the case of either the Kuboos or Tatasberg plutons. The northernmost portion of the Richtersveld Suite, however, shows a more prominent U-anomaly. The mean U-content of the samples collected on the pluton is 6 ppm, whereas in the more enriched portion it reaches 10 ppm. Despite the relative low mean U-contents, it is still higher than the clarke-value for granites (Darnley, 1982) and hence portions of the Richterveld Suite could still be viewed as a possible U-targets.

The Schwarzrand Formation defines a large but variable U-anomaly as a whole. According to Frick and Strauss (in press) the provenance of the Schwarzrand Formation was the U-enriched granitic and pegmatitic portions of the Vioolsdrift batholith and hence the possibility exists of U-bearing placer deposits in the quartzites and carbon-hosted deposits in the limestones. Although the Schwarzkalk Member of the Schwarzrand Formation appears to have yielded stream sediment samples containing high U-concentrations, the uniformly, slightly higher U-content than the surrounding sediments, can thus be viewed as a possible U-target.

The U grey scale map of the Naros pluton, depicted in Figure 5, also shows a relative high, but variable U-anomaly pattern, across the pluton. In the vicinity of the pegmatite deposits, as well as in the exposed areas close to the Orange River the U-content of the stream sediments is much higher. Although the mean U-content of the stream sediments collected on the Naros granite is only 12 ppm, it should be noted that a large portion of the samples are diluted by transported quartz. Taking this into consideration, it is possible that the U-content of the granite could be much higher and a further evaluation of the anomaly is thus justified.

From Figures 4 and 5 it is evident that a number of other regional U-anomalies are present in the Warmbad and Alexanderbay areas, and some of these anomalies are more pronounced than the five selected for this investigation. Since most of these anomalies occur in areas where the geology is not presently sufficiently understood, they were excluded.

V GEOCHEMISTRY OF THE INDIVIDUAL ANOMALIES

Multivariate statistical analysis was performed on the five geochemical anomalies which were selected on the basis of the regional geochemical maps. Since U behaves essentially as an incompatible lithophile element during both magmatic (Burt and Sheridan, 1981) and sedimentary processes, only the lithophile elements were selected from the data set during the multivariate regression. These include, in addition to U, elements such as Th, Zr, Y, Nb, Rb, Sr, P and Ti. Since U is often hosted in secondary Fe and Mn-oxides during weathering cycles (Rimsaite, 1982) or could be captured in calcrete together with elements such as V and Mo (Carlisle, 1980), these four elements were also included in the data set during the multivariate regressions.

A KUBOOS PLUTON

The stepwise multiple regression of all the elements as a function of U in all the samples taken from the well exposed portion of the Kuboos pluton showed that approximatly 61 percent of the U-values can be expressed as a linear function of Th, which would normally be expected in most granitic batholiths, since U and Th usually correlate positively in granitic rocks (Rogers, 1964 and Chatterjee and Muecke, 1982). This positive correlation is a consequence of the fact that U and Th usually concentrate in the same late phase minerals in granites (Ragland, 1964). The mineralogical data presented for the Kuboos granite showed that both the U and Th could be hosted either in the accessory apatite (monazite) or possibly zircon. The second regression cycle, however, showed that approximately 67 percent of the U-values can be accounted for as a linear function of both Th and Zr, thus indicating that a good correlation exists between Th and Zr (0,73978) and hence also between U and Zr (0,61430). This implies that at least 67 percent of all the U observed in the Kuboos pluton may substitute for Th in zircon.

The addition of Rb to the multiple regression equation accounts for a further 9 percent of the U present in the pluton, indicating that this U is either hosted in biotite or K-felspar. The excess U hosted in biotite, but not in zircon, could be present in the apatite inclusions in the biotite. The low correlation coefficient between U and P (0,26626), however, suggests that this is possibly not the case. As has been indicated earlier the K-feldspar, together with the plagioclase, are altered to epidote, and since the latter mineral can contain significant amounts of U (Hurley and Fairbairn, 1957) it is possible that this 9 percent of U may be hosted in epidote. The addition of Ti and Sr to the regression formula accounts for a further 7,5 percent of the U present in the Kuboos pluton, which indicates that this U is hosted in sphene.

As can be seen in Figure 6 an additional 2 percent of U can also be accounted for in terms of Fe and Mn, thus indicating the presence of a very small proportion of U in secondary Fe and Mn-oxide minerals. Cumulative, the regression procedure thus shows that 85,5 percent of the U in the Kuboos pluton can be accounted for as U which is included in zircon, epidote (altered feldspar) or biotite, sphene and iron oxides and that only 14,5 percent of the U observed in the total sample population cannot

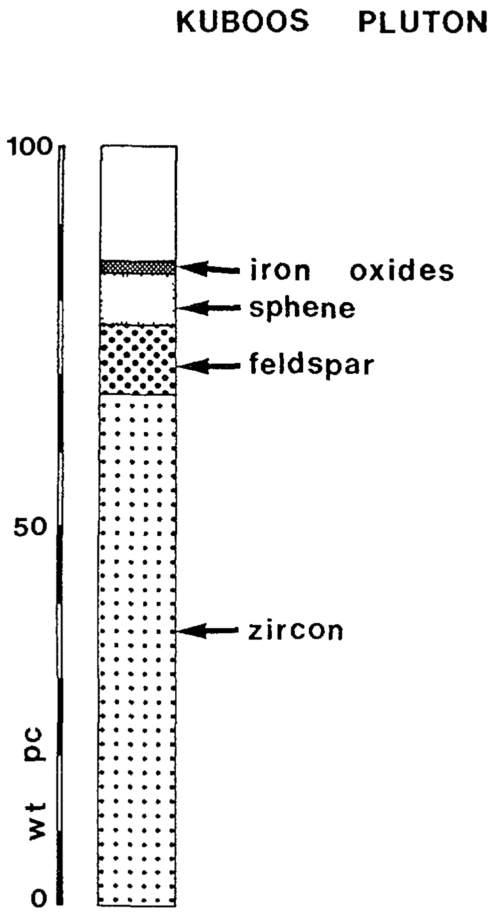

FIG. 6.

The weight percentage of U-bearing mineral phases in the Kuboos pluton as inferred from the stepwise multivariate regression.

be accounted for. This U may thus be present as uraninite or as a trace constituent in the other rock-forming minerals.

In Figure 7 the calculated U concentrations, using the regression coefficients determined above, are compared with the observed U concentrations. This diagram shows that the bulk of the U present in the samples collected on the Kuboos pluton can be accounted for by the elements (and mineral) depicted in Figures 6. Two anomalous populations consisting of 4 and 2 samples respectively do not appear to fall within the population defined by the regression coefficients, and may thus contain a U-bearing phase not considered in the regression equation. It

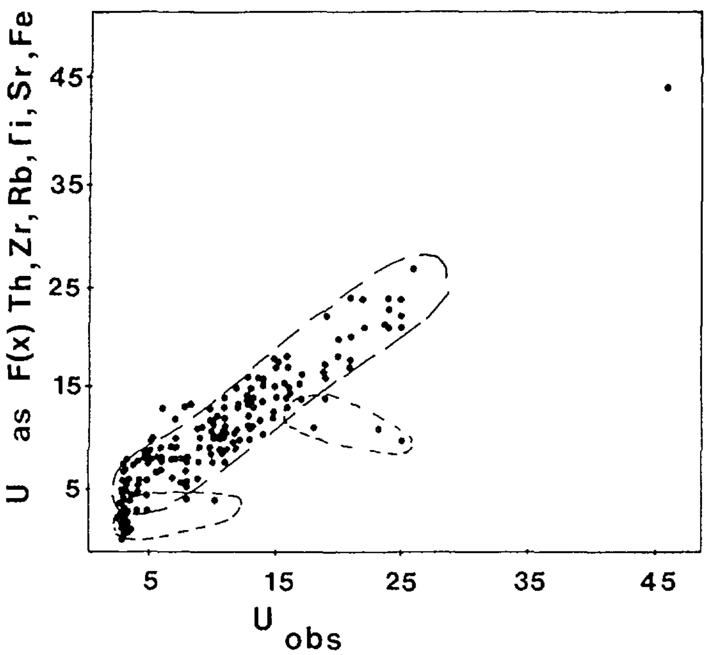

FIG. 7.

The calculated U-concentration, based on the regression coefficients plotted as a function of the observed U-contents in the samples from the Kuboos pluton.

is significant to note that both these populations contain slightly higher U-concentrations than would have been predicted from the regression coefficients, based on the calculated mineralogical composition. Two of the samples from this population contain approximatly 24 ppm U of which only roughly 13 ppm could be accounted for by U incorporated in any of the U-bearing mineral phases shown in Figure 6. The balance of the U-content may thus indicate the presence of a uranium-bearing mineral phase which is significantly enriched in U.

It is thus clear that the provenance areas where these two samples were collected may contain truely anomalous U-concentrations and would thus define higher priority exploration targets within the Kuboos pluton.

A fission tract study has been carried out on the stream sediment samples in order to verify the validity of the regression procedures applied above. This study has shown that most of the U is hosted in zircon, with smaller amounts being present in epidote, biotite, sphene and Fe-oxides. The two samples with anomalously high U-contents also contain some uraniferous apatite in addition to metamict zircon with high U-abundances. The fission tract data thus confirm that the mineralogical inferences based on the regression procedure are essentially correct, and that the anomalous samples have indeed been identified correctly. The latter samples, however, appear to contain two very uraniferous mineral phases instead of uraninite.

B TATASBERG PLUTON

The stepwise multiple regression indicates that 71,5 percent of the U present in the samples collected from the Tatasberg pluton can be accounted for in terms of a linear equation of Th. Since the mineralogical data showed that monazite, apatite and zircon are present in the Tatasberg granite, the U together with the Th could be hosted in any of these mineral phases. The U-concentrations have been plotted against P (Figure 8), in order to evaluate whether the U substitutes for Th in either apatite or monazite. This diagram shows that no correlation exists, thus the U possibly substitutes for Th in either zircon or Th-oxides. A further 8 percent (79,5 percent in total) of the U in the pluton can be accounted for as a function of both Zr and Th thus suggesting that 79,5 percent of the total U observed is hosted in zircon.

In Figure 9 the observed U concentration has been plotted as a function of the calculated U-concentration using only the regression coefficients for Th and Zr. This diagram shows that two sample populations can be distinguished, but that some overlap may exist between the populations in the low U concentration

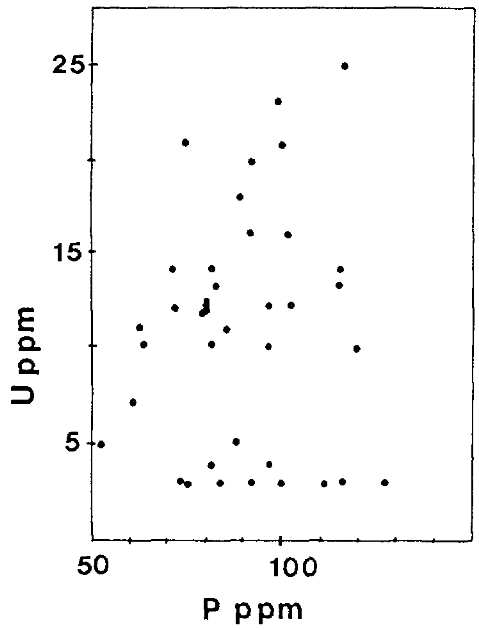

FIG. 8.

The uranium versus phosphorous content in the stream sediment samples from the Tatasberg pluton.

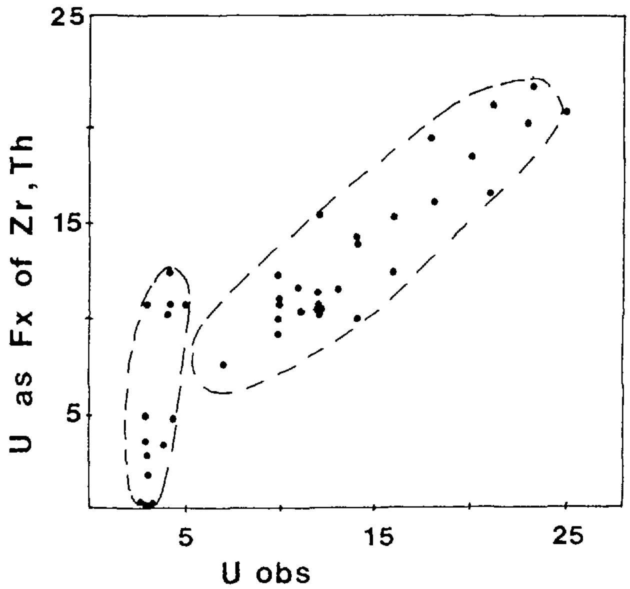

FIG. 9.

The calculated U-content based on the regression coefficients plotted as a function of the observed U-concentrations in the samples from the Tatsberg pluton.

ranges. The main population showing a more or less 1:1 correlation can be accounted for by the samples in which all the U is hosted in zircon. The second population, which consistently yields higher calculated U-contents than what was actually observed, represent samples in which the U content of the zircon grains must be much lower than those in the remainder of the samples or may include samples which carry U-impoverished mineral phases. These samples were all derived from the granite body which is partly covered by sand and may thus represent a mixed population in which zircons from different sources are present.

In order to explain the characteristics of this second population a further stepwise regression cycles were carried out, and this revealed that a further 4,5 percent of the U can be accounted for by the presence of samples in which the U is hosted in iron oxides (Figure 10). It is significant that the correlation coefficients between Fe and U as well as between Mn and U are fairly low, indicating that only a small portion of the Fe and Mn-bearing mineral phases contain any uranium. It is thus possible that the second population identified above can be accounted for by U hosted in Fe-oxides. Figure 10 further shows that only 16 percent of the uranium observed in the population of samples from the Tatasberg pluton cannot be accounted for by either the presence of iron oxides or zircon, and Figure 9 indicates that no sample contaings more U than would be predicted from the zircons can be identified. It is thus clear that the remaining 16 percent of the uranium is present as trace amounts in mineral phases, and hence, despite its high mean U content, the Tatasberg pluton can be viewed as an unattractive exploration target for uranium.

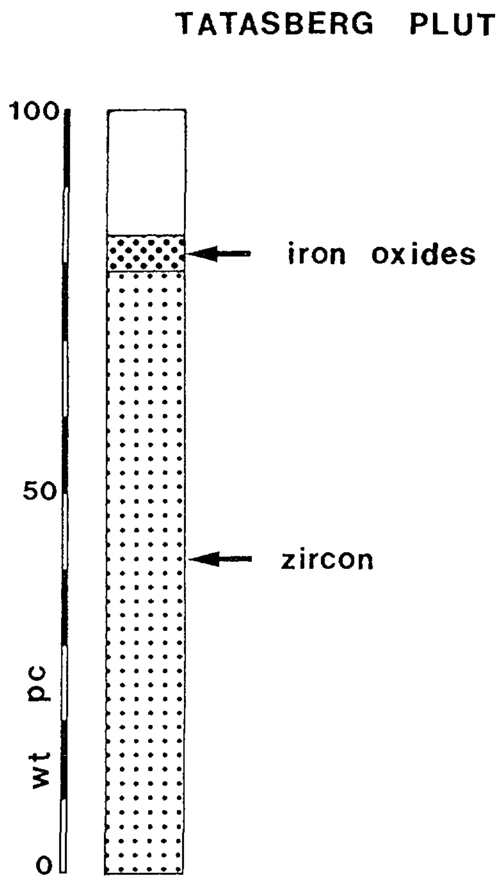

FIG. 10.

The weight percentage of U-bearing minerals in the Tatsberg pluton as deduced from the multivariate regression.

C RICHTERSVELD SUITE

The stepwise regression of all the elements against U indicates that in 50,5 percent of the U in the entire population can be expressed as a function of Th. In this case, however, the Th yields low correlation coefficients when regressed against Zr (0,00713) and P (0,03252) thus indicating that the Th is not hosted in either zircon, monazite or apatite. Similarly the U does not correlate with P, and even yields a small negative correlation coefficient (-0,06594). U also does not correlate with Zr (Figure 11). This indicates that neither the U nor the Th are hosted in either zircon or phosphates. The mineralogical data showed that fluorite is commonly present in the Richterveld

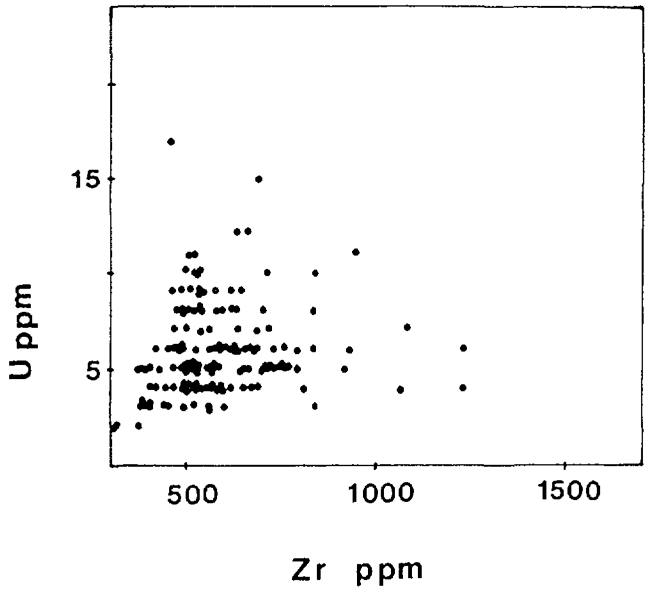

FIG. 11.

The uranium versus zirconium plot for the stream sediment samples from the Richtersveld Suite.

Suite, but unfortunately fluorine determinations were not available, hence it is possible that the Th and U could be hosted in fluorite (Davidson, 1982) or in thorianite.

Further stepwise regression indicates that a further 11,5 percent (62 percent in total) of the uranium can be accounted for in terms of a linear expression consisting of Y, Mn and Rb. Since the Mn would be expected to be present in Mn-oxides and the Rb would reflect the presence of altered feldspar (epidote) or biotite, it is concluded that a small percentage of the uranium is hosted in these minerals. The contribution of Y to the regression equation is more problematic and can be attributed to U-bearing xenotime or fluorspar. The regression of Y against P, however, shows a very low correlation coefficient (0,0719), which would favour the presence of Y in fluorite. In Figure 12 the possible mineralogical hosts of the U in the Richtersveld Suite is summarized, and this diagram reveals that at least 38 percent of the uranium cannot be accounted for by these minerals. This implies that

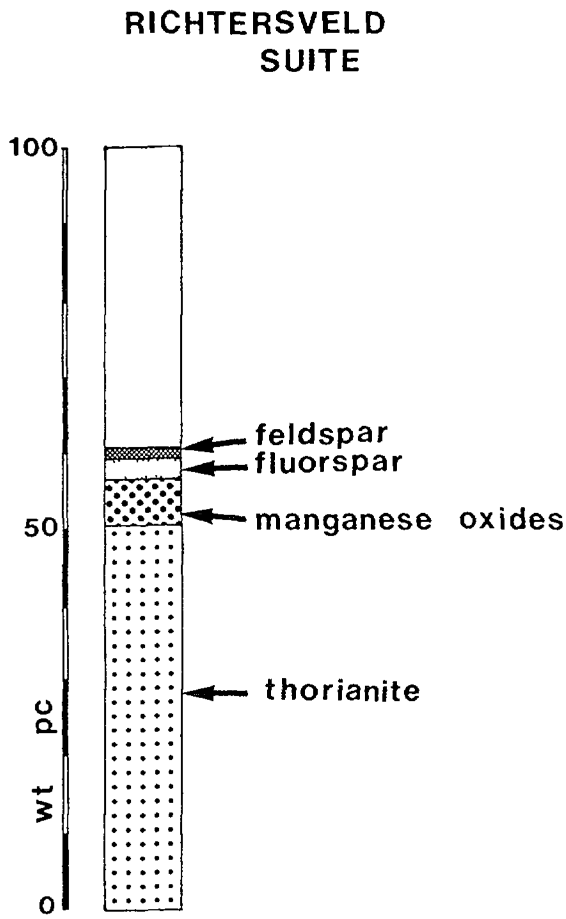

FIG. 12.

The possible weight percentage of U-bearing mineral phases in the Richtersveld Suite as deduced from the multivariate regression.

a large portion of the uranium is hosted as a trace constituent in a number of other rock-forming minerals, or that it is hosted in uraninite.

In Figure 13 the observed uranium values have been plotted against the calculated uranium concentration using the regression coefficients derived for Th, Y, Mn, and Rb. This diagram shows that in addition to the population which can be accounted for by the mineralogical hosts depicted in Figure 12, two more populations can be identified. The latter, however, contain less uranium than would be expected for samples in which the U is hosted in fluorite, thorianite, Mn-oxides and feldspar. These two populations thus consist of samples in which the uranium

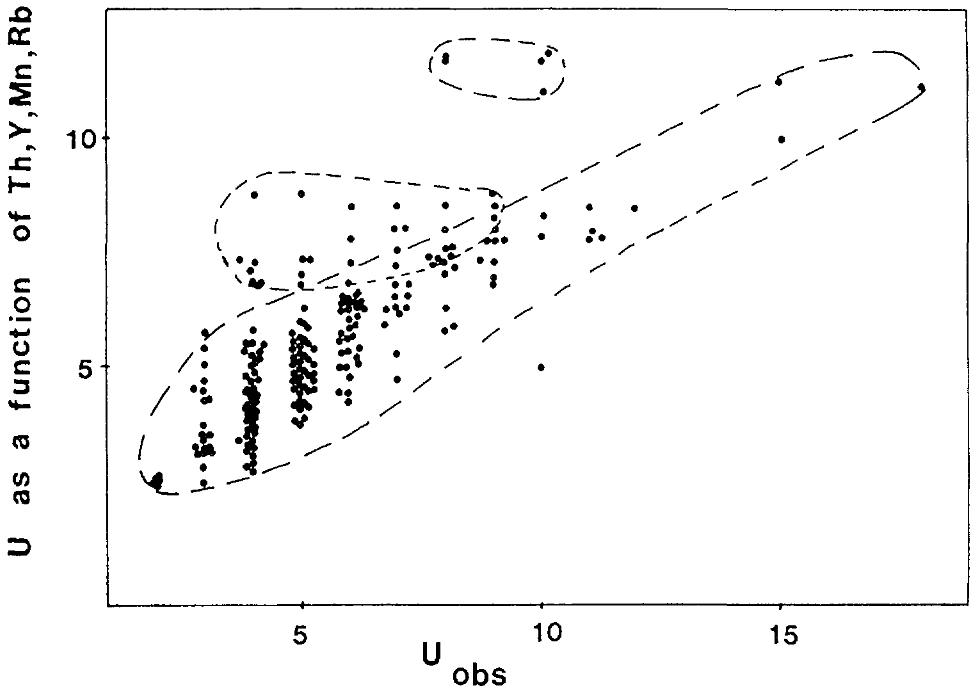

FIG. 13.

The calculeted U-content based on the regression coefficients plotted as a function of the observed U-concentrations in the samples from the Richtersveld Suite.

is dispersed as a trace constituent in the other rock-forming minerals and would represent unattractive targets. One sample, however, yields an uranium concentration of 10 ppm, whereas the mineralogical controls would indicate that it should contain only 5 ppm if all the uranium was hosted in thorianite, fluorspar, feldspar and Mn-oxides. This sample may thus contain uraninite and could serve as a possible exploration target.

The Richtersveld Suite as a whole, despite the relative low mean U-content, appears to be a higher priority exploration target than the Kuboos or Tatasberg plutons, because most of the uranium in this batholith is not hosted in zircon.

VI SCHWARZRAND FORMATION

The stepwise multiple regression against uranium in the samples from the Schwarzkalk Member of the Schwarzrand Formation indicates that 46,5 percent of the uranium can be accounted for as a linear function of thorium. A further 41,5 percent can be accounted for as a function of Sr, which implies that a total of 88 percent of the population can be accounted for by both Sr and Th. The Th was regressed against Zr to establish whether it is hosted in zircon, an a correlation coefficient of 0,83868 was obtained. This indicates that at least 46,5 percent of the uranium in the Schwarzkalk Member is hosted in detrital zircon. Since the Sr is hosted in the calcite, which comprises roughly 50 percent of the succession, the remaining 41,5 percent of uranium is hosted in calcite.

In order to establish whether other mineral phases also host significant amounts of uranium a further cycle of stepwise regression was undertaken, and this indicated that a remaining 4,5 percent of uranium can be accounted for as a function of P, Y, Rb and Fe. Mineralogicaly this suggests that some uranium could be hosted in feldspar, phosphates and iron oxides. The relative good correlation between Y and P indicates that most of the Y is hosted in phosphates as would be expected for marine limestones (Schofield and Haskin, 1964). Figure 14 shows the weight distribution of uranium in the different mineral phases in the Schwarzkalk Member and indicates that only some 7,5 percent of the uranium cannot be accounted for by the presence of these mineral phases. In order to evaluate whether any of this uranium may be present as uraninite which may serve as a priority target, the calculated uranium concentrations have been plotted against the observed concentrations in Figure 15. This shows that, except for a few samples in which the calculated U is slightly less than the observed U-content, all the samples plot as a single population.

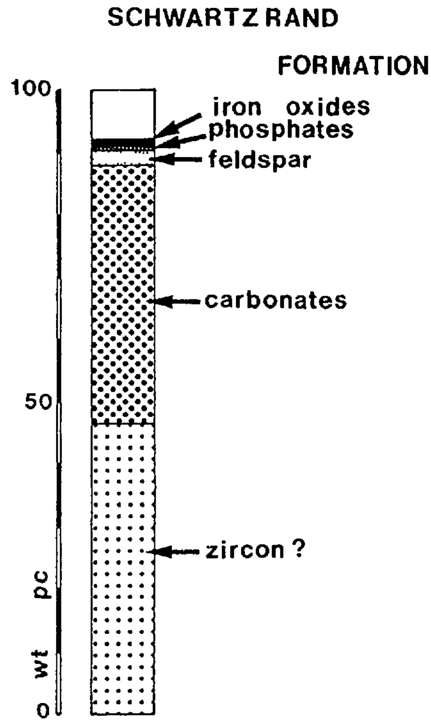

FIG. 14.

The weight percentage of U-bearing mineral phases in the Schwarzrand Formation as deduced from the multivariate regression.

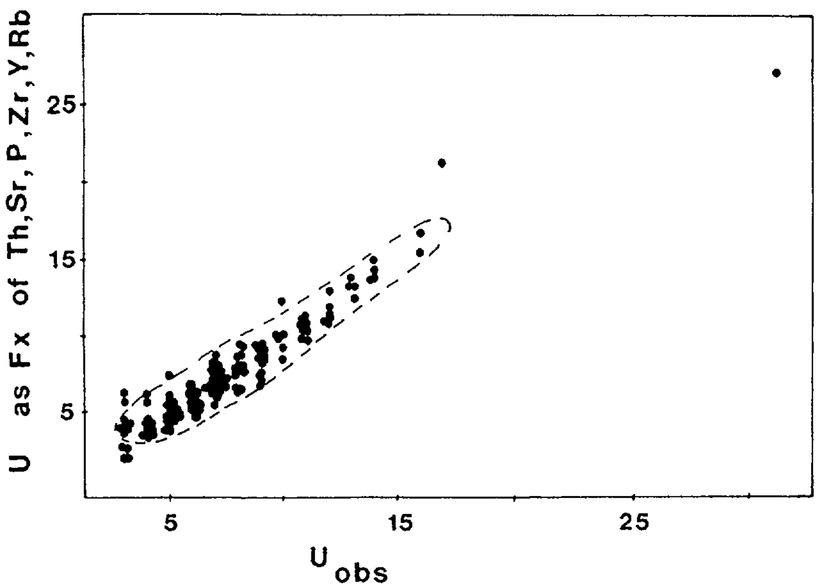

FIG. 15.

The calculated U-content, based on the regression coefficients, plotted as a function of the determined U-concentrations in the samples from the Schwarzrand Formation.

It is thus clear that the Schwarzkalk Member is an unattractive exploration target, and that all the uramiun is hosted either in detrital zircon or calcite. It is significant to note that limestone comprises roughly 50 percent of the succession and shale constitute the remainder. The multiple regression indicated that roughly 50 percent of the uranium is hosted in the limestone and the remainder in zircon in the shale. This shows that the geochemical data could have been used to calculate the average composition of the succession as a whole.

VII NAROS PLUTON

The Naros granite contains a few small pegmatite deposits which have been mined for columbite, tantalite and beryl (Hugo, 1974) but so far no uraninite occurrences have as yet been found. The multiple regression of U against the other elements indicates that 66 percent of the uranium can be expressed as a linear function of Zr and that an additional 14 percent can be expressed as a function of both Zr and Th. In Figure 16 the uranium concentration has been plotted against the Zr-content, and this diagram shows that a good correlation exists, thus confirming that the uranium is possibly hosted in zircon. Inspection of the data revealed that the sample which contain the highest uranium concentration does not appear to correlate with Zr. This suggests that some samples contain uranium which is hosted in another mineral phase, and that such a mineral is considerably enriched in uranium.

Further multiple regression cycles indicated that the remaining uranium can in part be accounted for by the addition of Sr, Fe and Ti to the regression equation. These elements account for a further 11,5 percent of the uranium. Taking into consideration

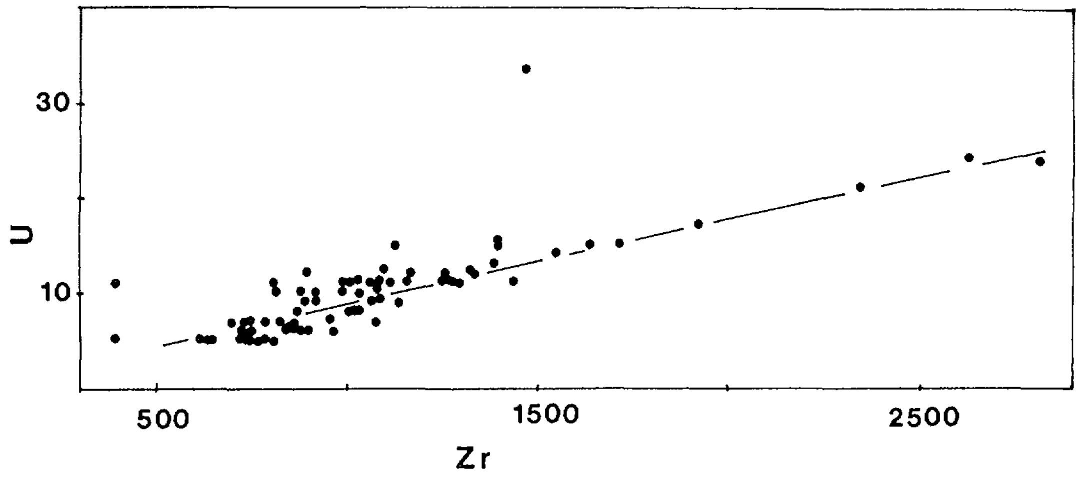

FIG. 16.

The uranium versus zirconium plot for the stream sediment samples from the Naros pluton.

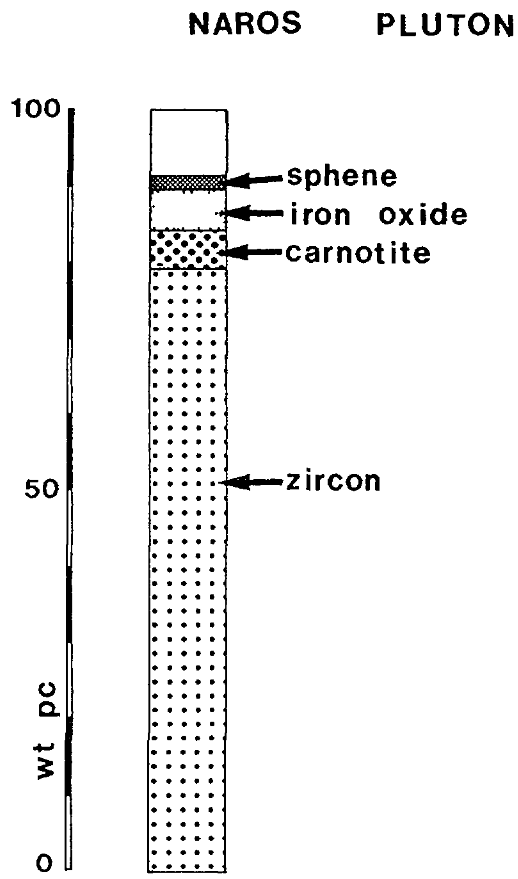

FIG. 17.

The weight percentage of U-bearing minerals in the Naros pluton as deduced from the multivariate regression.

that carnotite bearing calcrete nodules were often found in this area, and even constitute the Koboop calcrete hosted uranium deposit, it is concluded that the correlation with Sr would reflect the presence of such calcrete nodules. The Fe contribution can be ascribed to the presence of iron oxides and the Ti could be explained by the presence of sphene or ilmeno-rutile. In Figure 17 the percentage of uranium present in the different mineral phases in the Naros granite is illustrated, and from this diagram it is clear that only 8,5 percent of the uranium cannot be accounted for.

In order to evaluate whether this unaccounted uranium is disseminated in other rock-forming minerals, the calculated U-contents have been plotted against the observed concentrations in Figure 18. This diagram shows that the uranium content of all the samples, with the exception of one, can be accounted for in terms of the regression coefficients. The remaining sample contains 33 ppm uranium of which only 21 ppm can be accounted for by a combination of the U present in zircon, iron oxides, carnotite-bearing calcrete and sphene or ilmeno-rutile. Inspection

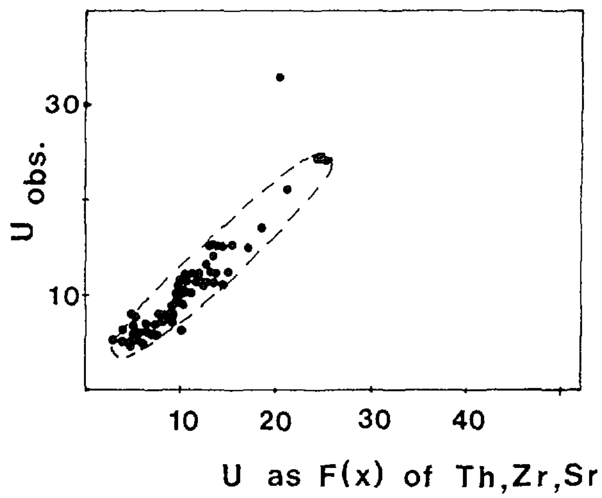

FIG. 18.

The calculated U-content, based on the regression coefficients, plotted as a function of the determined U-concentrations in the samples from the Naros pluton.

of the analytical data reveals that this sample is extremely enriched in Th, but not in any other element. This sample may thus be derived from an area where either uraninite or urano--thorianite is present in the provenance, and may thus serve as an exploration target.

VIII DISCUSSION AND CONCLUSIONS

The data presented show that a multiple regression technique can be used to identify sample populations in which U is hosted in a specific mineral phase. Although the technique was applied to uranium, no reason exists why it could not be applied to other elements, such as Cu, Zn or Th. It is further shown that the successive regression cycles allows the recognition of specific elements or combinations of elements which can be used to account for the other mineralogical hosts in which U occurs. In the one example, the Kuboos pluton, it was possible to verify quantitatively by means of a systematic fission tract study on the stream sediment samples that the mineralogical inferences, based on the chemical data, is valid.

In the case of the other plutons studied, however, the stream sediment samples were not studied mineralogically, *but* a superficial mineralogical and petrographical study was carried out on a few thin sections, in order to narrow the possible mineralogical hosts. This information is a prerequisite in the application of such a multivariate regression study.

The data showed that, beside identifying the mineralogical hosts for uranium it is also possible to evaluate the significance of a regional geochemical anomaly as a whole. In the case of the Tatasberg pluton, where almost 85 percent of all the uranium in the sample population can be accounted for by the presence of uranium in zircon and iron oxides, the pluton as a whole is an unattractive exploration target. This is true, even despite the relative high mean U-content in the stream sediment and rock samples from this pluton. The Richtersveld Suite, on the other hand, despite its low mean U-content, is an attractive exploration target, because only a small fraction of the uranium in the sample population can be accounted for in terms of U hosted in rock-forming minerals, and in this case the largest portion of the uranium appears to be hosted in either uraninite, fluorite or thorianite.

In addition to evaluating the significance of a regional anomaly, the multivariate procedure can also serve to identify specific exploration targets within a regional anomaly. The presence of such specific targets is identified when the calculated uranium content, based on the regression coefficients, are plotted as a function of the observed uranium content. Samples which contain substantially more uranium than would have been expected from the mineralogical constraints developed, would represent areas where the uranium is concentrated in other mineral phases which may be of economic significance. These samples thus indicate an unusual provenance for the stream sediment sample and justifies a follow-up study. Samples which contain less uranium than would be expected from the mineralogical constraints determined during the multiple regression could either indicate that two populations of a host mineral may be present with different uranium contents or that the uranium is present as a trace consitituent in a number of rock-forming minerals. In both these cases the evaluation of the results would cause a lower priority to be attributed to these areas within a regional anomaly.

Clearly, the possibility of identifying mixed populations, and the evaluation of second or third order correlations should also be considered. This was not done during this investigation. Evidence for the existence of such associated correlations were, however, found, but further research on the development of recognition criteria for the identification of these populations must still be carried out.

ACKNOWLEDGEMENTS

The authors wish to express their thanks to the Chief Director of the Geological Survey of South Africa for permission to publish the results of this investigation. Thanks are also due to Messers J.H. Strydom and S. Hine for assistance with the mathematical modelling used. Mr. M.D. Kohler kindly prepared the final copies of the illustrations for publication.

We are also indebted to Dr. F. Walraven and Mr. R. Dixon who kindly reviewed the manuscript and suggested several improvements. Our thanks are also due to Miss T Denyschen who assisted in the compilation of the geochemical maps which served as a basis for this investigation.

REFERENCES

Abbey, S., 1983. Studies in "standard samples" of silicate rocks and minerals 1969-1982. Canad. Geol. Surv. Pap. 83-15, 115pp.

Allsopp, H.L., Kostlin, E.E., Welke, H., Burger, A.L. Kroner, A., and Blignault, H.J. 1979. Rb-Sr and U-Pb geochronology of late Precambrian and early Proterozoic igneous activity in the Richtersveld and Southern South West Africa. Trans. geol. Soc. S. Afr., 82: 185-204.

Burt, D.M. and Sheridan, M.F., 1981. Model for the formation of uranium/lithophile element deposits in fluorine-rich volcanic rocks. Bull. Am. Assoc. Pet. Geol., 13:99-109.

Carlisle, D. 1980. Possible variations on the calcrete-gypcrete uranium model. Rept. U.S. Dept. Energy, unpubl. 38pp.

Chatterjee, A.K. and G.K. Muecke, 1982. Geochemistry and distribution of uranium and thorium in the granitoid rocks of the South Mountain Batholith, Nova Scottia: some genetic and exploration implications: in Uranium in Granites ed. Y.T. Maurice, Pap. 81-23, Geol. Surv. Canad., p.11-17.

Darnley, A.G., 1982. "Hot granites: some general remarks; in Uranium in granites: in Uranium in Granites, ed. Y.T. Maurice, Pap. 81-23, Geol. Surv. Canad., p.1-10.

Davidson, A., 1982. Petrochemistry of the Blackford Lake Complex near Yellowknife, Northwest Territories: in Uranium in Granites ed. Y.T. Maurice. Pap. 81-23, Geol. Surv. Canad., p. 71-79.

De Villiers, J. and P.G. Sohnge, 1959. The geology of the Richtersveld. Mem. Geol. Surv. S. Afr., 48, 295 pp.

De Villiers, J. and A.J. Burger. 1967. Note on the minimum age of certain granites from the Richtersveld area. Ann. Geol. Surv. S. Afr., 6: 83-84.

Du Plessis, G., 1979. n Metamorf- magmatiese studie van die Namaqualandse Metamorfe Kompleks langs die Oranje Rivier oos van Onseepkans. MSc-thesis, University of the Orange Free State, 139pp. (unpubl.).

Frick, C. and S.W. Strauss, (in press). Geochemical evolution of the Richtersveld area, South Africa, as deduced from regional geochemical maps of stream sediments. J. Geochem. Explor.

Germs, G.J.B., 1972. The stratigraphy and palaeontology of the Lower Nama Group, South West Africa. Precambrian Res. Unit, Univ. Cape Town, 12, 250pp.

Hugo, P.J., 1970. The pegmatites of Kenhardt and Gordonia districts, Cape Province. Mem. Geol. Surv. S. Afr., 58pp.

Hurley, P.M., and H.W. Fairbairn 1957. Abundance and distribution of uranium and thorium in zircon, sphene, apatite, epidote and monazite in granitic rocks. Trans. Am. Geophys. Union, 38: 930-950.

Nisbett, E.G., Dietrich, V.J., and Essenwein, A., 1979. Routine trace element determination in silicate minerals and rocks by X-ray fluorescence. Fortchr. Mineral., 57: 266-279.

Ragland. P.C., 1964. Autoradiographic investigation of naturally occuring materials: in The natural radiation environment ed. J.A.S. Adams and W.M. Lowder, Chicago University Press, Chicago, p.129.

Rimsaite, J., 1982. Mineralogical and petrochemical properties of heterogeneous granitoid rocks from radioactive occurrences in the Grenville Structural Province, Ontario and Quebec: in Uranium in Granites ed. Y.T. Maurice, Pap. 81-23, Geol. Surv. Canad., p. 19-30.

Rogers, J.J.W., 1964. Statistical tests of the homogeneity of the radioactive components of granitic rocks; In The natural radiation environment ed. J.A.S. Adams and W.M. Lowder, Chicago University Press, Chicago. p.51.

SACS 1980. Stratigraphy of South Africa, Part I. Lithostratigraphy of the Republics of South Africa, South West Africa/-Namibia and the Republics of Boputhatwana, Transkei, and Venda. Handb. Geol. Surv. S. Afr., 8, 690 pp.

Schofield, A., and Haskin, L., 1964. Rare-earth distribution patterns in eight terrestrial materials. Geochem. et Cosmochem. Acta., 28: 437-446.

AN ADP-SYSTEM TO PREDICT MASSIVE Cu-Zn ORE DEPOSITS USING MAPS OF DIFFERENT SCALES

V.V. KUOSMANEN, H.M. ARKIMAA, I.A. SUPPALA
Geological Survey of Finland,
Espoo, Finland

Abstract

This work is a part of the geodata integration project in the Exploration Department of the Geological Survey of Finland. The purpose of the project is mainly to develope methods for prediction of especially massive Cu-Zn ore deposits.

The basic idea of this work is that large ore deposits may be generated only by large geological processes due to large tectonic events. Indications of large geological structures and formations are therefore seen in reconnaissance scale geophysical, geochemical, etc. maps and remote sensing data. These are used to predict large areal favourability for ore deposits. But in order to properly predict field targets for exploration, geomaps and predictions in regional scale are needed simultaneously with the reconnaissance studies.

An ADP-system, composed of two main programs LOCUS and SCALEX, was designed to study map data of various 'scales' for prediction purposes. These programs were applied to geodata on a 330x420 km2 large test area and included two smaller, 60x75 and 30x50 km2 areas. All the areas are situated on the Archean-Early Proterozoic 'Main Sulphide Ore Belt' which contains 90 % of the known sulphide ore reserves in Finland. The data consisted gravimetric, magnetic and soil geochemical measurements and maps on Cu-Zn ore deposits in the reconnaissance scale and low altitude geophysical survey data such as magnetic, electromagnetic measurements and mineralization maps in the regional scale. All geophysical and geochemical data were gridded into pixel-image form.

Spatial frequencies of the geodata were enhanced in order to find structurally relevant combinations of different variables, e.g. to correlate maps of different spatial resolutions. These data were studied both visually and statistically in feature spaces (= variable spaces). It was found that features of ore deposits (from big to small) followed certain subspaces in these multidimensional feature spaces. These subspaces can be used to consider prediction of the biggest possible Cu-Zn deposits and in this respect to priorize local exploration targets for field checking.

---

1. GEOLOGICAL AND METHODOLOGICAL BACKGROUND

This work is a part of the geodata Integration and Analysis project in the Exploration Department of the Geological Survey of Finland. The purpose of the project is mainly to develope methods for prediction of ore deposits and to carry out computer aided map analyses for exploration cases.

The basic idea of this work is that large ore deposits may be generated only by large geological processes due to large tectonic events. Indications of large geological structures and formations are therefore seen in reconnaissance scale geophysical, geochemical, etc. maps and remote sensing data. These are used to predict large areal favourability for ore deposits. But in order to properly predict field targets for exploration, geomaps and predictions in regional scale are needed simultaneously with the reconnaissance studies.

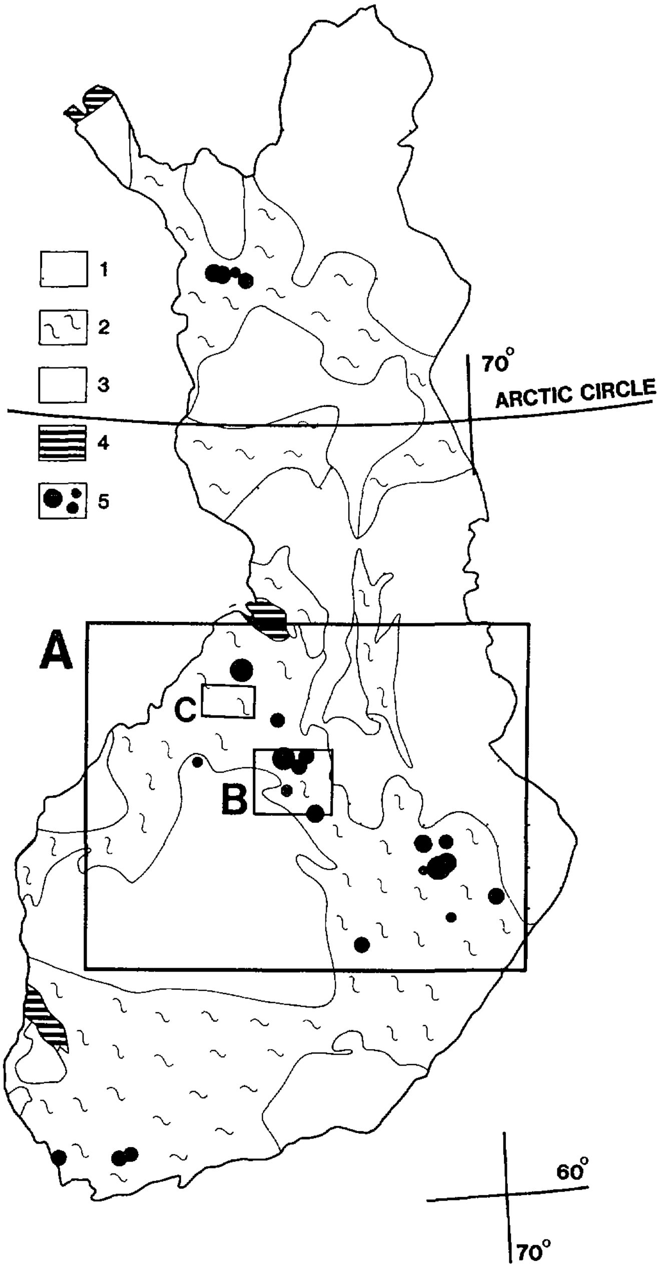

Figure 1. Test areas for the prediction study: (A) reconnaissance scale, (B) and (C) regional scale. Main bedrock units of Finland: 1) Archean basement, 2) Middle Precambrian schists, 3) Middle Precambrian plutonic granitoids, 4) Late Precambrian or later sedimentogenic rocks, 5) Locations and sizes of Cu, Zn and/or Pb ore deposits and prospects (Kahma et al.1976).

The bedrock of Finland consists of Archean basement gneisses in the N-NE, and middle Precambrian schists, migmatites and plutonites in the S-SE areas (Fig. 1). The Cu, Zn or Pb ore deposits (Fig. 1) are massive, mainly stratabound type. Their volcanocenic affinites range from mafic to felsic.

In Finland systematic computer aided geodata integration and analysis for exploration purposes by image classification and analysis were carried out by Kilpelä et al.1978, Talvitie 1979, Aarnisalo 1982 and 1984, Arkimaa 1982 and 1985 and Kuosmanen et al. 1985. Statistical approach to mineral potential appraisal in Finland was used by Tontti et al. 1979, Tontti et al. 1981 and Gaal 1984.

Mineral exploration in regional and reconnaissance scales is, especially in a glaciated terrain as in Finland, greatly facilitated by modern geophysical and geochemical surveys which nowadays produce maps of large coverage and spatial and spectral resolution. Remote sensing and other map data can be quickly integrated by automatic image processing. By this method many but often weak ore indications have been discovered. However, when structures revealing spatial linking of the ore indications are discovered, economically significant geological entities, e.g. alteration, etc. features are encountered (Barringer A.R. 1969, Sabins, F. 1986 p. 283).

This work reviews a computer aided mineral prediction system and a case history, both based on two geodata analyses and integration programs LOCUS (Kuosmanen et al. 1982) and SCALEX. The latter program was written during the current work. Image processing software (CSIRO 1986) and hardware (Technical Reseach Centre of Finland, Laboratory of Urban Planning and Building Design) were used to visualize the results. The ADP-programs LOCUS and SCALEX were designed to aid analysis of spatial linking of ore deposits in maps and feature spaces. LOCUS divides geomaps into various spatial components and SCALEX visualizes their 2- or 3-dimensional histograms by image processing system. Understanding of 3-dimensional histograms is facilitated by rotations.

Case studies on the use of the system were carried out in three test areas (Fig. 1), large A including the two smaller B and C. The area A represents here reconnaissance scale and B and C both represent regional scale.

2. THE PREDICTION SYSTEM

Flow chart (Fig. 2) illustrates how the two main programs LOCUS and SCALEX 'cooperate' in the study. The system is designed to handle spatially distributed pixel-map data in comparison to the ore features in the following order:

1) The original data is enhanced by program LOCUS in order to tailor more appropriate variables for prediction.

2) Features of the ore deposits are studied in the feature spaces of the tailored variables. This is made by SCALEX program.

3) Those subspaces which are connected to the ore deposits are separated from the feature spaces and prediction maps of various scales are prepared from the subspaces. These are made by SCALEX program.

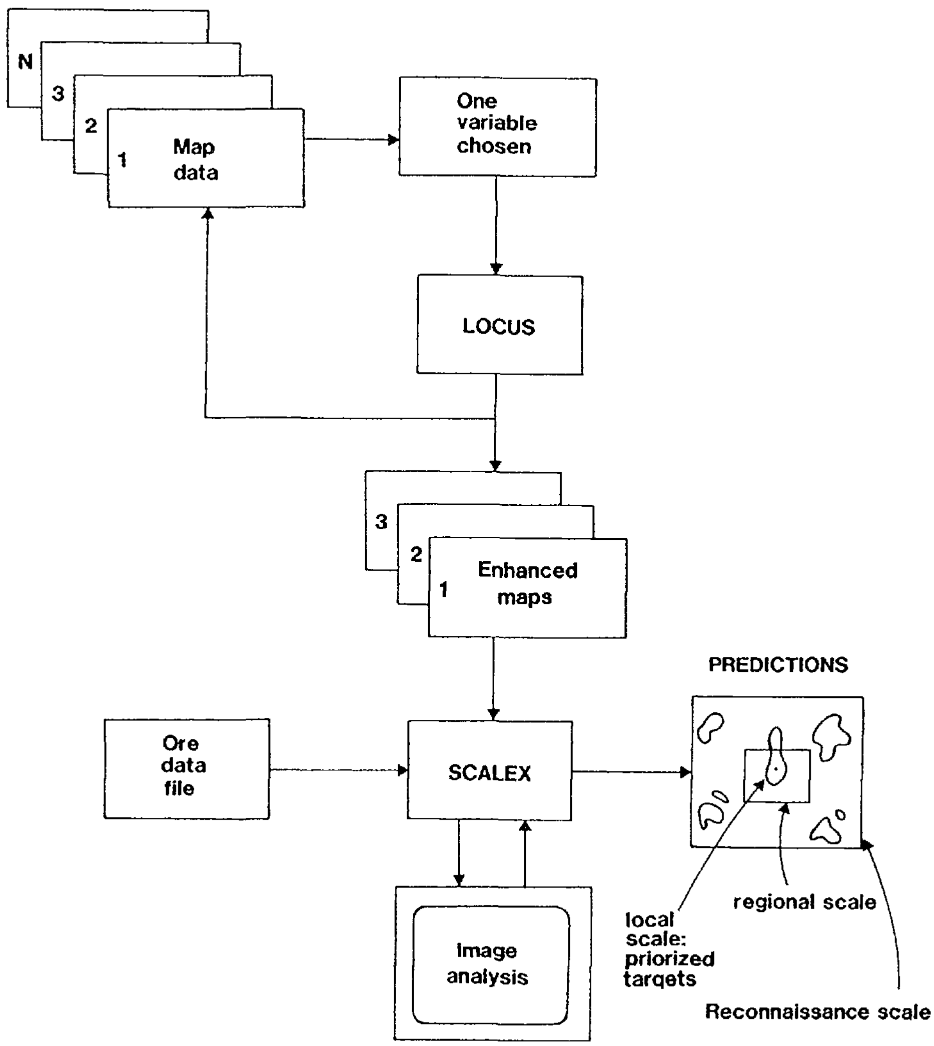

Figure 2. Flow chart of the ore prediction system. Explained in the text.

LOCUS program (Fig. 2) first executes spatial enhancement of digital geomaps (one variable /each run) and optional color and/or greytone plotting of the products. Patterns in maps can be flexibly enhanced, for example spatial frequencies, gradients and also more complex structural features such as texture can be enhanced by Fourier and convolution methods.

SCALEX program (Fig. 2) transforms the enhanced variables into 2- or 3-dimensional feature spaces in the form of 2- or 3-dimensional histograms. These are visualized by color monitor screening. The values of all variables, which originally vary between their minimum and maximun, are scaled to vary between 1 and 512 in the histogram. The 3-dimensional case is illustrated by rotation of the histogram. The positions of the 'ore containing pixels' are indicated by special symbols in the histograms.

Next, features of ore deposits, i.e. positions of 'ore containing pixels' in the feature space are studied, the favourable subspaces are delineated and separated. Fig. 3 illustrates how the separation is made by user-designable ellipsoids or cut-off values: The user can define a subspace by a group of ellipsoids by fixing their focal points and the constant sum of distances from their focal points. The user can also define a subspace by fixing cut-off values for each variable in the histogram. Contents of the ellipsoids, or an area where all variables simultaneously exeed fixed cut-off values, are transformed back from feature coordinates to geographic map coordinates to find the final targets.

These operations can be made systematically for maps of reconnaissance, regional and local scales. When targets of different scales match, these targets are suggested to be the most favourable (of high priority) in comparison with the other targets. If the size distribution of the ore deposits in the feature spaces shows a clear tendency, priorization of the targets can be made according to this tendency (see Fig. 3).

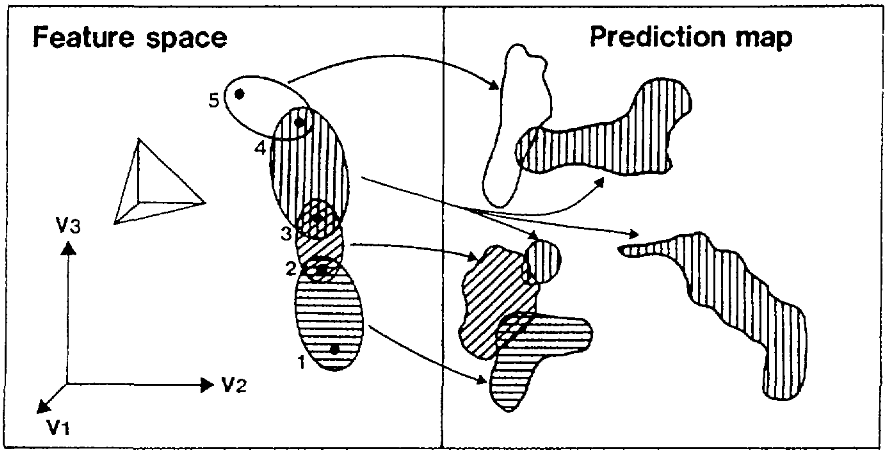

Figure 3. Ore potential subspaces are separated from the feature space of three variables to prediction map (in geographic coordinates) by user-designable ellipsoids or cut-off values. The latter ones are illustrated by a 'corner'. Features of the ore deposits may be selected to the role of training features 1-5, which define locations of the subspace ellipsoids.

3. A CASE STUDY

A case study was carried out separately for a reconnaissance scale area A (Fig. 1), 330x420 km2 and a regional scale area B (Fig. 1), 60x75 km2. An other regional scale area C (Fig. 1), 30x50 km2 was only tentatively tested.

3.1 RECONNAISSANCE SCALE

In the large test area A the data used for this experiment are the following:

Regional Bouguer gravity map (Geodetic Institute of Finland)
- average sampling distance 5km,
- gridded to 1x1km (Fig. 4)

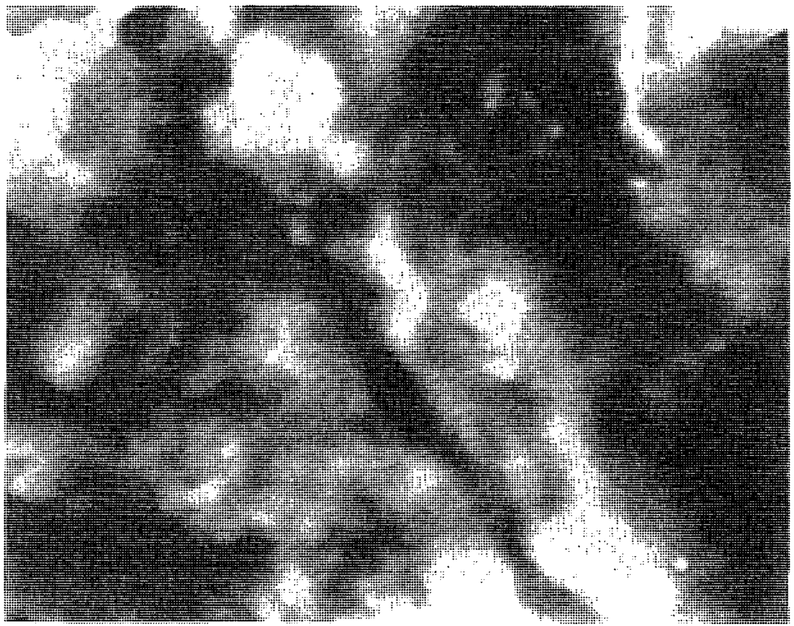

Figure 4. Bouguer gravity map of area A. Light tones indicate high and dark tones low Bouguer gravity anomalies.

Aeromagnetic total intensity (Geophysics Department of the Geological Survey of Finland; Korhonen, J. 1979)
- flight altitude 150 m, separation of flight lines 400m,
- gridded to 1x1km (Fig. 5)

Till geochemical maps (Geochemistry Department of the Geological Survey of Finland)
- Average sampling interval 10 km
- Elements: Cu, Zn, Ni, Cr, Ba, Th
- gridded to 1x1km

Cu, Zn and/or Pb ore deposits and prospects (Exploration Department of the Geological Survey of Finland; Kahma et al. 1976)
- areal distribution and relative metal content (Fig. 1, area A)

In the case of reconnaissance scale (area A) both the gravity and aeromagnetic maps were first high-pass filtered (Figs. 6 and 7) by LOCUS. Both the original and the filtered versions were studied by SCALEX.

Figure 5. Aeromagnetic total intensity, high altitude survey measurements in area A. Light tones indicate high and dark tones low anomalies.

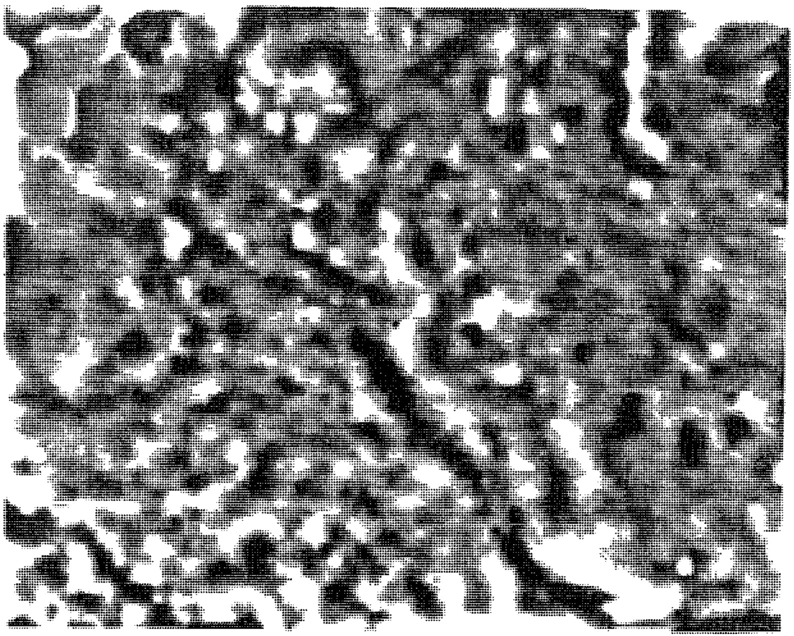

Figure 6. High-pass filtered Bouguer gravity map of area A. Tones as in the original map in Fig. 4.

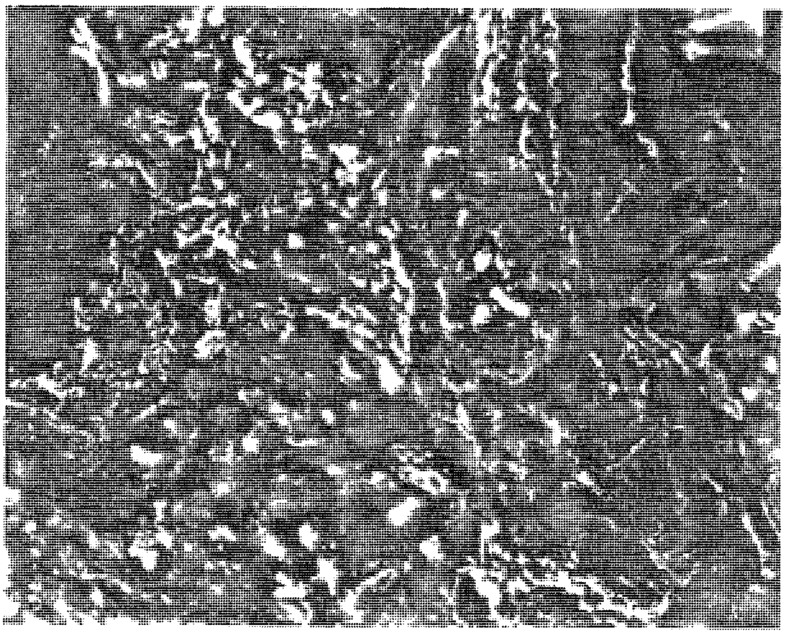

Figure 7. High-pass filtered aeromagnetig map of area A. Tones as in the original map in Fig. 5.

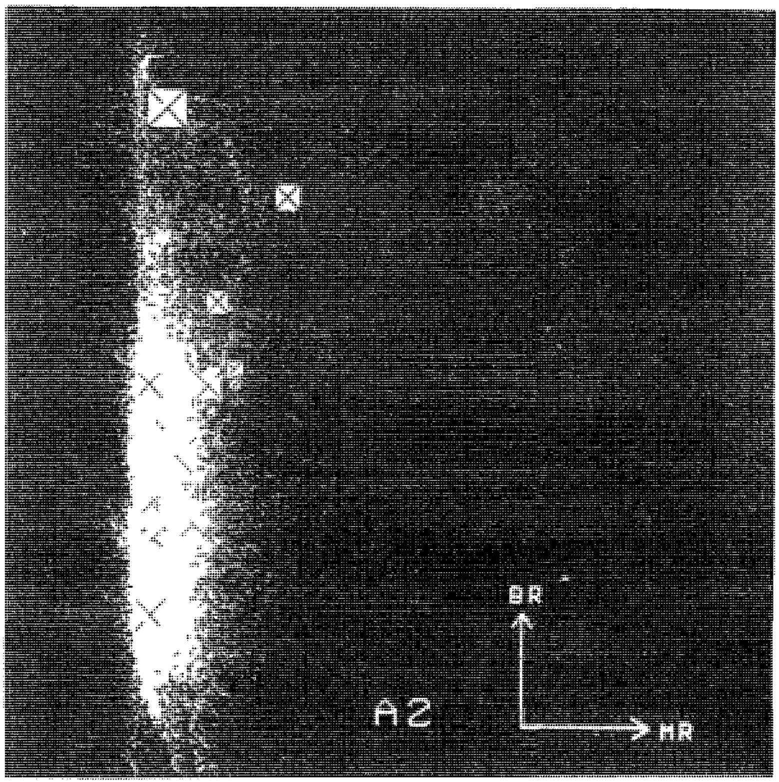

Figure 8. Two-dimensional histogram of Bouguer anomalies (BR, vertical axis) and aeromagnetic anomalies (MR,horizontal axis) in area A. The crossed boxes indicate features (anomaly combinations) and sizes of the ore deposits and prospects. (The drawn axes do not coincide with the origin.)

Fig. 8 gives an example of a 2-dimensional histogram, from area A, with two variables each being scaled from their domain (min,max) to (1,512). The vertical axis is Bouguer anomaly (Fig. 4) and the horizontal axis is magnetic anomaly (Fig. 5). Every combination of these anomalies per pixel is indicated by a light point in the histogram.

The positions of ore deposits in this feature space are indicated by boxes with crosses, the sizes of which are comparable to the metal equivalents (Kahma et al. 1976) in the respective ore deposits or prospects.

Fig. 9 shows a 3-dimensional case, when a third variable, i.e. high-pass filtered Bouguer-anomaly is revealed through rotation of the previous histogram clockwise 45 degrees around the (0,1,-1)-directed vector from the centerpoint (256,256,256).

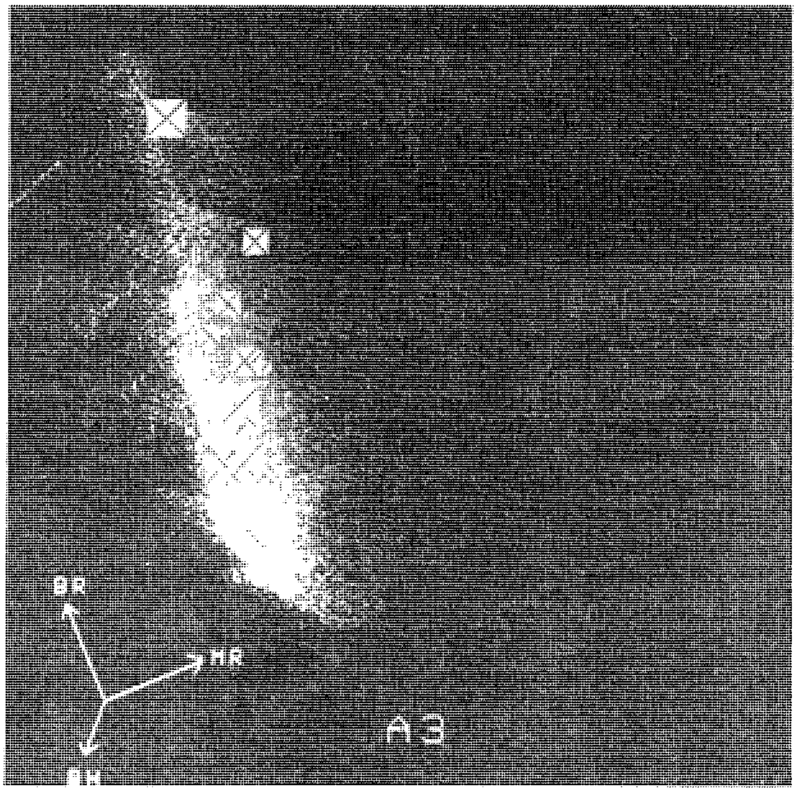

Figure 9. Picture of a three-dimensional rotated histogram of original Bouguer (BR), aeromagnetic (MR) and high-pass filtered Bouguer anomalies (BH) in area A. The boxes indicate the above anomaly features of the ore deposits and prospects. Box sizes are directly proportional to the sizes of the deposits and prospects. (The drawn axes do not coincide with the origin.)

It is immediately seen that the boxes corresponding to the ore deposits become closer to each other when compared to the non-rotated case, and are arranged roughly from big to small. The ore boxes become still closer to each other if the original magnetic map in this histogram is replaced by its hig-pass filtered version (Fig. 10). Enveloped by an ellipsoid, a subspace, including the known five biggest ore deposits (Vihanti, the most exceptional excluded), was transformed from the last histogram (feature

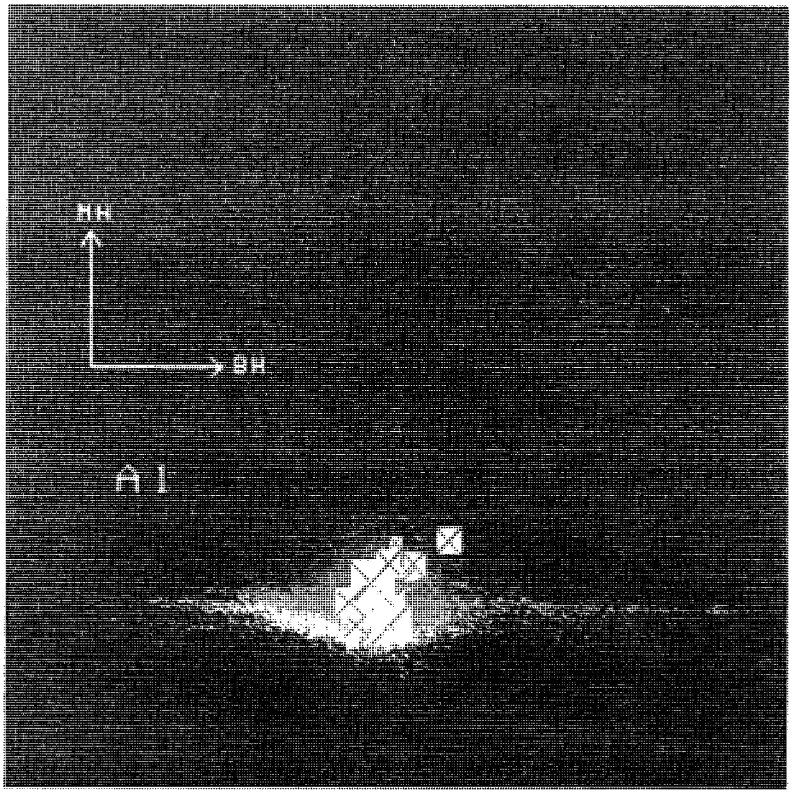

Figure 10. Two-dimensional histogram of high-pass filtered Bouguer (BH, horizontal axis) and high-pass filtered aeromagnetic (MH, vertical axis) anomalies in area A. The boxes indicating the ore deposits and prospects of various sizes are 'concentrated'. (The drawn axes do not coincide with the origin.)

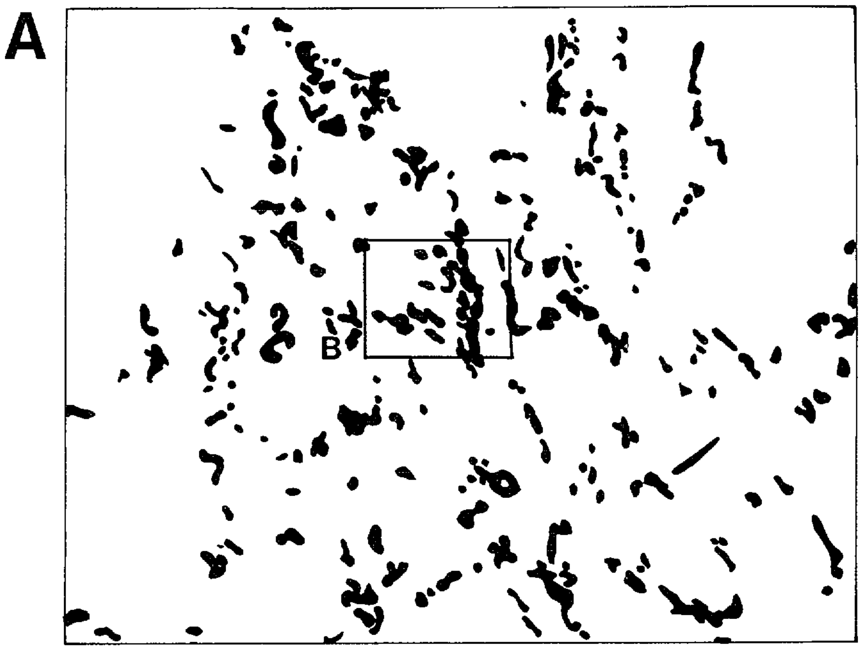

Figure 11. A reconnaissance scale Cu-Zn prediction map of area A. The black areas were transformed from the histogram (see Fig. 10) of filtered Bouguer and magnetic anomalies as explained in the text.

space) back to the map. Fig. 11 shows this back transformed map which is later on used to priorize the targets produced by the following study made in regional scale.

As to the till geochemical maps, only their applicability to this kind of analysis was tested - and found succesful: Relatively limited subspaces favourable for Cu-Zn ore deposits can be found and delineated.

3.2 REGIONAL SCALE

In the smaller test area B (60x75 km2) of regional scale, the data were airborne geophysical survey data and ore indications:

Low altitude magnetic total intensity (Geophysics Department of the Geological Survey of Finland)
- -Flight altitude 30-40m
- -Line separation 200m, average sampling interval 25m
- -Gridded to 100x100m2

Low altitude electromagnetic measurements (Geophysics Department of the Geological Survey of Finland; Peltoniemi 1982)
- -Sampling interval 50m
- -Flight altitude and grid as above
- -In-phase component
- -Out-of-phase component

Indications for Cu, Zn and Pb (Exploration Department of the Geol. Surv. Finland; Ore Deposit Databank, Gaal et al.1977)
- -Ore showings in the bedrock

Fig. 12a shows an example of the low altitude survey magnetic data and Fig. 12b its high-pass filtered version. The dark areas indicate here high magnetic field mostly connected to schists of volcano-sedimentary origin.
Fig. 13a shows the electromagnetic out-of phase map and Fig.13b its high-pass filtered version. The latter makes faults visible perhaps due to the ability of faults to contain electrolytic conductors.

The maps of regional scale were also studied by SCALEX: Three-dimensional histograms of all possible combinations of the original and the high-pass filtered versions were formed. An example showing a histogram between the original electromagnetic in-phase and out-of-phase components is seen in Fig. 14. The minimum of the variables is located in the bottom-left corner and the maximum in the upper-right corner. The vertical axis represents out-of-phase and horizontal in-phase component. The 'cloud' indicates the histogram and the (crossed) boxes indicate features of ore deposits/showings of different sizes. The boxes of ore features seem to be roughly arranged from big to small.

Figure 12a Low altitude survey aeromagnetic total intensity map of area B. Dark tones indicate high anomalies and light tones low anomalies.

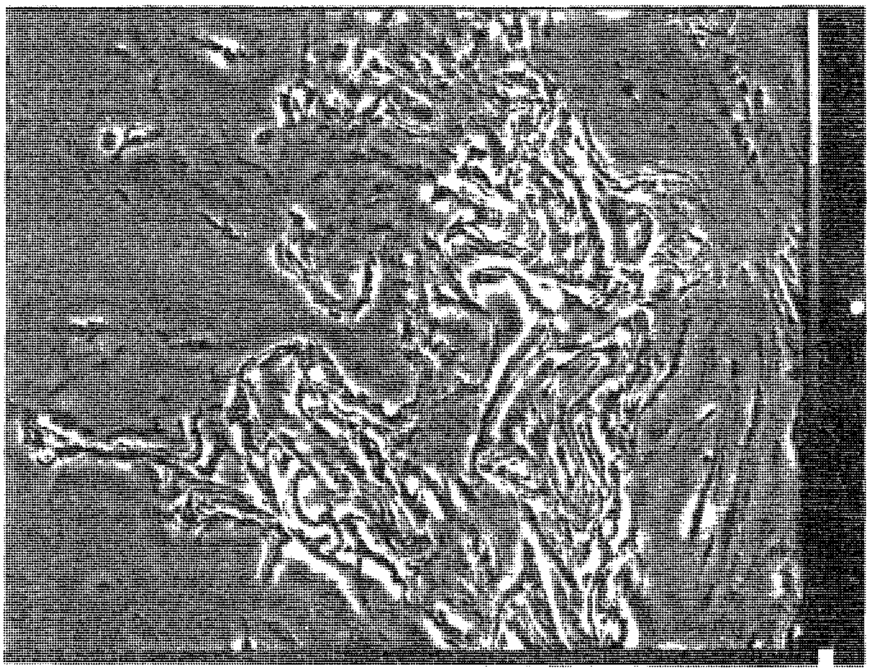

Figure 12b High-pass filtered low altitude survey aeromagnetic total intensity map of area B. Dark tones indicate high and light tones low local anomalies.

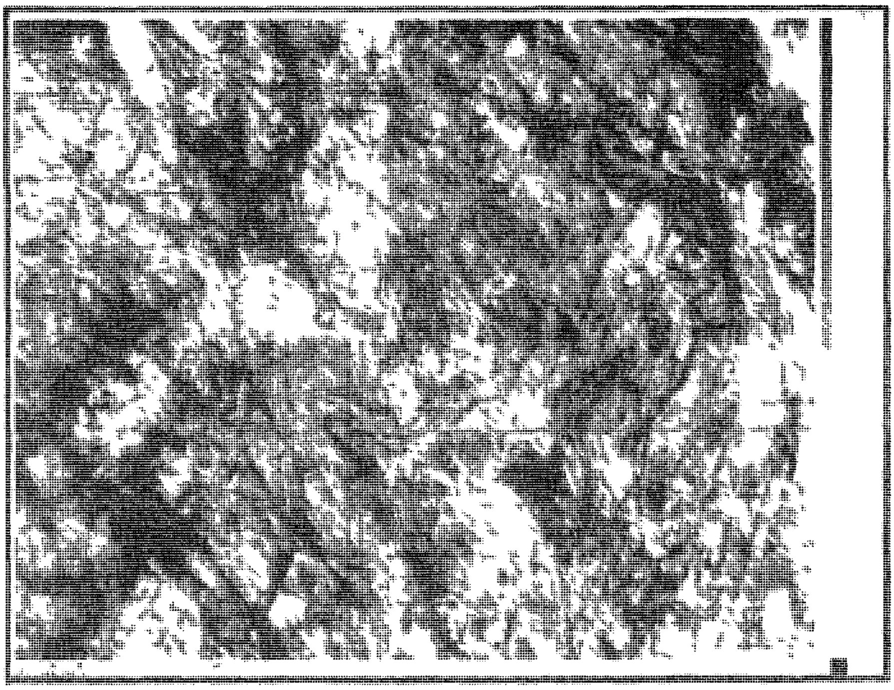

Figure 13a Low altitude survey electromagnetic out-of-phase map of area B. Dark tones indicate high and light tones low anomalies.

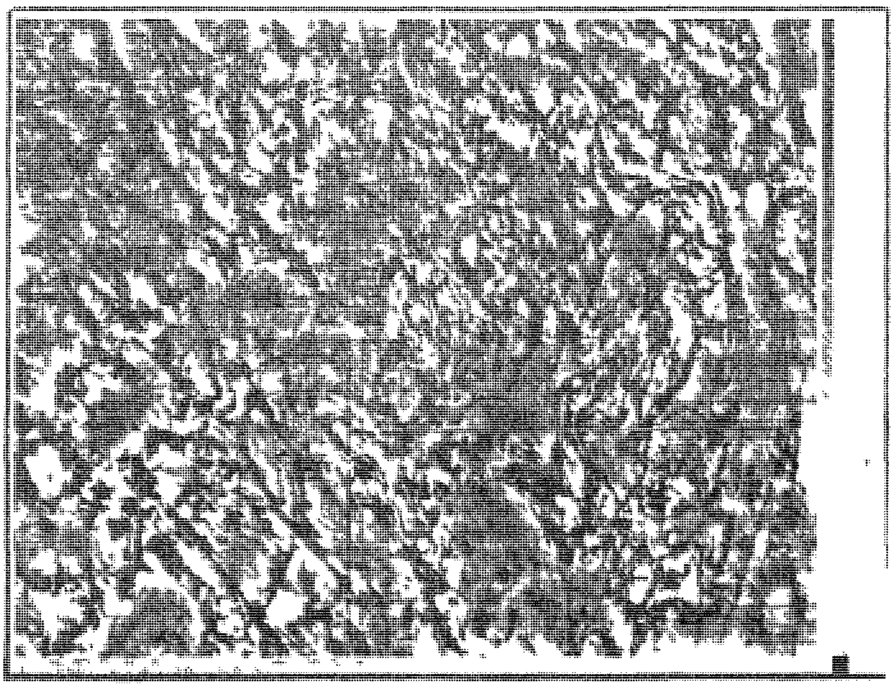

Figure 13b High-pass filtered low altitude survey electromagnetic out-of-phase map of area B. Dark tones indicate high and light tones low local anomalies.

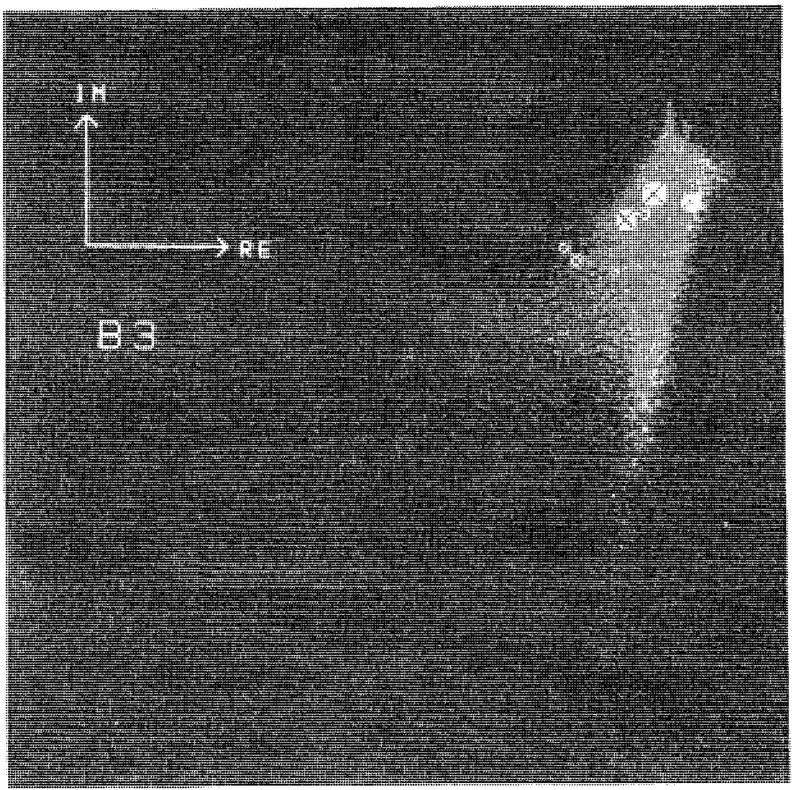

Figure 14. Two-dimensional histogram of the low altitude geophysical survey data, electromagnetic out-of-phase anomalies (IM, vertical axis) and in-phase anomalies (RE, horizontal axis). The features of ore deposits of various sizes are indicated by crossed boxes. (The drawn axes do not coincide with the origin.)

A subspace was separated from the 3-dimensional histogram of the high-pass filtered magnetic map and both electromagnetic components : such features (Fig. 15), where the high-pass filtered (Kuosmanen et al.1985) anomalies simultaneously exeeded specific limits, were transformed back to geographic coordinates. The limits are: magnetic > 239nT, in-phase anomaly < -45.1 ppm and out-of-phase < -67.4 ppm (Kuosmanen et al. 1985). The limits were defined in such a way that the biggest ore deposit (Pyhäsalmi) of area B becomes indicated by the minimum number of pixels. All the known Cu-Zn ore deposits and showings were precisely (+200m) pinpointed by the back transformed subspace (Fig. 15). Therefore, the additional back transformed pixels which do not coincide with the known ore indications may be - after priorization - favourable targets for local exploration.

4. PRIORIZATION OF THE TARGETS FOR EXPLORATION

In order to be able to start local exploration from the most favourable targets, the targets in regional scale were priorized by those in reconnaissance scale. In Fig. 15, the targets of various scales are superimposed and it is suggested that those where the predictions

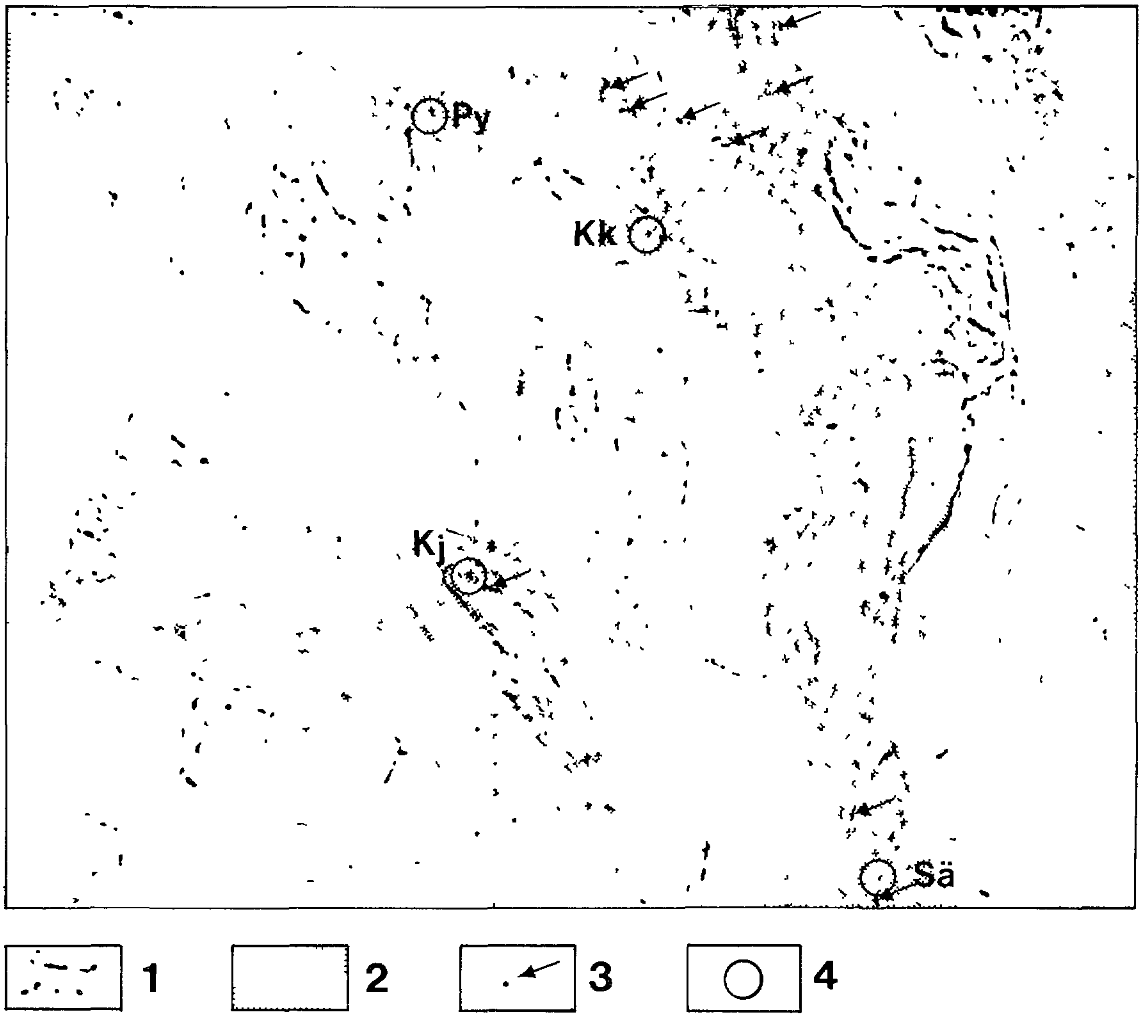

Figure 15. Superimposed predictions in area B. 1) Targets obtained from the histogram of the regional scale maps. 2) Targets obtained from the histogram of the reconnaissance scale maps. 3) Arrows indicate those predicted locations which coincide with ore showings. 4) The ore deposits of this regional scale test area: Py=Pyhäsalmi, Kk=Kalliokylä, Kj=Kangasjärvi, Sä=Säviä. Places where the targets (1) and (2) overlap are suggested to be favourable for Cu-Zn(-Pb) deposits.

of various scales coincide represent targets of higher priority, i.e. higher favourability for Cu-Zn ores.

More than twenty of these targets were field checked by the so called Multimethod Project at the Exploration Department of the Geological Survey of Finland. This work is not yet reported, but it was found that most of the targets contained signs of hydrothermal alteration and/or Fe, Cu or Zn sulphide mineralizations.

5. DISCUSSION

Visualization of the multidimensional feature spaces was found useful especially when the number of observations was large. These studies lead to a possibility to consider prediction of the biggest ore deposits in an area.

Any number of different variables can be studied by the suggested method. Visual investigation is restricted to a maximum of three variables at a time. However, the investigation can be repeated very quickly with a new combination of three variables.

For the test area C there were data only on low altitude geophysical surveys. These data were tentatively analyzed and the high-pass filtered versions indicated similar relations as those in area B.

The proposed method can be applied to geochemical and radiometric measurements and therefore also to uranium exploration.

ACKNOWLEDGEMENTS

The authors would like to thank the Geological Survey of Finland for the possibility to publish this paper. The Laboratory of Urban Planning and Building Design of the Technical Research Centre of Finland is thanked for offering use of their image processing and other facilities to the authors. Especially, senior research scientist Risto Kuittinen and research scientist Kaj Andersson from the laboratory are thanked for help during the investigation. Prof. Jouko Talvitie and Mr. Mikko Tontti, Lic Ph, are thanked for critical reading of the text.

REFERENCES

Aarnisalo,J.,Franssila,E.,Eeronheimo,J.,Lakanen,E. and Pehkonen,E. (1982): On the integrated use of Landsat, geophysical and other data in exploration in the Baltic Shield, Finland. The Photogrammetric Journal of Finland, Vol.9, No.1, pp.48-64.

Aarnisalo,J. (1984): Image processing and integration of geophysical and other data as a tool for mineral exploration in glaciated Precambrian terrain. In (Cook,J.,editor): Proceedings of the international symposium on remote sensing of environment: 'Remote Sensing for Exploration Geology', April 16-19 1984, Colorado Springs, Colorado, USA. Envir. Res. Inst. Mich., Ann Arbor, Michigan, USA, Vol.1, pp. 107-128.

Arkimaa,H. (1982): Some examples of multi-channel analyses of Landsat and geophysical data. The Photogrammetric Journal of Finland, Vol.9, No.1, pp.38-47.

Arkimaa,H.,Lindqvist,E. and Kuosmanen,V. (1985): Prediction of areas potential for Cu-Zn sulphide ore with the aid of low altitude aerogeophysical data and statistical methods. Abstracts, Geoexploration, Vol.23, No.3,p.416.

Barringer,A. (1969): Remote-sensing techniques for mineral discovery. Proceedings of the 9th Comm. Min. Met. Congress. London. pp. 649-690.

CSIRO (Commonwealth Scientific and Industrial Research Organization), Division of Information Technology, (1986): Disimp/Slip image processing and graphics software. Canberra, Australia.

Gaál,G.,Tontti,M.,Autio,H. and Lehtonen,M. (1977): Establishing a national ore data file in Finland. Journal Int. Assoc. Math. Geol.,Vol.9,No.3, pp.319-325.

Gaál,G. (1984): Evaluation of the mineral resource potential of central Finnish Lapland by statistical analysis of geological, geochemical and geophysical data. Geological Survey of Finland, Report of Investigation No.63, 69p.

Kahma,A.,Saltikoff,B. and Lindberg,E. (1976): Ore deposits of Finland, map in scale 1:1mill., Geological Survey of Finland.

Kilpelä,E.,Jaakkola,S.,Kuittinen,R.,Talvitie,J. (1978): Automated earth resources surveys using satellite and aircraft scanner data. Building Technology and Community Development, Technical Research Centre of Finland, Publ. 15, pp. 70-104.

Korhonen,J. (1979): Aeromagneettisten korkealentojen digitalisointi (in Finnish, Digitalization of aeromagnetic high-altitude survey data). Unpublished report Q 16.2/22.9/79/1, Geological Survey of Finland.

Kuosmanen,V.,Arkimaa,H. and Lindqvist,E. (1985): Structural positions of predicted and known Cu-Zn indications. In (Cook,J.,editor): Proceedings of the international symposium on remote sensing of environment: 'Remote sensing for Exploration Geology', April 1-4 1985, San Fransisco, California, USA. Environ. Res. Inst. Mich., Ann Arbor, Michigan,USA, pp.57-71.

Kuosmanen,V.,Tumanto,M. and Honkaranta,T. (1982): LOCUS - an image analysis ADP system to search for map patterns connected with ore indications. Unpublished report, Department of Geology and Bureau of Physical Computation, University of Helsinki, 56p.

Sabins,F. (1986): Remote sensing principles and interpretation. Second edition, Freeman & Co., 449p.

Talvitie,J. (1979): Remote sensing and geobotanical prospecting in Finland. Bull. Geol. Soc. Finland No.51, pp. 63-73.

Tontti,M.,Koistinen,E. and Lehtonen,M. (1979): Kotalahden nikkelivyöhykkeen monimuuttuja-analyysi (in Finnish, with English abstract: A multivariate analysis of the Kotalahti Nickel Belt). Geological Survey of Finland, Report of Investigation No.36, 58p.

Tontti,M.,Koistinen,E. and Seppänen,H. (1981): Vihannin Zn-Cu-malmivyöhykkeen geomatemaattinen arviointi (in Finnish, with English summary: Geomathematical evaluation of the Vihanti Zn-Cu Ore Zone). Geological Survey of Finland, Report of Investigation No. 54, 34p.

WORKING GROUP REPORTS

Working Group 1

REMOTE SENSING IN GEOLOGY

Members: **Y. Chong** (Singapore)
G.R. Garrard (United Kingdom)
N.V.A.S. Perumal (India)
J. Talvitie (Finland)

Introduction

Several aspects of remote sensing including physical phenomena and measurement techniques and use of different remote sensing systems as applicable to geological investigations, have been dealt with in the IAEA Technical Report Series No. 208.

The present report briefly reviews the application of remotely sensed data in geological mapping and integration of remotely sensed data with those of conventional techniques as presented in the Committee Meeting and identifies several advantages in the use of these data in all phases of mineral and uranium exploration programmes.

Remote sensing techniques are now effectively used in a wide variety of earth resources investigations including agriculture, forestry, hydrology and water management, exploration for minerals (uranium included) and hydrocarbons, urban development, ecology, siting of nuclear power plants and waste disposal. Remotely sensed data either from orbital or airborne platforms provide basic information on lithology, morphology and geological structures in regional or detailed scale, necessary for any earth resources study. Many geological problems which are difficult to or could not be solved through conventional methods alone are now being solved with the help of remote sensing. The synoptic view and regional structures readily provided by the satellite imagery are used to identify favourable environments for the occurrence of uranium and other minerals.

Physical Principles

The ability of the geologist or the interpreter to extract sound geological information from remotely sensed data largely depends on his or her understanding about the complex nature of physical principles, especially the reflection, absorption, scattering and emission of the electromagnetic (radiant) energy and the thermal properties of the geological materials, underlying the remotely sensed data, his knowledge about the geology of the area and his experience and skill in photointerpretation techniques. Optimum utilization of remotely sensed data are, however, be best achieved through enhancement of digital multispectral data using computer image processing techniques. The physical principles and their significance in remote sensing are briefly given in the above Technical Report.

Electromagnetic Spectrum and Platforms

The conventional and widely accepted definition of "remote sensing" denotes measurement of EM spectrum in the region of 0.4 µm to 25 cm which include, visible, near infrared (NIR), short wave infrared (SWIR), thermal infrared (TIR) and microwave. Applicability of remote sensing systems employing these spectral ranges from airborne and orbital platforms has been successfully demonstrated. Spectral data obtained through narrow bands generally provide better differentiation of geological materials. The spectral bands, 1.25 - 1.55 µm and 2.08 - 2.35 µm which have beem empirically established to be the most useful bands for differentiating various geological materials are included in the Thematic Mapper (TM) of the Landsat 4 and 5 series. Landsat TM data with 30 m ground resolution are now used to prepare excellent geological maps at 1:50,000 - 1:60,000 scale and with image enhancement techniques imagery can be used up to approximately 1:25,000 scale. This appears quite significant as maps of up to 1:100,000 scale, with 79 m ground resolution, were only possible with Landsat MSS data. Recent experiments also show that the thermal infra-red band (8 - 10.5µm) is fast gaining importance in geological remote sensing as several silicate and non-silicate rocks can be distinguished within this spectral range.

Significant developments in optical and scanning instruments have taken place in recent years leading to better spatial and spectral resolution from orbiting space platforms. This includes the use of steerable sensors to obtain stereoscopic imagery from, for example, the SPOT satellite.

Airborne surveys using airphoto cameras, multispectral scanners, radar instruments and spectrometers also play an important role in remote sensing both from a commercial and research orientated viewpoint. They will continue to do so until equivalent resolution, both spatial and spectral, is available from orbiting satellites.

Satellites at present in polar or geostationary orbits are given in Table 1 with their sensors, spectral range and spatial resolution. Proposed future systems for 1987 to 1995 are given in Table 2. Some improvements in spatial and spectral resolution are anticipated for Landsat TM and SPOT. Notably 20 m resolution for TM and a greater number of channels for SPOT. Most of the SAR instruments will have limited recording facilities, hence coverage, and some are anticipated as only research instruments. Even the Polar Orbiting Platforms proposed for 1995 at present do not appear to anticipate greater resolution than 10 m, 20 m or 30 m (at present available from SPOT) and not all instruments will have this resolution. The platforms are due to carry several instruments including weather sensors, multispectral scanners and radar. Due to power considerations it is unlikely that more than one to three radar scenes will be collected per orbit. At present the initial orbiting configuration is research orientated apart from the weather instruments and serious discussion is in progress about commercial collection and availability of data. Needless to say the loss of "Challenger" may affect the schedule for the USA platform.

Data Processing, Hardware and Software

Image processing techniques have been used to enhance single-band and multispectral remotely sensed data available in digital format. These processes, namely linear-streching, improve the visual contrast and colour balance from bulk processed hard copy enabling subtle geological features to be more easily distinguished. Other techniques such as histogram equalization, spatial filtering, simple and compound ratioing and principal component analysis of the different spectral bands have proved quite useful in interpretation of lithological and structural features.

Utilization of data from remote sensing, geophysical, geochemical and other compatible techniques is rapidly developing and the utility of the integrated approach for accelerating the pace of investigations in different phases leading to considerable savings in cost and manpower has been realized.

The hardware for digital data processing is available from many agencies. The data inputs in different formats are also available. One significant development in recent years has been the availability of low-cost, but very powerful desk-top computers capable for effective performance in image processing.

Today the software for effective processing of the remotely sensed data is available. On the other hand packages of automated data processing programmes for automated integrated data analysis need immediate development to meet the rapidly growing requirements of integrated data analysis involving several geoscience data sets.

TABLE I. Present Satellites (or Space Sensors).

Satellite	Sensor	Spectral Range (um)	No.of Bands	Spatial Resolution	Comments
Landsat 5	MSS	0.1-0.9	4	60x80 m)	Expires
	TM	0.3-2.5	6	30x30 m)	1987
	TM	8.0-13.5	1	120x120 m)	
SPOT 1	MSS	0.5-0.9	3	20x20 m	With stereoscopic imagery
	PAN	0.5-0.7	1	10x10 m (panchromatic)	
SEASAT	Radar	23 cm (L band)	1	25 m	Expired 1978
METEOSAT	MSS	0.4-1.1	1	2.5 km	Geostationary
	MSS	5.7-7.1	1	5.0 km	orbit
	MSS	10.5-12.5	1	5.0 km	
NOAA 7	AVHRR	0.5-1.1	2)		
	AVHRR	3.5-4.0	1)	1.1 or 4 km	
	AVHRR	10.0-12.5	2)		
NIMBUS 7	CZCS	0.4-0.8	5	800 m	Expired
		10.5-12.5	1	800 m	
SIR-A/B	Radar	L band	1	-	Limited cover.
Shuttle	Large format camera	0.4-0.9	3	-	Limited cover.

TABLE 2. Future Systems.

Satellite	Country/ Organisation	Launch Date	Sensors
Landsat 6/7	EOSAT	1988/1991	TM
SPOT 2/3	France	1987-8/1989-90	MSS + Panchromatic
SIR-C	NASA	1989	SAR
ERS-1	ESA	1989	SAR + Scatterometer
RADARSAT	Canada	1990/91	SAR + Scatterometer
JERS-1	Japan	1990	SAR + optical sensor
MOS-1	Japan	1986/87	Three radiometers
GEOSAT	U.S.A.	1984/85	Altimeter
TOPEX	USA/France	1988/89	Altimeter
NROSS	U.S.A.	1988/89	Altimeter, Scatterometer, radiometer.
POSEIDEN	France	1989/90	Altimeter Doris Tracking System.
TERS	Netherlands/ Indonesia	?	Optical Sensors.
Polar Platforms	USA/ESA/Canada Japan	1995?	Optical Sensors, Spectrometers, Radio-meter, e.g. TM?, SAR, Altimeter, AVHRR, a collection of sensors.

Working Group 2

GEOPHYSICAL TECHNIQUE

Members: **N. Njibaloh** (Cameroon)
Shuxin Zhao (China)
V.V. Kuosmanen (Finland)
J.N. Faurie (South Africa)
S.Potisat (Thailand)
G.R. Garrard (United Kingdom)

1. INTRODUCTION

A total of seven out of seventeen papers presented to the Technical Committee Meeting on Geological Data Integration and Analysis dealt with the subject of integrating different airborne geophysical survey results with one another, with geological data and etc. Some of them revealed new techniques while the others highlighted grey areas that still exist and need some clarification. Since data acquisition is the basis of any survey it could not be left out and was also discussed.

The panel tried to give a summary on the state-of-the-art of both data acquisition and integration of geophysicsal methods related to uranium exploration techniques as its present status and also proposed some recommendations for the future.

2. DATA ACQUISITION

2.1. General

Data acquisition is the take off point in exploration geophysics and its importance cannot be overemphasized. However, in the last few years acquisition of data is becoming more difficult due to many factors including:

i) Sophisticated digital instruments with low reliability under field conditions and their high maintenance costs.

ii) Lack of adequate and well-trained manpower in many countries.

iii) Problems inherent to the application of certain methods which have not yet been solved; for example, in airborne radiometric surveys, the correction of atmospheric radon distribution the variation of stripping factors with altitude or the attenuation of gamma radiation by thick lateritic and damp over burden, etc.

It is recommended that the physical basis of these phenomena in real geological situations be carried out and guidelines given to Member States or organizations involved in data acquisition. This could improve the degree of reliability of collected data.

2.2. Selection of Instruments

The technical specifications of all geophysical instruments are usually made available by the manufacturers. Though the choice of any instruments are based on such specificiations it is advisable that the users take into account geographical conditions under which they are going to be used, the procedure and conditions under which such specifications concerning calibrations, stripping factors, etc. were carried out.

With the development of DBS with enormous storage and retrieval potentials it is possible that future instruments will become multi-purpose and measuring many different geophysical parameters and their derivative or other transformations at the same time. We suggest that the IAEA in collaboration with manufacturers look into the possibility of serial production of instruments capable of measuring as many geophysical parameters as possible and their derivatives, ratios or other transforms where possible. In this respect it is worth mentioning that certain well-logging equipment have made considerable progress in theat direction. It is possible that the production of multi-purpose equipment for the measurement of magnetic, radiometric, spectrometric, electromagnetic parameters, etc., and their derivatives or transforms, where possible, could enhance integration and reduce cost of data acquisition.

2.3. Correction and Calibration

It is clear that within the next few years DBS will play an important role in geophysical data storage so the demand inuniformisation of calibrations of geophysical equipments, accuracy in the correction of different geophysical parameters will become more stringent.

We recommend that the IAEA make standard recommendations on the execution of calibrations and corrections involved in airborne radiometric and spectrometric survey and remote sensing techniques.

We also recommend that standard test paths for calibration or testing different airborne radiometric and spectrometric equipment be in different geographical regions. This will improve the compatibility of results obtained in different countries.

2.4. Results Presentation

The problem: Different organizations and countries have different presentations.

To be sure the different parameters are well represented they should be on the same format (scale). The different formats or scale should reflect the type of information expected, regional tectonic, structures, metallogenic provinces or ore bodies, etc.

We recommend that the IAEA make certain guidelines in this direction.

3. DATA INTEGRATION

A. Before integration procedures can be carried out a goal must be chosen with carefully selected limits.

B. The work carried out depends on finance, manpower and instrumentation available.

C. Selection of data: Regional databases facilitate data selection because they are easy to update and their structure can be changed.

Raw data selection must be related to the physical properties of the target.

Analog data requires a lot of preprocessing before it can be used and digital data collection is preferable.

Recommendations:

Primary ground earth data (i.e. field data and/or existing documents) should be collected and stored in the same database as the geophysical data. Any errors in the basic data should be corrected before getting it into the database.

D. Generation of effective variables

Raw data collected can be useful in its own right but often for integration it is more useful in a form related to the physical parameters of the target, e.g. total magnetic field maps would be more useful in the form of apparent magnetic susceptibility maps; and gravity data as apparent density; electromagnetic data as apparent conductivity, etc.

Digital data allows fast computer production of new variables, e.g. ratios U/Th, Th/K, U/K

E. Integration

Any integration method (e.g. Visual correlation, statistical correlation and modelling) of grouping data is part of the larger process of inversion.

Visual integration is valuable but ground truth data should always be kept in mind.

Modelling in 1-3 dimensions in geophysics is very time consuming and new more efficient methods must be studied.

Statistical methods are often too inflexible when very large airborne survey data sets are studied.

Image processing systems make integration methods easier because of fast screen display and transformation and modeling processes.

F. Predicted Targets

Successfully predicted targets provide keys for modelling which should be made available.

G. Ground Verification with Geology

Links between geologists and geophysicists are often not clear and ground truth might remain insufficient.

Verification of targets can be made by sampling target boundaries and if ther are errors the prediction must be corrected by interactions.

Prediction should be made at different scales, e.g. reconnaissance, regional and local, and these should be systematicallly related to each other.

GENERAL FLOW CHART FOR INTEGRATION

OF GEOPHYSICAL DATA

GOAL

FINANCE
MANPOWER
INSTRUMENTATION

SELECTION OF DATA SET

- KNOWN PHYSICAL PROPERTIES
- GEOLOGY

GENERATE EFECTIVE VARIABLES
U VALUES
U/Th VALUES
etc.

INTEGRATION
VISUAL, STATISTICAL, MODELLING, INVERSION

PREDICTED TARGETS

GROUND VERIFICATION GEOLOGY

T
A
R
G
E
T

4. FUTURE DATA USE AND STORAGE

Most of the geophysical data and some of the geological data collected at present costs a lot of money. Preparation of this data in digital format and processing of the data also costs a large amount of money. We feel that much of his data will be useful in future years and should not be lost. Some, however, will not be relevant and should be thrown away?!!

The following require decisions:

I) What data should be kept - raw or derived. Recommendations should be for raw data as processing factors change over the years.

II) How should it be stored? Paper copies are not a good form of storage so it should be by tape or optical disc.
Problems: -Tapes deteriorate over 10 years or less depending on storage conditions.
-Optical discs are at present unprooven.

III) How will we know what is available?
Cataloging is required at some central office - possibly IAEA where client confidential information (geophysical data, etc.) has been collected how long should there be before it is made publically available or should it not be made available?

IV) As new data is collected will it be stored as an update of an area or as a replacement, if it is the same type of data.

V) How long should we keep the data? And how long will it be useful to anyone?

These are all factors that should be considered as data collection becomes more digitally orientated and with the soaring costs of collection. The panel cannot answer all the questions but feel they should be posed and thought about over the next few years.

Working Group 3

THE INTERPRETATION OF GEOCHEMICAL EXPLORATION DATA

Members: **P. Abeysinghe** (Sri Lanka)
H.M.H.I. Ayesh (Jordan)
K. Busch (Federal Republic of Germany)
L.J. Dejonghe (Belgium)
B.B. Hambleton-Jones (South Africa)
G. Hatziyannis (Greece)
H. Kürzl (Austria)
M.E. Mostafa (Egypt)
A. Steenfelt (Denmark)
J. Talvitie (Finland)
J. Tomsic (Yugoslavia)
S. Uçakciouglu (Turkey)

1. INTRODUCTION

Geochemical exploration is one method within the broad spectrum of exploration techniques all of which should be integrated to assist in the final target selection.

The objective of this report is to recommend ways as to how the geochemical exploration data can be presented in a form which is complimentary and compatible with other exploration methodologies.

Discussion on detailed sampling and chemical analysis will not be included here as these have been dealt with elsewhere and in other relevant IAEA technical reports.

From the sampling point of wiew, on both reconnaissance and follow-up stages, drainage samples e.g. the stream sediment fine fraction or heavy mineral concentrates and stream water are often chosen as sample media. In addition, till, soil, lake sediment. plant material, ground water and gas may be applicable depending upon local circumstances.

Multi-element analysis of samples is preferable throughout the various exploration phases. However. dependant upon the uniqueness of the program only specialised elements may be selected for analysis. In general, this approach will be particularly useful in broadening the scope of interest within the area but care must be exercised to ensure the overall cost effectiveness of the program.

2. ANALYSIS AND PRESENTATION OF MULTIVARIATE GEOCHEMICAL DATA

2.1 Reconnaissance Level

The aim of reconnaissance geochemical surveys is to outline districts with potential mineral resources which may be geochemically characterised by either elevated contents of one or more elements, or by unusual geochemical signatures. In order to define these signatures it is necessary to establish, with the assistance of all available geological information, both the single and multi-element geochemical background variations which ultimately should represent, as closely as possible, the geochemistry of the underlying bedrock. This data can thus be used to define "ore indicating" deviations from the characteristic element background concentrations. When the geology is poorly known, the geochemical distribution patterns of single and multi- element associations provide valuable information in the interpretation of the underlying geology, particularly when it can be integrated with other regional data (e.g. airborne magnetics and gamma spectrometry, and other remote sensing data). For the purpose of geological interpretation, major elements and non ore-forming trace elements like Rb, Sr, Zr are very useful and should be included in the evaluation. Statistical treatment of the exploration data helps to reduce the "noise" due to sample and analytical errors and establish the significance of observed variations. The statistical procedures outlined below are relevant to the treatment of reconnaissance geochemical exploration data.

2.1.1. Data preparation and univariate statistical analysis

a. Geological domains
   Where possible, outline geological domains wherein the sampling density is limited to approximately 2 000 to 3 000 samples. This is especially recommended to avoid technical problems in data handling of larger sample sets and to reduce computing time.

b. Raw data documentation*

The first step is data verification firstly to ensure the elimination of data errors and secondly to establish empirical detection limits and analytical variance which can be done if necessary by an external laboratory control, see ([5] (Reimann and Wurzer, 1986). This is followed by display, description and summary of raw data, for example;

(i) Documentation of single elements on maps with point symbols. Map scales should be compatible with those of existing geological maps and with those of other exploratory data.

(ii) Documentation of single element frequency distributions for the whole data batch using histograms, cumulative frequency curves and graphical plots derived from Exploratory Data Analysis (EDA) such as density traces, box-plots and one dimensional scatter plots, from which estimates of frequency distribution parameters such as the central value and spread can be obtained. Robust and resistant methods are highly recommended [6] (Hoaglin et al. 1983). Graphic displays and maps are used in the preliminary testing of the conceptual models where mixed populations, inhomogeneities and the regional and local variations can be assessed.

c. Regional geochemical groupings

Group the regional data into geochemical units representing more or less homogeneous geographical, tectonic and geological environments. The interrelationships between these factors and the element behaviour inthe secondary environment are important with respect to the interpretation and delineation of anomalous areas.

---

* The methodology outlined here is mainly based on the work of [1] Tukey (1977) as its applications were tested and shown to be useful ([2] Garrett 1981, [3] Howarth 1984). Other useful literature on statistical treatment of geochemical exploration data is to be found in [4] Howarth (ed.) (1983).

A variety of clustering techniques are available to assist with the grouping, such as:

i Robust Principal Component Analysis (RPCA) provides basic information about the proportion of multivariate variability represented by each element. Elements having a high regional variability are those, which should be used in the grouping procedures. Additional information can be gained by mapping the scores of the first eigenvector, giving an overall impression of regional multivariate element behavior.

ii Non-linear mapping, "minimal Spanning Tree" (MST-method described by [7] (Friedmann and Rafsky, 1981) and similar non-parametric methods are extremely useful and efficient. However, all these methods require access to graphic terminals for interactive work.

iii The application of the Bi-Plotting Technique as described by [8] (R. Sinding-Larsen, 1974). Hierarchical cluster techniques are questionable in this respect because of the unknown number of natural clusters and the long computing time

d. Areal element distributions
After the establishment of regional groups the areal element distributions are evaluated by estimating regional background variations. This can be accomplished by using for example moving average techniques in which search areas and distance weighting can be varied, or geostatistics which provide estimates of regional element concentration levels taking into account the multi-directional spacial relationships between adjacent samples. As the application of the latter method assumes a homogeneous geochemical population the estimation is done separately for all groups. The results can be displayed on composite pixel maps which are ideally suited for integration with other geodata.

2.2. Regional Follow-up Level

Based on information from reconnaissance-level geochemical exploration and comparative studies with other reconnaissance geological. geophysical and remote sensing data, areas for follow-up exploration for particular commodities can be selected. The aim of the geochemical exploration at this level is to locate mineralised occurrences and to determine their geochemical characteristics.

2.2.1. Statistical analysis

In the established regional geochemical groups local anomalies or subgroups may be identified by applying further data analysis using the methods described in section 2.1.1b provided that the sampling density is high in relation to the size of the target. This is an attempt to refine the conceptual geochemical models of the mineralisation within the potential target areas. The subgroups do not necessarily represent homogeneous geographical environments but may be consistent with geochemical populations. The data can be further analysed by simple point related graphics and univariate data analysis using EDA.

If this is insufficient and uncertainties about interpretation still remain (for example the occurrence of false anomalies) some multi-variate data analysis techniques can be applied such as multiple regression and canonical correlation analysis.

It is important that the data structure fits the above mentioned statistical models otherwise results might be meaningless. To overcome these problems the application of robust statistics is highly recommended.

2.3. Local Level

The exploration at this level aims at outlining the extent of a mineralisation. The sampling density is high (100 to 250 samples per km^2) and sample material and chemical analysis is closely adapted to the geochemical nature of the mineral target. Likewise, the statistical treatment of the data depends very much on the complexity of the chemistry, mineralogy and structural setting of the mineralisation in question. In principle, the statistical treatment may again follow the methodologies described in chapter 2.2.1, but it is not possible to design a universal statistical line of approach. For the initial step, however, it is recommended to use techniques derived from "Exploratory Data Analysis" as mentioned in chapter 2.1.1. and to investigate the multivariate geochemical relations by graphical displays like scatterplots and multiple code symbols, as described by [9] Kuerzl, 1986.

At the local level various geophysical and geochemical prospecting methods are often intimately integrated and in the evaluation of the data it is recommended to use multivariate techniques in which geochemical as well as geophysical and geological parameters are included. However, care must be taken to include only relevant variables in the multivariate analysis.

The multivariate signature over a given target can be used to identify other potential targets in the explored area containing the same or similar geochemical characteristics.

REFERENCES

[1] TUKEY, J. W. (1977): Exploratory Data Analysis. Addison Wesley Publ. Comp., Reading, Mass.

[2] GARRETT, R.G. (1983): Opportunities for the 80s. Math. Geol. 15, 385-398.

[3] HOWARTH, R.J. (1984): Statistical Application in Geochemical Prospecting: A Survey of Recent Developments. Journ. of Geochem. Expl. 21, 41-61.

[4] HOWARTH, R. (ed.) (1983): Statistics and data analysis in geochemical prospecting. in: Govett G. J. S. (ed.), Handbook of exploration geochemistry, Vol. 2, Elsevier, Amsterdam.

[5] REIMANN, C. and WURZER, F. (1987): Monitoring Accuracy and Precision - Improvements by Introducing Robust and Resistant Statistics. Mikrochimica Acta (in press) - Proceedings of COBAC IV, Graz 1986.

[6] HOAGLIN, D. C., MOSTELLER, F. and TUKEY, J. W. (ed.) (1983): Understanding Robust and Exploratory Data Analysis. John Wiley and Sons, Inc., New York.

[7] FRIEDMAN, J. H. and RAFSKY, L. C. (1981): Graphics for the Multivariate Two Sample Problem. J. Am. Stat. Ass., Vol. 76, No. 374.

[8] SINDING-LARSEN, R. (1974): A computer method for dividing a regional geochemical survey area into homogeneous subareas prior to statistical interpretation. in: I. L. Elliott and W. K. Fletcher (Editors). Geochemical Exploration 1974. Elsevier. Amsterdam.

[9] KUERZL. H. (1986): Graphical displays of multivariate data on scatterplots and maps as an aid to detailed interpretation. IAEA-Publ.. in press.

Working Group 4

DATABASE MANAGEMENT SYSTEM

Members: **F. Wurzer** (Austria)
Yuxuan Xue (China)
G. Hatziyannis (Greece)
S.G. Tewari (India)
E. Hammerbeck (South Africa)

1. INTRODUCTION

The panel discussion on database management systems was initiated to compile the different experiences of the participants on that field valid for their work in their country. As a result some basic or fundamental guidelines concerning the whole field of capturing and storing geological data on computer systems shall be outlined.

2. WHY DATABASES ?

In any mineral exploration activity an enormous amount of data is generated which has to be coordinated, accessed and operated upon for monitoring the progress, making decisions, providing information for application of new strategies. An efficient way of handling such data is through a Database Management System rather than a conventional File Management System. The organization of data files in a database concept achieves three major objectives:

- Data Integration,
- Data Integrity,
- Data Independence;

and this concept also avoids much redundancy of data as in conventional File Management Systems.

There are various stages involved in uranium exploration activity, namely aerial reconnaissance by high sensitivity gamma-ray spectrometer, carborne surveys, ground surveys, trenching, drilling and finally mining and exploitation of an ore deposit. At all stages a wide variety of data is generated which has to be properly filed and linked for future use. This need was also stressed by the Advisory Group of Uranium Exploration and Regional Evaluation (Vienna, 1985)

Such data for most of the mines and prospects are kept under the control of private or government agencies. It is felt that such data is a national asset and should be preserved in databases before it is too late and it is either lost or may get disintegrated in such a way that proper collation may not be possible and it may need reevaluation of an area at enormous cost. Though detailed studies have not been done for computing the cost-benefit ratio in preserving the data in machine readable form, it is felt that it would be quite low, and governments should provide sufficient financial support to establishing databases for the proper long-term storage of geoscience data.

Also uranium exploration activity is multidisciplinary. Persons from many disciplines like geology, geophysics, geochemistry, drilling, mining, petrology, management, etc., are associated in the whole process. In a database approach each user can view the data to serve his special needs.

3. WHAT KIND OF DATABASES

While the need for a wide range of databases is recognized the panel discussion centered around those dealing with mineral deposits. The objective for a database must be clearly defined and great care must be taken to prevent the escalation of the database to incorporate related fields. At the same time structures must be created permitting the integration of such related field at some stage or another.

The following kinds of databases are considered essential for the comprehensive storage of data on mineral deposits:

(i) Mineral deposit inventories - detailing the name of the deposit, its location, the commodity(ies) present, information regarding the status (i.e. occurrence, prospect, deposit), and mining (i.e. mine, inactive mine, closed mine).

(ii) Description of orebodies - Details on the mineral deposits entered on the mineral inventory files.

(iii) Exploration - Exploration history and results, i.e. borehole database and results of exploration programmes.

(iv) Resources - Such databases should contain comprehensive original data from which resource calculations can be performed.

(v) Geology - An integrated database system on mineral deposits must be able to relate the deposit to its geological environment.

The following are examples of a few databases on mineral deposits that where discussed:

INTURGEO (International Uranium Geology Information System):

This system, installed at the IAEA in Vienna, consists of two files, one world-wide and the other on uranium deposits of the United States of America (See Appendix).

INDURGEO (Indian Uranium Geology Information System):

A planned dedicated database of uranium deposits of India, based on INTURGEO.

SAMINDABA (South African Mineral Deposits Database):

A comprehensive database covering most of the above-mentioned aspects on South African mineral deposits.

GEOSIS (Geoscience Spatial Information System):

A database that is being developed at the Ontario Geological Survey, attempting to integrate structured, digital data with unstructured graphical, and descriptive data.

4. HARDWARE REQUIREMENTS

The actual hardware requirements for a geological database system are strongly dependent on the amount of data which has to be handled. The basic hardware components for a database system are a computer and in addition the secondary storage units. The size of the used computer can range from a micro or personal computer up to a big mainframe computer, each with the corresponding storage units (e.g. floppy disks, hard disks, tapes). Geologists should really be encouraged to build their own databases to fulfill the basic requirement not to loose data. Database systems can also be established on microcomputers.

The choice of hardware is not that important, however there exist some problems concerning portability and compatibility, but it is up to the computer engineers to solve these problems.

The basic concept concerning hardware can be described as follows: The main task for database systems is to save data, time and cost, they can or should be established on available hardware. But to keep in mind national and international cooperation and to make it easier the problems of compatibility and portability must be borne in mind. So each small database system has to fit into a larger concept or system, at least the facilities for data exchange have to be provided.

5. SOFTWARE

Compatibility and portability are the most important problems concerning database management systems. As for hardware it has again to be said that each database which is built has to provide the open links to fit into a larger concept or system to provide data transfer, integration and access for national and international cooperation.

Commercial software can and should be used where available. Such products are also offered for microcomputers. In-house developments can be appropriate to solve special problems but they require more personnel to write the necessary programs.

There are basically three approaches which are also implemented in commercial database management systems. First, the hierarchical database systems; second, the network, and third, the relational database systems. The oldest systems have been the hierarchical ones and they are still in use, but may become obsolete. The disadvantages of these systems lie primarily in the strong hierarchical structure which is not necessarily the best model for real world data. The network approach is more appropriate to model data and to implement a database but for complex systems, and geological data sets most of the time have complex structures, retrievals may get very slowly and also update and maintaining of a network database can be a complex task. As the state-of-art in computer science the relational database systems can be recommended mostly. The main advantages of this approach are the simplicity of the corresponding data models, the simplicity of update and last not least the flexibility of retrieval operations. It is also a fact that the recently developed commercial systems are relational database systems and most of the present research in computer science is done in this field. M.T. Holroyd, in his paper, presents an interesting mathematical model to accomplish the applicability of relational database models to geoscience data.

Another point concerning software is the choice of the user interface. There are the two basic solutions, the users can communicate with the system via a menu or via a defined command language. Menu driven programs are very useful for unexperienced users. On the other hand, if users get accustomed to a database system they often do not like to go through all the offered menus they know their exact questions and they prefer a more direct route. Command language driven systems are more convenient for the latter requirements. It is also possible to have both to give the user the choice in which way he likes to communicate with the system.

6. PERSONNEL REQUIREMENTS AND TRAINING

The requirement of personnel for establishing a uranium database will depend on the exploration activity of the country. For designing the file structure and the schema a minimum of two trained persons is needed. They have to interact with as many users as possible so as to develop the optimum design.

In parallel the data has to be coded in machine readable form. For this job also a minimum of two data entry operators is needed to start with, which can be reviewed as the work expands. Apart from these two groups, one very senior officer is needed to take charge as a database administrator.

For the users, it is necessary to get involved in the project and to achieve this objective regular training programmes have to be organized for small groups of people. This will help to remove the fear of using a computerized information retrieval system. It should also be borne in mind that this training should also convince users that partially confidential information can be protected by implementing various levels of security.

During training it should also be impressed that a geologist, geophysicist, etc., can run their application programs using the data already available in the database, e.g. any type of statistical analysis.

7. SECURITY OF DATA

Database security is an important aspect which requires special attention during the design and operation of a system. This has a bearing not only on unauthorized access to database functions, the integrity of data, and the safeguarding of data of proprietory nature, but will to a large degree influence the confidence and participation of organizations and individuals in the systems.

In SAMINDABA database security is handled at three levels. Firstly, at the systems level the built-in options available with the DBMS apply. Secondly, at the applications level, special controls were introduced to determine at what level entry into the system is permitted, what actions may be performed and what data may be accessed. Thirdly, data of proprietory nature is specially flagged and the ownership of that data indicated, in order to restrict access to such data. Users who do not have access to proprietory data will not be aware that such data even exist in the database.

8. OUTPUT, INTERFACE TO APPLICATION PROGRAMS AND INTEGRATION OF DATA

A properly designed geological database must provide the user with a variety of outputs for retrieval of data, for report writing in specific formats and for the use of the files by other programs. The end user must be able to extract the required information in any form in order to incorporate it in a report, or to process it with specific application programs, even with another computer system. For the latter case the output files must be in the standard ASCII format, and the database must include a good report generator.

Since the database will not be a simple mineral inventory system but will contain various data sets with exploration, geological and mining data it must allow the integration and processing of these data sets with specific application programs or packages. Therefore it is necessary to interface the database with other packages or programs running in the same computer for direct access and processing of data such as statistical analysis, contouring and other graphic applications, ore reserve estimation, geostatistical analysis and kriging, filtering, image processing, etc.

For the integration of data suitable links must be designed between the various data sets. They will give the user the capability to integrate and overlay processed data from geological, geochemical, geophysical, metallogenic and mining data sets, allowing him to make valid conclusions.

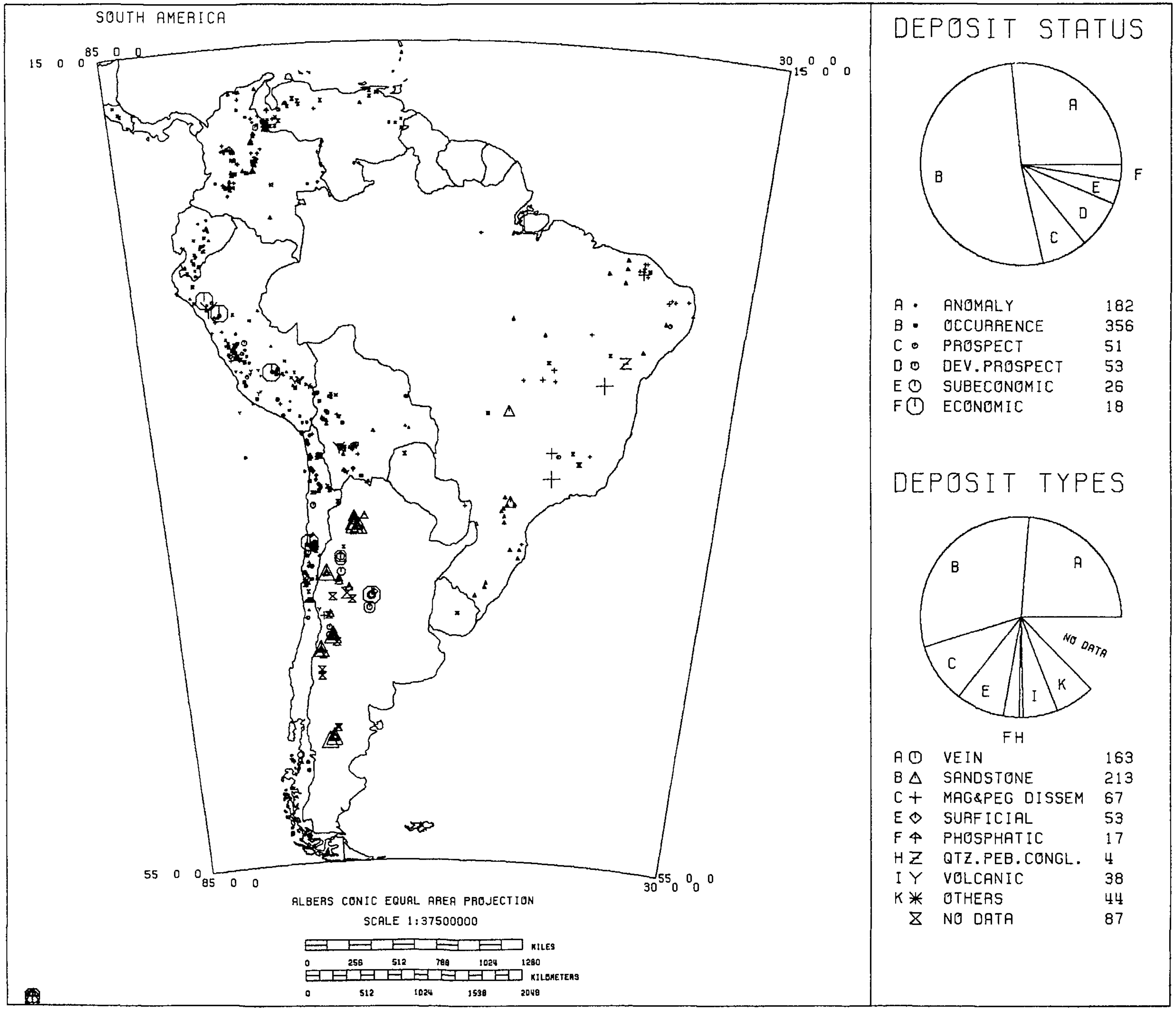

Appendix
Example of output and input form as given in the
IAEA International Uranium Geology Information System INTURGEO

INTERNATIONAL URANIUM GEOLOGY INFORMATION SYSTEM (INTURGEO) PAGE -: 1
URANIUM OCCURRENCE REPORT

OCCURRENCE -:	**WOODFORDS NO. 2**		**MAP NUMBER**	-:	**AUL-190**
COUNTRY	-:	AUSTRALIA	RECORDER	-:	SAZEDJ, F.
PROVINCE	-:	NEW SOUTH WALES	DISTRICT	-:	INVERELL
LATITUDE	-:	29°48'00"S	LONGITUDE	-:	151°09'00"E

GEOLOGIC CHARACTERISTICS -:

DEPOSIT TYPE	-:	VEIN	STATUS	-:	PROSPECT
HOST ROCK	-:	GRANITE	HOST AGE	-:	PERM-TRIASSIC
TECT.SETTING	-:		DEPOSIT SIZE	-:	_

TYPICAL MINERALOGY	IMPORTANT ORE CONTROLS	ALTERATION	TRACE ELEMENTS
URANOPHANE	QUARTZ-BRECCIA VEIN		

DEPOSIT SUMMARY

Woodfords No. 2 prospect, Gilgai, is several kilometres northeast of No 1 prospect. A narrow quartz vein within granite occupies a fissure striking 254 degrees and traceable for 5 km, but radioactivity is confined to a brown ferruginous quartz-breccia vein 90 m in length adjoining the southern wall of the barren quartz vein. The width of the breccia vein is from 20 to 90 cm A yellow to orange secondary uranium mineral encrusts haematite, limonite, and quartz, or is present as linings and fillings of small vughs The mineral has been tentatively identified as uranophane of beta-uranotil, and could derive from pitchblende or uraninite at depth (From: Willis J.L and Stevens B.P J , 1971 p. 43.)

REFERENCES -:

Willis J L and Stevens B P.J., 1971, Uranium· The Mineral Industry of New South Wales No. 43, Dep. of Mines, Geol. Survey of New South Wales, 1974.

SOURCE IAEA INTURGEO, REPORT XEAXIUOR 21/02/86

LIST OF PARTICIPANTS

AUSTRIA

Dr. H. Kürzl
Joanneum Research Society
Mineral Resources Research Division
Roseggerstr. 15, A-8700 LEOBEN

Mr. F. Wurzer
Joanneum Research Society
Mineral Resources Research Division
Roseggerstr. 15, A-8700 LEOBEN

BELGIUM

Mr. L.J. Dejonghe
Ministère des Affaires Economiques
Administration des Mines
Service Géologique de Belgique
Rue Jenner 13, B-1040 Bruxelles

CAMEROON

Mr. Njibaloh Ndah
Ministère des Mines et Energie
Direction Mines et Geologie, Yaounde

CHINA, PEOPLE'S REP.

Ms. Shuxin Zhao
Ministry of Nuclear Industry
Bureau of Geology
P.O. Box 183, Shijiazhuang
Province Hebei

Ms. Yuxuan Xue
Ministry of Nuclear Industry
Bureau of Geology
P.O. Box 1436, Beijing

DENMARK

Ms. A. Steenfelt
Grønlands Geologiske Undersøgelse
Øster Voldgade 10
DK-1350 Copenhagen K

EGYPT

Dr. M.E. Mostafa
Nuclear Materials Corporation
Scientific Information Department
P.O. Box 530
El Maadi, Cairo

FINLAND

Mr. V.V. Kuosmanen
Geological Survey of Finland
c/o VTT/MAA
Itätuulentie 2A
SF-02100 Espoo

Mr. J. Talvitie	Geological Survey of Finland Kivimiehentie 1 SF-02150 Espoo

GERMANY, FED. REP. OF

Dr. K. Busch	Bundesanstalt für Geowissenschaften und Rohstoffe Postfach 510153 D-3000 Hannover

GREECE

Mr. G. Hatziyannis	Institute of Geology and Mineral Exploration (IGME) 70, Messogion Str., Athens

HUNGARY

Mr. A. Várhegyi	Mecsek Ore Mining Enterprise Pécs, 39-es Dandár u. 19. H-7633 Budapest

INDIA

Mr. N.V.A.S. Perumal	Atomic Minerals Division Department of Atomic Energy 1-10-153/156, Begumpet Hyderabad 500 016
Mr. S.G. Tewari	Atomic Minerals Division Department of Atomic Energy College House, AMD Complex Begumpet, Hyderabad - 500 016

JORDAN

Mr. H.M.H.I. Ayesh	Arab Mining Company P.O. Box 20198, Amman

SINGAPORE, REP. OF

Prof. Y.Chong	Department of Physics National University of Singapore Kent Ridge

SRI LANKA

Mr. P. Abeysinghe	Geological Survey Department 48, Sri Jinaratana Rd., Colombo 2

SOUTH AFRICA

Dr. B. Hambleton-Jones	Atomic Energy Co. of South Africa, Ltd. Private Bag X256 Pretoria 0001

Mr. J.N. Faurie	Atomic Energy Co. of South Africa, Ltd. Private Bag X256 Pretoria 0001
Dr. E.C.I. Hammerbeck	Geological Survey of South Africa Private Bag X112 Pretoria 0001

THAILAND

Mr. S. Potisat	Department of Mineral Resources Mineral Resources Development Project Economic Geology Division Rama VI Rd., Bangkok 10400

TURKEY

Mr. S. Uçakciouglu	General Directorate of Mineral Research and Exploration Ankara

UNITED KINGDOM

Mr. G.R. Garrard	Hunting Geology and Geophysics Ltd. Elstree Way, Borehanwood Herts WD6 1SB

YUGOSLAVIA

Mr. M. Pecnik	Geoloski Zabod Ljubljana Dimiceva 16 61000 Ljubljana
Mr. J. Tomsic	Geoloski Zabod Ljubljana Dimiceva 16 61000 Ljubljana

HOW TO ORDER IAEA PUBLICATIONS

An exclusive sales agent for IAEA publications, to whom all orders and inquiries should be addressed, has been appointed in the following country:

UNITED STATES OF AMERICA	UNIPUB, 4611-F Assembly Drive, Lanham, MD 20706-4391

In the following countries IAEA publications may be purchased from the sales agents or booksellers listed or through major local booksellers. Payment can be made in local currency or with UNESCO coupons.

ARGENTINA	Comisión Nacional de Energía Atómica, Avenida del Libertador 8250, RA-1429 Buenos Aires
AUSTRALIA	Hunter Publications, 58 A Gipps Street, Collingwood, Victoria 3066
BELGIUM	Service Courrier UNESCO, 202, Avenue du Roi, B-1060 Brussels
CHILE	Comisión Chilena de Energía Nuclear, Venta de Publicaciones, Amunategui 95, Casilla 188-D, Santiago
CHINA	IAEA Publications in Chinese: China Nuclear Energy Industry Corporation, Translation Section, P.O. Box 2103, Beijing IAEA Publications other than in Chinese: China National Publications Import & Export Corporation, Deutsche Abteilung, P.O. Box 88, Beijing
CZECHOSLOVAKIA	S.N.T.L., Mikulandska 4, CS-116 86 Prague 1 Alfa, Publishers, Hurbanovo námestie 3, CS-815 89 Bratislava
FRANCE	Office International de Documentation et Librairie, 48, rue Gay-Lussac, F-75240 Paris Cedex 05
HUNGARY	Kultura, Hungarian Foreign Trading Company, P.O. Box 149, H-1389 Budapest 62
INDIA	Oxford Book and Stationery Co., 17, Park Street, Calcutta-700 016 Oxford Book and Stationery Co., Scindia House, New Delhi-110 001
ISRAEL	Heiliger & Co. Ltd. 23 Keren Hayesod Street, Jerusalem 94188
ITALY	Libreria Scientifica, Dott. Lucio de Biasio "aeiou", Via Meravigli 16, I-20123 Milan
JAPAN	Maruzen Company, Ltd, P.O. Box 5050, 100-31 Tokyo International
PAKISTAN	Mirza Book Agency, 65, Shahrah Quaid-e-Azam, P.O. Box 729, Lahore 3
POLAND	Ars Polona-Ruch, Centrala Handlu Zagranicznego, Krakowskie Przedmiescie 7, PL-00-068 Warsaw
ROMANIA	Ilexim, P O. Box 136-137, Bucharest
SOUTH AFRICA	Van Schaik Bookstore (Pty) Ltd, P.O. Box 724, Pretoria 0001
SPAIN	Díaz de Santos, Lagasca 95, E-28006 Madrid Díaz de Santos, Balmes 417, E-08022 Barcelona
SWEDEN	AB Fritzes Kungl. Hovbokhandel, Fredsgatan 2, P.O. Box 16356, S-103 27 Stockholm
UNITED KINGDOM	Her Majesty's Stationery Office, Publications Centre, Agency Section, 51 Nine Elms Lane, London SW8 5DR
USSR	Mezhdunarodnaya Kniga, Smolenskaya-Sennaya 32-34, Moscow G-200
YUGOSLAVIA	Jugoslovenska Knjiga, Terazije 27, P.O. Box 36, YU-11001 Belgrade

---

Orders from countries where sales agents have not yet been appointed and requests for information should be addressed directly to:

Division of Publications
International Atomic Energy Agency
Wagramerstrasse 5, P.O. Box 100, A-1400 Vienna, Austria